Vol. 65 December, 1961 No. 12

THE JOURNAL OF PHYSICAL CHEMISTRY

(Registered in U. S. Patent Office)

CONTENTS

NOTES

THE JOURNAL OF PHYSICAL CHEMISTRY

(Registered in U. S. Patent Office)

Published monthly by the American Chemical Society at 20th and Northampton Sts., Easton, Pa.

Second-class mail privileges authorized at Easton, Pa. This publication is authorized to be mailed at the special rates of postage prescribed by Section 131.122.

The *Journal of Physical Chemistry* is devoted to the publication of selected symposia in the broad field of physical chemistry and to other contributed papers.

Manuscripts originating in the British Isles, Europe and Africa should be sent to F. C. Tompkins, The Faraday Society, 6 Gray's Inn Square, London W. C. 1, England.

Manuscripts originating elsewhere should be sent to W. Albert Noyes, Jr., Department of Chemistry, University of Rochester, Rochester 20, N. Y.

Correspondence regarding accepted copy, proofs and reprints should be directed to Assistant Editor, Allen D. Bliss, Department of Chemistry, Simmons College, 300 The Fenway, Boston 15, Mass.

Business Office: Alden H. Emery, Executive Secretary, American Chemical Society, 1155 Sixteenth St., N. W., Washington 6, D. C.

Advertising Office: Reinhold Publishing Corporation, 430 Park Avenue, New York 22, N. Y.

Articles must be submitted in duplicate, typed and double spaced. They should have at the beginning a brief Abstract, in no case exceeding 300 words. Original drawings should accompany the manuscript. Lettering at the sides of graphs (black on white or blue) may be pencilled in and will be typeset. Figures and tables should be held to a minimum consistent with adequate presentation of information. Photographs will not be printed on glossy paper except by special arrangement. All footnotes and references to the literature should be numbered consecutively and placed in the manuscript at the proper places. Initials of authors referred to in citations should be given. Nomenclature should conform to that used in *Chemical Abstracts*, mathematical characters be marked for italic, Greek letters carefully made or annotated, and subscripts and superscripts clearly shown. Articles should be written as briefly as possible consistent with clarity and should avoid historical background unnecessary for specialists.

Notes describe fragmentary or incomplete studies but do not otherwise differ fundamentally from articles and are subjected to the same editorial appraisal as are articles. In their preparation particular attention should be paid to brevity and conciseness Material included in Notes must be definitive and may not be republished subsequently.

Communications to the Editor are designed to afford prompt preliminary publication of observations or discoveries whose value to science is so great that immediate publication is imperative. The appearance of related work from other laboratories is in itself not considered sufficient justification for the publication of a Communication, which must in addition meet special requirements of timeliness and significance. Their total length may in no case exceed 1000 words or their equivalent. They differ from Articles and Notes in that their subject matter may be republished.

Symposium papers should be sent in all cases to Secretaries of Divisions sponsoring the symposium, who will be responsible for their transmittal to the Editor. The Secretary of the Division by agreement with the Editor will specify a time after which symposium papers cannot be accepted. The Editor reserves the right to refuse to publish symposium articles, for valid scientific reasons. Each symposium paper may not exceed four printed pages (about sixteen double spaced typewritten pages) in length except by prior arrangement with the Editor.

Remittances and orders for subscriptions and for single copies, notices of changes of address and new professional connections, and claims for missing numbers should be sent to the American Chemical Society, 1155 Sixteenth St., N. W., Washington 6, D. C. Changes of address for the *Journal of Physical Chemistry* must be received on or before the 30th of the preceding month.

Claims for missing numbers will not be allowed (1) if received more than sixty days from date of issue (because of delivery hazards, no claims can be honored from subscribers in Central Europe, Asia, or Pacific Islands other than Hawaii), (2) if loss was due to failure of notice of change of address to be received before the date specified in the preceding paragraph, or (3) if the reason for the claim is "missing from files."

Subscription rates (1961): members of American Chemical Society, $12.00 for 1 year; to non-members, $24.00 for 1 year. Postage to countries in the Pan-American Union $0.80; Canada, $0.40; all other countries, $1.20. Single copies, current volume, $2.50; foreign postage, $0.15; Canadian postage, $0.10; Pan-American Union, $0.10. Back volumes (Vol. 56–64) $30.00 per volume; foreign postage, per volume $1.20, Canadian, $0.40; Pan-American Union, $0.80. Single copies: back issues, $3.00; for current year, $2.50; postage, single copies: foreign, $0.15; Canadian, $0.10; Pan-American Union, $0.10.

The American Chemical Society also publishes *Journal of the American Chemical Society, Chemical Abstracts, Industrial and Engineering Chemistry*, International Edition of *Industrial and Engineering Chemistry, Chemical and Engineering News, Analytical Chemistry, Journal of Agricultural and Food Chemistry, Journal of Organic Chemistry, Journal of Chemical and Engineering Data, Chemical Reviews, Chemical Titles* and *Journal of Chemical Documentation*. Rates on request.

COMMUNICATION TO THE EDITOR

THE JOURNAL OF
PHYSICAL CHEMISTRY

VOL. LXV

1961

EASTON, PA.
MACK PRINTING COMPANY
1961

THE JOURNAL OF
PHYSICAL CHEMISTRY

(Registered in U. S. Patent Office) (© Copyright, 1962, by the American Chemical Society)

VOLUME 65 JANUARY 9, 1962 NUMBER 12

ION-EXCHANGE IN CONCENTRATED ELECTROLYTE SOLUTIONS. I. THE SYSTEM LITHIUM CHLORIDE–ALKALI CHLORIDE–DOWEX-50

BY WALTER A. PLATEK[1a] AND JACOB A. MARINSKY[1b]

Department of Chemistry, University of Buffalo, Buffalo, N. Y.

Received April 27, 1961

The ion-exchange behavior of trace components has been studied by measuring the variation of selectivity, K_{Li}^{M}, as a function of external LiCl molality using Dowex-50 in the Li form. A molality range of 0.1 to 13.5 has been investigated with the trace component MCl, including NaCl, RbCl, CsCl and HCl, respectively. The effect of temperature in the range of 25–170° also has been studied to facilitate evaluation of thermodynamic exchange functions for these systems. The results are considered primarily on the basis of ionic hydration and binding.

Introduction

Numerous investigations have been reported in the field of ion-exchange in concentrated electrolyte media. These investigations, however, have been concerned primarily with separations and/or the elucidation of formation constants for metal complexes in the aqueous systems rather than with the thermodynamic behavior of the exchange system.[2,3]

The reaction under consideration in this study was

$$\overline{\text{LiCl}} + \text{MCl} \rightleftarrows \overline{\text{MCl}} + \text{LiCl} \qquad (1)$$

where M is an alkali metal cation and the barred terms refer to species in the resin phase. The thermodynamic equilibrium constant for the above reaction is

$$K_a = \frac{\overline{a_{\text{MCl}}}\, a_{\text{LiCl}}}{a_{\text{MCl}}\, \overline{a_{\text{LiCl}}}} = \frac{\overline{\gamma_{\pm\text{MCl}}{}^2}\, \overline{m_{\text{M}^+}}\, \gamma_{\pm\text{LiCl}}{}^2\, m_{\text{Li}^+}}{\gamma_{\pm\text{MCl}}{}^2\, m_{\text{M}^+}\, \overline{\gamma_{\pm\text{LiCl}}{}^2}\, \overline{m_{\text{Li}^+}}} \qquad (2)$$

and is made equal to unity by selecting the same standard state for the aqueous and resin phases. The symbol a is the activity, $\gamma\pm$, the mean activity coefficient and m, the molal concentration of the species under consideration. Other distribution expressions are more readily obtained experimentally such as the selectivity coefficient

$$K = \frac{\overline{m_{\text{M}^+}}\, m_{\text{Li}^+}}{m_{\text{M}^+}\, \overline{m_{\text{Li}^+}}} = \frac{\gamma_{\pm\text{MCl}}{}^2\, \overline{\gamma_{\pm\text{LiCl}}{}^2}}{\overline{\gamma_{\pm\text{MCl}}{}^2}\, \gamma_{\pm\text{LiCl}}{}^2} \qquad (3)$$

and the modified selectivity coefficient, K', which involves aqueous phase activity coefficients

$$K' = K\,\frac{(\gamma_{\pm\text{LiCl}}{}^2)}{(\gamma_{\pm\text{MCl}}{}^2)} \qquad (4)$$

The K' coefficient leaves the variation in observed selectivity due only to activity coefficients in the resin phase. A subsequent paper in the series will attempt the calculation of these resin phase activity coefficients and thus an independent determination of K from the osmotic coefficients of a mixed electrolyte–resinate system.

In this work, K was studied as a function of the external LiCl concentration over a range from 0.1 to 13.5 molal. The cation M (= Na, Rb or Cs), was present in initial concentrations ranging from 10^{-2} molal to trace amounts so that the mole fraction of lithium containing species in each phase was essentially unity. In all experiments where HCl was the minor component, its molality was 0.1. Activity coefficients for LiCl in the aqueous phase are identical to those for pure LiCl solutions; the activity coefficients for trace MCl in the presence of LiCl can be calculated up to saturation molalities of MCl by use of the Harned–Cooke[4] equation in the form

$$\log \gamma_{0(\text{MCl})} = \log \gamma_{\text{MCl}(0)} + \alpha m + \beta m^2 \qquad (5)$$

where $\gamma_{0(\text{MCl})}$ is the activity coefficient of a trace of MCl in the presence of LiCl at molality m,

---

(1) (a) Taken in part from the dissertation submitted by Walter A. Platek in partial fulfillment of the requirements for the Ph.D. degree in February 1961; (b) Author to whom requests for reprints are to be addressed. Dept. of Chemistry, Univ. of Buffalo, Buffalo, N. Y.

(2) (a) R. M. Diamond, *J. Am. Chem. Soc.*, **77**, 2978 (1955); (b) K. A. Kraus and F. Nelson, "Proceedings of the International Conference on the Peaceful Uses of Atomic Energy" (Geneva, 1955), vol. 7, pp. 113, 131, United Nations, 1956.

(3) F. W. E. Strelow, *Anal. Chem.*, **32**, 1185 (1960).

(4) R. A. Robinson and C. K. Lim, *Trans. Faraday Soc.*, **49**, 1144 (1953).

$\gamma_{MCl(0)}$ is the activity coefficient of pure MCl at molality m, and the terms α and β are experimentally determined parameters. At molalities of MCl above saturation, the term $\gamma_{MCl(0)}$ is calculated by extension of the 3-parameter form of the Debye–Hückel equation normally used in concentrated solutions.

The exchange reactions also were studied as a function of temperature so that the various thermodynamic functions of the exchange process could be evaluated.

Experimental Procedure

A. **Materials.**—The resin, Dowex-50-X-8, was kindly supplied by the Dow Chemical Company. Lithium chloride, reagent grade and sodium chloride, C.P., were purchased from J. T. Baker Company and used without further purification. Gamma emitting carrier-free radioactive nuclides 19.5 d Rb^{86} and 2.3 y Cs^{134} were purchased from the Radioisotopes Division of the Oak Ridge National Laboratories. The carrier-free 2.6 y Na^{22} was purchased from Nuclear Science and Engineering Corporation. Deionized water was used in the preparation of all solutions. All solutions were stored in polyethylene bottles to prevent exchange between the solution and the glass.

B. **Experimental.**—All equilibrations of aqueous systems conducted at temperatures up to 75° were carried out in 25-ml. erlenmeyer flasks which had been cleaned previously with hot nitric acid. Parr peroxide bombs were used for all runs made above 75°. Each experiment was made in duplicate. Ten-ml. portions of a specified LiCl stock solution and either 2 ml. of deionized water or 2 ml. of radioactive Na, Rb or Cs (sometimes with added carrier) in very dilute HCl (pH >5) in that order were added by means of a pipet to 1.000-g. samples of oven dried 20 to 50 mesh resin in the lithium form. The exchange of Li^+ and H_3O^+ ions was studied using 0.1 M HCl. An equivalent amount of resin which had been previously stored over water was used in experiments using LiCl solutions of molality less than unity in place of dry resin to prevent bead fracture. The flask was covered with a polyethylene stopper and shaken at a speed sufficient to keep the resin particles from settling. Samples equilibrated at temperatures other than ambient were shaken by attaching them to an extension arm of the shaking machine which extended through a hole into the oven.

The temperature was not controlled for equilibrations carried out at ambient conditions (24°) and varied by ±2°. A temperature constant to ±0.2° was maintained by use of a forced air circulating oven at temperatures other than ambient.

The selectivity was studied as a function of time in the first experiments conducted at the various ionic strengths employed to determine the time that was needed to achieve equilibrium. As much as 120 hours was needed at an external molality of 13.5. Highly concentrated salt solutions are quite viscous and diffusion of the species present is slow.

A centrifugation technique similar to that employed by Pepper[5] was used to separate the resin from the aqueous phase as completely as possible. Samples run at elevated temperatures were quenched in an ice-bath before centrifugation. Centrifugation, continued until successive five minute centrifugations showed no loss in sample weight, required 20–30 minutes. After transfer of the sample, the empty frit was weighed and the total weight of resin, water and invaded electrolyte determined by difference.

This centrifugation procedure does not remove all the surface adsorbed liquid from the resin beads. Analogous experiments carried out with spherical glass beads of mesh size 60–80 showed an upper limit of surface adsorption of 0.0163 g. of solution per g. of beads when contacted with 13.5 molal LiCl. The adsorption by 20–50 mesh material is even less and usually is neglected. Kraus[6] has reached the same conclusion from studies carried out in more dilute solutions.

The radioactive samples were placed in 13 × 100 mm. test-tubes and the activity measured in a 1-1/4″ by 2″ well-type sodium iodide, thallium activated, γ-ray scintillation crystal detector. To maintain the same geometry in all cases, the resin samples were centrifuged to the same height as the aqueous samples.

Aliquot portions of the aqueous solution after centrifugation were diluted and analyzed for chloride (= lithium) by the standard Mohr method. The resin was placed on a medium porosity glass-fritted funnel and was eluted slowly under slight suction with about 100 ml. of water to determine the amount of imbibed electrolyte. Chloride analysis of this eluent, after concentration by evaporation if necessary, also was done by the Mohr method.

Results

Table I contains the experimentally observed trace selectivities (K) as a function of the external LiCl molality. The resin water content and internal molalities (invaded electrolyte and exchange sites) which are used in determining the selectivity also are listed.[7] The modified selectivity coefficients (K') were calculated by use of the 2-parameter form of the Harned rule[4] (equation 5) to obtain activity coefficients for species present at essentially zero concentration in media of ionic strengths up to saturation of MCl; at higher molalities the extended Debye equation was used to obtain activity coefficients of pure MCl prior to use of the Harned rule. The Harned coefficients for RbCl were interpolated from those for the other alkali metals; values of $\alpha = 0.014$ and $\beta = 0$ were used. The selectivities at a molality of 0.1 have been modified by using the pressure–volume correction as calculated by Myers and Boyd[8] and are listed on the last line of the table. This correction is not needed at higher molalities. Again the RbCl correction was interpolated. The value for $K_{Li}{}^{Na}$ at 0.1 molal is in excellent agreement with that obtained by Soldano[9]; the value for $K_{Li}{}^{Cs}$ is somewhat lower than the Soldano value and may be due to a small variation in the resin cross-linkage; the Cs–Li exchange reactions would be most sensitive to this variable.

The invasion data that were obtained in the experimental program (column 3 of Table I) have been used as shown below to evaluate the $\overline{\gamma_{\pm LiCl}}$ values that are given in Table II. These values agree quite well with those previously obtained by Gregor.[7] These $\overline{\gamma_{\pm LiCl}}$ values were calculated from the condition that the chemical potential of a given component, in this case, LiCl, must be the same in both phases at equilibrium. The lithium ion in the resin phase comes from two sources, the resin bound Li^+ and the invaded LiCl. Thus

$$\overline{m_{Li^+}} = \overline{m_{R^-}} + \overline{m_{Cl^-}}$$

The $\overline{\gamma_{\pm CsCl}}$ values that also are listed in Table II were evaluated from equation 3 of the introduction using the $\overline{\gamma_{\pm LiCl}}$ values obtained as described above and the $\gamma_{\pm CsCl}$ values calculated from the modified Harned equation described earlier. It is important to keep in mind that these CsCl activity coefficients refer to "essentially zero" CsCl in highly concentrated solutions of either pure LiCl or a mixture of LiCl and LiR.

The compilation of invasion data at low ionic strength was not attempted during the experi-

---

[5] K. W. Pepper, D. Reichenberg and D. K. Hale, *J. Chem. Soc.*, 3129 (1952).

[6] F. Nelson and K. A. Kraus, *J. Am. Chem. Soc.*, **80**, 4154 (1958).

[7] H. P. Gregor and M. H. Gottlieb, *ibid.*, **75**, 3539 (1953).

[8] G. E. Myers and G. E. Boyd, *J. Phys. Chem.*, **60**, 521 (1956).

[9] B. Soldano and Q. V. Larson, *J. Am. Chem. Soc.*, **77**, 1331 (1955).

TABLE I

SELECTIVITY DATA—DOWEX-50

External molality LiCl	Water content g. H_2O/g. dry resin	Molality LiCl(r)	Molality LiR	M = Na K	M = Na K'	M = Rb K	M = Rb K'	M = Cs K	M = Cs K'	M = H_2O K	M = H_2O K'
13.5	0.2808	8.65	15.9	0.86	2.34	0.98	304	0.70	2890	6.53	6.27
11.1	.3347	5.91	13.6	1.09	4.02	1.39	197	0.99	898		
8.80	.4270	4.19	10.6	1.14	3.74					4.96	3.64
5.69	.6042	2.06	7.44	1.30	3.04	2.64	34.8	2.16	57.4		
2.89	.8229	0.606	5.51	1.29	1.66	3.80	11.2	3.48	14.3		
0.862				1.87	2.28	5.22	8.65	6.50	12.9		
0.1	.889	...	5.09	1.72	1.75	5.84	6.18	6.60	7.25		
0.1[a]	.889	...	5.09	1.83	1.85	6.40	6.95	7.45	8.10		

[a] πV correction applied.

TABLE II

ACTIVITY COEFFICIENTS

External molality LiCl	Internal molality LiCl + LiR	$\gamma_{\pm\text{LiCl}}$	$\overline{\gamma_{\pm\text{LiCl}}}$	$\gamma_{\pm\text{CsCl}}$	$\overline{\gamma_{\pm\text{CsCl}}}$
13.5	24.5	24.5	22.0	0.387	0.417
11.1	19.5	12.9	13.2	.428	.430
8.80	14.8	6.45	7.37		
5.69	9.50	2.42	3.09	.467	.405
2.89	6.12	1.05	1.50	.503	.382
0.862	~5.2	0.774	(1.16)	.547	(.322)

mental program and the estimate of $\overline{\gamma_{\pm\text{LiCl}}}$ in the system that was equilibrated with 0.86 molal LiCl is based upon linear extrapolation of the plot of $\overline{\gamma_{\pm\text{LiCl}}}/\gamma_{\pm\text{LiCl}}$ values *versus* external molality.

A plot of the $\gamma_\pm$ values *versus* ionic strength for LiCl and CsCl in aqueous LiCl–trace CsCl mixtures and in the imbibed resinate system. LiCl, LiR–trace CsCl, CsR, respectively, is presented in Fig. 1 to facilitate a comparison of $\overline{\gamma_\pm}$ values at the ionic strengths, m_{LiCl} and $\overline{m_{\text{Li}^+}}$, which result when the resin is equilibrated with a salt solution, thereby demonstrating the effect on $\gamma_\pm$ of the presence of resinate ions. Lines are drawn between the $\gamma_\pm$ values assigned to the salts in the resin and solution phases at equilibrium to demonstrate molality relationships in the resin and aqueous phases.

The variation of K with temperature is shown in Fig. 2 for Na–Li exchanges and in Fig. 3 for Rb–Li and Cs–Li exchanges. Plots of log K *vs.* $1/T$ for all cations studied appear to be linear within the limits of experimental error at all the molalities studied. Since there is some scatter of the data, the possibility of minimal curvature in several of the plots is not excluded. In any case, the value of ΔH as obtained from the slope is essentially un-

$$\left(\frac{\text{d}\log K}{\text{d}(1/T)} = \frac{-\Delta H}{2.3R}\right)$$

affected by temperature. This result is in agreement with a column chromatographic study of alkali cation–sodium exchange reactions carried out by Kraus[10] in dilute solution. The value of ΔH for the exchange reactions does not appear to be a function of the molality as soon as an appreciable amount of non-exchange electrolyte has entered the resin phase.

A study of non-exchange electrolyte invasion as

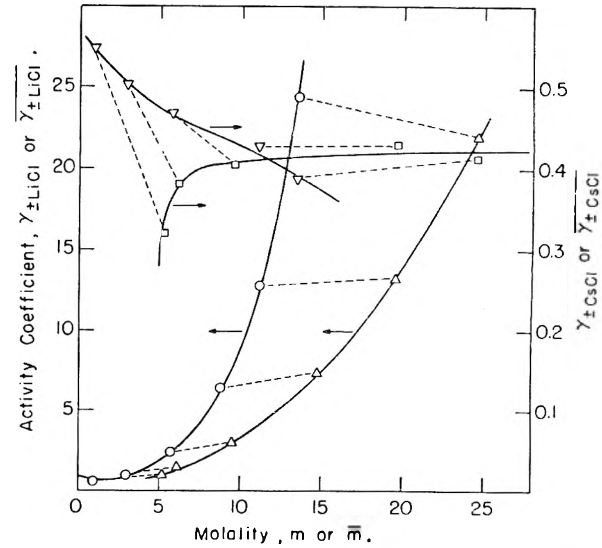

Fig. 1.—Plot of the activity coefficients in a given phase as a function of the molality of that phase. For the aqueous phase, $m = m_{\text{LiCl}}$; for the resin phase, $\overline{m} = \overline{m_{\text{LiCl}}} + \overline{m_{\text{LiR}}}$. Dashed lines are used as tie lines to connect the $\gamma_\pm$ values for a given species which result from the same experiment. $\gamma_{\pm\text{LiCl}}$, ○; $\overline{\gamma_{\pm\text{LiCl}}}$, △; $\gamma_{\pm\text{CsCl}}$, ▽; $\overline{\gamma_{\pm\text{CsCl}}}$, □.

a function of temperature shows that the ratio $\overline{\gamma_{\text{LiCl}}}/\gamma_{\text{LiCl}}$ is very nearly independent of temperature. Using this experimental fact, the ratio of $\overline{\gamma_{\text{MCl}}}/\gamma_{\text{MCl}}$ also should be only slightly affected by temperature. The minimal variation of K with temperature is consistent with this observation and indicates that the electrolyte in solution and resin phases is similarly affected by temperature.

The modified thermodynamic functions ($\Delta F'$, $\Delta H'$ and $\Delta S'$) that have been evaluated from the data are given in Table III and refer to the process of transfer of ions from an idealized aqueous solution into the resin phase under the conditions of the experiment at 25°. The approximation that K' varies exactly as K is necessary for the evaluation of $\Delta H'$ and introduces inherent error in its value.

Experimental osmotic coefficients that have been obtained by Patterson, Gilpatrick and Soldano[11] at 99.6° for NaCl, CsCl and LiCl at various concentration values demonstrate the effect of temperature on the ratio of $\gamma_{\text{LiCl}}/\gamma_{\text{MCl}}$ and these data may be used to estimate its effect on K'. The

---

[10] K. A. Kraus and R. J. Raridon, *J. Phys. Chem.*, **63**, 1901 (1959).

[11] C. S. Patterson, L. D. Gilpatrick and B. A. Soldano, private communication, 1959.

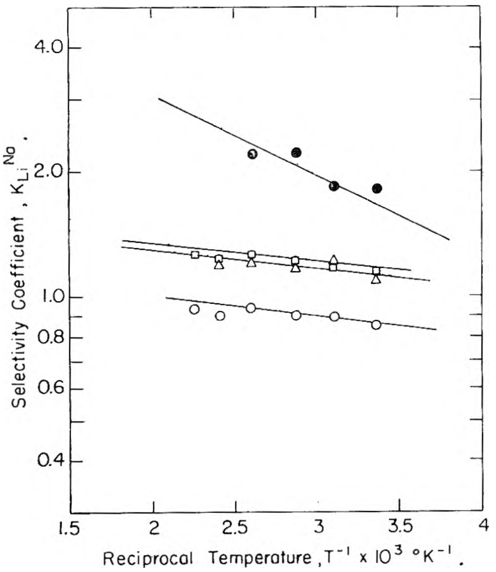

Fig. 2.—Selectivity coefficient, $K_{\mathrm{Li}}^{\mathrm{Na}}$, as a function of temperature: 13.5 molal, ○; 11.1 molal, △; 8.80 molal, □; 0.1 molal, ●.

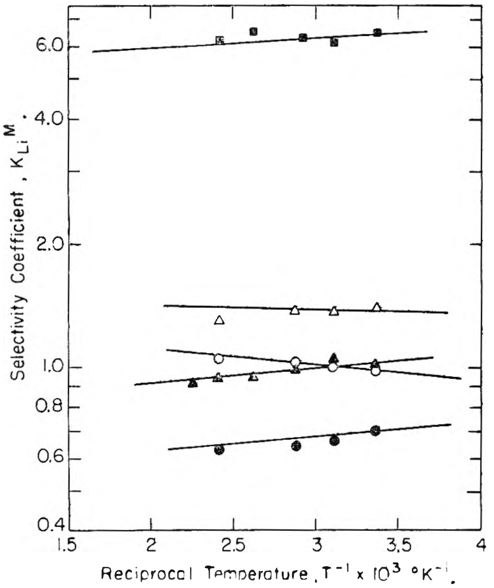

Fig. 3.—Selectivity coefficient, $K_{\mathrm{Li}}^{\mathrm{M}}$, as a function of temperature: $K_{\mathrm{Li}}^{\mathrm{Rb}}$, 13.5 molal, ○; 11.1 molal, △; $K_{\mathrm{Li}}^{\mathrm{Cs}}$, 13.5 molal, ●; 11.1 molal, ▲; 0.862 molal, ■.

TABLE III

THERMODYNAMIC EXCHANGE FUNCTIONS AT 25°

Exchange	External LiCl molality	$\Delta F'$, cal./mole	$\Delta H'$, cal./mole	ΔS, cal./mole deg.
Na–Li	0.1	−387	−852	−1.56
	8.80	−791	−227	1.89
	11.1	−832	−227	2.03
	13.5	−498	−227	0.91
Rb–Li	11.1	−3140	−218	10.5
	13.5	−3410	−141	11.0
Cs–Li	0.862	−1520	+178	5.70
	11.1	−3890	+178	13.6
	13.5	−4250	+178	14.9

deviations at 99.6° from osmotic properties at room temperature are slight except for LiCl whose osmotic coefficient decreases substantially as the concentration increases. The value of this difference ($\phi_{25°} - \phi_{99.6°}$) increases from 0.03 to 0.16 between molalities of 1 and 4, respectively. The true values of K' therefore should become increasingly smaller than the tabulated K' values as the temperature increases since it was assumed that $\gamma_{\mathrm{LiCl}}/\gamma_{\mathrm{MCl}}$ is independent of temperature. The true $\Delta H'$ values thus are slightly larger than the tabulated values leading to slightly larger values of $\Delta S'$ than are reported. In any case the values as reported permit a valid qualitative interpretation of the ion-exchange process.

No comparable data have been previously reported in the literature for the concentrated systems studied. Cruickshank and Meares[12] have, however, investigated the Na–Li exchange in 0.1 molal LiCl at 25° measuring ΔH calorimetrically. A 10% cross-linked resin was used in their experiments and a significant exchange of ions was involved. Since selectivity is strongly dependent on the mole fraction exchanged and on the cross-linkage of the resin, the discrepancy between their ΔF value of −425 cal./mole and the ΔF value of −387 cal./mole that is reported herein is to be expected, even though the actual discrepancy is lowered somewhat by including a pressure–volume term correction in the evaluation of K.

The large difference between the calorimetrically measured ΔH value of −1634 cal./mole and the −852 cal./mole estimated for ΔH from the plot of log K *vs.* $1/T$ in Fig. 2 is probably due to the different behavior of K and K' with temperature. It also may be due in part to disturbance of the equilibrium reached at the elevated temperatures during cooling and separation of phases. This potential source of error in the dilute systems is essentially eliminated in the more concentrated systems that were studied due to slowing of diffusion processes in the increasingly viscous aqueous phase. Recall that 120 hours were needed to achieve equilibrium in 13.5 molal LiCl at 25° using 20–50 mesh resin particles.

Discussion

If the ion-exchange system can be handled adequately by a model which considers that it is (1) a highly concentrated electrolyte solution which contains only one freely diffusible ion and also (2) a cross-linked network with a volume-dependent free energy term, the preceding ion-exchange experiments carried out in concentrated solution should prove a good test of the model. The system of resin invaded electrolyte can be treated in the same fashion as the somewhat analogous mixture of two salts having a common ion if the above restrictions are considered. The limitation on the treatment is our knowledge of concentrated electrolyte solutions.

The basic considerations of ion-exchange in concentrated electrolyte solution already have been briefly discussed by Diamond.[2] The most important of these with regard to the present study is the breakdown of the hydration spheres and the consequent changes in the effective sizes of ions. A pressure–volume effect is important at low molali-

---

[12] E. H. Cruickshank and P. Meares, *Trans. Faraday Soc.*, **49**, 1144 (1953).

ties. It becomes negligible for exchange reactions of the alkali metal ions at molalities above unity. The external water activity at this concentration is lowered, reducing greatly the swelling of the resin matrix and thus the corresponding internal tension, π. The volume due to the invaded electrolyte is not sufficient to compensate for the deswelling caused by lowering the water activity. In addition, the pressure–volume term for an exchange system arises from the difference in partial molar volumes of the electrolyte within the resin phase, $\bar{V}_{\text{MCl}} - \bar{V}_{\text{NCl}}$, and this difference of two numbers of the same magnitude coupled with the decrease in π tends to make this term completely negligible at the higher molalities. Complex ion formation in the concentrated aqueous chloride solutions is unimportant for the alkali metal cations.

The normal order of ion-exchange selectivity that is observed with Dowex-50 in dilute solutions of the alkali metal ions, ammonium ion and hydrogen ion is

$$\text{Cs} > \text{Rb} > \text{K} \approx \text{NH}_4 > \text{Na} > \text{H} \approx \text{Li}$$

This sequence correlates well with the order of increasing hydrated ionic radii. The resin phase is only 5 molal in lithium ions as long as little or no invasion occurs; the exchanging species are still fully hydrated ions. Actually, the order is in more general terms the order of increasing activity coefficients in the region of 2 molal. The effect of electrolyte concentration on this order of selectivity may be seen from the selectivities in Table I. For example, the sequence in 13.5 molal LiCl is shifted to H >> Li > Rb > Na > Cs (K and NH_4 were not studied) and is indicative of the relative change of the hydrated ionic radii in concentrated solutions. The resin phase is about 25 molal in lithium ions and 16 molal in matrix sulfonate ion; if one allows that each sulfonate has associated with it one molecule of water,[13] only 1.5 water molecules remain per Li^+ ion. Neglecting the sulfonate water, there are still only 2.2 water molecules per cation. The order of ion sizes and thus of selectivity is the order of increasing bare ionic radii. This change in selectivity has been brought about by the presence of non-exchange electrolyte in the resin phase coupled with the lowering of the water activity inside the resin phase because of the lowered external water activity. The dehydration effect is not completed at an external molality of 13.5 because Na is still a little less preferred than Rb.

The fact that sodium–lithium exchange systems exhibit a shallow maximum in K' before the most concentrated region is probably due to inadequacy of the approximations used to obtain the activity coefficients for trace NaCl in these concentrated solutions.

Dehydration is thus a most important factor in the ion-exchange process when a significant amount of invasion has taken place. This fact is substantiated further from the values of modified entropy of exchange ($\Delta S'$) that are observed for the exchange process. There is an increase in $\Delta S'$ when electrolyte concentration and difference in atomic number between the exchanging ions increase. Comparing at 25° the observed values (Table III) with the standard entropies of hydration for cations (Table IV) as calculated by Latimer[14] using standard states of 1 mole per liter of gaseous ions and one molal aqueous solution, the difference in $\Delta S_h'$ values of the pairs of ions involved is seen to be of the same order of magnitude and direction that is observed experimentally approaching the higher limit as hydration in the resin phase decreases.

TABLE IV

m	M	$\Delta S'$ Dowex-50	$(\Delta S'_{h(M)} - \Delta S'_{h(Li)})$
11.1	Na	2.0	5
11.1	Rb	11.	16
11.1	Cs	14.	18

Hydration changes are less important in the ion-exchange process at dilute external concentration, the $\Delta S'$ having a negative instead of a positive value. This is a reasonable result since breakdown of hydration spheres at low imbibement cannot be significant; the internal molality is 5.09.

The presence of invaded electrolyte in a cross-linked polyelectrolyte should result in a net increase in entropy. Even though the swollen volume is lowered because of a lower water activity, ion-pair formation, which neutralizes the charge sites on the resin matrix, and a smearing of the electric field due to these matrix sites by the excess non-electrolyte both tend to weaken the repulsive forces holding the chains in place. As a result the chains are free to move and the entropy change should increase as the amount of invasion increases. The larger the entropy change in these systems, the stronger is the binding or ion pair formation between cation M and the matrix; thus the K' values lie in the order Cs > Rb > Na as is expected.

The enthalpies of exchange represent the transfer of an M ion which is more or less fully hydrated into the resin phase with the subsequent removal of a Li ion from the resin phase. The net result is that the M ion which needs less water for hydration moves into an environment of less water and the lithium which requires more water moves to an environment of substantially more water; this process should result in only a small net enthalpy change since it involves both a dehydration and a rehydration and should have a positive value for these systems. The fact that only Cs–Li exchanges have a positive $\Delta H'$ indicates that the hydration effect also should be applied to the matrix.

Acknowledgment.—Financial support of portions of this study from the National Science Foundation and through Contract No. At (30-1)-2269 with the U. S. Atomic Energy Commission is gratefully acknowledged.

---

[13] E. Glueckauf and G. P. Kitt, *Proc. Roy. Soc. (London)*, **A228**, 322 (1955).

[14] W. M. Latimer, K. S. Pitzer and C. M. Slansky, *J. Chem. Phys.*, **7**, 108 (1939).

ION-EXCHANGE IN CONCENTRATED ELECTROLYTE SOLUTIONS. II. THE SYSTEM LITHIUM CHLORIDE-ALKALI CHLORIDE-ZEOLITE

By WALTER A. PLATEK[1a] AND JACOB A. MARINSKY[1b]

Department of Chemistry, University of Buffalo, Buffalo, N. Y.

Received April 27, 1961

The ion-exchange behavior of trace components has been studied by measuring the variation of selectivity, $L^M{}_{Li}$, as a function of external LiCl molality using a Linde "Molecular Sieve" as the exchanger. A molality range of 0.1–13.5 has been investigated with the trace component MCl including NaCl, RbCl and CsCl. The exchange reactions also have been studied as a function of temperature in the range 25–97.5° and in fused LiCl at 650°. The thermodynamic exchange functions have been calculated, and the zeolite exchanger compared to a typical organic exchanger.

Introduction

Although the synthetic zeolite materials appear to offer certain advantages for ion exchange, the bulk of scientific work with these materials has been in the area of preparation of new cationic forms rather than in the study of exchange.[2] Their exchange behavior in concentrated solutions has only recently been considered.[3] The structure of the NaA zeolite, however, has been very well characterized by X-ray studies.[2,4] The cation locations, pore openings and pore volumes are all well defined, offering the advantage of a known structure which is also quite inflexible as contrasted with a swelling cross-linked organic ion-exchange resin. The A zeolite is also quite temperature stable under normal conditions so that exchange in fused salt media can be studied.

The reaction under consideration in this study was

$$\overline{\mathrm{LiCl}} + \mathrm{MCl} \rightleftarrows \overline{\mathrm{MCl}} + \mathrm{LiCl}$$

where M is an alkali metal cation and the barred terms refer to the species in the resin phase. The thermodynamic equilibrium constant for the above reaction is

$$K_a = \frac{\overline{a_{\mathrm{MCl}}}\,a_{\mathrm{LiCl}}}{a_{\mathrm{MCl}}\,\overline{a_{\mathrm{LiCl}}}} = \frac{\overline{\gamma_{\pm\mathrm{MCl}}{}^2}\;\overline{m_{\mathrm{M}^+}}\;\gamma_{\pm\mathrm{LiCl}}{}^2\;m_{\mathrm{Li}^+}}{\gamma_{\pm\mathrm{MCl}}{}^2\;m_{\mathrm{M}^+}\;\overline{\gamma_{\pm\mathrm{LiCl}}{}^2}\;\overline{m_{\mathrm{Li}^+}}} \qquad (1)$$

and is made equal to unity by selecting the same standard state for the aqueous and resin phases. The symbol a is the activity, $\gamma_\pm$ is the mean activity coefficient and m is the molal concentration of the species under consideration. Other distribution expressions more readily obtained experimentally are the selectivity coefficient

$$K = \frac{\overline{m_{\mathrm{M}^+}}\;m_{\mathrm{Li}^+}}{m_{\mathrm{M}^+}\;\overline{m_{\mathrm{Li}^+}}} = \frac{\gamma_{\pm\mathrm{MCl}}{}^2\;\overline{\gamma_{\pm\mathrm{LiCl}}{}^2}}{\overline{\gamma_{\pm\mathrm{MCl}}{}^2}\;\gamma_{\pm\mathrm{LiCl}}{}^2} \qquad (2)$$

and the modified selectivity coefficient, K', which involves aqueous phase activity coefficients.

$$K' = K\left(\frac{\gamma_{\pm\mathrm{LiCl}}{}^2}{\gamma_{\pm\mathrm{MCl}}{}^2}\right) \qquad (3)$$

Experimental

A. Materials.—The calcium A zeolite was kindly supplied by the Linde Company. It was converted to the Li form by treatment with concentrated LiCl solutions as described by Barrer.[3] A lithium content of 4.22% was found for the anhydrous exchanger, comparing favorably with a calculated value of 4.20% based on a stoichiometry of $\mathrm{Li_2O \cdot Al_2O_3 \cdot 2SiO_2}$. Sodium and calcium were absent. Reagent grade lithium chloride was purchased from J. T. Baker Co. and used without further purification. γ-Emitting, carrier-free radioactive nuclides 19.5 d $\mathrm{Rb^{86}}$ and 2.3 y $\mathrm{Cs^{134}}$ were purchased from the Radioisotopes Division of the Oak Ridge National Laboratories. The carrier-free 2.6 y $\mathrm{Na^{22}}$ was purchased from Nuclear Science and Engineering Corporation. Deionized water was used in the preparation of all solutions. All solutions were stored in polyethylene bottles.

B. Equilibration Procedure.—The procedures were fundamentally the same as those described in the previous paper.[5] Some modification was required, however. It is difficult to use the zeolite in the anhydrous form because it has a strong tendency to pick up water. The exchanger was therefore stored over saturated ammonium chloride solutions to obtain a constant water content. One-gram samples of the exchanger in the hydrated condition were used to provide about the same capacity as was obtained with Dowex-50.

For exchanges at 11.1 and 13.5 molal, 27 hours was found to be required to achieve equilibrium. The shorter time compared to the Dowex-50 (120 hours) is attributable to the larger available surface of the zeolite sample. If the zeolite was allowed to stand in contact with these strong aqueous solutions for longer periods of time (48 hours or more), the selectivity decreased slightly and traces of aluminum were found in the mother liquor. The zeolite structure, however, remains intact as evidenced by X-ray studies kindly performed by the Linde Company. This effect was not observed at the lower molalities, where five hours was sufficient to reach equilibrium, and is apparently due to a slight attack on the zeolite lattice by high concentrations of chloride ion in the presence of water. The Molecular Sieve exchanger in contact with aqueous chloride solutions at temperatures above 110° decomposes to another artificial zeolite type previously reported by Barrer[6] and designated by him as the A phase. Identification was made by comparison of the X-ray powder patterns made available to us by the Linde Company. For this reason the selectivity was studied only in the range from 25–97.5°.

Alumino-silicates have a tremendous surface area and thus present a much more serious problem of adsorption of electrolyte on the exchanger surface than do the organic exchangers. Anhydrous acetone was used to remove the adsorbed alkali halides. The halides are sufficiently soluble so that the adsorbed surface film can be removed and the acetone molecule is too large to enter the ~ 4 Å. pore of the zeolite. Thus the invaded electrolyte and water which are located within the cavity are not affected. After centrifugation to remove the exchange liquor, the exchanger was collected on a frit washed 5 times with 20-ml. portions of anhydrous acetone and centrifuged 5 minutes to remove the wash liquor. The filter cake was not stirred until most of the surface water was removed by the first two washings. After the final washing, the material on the frit was centrifuged for 15–20 minutes to remove most of the residual acetone. Constant weight was not employed as a criterion for acetone removal because of the highly adsorptive character of the zeolite. The now moderately dry powdery filter cake was

---

[1] (a) Taken in part from the dissertation submitted by Walter A. Platek in partial fulfillment of the requirements for the Ph.D. degree in February 1961; (b) author to whom requests for reprints are to be addressed: Dept. of Chemistry, Univ. of Buffalo, Buffalo, N. Y.

[2] R. M. Barrer and E. A. D. White, *J. Chem. Soc.*, 1561 (1952).

[3] R. M. Barrer and W. M. Meier, *ibid.*, 299 (1958).

[4] D. W. Breck, *et al.*, *J. Am. Chem. Soc.*, **78**, 5963, 5972 (1956).

[5] W. A. Platek and J. A. Marinsky, *J. Phys. Chem.*, **65**, 2113 (1961).

[6] R. M. Barrer and E. A. D. White, *J. Chem. Soc.*, 1267 (1951).

removed from the frit easily by means of a stainless steel spatula.

The invaded electrolyte is not easily washed out and the samples had to be dissolved prior to chloride analysis. The samples were transferred from the test-tube with about 10 ml. of water. All adhering material was washed out in 2 additional 5-ml. water washes. Thirty ml. of concentrated nitric acid then was added to dissolve the zeolite. The solution was placed in an ice-bath and the *p*H was adjusted to be tween 0.5-1 by the addition of 6 *M* NaOH. The samples then were titrated for chloride by the standard Volhard procedure using excess $AgNO_3$ and back-titration with KCNS using ferric alum as the indicator and nitrobenzene as the coating agent for the AgCl precipitate.

Water content was determined by ignition at 800° after the material had come to isopiestic equilibrium with the desired salt solution (either the same salt solution with which it was equilibrated or an isopiestic standard). The acetone-washed samples were surface dried for one hour at 80° to remove the adsorbed acetone so that it would not interfere with the isopiestic equilibrium.

C. Exchange in Anhydrous Melts.—Anhydrous LiCl was prepared by vacuum drying at 450° in an HCl atmosphere using the best features of the methods of Boston[7] and Gardner.[8] The anhydrous zeolite was prepared by heating under vacuum at 350° until pressure of 10^{-5} mm. was obtained.[4] Radioactive tracers were prepared in the anhydrous form by first evaporating an aliquot of stock solution at 80° in a 20-ml. alundum crucible. The alundum crucible which also was used as the reaction vessel then was ignited at 450°. Approximately 5 g. of anhydrous LiCl and 1 g. of anhydrous zeolite were then transferred into the alundum reaction vessel in a dry box under an atmosphere of dry nitrogen. The samples were weighed accurately by difference in ground-glass-stoppered weighing bottles. The alundum crucible was inserted into a 30-ml. silica crucible, covered with a tightly-fitting silica lid and placed in a P_2O_5 desiccator to prevent any entry of moisture during the transfer from the dry box to the furnace which was kept at 200°. The temperature was raised to 660° during the course of one hour and held at that temperature for 8 hours. This time previously had been found sufficient to achieve equilibrium by Barrer during his inclusion studies in a variety of melts and exchangers.[3] The temperature was held constant to ±5° by means of a Honeywell Pyr-O-Vane regulator. At the end of this time the sample was removed from the furnace and transferred immediately to a P_2O_5 desiccator. Gradual cooling was not used because a shift in the equilibrium could be caused by gradual temperature changes.

The phase separation was accomplished in a dry box under a nitrogen atmosphere. A 20-minute nitrogen flush was used before the sample was removed from the desiccator. The solidified melt was removed from the crucible and transferred to a 400-ml. beaker with a stainless steel spatula. The crucible and spatula were rinsed with 30–40 ml. of anhydrous acetone. After the addition of 150 ml. of anhydrous acetone, the residue was stirred with a magnetic stirrer. The residue, after suction filtration, was finely ground twice in a mortar and pestle and the leaching procedure was continued until the filtrate was free of chloride ion. About 1.5 liters of acetone was found to be sufficient for the complete leach of a 5-g. sample of LiCl.

The acetone leach was evaporated nearly to dryness and the residue dissolved in water and diluted to 100 ml. in a volumetric flask. The leached resin was dissolved in 70% nitric acid and diluted with water to 500 ml. in a volumetric flask. Two-ml. samples of both the leach and the dissolved resin were withdrawn for activity measurement. The chloride contents were obtained as described above.

X-Ray powder patterns of an equilibrated sample containing only LiCl and LiA, which had been cooled slowly over a period of six hours to prevent phase changes due to large temperature gradients, were obtained. The pattern was identical to that obtained for pure LiA indicating that the zeolite structure is not attacked by the anhydrous melt. The sensitivity of the X-ray analysis method was sufficient for the determination of the basic zeolite pattern but did not permit determination of the presence of definite inclusion compounds.

Results and Discussion

The variation of trace selectivity (*K*) as a function of the external LiCl molality is shown in Table I. The modified selectivity coefficients, *K'*, were calculated by use of the Harned rule as described previously.[5] Also tabulated are the water content and the internal molalities which were used to obtain the resin phase activity coefficients. These selectivities are substantially higher than those observed using Dowex-50 as the exchanger. The significant differences observed with organic and zeolite exchangers result from structural differences. The Dowex-50 is only 8% cross-linked and its skeletal structure is quite flexible; even at water activities approaching unity, resistance to osmotic diffusion of water is small and there are a large number of sites made available for adsorption in the space between the separated polymer segments. The internal network of the zeolite exchanger, on the other hand, is made up of short, inflexible, uniform links which limit the maximum uptake of water to the amount which will fill the fixed pore volume and form a "surface layer or layers." The zeolite in contact with the less concentrated aqueous systems thus is not appreciably diluted due to osmotic diffusion of H_2O. With increasing electrolyte concentration, there is no contraction and thus no water loss except that due to displacement by the invading ions. There is some modification of the water content with changes in water resulting from changes in the surface layer or layers. The relative molality is not enhanced by contraction of the exchanger matrix as it is with the organic exchanger.

The activity coefficients of the internal electrolyte have been calculated with the aid of the Donnan equation. The activity coefficient values of LiCl in the zeolite and aqueous phase are shown in Fig. 1; the values for Dowex-50 obtained in the preceding paper[5] also are included for comparison. The lines connect experiments at the same external molality. The low values for the activity coefficient of LiCl inside the zeolite which are obtained when the exchanger is equilibrated with 3–5 molal salt solutions result from its inflexible structure. This behavior is analogous to that observed with highly cross-linked organic exchangers.[9] The zeolite is highly "cross-linked" and the free osmotic transfer of water into the exchanger phase is greatly hindered at high water activities. A relationship of the type suggested by Glueckauf[9] for highly cross-linked exchangers

$$\ln a_J = \ln \overline{a_J} + \pi \overline{V_J}$$

should hold for this system also. The swelling pressure, π, is not available by the methods used with resinous exchangers since the zeolite cannot be made in an "uncross-linked" form without destroying its structure, but must be much larger than in organic exchangers at high water activity. The value of $\overline{a_J}$ and consequently the value of $\overline{\gamma_J}$, must be smaller as a result.

An operational picture is as follows: the net negative charge of the inflexible ring of oxygen atoms of the zeolite at the pore opening electro-

---

[7] C. R. Boston and G. P. Smith, *J. Phys. Chem.*, **62**, 409 (1958).

[8] H. J. Gardner, C. T. Brown and G. J. Janz, *ibid.*, **60**, 1458 (1956).

[9] E. Glueckauf, *Proc. Roy. Soc.* (*London*), **214A**, 207 (1952).

TABLE I

SELECTIVITY DATA—ZEOLITE

External molality LiCl	Water content g. H_2O / g. dry exchanger	Molality LiCl (r)	Molality LiR	$\overline{\gamma_{\pm LiCl}}$	$\overline{\gamma_{\pm LiCl}}$ / $\gamma_{\pm LiCl}$	M = Na		M = Rb		M = Cs	
						K	*K'*	*K*	*K'*	*K*	*K'*
13.5	0.2553	3.56	28.9	30.7	1.25	1.90	5.12	3.59	1110	19.3	35,900
11.1	.2611	2.51	28.4	16.2	1.26	2.45	9.04	5.71	811	43.4	24,800
5.69	.2836	1.80	26.6	1.93	0.80	6.55	15.3	45.1	595	208	5,570
2.89	.2844	1.47	26.0	0.477	0.45	11.4	14.7	63.4	188	321	1,320
0.862						9.40	11.5				
0.1			∽18.0			6.66	6.74	6.98	7.40	250	275

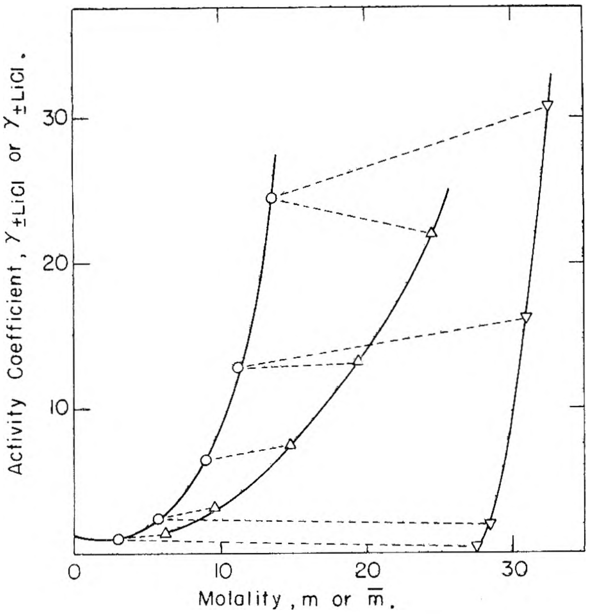

Fig. 1.—Plots of the activity coefficient in a given phase as a function of the molality of that phase. For the aqueous phase, $m = m_{LiCl}$; for the resin phase, $\overline{m} = \overline{m}_{LiCl} + \overline{m}_{LiR}$ Dashed lines are used as tie lines to connect the $\gamma_{\pm}$ values which result from the same experiment. Also included for comparison are $\overline{\gamma_{\pm LiCl}}$ values obtained previously[5] with Dowex-50: $\gamma_{\pm LiCl}$, O; $\overline{\gamma_{\pm LiCl}}$, ∇; $\overline{\gamma_{\pm LiCl}}$ (Dowex-50), Δ.

statically prevents the entrance of the anion and thus by virtue of the need to preserve electroneutrality prevents the cation from entering the pore. At high external electrolyte concentration, there is opportunity for leakage through the electric field barrier because of a sizable concentration gradient across the phase boundary. The negative field due to the rigid ring of O atoms is neutralized sufficiently by the cations of the invading electrolyte, permitting the smaller dehydrated cation to enter the pore and bring with it the anion to preserve electroneutrality. Penetration of the electrolyte is restricted because cations of the matrix and the matrix itself prefer water rather than additional electrolyte so as to satisfy their hydration requirements as much as possible. The restriction of invasion of Dowex-50 by electrolyte is less effective since the field due to the negative charge of its matrix is variable. In contact with dilute solutions the organic matrix expands and a minimum potential energy is achieved reducing the negative field and thereby facilitating the invasion process.

The exchange process itself involves removal of a "hydrated" ion from the solution. The ion is dehydrated[5] and then replaces a matrix cation on the pore opening. Alternately the process may consist of passing the cation, either hydrated or unhydrated, into the interior of the large cavity and then dehydrating it further, if necessary, and replacing one of the matrix cations in the pore with it. The order of selectivity in dilute solutions depends then on the ease of dehydration of the cation which is Cs > Rb > Na > Li and the relative binding energy of the ions which is in the reverse order. The magnitude of the selectivity constant at a given molality depends on the difference in the free energy needed to dehydrate the respective cations from the state in which they are present in the solution to the bare ion of the matrix and the relative stability increase produced by the exchange itself. The relative binding strengths lie in the order Li > Na > Rb > Cs, the smaller dehydrated ion being most strongly bound. The situation is such that in dilute solution the energy of dehydration is so much greater for Li^+ that the less strongly hydrated ion enters the resin phase more easily. When hydration spheres are broken in the external phase, as a result of concentration increase, the zeolite behavior approaches that of the organic exchanger with Li competing more successfully for resin sites. Crossovers are not encountered at the electrolyte concentrations employed during this study; undoubtedly such crossover would occur at higher external molalities (see Table I).

From external molalities of 0.1 to 2.5, a small but distinct rise in *K* is observed for the zeolite exchanges. The selectivity coefficients at 0.1 and 0.862 molal were questioned in the first experiments since only a small fraction of the original activity was left in the aqueous phase at equilibrium. The calculation of *K* then is strongly dependent on a very small number and the possibility of difficulty due to colloidal suspension was suspected; subsequent experiments using approximately 5–10 times the amount of tracer and smaller resin samples of 0.1000 and 0.0100 g. (10 and 1% of the original samples) confirmed the earlier results. This maximum is explained adequately by the behavior of the $\pi(\bar{V}_{Li} - \bar{V}_M)$ term. As π decreases with concentration this term, which is negative since bare ions are present in the zeolite, increases from a large negative value to a limit of zero at low external water activity.

Barrer[3] discusses the conversion of one salt form to another and ion sieve properties primarily on the basis of bare ion sizes as compared to the pore size. This is consistent with our conclusions

TABLE II

SELECTIVITY AS A FUNCTION OF TEMPERATURE, K_{Li}^{M}

Temp., °C.	M = Na				M = Rb External LiCl molality			M = Cs		
	0.862	11.1	13.5	Melt	11.1	13.5	Melt	11.1	13.5	Melt
25	9.40	2.45	1.90		5.71	3.59		43.4	19.3	
50	9.95	2.36	2.02		8.70			28.4	17.5	
75	11.1		2.46		9.90	7.19			14.7	
97.5		3.05	2.46		18.6	10.9		25.8		
650				78.4			246			63.1

that the hydration within the exchanger phase must be very slight indeed since the Li molality is so high. The order of exchange selectivity and the relative differences that are observed in this study between the various cationic selectivities are different from results observed with the Na form by earlier investigators[4] where the extent of exchange follows the order Rb > Li > Cs and the values are quite similar, *i.e.*, 36, 33, 31%, respectively. These extent of exchange values refer to the per cent. exchange observed when one equivalent of exchanger is contacted with one equivalent of exchange electrolyte at an ionic strength of 0.2. Since the results observed in this study refer to trace selectivity (Cs > Rb > Na > Li), and selectivity is strongly dependent on the mole fraction exchanged, the differences are not surprising. Lack of interstitial space is not a problem with relatively small cations of the alkali metal series. Assuming that the LiA α-sites are governed by a cationic diameter of 4.5 Å (the same as for NaA) or larger, all of these cations on the basis of their distance of closed approach values when hydrated, a_0, are capable of entry into this pore. Only the dehydrated Li and Na ions can enter the pore of the β-cavity where the maximum diameter is 2.5 Å. It is here in the β-cavity that interstitial $LiAlO_2$ exists and complete exchange would be possible only if this region were accessible to the exchanging species.

The variation in selectivity as a function of temperature is shown in Table II. Since the plots of log K *vs.* $1/T$ are linear within experimental error, ΔH is constant over the limited temperature range from 25 to 97.5° that was investigated with the aqueous systems. Since the bare ions are present in an anhydrous melt, the selectivities for the zeolite exchanger in a melt might be expected to be similar to those extrapolated from Table I to the region beyond an external LiCl molality of 13.5. The effect of temperature on the exchange process as demonstrated in Table II must also be considered. If the values for selectivity coefficients obtained at an external molality of 13.5 are extrapolated linearly to a temperature of 948°K. ($1/T = 1.05 \times 10^{-3}$), selectivity coefficients of ~4.6, ~150 and ~3.9 are obtained for Na, Rb and Cs exchanges, respectively, as compared to the measured values of 78.4, 246 and 63.1 A long linear extrapolation of this sort, however, is very questionable not only because of the change in the nature of the system but also especially since the experimentally observed linear range is short and there is some scatter so that the best straight line must be drawn. It appears from these crude data that water does play a definite role in the exchange process.

The increase in invaded electrolyte to a value of 1.42 mm. LiCl/dry g. of zeolite follows directly the electrostatic considerations previously mentioned.

The fact that rubidium is strongly preferred in the melt is also in agreement with the selectivity observed in the aqueous systems at various temperatures.

Further work of this type is presently in progress by one of us in the system pyridine hydrochloride–Dowex-50–alkali metal chloride. This system will enable measurements to be made both in aqueous solution and in the anhydrous melt in the same temperature range (145–170°), thus doing away with the need of any extrapolation to ascertain the role of water in the exchange process.

The modified thermodynamic exchange functions ($\Delta F'$, $\Delta H'$ and $\Delta S'$) as calculated by the methods used previously[5] are listed in Table III. While the $\Delta H'$ and $\Delta S'$ values for Na–Li exchanges are comparable to those observed with the organic exchangers in concentrated solutions, the $\Delta H'$ values for Rb–Li and Cs–Li values are an order of magnitude larger while $\Delta S'$ is less positive for the Rb–Li system and more positive for the Cs–Li system.

TABLE III

THERMODYNAMIC EXCHANGE FUNCTIONS

Exchange	External LiCl molality	$\Delta F'$, cal./mole	$\Delta H'$, cal./mole	$\Delta S'$, cal./mole deg.
Na–Li	0.862	−1460	−714	2.50
	11.1	−1270	−650	2.08
	13.5	− 999	−714	0.96
Rb–Li	11.1	−3950	−3240	2.38
	13.5	−4170	−3160	3.38
Cs–Li	11.1	−5970	+1680	25.7
	13.5	−6260	+1350	25.6

The operational picture presented in the previous paper is still applicable. Dehydration and binding again are the important factors in the exchange process. Comparison of $\overline{\gamma}_{\pm \mathrm{LiCl}}$ values characterizing the organic and inorganic exchanger show that ion binding (ion-pair formation) is greater in the zeolite. The larger ΔH values for the Cs–Li exchange reaction thus reflect the effect of this increased binding in the resin phase. The behavior of the Rb–Li exchange is anomalous.

The importance of dehydration on the entropy change is reflected in the rather large $\Delta S'$ value obtained for the Cs–Li exchange reaction. Again a smaller $\Delta S'$ value for the Rb–Li exchange is anomalous.

In the zeolite exchanger, the matrix is fixed and neutralization of charge, both due to binding and the presence of non-exchange electrolyte, will affect additional contribution to the entropy a little differently than in the organic exchanger. The neutralization of the charge does decrease the field due to charged matrix. This increases the entropy since the ions are no longer lined up by the field, but the volume of the resin does not expand in this process.

A possible explanation for the peculiar behavior of Rb could be a slightly different positioning of this alkali metal cation on the zeolite lattice which could be brought about by the influence of the non-exchange electrolyte. The slightly smaller unit cell of the LiA as compared to NaA and KA is justification of this hypothesis.

(LiA = 12.105 (in kX.)
NaA = 12.273, and KA = 12.280)

Acknowledgment.—Financial support of portions of this study from the National Science Foundation and through Contract No. At(30-1)-2269 with the U S. Atomic Energy Commission is gratefully acknowledged.

X-RAY DIFFRACTION STUDY OF STRAIGHT CHAIN (C_1 TO C_{14}) CARBOXYLIC ACIDS

By William L. Baun

Directorate of Materials and Processes, Aeronautical Systems Division, Wright-Patterson Air Force Base, Ohio

Received May 4, 1961

X-Ray diffraction effects in solid state saturated fatty acids are shown with emphasis on short chain fatty acids normally liquid at room temperature. Long and short spacings are determined and compared with early work, anisotropic thermal expansion is noted, polymorphic tendencies are investigated and other variable temperature effects are discussed.

Introduction

In the last forty years well over one hundred papers have appeared in the literature concerning the study of fatty acids by X-ray diffraction. Much of the data obtained from these solid state studies has been summarized by Francis and Piper,[1] and more recently by Von Sydow.[2] Most of the investigations report data on the solid series of saturated fatty acids containing from 12–46 or more carbon atoms. Information is sketchy on acids normally liquid at room temperature, *i.e.*, methanoic (formic) to decanoic (capric), even though this series of acids was among the first to be investigated by X-ray diffraction.[3–5] Data taken from these early works do not agree among themselves and are not complete, probably because of low temperature experimental difficulties and impurities in the acids available at the time.

The present work was undertaken to study X-ray diffraction effects in solidified fatty acids with emphasis on short chain saturated fatty acids that are normally liquid at room temperature. Long and short spacings are determined, anisotropic thermal expansion is shown, and polymorphic tendencies are investigated using pure acids and modern X-ray equipment.

Experimental

Materials.—The monocarboxylic acids C_6, C_8, C_{12} and C_{14}[6] were 99.8% pure and were obtained from Applied Science Laboratories.[7] The remainder of the acids were either prepared in this Laboratory or were purified from Eastman or Matheson Coleman and Bell products.

Equipment.—A Philips[8] diffractometer equipped with a scintillation counter was employed for a majority of the measurements. Beam exit slits of 1/6 to 1° were used depending on the diffraction angle. Nickel filtered copper radiation was used in all cases. The diffractometer was equipped with a simple low temperature specimen mount similar to one described by this author for pressed samples.[9] The mount was modified so that liquids or powders could be accommodated in a depression milled in a copper block. The copper specimen holder was insulated from the diffractometer by a Teflon block which was bolted to the diffractometer to increase rigidity and minimize drag effects from the feed tube. The feed tube carried cold gas into the copper block where the gas circulated beneath the sample. The gas then emerged and a curved piece of tubing in the block sprayed the cold gas on the surface of the sample. The Philips can-type scatter shield with one mil Mylar covering the can slit was used as a container to provide a pressure of dry gas within the vessel and thereby reduced sample icing problems. This mount was used mainly for recording side spacings of acids and noting preferred orientation in these compounds. At times, one mil Mylar was used to cover the sample itself to reduce evaporation, especially in such acids as butanoic and pentanoic. For determination of side spacings, the samples were powdered in an agate mortar at solid CO_2 or liquid nitrogen temperatures and packed into the depression in the copper block. Long spacings were determined by allowing a thin layer of acid to crystallize on a ground glass slide cooled by a stream of dry nitrogen. Temperature was controlled by varying the flow of dry nitrogen through a copper coil immersed in liquid nitrogen or a solid CO_2–acetone mixture.

Powder patterns for several acids were recorded on film using a Philips 114.6 mm. Debye–Scherrer camera adapted for moderately low temperatures by flowing cold nitrogen into a piece of quarter inch copper tubing threaded into a hole in the camera cover just opposite the rotating sample. The sample was contained in a capillary to prevent evaporation.

Results and Discussion

Table I shows long and short spacing data for the saturated fatty acids C_1 to C_{10}. Comparisons of literature long spacing values also are shown. As can be seen, the literature data do not agree well, but the very early work by Gibbs[3] compares favorably with the long spacings reported here. Long spacing data in this table were calculated from an

---

[1] F. Francis and S. H. Piper, *J. Am. Chem. Soc.*, **61**, 5771 (1939).

[2] E. Von Sydow, *Arkiv Kemi*, **9**, 231 (1956).

[3] R. E. Gibbs, *J. Chem. Soc.*, **125**, 2622 (1924).

[4] R. M. Morrow, *Phys. Rev.*, **31**, 10 (1928).

[5] J. J. Trillat, *Z. Physik*, **64**, 191 (1930) (A review).

[6] Notation C_n refers to total number of carbon atoms in acid and will be used through the paper.

[7] Applied Science Laboratories, State College, Pennsylvania.

[8] Philips Electronics, Inc., Mt. Vernon, New York.

[9] W. L. Baun, *Appl. Spectroscopy*, **13**, 79 (1959).

average of the best resolved and highest order lines due to the long spacing. The long spacings were obtained by inducing preferred orientation and enhancement of the long spacing by crystallizing thin layers of the acid on a ground glass slide. Crystallizations were carried out both from the melt and from solvents. Toluene, benzene and acetone were used during the solvent crystallization phase of this work. Short spacings were determined from samples ground and packed into a copper holder at liquid nitrogen or solid carbon dioxide temperatures. Intensities shown with short spacings probably are almost meaningless since preferred orientation is very pronounced in these compounds. No attempt was made to obtain each acid pattern at the same temperature. Rather, each acid was run at about thirty degrees below its melting point in an attempt to put these patterns on the same basis as the solid acids in the range C_{14} to C_{18}, which melt thirty to forty degrees above room temperature. A change in temperature has a striking effect on the short spacings as will be shown later, while long spacings are virtually unaffected by moderate changes in temperature. The latter is in agreement with early observations by Muller[10] and Slagle and Ott.[11]

Table I

Fatty Acid Spacing Data, C_1 to C_{10}

No. C Atoms	Name	Long spacing, Å.	Short spacing d, Å. $\left(\frac{I}{I_1}\right)$	Lit. long spacing, Ref. 3,	4,	5
1	Methanoic (formic)	5.14	4.52(10), 3.92(25) 3.68(100), 3.32(10)	5.19	5.2	
2	Ethanoic (acetic)	6.65	4.35(100), 3.91(20) 3.67(40), 3.46(70) 2.88(40)	6.66	5.9	
3	Propanoic (propionic)	7.05	5.52(10), 4.70(50) 4.19(100), 3.89(10) 3.66(10), 3.44(5) 2.85(60), 2.65(50) 2.63(30), 2.14(5) 1.579(10)	6.75	6.0	8.5
4	Butanoic (butyric)	9.45	7.60(40), 4.07(100) 3.93(70), 3.78(100) 3.69(40)	9.65	8.5	9.2
5	Pentanoic (valeric)	12.63	7.25(50), 4.82(50) 4.44(100), 3.88(40) 3.65(50), 3.60(100) 3.46(20)	10.1	10.2	12.2
6	Hexanoic (caproic)	14.25	4.05(100) 3.90(25), 3.67(30) 3.42(35)	14.6	12.8	12.4
7	Heptanoic (enanthic)	16.23	4.36(50), 3.88(50) 3.75(100), 3.65(40) 3.43(40)	16.4	14.5	14.5
8	Octanoic (caprylic)	18.65	4.10(100), 3.91(20) 3.67(10)	19.0	17.0	
9	Nonanoic (pelargonic)	20.73	4.40(40), 4.27(70) 4.00(100), 3.89(65) 3.43(30)	22.9	18.4	
10	Decanoic (capric)	23.10	4.13(90), 3.87(25) 3.78(100) (room temp.)	23.3	20.3	

If long spacings of compounds in a homologous series such as the saturated acids are plotted against the number of carbon atoms in the chain, a straight line (or straight lines if more than one polymorphic form exists) is obtained. These straight line relationships have been shown by many authors. Bailey[12] has collected data from the literature and plotted them for all the polymorphic forms of the saturated acids having from 11–24 carbon atoms. Francis, Collins and Piper[13] show linear relationships for acids, alcohols, esters and iodides having from 16–46 carbon atoms. When long spacing data from Table I for the lower acids is plotted against number of carbon atoms, the linear relationship begins to fail about C_4, where apparently the influence of the terminal groups begins to overcome packing due to the long chain. Spacings in lead and zinc salts of saturated fatty acids likewise deviate from linearity at about the same point as the acids themselves.[14] It is interesting to note that the long spacings digress from linearity in the same place as a plot of melting point as a function of chain length. In the linear portion of the line, an equation for line slope may be written which enables one to calculate average long spacings for any acid. The equation for short chain saturated acids is L. S. $= 2.22N + 0.86$, where N is the number of carbon atoms in the acid.

The only acid in this group for which complete crystallographic data could be found was decanoic, the only naturally solid acid shown in Table I. This data shows decanoic acid to be monoclinic as are most of the acids with a C_0 lattice parameter of 30.5 Å. and a β angle of 130.9°.[15] Since the long spacing which is shown in Table I is merely a projection of the C_0 parameter, the long spacing may be calculated by L.S. $= C_0 \sin \beta$. This calculation using The Powder Data File value for C_0 gives a long spacing of 23.06 Å., which is in excellent agreement with the value 23.10 from Table I, especially since C_0 was given to only one decimal place and the calculated long spacing should be rounded off to 23.1 Å.

Polymorphism.—X-Ray diffraction examination of long chain solid fatty acids has revealed that they exist in more than one form. The transformation and existence of these forms are dependent on temperature, purity of the acid, rate of crystallization, and solvent used for crystallization.[2] Three different sets of long spacings have been recorded for the very long chain acids with an even number of carbon atoms and four different sets for the acids with an odd number of carbon atoms. In decreasing order of long spacing size these phases are called, respectively, A, B and C; and A′, B′, C′ and D′. Since short spacings are virtually identical in each phase, this indicates that there is similar packing of long chains, and that polymorphism results from different modes of carboxyl union, causing different angles of tilt in the lattice. Figure 1 shows diffractometer patterns for two forms of the C_{13} acid (tridecanoic). In these traces, the C′ form was obtained by allowing the acid to melt, recrystallize, and then holding the temperature at 40° during the run. The acid then

---

(10) A. Muller, *Proc. Roy. Soc.* (London), **A127**, 417 (1930).

(11) F. B. Slagle and E. Ott, *J. Am. Chem. Soc.*, **55**, 4397 (1933).

(12) A. E. Bailey, "Melting and Solidification of Fats," Interscience Publishers, New York, N. Y., 1950, pp. 118–119.

(13) F. Francis, F. J. E. Collins and S. H. Piper, *Proc. Roy. Soc.* (London), **A158**, 691 (1937).

(14) W. L. Baun, unpublished results.

(15) T. R. Lomer, University of London, The Powder Data File, Card No. 8-527 A.S.T.M., 1916 Race Street, Philadelphia, Pennsylvania.

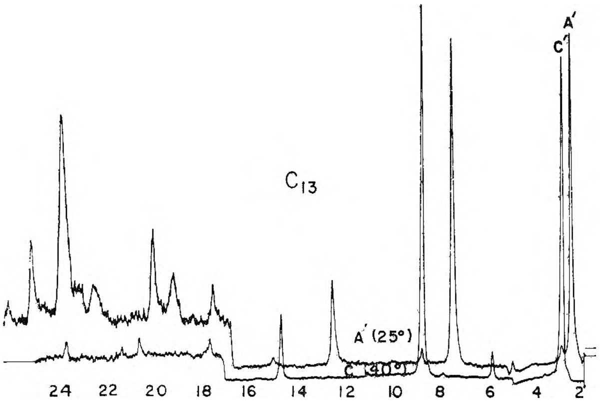

Fig. 1.—Diffractometer traces of two polymorphic forms of tridecanoic acid (Cu Kα radiation).

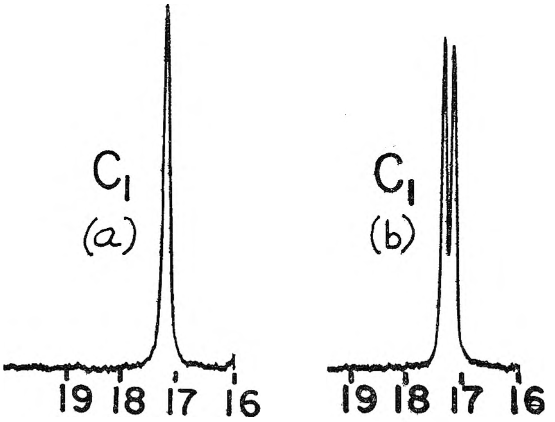

Fig. 2.—Line splitting phenomena in 5.14 Å. peak of methanoic acid.

was allowed to cool to room temperature and a pattern was taken of the resulting A' phase. As can be seen, the transformation is not complete, and a small amount of C' still exists with A'. Since scale expansions were affected at 5° 2θ and at 17° 2θ to show detail, the intensities shown are not on the same relative basis.

The effect of acid crystallization from solvents was investigated in the solid acids by crystallizing the C_{11} (undecanoic) acid first from the melt and then from benzene and acetone. The A' modification was formed with both solvents, while the C' form resulted from solidification from the melt. Table II shows long spacing data and data from the literature for C_{11} through C_{14}; these acids being those melting in a range within about 30° above room temperature. As can be seen, agreement of these long spacings with literature values is very good. Calculation of the long spacing from complete crystallographic data for dodecanoic acid (Powder Data File Card No. 8-528) gives a long spacing value of 27.45 Å., exactly that reported here. Data for tetradecanoic acid (Powder Data File Card No. 8-786) give a long spacing value of 31.51 Å., which does not agree as closely with the experimental data shown as do the values for decanoic and dodecanoic acids.

The long spacings for A' and C' forms shown in Table II for the first two solid, odd acids were easily observed using the diffractometer. However, observation of polymorphism in the normally liquid acids proved much more difficult, with hints of phase changes recorded usually only fleetingly.

Table II

Long Spacings for Solid Saturated Fatty Acids

No. C atoms	Name	Long spacing, Å. A or A'	Long spacing, Å. C or C'	Long spacing, Å. from lit. A or A'	Long spacing, Å. from lit. C or C'
11	Undecanoic	30.16	25.50	30.1(17)	25.4(17)
12	Dodecanoic		27.45		27.4(16) 27.18(12)
13	Tridecanoic	35.35	30.0	35.3(16)	30.0(16) 29.8(12)
14	Tetradecanoic		31.60	36.64(12)	31.5(16) 31.6(1)

One phenomenon encountered in nearly all the acids is illustrated in Fig. 2. The line shown here of methanoic acid at 5.14 Å. is recorded (a) at low temperature after crystallization from the melt, and (b) just as crystallization takes place. Most observations indicate that this is an effect similar to a stacking fault in a metal or alloy, rather than the appearance of a second phase.

Each of the acids was crystallized from acetone and benzene (toluene, for lower temperatures) in an attempt to induce phase changes. The even acids gave the same long spacings as when solidified from the melt. The odd acids, however, showed some change, usually very slight. Crystallization from the acetone usually gave two spacings in C_9, C_7, C_5 and C_3. These spacings did not seem too well defined and seldom gave more than three or four orders of the long spacing. The short spacings remained about the same as when crystallization occurred from the melt.

Orientation.—In these compounds, as with most organic materials, sample preparation is quite important because of preferred orientation effects. Figure 3 shows three diffractometer traces of propanoic acid, each prepared differently. As can be seen from this figure the long spacing, 7.05 Å., remains approximately the same regardless of the crystallization method, along with the short spacings. There is a marked difference in the appearance and intensity of spacings intermediate between the long and short spacings in this compound according to the method of recrystallization. The occurrence of fairly large spacings between long spacings and short spacings is common in the short chain acids with five or less carbon atoms. In these compounds the terminal groups apparently begin to influence the molecular packing, while in longer acids packing is influenced only by the aliphatic chain. The packing effect of long chain substitutions is seen in many compounds such as substituted amides, anilides, phenols and, recently, ferrocenes.[18]

In very short chain acids the problem of preferred orientation did not seem nearly as serious as with the long chain compounds. In fact, intensities from the diffractometer trace of ethanoic acid compared very favorably with a powder pattern taken at a low temperature in a Debye–Scherrer camera. Figure 4 shows a pattern taken of a cylindrical (capillary) sample of ethanoic acid and the corresponding pattern obtained with the diffractometer. Both the position and intensities of the lines agree well although the particle size is not optimum in

(16) F. Francis, S. H. Piper and T. Malkin, *Proc. Roy. Soc.* (London), **A128**, 214 (1930).

(17) G. M. deBoer, *Nature*, **119**, 634 (1937).

(18) W. L. Baun, *Anal. Chem.*, **31**, 1308 (1959).

the cylindrical sample. This figure also serves to illustrate the advantage, insofar as time is concerned, of using the diffractometer in work such as this. The sample preparation, alignment, exposure and development for the Debye photograph took approximately seven hours, while the procedure using the diffractometer took only 30 minutes. Time also is saved since one records only the patterns which show desired phase changes or effects and does not record many unusable patterns as with the film method; that is, the pattern may be quickly checked by hand-scanning the diffractometer to see if the desired crystallization has been obtained. With film methods, one must wait for several hours before he knows whether a crystallization has been a success.

Mixtures.—The study of mixtures of fatty acids, particularly binary mixtures, has been carried on by many investigators[19] and has added much to the understanding of melting and solidification of fatty compounds. Slagle and Ott[20] have examined long spacings from binary mixtures of fatty acids C_{10} to C_{18} and varied chain length differences from one to eight carbon atoms. In all cases, mixed crystal formation was established and some binary mixtures formed a continuous series of solid solutions conforming to Vegard's law.[21] Some systems, although exhibiting solid solution, give different spacings according to sample treatment and thus make data interpretation quite difficult. Also there appears to be disagreement as to the sharpness of mixture lines. Francis, Collins and Piper[13] state that mixture lines are broad and poorly defined, while Slagle and Ott[20] claim that mixture lines are comparable to pure acids.

The results of the study of binary mixtures of both solid and liquid fatty acids show partial agreement with both of the above sets of authors. The solid systems studied were C_{10}–C_{12}, C_{12}–C_{14} and C_{14}–C_{16}. The liquid mixtures studied were more extensive and in some cases varied by more than two carbon atoms. Complete phase diagrams of the systems were not compiled since only binary mixtures containing 50 mol % of each component were studied. In most mixtures where complete solid solution was indicated, the first-order line due to the long spacing was as intense and nearly as well resolved as that line from either of the pure acids. However, fewer orders of reflection were recorded in mixtures and higher order lines were less sharp than in pure acids. Mixtures tended to crystallize from solvents in more than one polymorphic form much more readily than did the corresponding acids alone. Further, at times when more than one form was present, both phases did not exhibit the same degree of crystallinity or order and sometimes a broad peak was observed very close to a sharp peak. Only with difficulty were these peaks resolved, and on film they gave the impression of a broad line.

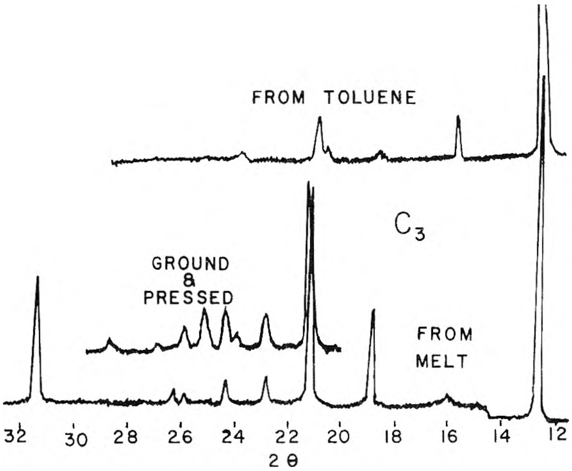

Fig. 3.—Effects of specimen preparation and preferred orientation on the pattern of propanoic acid (Cu Kα radiation).

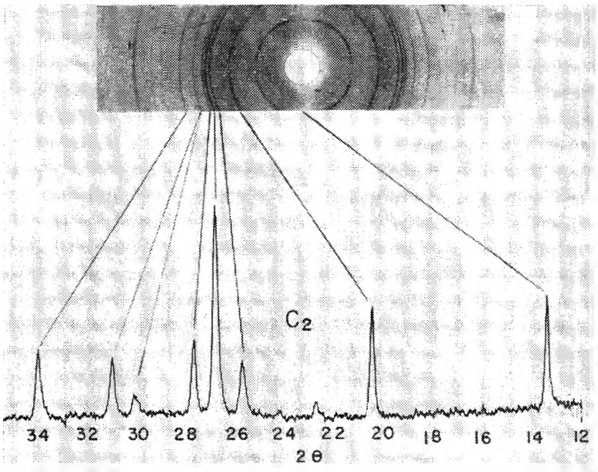

Fig. 4.—Debye–Scherrer powder pattern for ethanoic acid from a cylindrical sample (top) compared to a flat plate diffractometer trace (−25°) (Cu Kα radiation).

In mixtures normally solid at room temperature, mixed crystal formation was established in all cases even when chain length difference exceeded four carbon atoms. In the lower acids, however, one observes all of the possible effects, *i.e.*, complete solubility, partial solubility and complete insolubility. Figure 5a is the diffractometer trace of a mixture of hexanoic and octanoic acids. This pattern shows the long spacing to be midway between the normal spacing of each acid, indicating complete solubility and mixed crystal formation. In this particular mixture, no well defined higher orders of the long spacing appear. The very weak, broad line at 16° 2*θ* is probably the third order of the long spacing. An indication of partial solid solution is seen in a mixture of short acids differing by four carbon atoms as shown by Fig. 5b. This figure shows a mixture of a liquid acid (hexanoic) and a solid acid (decanoic). Here, a long spacing is observed in a position giving a shorter spacing than decanoic acid and also a poorly defined spacing is seen that is considerably larger than hexanoic acid. Complete insolubility is shown in a low temperature diffractometer trace of ethanoic acid and hexanoic acid (Fig. 5c). No evidence for mixed crystal formation is seen, with spacings occurring in the same positions as in the pure acids.

Short spacings of mixtures were approximately the same intensity and shape as in pure acids, with lines at 4.1 and 3.7 Å. being the most dominant.

---

[19] For a review see ref. 13, chapter IV.

[20] F. B. Slagle and E. Ott, *J. Am. Chem. Soc.*, **55**, 4404 (1933).

[21] L. Vegard, *Z. Physik*, **5**, 17 (1921).

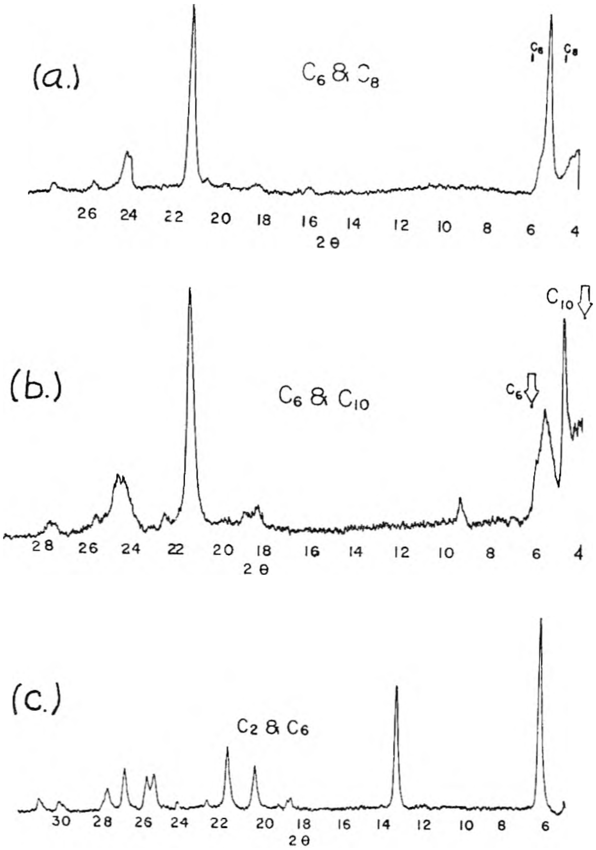

Fig. 5.—Diffractometer traces of binary mixtures of saturated fatty acids (50 mole % each) (Cu Kα radiation): (a) hexanoic and octanoic acids (complete solubility); (b) hexanoic and decanoic acids (partial solubility); (c) hexanoic and ethanoic acids (complete insolubility).

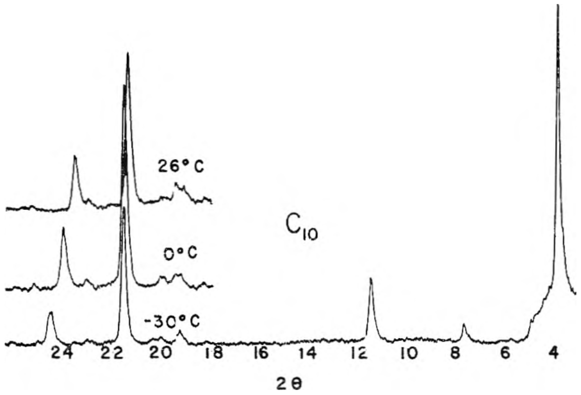

Fig. 6.—Diffractometer traces of decanoic acid showing anisotropic effects in short spacings. Short spacing at 3.7 Å. occurs near 24°2 θ; spacing at 4.1 Å. occurs near 22°2 θ (Cu Kα radiation).

The absolute values of mixture short spacings were found to be somewhat different from pure acids. In all cases, corresponding short spacings were larger in solid solution mixtures than in pure acids or mechanical mixtures of saturated acids. All side spacings were not increased the same amount, however. The peak at 3.7 Å. was affected much more than the one at 4.1 Å. For instance in the C_{12}–C_{14} (50 mole % each) mechanical mixture, lines were recorded at 4.14 and 3.71 Å. After melting and resolidification short spacings were calculated to be 4.16 and 3.83 Å. giving a Δd for the larger line of 0.01 Å. and a Δd for the smaller line of 0.12 Å. The 3.7 line also is the line most affected by temperature changes in the pure acids, as will be shown later.

Thermal Expansion.—Since long chain compounds in general exhibit anisotropy in many properties, it is not surprising that thermal expansion varies considerably depending on direction. Early work on paraffins[11] indicates that long chain compounds contract about 2% along the *b*-axis, 7% along the *a*-axis, but scarcely at all along the long chain *c*-axis when liquid air measurements are compared with room temperature values. Measurements made in this work on both liquid and solid fatty acids gave values of from 20–28 × 10^{-4} Å./°C. for the interplanar distance of 3.7 Å., which was indexed as having the Miller indices (200). The strongest short spacing at 4.1 Å. gave expansion values of from 5–7 × 10^{-4} Å./°C. This line was indexed as the (110). The ratio of expansion of (200) to (110) averaged about 3.5 to 1, which agrees fairly well with the early data on paraffins referenced above where probably the two strongest short spacing lines were assumed to be either projections of, or directly due to, the *a*- and *b*-axes. The numerical values shown are *d*-value changes with temperature and should not be confused with the coefficient of thermal expansion. Figure 6 shows the short spacing changes with changes in temperature for decanoic acid. Long spacings for each temperature are not shown since they vary little and only complicate the figure. For this acid, the short spacing near 3.7 Å. has a thermal expansion of 28 × 10^{-4} Å./°C., while the spacing near 4.1 Å. has a thermal expansion of 7 × 10^{-4} Å./°C. More comprehensive measurements of thermal expansion are being made in this Laboratory on acids and other long chain compounds using only lines indexed as (*h*00), (0*k*0) and (00*l*). From these measurements, calculations will be made of the coefficient of thermal expansion and the change in unit cell volume.

A RECORDING EFFUSION BALANCE FOR PHASE DIAGRAM INVESTIGATIONS: U–Cd, U–Zn AND Ce–Zn SYSTEMS[1]

BY EWALD VELECKIS, CHARLES L. ROSEN AND HAROLD M. FEDER

Chemical Engineering Division, Argonne National Laboratory, Argonne, Illinois

Received May 5, 1961

An apparatus for the determination of the volatility of one component of a system over a wide range of compositions is described. The apparatus, which couples a Knudsen effusion crucible with a recording balance, permits the investigator to make a rapid survey of phase boundary locations and, simultaneously, to observe the decomposition pressures of the phases involved. Three test systems were studied. The results corroborated, modified or extended previously known phase diagrams. In the U–Cd system only the one (known) intermetallic compound, UCd_{11}, was found. Between 420 and 500° the U–Zn system study disclosed a single intermetallic phase, $UZn_{8.5-12}$. Only the end member of this solid solution range, $UZn_{8.5}$, had been described previously. In the Ce–Zn system eight intermetallic phases were found: $CeZn_{11}$, Ce_2Zn_{17}, $CeZn_{\sim 7}$, $CeZn_{3.8-6.2}$, $CeZn_2$, CeZn, Ce_2Zn and Ce_4Zn. Of these eight phases, three had been known, two had been suspected, and three had been indicated by indirect evidence.

Introduction

Numerous techniques (*e.g.*, X-ray diffraction, metallography) are available to the investigator who seeks to determine the location of sub-solidus phase boundaries in metallic systems. Alternatively, the isothermal variation of the activity of one of the components across the successive homogeneous and heterogeneous phase fields may be measured by suitable methods (*e.g.*, e.m.f., vapor pressure) to define the phase boundaries as well as to yield significant thermodynamic information.[2] In general, such methods require the preparation of a large number of stable alloys of well-defined compositions and are seldom rapid. However, if one of the components of an alloy is very much more volatile than the other, the preparation of a series of alloys at closely spaced compositions can be accomplished by evaporation. Elliott and Lemons[3] successfully used evaporation to prepare alloys within the rather narrow limits of the phase $CeCd_{\sim 6}$. In their apparatus the compositions were determined by weighing the cadmium added to or subtracted from the alloys. The tubular glass arms of their balance formed a closed system for the isopiestic equilibration of the alloys with pure cadmium so that the desired activity measurements could be accomplished. The apparatus to be described in this paper also provides a means for determining the volatility of one component of a system as a function of its composition. It is intended for the rapid survey of phase boundary locations in suitable systems.

Theory

Suppose a Knudsen effusion crucible containing some alloy is suspended from one arm of a balance within an evacuated space. Suppose also that the following conditions are satisfied: (a) only one component of the alloy is appreciably volatile; (b) the vapor species is known; (c) the vapor is emitted from the cell by effusive flow only.[4] Under these conditions, as the cell absorbs heat isothermally from its surroundings, the rate of weight loss is proportional to the pressure prevailing in the effusion cell at any time, and the integrated weight loss is simply related to the overall composition of the alloy in the effusion cell at the same time. The relevant equations for a binary alloy are

$$P_{\mathrm{obs}} = 17.1435 \sqrt{\frac{T/M_1'}{ka}}\,\dot{w} \qquad (1)$$

and

$$r = r_0 - \frac{M_2 \Delta w}{M_1 w_2} \qquad (2)$$

where P_{obs} is the observed pressure of the gas in the effusion cell in mm.; T, the absolute temperature in °K.; M_1', the molecular weight of the effusing species; $\dot{w}$, the rate of weight loss in grams per second; k, the Clausing short channel correction factor[5,6]; a, the area of the orifice in cm.^{2}; r_0 and r, the atom ratios of volatile to non-volatile component in the alloys initially and at any time, respectively; M_1 and M_2, the atomic weights of the volatile and non-volatile components, respectively; Δw, the total weight loss at any time; and w_2, the weight of the non-volatile component in the effusion crucible. The last quantity may be determined by analysis of the initial alloy, by the weight of the residue after complete evaporation of the volatile component, or from the composition of some known intermediate phase.

If the total weight of the effusion crucible *vs.* the time elapsed from the beginning of evaporation is plotted, the slope of the curve at any point is the rate of weight loss. The information derived from such a plot may, by means of equations 1 and 2, be redrawn as a pressure–composition isotherm. The continuous effusion method for the determination of pressure–composition isotherms also has been used by Blackburn[7] in a study of the uranium–oxygen system.

The equilibrium form of a pressure–composition isotherm (shown in Fig. 1) is well known. It consists of a series of constant pressure plateaus in the heterogeneous phase fields connected by a series of descending curves in the homogeneous phase fields. If the composition range of a homogeneous phase is very narrow, the corresponding

---

[1] This work was performed under the auspices of the U. S. Atomic Energy Commission.

[2] See, *e.g.*, the discussion by C. Wagner, "Thermodynamics of Alloys," Addison-Wesley Press, Inc., Cambridge, Mass., 1952, Section 1-10.

[3] G. R. B. Elliott and J. F. Lemons, *J. Phys. Chem.*, **64**, 137 (1960).

[4] M. Knudsen, "Kinetic Theory of Gases," Methuen, Ltd., London, 1934.

[5] P. Clausing, *Z. Physik*, **66**, 471 (1930).

[6] P. Clausing, *Ann. Physik*, **12**, 961 (1932).

[7] P. E. Blackburn, *J. Phys. Chem.*, **62**, 897 (1958).

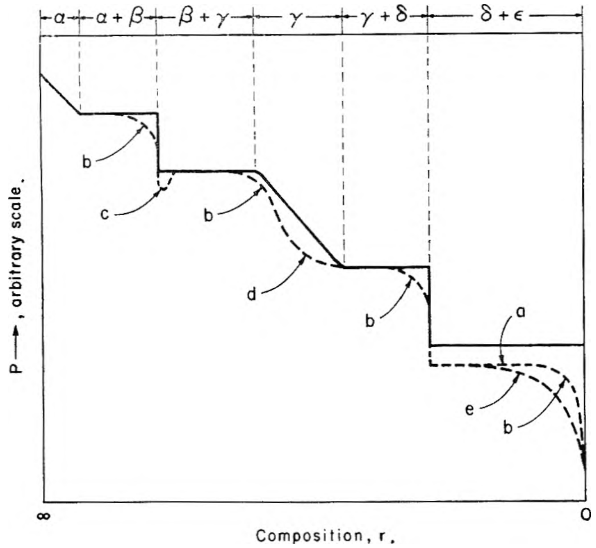

Fig. 1.—Pressure–composition isotherm. Solid line, idealized version; dashed line, dynamic effects: (a) low evaporation coefficient from the δ phase; (b) depletion of the α, β, γ and δ phases; (c) delayed nucleation of the γ phase; (d) a diffusion limited process in the γ solid solution; (e) a diffusion barrier of ϵ on the surface of the δ phase.

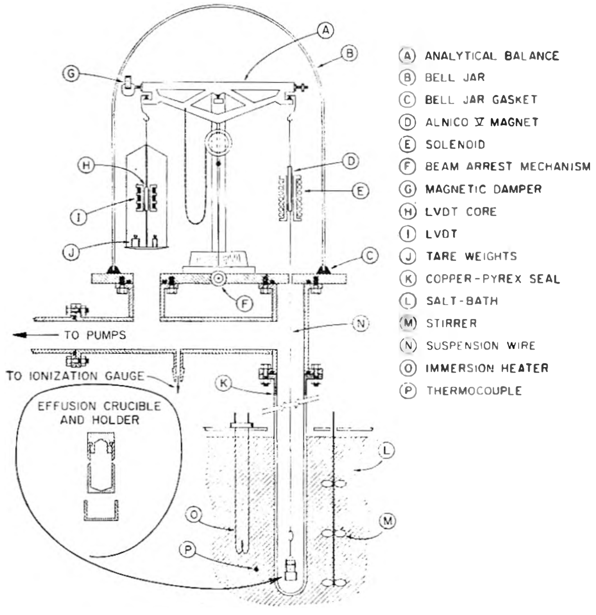

Fig. 2.—Schematic diagram of the recording effusion balance.

descending curve is nearly vertical. At the temperature at which a miscibility gap develops in a homogeneous phase (the "consolute" temperature) the descending curve shows a horizontal inflection.

When vapor pressures are measured dynamically, as in effusion, departures from equilibrium behavior may occur as a result of the unfavorable kinetics of certain solid–vapor or solid–solid transformations. Some examples of such behavior, which invariably decrease the observed pressure, are as follows. (a) The evaporation coefficient, α, of the vapor from the surface of the evaporating phase is small. The observed vapor pressure is related to the equilibrium pressure by the equation[8]

$$P_{\text{obs}} = P_{\text{eq}}(1 + ka/\alpha A)^{-1} \tag{3}$$

where A is the evaporating area of the phase in question. (b) The evaporating area is insufficiently large relative to the effective orifice area. At the end of a pressure plateau, as the volatile-rich phase disappears, this "depletion" effect always should occur to some degree and produce rounding of the otherwise square-cornered isotherms. (c) Evaporation from a homogeneous phase takes place more rapidly than nucleation of the succeeding phase. Should this occur supersaturation is accompanied by a continuous decrease in volatility and the onset of nucleation by a characteristic rapid increase in volatility. (d) Evaporation from the surface of a solid solution takes place more rapidly than diffusion within the solid. Should this occur the observed pressures will be characteristic of the composition of the depleted surface. (e) Evaporation from a heterogeneous mixture takes place with formation of a surface layer through which diffusion does not take place sufficiently rapidly to maintain the saturation pressure. The effects of these kinetic factors on the form of an idealized isotherm are illustrated in Fig. 1.

Experimental

The Balance.—The weight of the effusion crucible was monitored by means of a continuous recording vacuum balance,[9] represented schematically in Fig. 2. A chain-adjustable analytical balance was solidly fastened to a heavy brass base plate and the beam arrest and chain adjusting controls were brought out through the base plate *via* vacuum seals. The sensor for balance beam movements was a linear, variable, differential transformer (Schaevitz Engineering Co., Pennsauken, N. J., LVDT Model 0335-LT) rigidly mounted on an elevating screw for adjustment of the balance zero. Restoring force was provided by an Alnico V bar magnet centered in a rigidly mounted solenoid. The solenoid-magnet combination provided a repulsive force[10] of 84 mg./ma. The weight of the suspended effusion crucible and holder was sufficient to counteract lateral forces due to misalignment of the magnet and solenoid. Motion of the LVDT core from its null position produced a signal which was amplified ($\times 10^6$) to drive a reversible, two phase a.c. servomotor (Minneapolis–Honeywell No. 356358-1). The servomotor actuated the shaft of a 10-turn helical potentiometer through an adjustable-ratio speed reducer. The potentiometer setting controlled the solenoid current and, therefore, the repulsive force upon the magnet, to complete the feedback loop. The solenoid current was recorded on a strip chart. The balance system was calibrated with analytical weights. A typical calibration factor was 0.942 ± 0.005 chart divisions per mg. and the traces were estimated to two-tenths of a division. The slopes of straight line portions of the traces were measured graphically and a mechanical derivimeter (Gerber Instrument Co., Hartford, Conn.) was satisfactory for the curved portions.

In order to isolate the balance from vibrations the apparatus was shock-mounted and the mechanical forepump was connected to the system by looped and suspended rubber hoses. Thus isolated, the balance required only minimum attention during operation and was stable for periods as long as 36 hours.

The Effusion Apparatus.—The effusion crucible was suspended in a two-inch diameter Pyrex or stainless steel tube which was immersed to a depth of 12 inches in a thermostated, 50-liter molten salt-bath. The temperature of the bath, measured near the Pyrex tube with a calibrated Chromel–Alumel thermocouple, was maintained within 0.5° dur-

---

(8) R. Speiser and H. L. Johnston, *Trans. Amer. Soc. Metals*, **42**, 283 (1950); K. Motzfeldt, *J. Phys. Chem.*, **59**, 139 (1955).

(9) Continuous recording vacuum balances are now available from W. Ainsworth and Sons, Inc., Denver, Colorado.

(10) In order to obtain stable operation of the balance the force between the solenoid and the magnet must be repulsive rather than attractive, C. Groot and V. H. Troutner, *Anal. Chem.*, **29**, 835 (1957).

ing a run. By a separate measurement under effusion conditions, the crucible temperature was found to differ from the bath temperature by not more than 0.2°.

Effusion Crucibles.—Crucibles were machined from ½ inch diameter tantalum rods. A threaded lid (7/16-40 NF thread) was screwed into the crucible after the sample was introduced. The lid was well-seated and no vapor seepage through the threads was observed. Two effusion holes were drilled through the sides of the crucibles at opposite ends of a diameter. The usual practice of drilling the effusion hole in the lid must be avoided because the vertical momentum of the effusing beam then is recorded as an added weight which changes during the course of a run. To approximate ideal orifices, the holes were reamed to knife-edge thinness. Effective orifice areas were determined by calibration with pure solid or liquid zinc. Zinc was chosen because excellent vapor pressure data[11] are available and because it is the volatile component in two of the systems studied. The calibration temperatures were close to those of the actual runs and orifice expansion corrections were insignificant. The effective orifice areas, *ka*, for crucibles B and C were $1.71_8 \times 10^{-3}$ cm.^{2} and $5.17_3 \times 10^{-3}$ cm.^{2}, respectively. The approximate single-hole Clausing correction factors were 0.697 and 0.531, respectively.

Alloy Preparations.—Alloys were prepared from pure (> 99.5%) metals. Cerium or uranium was dissolved in the appropriate liquid metal and cooled to precipitate the first intermetallic phase in the form of a bed of fine crystals intimately mixed with excess solvent. The bed material was removed and powdered for analysis. Approximately 300 mg. of finely powdered alloy was used in each run.

Procedure.—The entire system was evacuated to a background pressure of 10^{-5} mm. or less, purified helium at a pressure of 200 mm. was introduced, and the crucible was brought to temperature by raising the salt-bath. The purpose of the helium was to speed up heat transfer between the bath and the crucible and to prevent premature effusion during the heating period. After thermal equilibrium was reached, effusion was initiated by rapid evacuation and terminated by admission of helium to the system. Cooling the crucible in helium also prevented freezing of metal vapors in the threads of the lid and facilitated disassembly.

Results

Three systems of increasing complexity were investigated by means of the effusion balance. In all three the effusing vapor was assumed to be monatomic zinc or cadmium and pressures were computed by the use of equation 1 without correction for the effects of evaporation coefficients.

U–Cd.—The phase diagram of the uranium–cadmium system has been established by conventional methods.[12] In the temperature interval in which the effusion runs were made (320–380°) the system was reported to have only one intermetallic compound, UCd_{11}. A typical isotherm is shown in Fig. 3. The simple form of the isotherm obtained, two plateaus separated by a sharply decreasing pressure region, immediately confirmed the proposed phase diagram and the composition of the intermetallic compound. The only non-equilibrium features which were evident were the rounding of corners due to depletion and a small dip due to delayed nucleation of uranium metal.

U–Zn.—The phase investigation of the uranium–zinc system by Chiotti, *et al.*,[13] indicated the existence of a single intermetallic phase with a narrow homogeneity range, which was tentatively assigned the formula UZn_9. This phase was later designated by Makarov and Vinogradov[14] as

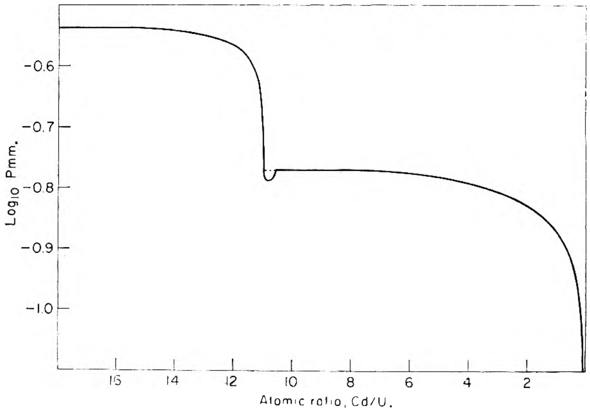

Fig. 3.—U–Cd system: vapor pressure–composition isotherm at 350°.

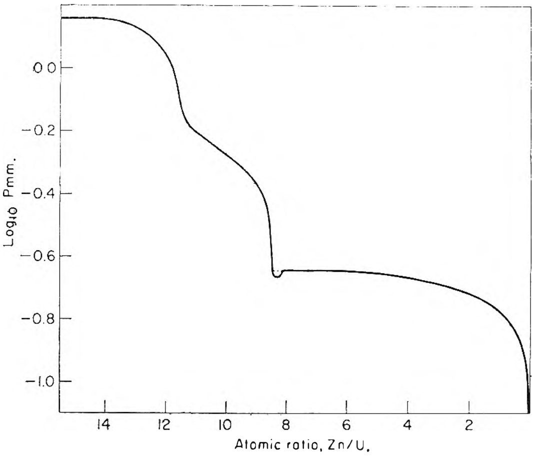

Fig. 4.—U–Zn system: vapor pressure–composition isotherm at 504°.

U_2Zn_{17} as a result of an X-ray structural study. Their suggestion that zinc deficiencies down to U_2Zn_{15} might exist was not supported by any evidence. Further work by Vold[15] on material of this composition showed the existence of two polymorphic forms, of which the high temperature form was isomorphous with Th_2Zn_{17} and the low temperature form with Th_2Ni_{17}. The shape of a typical isotherm for this system, shown in Fig. 4, was found to be quite reproducible in thirteen runs at 420–504°. Because of the supposed existence of a single intermetallic phase with a narrow range, the shape of the isotherm between $UZn_{\sim 12}$ and $UZn_{8.5}$ was unexpected. Two alternate, extreme interpretations of the isotherms in this region could be made. (a) Phases with narrow ranges of homogeneity exist at the compositions $UZn_{\sim 11.5}$ and $UZn_{8.5}$ and no plateau pressure was found in the intermediate region owing to kinetic factors. (b) A single phase with a homogeneity range from $UZn_{\sim 12}$ to $UZn_{8.5}$ exists. The issue was resolved in favor of (b) by stopping the effusion runs at various compositions in the range of interest and subjecting the residues to X-ray diffraction analysis. The alloys prepared at 460° and rapidly cooled to room temperature were found[16] to form a

---

[11] R. F. Barrow, *et al.*, *Trans. Faraday Soc.*, **51**, 1354 (1955).

[12] A. E. Martin, I. Johnson and H. M. Feder, *Trans. AIME*, 221, 789 (1961).

[13] P. Chiotti, H. H. Klepfer and K. J. Gill, *J. Metals, Trans.*, **9**, 51 (1957).

[14] E. S. Makarov and S. I. Vinogradov, *Kristallografiya*, **1**, 634 (1956).

[15] C. L. Vold, M.S. Thesis, Iowa State College, 1959.

[16] R. Schablaske and B. Tani, to be published.

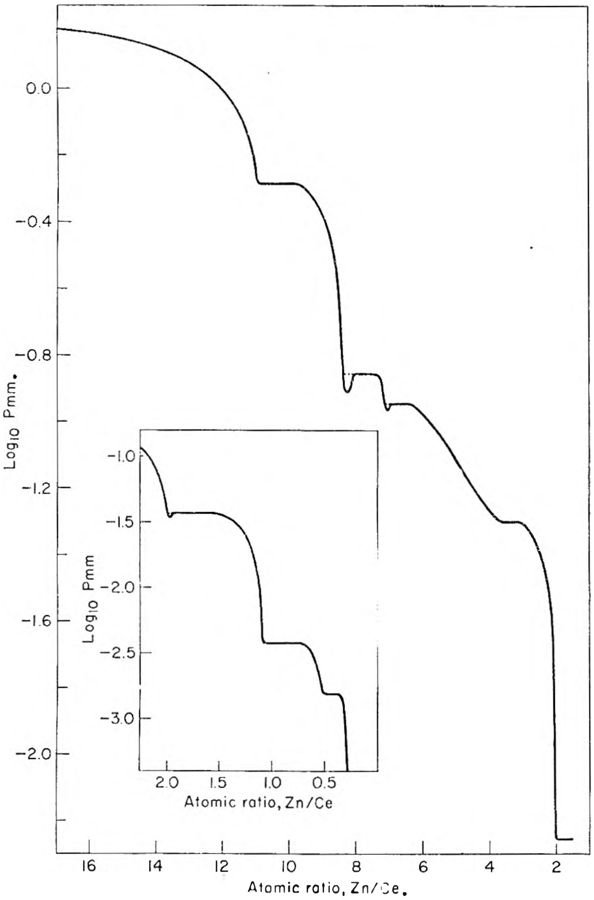

Fig. 5.—Ce-Zn system: vapor pressure–composition isotherm at 512° (crucible B). Insert shows a Ce-rich portion of the isotherm at 570° (crucible C).

continuous series of solid solutions beginning at $UZn_{8.5}$ (with the Th_2Ni_{17} structure). In these solid solutions one of the four uranium atoms in the U_2Zn_{17} unit cell is partially replaced by a pair of zinc atoms. The hypothetical end member of the series is UZn_{12}, whose structure is a variant of $TiBe_{12}$. The inflected form of the descending portion of the isotherm probably is indicative of a tendency for the solid solution to unmix at higher or lower temperatures.

At 450, 460 and 470° the decomposition pressures of U_2Zn_{17} were measured with both crucibles B and C. The crucible with the smaller orifice gave observed pressures 8% higher than the crucible with the larger orifice. This indicated a small but appreciable departure from solid–vapor equilibrium due to finite orifice areas.

Ce–Zn. — The published[17] phase diagrams of the very complex cerium–zinc system and the closely allied lanthanum–zinc system are incomplete. In the cerium system the reported intermediate phases are $CeZn_{11}$[18] and $CeZn_9$,[19] both stable within an undetermined range of homogeneity, and CeZn.[20] Thermal analysis[19] also indicated the likelihood of the existence of three additional, peritectically formed phases between 11 and 30 atom % Ce. Finally, from electrochemical potential measurements, it was reported[21] that Ce_2Zn and Ce_4Zn also exist. Thus a total of eight intermediate phases were suspected in the cerium–zinc system.

Because of the wide variation of zinc pressure in the cerium–zinc system two typical isotherms obtained with the effusion balance are shown in Fig. 5. It is evident that eight intermediate phases succeed one another: $CeZn_{11}$, Ce_2Zn_{17}, $CeZn_{\sim 7}$, $CeZn_{3.8-6.2}$, $CeZn_2$, CeZn, Ce_2Zn and Ce_4Zn. The first two appear to have quite narrow ranges of homogeneity. It may be noted that the replacement of the phase previously labeled $CeZn_9$ by Ce_2Zn_{17} is similar to the replacement of $ThZn_9$[22] by Th_2Zn_{17}[14] and of UZn_9[13] by U_2Zn_{17}[14]. This replacement was foreshadowed by Heumann[23] on the basis of purely geometrical arguments. The phase of apparent composition $CeZn_{\sim 7}$, which showed delayed nucleation, is new; further work is required to elucidate its structure and range of homogeneity. The phase in the vicinity of $CeZn_5$ may be the analog of $LaZn_5$.[24] The former appears to have a homogeneity range from $CeZn_{3.8}$ to $CeZn_{6.2}$; the isotype of this structure, $CaCu_5$, is also known to form solid solutions. It is interesting to note that the Ce–Cd system, however, has been reported to contain both $CeCd_{4.5}$[25] and $CeCd_6$[4,25] as distinct phases. The new phase $CeZn_2$ has as its analog $LaZn_2$.[26] The phase CeZn actually appears to occur at $CeZn_{1.1}$; the departure from the usual stoichiometry of phases having the CsCl structure requires further confirmation. Finally, it is seen that the existence of the compounds Ce_2Zn and Ce_4Zn appears to be confirmed even though Hansen[17] seems to consider them questionable because they were not found in the La–Zn system.

Discussion

The effusion balance, when applied to the study of three test systems with known or partially known phase diagrams, has been shown to be capable of corroborating the existence of known phases (UCd_{11}, $CeZn_{11}$, CeZn), proving the existence of suspected phases ($CeZn_{\sim 7}$, $CeZn_2$, Ce_2Zn and Ce_4Zn), modifying a previous formulation (Ce_2Zn_{17} for $CeZn_9$), and indicating ranges of homogeneity ($UZn_{8.5-\sim 12}$, $CeZn_{3.8-6.2}$). As a result of this study some limitations of the effusion balance have been revealed.

1. The system to be studied should contain not more than one relatively volatile component, and its pressure at the desired temperature and concentration should lie between about 10^{-3} and 1 mm. The lower limit is set by the time required to effect gross changes of composition by evaporation; the upper limit is set by the requirement that

---

[17] M. Hansen and K. Anderko, "Constitution of Binary Alloys," 2nd Edition, McGraw-Hill Book Co., Inc., New York, N. Y., 1958.

[18] M. J. Sanderson and N. C. Baenziger, *Acta Cryst.*, **6**, 627 (1953).

[19] J. Schramm, *Z. Metallkunde*, **33**, 358 (1941).

[20] A. Iandelli and E. Botti, *Gazz. chim. ital.*, **67**, 638 (1937).

[21] F. Clotofski, *Z. anorg. u. allgem. Chem.*, **114**, 16 (1920).

[22] H. Nowotny, *Z. Metallkunde*, **37**, 31 (1946).

[23] T. Heumann, *Nachr. Akad. Wiss. Göttingen. Math. Phys. Kl.*, **A2**(1), 1 (1950).

[24] H. Nowotny, *Z. Metallkunde*, **34**, 247 (1942).

[25] A. Iandelli and R. Ferro, *Gazz. chim. ital.*, **84**, 463 (1954).

[26] F. Laves, *Naturwissenschaften*, **27**, 65 (1939); L. Rolla and A. Iandelli, *Ricerca sci.*, **20**, 1216 (1941).

the volatility should be readily related to a true vapor pressure.

2. A more significant limitation, particularly for new systems, is the possibility of obtaining isotherms whose interpretation is ambiguous. The range of existence of the intermetallic phase in the uranium–zinc system, for example, could not be established without the aid of supplementary X-ray data. The most likely sources of ambiguity are the kinetic factors limiting the attainment of solid–vapor and solid–solid equilibrium. In this study examples of the effects of these kinetic factors were observed, but the phase boundaries were not obscured.

Certain advantages and special capabilities of the effusion balance also were noted: 1. The speed and simplicity with which phase boundary locations were determined compared very favorably with the time consumption and complexity of conventional methods; 2. The effusion balance was most precise for the measurement of changes in alloy composition at the beginning of evaporation. This feature is particularly valuable for the investigation of alloys over short ranges of composition, *e.g.*, between 16.31 wt. % Ce ($CeZn_{11}$) and 20.15 wt. % Ce (Ce_2Zn_{17}), and it should be useful for unraveling the complex phase relations in dilute amalgams.

In principle, the effusion balance may be used to obtain the activity of the volatile component in a binary system over the entire range of composition, and hence, by the Gibbs–Duhem relation, the thermodynamic properties of the non-volatile component and of each phase. The evaluations of these properties for the three binary systems studied have been deferred to later papers. Finally, the thermodynamic properties of certain binary systems may be best evaluated by investigating a ternary system in which the activity of a third component is measured at constant ratios of the other two (Darken's method[27]). The utility of the effusion balance for this and similar purposes[28] is obvious.

Acknowledgments.—The authors wish to thank P. Bergland and N. Goetzinger for technical assistance, R. Schablaske and B. Tani for their X-ray investigations, and Prof. Scott E. Wood for some helpful discussions.

(27) L. S. Darken, *J. Am. Chem. Soc.*, **72**, 2909 (1950).

(28) T. Yokokawa, A. Doi and K. Niwa, *J. Phys. Chem.*, **65**, 202 (1961).

THE EFFECT OF DISSOLVED ALKALI HALIDES ON THE RAMAN SPECTRUM OF WATER[1]

By J. W. SCHULTZ AND D. F. HORNIG

Metcalf Research Laboratory, Brown University, Providence, R. I.
Frick Chemical Laboratory, Princeton University, Princeton, N. J.

Received May 13, 1961

The Raman spectra of aqueous solutions of LiCl, LiI, KF, KI, CsF and CsI have been studied at several concentrations. The striking conclusion is that the intensity of both the bending and stretching vibrations are strongly affected by the nature of the anion, decreasing slightly in the presence of F^-, increasing slightly with Cl^- and increasing up to eight times in the presence of I^-. Equally striking is the observation that there is no detectable effect of the cation, *i.e.*, LiI and CsI yielded substantially identical spectra. There is no evidence for the presence of more than one kind of water molecule, either in pure water or in any of the solutions.

Introduction

It has been observed recently[2] that dissolved KBr produces a surprisingly large change in the intensity of Raman scattering from water (*e.g.*, the total scattering in the stretching region increased by 30% in going from pure water to 3.5 M KBr and that in the bending region by a factor of three). A similar but smaller effect occurred in aqueous HCl, although here the observations were complicated by the presence of OH_3^+ ions, while KOH in solution reduced the scattering intensity from all bands. These effects were so large that they seemed to merit further investigation for the light they might shed on the nature of the hydration of ions and the effect of dissolved ions on the structure of water. We therefore undertook to investigate the Raman spectra of H_2O, D_2O and of solutions of a series of alkali halides, utilizing a photoelectric Raman Spectrograph which enabled us to study band shapes, intensities and depolarization ratios as well as frequencies.

Previous investigations of the Raman spectrum of water have been reviewed extensively by Hibben[3] and Dorsey.[4] A more recent investigation was carried out by Narayanaswamy.[5] There also have been numerous investigations of the Raman spectra of electrolytic solutions,[3] but in the light of Busing's work we decided to investigate this very simple class of electrolytes in which the size of ions of either charge could be varied and the number of possible complicating effects minimized.

Experimental

The Raman spectra were obtained on a photoelectric spectrophotometer of Littrow design, the dispersing elements consisting of 30 and 60° medium flint glass prisms. One face of the 30° prism was silvered and served as the Littrow

---

(1) Based on a thesis presented by J. W. Schultz in partial fulfillment of the requirements for the Ph.D. degree, Brown University, April 1957. Presented at the meeting of the American Chemical Society, New York, Sept. 7, 1958.

(2) W. R. Busing and D. F. Hornig, *J. Phys. Chem.*, **65**, 284 (1961).

(3) J. H. Hibben, "The Raman Effect and Its Chemical Applications," Reinhold Publ. Corp., New York, N. Y., 1939.

(4) N. F. Dorsey, "Properties of Ordinary Water-Substance," Reinhold Publ. Corp., New York, N. Y., 1940.

(5) P. K. Narayanaswamy, *Proc. Indian Acad. Sci.*, **27A**, 311 (1948).

mirror. The aperture of the monochromator was approximately $f/6$ while the dispersion at 4358 Å. was 77 cm.$^{-1}$/mm. The light entering the monochromator was chopped at 30 c.p.s. and detected by an E.M.I. 6094B photomultiplier. The a.c. signal was amplified, rectified and fed to a standard recorder. Both the prism and chart drives were driven by synchronous motors. An automatic piping device inserted markers at regular intervals of the prism drive. The monochromator was calibrated using an argon lamp, the wave lengths having been obtained from the "M.I.T. Wave-Length Tables."[6]

The exciting lamps were of the Toronto type,[7] the design having been modified for vertical operation and to fit the shorter cells used in liquid work. These lamps were in the shape of inverted J's, the mercury being contained in the two ends. Kovar caps graded to Pyrex made electrical contact with the mercury. The ends of the lamps containing mercury were jacketed so that tap water could be used to cool the mercury. The straight sections of the lamps also were jacketed, but in this case the water coolant temperature was about 60° to avoid condensation of mercury. The curved sections of the lamps were left unjacketed. The total power put into the lamps was 660 watts, but only half of the total discharge length was actually used to illuminate the sample. The two lamps were surrounded by reflectors which were elliptical sections, the open ends of the reflectors being convenient in keeping the sample at room temperatures by an air blast. Some spectra also were obtained with a totally enclosed source unit employing a diffuse MgO reflector and 6 General Electric AH-11 mercury lamps.

All quantitative measurements were made in a sample cell of approximately 100-ml. volume. This cell was jacketed to filter out unwanted mercury lines. The filter solution used for all quantitative measurements was a 16% solution of *m*-dinitrobenzene in benzene which transmitted only 0.08% of the 4047 Å. mercury line. It was important to eliminate this line since the OH stretching band excited by it would have overlapped the OH bending band excited by the 4358 Å. mercury line. Although the same filter solution was used many times, no decomposition by the mercury arcs was detected. An air blast was sufficient to keep the sample near room temperature and it was unnecessary to circulate the filter solution.

All samples except those of heavy water were filtered through either a "fine" sintered Pyrex glass büchner funnel or a micro metallic stainless steel büchner of 5 μ pore size. Allowing the samples to stand overnight before filtering aided in removing suspended matter. The heavy water was quite free of scattering material and was left unfiltered to avoid any exchange with atmospheric moisture. All salts were either reagent grade or stated by the manufacturer to be better than 99% pure. Nevertheless, it was found necessary to neutralize the LiI with HI and then recrystallize the salt twice as $LiI \cdot 3H_2O$ to eliminate I_2. The CsF was very acidic and was neutralized with CsOH. The presence of dissolved silica in the CsF samples gave rise to a broad fluorescence band which was troublesome at high concentrations. The LiI, LiCl and CsI solutions were analyzed by standard volumetric methods, the CsF solutions by precipitating and weighing fluoride as PbClF and the KF solutions by measuring the refractive indices. The KI solutions were prepared from weighed amounts of reagent grade dried KI. A crystal of sodium thiosulfate was added to each iodide sample to prevent discoloration of the samples by the mercury lamps.

Depolarization measurements in the OH stretching region of H_2O and in the OD stretching region of D_2O were obtained by the method of Rank and Kagarise.[8] Chloroform was used to correct the observed depolarization ratios.

Experimental intensities of both the bending and stretching bands in salt solutions referred to pure water as a standard were obtained. Since the bands in the salt solutions were little altered in frequency from pure water, and since the depolarization ratio was little affected, if at all, it was unnecessary to correct the observed intensities for the varying sensitivity of the detector and transmission of the optics with wave length or for polarization introduced by the optics. However, over the wide range of concentrations employed there was considerable variation in refractive index and it was necessary to take the variation in incident intensity with refractive index into account. A modification of the method proposed by Bernstein and Allen[9] was used to obtain a correction curve. The relation between the intensity of a Raman line in a pure material and in solution in an inert solvent should be given approximately by the expression

$$I_s K(n_s) n_s^2 = I_v K(n_v) n_v^2 \qquad (1)$$

where I is the experimentally observed intensity, n is the refractive index, s refers to the solute and v to the volume fraction of the material in solution. The term in n^2 is the correction relating to the solid angle of light flux from each scattering point which reaches the spectrometer while $K(n)$ corrects collectively for other losses of incident radiation related to the refractive index. By measuring the intensities for a pure solute and solutions of the solute, one can obtain values for $K(n)/K(n_s)$ as a function of refractive index. These "correction factors" were obtained by measuring the 458 cm.$^{-1}$ Raman line of CCl_4 in pure CCl_4 and in solutions of CCl_4 in various hydrocarbons. While this limited the measured range of the correction factors from $n = 1.39$ to $n = 1.45$, an approximate calculation based on the geometry of our source indicated that the correction factor was nearly linear in the refractive index for refractive indices less than that of glass and nearly constant for refractive indices equal to or greater than that of Pyrex. The following equation therefore was used to correct the experimental intensities

$$\frac{I}{I_0} \frac{n^2_{\text{sample}}}{n^2_{H_2O}} \frac{\rho_{H_2O}}{\rho_{\text{sample}}} \frac{K(n_{\text{sample}})}{K(n_{H_2O})} = \frac{S}{S_0} \qquad (2)$$

where S is the scattering per molecule and ρ is the concentration of water in moles per liter. The concentrations were calculated from data in the International Critical Tables except for CsF, for which it was measured. The experimental intensities were measured by obtaining the spectrum of pure water, of one or two samples of solution, and then of pure water again. In this manner drifts in the intensity of the exciting radiation were accounted for. The areas under the bands were measured with a planimeter directly from the original spectra; the frequency scale was very nearly linear across any one band.

Experimental Results

The OH and OD stretching regions of H_2O and D_2O, respectively, are shown in Figs. 1 and 2. It is clear from these spectra that there are at least two major components of the band and there is some suggestion of a weak third component on the high frequency edge. This is as expected since the overtone of the bending frequency (2 × 1650 cm.$^{-1}$ in H_2O), the symmetric stretching frequency (ν_1) and the asymmetric stretching frequency (ν_3) should all appear in this region. The first two of these ought to be polarized (*i.e.*, $\rho < 6/7$) and ν_3 should be depolarized (*i.e.*, $\rho = 6/7$). The depolarization as a function of frequency in the OH and OD stretching regions is plotted in Fig. 3. It resolves plainly the highly polarized low frequency component, in all probability $2\nu_2$, and the polarized central component, which is therefore probably ν_1. There is only a suggestion, particularly in the O–D band, that the depolarization ratio is rising toward the value expected for ν_3 at the high frequency end of the range in which measurements could be taken.

The effect of temperature on the OH stretching region over the range from 2 to 95° is illustrated in Fig. 4. As the temperature is raised the low frequency component decreases considerably in intensity, the central component a little and the scat-

---

(6) G. R. Harrison, Editor, "M.I.T. Wave-Length Tables," John Wiley and Sons, Inc., New York, N. Y., 1939.

(7) See, for example, B. Stoicheff, *Can. J. Phys.*, **32**, 330 (1954).

(8) D. G. Rank and R. E. Kagarise, *J. Opt Soc. Am.*, **40**, 89 (1950).

(9) H. J. Bernstein and G. Allen, *ibid.*, **45**, 237 (1955).

TABLE I

MEASUREMENTS ON SOLUTION SPECTRA

Salt	Molar concn.	Mole ratio	$n^{22}D$	Bending region: ν of max.	Band width	I/I_0	S/S_0	Stretching region: ν of max.	Band width	I/I_0	S/S_0
LiI	2.0	0.039	1.374	1643	91	2.90	2.66	3478	265	1.16	1.06
LiI	4.0	.085	1.414	1638	80	5.18	4.57	3473	220	1.38	1.22
LiI	5.9	.138	1.456	1633	70	8.39	7.33	3475	202	1.62	1.42
LiI	7.9	.200	1.496	1638	64	8.38	7.99	3466	200	1.69	1.61
KI	2.0	.040	1.373	1643	96	2.66	2.50	3473	241	1.13	1.06
KI	5.0	.120	1.431	1635	80	6.12	5.88	3475	200	1.43	1.37
KI	6.1	.159	1.456	1630	76	7.53	7.40	3473	185	1.47	1.44
CsI	1.3	.026	1.364	1645	97	2.40	2.28	3475	304	1.09	1.04
CsI	2.6	.056	1.395	1638	93	3.22	3.04	3476	240	1.11	1.05
LiCl	2.0	.038	1.351	1643	122	1.11	1.06	3437	331	1.04	1.00
LiCl	5.0	.100	1.374	1652	113	1.31	1.24	3448	261	1.10	1.04
LiCl	8.0	.173	1.395	1648	90	1.42	1.36	3443	241	1.17	1.12
LiCl	11.0	.259	1.412	1650	88	1.90	1.87	3441	231	1.19	1.17
LiCl	13.7	.348	1.427	1646	93	2.31	2.38	3445	236	1.15	1.18
KF	2.9	.054	1.345	1653	116	0.75	0.74	3441	396	0.96	0.95
KF	4.6	.089	1.350	1652	112	.77	.77	3439	386	.89	.89
KF	7.5	.155	1.356	1637	151	.76	.80	3432	380	.79	.81
KF	10.5	.231	1.360	1637	142	.63	.68	3422	386	.73	.80
CsF	3.6	.071	1.360	1640	117	.64	.62	3434	400	.91	.88
CsF	7.2	.160	1.381	1641	131	.64	.65	3431	398	.77	.78
CsF	10.3	.257	1.398					3410	406	.69	.75
H_2O			1.332	1640	126	1.00	1.00	3439	407	1.00	1.00
D_2O				1208	67			2532	306		

tering near 3600 cm.$^{-1}$ is somewhat increased. When alkali halides are dissolved in water there is a marked change in the shape of the band. As pointed out by Busing and Hornig,[2] the intensity of the low frequency component diminishes and that of the central component increases markedly. The spectra of water with dissolved LiI is shown in Fig. 5; the spectra obtained with KI or CsI are indistinguishable. The shape of the band is the same but the intensity changes are much smaller with LiCl or CsCl. When KF or CsF are dissolved, the intensity changes are minor but there appears to be some broadening of the components so that the band is less well resolved. There also appears to be a slight downward shift in the frequency of the central peak, ν_1.

The bending regions in H_2O and D_2O are shown in Figs. 6 and 7. The two peaks in each case arise from the bending vibration, ν_2, and its combination with librational motion of the molecule. Both bands are symmetrical and while their width indicates some statistical distribution in the molecular environment, there is nothing to suggest the presence of more than one local structure for the water. When salts are dissolved in the water the intensity of the bending band is increased remarkably for iodides, increased slightly for chlorides and decreased slightly for fluorides; the frequency, width and shape of the band remain quite unaffected. All of these features are illustrated in Fig. 8, which is typical of all of the salts. In both the stretching and bending regions no new peaks which could be ascribed to water of hydration were observed, even when the mole ratio of alkali halide to water was as high as 0.200.

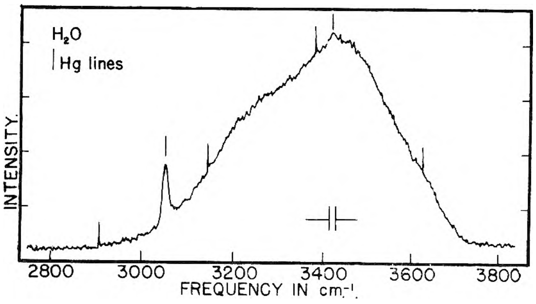

Fig. 1.—Raman spectrum of the OH stretching region in water.

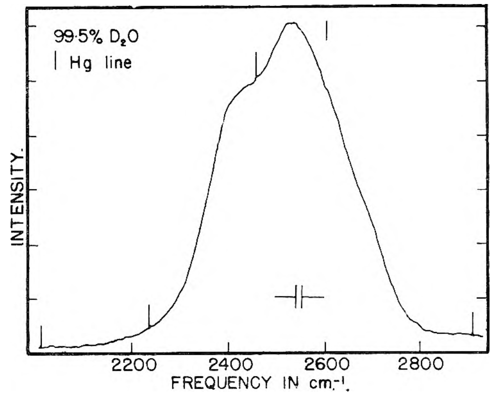

Fig. 2.—Raman spectrum of the OD stretching region in liquid D_2O.

The experimental intensities, corrected intensities, frequencies of the maxima, band widths at half maximum intensities, refractive indices of the solutions and concentrations are all given in Table I. The experimental intensities are proportional to the total area under the bands; no effort was made to distinguish the components in the stretching region for this purpose. The precision of the

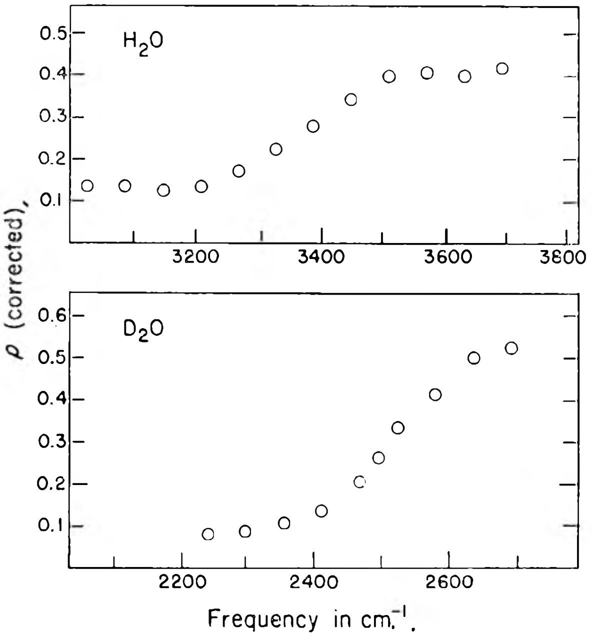

Fig. 3.—Depolarization ratios in the stretching regions of ordinary and heavy water.

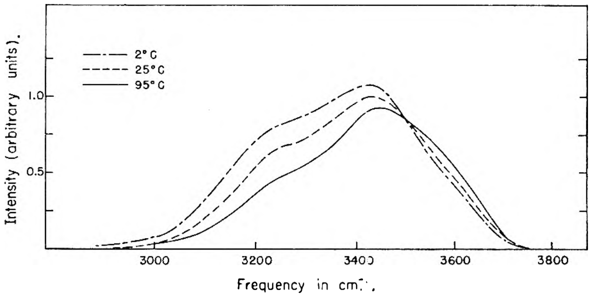

Fig. 4.—The effect of temperature on the OH stretching region.

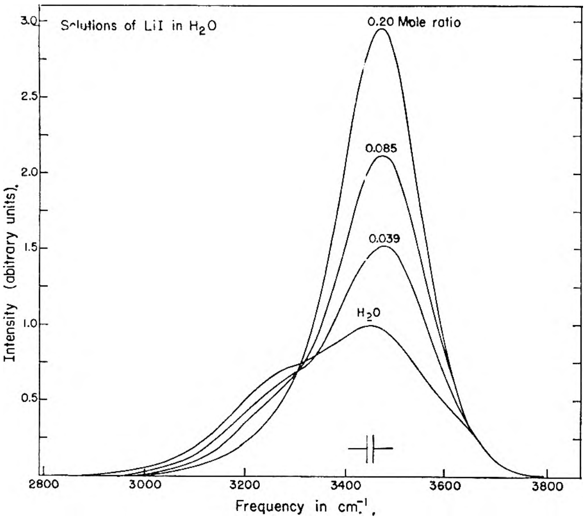

Fig. 5.—Raman spectra of the OH stretching region of LiI solutions.

experimental intensities is about ±3% in the stretching and ±6% in the bending region. It is hard to estimate the magnitude of the systematic errors which might have been introduced.

Analysis of the Stretching Region.—It was found by Busing[2] that the stretching region in KBr solutions could be represented quite well as a superposition of two Gaussian lines of constant frequency and width but of amplitude depending on composition. It seemed desirable to attempt a similar analysis for our solution, but since most investigators have found a weak peak near 3600 cm.$^{-1}$ as well as the two main peaks, the analysis was carried out on the assumption that the spectra could be represented as a superposition of three peaks, *i.e.*, that the observed spectrum could be described by an equation of the form

$$I(\nu) = \sum_{i=1}^{3} f(B_i, W_i, \nu_i^0, \nu) \qquad (3)$$

where B is an amplitude parameter, W a width parameter and ν^0 a position parameter. Two functions, f, were considered, the Gaussian and the Lorentz functions. The two functions are very similar above half height but the base of the Lorentz function is much broader and it has extended "wings." The measured intensities as a function of frequency were fitted by least squares to the equation

$$I_j = \sum_i B_{ij} \exp[-(\nu - \nu_i^0)^2/H_i^2]; \; i = 1, 2, 3;$$

$$W_i = 2\sqrt{\ln 2}\, H_i \qquad (4)$$

for a Gaussian fit, and to

$$I_j = \sum_i \frac{B_{ij}}{1 + (\nu - \nu_i^0)^2/H_i^2} \qquad (5)$$

for the Lorentz function. In eq. 4 and 5 the subscript j refers to spectra obtained with unpolarized, parallel polarized or perpendicularly polarized light; W_i is the full width at half height.

The least squares calculations were programmed and carried out for us on the Oracle computer of the Oak Ridge National Laboratory by Dr. W. R. Busing. About 60 observed points each were used in the O–H and O–D stretching region, each point having three intensity values corresponding to the three kinds of illumination. The points were taken from smoothed experimental curves and were given a weight of one-half in the vicinity of mercury lines. The "tails" were not considered either as important or as reliable as the peak regions and also were given less weight. The parameters obtained with the Gaussian curve are given in Table II, along with the standard deviations. It is apparent that the errors are much greater for the high frequency component than for the other two, undoubtedly because it is much weaker and nearly buried under the others. The fit is also much worse for D_2O, particularly for components II and III, which are very badly overlapped.

When the bands were fitted to Lorentz functions with all parameters varied the calculation did not converge and a unique solution was impossible. This was certainly caused by the much broader base of these functions which increased the overlap of the three components and made the parameters of any one component highly dependent on those of the other two. A reasonable fit was obtained when the position and line width parameters were

TABLE II

GAUSSIAN FIT OF OH AND OD STRETCHING BANDS[a]

Parameter	H_2O, cm.$^{-1}$	Std. deviation	D_2O, cm.$^{-1}$	Std. deviation
ν_{I}°	3260.8	+2.3	2405.4	+ 2.5
ν_{II}°	3460.0	1.6	2522.7	1.3
ν_{III}°	3612.5	2.8	2616.7	6.4
H_{I}	161.0	1.9	100.7	1.6
H_{II}	124.9	2.4	68.9	2.6
H_{III}	77.9	3.1	95.1	4.7
$B_{I\ un}$	148.2	1.8	285.0	3.4
$B_{II\ un}$	193.0	2.9	223.5	25.0
$B_{III\ un}$	47.3	3.5	197.3	12.0
$B_{I} \perp$	215.6	2.2	302.3	3.3
$B_{II} \perp$	236.3	4.1	200.0	21.0
$B_{III} \perp$	59.3	4.3	156.9	10.0
$B_{I\ \parallel}$	59.2	1.3	80.6	2.1
$B_{II\ \parallel}$	136.8	1.5	108.2	14
$B_{III\ \parallel}$	35.7	2.4	113.2	6.4
$\Sigma w[I(\text{obsd.}) - I(\text{calcd.})]^2$		0.00076		0.00238
$\Sigma w I^2(\text{obsd.})$		2.9281		4.1545
$\sqrt{\dfrac{\Sigma w([I(\text{obsd.}) - I(\text{calcd.})]^2}{\Sigma w I^2(\text{obsd.})}}$		1.6%		2.4%

[a] w = statistical weight.

carried over from the Gaussians and only the amplitudes were varied, but the over-all fit was then much poorer than with the Gaussian line shapes.

The spectra of 4 and 7.9 *M* LiI solutions were fitted only to Gaussians, using unpolarized spectra. In the case of the more concentrated solution the results were anomalous when three Gaussians were used and the final fit was made with only two. The results are listed in Table III.

It is apparent that the parameters from the best least squares fit are not entirely in agreement with values that might be estimated by visual inspection of the spectra in Figs. 1 and 2. One therefore must conclude that the degree of overlap between the components is sufficient so that other sets of parameters might have given almost as satisfactory an over-all fit. In particular, the parameters for the high frequency component (III) are most uncertain.

There are a number of checks which can be applied to the parameters. Assuming that the components in the OH and OD stretching regions of H_2O and D_2O have the same origins it would be expected that the depolarization ratios for corresponding peaks would be similar. The least squares fit gave the depolarization ratios, using Gaussian line shapes

	ρ_{I}	ρ_{II}	ρ_{III}
H_2O	0.27	0.58	0.60
D_2O	0.27	0.54	0.72

where I, II and III are in order of increasing frequency.

The values for H_2O and D_2O are in reasonably satisfactory agreement but ρ_{I} is somewhat greater in both cases than would have been expected from Fig. 3. ρ_{III} in both cases seems slightly low since if band III is ν_3, the asymmetric stretching frequency, a value of 6/7 is expected. These discrepancies would occur if, because of the great overlap of the components in the experimental spectra, the parameters of Table II had ascribed to components I and III a part of the total intensity which really belonged to II.

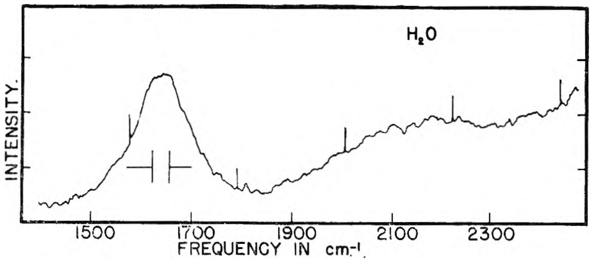

Fig. 6.—Raman spectrum of the bending region in water.

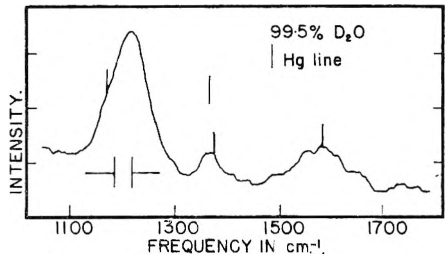

Fig. 7—Raman spectrum of the bending region in heavy water.

Another check can be made on the line widths. If their source is primarily the linear variation in O–H force constant caused by variations in the O–O distance, one expects that for any distribution of O–O distances whatever the ratio H/ν should be the same for H_2O and D_2O and $H_{D_2O}/H_{H_2O} = 0.7$. The observed quantities are

	I	II	III
$(H/\nu)_{H_2O}$	0.049	0.036	0.020
$(H/\nu)_{D_2O}$	.042	.027	0.034
H_{D_2O}/H_{H_2O}	.63	.55	1.22

For the two lower frequency components the ratios of line widths in H_2O and D_2O are similar but definitely lower than anticipated from the simple hypothesis above; they are consistent with the ratio 0.53 observed for the bending band. However, the

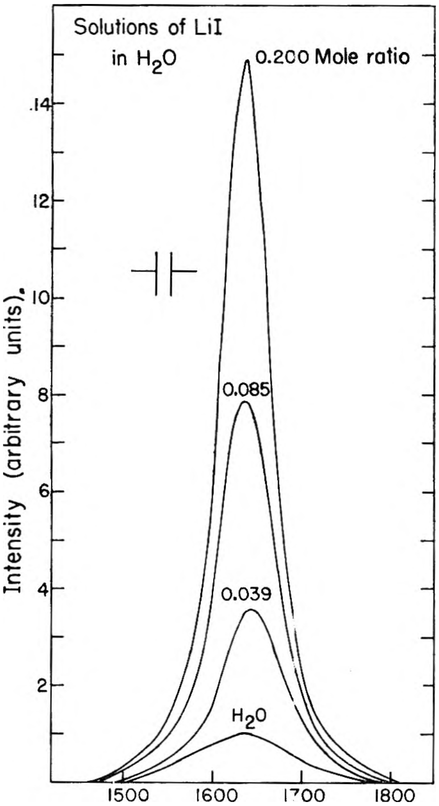

Fig. 8.—Raman spectra of the bending region of LiI solutions.

line width parameter, H, definitely seems too large for component III in D_2O, probably by a factor of at least two.

Still another check is possible from the intensities, which are proportional to the product BH. Assuming that the molecular polarizability parameters are the same in H_2O and D_2O, the relative intensities for the three components should be approximately the same for H_2O and D_2O in the absence of Fermi resonance. The situation is complicated because $2\nu_2$ and ν_1 are of the same symmetry type and may interact by Fermi resonance. As a consequence, $2\nu_2$ (component I) may "borrow" intensity from ν_1 (component II) but to a good approximation the sum of their intensities is unchanged by the Fermi resonance. Since ν_3 (component II) may not interact with either of the others we expect that even in the presence of Fermi resonance the intensity ratio III/(I + II) should be the same in H_2O and D_2O. A further consequence of resonance is that if $2\nu_2$ "borrows" intensity from ν_1 the relative intensity of component II must be equal to or greater than that of I.

The relative intensities given by the products BH from Table II are

	H_2O	D_2O
I	1.00	1.00
II	1.07	0.54
III	0.16	0.65

These ratios are very different for H_2O and D_2O; furthermore, the relative intensity of II in D_2O seems much too low. However, it is significant that the sum of the relative intensities of components II and III, 1.23 and 1.19, respectively, is almost the same in the two compounds. Inspection of Figs. 1 and 2 shows that components II and III are very badly overlapped so that the division of intensities during the least squares fitting process is uncertain, depending highly on the accuracy to which the shape of each component is Gaussian. It seems apparent that in the least squares fitting process the intensity assigned to component III in D_2O was much too great.

It seems worthwhile therefore to inquire as to the distribution of intensity if the intensity of III in D_2O were assigned by assuming the ratio III/(I + II) to be the same in D_2O as in H_2O and I to be correct. This yields the revised distribution

	H_2O	D_2O
I	1.00	1.00
II	1.07	1.03
III	0.16	0.16

This result seems thoroughly reasonable.

Since we had concluded previously that the width parameter, H_{III}, was approximately twice too large in D_2O, this result implies that the amplitude parameter, B_{III}, is also about twice the correct value. It also implies that the amplitude B_{II} in D_2O should be increased, perhaps as much as four times.

From the results of the previous discussion, as in the previous work of Busing and Hornig,[2] one can conclude that the stretching regions in H_2O and D_2O can be adequately represented as a superposition of Gaussian components which may be identified as $2\nu_2$, ν_1 and ν_3, respectively. Comparison of Table II and Table III shows that when LiI is dissolved at any concentration up to 7.9 M there is very little effect on either the central frequencies or the widths of the component lines. In view of the close similarity of the various spectra the same observation applies to them. Therefore, we can find no evidence of a significant further perturbation by the ions on the molecular frequencies, despite the fact that the hydrogen bonds in pure water have perturbed the stretching frequencies of the free molecule by about 200 cm.$^{-1}$ and it might have been presumed that the hydrogen bond arrangement would be disturbed by the presence of ions.

The really big effect of the dissolved ions is to decrease the intensity of I and to increase the intensity of II dramatically, a result previously obtained by Busing for KBr solutions.[2] The question of the origin of this effect and its relation, if any, to the structure of the solutions is an important one. Since overtones are normally very weak, the intensity of I ($2\nu_2$) suggests a strong Fermi resonance with II (ν_1). If it is assumed that in the absence of Fermi resonance $2\nu_2$ would have substantially zero intensity compared to ν_1, the relative intensities of the lines observed are related to the separation of the observed components and those of the unperturbed levels by the expression

$$\frac{I_{2\nu_2}}{I_{\nu_1}} = \frac{\delta - \delta_0}{\delta + \delta_0}; \quad \nu_1 + 2\nu_2 = \nu_1^0 + 2\nu_2^0 \qquad (6)$$

where δ is the observed separation and δ_0 the unperturbed separation.

For H_2O, $\delta = 200$ cm.$^{-1}$, and the intensity ratio

TABLE III

GAUSSIAN FIT OF OH STRETCHING REGION IN 4.0 AND 7.9 M LiI SOLUTIONS[a]

Parameter	4.0 M	Std. deviation	7.9 M	Std. deviation
ν I°	3283.7	+8.7	3269.0	±10.4
ν II°	3477.4	1.3	3469.6	1.2
ν III°	3623.9	2.7		
H_{I}	144.6	5.4	112.8	10.6
H_{II}	116.0	1.8	118.5	1.3
H_{III}	61.1	4.4		
B_{I}	49.0	1.7	31.4	1.9
B_{II}	203.5	2.2	289.3	1.5
B_{III}	16.2	1.8		
$\Sigma w[I(\text{obsd.}) - I(\text{calcd.})]^2$		0.0000322		0.000402
$\Sigma wI^2(\text{obsd.})$		0.47876		0.80876
$\sqrt{\dfrac{\Sigma w[I(\text{obsd.}) - I(\text{calcd.})]^2}{\Sigma wI^2(\text{obsd.})}}$		0.82%		2.2%

[a] w = statistical weight.

predicted by eq. 6 for various values of δ_0 is

$I_{2\nu_2}/I_{\nu_1}$	$2\nu_2^0$, cm.$^{-1}$	ν_1^0, cm.$^{-1}$	δ_0, cm.$^{-1}$
1.00	3361	3361	0
0.80	3350	3372	22
.60	3336	3386	50
.40	3318	3404	86
.20	3294	3427	133

and for D_2O, for which $\delta = 117$ cm.$^{-1}$

1.00	2464	2464	0
0.80	2457	2471	15
0.60	2449	2479	30

It is clear that relatively large intensity variations can result from small shifts in the zero-order frequencies. Since in both H_2O and D_2O the ratio $I_{2\nu_2}/I_{\nu_1}$ is certainly between 0.8 and 1.0, the zero-order frequencies of $2\nu_2^0$ and ν_1^0 nearly coincide, $2\nu_2^0$ lying between 3350 and 3361 cm.$^{-1}$ for H_2O and 2457 and 2464 cm.$^{-1}$ in D_2O (with corresponding narrow ranges for ν_1^0). At first sight the value of $2\nu_2^0$ seems high since the fundamental, ν_2, occurs at 1640 cm.$^{-1}$.

It seems likely, nevertheless, that this interpretation is correct and that the opposite behavior of I and II, when salts are dissolved or water is heated, is related to small changes in the unperturbed frequencies rather than to significant structural effects.

The ratio, $I_{2\nu_2}/I_{\nu_1}$, is 0.30 for 4.0 M LiI and 0.098 for 7.9 M LiI. Since $\delta = 193$ and 200 cm.$^{-1}$ at the two concentrations the intensities can be accounted for if $\delta_0 = 104$ and 164 cm.$^{-1}$.

Discussion

The results from Table I are plotted in Figs. 9 and 10. The total stretching intensity per molecule was plotted rather than those of individual components since it did not depend on the rather uncertain dissection of the band. Moreover, in the presence of strong Fermi resonance it is only the sum of the intensities of I and II which is important, while that of III is negligible in comparison.

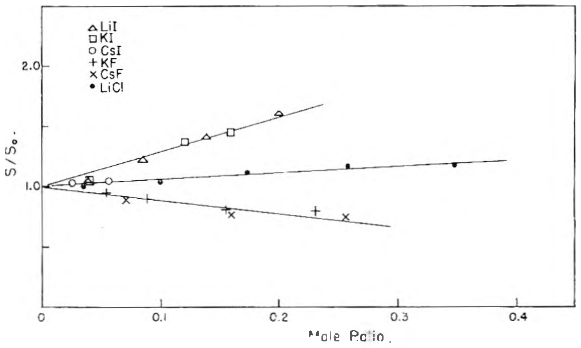

Fig. 9.—The effect of dissolved ions on the scattering per molecule, relative to pure H_2O, in the stretching region.

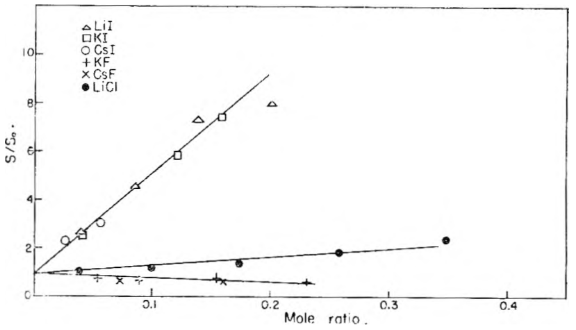

Fig. 10.—The effect of dissolved ions on the scattering per molecule, relative to pure H_2O, in the bending region.

The empirical conclusions are clear and striking. Both stretching and bending vibrations are affected in a parallel way. The F^- ions decrease the scattering intensity slightly, as did OH^- in Busing's work. The other halide ions increase the scattering intensity per water molecule. In the case of a saturated LiI solution, the scattering per water molecule is eight times greater in the bending region and 60% greater in the stretching region than in pure H_2O. Even more striking is the fact that within experimental error there is no cation effect whatever, the results for Li^+ and Cs^+ being substantially identical at equal concentrations. The data of Figs. 9 and 10 can be fitted to the equation

$$S/S_0 = 1 + ar \qquad (7)$$

where r is the mole ratio and a is the slope of the line. The values for the various anions are

	Bending	Stretching
I^-	39	2.8
(Ref. 1) Br^-	*ca.* 27	*ca.* 3.4
Cl^-	3.5	0.6
F^-	−1.9	−1.0

Actually the effects must be even bigger than these numbers suggest. If we divide all water molecules into "affected" and "unaffected" molecules, with N_a and N_u being the number of each, and designate the scattering per molecule of each kind by S_a and S_0, the observed average scattering per molecule would be

$$S = \frac{N_uS_0 + N_aS_a}{N_a + N_u} \tag{8}$$

If each dissolved anion "affects" n water molecules, $N_a = nN_d$, where N_d is the number of dissolved molecules, and eq. 8 becomes, in terms of the mole ratio $N_d/(N_a + N_u) = r$, after inserting eq. 7

$$S_a/S_0 = a/n + 1 \tag{9}$$

Hence the relative scattering per affected molecule (S_a/S_0) if $n = 4$ is

	Bend	Stretch
I^-	10.9	1.7
(Ref. 1) Br^-	7.8	1.8
Cl^-	1.9	1.1
F^-	0.5	0.7

or for $n = 6$

	Bend	Stretch
I^-	7.6	1.4
(Ref. 1) Br^-	5.5	1.5
Cl^-	1.6	1.1
F^-	0.7	0.8

The large effect of I^- might be caused either by the large changes in the scattering per molecule suggested in the previous tables or by a large increase in the number of molecules affected. If we assume that $n = 4$ for Cl^-, then if the specific effect of I^- were to be the same as for Cl^-, the number of affected water molecules per I^- ion would have to be 20.

We have not yet been able to account for these effects quantitatively. However, the effect of the anions can be put into reasonable qualitative perspective. On both theoretical and empirical grounds the intensity of Raman scattering decreases as the polarity of a bond increases. In our case the reference scattering, S_0, is that of pure water with OH...O hydrogen bonds. If the hydrogen bond to F^- is stronger than that in pure water, the OH...F^- bonds would be more highly polarized than those in pure water and the scattering intensity correspondingly reduced. On the other hand, all of the other halide ions are larger than a water molecule so that the O–H...X^- bonds must be longer than in water, hence weaker and less polarized. This would lead to an intensity enhancement in the observed order. However, since the range in ionic radius is only from 1.36 (F^-) to 2.16 Å. (I^-) this does not seem sufficient to account for a range in scattering power from 0.53 (F^-, $n = 4$) to 7.6 (I^-, $n = 6$) although it might be sufficient to account for the range in the stretching intensities of 0.73 (F^-, $n = 4$) to 1.4 (I^-, $n = 6$).

Another factor which must come into play, though, is that whereas F^- can replace H_2O in the water structure, the other halide ions become increasingly too large and must necessarily distort the water structure in their vicinity. Thus, with I^- for example, not only is the O–H...I^- bond weaker but a number of O–H...O bonds in the vicinity of the ion also must be loosened, thereby contributing further to the total effect.

As for the absence of a cation effect, we have no explanation whatever. Certainly a small ion like Li^+ (radius = 0.60 Å.) must interact strongly with the water dipole, presumably with the lone pairs of the oxygen. The apparent conclusion, then, is that the interaction of the positive ion with the oxygen produces no detectable polarization of the OH bonds in comparison with the effect of the negative ions. It may be that since all of our solutions were concentrated, the ions existed as pairs or clusters in which the relatively smaller positive ions were shielded. However, in concentrated solutions of $EuCl_3$, Brady found an ordered sheath of H_2O around the Eu^{3+} with Cl^- ions also incorporated in the second layer in ordered fashion.[10]

In summary, then, the solution of halogen ions strongly affects the intensity of Raman scattering from water molecules, approximately inversely to the strength of the O–H...X^- bonds, with an additional contribution due to the breakdown of the local water structure about the larger ions. On the other hand, in going from Li^+ to K^+ or Cs^+ there appears to be no effect whatever and for this we have no present explanation. Finally, it should be noted that we have found no evidence whatever for the presence of more than one kind of water molecule in either pure water or the solutions.

Acknowledgment.—We should like to acknowledge the assistance of Dr. W. R. Busing who performed the least squares analysis, assisted us with the instrument and engaged in many stimulating discussions. We should also like to acknowledge the support of the Office of Naval Research.

---

[10] C. W. Brady, *J. Chem. Phys.*, **33**, 1079 (1960).

LOW PRESSURE, FAST FLOW PYROLYSIS OF METHYLAMINES

BY G. W. MEADOWS AND J. J. KIRKLAND

Industrial and Biochemicals Department, E. I. du Pont de Nemours & Co., Inc., Wilmington, Delaware

Received May 15, 1961

The pyrolysis of monomethylamine under conditions of low pressure, short contact time and rapid quenching produced relatively high yields of hexahydro-1,3,5-trimethyl-s-triazine and N-methylglycinonitrile, and smaller quantities of glycinonitrile. A solid, believed to be a poly-N-2-(methylene methylimino)-acetamidine, was recovered from the quenching surface. Under similar pyrolysis conditions, dimethylamine and trimethylamine gave the same liquid products, plus N,N-dimethylglycinonitrile, the principal product in the case of dimethylamine. It is suggested that methyleneimine, N-methylmethyleneimine, and hydrogen cyanide, which are formed in the pyrolysis zone, undergo addition reactions on condensation to give the observed products.

Introduction

Previous studies of the thermal decomposition of methylamines have shown that a wide variety of products may be formed, depending on the pyrolysis conditions. These materials range from gases, such as hydrogen cyanide, ammonia, hydrogen and various hydrocarbons[1-4] to complex unidentified oils and solids.[5,6] Reaction mechanisms have been proposed in which methyleneimine and N-methylmethyleneimine are postulated as intermediate products, which may either decompose further or polymerize.[5,6] The transient formation of N-methylmethyleneimine has been suggested to account for products obtained from the pyrolysis of ethylamine,[7] the photolysis of di- and trimethylamine[8] and the decomposition of dimethylamine by high frequency electric discharge.[9] Methyleneimine was believed to be produced in the thermal decomposition of dimethylazide.[10] On the other hand, a free radical mechanism, which does not involve imine intermediates, has been advanced to explain the occurrence of methylhydrazines in the products obtained by cracking dimethylamine.[11]

A study of the pyrolysis of the methylamines was undertaken in order to identify the complex oils and solids previously reported. Pyrolysis conditions giving rise to optimum yields of these materials were investigated.

Experimental

Materials.—The methylamines used were commercial cylinder gases and samples analyzed by gas chromatography were found to contain only small amounts (less than 2%) of air and other amines. Removal of these impurities by repeated vacuum distillation, in the case of methylamine, did not result in any difference in behavior on pyrolysis compared with gas taken directly from a cylinder.

Apparatus.—The pyrolysis chamber was a 25-mm. "Vycor" tube, heated by a resistance furnace, the temperature inside the pyrolysis tube being measured with a thermocouple which could be positioned along the axis of the tube by sliding it inside a "Vycor" sleeve. A steady supply of amine was obtained by passing cylinder gas into a five-liter buffer bulb, and regulating the flow from this bulb to the furnace by means of a needle valve. The pressure in the reaction zone was measured with a mercury manometer, and flow rates were determined by means of a calibrated rotameter.

An ice-cooled finger was situated two inches from the end of the pyrolysis chamber, and gases impinged on this finger 1–2 msec. after leaving the hot zone. The resulting quenched gases then passed through Dry Ice and liquid nitrogen traps, and the uncondensed products, mainly hydrogen and methane, were pumped from the system. In order to achieve high flow rates and maintain low pressures in the furnace, there were no valves in the trapping system. Five hundred-ml. traps were used so that large amounts of condensate could be collected without restricting the rate of removal of gaseous products.

Procedure.—The apparatus was evacuated to 10^{-2} mm. pressure, and the furnace was brought to temperature. The temperature of the pyrolysis tube was checked at 2″ intervals along the tube, and the power input was adjusted to keep the temperature constant to ±4° over a 9 to 10″ hot zone. The refrigerants were applied to the quenching finger and the receiving traps, and the amine then was admitted to the pyrolysis chamber at the desired flow rate. The pressure was established by adjusting a valve in the line, through which noncondensable products were removed.

At the end of a run the amine was shut off and the apparatus was filled with nitrogen. The refrigerated traps then were disconnected, stoppered and transferred to a distillation apparatus. After pumping out the nitrogen, the traps were warmed to about 25° and the volatile products were distilled into a liquid nitrogen-cooled trap. The condensate was re-evaporated into a calibrated volume, and the total amount of gaseous condensable products and undecomposed amine was measured.

The gaseous fraction was analyzed by gas chromatography and components of the gas were identified by infrared spectrophotometric analysis and by peak retention times.

The liquid products, which remained in the traps after distilling off the volatile fraction, also were qualitatively analyzed by gas chromatography. A column of 25% (by weight) "Carbowax" 400, suspended on sodium hydroxide-treated, 80/100 mesh "Celite" 545, was used at a temperature of 125° and a helium carrier gas flow rate of 50 cc. per minute.

In addition to the gaseous and liquid products, a solid deposit was collected on the quenching finger. This was removed from the finger as a flexible, transparent film, and was characterized by chemical and infrared analysis.

Results

Monomethylamine.—The volatile fraction consisted of ammonia and monomethylamine. The composition of the gas was calculated using gas chromatography peak area calibrations, and this was checked by measuring the average molecular weight of the mixed gases. No monomethylamine was found in the gaseous fraction recovered from the pyrolysis at 1100°, and infrared analysis of this gas showed hydrogen cyanide and ammonia were the major constituents. Gas chromatographic analysis showed only ammonia to be present, since hydrogen cyanide was not eluted from the alkaline column. Calculations from peak area indicated

---

(1) M. A. Muller, *Bull. soc. chim.*, **45**, 439 (1886).

(2) L. J. Jolley, *J. Chem. Soc.*, 1957 (1934).

(3) H. J. Emeleus and L. J. Jolley, *ibid.*, 929 (1935).

(4) M. W. Travers, *Trans. Faraday Soc.*, **33**, 1342 (1937).

(5) J. Romney, *Ber.*, **11**, 835 (1878).

(6) A. G. Carter, P. A. Bosanquet, C. G. Silcocks, M. W. Travers and A. F. Wilshire, *J. Chem. Soc.*, 495 (1939).

(7) C. D. Hurd and F. L. Carnahan, *J. Am. Chem. Soc.*, **52**, 4151 (1930).

(8) C. H. Bamford, *J. Chem. Soc.*, 17 (1939).

(9) F. O. Rice and C. J. Grelecki, *J. Am. Chem. Soc.*, **61**, 824 (1957).

(10) F. O. Rice and C. J. Grelecki, *ibid.*, **61**, 830 (1957).

(11) H. A. Taylor, *J. Phys. Chem.*, **36**, 1960 (1932).

Table I

Pyrolysis of Methylamine

Run no.	Temp.,[a] °C.	Press., mm.	Contact time sec.	% Amine dec.	Mole ratio NH_3/CH_3NH_2 dec.	Liquid products recovered, % wt. of CH_3NH_2 dec. Total	Trap A (Dry Ice)	Trap B (liquid N_2)
1	860	5.0	0.28	54	0.302	52	..	..
2	900	5.0	.27	83	.228	49	..	..
3	945	2.5	.20	80	.319	40	..	..
4	960	2.0	.09	68	.345	56	..	..
5	945	1.5–2.0	.017	25	.325	75	20	55
6	1005	1.0	.011	62	.445	62	28	34
7	1000	1.0	.011	55	.405	55	30	25
8[b]	1000	1.0	.011	..	...	57	33	24
9	995	2.0	.022	70	...	58	45	13[c]
10	1015	2.0–2.5	.027	>80	...	77	74[d]	3[d]
11	1050	1.5	.016	71	.310	68	58	10
12	1055	1.5	.016	87	.375	63	56	7
13	1100	3.0	.049	100	.039	[e]	..	..

[a] Temperature variation along pyrolysis tube ±4°. [b] Long duration pyrolysis to prepare 30–40 g. of liquid products. [c] Pale brown liquid collected in trap B. [d] Dark brown liquid in both traps. [e] Dark viscous liquid collected in trap A amounted to only 5% of the amine decomposed. Non-volatile brown liquid accumulated between furnace and trap A. The gaseous fraction was found to be mainly HCN.

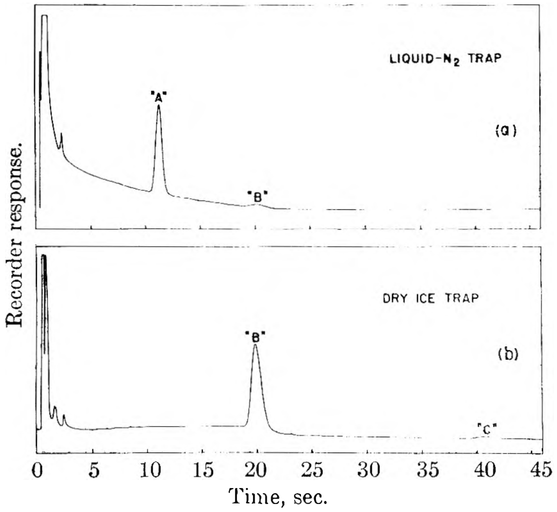

Fig. 1.—Gas chromatographic separation of liquids from monomethylamine pyrolysis: "A"—hexahydro-1,3,5-trimethyl-s-triazine; "B"—N-methylglycinonitrile; "C"—glycinonitrile.

that the gas contained 14 mole % ammonia. The total amount of hydrogen cyanide recovered corresponded to 29.4 mole % of the amine pyrolyzed, and this high conversion coincided with a large decrease in the yield of non-volatile products.

The extent of amine decomposition over a range of conditions studied and the amounts of ammonia and non-volatile pyrolysis products recovered are summarized in Table I. It was found that non-volatile products were best obtained at furnace temperatures of 1000–1050°, contact times of 0.01 to 0.02 second and pressures below 2 mm.

Gas chromatographic analysis of the contents of the liquid nitrogen and Dry Ice traps showed peaks corresponding to the volatile constituents identified previously, together with other components having longer retention times (Figs. 1a and 1b). Highly purified samples of these components were obtained by low pressure distillation, followed by preparative-scale gas chromatography,[12] using a 6-foot, 31-mm. i.d. column of "Carbowax" 400 supported on sodium hydroxide-treated "Celite" 545, and operated at a temperature of 125° with a helium carrier gas flow of 2.8 liters per minute.

The purified materials were identified as hexahydro-1,3,5-trimethyl-s-triazine, N-methylglycinonitrile and glycinonitrile (Table II). The triazine was obtained mainly from the fraction condensed in the liquid nitrogen trap and aminonitriles from the Dry Ice trap. A sample of hexahydro-1,3,5-trimethyl-s-triazine was prepared from formaldehyde and methylamine, and the infrared absorption curve was identical with that of the purified component from the pyrolysis of methylamine. Hydrolysis of the N-methylglycinonitrile fraction with barium hydroxide, followed by acidification with carbon dioxide,[13] yielded a crystalline product which was identified as sarcosine by infrared analysis.

Solid Products.—In addition to the gaseous and liquid products obtained from the pyrolysis of monomethylamine, a solid product was formed. This material was removed from the quenching finger as a clear flexible film. It was slightly hygroscopic when first exposed to air, but quickly lost this characteristic on standing in contact with the atmosphere. Under the conditions used to obtain the liquid products in good yield, the solid material produced amounted to less than 1% by weight of the amine decomposed. It was found that somewhat higher pressure and lower temperature favored the formation of this product, and also that the yield was dependent on the flow rate and quenching temperature. Figure 2 shows the relationship between the amount of solid polymer formed and contact time and furnace temperature. The yields are expressed as the percentage by weight of the amine decomposed.

Elementary analyses on several films are given in Table III. In all cases, the films were exposed to air, at least overnight, before analysis. The analyses are consistent with an empirical formula C_4H_8-

---

(12) J. J. Kirkland, in V. J. Coates, *et al.*, eds., "Gas Chromatography," Academic Press, New York, N. Y., 1958, pp. 203–222.

(13) J. H. Ford, "Organic Syntheses," Coll. Vol. III, John Wiley and Sons, Inc., New York, N. Y., 1955, p. 34.

TABLE II

Analysis or determination	Hexahydro-1,3,5-trimethyl-s-triazine, $C_6H_{15}N_3$ Theory or reported	Hexahydro-1,3,5-trimethyl-s-triazine, $C_6H_{15}N_3$ Found	N-methylglycinonitrile $C_3H_6N_2$ Theory or reported	N-methylglycinonitrile $C_3H_6N_2$ Found	Glycinonitrile $C_2H_4N_2$ Theory or reported	Glycinonitrile $C_2H_4N_2$ Found	N,N′-Dimethylglycinonitrile $C_4H_8N_2$ Theory or reported	N,N′-Dimethylglycinonitrile $C_4H_8N_2$ Found
Carbon, %	55.8	56.3, 56.1	51.4	51.6	42.8	43.5, 43.8	57.2	57.4, 57.4
Hydrogen, %	11.9	11.8, 11.6	8.6	8.7	7.2	7.4, 7.3	9.5	9.7, 9.8
Nitrogen, % (Dumas)	32.5	32.5, 32.0	40.0	39.2, 39.3[d]	50.0	45.1, 45.2	33.3	33.4, 33.1
Neut. equiv.[a]	43.0	43.8	70	70, 73, 72	56	61	84	85
Mol. wt.[b]	129	126, 131	70	71, 73	56	58, 69	84	82, 94
B.p., ° C.	162.5	162	...	....	....	....	137–138	137.5
Derivative, m.p., ° C.	96[c]	101.5–102.5	...	....	164–166.5[e] (with dec.)	165 (with dec.)	...	...
Refractive index	...	...	n^{19}D 1.4604–1.4632	n^{25}D 1.4604				

[a] Titration with 0.1 *N* perchloric acid in glacial acetic acid. [b] Cryoscopic method, benzene solvent. [c] Reaction with CS_2 to form $C_6H_{10}N_2S_2$, M. Delépine, *Bull. soc. chim. France*, [3] 15, 89 (1896). [d] Sealed tube Kjeldahl method. [e] Reaction with picric acid in alcohol to form picrate salt.

$N_{3-x}O_x$, assuming that oxygen constitutes the balance of material.

TABLE III

ANALYTICAL INFORMATION ON SOLID POLYAMINE

Sample	%, C	%, H	%, N	% C,H,N	Elemental formula[a]
1	48.89	8.08	35.39	92.36	$C_{4.1}H_{8.1}N_{2.5}O_{0.5}$
2	46.92	7.95	38.55	93.62	$C_{3.9}H_{8.0}N_{2.7}O_{0.4}$
3	50.50	7.90	39.26	97.66	$C_{4.2}H_{7.9}N_{2.8}O_{0.2}$
4	50.07	7.76	37.14	94.97	$C_{4.2}H_{7.8}N_{2.7}O_{0.3}$
5	49.06	8.42	35.49	92.97	$C_{4.1}H_{8.4}N_{2.6}O_{0.4}$
6	47.87	7.79	41.65	97.31	$C_{4.0}H_{7.8}N_{3.0}O_{0.2}$

[a] Assuming material not accounted for in analysis is oxygen.

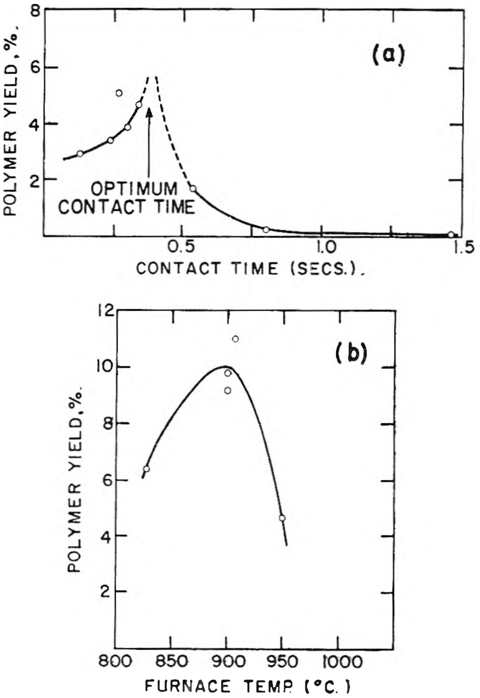

Fig. 2.—Relationship between polymer yield and (a) contact time at 950° and 5 mm. pressure; (b) pyrolysis temperature at 0.3 and 0.35 sec. contact time and 5 mm. pressure.

Additional information on the composition of the solid pyrolysis product was obtained by infrared studies using a Perkin–Elmer Model 21 infrared spectrophotometer with a sodium chloride prism. A spectrum was run first on a freshly prepared film and re-run on the same sample after aging under various conditions. The original spectrum showed close similarities with the curves for N-methylglycinonitrile and glycinonitrile. Absorptions characteristic of bonded N–H (3.05 μ); C–H stretching (3.55 μ); C–H deformation (6.85 and 7.35 μ) and rather weak $C{\equiv}N$) (4.48 and 4.55 μ) were noted. In addition, a band at 6.12 μ suggested N–H deformation absorption. Exposure to the atmosphere produced a decrease in the absorption intensity due to bonded N–H and $C{\equiv}N$ and a slight decrease in C–H, which showed up in the weakest band at 6.85 μ. The increased absorption at 5.95 μ was probably due to the formation of C=O, possibly as part of an amide group. The absorption intensity at 6.12 μ remained unchanged, and two new unidentified peaks appeared at 12.26 and 14.90 μ. The absorption spectra obtained after a further period of 11 days, during which the film was stored in a desiccator, showed essentially no change. However, after again exposing the film to the atmosphere for 32 days, changes in absorption intensity were evident at the same wave lengths previously noted. The stronger C–H absorptions at 3.55 and 7.35 μ also showed slight decreases in intensity after prolonged exposure to the atmosphere.

On the basis of the above observations, it was concluded that the solid product was a basic polymer containing $>NH$; $>C{=}NH$; $>C{=}NR$ and –CN groups, the imine and nitrile groups being susceptible to hydrolysis in the presence of moisture, as shown below

$$>C{=}NH + H_2O \longrightarrow >C{=}O + NH_3 \qquad (1)$$

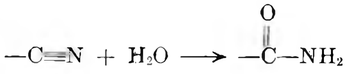

$$-C{\equiv}N + H_2O \longrightarrow -\overset{\overset{\displaystyle O}{\|}}{C}-NH_2 \qquad (2)$$

It is suggested that the film is a polymer, consisting of a polyamine chain with methyl and imine substituents and an empirical formula $(C_4H_9N_3)_x$.

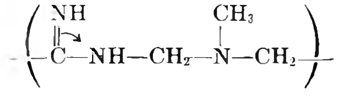

$$\left(-\overset{\overset{\displaystyle NH}{\|}}{C}-NH-CH_2-\overset{\overset{\displaystyle CH_3}{|}}{N}-CH_2-\right)$$

TABLE IV

PYROLYSIS OF DIMETHYLAMINE AND TRIMETHYLAMINE

Run no.	Temp.,[a] °C.	Press., mm.	Contact time, sec.	% Amine dec.	Mole ratio NH$_3$/Amine dec.	Mole ratio C$_2$H$_4$/Amine dec.	Liquid products recovered, % wt. of Amine decomp. Total	Trap A (Dry Ice)	Trap B (liq. N$_2$)
				Dimethylamine					
1	800	5.0	0.30	85	0.281	0.024	45	16	29
2	855	2.0	.030	93	.244	.075	63	35	28
3[b]	850	2.0	.030	90		...	64	36	28
4	945	3.0	.46	100	.225	...	[c]	..	..
				Trimethylamine					
1	770	1.0	.016	<10	...	...	..	..	..
2	795	3.0	.045	84	.015	.158[d]	35	9	26
3[b]	790	3.0	.045	80	...	...	46	16	30
4	850	4.0	.057	98	.017	.268[d]	34	22	12
5	955	3.0	.39	100	< .01	.765[d]	[c]	..	..

[a] Temperature variation along pyrolysis tube ±4°. [b] Long duration pyrolyses to prepare 60–70 g. of liquid products. [c] Black viscous liquid collected in trap A. [d] Traces of acetylene also found in gaseous fraction.

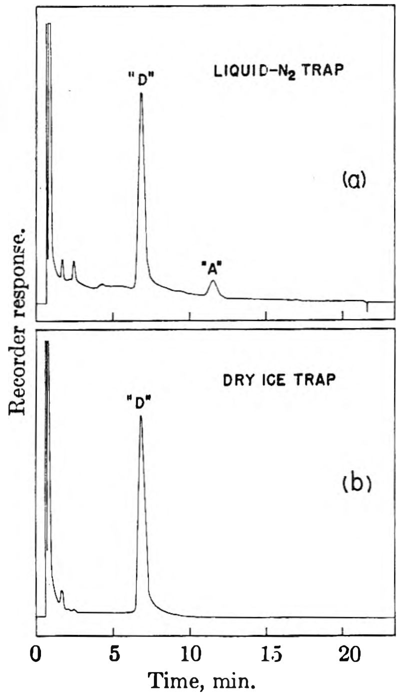

Fig. 3.—Gas chromatographic separation of liquids from dimethylamine pyrolysis: "A"—hexahydro-1,3,5-trimethyl-s-triazine; "D"—N,N-dimethylglycinonitrile.

Dimethylamine and Trimethylamine.—A more limited study of the pyrolysis of dimethylamine and trimethylamine was made using the low pressure, fast flow technique employed in the case of monomethylamine. The volatile and liquid products were separated and identified, using the same procedure.

The amine conversion and the amounts of gaseous and liquid products obtained are summarized in Table IV. It was found that in order to avoid the formation of hydrogen cyanide and the production of black viscous tarry products, it was necessary to use progressively milder conditions, with increasing methyl substitution on the amine nitrogen.

Infrared and gas chromatographic analyses of the condensed gaseous products showed that slightly less ammonia was obtained from dimethylamine and much less from trimethylamine. Traces of ethylene also were obtained from the dimethylamine pyrolysis and in the case of trimethylamine ethylene was a major component of the volatile fraction, with a small amount of acetylene also being evident.

Gas chromatographic analysis of the condensed products from the dimethylamine pyrolysis showed the presence of a new and major component in addition to the triazine obtained from monomethylamine (Figs. 3a and 3b). This material was isolated and purified as previously described, and identified as N,N-dimethylglycinonitrile (Table II). The characterization was confirmed by infrared analysis.

All four of the compounds obtained from the cracking of monomethylamine and dimethylamine were found in the pyrolysis products of trimethylamine (Figs. 4a and 4b). The major pyrolysis product found in the liquid nitrogen trap was hexahydro-1,3,5-trimethyl-s-triazine, with much smaller quantities of N,N-dimethylglycinonitrile and N-methylglycinonitrile in evidence (Fig. 4a). The Dry Ice trap contents were composed mainly of N-methylglycinonitrile, with smaller amounts of N,N-dimethylglycinonitrile and glycinonitrile also present (Fig. 4b).

Solid Product.—The basic polymer which collected on the quenching finger as a transparent flexible film in the pyrolysis of monomethylamine also was obtained from dimethylamine; however, this product was not recovered from the pyrolysis of trimethylamine.

Infrared analysis of films prepared from dimethylamine showed them to be practically identical with those obtained from monomethylamine, the only difference being a weak band at 6.00 μ, most probably due to olefinic unsaturation. The close similarity with the absorption spectrum of the monomethylamine product implies that the structure is essentially the same, with an olefinic substituent present at a few sites along the polymer chain.

Discussion

Methyleneimine and N-methylmethyleneimine have been postulated as intermediates in the exhaustive cracking of monomethylamine

$$NH{=}CH_2 \longrightarrow HCN + H_2$$
$$CH_3N{=}CH_2 \longrightarrow HCN + CH_4$$
$$NH{=}CH_2 + CH_3NH_2 \longrightarrow HCN + CH_4 + NH_3$$

It is suggested that the products obtained in this work are formed when the active species leaving the pyrolysis zone are rapidly quenched and condensed

(A) $CH_3N{=}CH_2 \longrightarrow (CH_3N{-}CH_2)_3$

(B) $CH_3N{=}CH_2 + HCN \longrightarrow CH_3NHCH_2CN$

(C) $NH{=}CH_2 + HCN \longrightarrow NH_2CH_2CN$

(D) $HCN + NH{=}CH_2 + CH_3N{=}CH_2 \longrightarrow$

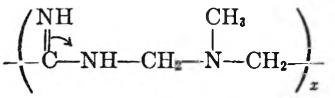

$$-\left(\overset{NH}{\overset{\|}{C}}{-}NH{-}CH_2{-}\overset{CH_3}{\overset{|}{N}}{-}CH_2{-}\right)_x$$

These reactions indicate that the relative proportions of the various products will depend upon the amounts of hydrogen cyanide and imines formed in the pyrolysis zone. Decomposition of the imines, giving hydrogen cyanide, ammonia and gaseous hydrocarbons is minimized at the lowest temperatures and shortest contact times. These conditions favor the production of cyclic triazine and solid polymer. Only small amounts of N-methylglycinonitrile and glycinonitrile are formed. As the conditions are made more severe, the solid polymer and the cyclic triazine yields decrease, with a corresponding increase in the amount of N-methylglycinonitrile. This is due to the formation of more HCN, which results in a greater opportunity for the production of the aminonitrile by reaction B. Since neither glycinonitrile nor the solid polymer are formed as the temperature and contact time are increased, it is concluded that methyleneimine is decomposed more readily to hydrogen cyanide than is N-methylmethyleneimine. Under the most extreme conditions, both imines decompose completely to gaseous products and black tars.

The imine intermediates also appear to be produced from dimethylamine and trimethylamine, since the same products were obtained as in the monomethylamine pyrolysis.

The greater complexity of the secondary and tertiary amines also results in other side reactions. Increasing amounts of unsaturated hydrocarbons and less ammonia were obtained in the sequence mono-, di- and trimethylamine. Thus the conditions which give rise to the polyamines and aminonitriles are progressively milder, and the optimum yields of liquid products are less the more complex the amine, as shown in Table V.

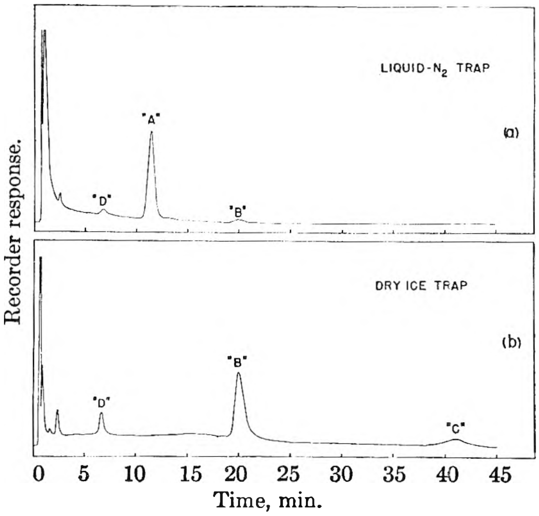

Fig. 4.—Gas chromatographic separation of liquids from trimethylamine pyrolysis: "A"—hexahydro-1,3,5-trimethylglycinonitrile; "C"—glycinonitrile; "D"—N,N-dimethylglycinonitrile.

TABLE V

OPTIMUM CONDITIONS FOR 80–90% CONVERSION OF AMINES WITHOUT PRODUCING HYDROGEN CYANIDE

Amine	Temp., °C.	Press., mm.	Contact time, sec.	% Yield liquid products
Monomethyl-	1000–1050	1.5–2	0.1–0.02	50–70
Dimethyl-	800– 860	2–5	*ca.* 0.03	45–65
Trimethyl-	800– 850	3–4	0.04–0.06	35–45

The formation of N,N-dimethylglycinonitrile, from both dimethylamine and trimethylamine, cannot be explained by addition reactions between the various intermediates described above. Since N,N-dimethylglycinonitrile was not obtained from monomethylamine, its formation must be related to the presence of two methyl groups on the original amine nitrogen. The only analogous process producing this compound would be an addition reaction between acetonitrile and N-methylmethyleneimine.

$$CH_3N{=}CH_2 + CH_3CN \longrightarrow (CH_3)_2N{-}CH_2CN$$

While acetonitrile was not observed in any of the gas chromatographic analyses, it was detected by mass spectrometric analysis in a sample of the volatile components recovered from one pyrolysis.

THE PHOTOLYSIS OF TRAPPED FREE RADICALS PRODUCED BY IONIZING RADIATION[1]

By RUSSELL H. JOHNSEN

Department of Chemistry, Florida State University, Tallahassee, Florida

Received May 20, 1961

A study of the changes in yields resulting from the subsequent exposure of γ-irradiated alcohols to ultraviolet and visible light at $-190°$ is reported. It is presumed that trapped free radicals are being photolyzed by this treatment. The chemical consequences thereof can be correlated with previously reported changes in e.s.r. spectra of γ-irradiated alcohols brought about by illumination with ultraviolet light. The study thus provides additional evidence as to the structure of the trapped radicals.

Introduction

The radiation chemistry of the lower aliphatic alcohols has been studied in a number of laboratories. An extensive survey of the stable chemical products resulting from the He^{++} bombardment of liquid alcohols was conducted by McDonnell and Newton.[2] The most studied of the series, methanol, has been further investigated by Burton,[3] Lichtin,[4] and Baxendale.[5] Ethanol and deuterioethanol have been investigated by Burr,[6] as well as by the previously mentioned groups.

A number of studies of the lower alcohols irradiated in the solid state have been made using the techniques of electron spin resonance.[7] The e.s.r. spectra of alcohol free radicals produced by the abstraction reaction of OH radicals from photolyzed H_2O_2 also have been studied by Symons, *et al.*[8]

No information on the chemical effects of irradiation in the solid state has been reported nor has there been any extensive attempt to correlate the e.s.r. data with the information available for the liquid state irradiation in the synthesis of an over-all mechanism for the decomposition of this class of compounds.

The optical absorption spectra of samples irradiated at low temperatures as well as those produced by photochemically generated $OH\cdot$ radicals have been determined. The influence of photolyzing on the two principal absorption regions as well as on the e.s.r. spectrum has been discussed.[7]

In a recent communication[9] we reported that this type of photolysis has a sometimes dramatic effect on the over-all radiation chemistry of ethanol. In this paper extension of this technique to a number of other systems is reported. Included are studies on methanol, ethanol and 1-propanol.

The lower alcohols, upon γ- or X-irradiation in the solid state at 77°K. give relatively simple paramagnetic resonance spectra. Methanol yields a three-line, ethanol and 1-propanol each a five-line spectrum. These have been ascribed to species resulting from the removal of a hydrogen adjacent to the hydroxyl group: ($\dot{C}H_2OH$, $CH_3\dot{C}HOH$, $CH_3CH_2\dot{C}HOH$). The free H-atom is not detected under these conditions. These formulations are also consistent with the formation of the corresponding glycols which are among the chief products observed in radiolyses in the liquid state.

It has been suggested by Livingston, *et al.*,[10] that the absorption in the visible region (5,000 Å.) is associated with a paramagnetic precursor to the alcohol radical ($R\dot{C}HOH$), which in turn is possibly responsible for the absorption observed in the ultraviolet region. When γ-irradiated samples are exposed to visible light the colored species disappear. When bleaching is carried out with ultraviolet light the paramagnetism disappears or the e.s.r. spectrum is altered, depending upon the wave lengths employed and the alcohol under investigation. It is these effects, in terms of the resulting stable products, that we have set out to investigate in this research.

We also have found, in addition to these photolytic effects, that change of state alone has some consequences worthy of comment.

Experimental

A. **Materials and Purification.**—The alcohols used in these studies were reagent grade and were further purified by a variety of techniques peculiar to those impurities detected by vapor phase chromatography. In each case the materials finally used were shown to be homogeneous by vapor chromatographic standards. The methanol used was purified by repeated fractional distillation, dried over calcium oxide and subjected to a final fractional distillation in which material boiling over a range of 0.5° was collected. This material was stored in a vacuum line and subjected to two bulb-to-bulb distillations before being used. The ethanol was treated in a similar manner, in addition to which it first was treated with silver oxide to remove aldehydic impurities. 1-Propanol was purified in a manner similar to that described for methanol.

B. **Irradiation Procedures.**—For those samples upon which analyses of the gaseous products were to be performed a 275 curie Cobalt-60 source was used. Samples were sealed in Pyrex ampoules following degassing and irradiated in a dewar flask under liquid nitrogen when appropriate. The dose rate as determined by the Fricke dosimeter was approximately 1.80×10^{17} e.v./g./min. A $G(Fe^{+++})$ of 15.5 was employed and energy absorbed in the samples was corrected for differences in electron density. Total doses are recorded with the analytical results.

In order to analyze for liquid products a much higher total dose was required and for these irradiations X-rays from a 3 mev. Van de Graaff accelerator were employed. Dose rates under the conditions employed were of the order of 2.5×10^{18} e.v./g./min. The formate dosimeter of Hardwick[11] was employed in these irradiations and dosimeter

---

[1] This work was supported in part by the U. S. Atomic Energy Commission under contract AT-(40-1)-2001.

[2] W. McDonnell and A. S. Newton, *J. Am. Chem. Soc.*, **76**, 4651 (1954).

[3] G. Meshitsuka and M. Burton, *Radiation Research*, **8**, 285 (1958).

[4] N. Lichtin, *J. Phys. Chem.*, **63**, 1449 (1959).

[5] J. Baxendale, *J. Am. Chem. Soc.*, **80**, 4125 (1958).

[6] J. G. Burr, *ibid.*, **79**, 751 (1957).

[7] R. S. Alger, T. H. Anderson and L. A. Webb, *J. Chem. Phys.*, **30**, 695 (1959).

[8] M. C. R. Symons and M. Townsend, *ibid.*, **25**, 1299 (1956).

[9] R. H. Johnsen, *J. Phys. Chem.*, **63**, 2088 (1959).

[10] H. Zeldes and R. Livingston, *J. Chem. Phys.*, **30**, 40 (1959).

[11] T. Hardwick and U. S. Guenter, *J. Phys. Chem.*, **63**, 896 (1959).

solution and alcohols were irradiated simultaneously to provide a continuous monitoring of samples and also to provide a dosimetry check on each run since it was found that machine settings could not be reproduced with complete reliability from run to run.

Irradiation was carried out in either 8-mm. Pyrex ampoules or 6-mm. Vycor ampoules. Approximately 5 ml. of sample was employed in each run, and each sample was run in triplicate.

C. **Photolysis Procedures.**—Photolyses at liquid nitrogen temperatures were carried out in unsilvered quartz dewars upon which a stream of air was directed to prevent condensation. Bleaching in the ultraviolet region was accomplished using a 1 kw. AH-6 high pressure mercury arc lamp with a quartz jacket and a quartz-windowed water filter. Ultraviolet photolyses were carried out in both Pyrex and Vycor ampoules, as noted in the section on results.

D. **Analytical Procedures.** (i) **Gaseous Products.**—A modified Saunders–Taylor[12] procedure was employed for the gaseous products volatile at liquid nitrogen temperature, those gases volatile at −78° but not at −196° were analyzed by means of vapor phase chromatography using a silica gel column with helium carrier gas.

(ii) **Liquid Products.**—The vicinal glycols were analyzed by the usual periodic acid oxidation method.[2] Other liquid products were determined by vapor fractometry using a Perkin–Elmer Column "F" calibrated quantitatively for the various products determined.

Results

In Tables I, II and III are recorded the yields of gaseous products for the three alcohols investigated. Results are reported for irradiations carried out at room temperature, on solid samples at −196° which were allowed to thaw in the dark, and on solid samples which were bleached before thawing. In addition, the effect of allowing the solid samples to anneal at −190° in the dark before bleaching is reported. In Table IV are the results of analyses for certain liquid products resulting from the radiolysis of each of these three alcohols. In all cases yields are calculated on the basis of ionizing radiation absorbed only.

TABLE I

GASEOUS RADIOLYTIC PRODUCTS FROM METHANOL

Conditions of irradiation	100 e.v. yields H_2	CH_4	CO	C_2H_6	Total dose, e.v./g.
Liquid 26°	5.66	0.57	0.45	0.14	1×10^{19}
Solid −190°, warmed in dark	3.60	1.56	0.33	0.10	1×10^{19}
Solid −190°, VSB. bleach	3.64	1.40	0.26	0.85	1×10^{19}
Solid −190°, U.V. bleach	22.60	10.70	6.55	4.00	2.5×10^{18}
Solid −190°, U.V. bleach, annealed −190°	20.00	10.65	6.18	4.05	2.5×10^{18}

TABLE II

GASEOUS RADIOLYTIC PRODUCTS FROM ETHANOL

Conditions of irradiation	100 e.v. yields H_2	CH_4	CO	C_2H_6	C_2H_4	Total dose, e.v./g.
Liquid 26°	5.53	0.80	0.10	0.30	0.27	1×10^{19}
Solid −190°, warmed in dark	4.60	0.30	0.01	0.41	0.35	1×10^{19}
Solid −190°, VSB. bleach	5.87	0.42	0.30	0.28	0.33	1×10^{19}
Solid −190°, U.V. bleach	34.00	12.10	8.85	6.88	1.78	2.5×10^{18}
Solid −190°, bleached U.V., annealed −190°	23.40	8.20	5.60	6.25		2.5×10^{18}

A number of miscellaneous but pertinent observations also were made during these experiments which should be mentioned.

(i) **Total Dose Effect in Liquid Ethanol.**—The measured energy yield $G(H_2)$ was found to be inversely proportional to the total dose absorbed over a dose range of 10^{18} to 10^{22} e.v./g.

(ii) **Effect of Ultraviolet Light on Solid Alcohols.**—When purified alcohols were irradiated with the AH-6 arc at liquid nitrogen temperatures no change was observed in their constitution as measured by v.p.c. analysis.

(iii) **Effect of Ultraviolet Light on Some of the Stable Products of Radiolysis.**—Samples of ethanol were irradiated with γ-rays at −196° and then allowed to melt. After refreezing they were photolyzed in the usual manner. Such samples gave the same results as those allowed to melt without photolysis, *i.e.*, "dark" samples.

Discussion of Results

A. Comparison of Solid State Irradiation with Liquid State.—The data shows considerably more scatter when irradiations are carried out in the solid state rather than in the liquid state. Thus "*G*" values for liquid state radiolyses are reproducible to within ±1%, while for solid state experiments, when no subsequent photolysis was carried out, "*G*" values were reproducible to only ±5%. The values reported in Tables I–IV represent the average of at least three runs for each listed condition. The effect of going to the solid state (and lower temperature) for the gaseous products is in general to lower yields. There are several notable exceptions, however: the yield of methane from methanol is increased by a factor of 3, the yield of hydrogen from propanol is slightly increased and, most interestingly, propane appears as a product from solid propanol while in the liquid state only ethane and ethylene are found. The effect of irradiation in the solid state on the liquid products is in general to decrease the yield of the glycol and increase the yield of the corresponding aldehyde.

The effect of irradiation on a glassy sample compared to a crystalline one relative to the efficiency of caging and therefore the relative importance of recombination reactions has been remarked upon by Willard,[13] Livingston[10] and others. In general glassy conditions seem to lead to a greater extent of radiolytic decomposition. We have made some attempts to produce and radiolyze both states under controlled conditions, especially methanol. These efforts so far have not been successful.

B. The Effect of Bleaching Solid Alcohols. (i) **On the Gaseous Products.**—In general it can be said that rather dramatic effects are observed when the γ-irradiated solid alcohols are bleached with the light of the AH-6 mercury arc lamp. For example; the ratio of hydrogen yield in bleached samples to samples thawed in the dark is 6.6, 7.9, 4.4 for methanol, ethanol and 1-propanol, respectively. The yields of carbon monoxide are also markedly enhanced, from 0.43 to 6.55 in the case of methanol, 0.01 to 8.85 in the case of ethanol and from 0.04 to 4.10 in the propanol case.

In some cases ultraviolet bleaching was followed by a 12 hour period of annealing at −190° before the sample was melted. Under such conditions

---

[12] K. W. Saunders and H. A. Taylor, *J. Chem. Phys.*, **9**, 616 (1941).

[13] T. O. Jones, R. H. Luebbe, Jr., J. R. Wilson and J. E. Willard, *J. Phys. Chem.*, **62**, 9 (1958).

TABLE III

GASEOUS RADIOLYTIC PRODUCTS FROM 1-PROPANOL

Conditions of irradiation	100 e.v. yields							Total dose, e.v./g.
	H_2	CH_4	CO	C_2H_6	C_2H_4	C_3H_8	C_3H_6	
Liquid 26°	4.09	0.10	0.27	0.50	0.12	0	0	1×10^{19}
Solid −190°, warmed in dark	4.42	.04	.12	.12	.09	0.12	0.10	1×10^{18}
Solid −190°, VSB. bleach	4.90	.06	.06	.60				1×10^{18}
Solid −190°, U.V. bleach	19.30	.22	4.10	4.0*	.30*	7.0*	Trace	2.5×10^{18} *2.0×10^{20}
Solid −190°, bleached U.V., annealed −190°	17.30	.86	3.20	4.0*		7.0*	Trace	2.5×10^{18} *2.0×10^{20}

TABLE IV

LIQUID PRODUCTS FROM ALCOHOL RADIOLYSES

Alcohol	Conditions	100 e.v. yields			Dose, e.v./g.
		Glycol	R'CHO	Others	
	Liquid	2.10	1.0	∽0(H_2O)	∽2×10^{20}
Methanol	Dark	1.77	0.8	2.5(H_2O)	
	Bleach	3.5	0	5.5(H_2O)	
				Ether H_2O	
	Liquid	1.95	1.40	0.03 v.s.	∽2×10^{20}
Ethanol	Dark	0.84	2.40	.07 v.s.	
	Bleach	1.38	4.22	.07 2.2	
				Acetone	
	Liquid	1.43	0.72	0.23	∽2×10^{20}
1-Propanol	Dark	1.13	2.19	.36	
	Bleach	1.38	3.41	.82	

it was assumed that any reversibility in the photolytic process would be revealed. Examination of Tables I, II and III shows that indeed there is some evidence of reversibility, yields of decomposition products being generally somewhat diminished by the annealing treatment.

(ii) **On the Liquid Products.**—The effect of ultraviolet bleaching in all cases is to increase the yields of all products over the amounts found in the "dark" radiolyses. In some cases, however, the yields are still not equal to what they were in the liquid state radiolyses. The increased yields of liquid products resulting from bleaching were quite unexpected since it was assumed that the enhanced yields of gaseous decomposition products were the result of the photolysis of the precursors of these liquid products.

(iii) **The Effects of Bleaching with Visible Light.**—The study of the effect of bleaching the solid alcohols with visible light was confined to the gaseous products. Examination of Tables I, II and III reveals that in general exposure to visible light before melting results in a small enhancement of decomposition. This is consistent with the results of Livingston and others who have studied the effect of such bleaching on the e.s.r. spectra.

Conclusions

A number of tentative conclusions concerning the mechanism of the radiolytic decomposition of these alcohols can be made on the basis of the observed behavior of the trapped free radicals under photolysis.

(i) The yields of carbon monoxide from methanol and ethanol which have been photolyzed show excellent correlation with the yields of free radicals estimated by Alger, *et al.*, from e.s.r. measurements.[7] This strongly suggests that the radicals measured by e.s.r. are quantitatively photolyzed to produce carbon monoxide. This is consistent with the suggestion of Voevodsky[14] that the effect of ultraviolet bleaching is to dissociate the methanol radical as

$$CH_3OH \rightsquigarrow \dot{C}H_2OH + H\cdot \qquad (1)$$

$$\dot{C}H_2OH \overset{h\nu}{\rightleftarrows} \dot{C}HO + H_2 \qquad (2)$$

$$\dot{C}HO \rightleftarrows CO + H\cdot \qquad (3)$$

That the bleaching is partially reversible as suggested by Voevodsky is attested to by the lower yields obtained when a period of annealing, prior to melting, follows the bleaching process. The formyl radical seems to be a reasonable postulate in the light of the reported behavior of the e.s.r. spectrum of the methanol radical upon bleaching. The original triplet is transformed by bleaching into a doublet with approximately 134 gauss splitting. A similar doublet (135 gauss splitting) has been reported in irradiated formic acid and was attributed to the $H\dot{C}O$ radical.[15]

Bleaching of γ-irradiated ethanol transforms the e.s.r. quintet into a quartet which can be ascribed to the methyl radical. This is consistent with the following sequence of events which is analogous to that postulated for methanol.

$$CH_3CH_2OH \rightsquigarrow CH_3\dot{C}HOH + H\cdot \qquad (4)$$

$$CH_3\dot{C}HOH \overset{h\nu}{\rightleftarrows} CH_3\cdot + CHOH \qquad (5)$$

$$CHOH \rightleftarrows CO + 2H\cdot \qquad (6)$$

Thus, each radical ultimately gives rise to a molecule of carbon monoxide. Values of G(Radical) from methanol and ethanol have been reported as 7.0 and 9.0, respectively.[7] The yields of carbon monoxide obtained in this work were 6.55 and 8.85 for these two alcohols. G(Radical) has not been reported for the 1-propanol case, but a yield of 4.1 for CO suggests a G(Radical) = 4.0. This, however is not consistent with a "dark" $G(H_2)$ of 4.4 as suggested below.

(ii) The yields of hydrogen obtained in the "dark" experiments in the cases of methanol and ethanol are almost exactly one-half the yields of G(Radical) and/or G(CO). This suggests that at −190° either the hydrogen atoms produced in the primary dissociation (equations 1 and 4) react by recombination, which seems rather unlikely, or the *initial* yield of free radicals is one-half of that observed and each hydrogen atom produces a second radical by abstraction. In the case of 1-

---

(14) V. V. Voevodsky, Abstracts, 4th International Symposium on Free Radical Stabilization, 1959.

(15) W. Gordy, Ard and Shields, *Proc. Natl. Acad. Sci. U. S.*, **41**, 996 (1955).

propanol this simple relationship is not observed, as pointed out above. Two possible explanations for this discrepancy suggest themselves: (a) the primary free radical can undergo two modes of photolysis, only one of which leads to CO or (b) the hydrogen abstraction reactions following initial radical formation produce radicals which are not photolyzable to CO, and it is only the initially produced radicals which lead to this product. The observed yields of aldehyde and glycol from the solid state irradiations suggest that the latter explanation is the correct one.

The greatly enhanced yield of hydrogen observed when the irradiated alcohols are photolyzed is in part explained by the formation of additional glycol and aldehyde as noted below, but a substantial fraction cannot be accounted for in this way. This hydrogen therefore must arise from the photolysis of the free radical that is also responsible for the formation of carbon monoxide as shown in equations 1 through 6. The yield of hydrogen observed can largely be accounted for if one makes the following assumptions. In the case of methanol each $\dot{C}H_2OH$ radical produces one molecule of hydrogen and one free hydrogen atom which reacts by abstraction to produce a second molecule. Thus, assuming that the initially produced H-atom reacts at −196° by abstraction, each $\dot{C}H_2OH$ radical produces 2.0 molecules of additional hydrogen. In the case of ethanol each $CH_3\dot{C}HOH$ radical photolyzed produces two H-atoms by photolysis which react by abstraction for a total of 2.0 additional molecules of hydrogen.

On the basis of these assumptions the calculated value of $G(H_2)$ is 17.50. On photolysis the observed yield of aldehyde and glycol would give rise to an additional 3.5 molecules of hydrogen for 21.0 molecules of H_2 per 100 e.v. The observed value is 23.0. In the case of ethanol 28.0 molecules are predicted and a total of 34.0 are observed.

(iii) In none of the cases so far studied does the observed yield of carbonyl plus glycol (in the absence of bleaching) account for the number of free radicals indicated by e.s.r. or the carbon monoxide produced on bleaching. Thus for ethanol, where G(Radical) is approximately 9.0, the maximum number of initial free radicals calculated on the basis of the acetaldehyde plus glycol yield is 6.5. This figure is arrived at assuming that both aldehydes and glycols arise from bimolecular radical reactions involving, on the one hand, disproportionation and, on the other, combination. This mechanism is postulated on the basis of certain anomalous l.e.t. effects which have been observed in this and other[16] laboratories, and are currently under further study.

The observed discrepancy between G(Radicals) and $2G$(aldehyde + glycol) is probably the result of other reaction paths open to free radicals of this type. For example hydrogen abstraction, leading to alkoxyl radicals and ultimately the production of ethers, has indeed been observed in the case of ethanol. The low yields of these compounds in the case of the low molecular weight alcohols is probably due to their considerable volatility resulting in losses during sample handling.

(iv) The observation that bleaching with ultraviolet light results in either the destruction or substantial alteration of the initially produced free radicals raises a problem in connection with the further observation that carbonyl compounds and glycols are nevertheless found in bleached samples. One possible explanation for the formation of these products involves the influence of the paramagnetic free radicals on the surrounding alcohol matrix. Tsubomura and Mulliken[17] and others have shown that oxygen and other paramagnetic substances are capable of producing weak complexes with alcohols, the absorption of which is shifted to appreciably longer wave lengths. It can be speculated that in these experiments the alcohol free radicals complex with the substrate and bleaching then results in the photolysis of the nearest neighbors at wave lengths which would not affect the unperturbed alcohol molecules. Preliminary experiments have been conducted in which the photochemistry of ethanol as a function of added oxygen has been studied. There is considerable evidence for the formation of an oxygen–alcohol complex and indeed, photochemical decomposition to produce acetaldehyde occurs (in the presence of oxygen) at wave lengths which are ineffective in oxygen-free systems.[18] This effect is also under further investigation.

Acknowledgments.—The author wishes to thank Messrs. D. Hoernschemeyer and M. Riggenbach for assistance with the chemical analysis and Mr. K. Chellis for performing the Van de Graaff irradiations.

---

[16] W. R. McDonell and S. Gordon, *J. Chem. Phys.*, **23**, 208 (1955).

[17] H. Tsubomura and R. S. Mulliken, *J. Am. Chem. Soc.*, **82**, 2411 (1960).

[18] D. A. Becker, M.S. Thesis, Florida State University, 1961.

THE EXCESS VOLUME OF MIXTURES OF CYCLOHEXANE AND SOME NORMAL ALKANES

BY JOSÉ GÓMEZ-IBÁÑEZ AND CHIA-TSUN LIU

Hall Laboratory of Chemistry, Wesleyan University, Middletown, Connecticut

Received May 27, 1961

The excess volumes of binary mixtures of cyclohexane with *n*-hexane and with *n*-dodecane have been determined at 15, 25 and 35°. Over the measured range, the excess volume of these systems is independent of the temperature, and the magnitude of the effect observed, when related to some partial data existing for two other cyclohexane–paraffin systems seems to be related to the length of the normal alkane. In the case of cyclohexane and *n*-hexane the experimental data available are compared with those predictable from modern theories of solutions resulting in a qualitative, but not quantitative agreement. The agreement is somewhat better when reference is made to less refined theories of solutions, pointing to the continuing need for more data on simple systems as well as the re-examination of the range of validity of present theories.

The importance of the excess volume of mixing and its relation to all other thermodynamic functions has been emphasized consistently by modern theories of solutions.[1-5] Theories based on a cell model,[3] as well as those based on the theorem of corresponding states,[4,5] predict a contraction in volume when dispersion forces are involved and the molecules are of the same size. Small differences in size, on the other hand, are made to account for a large, positive excess volume of mixing.

It is of particular interest then to undertake a systematic study of the way in which known and regular variations in the size and shape of the molecules affect the excess thermodynamic functions. Reports of measurements of the excess volume of binary mixtures are not frequent in the literature and, as part of a program of study of the thermodynamic properties of binary mixtures of non-electrolytes, we have measured the densities of a few mixtures of hydrocarbons. We report here the results of our measurements of the systems formed by cyclohexane with *n*-hexane and with -*n* dodecane.

Experimental

Materials.—All the materials used were Matheson Coleman and Bell reagents. Spectroquality grade cyclohexane was fractionally distilled over sodium wire and the density of the middle portion was found to be 0.77395 g./cm.^{3} at 25°. *n*-Hexane (b.p. 68–69°) and *n*-dodecane (b.p. 111–114° (30 mm.)) were further purified by repeated fractional distillation of the middle fraction over sodium wire. The boiling points of the final distillation products were 68.76–68.78° for *n*-hexane and 216.3° for *n*-dodecane.

Procedure.—The densities of the pure hydrocarbons and of their mixtures were measured at 15, 25 and 35° in a pycnometer similar to those used and described by Mathot and Desmyter[6] and by Tacker and Rowlinson.[7] It consisted of a cylindrical bulb of approximately 10 cm.^{3} provided with two parallel graduated capillary tubes (10 cm. in length and 0.015 cm.^{2} in cross-section), both fitted with a ground cap.

The pycnometers were calibrated at 15, 25 and 35° using air and CO_2-free water obtained by redistilling four times condensed steam taken from the steam system of the laboratory. All weighings were carried out in a constant temperature room and in each instance the temperature in the balance case was measured to 0.2°, the relative humidity to 1%, and the barometric pressure to 0.1 mm. The densities of the water were taken as 0.99913, 0.99823 and 0.99567 g./cm.^{3} for the temperatures of 15, 25 and 35°, respectively.

In the mixing experiments the substance with the higher boiling point was introduced first into the pycnometer and, after weighing, the second component was added until the liquid level would come up to the middle part of the scale on the capillary. The pycnometer then was covered with the cups, repeatedly tilted to ensure mixing, weighed and immersed in the thermostat until the levels of the liquid in the capillaries showed no change. It then was allowed to stand in the constant temperature room, and weighed again.

The observed weights were corrected to vacuum, for evaporation loss, for the displacement of air by both the liquid and vapor phases and for the weight of each component in the vapor phase after mixing has taken place. In correcting for the weight of the vapor above the meniscus of the pycnometer Raoult's law was assumed to be obeyed, and in making all buoyancy corrections the true density of air was used as obtained from the appropriate equation.[8] The vapor pressure of *n*-dodecane was neglected.

The atomic weights used are 12.010 for carbon and 1.008 for hydrogen.

The most significant error arises from the reading of the liquid levels in the pycnometer. This reading can be made accurately within ±0.1 of a division (1 mm.). One unit of the capillary scale has an approximate volume of 0.003 cm.^{3}, depending upon the temperature, and since there are two capillary tubes, the error involved in reading the volume is ±0.0006 cm.^{3}. Weighing has been carried out with an accuracy better than ±0.0001 g., corresponding to a volume difference of 0.0002 cm.^{3}. Errors arising from uncertainty in the volume above the meniscus in the pycnometer and from the assumption that the vapor obeys Raoult's law are supposed not to exceed more than ±0.0002 cm.^{3}. Hence the total errors in the volume measurement are less than ±0.001 cm.^{3}. Since the pycnometer has a volume of approximately 10 cm.^{3}, the percentage error will not exceed ±0.01%.

The temperature of the thermostat was maintained in each case within ±0.005°, a sufficient accuracy when compared with the errors involved in the weighing and in the volume reading.

Results

The values reported in Table I for the densities of the pure hydrocarbons at 15, 25 and 35° are each the average of several measurements and are accurate to within 0.0001 g./cm.^{3} or better. Comparison is made in the table with other values found in the literature. The three calculated molar volumes of cyclohexane and *n*-hexane all fall in a straight line when plotted against the temperature. Columns 5 and 6 in the table give, respectively, the values of dV/dT and α, the coefficient of thermal expansion, at 25°, obtained from the slope of the line. The values for *n*-dodecane deviate only slightly from a straight line.

The values obtained for the excess volume of mixing for the systems cyclohexane + *n*-hexane

---

[1] G. Scatchard, *Trans. Faraday Soc.*, **33**, 160 (1937).

[2] H. C. Longuet-Higgins, *Proc. Roy. Soc.* (London), **A205**, 247 (1951).

[3] I. Prigogine and V. Mathot, *J. Chem. Phys.*, **20**, 49 (1952).

[4] I. Prigogine, A. Bellemans and A. Englert-Chwoles, *ibid.*, **24**, 518 (1956).

[5] R. L. Scott, *ibid.*, **25**, 193 (1956).

[6] V. Mathot and A. Desmyter, *J. Chem. Phys.*, **21**, 782 (1953).

[7] R. Tacker and J. S. Rowlinson, *Trans. Faraday Soc.*, **50**, 1036 (1954).

[8] "International Critical Tables," Vol. I, McGraw-Hill Book Co., Inc., New York, N. Y., p. 71.

TABLE I

DENSITIES OF CYCLOHEXANE, n-HEXANE AND n-DODECANE

Hydrocarbon	t, C.	d, g./cm.^{3} (this work)	Other values in the lit.	dV/dT, cm.^{3}/deg. (25°)	$\alpha \times 10^{-3}$, deg.$^{-1}$
Cyclohexane	15	0.78318	0.78310[9]		
	25	.77395	.77389[9]; 0.77382[10] .7764[11]	0.132	1.22
	35	.76458	.7690[12] (30°)		
n Hexane	15	.66390			
	25	.65488	.65481[9]; 0.6548[13] .65892[14]; .6863[11]	0.180	1.37
	35	.64602	.64603[15]		
n Dodecane	15	.75244			
	25	.74557	.74516[9]; 0.74514[15] .74542[16]	0.219	0.96
	35	.73812	.73800[15]		

TABLE II

EXCESS VOLUME IN MIXTURES OF CYCLOHEXANE WITH HEXANE AND WITH DODECANE

	Cyclohexane (x_1) + n-Hexane (x_2)		Cyclohexane (x_1) + n-Dodecane (x_2)	
	Mole fraction x_1	V^E, ml./mole	Mole fraction x_1	V^E, ml./mole
15°	0.20314	0.063	0.37463	0.403
	.24855	.088	.49847	.509
	.35292	.110	.55987	.551
	.55392	.156	.65342	.560
	.73146	.157	.74165	.537
	.78942	.138	.79426	.480
	.81678	.118	.84327	.412
			.90907	.265
			.95318	.134
25°	0.13194	0.038	0.45797	0.504
	.28094	.086	.56371	.554
	.38635	.117	.63629	.549
	.49893	.138	.67103	.559
	.62808	.153	.76445	.505
	.71271	.174	.80594	.467
	.86203	.088	.81670	.445
			.88783	.304
35°	0.13189	0.053	0.45787	0.399
	.27451	.085	.56359	.552
	.38647	.125	.63625	.574
	.43647	.131	.67097	.547
	.49897	.153	.76442	.534
	.62820	.176	.80587	.464
	.71277	.157	.81664	.451
	.86201	.086	.88779	.322

and cyclohexane + n-dodecane are given in Table II. The values obtained show that, in each of the two systems, the differences in the excess volume at the three temperatures considered here are of the order of magnitude of the experimental error.

Using all the data obtained at the different temperatures, equations expressing the change in excess volume with mole-fraction (x) and with volume fraction (ϕ) were computed by the method of least squares for each of the two systems.

Cyclohexane (1) − n-hexane (2)

$$V^E = x_1x_2\,[0.599 + 0.351(x_1 - x_2) + 0.00815(x_1 - x_2)^2] \quad (1)$$

$$\frac{100V^E}{V_1 + V_2} = \phi_1\phi_2\,[0.527 + 0.237(\phi_1 - \phi_2) - 0.0716(\phi_1 - \phi_2)^2] \quad (1')$$

Cyclohexane (1) + n-dodecane (2)

$$V^E = x_1x_2\,[2.022 + 1.532(x_1 - x_2) - 0.00164(x_1 - x_2)^2] \quad (2)$$

$$\frac{100V^E}{V_1 + V_2} = \phi_1\phi_2[1.532 - 0.317(\phi_1 - \phi_2) - 0.456(\phi_1 - \phi_2)^2] \quad (2')$$

The above equations are assumed here to be valid over the temperature range 15–35°. Table III shows the variance or mean square error of the coefficients.

TABLE III

MEAN SQUARE ERRORS OF THE COEFFICIENTS IN EQUATIONS 1, 1′, 2 AND 2′

Equation	Coefficient 1st	2nd	3rd
1	0.014	0.027	0.069
1′	.011	.022	.056
2	.027	.151	.254
2′	.013	.034	.099

There are no values reported in the literature for the system cyclohexane + n-dodecane with which to compare ours. For the system cyclohexane + n-hexane there is a set of measurements by Klapproth[11] and three single determinations around x = 0.5 by Mathieson and Thynne.[13] Klapproth's values are much lower than ours (V^E = 0.10 as contrasted with 0.15 ± 0.01 at x = 0.5), while Mathieson and Thynne's are higher than ours (0.19 at x = 0.5). The magnitude of the errors involved is not indicated in either case. We will adopt our values for the purpose of the discussion which follows since they have been obtained over a wider range of composition and are self consistent.

Discussion

Equations 1 and 2 for the systems n-hexane and cyclohexane and n-dodecane and cyclohexane are represented graphically in Fig. 1. Neither of the two curves is symmetric about the composition axis, the maximum appearing on the cyclohexane-rich side (around x = 0.6). Although less pronounced, the asymmetry is retained when the composition is expressed as volume fraction.

Temperature Independence of the Excess Volume.—The temperature independence of the excess volume of the two systems over the range 15–35° is unexpected and probably the most interesting result of the present study. The fact that $(\partial V^E/\partial T) = 0$ establishes certain relationships among some of the thermodynamic differential coefficients. Thus, for the systems under consideration

---

(9) "Selected Values of Physical and Thermodynamic Properties of Hydrocarbons and Related Compounds," American Petroleum Research Project 44, Carnegie Press, Pittsburgh, Penna., 1953.

(10) C. R. Brown, A. R. Mathieson and J. C. P. Thynne, *J. Chem. Soc.*, 4141 (1955).

(11) H. Klapproth, *Nova Acta Leopoldina*, **9**, 305 (1940).

(12) F. Danusso, *Rend. reale accad. naz. Lincei*, **13**, 131 (1952).

(13) A. I. Vogel, *J. Chem. Soc.*, 133 (1946).

(14) A. R. Mathieson and J. C. P. Thynne, *ibid.*, 3708 (1956).

(15) R. M. Deanesly and L. T. Carleton, *J. Phys. Chem.*, **46**, 1104 (1941). (Calculated from their data).

(16) A. F. Shepard, A. L. Henne and T. Midgley, Jr., *J. Am. Chem. Soc.*, **53**, 1948 (1931).

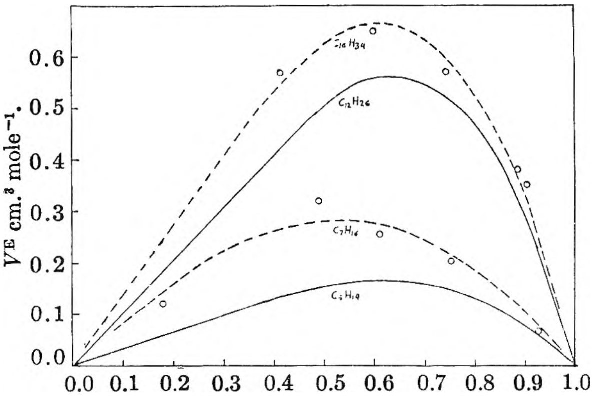

Fig. 1.—Excess volume of mixtures of cyclohexane and *n*-alkanes: full line, present work; broken line and ○: Danusso's work.

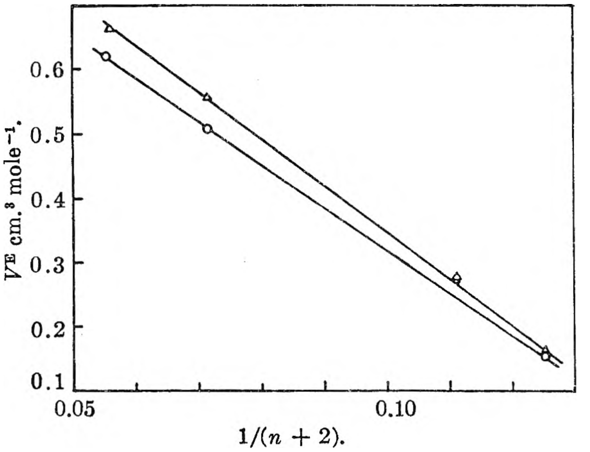

Fig. 2.—Relation between excess volume and chain length at mole-fractions of cyclohexane: ○, $x = 0.5$; △, $x = 0.6$.

$$\left(\frac{\partial H^E}{\partial T}\right)_P = \left(\frac{\partial E^E}{\partial T}\right)_P; \quad \left(\frac{\partial E^E}{\partial P}\right)_T = \left(\frac{\partial F^E}{\partial P}\right)_T$$

$$\left(\frac{\partial H^E}{\partial P}\right)_T = \left(\frac{\partial G^E}{\partial P}\right)_T = V^E; \quad \left(\frac{\partial F^E}{\partial T}\right)_P = \left(\frac{\partial G^E}{\partial T}\right)_P = -S^E$$

and also

$$\left(\frac{\partial S^E}{\partial P}\right)_T = \left(\frac{\partial S^E}{\partial V}\right)_T = 0 \qquad (3)$$

A random model, based on weak interactions independent of the temperature, would lead to the same last expression.[17]

Effect of Paraffin Length on the Excess Volume.—The excess volume observed is much larger with *n*-dodecane than with *n*-hexane, suggesting a possible dependence of the excess volume upon the length of the paraffin chain. Excess volume data have been reported for two other systems involving cyclohexane and a normal paraffin. Danusso[12] has reported density measurements at 30° for the systems cyclohexane and *n*-heptane and cyclohexane and *n*-hexadecane. From his data we have calculated the following two equations by the method of least squares

cyclohexane and *n*-heptane

$$V^E = x_1x_2\,[1.002 + 0.1339(x_1 - x_2)] \qquad (4)$$

cyclohexane and *n*-hexadecane

$$V^E = x_1x_2[2.475 + 1.384(x_1 - x_2)] \qquad (5)$$

A two-term equation has been obtained in each case representing fairly well the excess volumes. Mathieson and Thynne[14] also have reported two single measurements around $x = 0.5$ and at 25° for the cyclohexane and *n*-heptane system. Their values are here again higher than those of Danusso. As Danusso's data cover a wider range of composition and extend to two systems, we are using them here for purposes of correlation, and equations 4 and 5 also are represented in Fig. 1. The similarity of the curves is noticeable in the case of *n*-hexadecane, but not so much in the case of *n*-heptane, where the experimental point about $x = 0.5$ seems to impart to the curve a large measure of symmetry.

The increase in the excess volume of mixing with increasing length of the *n*-paraffin chain exhibited by the four curves represented in Fig. 1 suggests some possible empirical relationship. No simple, direct relationship could be obtained between V^E, the excess volume per mole, and n, the number of carbon atoms in the chain. On the other hand, when the excess volume for the four systems is plotted against the function $1/(n + 2)$, as shown in Fig. 2, a straight line can be drawn through those points which correspond to the mole-fraction of the maximum, *i.e.*, $x = 0.6$. At $x = 0.5$, the point representing the excess volume of cyclohexane and *n*-heptane fails to fall on the straight line determined by the other three systems, perhaps for the reason indicated at the end of the previous paragraph. Previously van der Waals and Hermans[18] have shown that the molar volumes of pure *n*-alkanes are a linear function of $n/2 + 1$, rather than of n, and have postulated that $-CH_3$ and $-CH_2-CH_2-$ are to be considered as equivalent units in the hydrocarbon chain. It is on this basis that an attempt has been made to extend to hydrocarbons the theorem of corresponding states.[19] Our data also shows a linear relationship when plotted against $1/(n/2 + 1)$ but an alternate interpretation could be to assign to each terminal hydrogen the same volume as that of a $-CH_2-$ group.

It is of interest that such relationships also can be found in the case of mixtures of the paraffins with cyclohexane. This would seem to indicate that the intermolecular forces are in all cases the same and that, if the interactions are small, the presence of cyclohexane will not interfere appreciably with the alkane–alkane interaction. The observed differences in behavior then could be expressed in terms of a single parameter, in this case the increase in the number of units present in the paraffin chain, and a consistent set of data should make it possible to express V^E by means of a single equation in terms of x, the mole fraction, and the parameter $1/(n + 2)$ or $2/(n + 2)$.

The System Cyclohexane and *n*-Hexane.—Of all the systems here considered, cyclohexane and *n*-hexane is the one for which the most complete

---

[17] J. H. Hildebrand and R. L. Scott: "The Solubility of Non-electrolytes," 3rd edition, Reinhold Publ. Corp., New York, N. Y., 1950, pp. 137–139.

[18] J. H. van der Waals and J. J. Hermans, *Rec. trav. chim.*, **68**, 181 (1949).

[19] I. Prigogine, "The Molecular Theory of Solutions," North Holland Publishing Co., Amsterdam, 1957, Ch. XVI.

thermodynamic information is available. Mathot[20] has measured the excess free energy and the heat of mixing for this system at 25°, while Mathieson and Thynne[14] have measured the heat of mixing at the same temperature with results which are in essential agreement. With the available information it is possible to compare the experimental results with those predictable from recent theories of solutions. The calculations summarized in Table IV have been made for the simple case of dispersion forces.

TABLE IV

EXPERIMENTAL AND CALCULATED VALUES FOR THE EXCESS THERMODYNAMIC FUNCTIONS OF THE SYSTEMS CYCLOHEXANE AND n-HEXANE AT 25°, FOR AN EQUIMOLAR MIXTURE $x_1 = x_2 = 0.5$

	Values for the parameters	G^E, $\frac{\text{cal.}}{\text{mole}}$	H^E $\frac{\text{cal.}}{\text{mole}}$	V^E, $\frac{\text{cm.}^3}{\text{mole}}$
Prigogine, *et al.*	$\delta = 0.09$;	63		0.66
	$\rho = 0.06$			
Scott	$\eta = -0.025$;	54		0.61
	$\xi = 0.095$			
Experimental		17	51	0.15

For calculations involved in Prigogine's theory[4,19] values for the parameters have been obtained from the critical data of Kobe and Lynn.[21] Since both δ and ρ are small, it should make no difference whether cyclohexane or n-hexane are taken as reference. The values for η and ξ are taken from Scott's original paper.[5]

Both theories agree, but only qualitatively, with the experimental results. It should be pointed out that applying either theory to the present system probably stretches too far their ranges of validity. Both theories are based on the theorem of corresponding states but, unlike the corresponding states theory first formulated by Longuet-Higgins,[2] they are not limited to the first-order terms in the molecular and interaction parameters. Their postulates are, of necessity, more stringent, and the theories should apply more properly to mixtures of small, non-polar, spherically-symmetric molecules, *i.e.*, to systems formed by condensed gases. Even then the discrepancies reported between theory and experiment for such systems are as large in some cases as the ones reported here.[22]

If, on the other hand, we restrict ourselves to the first-order theory, we can compute the Longuet-Higgins parameter d_{12} which is related to the molecular interactions and is given explicitly by the expressions[2]

$$x_1x_2d_{12} = \frac{G^E}{RT - Q_0} = \frac{H^E}{T\frac{dQ_0}{dT} - Q_0} = \frac{V^E}{V_0\,(p\,\beta_0 - T\alpha_0)}$$

where Q_0 ($= E_0 - RT$) is the latent heat of conversion of one mole of the reference liquid to the vapor state at zero pressure, and α_0 and β_0 are the coefficients of thermal expansion and isothermal compressibility, respectively, of the reference substance.

Since $p\beta_0$ is negligible compared to $T\alpha_0$, we also can write[2,23]

$$\frac{V^E}{G^E} = \frac{\alpha_0 T}{(-E_0/V)} = \frac{\alpha_0 T}{\delta^2}$$

where $-E_0/V$ is now the so-called cohesive energy density and δ the solubility parameter. Table V shows the values for d_{12} calculated at $x = 0.5$ from the experimentally determined G^E, H^E and V^E and also the average value of α_0T/δ^2, which is 75% of the experimental V^E/G^E.

TABLE V

COMPARISONS AT $x = 0.5$

Reference substance	d_{12} ($\times 10^{-2}$) from G^E	H^E	V^E	$\alpha_0 T/\delta^2$ (cm.^{3} cal. 10^{-3})	V^E/G^E (cm.^{3} cal.$^{-1}$ 10^{-3})	$\beta_0/1 + \alpha_0 T$ (cm.^{3} cal.$^{-1}$ 10^{-3})	V^E/H^E (cm.^{1} cal.$^{-3}$ 10^{-3})
n-Hexane	0.98	1.8	1.1	7.8			
Cyclohexane	0.93	1.8	1.5	5.4			
(Average)				(6.6)	8.8	3.6	2.9

We finally turn to the formulation of what sometimes is referred to as the solubility-parameter theory. Scatchard[1] obtained originally the relation

$$V^E = \beta_0 E_v{}^E = \beta_0 G_p{}^E$$

With an average for β_0 of 5×10^{-3} cm.^{3} cal.$^{-1}$ the expression yields only half the experimental value of V^E/G^E. Also, because the differential coefficients (3) correspond to some of the assumptions of the theory, we can write[17]

$$H^E = E_v{}^E\,(1 + \alpha_0 T)$$

from which

$$\frac{V^E}{H^E} = \frac{\beta_0}{1 + \alpha_0 T}$$

showing (Table V) a similar agreement between the calculated and the experimental values.

---

(20) V. Mathot, *Bull. soc. chim. Belges*, **59**, 111 (1950).

(21) K. A. Kobe and R. E. Lynn, Jr., *Chem. Revs.*, **52**, 117 (1953).

(22) For a summary of the results obtained for some condensed systems see N. G. Parsonage and L. A. K. Stavely, *Quart. Revs.* (London), **13**, 306 (1959).

(23) R. L. Scott, *Discussions Faraday Soc.*, **15**, 44 (1953).

KINETIC AND MAGNETIC STUDIES ON SUPPORTED NICKEL OXIDE CATALYSTS

By G. T. Rymer, Joanne M. Bridges and J. R. Tomlinson

Gulf Research & Development Company, Pittsburgh 30, Pa.

Received May 29, 1961

Magnetic and kinetic studies have been made on a series of catalysts consisting of nickel oxide supported on γ-alumina and on silica. Magnetic susceptibility studies have shown nickel is present in all cases as Ni^{+2}. Low susceptibility values obtained for some samples have been attributed to the presence of antiferromagnetic NiO. The kinetics of CO oxidation over those catalysts obeyed first-order kinetics for nickel on alumina at low concentrations. For the nickel on silica and the highest concentrations of nickel on alumina, the rate data obeyed an Elovich equation. These results have been interpreted in terms of a two-phase model for the supported nickel oxide catalysts.

Introduction

The importance of electronic structure in determining the catalytic activity of systems containing transition-metal ions has been demonstrated on numerous occasions. In the field of supported transition-metal oxide catalysts, Selwood[1] has characterized many systems by magnetic analysis. In several cases he has shown the influence of the support upon the electronic structure of the supported transition-metal ion and has developed a theory of "valence inductivity" to explain this influence.

In a recent publication[2] from this Laboratory, the magnetic susceptibilities of supported cobalt oxide catalysts were interpreted in terms of a model in which the cobalt was considered to exist in two distinct phases. The two phases were designated as a magnetically dilute δ-phase associated with the support lattice and a magnetically concentrated β-phase similar to the bulk oxide. The relative proportions of the two phases were found to be dependent upon the type of support used and the amount of cobalt supported. This proposed model was the natural outgrowth of consideration of the impregnation and calcination steps in the catalyst preparation. The δ-phase was believed to arise from adsorption of the cobalt ions on the support, while the β-phase was formed by occlusion and subsequent calcination of the cobalt solution in the pores of the support.

There is one point of similarity between Selwood's "valence inductivity"[3] and the two-phase model. This is that both theories postulate an interaction between the transition-metal ion and the support. That these effects should be most prominent with catalysts of low metal content is obvious. Selwood postulates that the supported transition-metal oxide imitates in some cases the crystal structure of the support and that the valence of the support cation is thereby induced into the transition-metal ion. Our theory postulates that the transition-metal ions, adsorbed during impregnation, are incorporated upon dehydration of the catalyst into the surface lattice which we designate as the δ-phase.

It should be noted that the concept of a two-phase model was considered and rejected in an earlier work by Selwood.[4] Nevertheless, we believe that the two-phase model offers an additional insight into the structure of supported metal oxide systems, thus providing a basis for an understanding of the kinetics over these catalysts. The primary innovation of the two-phase model is the existence and mode of formation of the δ-phase.

The present investigation of the supported nickel oxide system was undertaken to determine if a second catalyst system could be interpreted in terms of a similar two-phase model. Although susceptibility studies[5] on supported nickel oxides have been made, it was thought necessary to repeat these investigations in order to obtain magnetic and kinetic results on the same series of catalysts.

Experimental

Sample Preparation.—Alumina, prepared from $Al(NO_3)_3 \cdot 9H_2O$ (J. T. Baker C.P.), was calcined at 500° for 6 hours. The product was identified by X-ray diffraction as γ-alumina containing a small percentage of η-alumina. The B.E.T. surface area was 190 m.^{2}/g. Silica prepared by the hydrolysis of ethyl orthosilicate was calcined at 500° for 6 hours. This material had a B.E.T. surface area of 580 mg.^{2}/g. Impurities present were less than 0.01% as determined by spectrographic analysis. Both the Al_2O_3 and the SiO_2 were ground to 50–140 mesh before impregnation with nickel nitrate.

Supported nickel catalysts were prepared by impregnation with varying concentrations of $Ni(NO_3)_2 \cdot 6H_2O$ (Baker C.P.). The samples were oven dried at 100° for 2 hours, then calcined for 6 hours at 500°. Two series of $Ni-Al_2O_3$ catalysts were prepared. The first series ranged in concentration from 1.12 to 4.25 wt. % nickel, the second series from 2.47 to 9.69 wt. % nickel. All $Ni-Al_2O_3$ samples, after calcination, were light green with the exception of the 9.69 wt. % sample, which was black. All $Ni-SiO_2$ samples were black after calcination. A plot of nickel concentration on alumina and silica *vs.* the final molarity of the impregnating solution is given in Fig. 1.

Nickel oxide was prepared by calcining $Ni(NO_3)_2 \cdot 6H_2O$ (Baker C.P.) for 24 hours at 500°. X-Ray diffraction patterns indicated the product to be NiO. Chemical analysis showed that the gray-green calcined product contained 78.9% Ni, compared with 78.6% Ni for stoichiometric NiO.

Magnetic Susceptibility Measurements.—A Ding's G.M.-1 four-inch electromagnet with a 1.25-inch gap was used for susceptibility measurements. The pole caps were truncated cones with a 30° bevel on the flat faces. Magnet current was controlled by a modified Sorenson "Nobatron" power supply. The sample, contained in a spherical quartz bucket 4 mm. in diameter, was suspended in the magnet gap by a quartz fiber attached to a quartz spiral spring. The spring, which had a sensitivity of 3 mm./mg., was in turn attached to a vacuum micromanipulator used to position the sample accurately at the point where the value of

---

[1] P. W. Selwood, "Magnetochemistry," Interscience Publishers, Inc., New York, N. Y., 1956.

[2] J. R. Tomlinson, R. O. Keeling, Jr., G. T. Rymer and J. M. Bridges, Preprints of the Second International Congress on Catalysis, Paper No. 90, Paris, July 1960.

[3] P. W. Selwood, "Advances in Catalysis," Vol. III, Academic Press, Inc., New York, N. Y., 1951, p. 57.

[4] P. E. Jacobson and P. W. Selwood, *J. Am. Chem. Soc.*, **76**, 2641 (1954).

[5] F. N. Hill and P. W. Selwood, *ibid.*, **71**, 2522 (1949).

$H(dH/dx)$ was maximum. The sample, fiber and spring were vacuum enclosed. Forces precise to 1 μg. were determined by measuring displacements with a Gaertner cathetometer and microscope. Temperature control at the low temperatures was achieved by cryostatic liquids contained in a glass Dewar which could be placed around the sample in the magnetic field. Temperatures to 300° were obtained by means of a d.c. operated platinum heater winding between the walls of the sample housing.

The magnetic field was calibrated by determining at constant magnet current the force on a 75 mg. platinum standard as a function of the vertical position, x, in the field. From the force, spring sensitivity and the susceptibility of platinum,[6,7] values of $H(dH/dx)$ were calculated and plotted as a function of x. Graphical integration of this curve from maximum $H(dH/dx)$ to a position above the magnet where $H(dH/dx)$ is negligible yields $H^2/2$ at the sample position.

Catalyst samples weighing 20 mg. were pretreated *in situ*. These samples were evacuated at room temperature for 16 hours and then were maintained in a helium atmosphere. Susceptibility measurements were made at three temperatures, 77, 194 and 295°K., for the $Ni-Al_2O_3$ samples. Additional measurements were made at higher temperatures on several samples. At each temperature, measurements were made at five field strengths over the range 4200 to 7760 oersteds. Susceptibility *vs.* reciprocal field plots were linear and parallel with small positive slopes in the temperature range 194 to 580°K. At 77°K. a slight anomaly was observed. The positive slopes of the plots for $Ni-SiO_2$ increased; for $Ni-Al_2O_3$ the slopes became negative. These cryomagnetic peculiarities are not unique; Van Vleck[8] cites other examples and suggests theoretical explanations.

Kinetic Measurements.—The activity studies for the oxidation of carbon monoxide were made using the rising temperature reactor described previously.[2,9,10] Flow rates ranging from 40 to 200 cc./min.(STP) were used in this investigation. These flow rates were maintained to within 1 cc./min.(STP). The composition of reactant gases was 5% carbon monoxide and 95% oxygen. Both gases (Matheson) had been dried previously by passage over magnesium perchlorate.

The extent of reaction was followed by thermal conductivity. Since carbon monoxide and oxygen have essentially the same thermal conductivities, which differ appreciably from that of CO_2, any change which occurred in the thermal conductivity of the product stream was a direct measure of the extent of reaction. The thermal conductivity cells were calibrated by metering appropriate mixtures of carbon monoxide, oxygen and carbon dioxide. For the composition of reactant gases used it was found that the thermal conductivity varied linearly with conversion.

In studying the oxidation of carbon monoxide over the Al_2O_3 which was used in these investigations, it was found that the support had considerable activity if it had been evacuated previously at 500°. A similar phenomenon was reported in an earlier investigation.[10] However, this activity could be eliminated by flowing an oxygen stream which had been saturated with water at room temperature over the catalyst at 300°. Therefore, to avoid any interpretational difficulties regarding the activity of the supported nickel catalysts, the catalysts were pretreated in this manner. This pretreatment had no effect on the activity of the NiO. In all activity studies the temperature of the catalysts was maintained below 310° to prevent subsequent dehydration of the alumina. Reproducibility of the data indicated no subsequent dehydration of the alumina during the studies.

The catalysts then were stabilized in the reactant stream at a feed rate of 200 cc./min.(STP) for three hours at 300°. Rising and falling temperature runs then were made over the range of feed rates already mentioned. In studying the $Ni-Al_2O_3$ catalysts containing less than 4 wt. % nickel, it was found that the maximum conversions obtained at 300° at a flow rate of 40 cc./min.(STP) were in the order of magnitude of 10 to 20%. For conversions below 10% the rising temperature technique was not practicable because of base line drift of the recorder. It was, therefore, decided for those $Ni-Al_2O_3$ catalysts having only slight activity that reaction kinetic data should be obtained using the reactor on an isothermal basis. The procedure was identical with that for the rising temperature technique except that the reactor was kept at a constant temperature using a Foxboro controller which maintained the temperatures in this investigation to within 1°. Conversions were determined at feed rates of 40, 65, 112, 150 and 200 cc./min. (STP) at three temperatures in the range of 230–307°. During the isothermal studies the base line of the recorder was adjusted at regular intervals.

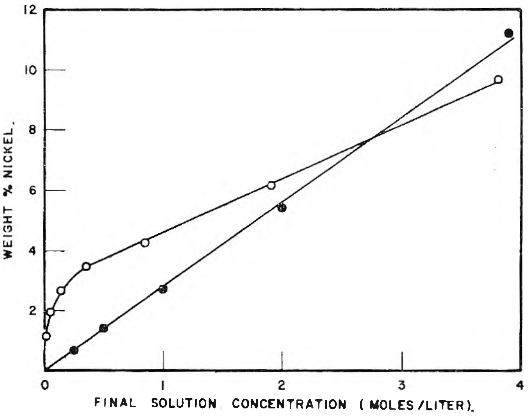

Fig. 1.—Weight per cent. nickel in the catalyst as a function of the concentration of the impregnating solution: ○, nickel on Al_2O_3; ●, nickel on SiO_2.

In the case of NiO, all the $Ni-SiO_2$ catalysts, and the $Ni-Al_2O_3$ containing above 4 wt. % Ni, it was possible to use the rising temperature technique. Rising and falling temperature runs were made at feed rates of 40, 65, 112 and 200 cc./min.(STP). In all cases it was found that at a rate of temperature change of 1°/min. the activities of the rising and falling temperature runs agreed. In this way it was assured that steady-state catalyst conditions had been obtained. Since two different techniques were being used, it seemed necessary to ascertain that both techniques would yield the same results. Therefore the 4.40 wt. % $Ni-Al_2O_3$ catalyst was tested using both the rising temperature and the isothermal methods. The results were identical within experimental error.

Results

Magnetic.—The magnetic susceptibility of the nickel in the $Ni-Al_2O_3$ and $Ni-SiO_2$ catalysts and in bulk NiO, measured at various temperatures, is given in Table I.

The $Ni-Al_2O_3$ data are well represented by the Curie–Weiss function, $x = C/T + \Delta$, with average deviations of about 0.5%. The effective Weiss constants, Δ, and the effective moments, as calculated by $\mu = 2.84\sqrt{C}$, were obtained by least squares. With the exception of the 9.69 wt. % Ni catalysts, the moments of the $Ni-Al_2O_3$ series were essentially constant yielding an average value of 3.23 ± 0.02 Bohr magnetons. The 9.69 wt. % Ni yielded a slightly lower moment of 3.05 μ_B. For all samples a small Weiss constant which was less than 10°K. was found.

At all temperatures studied the susceptibilities of the $Ni-SiO_2$ catalysts are about a third of the values for the $Ni-Al_2O_3$ catalysts. Up to 300° the data can be represented by a Curie–Weiss function from which a moment of 2.1 Bohr magnetons and effective Weiss constants of 50–60°K. can be calcu-

---

(6) J. W. Mayo and T. Pankey, *Rev. Sci. Instr.*, **29**, 429 (1958).

(7) F. E. Hoare and J. C. Walling, *Proc. Phys. Soc. (London)*, **B64**, 337 (1951).

(8) J. H. Van Vleck, "The Theory of Electric and Magnetic Susceptibilities," Oxford University Press, Oxford, 1932, p. 307.

(9) J. M. Bridges and G. Houghton, *J. Am. Chem. Soc.*, **81**, 1334 (1959).

(10) J. M. Bridges, D. S. MacIver and H. H. Tobin, Preprints of the Second International Congress on Catalysis, Paper No. 110, Paris, July 1960.

TABLE I

SUSCEPTIBILITY PER GRAM OF NICKEL AS A FUNCTION OF TEMPERATURE

Wt. % nickel	Support	$\chi \times 10^6$ at 77°K.	$\chi \times 10^6$ at 194°K.	$\chi \times 10^6$ at room temp.[a]		$\chi \times 10^6$ above room temp.					
1.12	Alumina	281.6	111.7	74.7	(297)						
1.94	Alumina	264.5	107.9	74.0	(298)						
2.47	Alumina	296.4	115.5	75.6	(298)						
2.64	Alumina	266.8	106.5	71.3	(296)						
3.21	Alumina	273.5		74.1	(300)						
3.48	Alumina	291.4	118.9	78.9	(297)						
4.25	Alumina	271.6	112.2	75.4	(296)						
4.40	Alumina	280.3	114.1	77.4	(291)						
6.06	Alumina	264.4	110.3	75.8	(295)	57.5	(373)	49.0	(443)	41.7	(534)
9.69	Alumina	226.5	96.1	64.9	(294)	44.0	(437)	40.1	(481)	35.8	(573)
2.67	Silica	65.3	35.3	25.6	(296)						
5.42	Silica	74.1	39.4	26.4	(294)	25.4	(326)	22.5	(391)	22.1	(568)
11.22	Silica	74.9	38.8	25.8	(294)	24.5	(316)	22.0	(405)		
Bulk NiO	....	10.5	10.8	11.7	(294)	13.2	(414)	15.4	(518)	15.7	(570)

[a] Actual temperatures in degrees Kelvin for room temperature and above are given in parentheses.

lated. However, above 300° a Curie–Weiss plot of the data showed curvature toward the temperature axis.

Magnetic measurements on a sample of bulk NiO prepared from the nitrate gave comparatively low values of susceptibility which decreased with decreasing temperature consistent with the antiferromagnetic properties ascribed to this material and which were almost identical with those reported by Singer.[11]

Kinetic.—The theory of a rising temperature flow reactor was developed in a previous paper.[9] It will be briefly summarized here. In the case of a flow reactor the steady state of mass balance may be written as[12]

$$r\mathrm{d}A = F\mathrm{d}x \qquad (1)$$

where

r = reaction rate (moles/min.-m.^{2})
A = surface area of the catalyst (m.^{2})
F = feed rate of the charge (g./min.)
x = moles of reactant converted per g. of feed

In the field of catalytic reactions it is common practice to consider that the reaction rate may be expressed by an equation of the form

$$r = k\Pi p_i^{n_i} \qquad (2)$$

where

k = temp. dependent velocity constant
p_i = partial pressure of the ith reactant
n_i = reaction order of the ith reactant

Equations 1 and 2 may be integrated to yield the following general equation

$$k\frac{A}{F} = \Psi \qquad (3)$$

where

$$\Psi = \int_0^x \frac{dx}{\Pi p_i^{n_i}} \qquad (4)$$

The rate constant k may be expressed by the Arrhenius equation

$$k = Be^{-E/RT} \qquad (5)$$

where B is the frequency factor and E is the activation energy. Combining equations 3 and 5, we obtain

$$\ln F + \ln\Psi = -E/RT + \ln(AB) \qquad (6)$$

In the case of a rising temperature reactor, equation 6 may be used to obtain values of E without any knowledge of ψ, providing ψ has no temperature dependency. Conversion–temperature values may be obtained for a number of feed rates, and ln F then may be plotted against $1/T$ for those temperatures at which identical conversions are obtained. The slopes of the resulting straight lines are equal to $-E/R$. However, in the field of heterogeneous catalysis, it is found quite frequently that a simple rate equation of the form of equation 2 is not applicable to the rate data and that ψ is actually temperature dependent. When this occurs, the activation energies obtained from the ln F *vs.* $1/T$ plots vary with conversion, and, if the dependency is large, the individual plots are curved. It then is necessary to obtain, by means of interpolation of these plots, values of conversion as a function of feed rate at any given temperature. These data then are applied to equation 1 by selecting a rate equation which will represent the data. In this investigation the latter approach was used and all the data from rising temperature runs were reduced to an isothermal basis.

For those catalysts containing less than 6 wt. % Ni on Al_2O_3, a first-order rate law was obeyed

$$r = kp_{CO} = k'(1 - f)x^0 \qquad (7)$$

where

$k' = \frac{kP}{n^0}$ P = total pressure

x^0 = moles of CO at the inlet of the reactor/g. of feed
n^0 = moles of feed/g. of feed
f = x/x^0 = fraction CO converted to CO_2

When equation 7 is substituted in equation 1, and then integrated the result is

$$\frac{k'A}{F} = -\ln(1 - f) \qquad (8)$$

Typical first-order rate plots are shown for these catalysts in Fig. 2.

In the case of NiO, 9.69 wt. % Ni–Al_2O_3, and the Ni–SiO_2 catalysts, it was necessary to use an Elovich equation to fit the data

$$r = ke^{-\alpha p_{CO_2}} = ke^{-\alpha' x^0 f} \qquad (9)$$

---

(11) J. R. Singer *Phys. Rev.*, **104**, 929 (1956).

(12) O. A. Hougen and K. M. Watson, "Chemical Process Principles," Vol. III, John Wiley and Sons, Inc., New York, N. Y., 1943.

TABLE II

KINETIC DATA FOR CO OXIDATION OVER NiO AND SUPPORTED NiO CATALYSTS

Wt. % nickel	Support	Technique[a]	Temp. region[b], °C.	Rate equation	$r_s \times 10^4$ at 240°, moles/min.-g. Ni	E, kcal./mole
Bulk NiO	...	RT	166–187	Elovich	2.3	16
1.94	Al_2O_3	I	238–297	First order	0.80	10
2.64	Al_2O_3	I	243–308	First order	.90	12
3.21	Al_2O_3	I	245–294	First order	.72	14
4.40	Al_2O_3	I	233–304	First order	.80	13
4.40	Al_2O_3	RT	253–290	First order	.77	11
9.69	Al_2O_3	RT	203–253	Elovich	2.3	11
2.67	SiO_2	RT	240–268	Elovich	9.2	13
11.22	SiO_2	RT	152–166	Elovich	40	20

[a] The experimental technique refers to the method used in determining the kinetic data. RT indicates the rising temperature method and I the isothermal method. [b] The temperature region is that in which the catalytic investigations were made.

where

α = a temp. dependent parameter

$$\alpha' = \frac{\alpha P}{n^0}$$

To test the validity of using this equation, conversion was plotted *versus* reciprocal space velocity for each catalyst, and the slopes of these curves, which correspond to r in equation 9, were measured at various conversions. Log r then was plotted *versus* conversion according to equation 9. The resulting plots were found to be linear. The reaction data also were fitted to the integrated form of the Elovich equation

$$\alpha' x^0 f = \ln \alpha' kA + \ln \left(\frac{1}{F} + \frac{1}{\alpha' kA}\right) \qquad (10)$$

The fit of the reaction data to the integrated form of the equation is shown in Fig. 3. In Table II a summary is given of the reaction conditions under which each catalyst was tested and of the rate data and activation energies obtained. For the purpose of comparing relative activities, the specific rate, r_s, is listed. This parameter refers to the differential reaction rate at infinite space velocity per gram of nickel at 240°. A temperature of 240° for comparing rates was chosen because rate data had been obtained for all catalysts except NiO and 11.22 wt. % Ni–SiO_2 at or near this temperature. In calculating rates the experimentally determined rate constants and the apparent activation energies were used. The specific rates are estimated to be precise to within 10%, and the activation energies to within 2 kcal./mole.

Discussion

For the Co–Al_2O_3 system[2] it was concluded that the formation of the two phases of cobalt was dependent upon two well-known characteristics of alumina and perhaps other catalyst supports. First, alumina has the ability to adsorb transition-metal ions from an impregnating solution, and, second, it is capable of occluding this solution in its pores. It was postulated that in the dehydration of the catalyst the adsorbed transition-metal ion became incorporated into the alumina lattice, forming the magnetically dilute δ-phase. In the dehydration and subsequent decomposition of the occluded solution during calcination, a β-phase consisting of the transition-metal oxide was formed.

In order to determine if the two-phase model is applicable to the supported nickel oxide system, the sample preparation will be considered first. As may be seen in Fig. 1, the weight per cent. of nickel on silica is directly proportional to the final concentration of the impregnating solution. In addition, there was no detectable change in the solution con-

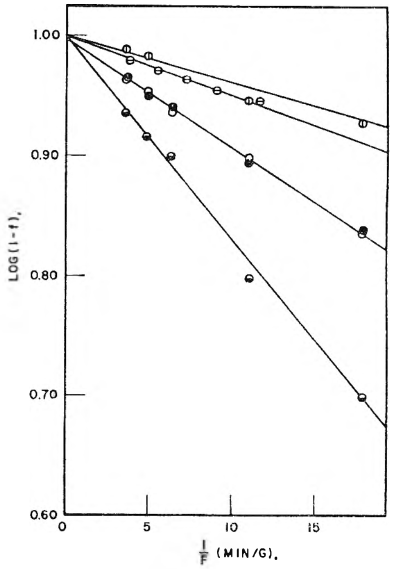

Fig. 2.—First-order rate plots for Ni/Al_2O_3 catalysts containing less than 5 weight % Ni: ◒, 4.40 wt. % Ni/Al_2O_3 at 304°; ●, 3.21 wt. % Ni/Al_2O_3 at 294°; ○, 2.64 wt. % Ni/Al_2O_3 at 308°; ∋, 4.25 wt. % Ni at 250°; ⦶, 1.94 wt. % Ni at 297°.

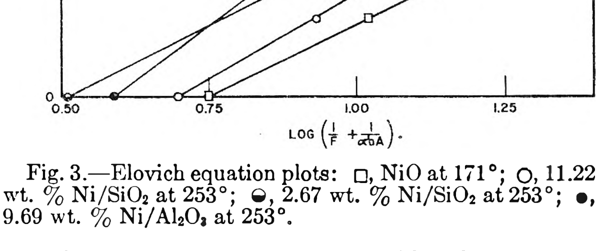

Fig. 3.—Elovich equation plots: □, NiO at 171°; ○, 11.22 wt. % Ni/SiO_2 at 253°; ◒, 2.67 wt. % Ni/SiO_2 at 253°; ●, 9.69 wt. % Ni/Al_2O_3 at 253°.

centration before and after impregnation. This result is to be expected if the nickel is retained only by occlusion of the solution in the pore structure of the support. In the case of nickel on alumina the weight per cent. nickel at first increases quite rapidly with the final concentration of the impregnating solution, and then levels off to a linear dependence at higher solution concentrations. The impregnation produced a marked decrease in the nickel concentration of the impregnating solutions. This decrease is evidence of the adsorption of nickel ions by the alumina. The linear dependence at higher solution concentrations indicates the simultaneous occlusion of the solution in the pore structure of the alumina. Thus it would appear that the observations during sample preparation are in accordance with the previously postulated steps in the formation of the two phases.

As a result of these impregnation studies, it appears that the β-phase should be essentially absent in the alumina supported catalysts of lowest nickel content by virtue of the extremely low concentration of the occluded solution. Hence, magnetic studies on alumina supported catalysts of low nickel content should yield the properties of the δ-phase. It also seems safe to assume that the δ-phase is absent in the case of the silica-supported samples.

The interpretation of the magnetic data in terms of δ- and β-phases is complicated when the probable nature of the β-phase is considered. The β-phase should be the stable form of the transition metal oxide which in this case is NiO. Nickel oxide in its bulk form is antiferromagnetic and exhibits a quite low susceptibility. However, when supported, part of the NiO will be dispersed and consequently this portion will have a lower Curie temperature than bulk NiO. As a result the dispersed portion of the bulk NiO will be paramagnetic in the temperature region investigated. It should, therefore, have a moment comparable to that for Ni^{++} in octahedral symmetry and a non-zero Weiss constant since exchange forces will not be entirely eliminated.

For nickel oxide supported on alumina there exists the possibility that the δ-phase and the two forms of the β-phase are present. It is impossible to calculate the distribution of these three types of nickel ions. However, an examination of the magnetic data leads us to believe that the δ-phase predominated at least out to 6% nickel. As seen in Table I, the magnetic moment for the $Ni-Al_2O_3$ catalysts, with the exception of the 9.69 wt. % sample, was independent of concentration and was calculated to be 3.23 ± 0.02 Bohr magnetons. This value is quite close to the accepted experimental value ($3.2\mu_B$)[13] and the theoretical value ($3.4\mu_B$)[13] for Ni^{++} in octahedral symmetry. For tetrahedral symmetry, the experimental value is $3.9\mu_B$.[13] These results suggest that for these catalysts the Ni was present as octahedrally coördinated Ni^{++}. The fact that there was no decrease in moment for any of these catalysts eliminates the possibility that any of the nickel was present as antiferromagnetic NiO. In addition, for all of these catalysts the Weiss constant was essentially zero. This result indicates that the nickel ions were magnetically dilute and also eliminates the possibility that any appreciable quantity of the nickel was present as paramagnetic bulk NiO. Therefore, it appears that for the nickel oxide supported on alumina the δ-phase predominates up to 6 wt. % nickel. The decrease in moment to $3.04\mu_B$ for the 9.69% $Ni-Al_2O_3$ is believed to be outside experimental error. It is most likely that for this catalyst a small portion of the nickel is in the form of antiferromagnetic NiO.

For the nickel oxide supported on silica, for which the δ-phase has been assumed to be absent, it is possible to estimate the proportions of antiferromagnetic and paramagnetic forms of NiO in the β-phase. As a first approximation, the susceptibility value of bulk NiO was assigned to the antiferromagnetic form and the susceptibility value equivalent to the δ-phase was assigned to the paramagnetic form. (In this approximation it has been necessary to ignore the exchange forces which would make the susceptibility of the paramagnetic form lower than that of the δ-phase since there is no way to estimate these forces quantitatively.) It was calculated that these samples contain 25% of the paramagnetic form and 75% of the antiferromagnetic form. This distribution accounts for the susceptibility of the three samples over the temperature region studied. It should be noted that for any substance which is predominantly antiferromagnetic, the Curie–Weiss law is not applicable. Therefore, the observed moment of $2.1\mu_B$ mentioned in the Results section for theses amples is meaningless and the fit of the data to a Curie–Weiss law was fortuitous.

In summary, for the $Ni-Al_2O_3$ catalysts containing 6 wt. % nickel and less, the nickel is believed to exist predominantly as the δ-phase. For the 9.69 wt. % $Ni-Al_2O_3$, it is believed that a portion of the nickel is in the antiferromagnetic β-form, and for the $Ni-SiO_2$ catalysts it is estimated that 75% of the nickel is in the form of the antiferromagnetic NiO. It has been assumed that the δ-phase was absent in the $Ni-SiO_2$ catalysts.

The rate data summarized in Table II also separate the catalysts into two distinct groups. The kinetic results of the first group, consisting of those catalysts containing less than 6 wt. % nickel supported on alumina, may be characterized as follows: (1) the reaction data for CO oxidation fitted a first-order rate equation; (2) the specific rates, r_s, were constant within the limits of experimental uncertainty; and (3) the activation energies also were constant. All the other catalysts studied fall into the second group, and for these the kinetic results have the following distinguishing features: (a) the reaction data fitted an Elovich equation; (b) the specific rates were not constant and were of a much higher order of magnitude than those found for the first group of catalysts; (c) the activation energies were not constant.

The results of the magnetic susceptibility studies interpreted in terms of a two-phase model have indicated that in the first group of catalysts all or almost all of the nickel ions were incorporated in the δ-phase while in the second group the nickel ions

---

(13) B. N. Figgis, *Nature*, **182**, 1568 (1958).

existed either entirely (*e.g.*, Ni–SiO_2) or to a measurable extent (9.69 wt. % Ni–Al_2O_3) in the β-phase. It would appear then that the δ- and β-phases act quite differently as catalysts.

Consider those catalysts in which only the β-phase was present. Catalytically they resembled NiO in that CO oxidation over them followed the Elovich equation. Parravano[14] found that CO oxidation over NiO containing appreciable amounts of chemisorbed oxygen also followed this rate equation. Since NiO tends toward black when it contains excess oxygen,[15,16] it is logical to assume that the black β-phase catalysts contain oxygen enriched NiO. In order to consider the kinetic results for the β-phase catalysts in greater detail, much more would have to be known about their chemisorptive properties. It should be noted that the difference in activation energies for these catalysts may be due to differences in the temperature regions in which they were studied.

Next consider the catalysts in which only the green δ-phase was present. It is believed that the nickel ions incorporated in the alumina lattice lacked the strong oxygen chemisorption properties of NiO. Kinetically the δ-phase catalysts have a striking similarity to Parravano's[14] NiO which lacked chemisorbed oxygen. The kinetics for CO oxidation over this catalyst were also first order, the activation energy was 13 kcal./mole, and the rate was much slower than that obtained for a NiO catalyst with chemisorbed oxygen. The fact that the specific rates, *i.e.*, the rates per unit weight of supported nickel, over the δ-phase catalysts were constant is indicative that for these catalysts all the nickel ions were accessible for the reaction and, therefore, that they were well dispersed. The constant values of the activation energies indicate that only one phase was present in these catalysts.

One catalyst, the 9.69 wt. % Ni–Al_2O_3, did contain both phases. Here it appears that the enhanced activity of the β-phase overshadowed that of the δ-phase. As a result, the kinetics resembled those for the catalysts in which only the β-phase was present.

---

[14] G. Parravano, *J. Am. Chem. Soc.*, **75**, 1448 (1953).

[15] R. P. Marcellini, R. E. Ranc and S. J. Teichner, Preprint No. 7, Second International Congress on Catalysis, Paris, July 1960.

[16] R. Newman and R. M. Chrenko, *Phys. Rev.*, **114**, 1507 (1959).

FLUORINE BOMB CALORIMETRY. III. THE HEAT OF FORMATION OF BORON TRIFLUORIDE[1-3]

By STEPHEN S. WISE, JOHN L. MARGRAVE, HAROLD M. FEDER AND WARD N. HUBBARD

Argonne National Laboratory, Argonne, Ill., and University of Wisconsin, Madison, Wis.

Received June 3, 1961

The heat of formation of boron trifluoride has been measured by direct combination of the elements in a bomb calorimeter. $\Delta Hf°$ at 25° was found to be -270.10 ± 0.24 kcal. mole^{-1}.

Recent interest in boron–hydrogen compounds as high-energy fuels and in refractory borides as structural materials for high temperatures has increased the need for high precision thermochemical data for boron compounds. The existence of glassy (amorphous) B_2O_3, the sub-oxides B_2O_2, B_3O and B_7O, and various hydrated oxides and sub-oxides, however, has made the interpretation of experimental heats of combustion of boron and its compounds in oxygen quite difficult. For example, the oxygen bomb combustion of boron has yielded values for the heat of formation of boric oxide which vary over a range of 80 kcal. mole^{-1}. It has required pyrolysis and hydrolysis reaction heats to yield an unequivocal result[4] for this important quantity. Fluorine is a stronger oxidant than oxygen and, in addition, it has the special advantage, in reactions with boron compounds, of forming a volatile reaction product, BF_3. Thus, the heat of formation of BF_3 must be known with high reliability if accurate heats of formation for other boron compounds are to be determined by fluorine bomb calorimetry.[5]

The presently accepted value for the heat of formation of BF_3 was calculated from the heat of solution of BF_3 (gas) in water[6-8] and the heat of solution of B_2O_3 in aqueous HF[9,10] Since there is some uncertainty about the exact composition of the solutions obtained in the above processes, the uncertainty in the "best" value[4] for $\Delta Hf°_{298.15}$ of BF_3(gas) (270 kcal. mole^{-1}) is rather large, 2 kcal. mole^{-1}. In this work, high-purity crystalline boron (99.4%) was allowed to react with fluorine in a nickel combustion bomb to give the first reported direct determination of the standard heat of formation of BF_3(gas).

Experimental

Calorimeter and Bomb.—The bomb, calorimetric system and operational procedure were similar to those described

---

[1] This work was performed under the auspices of the U. S. Atomic Energy Commission.

[2] Presented in part at the 139th National Meeting of the American Chemical Society in St. Louis, March, 1961.

[3] Abstracted from a thesis submitted by S. S. Wise to the faculty of the University of Wisconsin in partial fulfillment of the requirements for the Ph.D. degree.

[4] W. H. Evans, D. D. Wagman and E. J. Prosen, Natl. Bur. Standards Report No. 6252, December 15, 1958.

[5] E. Greenberg, J. Settle, H. M. Feder and W. N. Hubbard, *J. Phys. Chem.*, **65**, 1168 (1961). Paper I of this series.

[6] H. Hammarl, *Compt. rend.*, **90**, 312 (1890).

[7] A. W. Laubengayer and D. S. Sears, *J. Am. Chem. Soc.*, **67**, 164 (1945).

[8] A. W. Laubengayer and G. R. Finlay, *ibid.*, **65**, 884 (1943).

[9] O. Mulert, *Z. anorg. Chem.*, **75**, 198 (1912).

[10] J. Thomsen, "Thermochemische Untersuchungen," Vol. I, II, III, IV, Verlag J. A. Barth, Leipzig, 1882–1886.

in Paper I of this series,[5] except that a soft aluminum gasket was substituted for the gold gasket used to seal the head of the bomb to the body. The masses of all combustion samples were determined to 0.01 mg. on a semi-micro analytical balance. The mass of the calorimeter water was determined to 0.05 g. on a 10-kg. capacity balance.

Calibration.—The energy equivalent of the calorimeter was determined in the standard manner[11] using benzoic acid NBS standard sample 39g, under prescribed conditions. No nitric acid or carbon monoxide were observed as combustion products. The mean of eleven combustions gave 3570.36 cal. deg.$^{-1}$ as the energy equivalent of the calorimetric system. The standard deviation of the mean was 0.24 cal. deg.$^{-1}$ or 0.007%.

Materials.—Crystalline boron was prepared by the United States Borax and Chemical Corporation[12] by recrystallization of Moissan boron at temperatures in excess of 2000°. The X-ray powder diffraction patterns of this material corresponded to those of the β-rhombohedral (high temperature) form.[13] Specific chemical analyses showed that the sample contained 0.24% carbon, 0.15% iron, 0.12% manganese, 0.05% silicon, 0.05% oxygen, 0.007% magnesium, 0.0004% hydrogen, and, by difference, 99.38% boron. Spectrochemical analysis detected no other impurities.

High-purity titanium wire (4 mil diameter) was obtained from the A. D. McKay Co. No chemical analysis was made on this fuse wire because only 3 mg. was consumed per run.

The fluorine used in the calorimetric experiments was purified by distillation in a low temperature still.[5] Mercury titration analysis[14] showed the distilled fluorine to be 99.94% pure. A mass spectrometric analysis of the impurity fraction indicated that the fluorine contained 0.04% oxygen, 0.01% nitrogen, and traces of helium and argon.

Combustion Technique.—Boron crystals larger than 325 mesh could be kept in contact with fluorine for at least four hours with no detectable weight change. Quite large crystals, when ignited, tended to shatter and be scattered away from the combustion zone. A sieved fraction (−100 +325 mesh) was found to give smooth combustion without excessive hot spots if the temperature of the burning boron was lowered by dilution of the fluorine with inerts. A mixture of 2500 mm. of fluorine with 2000 mm. of argon in a 0.35 liter bomb was adequate to ensure essentially complete combustion of the boron sample. To ignite the sample a titanium fuse wire, suspended from nickel electrodes above a mound of boron crystals, was fired electrically. Molten droplets of fuse ignited the boron.

The selection of a suitable sample support material was difficult. High-fired ceramic alumina and massive nickel were tried and rejected because of significant reactions with fluorine near the combustion zone. Ceramic calcium fluoride was chemically satisfactory, but in the commercially available thicknesses it was found to shatter from thermal shock. A satisfactory sample support arrangement consisted of a thin shell of calcium fluoride supported by a massive nickel dish; if the shell was thin enough, it remained intact during the combustion. Each shell was made by melting and spreading 1.5 g. of reagent grade calcium fluoride in a platinum dish; by gentle manipulation the solidified melt could be removed from the platinum without cracking. In several of the runs a secondary support plate of ceramic calcium fluoride was inserted between the shell and nickel dish.

The bomb, with nickel electrodes and nickel dish in place, was treated with one atmosphere of fluorine for eight hours at 110° before the calorimetric series was begun. The bomb and its internal fittings were washed with water and dried after every run. The internal fittings were weighed after each run and were found to lose 0.3 mg. per run. Blank runs have shown that this loss in weight occurs because of exposure of freshly washed nickel surfaces to fluorine rather than as a result of boron combustion.

The boron sample was weighed directly on the calcium fluoride shell; the unburned boron remained on the shell in all acceptable runs. The completeness of combustion was determined by recovery of unburned boron. The combustion residue was heated in 1 *M* aluminum chloride solution to dissolve calcium fluoride. Boron in the undissolved residue was determined by solution in nitric acid and titration as the mannitol complex.[15] In none of the acceptable runs was the amount of unburned boron in excess of 0.30 mg. or 0.2% of the starting sample. Most of the unburned titanium fuse remained attached to the nickel electrodes, but some was found as small beads on the interior bomb surfaces. The beads were gently scraped off, combined with the rest of the recovered fuse, washed with distilled water, dried and weighed.

The product gases from several of the calorimetric runs were discharged into an 8 cm. nickel spectrometer cell with silver chloride windows. The only identifiable bands in the infrared spectrum, other than those of BF_3, were attributable to CF_4 and SiF_4 formed from carbon and silicon impurities in the boron sample.

Results

The data for eight acceptable runs out of a total of 15 made are summarized in Table I. They refer to a standard state temperature of 25°. All energies are expressed in terms of the defined calorie equal to (exactly) 4.1840 absolute joules and all weights were corrected to *in vacuo*. The corrections to standard states were applied in the usual manner[16] with suitable modifications for fluorine bomb calorimetry.[17] The entries in Table I are: (1) the mass of the crystalline boron sample corrected for recovered unburned material; (2) the observed increase in the calorimeter temperature, corrected for heat exchange between the calorimeter and its surroundings; (3) the energy equivalent of the calorimeter multiplied by the corrected temperature increase; (4) the energy absorbed by the contents of the bomb during the hypothetical isothermal process at 25°; (5) the electrical energy input for ignition of the fuse; (6) the energy from the combustion of the titanium fuse; (7) the net correction due to the hypothetical compression and decompression of the bomb gases; (8) the energy change per gram of boron sample burned, with the reactants and products in their respective standard states at 25°; (9) the average energy change per gram of sample for eight experiments; (10) the energy correction per gram of sample for 0.62% impurities in the sample; and (11) the energy change per gram of boron for the reaction

$$B(c,\beta) + 3/2F_2(g) = BF_3(g) \qquad (1)$$

For calculation of item (4) the following heat capacities were used; $C_p = 0.105_8$, 0.245 and 0.205_2 cal. deg.$^{-1}$ g.$^{-1}$ for Ni[18], B(c)[19] and CaF_2[18], respectively; $C_v = 5.50$, 2.983 and 10.07 cal. deg.$^{-1}$ mole^{-1} for F_2[20], Ar[21] and BF_3[19], respectively. For item (6)

---

[11] J. Coops, R. S. Jessup and K. van Nes, "Experimental Thermochemistry," F. D. Rossini, Editor, Interscience Publishers, Inc., New York, N. Y., 1956, Chapter 3.

[12] "Boron Synthesis, Structure, and Properties," J. A. Kohn, W. Nye and G. K. Gauli, Editors, Plenum Press, Inc., New York, N. Y., 1960, p. 38.

[13] J. L. Hoard and A. E. Newkirk, *J. Am. Chem. Soc.*, **82**, 70 (1960).

[14] G. T. Armstrong and F. S. Jessup, *J. Research Natl. Bur. Standards*, **64A**, 49 (1960).

[15] W. W. Scott, "Standard Methods of Chemical Analysis," 5th ed., D. Van Nostrand Co., Inc., New York, N. Y., 1939, p. 176.

[16] W. N. Hubbard, D. W. Scott and G. Waddington, Chapter 5 in ref. 11.

[17] W. N. Hubbard, "Experimental Thermochemistry," Vol. II, H. A. Skinner, Editor, Interscience Publishers, Inc., New York, N. Y., 1961, chapter 5.

[18] "Selected Values of Chemical Thermodynamic Properties," Natl. Bur. Standards Circular 500, U. S. Govt. Printing Office, Washington, D. C., 1951.

[19] W. H. Evans, E. J. Prosen and D. D. Wagman, Chapter V, "Thermodynamic and Transport Properties of Gases, Liquids and Solids," The American Society of Mechanical Engineers, McGraw-Hill Book Co., Inc., New York, N. Y., 1959, p. 226.

TABLE I

RESULTS OF BORON COMBUSTION EXPERIMENTS[a]

(1) m, g.	0.17030	0.17205	0.16335	0.16094	0.16230	0.16097	0.16370	0.16187
(2) Δt_c, deg.	1.18434	1.19610	1.13540	1.12248	1.12903	1.12205	1.13703	1.12409
(3) ϵ (calor.) $(-\Delta t_c)$, cal.	−4228.58	−4270.57	−4053.84	−4007.66	−4031.04	−4006.12	−4059.61	−4013.41
(4) ΔE contents, cal.[b]	−13.65	−14.35	−13.70	−11.24	−11.05	−11.00	−14.98	−13.91
(5) ΔE ignition, cal.	0.20	0.20	0.20	0.20	0.20	0.20	0.20	0.20
(6) ΔE titanium fuse, cal.	18.16	13.23	11.34	14.14	8.22	14.47	11.34	9.78
(7) ΔE gas, cal.[c]	0.15	0.14	0.14	0.12	0.13	0.13	0.14	0.13
(8) $\Delta E_c°/M$, cal. g.$^{-1}$	−24802	−24826	−24829	−24882	−24852	−24864	−24819	−24818
(9) Average $\Delta E_c°/M$ for sample					−24837 cal. g.$^{-1}$			
Std. dev. of mean					±9 cal. g.$^{-1}$			
(10) Energy correction for 0.62% impurities					57 cal. g.$^{-1}$			
(11) $\Delta E_c°/M$ for crystalline boron					−24935 cal. g.$^{-1}$			

[a] The symbols employed are explained in ref. 16. [b] ΔE contents $= \epsilon^{i}(\text{cont.})(t_i - 25) + \epsilon^{f}(\text{cont.})(25 - t_f + \Delta t_{\text{corr.}})$. [c] ΔE gas $= \Delta E^{i}\,(\text{gas})]_0^{P^i(\text{gas})} + \Delta E^{f}\,(\text{gas})]^0_{P^f(\text{gas})}$.

titanium was assumed to burn to TiF_4. The standard heat of formation of TiF_4 has been reported recently by Gross[22] as −393.7 kcal. mole^{-1}. The second virial coefficient and its temperature derivative for the gas mixture are required for the calculation of item 7. They were estimated[23] from the force constants of F_2[24], Ar[23] and BF_3[25]. All other corrections to the standard state were negligible. Item 8, $\Delta E_c°/M$, is just the sum of items 3 through 7 divided by the mass of sample reacted.

The thermal correction for impurities in the sample was made on the following basis. Carbon and oxygen were assumed to be present in the sample as B_4C and B_2O_3, respectively. Hydrogen, iron, manganese, magnesium and silicon were assumed to be present as the elements. The products of these impurities were taken as CF_4, O_2, HF, FeF_3, MnF_2, MgF_2 and SiF_4, respectively. The required heats of formation were taken from reference 18, except for CF_4[26], B_2O_3[27] and B_4C[27].

Derived Data.—The following data were derived for the formation of gaseous BF_3 at 25°

Energy of formation, $\Delta Ef° = \Delta E_c° = -269.80 \pm 0.24$ kcal. mole^{-1}

Heat of formation, $\Delta Hf° = -270.10 \pm 0.24^{1}$ kcal. mole^{-}

Entropy of formation, $\Delta Sf° = -13.38$ cal. deg.$^{-1}$ mole^{-1}

(Gibbs) free energy of formation, $\Delta Gf° = -266.11 \pm 0.24$ kcal. mole^{-1}

The atomic weight of boron was taken as 10.82 g. (g.-atom.)$^{-1}$.[28] The entropies, S^0, at 25° of B(c),[27] BF_3(g)[27] and F_2(g)[29] were taken as 1.42, 60.72 and 48.45 cal. deg.$^{-1}$ mole^{-1}, respectively. The uncertainties given in these estimates are uncertainty intervals[30] equal to twice the combined standard deviations arising from known sources.

Conclusion

The standard heat of formation of gaseous boron trifluoride has been determined to be −270.10 ± 0.24 kcal. mole^{-1} by direct combination of the elements in a nickel bomb calorimeter. The uncertainties in the value derived from the direct reaction are believed to be considerably less than those in the value −270 ± 2 kcal. mole^{-1} derived[4] from heat of solution data, although the values are in essential agreement. Preliminary values of −270.8 and −271.6 kcal. mole^{-1} for two different boron samples have been reported by Gross, *et al.*,[31] who observed the direct combination of the elements in a glass calorimeter. The source of the discrepancy between their results and ours is not apparent at this time.

NOTE ADDED IN PROOF.—The proposed revision of atomic weights to a basis C^{12} = 12.0000 (International Union of Pure and Applied Chemistry, Information Bulletin 14B, 1961) will, when accepted, effect numerous changes in thermochemical constants. If the atomic weight of boron is revised from 10.82 to 10.811 ± 0.003 (the uncertainty includes that due to natural variation in isotopic composition), the derived data should be revised to: $\Delta Ef° = -269.58 \pm 0.29$, $\Delta Hf° = -269.88 \pm 0.29$, $\Delta Gf° = -265.89 \pm 0.29$ kcal. mole^{-1}.

Acknowledgments.—The assistance of Messrs. R. W. Bane, B. D. Holt, J. F. Goleb, R. V. Schablaske and R. J. Meyer in the performance of special analyses is gratefully acknowledged.

---

(20) W. H. Evans, T. R. Munson and D. D. Wagman, *J. Research Natl. Bur. Standards*, **55**, 147 (1955).

(21) "Tables of Thermodynamic and Transport Properties of Air, Ar, CO_2, CO, H_2, N_2, O_2 and Steam," Joseph Hilsenrath, *et al.*, Pergamon Press, New York, N. Y., 1960. p. 75–137.

(22) P. Gross, C. Hayman and D. L. Levi, "XVIIth Int. Congress of Pure and Applied Chemistry, Abstracts," Vol. 1, Inorganic Chemistry, A-405, 1959.

(23) J. O. Hirschfelder, C. F. Curtiss and R. B. Bird, "Molecular Theory of Gases and Liquids," John Wiley and Sons, Inc., New York, N. Y., 1954.

(24) D. White, J. H. Hu and H. L. Johnston, *J. Chem. Phys.*, **21**, 1149 (1953).

(25) G. L. Brooks and C. J. G. Raw, *Trans. Faraday Soc.*, **54**, 972, (1958).

(26) (a) D. W. Scott, W. D. Good and G. Waddington, *J. Am. Chem. Soc.*, **77**, 245 (1955). (b) C. A. Neugebauer and J. L. Margrave, *J. Phys. Chem.*, **60**, 1318 (1956).

(27) W. H. Evans, D. D. Wagman and E. J. Prosen, NBS Report No. 4943, August 1956.

(28) E. Wichers, *J. Am. Chem. Soc.*, **80**, 4121 (1958).

(29) G. B. Skinner and H. L. Johnston, *ibid.*, **73**, 4549 (1951).

(30) F. D. Rossini, Chapter 14, in ref. 11.

(31) P. Gross, C. Hayman, D. L. Levi and M. C. Stuart, Fulmer Research Institute Report No. R146/4/23, Nov. 1960.

IODINE CYANIDE AS A SCAVENGER IN THE RADIOLYSIS OF LIQUID BENZENE[1]

By Gordon Hughes

Department of Inorganic and Physical Chemistry, The University, Liverpool, England

Received June 5, 1961

Decomposition yields in the radiolysis of benzene have been measured using ICN as scavenger. The results are not readily explained in terms only of free radical reactions and indicate that processes of charge (or energy) transfer are taking place.

The radiation chemistry of liquid benzene has been widely investigated.[2-4] The yield of hydrogen gas evolved[2] and the radical yield as measured by conventional scavengers *e.g.*, DPPH,[5] I_2[6] are both low in comparison with the corresponding yields for alkanes. Because of this, benzene has been regarded as fairly inert to radiation damage. Scavenger studies have, in the main, been confined to low concentrations *i.e.*, $<10^{-3}$ *M*, since such studies have been determined largely by considerations of either solubility or of difficulties in product analysis.

It is known, however, that in other systems, *e.g.*, water, the effect of solute concentration may be quite marked. In some cases, ionic precursors of the radical products may be captured at suitably high concentrations of scavenger.[7] It seems desirable then that more information be obtained on the effect of scavenger concentration in benzene.

The use of ICN as a radical scavenger in methanol already has been investigated and results consistent with other scavengers were obtained.[8] The effect of ICN in the radiolysis of benzene now has been investigated. This was thought to be a suitable system for study since ICN is moderately soluble in benzene so that a wider range of concentrations may be investigated. Moreover, since the solution is colorless, the determination of products, *e.g.*, I_2, is straightforward even in the presence of a large excess of scavenger.

Experimental

The experimental details are similar to those outlined in an earlier communication.[8]

Benzene was purified by successive recrystallizations and distillation. Solutions of ICN in benzene were made up by weighing and degassed by freezing, pumping and thawing *in vacuo*. This cycle of operations was repeated three times. The production of I_2 was followed spectrophotometrically, and, in addition, the irradiated solutions were examined for the formation of organic iodide, using $I^{131}CN$, and for organic cyanide, using $IC^{14}N$.

Solutions were irradiated with 0.661 Mev. γ-rays at a dose rate of 1.92×10^{18} e.v./ml./min.

Results

Figure 1 shows the results for the production of I_2. Initially the rate of production of I_2 is independent of dose but decreases at higher doses, this effect being more marked at low concentrations of ICN. Finally, when most of the ICN has reacted, product I_2 is consumed. The initial yield of I_2 increases considerably with ICN concentration but appears to approach a limiting value at high concentrations, as shown in Fig. 2. This effect of concentration is in marked contrast to the methanol system, where $G(I_2)$ was equal to 3.4 and was independent of ICN concentration.[8]

In Fig. 3, the production of organic iodide, as measured by the uptake of I^{131} by the benzene, is compared with the corresponding I_2 production. After a sufficient concentration of iodine has been established ($\sim 5 \times 10^{-5}$ *M*), the production of organic iodide is linear with dose and independent of ICN concentration, and corresponds to $G(\mathrm{RI}) = 0.6$. This is approximately the same value as obtained in the radiolysis of benzene–I_2 solutions, and suggests that similar reactions are occurring in both systems. No attempt was made to identify the organic iodide, but it is likely to be phenyl iodide.

When $IC^{14}N$ was used as a scavenger, extraction of the irradiated liquid with sodium sulfite to remove unreacted $IC^{14}N$, followed by acid hydrolysis, showed the presence of a C^{14} containing solid residue. When inactive phenyl cyanide was added to the irradiated solution prior to hydrolysis, it was shown that the active constituent behaved chromatographically identically with the benzoic acid produced. It may be assumed then that phenyl cyanide is a product of the reaction. It was estimated that $G(\mathrm{PhCN}) \simeq 1$ at 5×10^{-3} *M* ICN.

Discussion

Reactions leading to the production of I_2 in the methanol–ICN system[8] were

$$\mathrm{H} + \mathrm{ICN} \longrightarrow \mathrm{HCN} + \mathrm{I} \qquad (1)$$

$$\mathrm{CH_2OH} + \mathrm{ICN} \longrightarrow \mathrm{CH_2O} + \mathrm{HCN} + \mathrm{I} \qquad (2)$$

However, results in the cyclohexane–ICN system indicated that alkyl radicals, in so far as they do not possess marked reducing properties, did not react with ICN but were consumed by reaction with product I_2.

If the production of I_2 in ICN–benzene solutions is to be explained in terms only of free radical reactions then the magnitude of $G(I_2)$ suggests that hydrogen atoms are produced in appreciable yield. Thus the radiolysis of benzene might be represented formally by the equations

$$\mathrm{C_6H_6} \rightsquigarrow \mathrm{C_6H_5} + \mathrm{H} \qquad (\mathrm{A})$$

$$\mathrm{C_6H_6} \rightsquigarrow \mathrm{P} + 2\mathrm{H} \qquad (\mathrm{A}^1)$$

where process A^1 represents the production of hydrogen atoms accompanied by some non-radical products. Hydrogen atoms then might react as in

---

[1] The work reported in this paper was performed under the auspices of the Atomic Energy Commission.

[2] J. P. Manion and M. Burton, *J. Phys. Chem.*, **56**, 560 (1952).

[3] W. N. Patrick and M. Burton, *J. Am. Chem. Soc.*, **76**, 2626 (1954).

[4] S. Gordon, A. R. Van Dyken and T. F. Doumani, *J. Phys. Chem.*, **62**, 20 (1958).

[5] L. Bouby, A. Chapiro, M. Magat, *et al.*, "International Conference on Peaceful Uses of Atomic Energy, Geneva," 1955, vol. 7, p. 526.

[6] E. N. Weber, P. F. Forsyth and R. H. Schuler, *Radiation Research*, **3**, 68 (1955).

[7] J. H. Baxendale and G. Hughes, *Z. physik Chem.*, **14**, 336 (1958).

[8] G. Hughes and W. M. Garrison, *J. Phys. Chem.*, **64**, 695 (1960).

reaction 1 and phenyl radicals be scavenged by product I_2

$$C_6H_5 + I_2 \longrightarrow C_6H_5I + I \qquad (3)$$

since it is probable that, like alkyl radicals, they would not react with ICN. If the primary process A then is unaffected by the addition of ICN, it would be expected that the yield of phenyl iodide would be the same as that in the benzene–I_2 system. This is observed to be the case and indicates that $G(-C_6H_6)$ *via* process $A \simeq 0.6$. However, in order completely to reconcile the above scheme for the benzene–I_2 system, it must be assumed that all H atoms, at low concentrations of I_2, react *via*

$$H + C_6H_6 \longrightarrow C_6H_7\cdot \qquad (4)$$

and that moreover, the $C_6H_7\cdot$ radical does not react with I_2. This is not surprising since in the process of bond formation the resonance energy of interaction of the unpaired electron with the conjugated double bonds will be lost so that the reaction may not be very exothermic.

The effect of ICN concentration then would be attributed to competition between reactions 4 and 1. There is as yet, however, no good evidence for the production of such a high yield of hydrogen atoms in the radiolysis of benzene. Moreover the mechanism outlined above does not account for the production of phenyl cyanide. It thus would appear that reactions in addition to these simple free radical reactions must be taking place.

It is possible that processes of charge [or energy] transfer may be responsible for the production of I_2. If in addition to the free radical decomposition process A, the radiation decomposition of benzene is represented by

$$C_6H_6 \rightsquigarrow C_6H_6^+ + e \qquad (B)$$

then ICN might act as an efficient electron scavenger, the reaction

$$ICN + e \longrightarrow I + CN^- \qquad (5)$$

being approximately 20 kcal. exothermic in the gas phase. Charge neutralization would lead to

$$C_6H_6^+ + CN^- \longrightarrow C_6H_6CN\cdot \qquad (6)$$

or

$$C_6H_6^+ + CN^- \longrightarrow C_6H_6 + CN\cdot \qquad (7)$$

followed by

$$CN\cdot + C_6H_6 \longrightarrow C_6H_6CN\cdot \qquad (8)$$

It is not possible at present, to distinguish between the above scheme and that involving energy transfer. If excited benzene molecules are formed

$$C_6H_6 \rightsquigarrow C_6H_6^* \qquad (C)$$

(these excited species may be produced directly or by the reaction

$$C_6H_6^+ + e \longrightarrow C_6H_6^* \qquad (9)$$

energy may be transferred and lead to dissociation of the ICN.

$$C_6H_6^* + ICN \longrightarrow C_6H_6 + I + CN \qquad (10)$$

followed by reaction 8. The radical $C_6H_6CN\cdot$ might, like alkyl radicals, be scavenged by I_2. Calculations indicate that of the various possible reactions, the reaction

$$C_6H_6CN\cdot + I_2 \longrightarrow C_6H_5CN + HI + I \qquad (11)$$

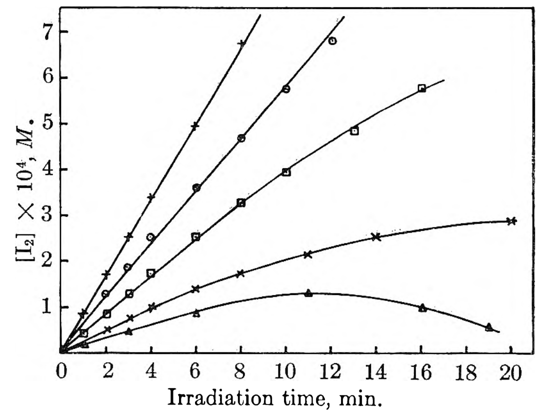

Fig. 1.—Production of I_2 in ICN–benzene solutions. Molarity of ICN: +, 3.6×10^{-2} *M*; ⊙, 1.1×10^{-2} *M*; ⊡, 5.0×10^{-3} *M*; ×, 1.0×10^{-3} *M*; ◬, 5.0×10^{-4} *M*.

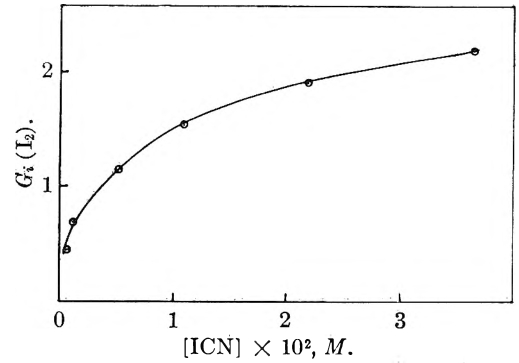

Fig. 2.—Effect of [ICN] on initial yields of I_2.

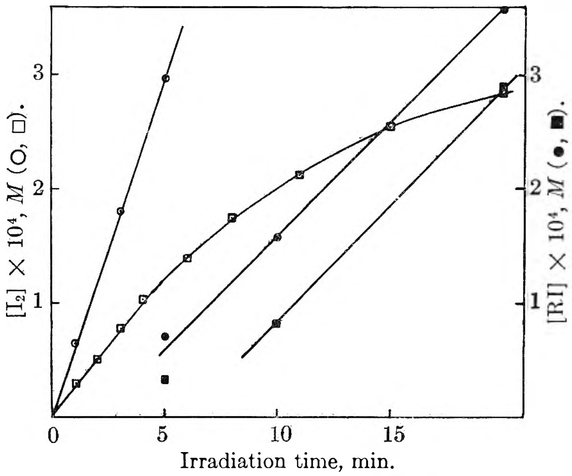

Fig. 3.—Comparison of production of I_2 and RI. Ordinate (open circles and squares), $[I_2] \times 10^4$, *M;* (full circles and squares), $[RI] \times 10^4$, *M*. Abscissa, irradiation time, min. ⊙, ● 1.1×10^{-2} *M* ICN; ⊡, ■ 1.0×10^{-3} *M* ICN.

is the most exothermic. This would be followed by the reaction

$$HI + ICN \longrightarrow I_2 + HCN \qquad (12)$$

which is known to be rapid.[9] On this basis, the products of reaction ought to be phenyl iodide by process A and phenyl cyanide by process B or C. If these are entirely independent processes then $G(C_6H_5I) \simeq 0.6$ and $G(C_6H_5CN) \simeq G(I_2)$. This is in agreement with experimental observations.

The dependence of $G(I_2)$ on ICN concentration

---

[9] R. B. Mooney and H. G. Reid, *J. Chem. Soc.*, 1318 (1933).

then would arise since at low concentrations of ICN the reaction

$$\mathrm{ICN} + e \longrightarrow \mathrm{I} + \mathrm{CN}^- \qquad (5)$$

could not compete so effectively with the reaction

$$C_6H_6^+ + e \longrightarrow C_6H_6^* \qquad (9)$$

If processes of energy transfer are involved, then this implies that the reaction

$$C_6H_6^* + \mathrm{ICN} \longrightarrow C_6H_6 + \mathrm{I} + \mathrm{CN} \qquad (10)$$

is in competition with a reaction

$$C_6H_6^* \longrightarrow \text{products} \qquad (13)$$

It is difficult to state with precision the processes responsible for I_2 production. The results obtained in this work do indicate, however, that reactions other than those normally invoked in the radiation chemistry of benzene must be taking place. It then would appear that the degree of radiation inertness of benzene is very dependent on the nature of the scavenger used.

Since the ionization potential of benzene is not very different from that of hexane, it might be expected that the radiation yields of primary products, *e.g.*, ions and excited molecules, are not very different in the two species. That there is considerable difference in the net decomposition has been attributed to the fact that energy can be distributed readily throughout the benzene ring, thus reducing the localization of energy in any particular bond, and hence the possibility of rupture of that bond. In principle, it ought to be possible, by the choice of suitable scavengers, to measure the yield of primary products.

It is unlikely that iodine would be suitable in detecting ionic precursors since even if an electron were captured

$$I_2 + e \longrightarrow \mathrm{I} + \mathrm{I}^- \qquad (14)$$

charge neutralization with the benzene ion would lead to

$$C_6H_6^+ + \mathrm{I}^- \longrightarrow C_6H_6 + \mathrm{I} \qquad (15)$$

In so far as the iodine atom is chemically fairly unreactive, dimerization to give I_2 would occur

$$\mathrm{I} + \mathrm{I} \longrightarrow I_2 \qquad (16)$$

so that no net decomposition would be observed. The effect of high concentrations of iodine has been examined but little published data are available. The system appears to be complex.[10]

It has been claimed that CF_4 reacts with some ionic intermediate in the radiolysis of benzene–CF_4 solutions,[11] and this might be a promising system for further investigation. The essential characteristic of a suitable scavenger, as ICN, is that processes of charge capture, etc., should lead to the formation of a reactive radical which results in some net decomposition.

Thanks are due to the Bio-organic chemistry group of the Lawrence Radiation Laboratory, University of California, for the irradiation facility and to Dr. W. M. Garrison for valuable discussion during the course of this work.

[10] R. H. Schuler, *J. Phys. Chem.*, **62**, 39 (1958).

[11] P. Y. Feng and L. Mamula, *J. Chem. Phys.*, **28**, 507 (1958).

SOLID–LIQUID PHASE EQUILIBRIA AND SOLID COMPOUND FORMATION IN ACETONITRILE–AROMATIC HYDROCARBON SYSTEMS

By J. Rex Goates, J. Bevan Ott and Allen H. Budge

Department of Chemistry, Brigham Young University, Provo, Utah

Received June 6, 1961

Solid–liquid phase diagrams were obtained from time–temperature cooling curves for the binary systems containing acetonitrile with benzene, toluene and *p*-xylene. A solid phase compound with an incongruent melting point and a composition of one acetonitrile to two benzene molecules was identified in the first of these systems. A number of other acetonitrile–aromatic compounds were screened for possible compound formation. No evidence for 1:2, 1:1 or 2:1 solid compounds was found for acetonitrile with *o*-xylene, *m*-xylene, pseudocumene, anisole, chlorobenzene, nitrobenzene or α,α,α-trifluorotoluene. A solid phase transition in acetonitrile is reported, and the freezing point of acetonitrile is compared with a wide range of values found in the literature.

Prausnitz and Anderson[1] have measured volume changes on mixing for the system acetonitrile–benzene and found an "S" shaped volume change *vs.* composition curve, typical of systems that form stable complexes in the liquid state. They also pointed out that the freezing point measurements of Joukovsky[2] indicate that a solid phase compound may form in this system. Although Joukovsky reported no compound, peculiarities in the graph of his freezing point *vs.* composition data suggest that had the data been more detailed a compound might have been found.

These results suggested an investigation of compound formation in acetonitrile–aromatic compound systems in general. This paper reports the results of an investigation of the solid–liquid phase equilibrium properties of several such systems.

Experimental

Chemicals.—Reagent grade benzene and *p*-xylene were rapidly distilled over sodium metal. The center third cut of each distillation then was fractionally crystallized several times. Phillips Petroleum research grade toluene and Eastman spectro grade acetonitrile were used without special purification. Calculations made on the change of the melting point with fraction melted showed the liquid soluble–solid insoluble impurities to be 0.03 mole % in the benzene, 0.05 mole % in the *p*-xylene, 0.05 mole % in the toluene and 0.20 mole % in the acetonitrile.

A number of other chemicals were used in only a few ex-

[1] J. M. Prausnitz and R. Anderson, private communication.

[2] N. I. Joukovsky, *Bull. soc. chim. Belges*, **43**, 397 (1934).

ploratory measurements to check on the presence or absence of compound formation. These were either reagent or research grade chemicals that were used without further purification.

Temperature Scale.—Temperatures were measured with a Leeds and Northrup calibrated strain-free platinum resistance thermometer in combination with an L. & N. high precision resistance recorder. The calibration was checked against the ice point (273.150°K.); the freezing points of toluene (178.16°K.), mercury (234.29°K.), *o*-xylene (247.97°K.), benzene (278.683°K.) and *p*-xylene (286.41°K.); the transition point of sodium sulfate decahydrate (305.534°K.); and two Bureau of Standards calibrated mercury thermometers (298.15 and 323.15°K.). All melting points were corrected for impurities by using the intercept of the plot of temperature of melting *vs.* the reciprocal of the fraction melted as the true melting point of the compound.

On the basis of these measurements a small linear correction was made on the calibration, after which the Callendar equation gave the correct temperature at the previously mentioned points to within 0.01°, with the exception of *o*-xylene and toluene, which were within 0.05°. On the basis of these checks, the thermometer calibration is considered accurate to at least 0.05° over the range of 175–325°K.

The calibration was rechecked periodically at the mercury freezing point, ice point, and sodium sulfate transition temperature. No changes were found in the resistance of the thermometer even after six months of almost constant cooling and warming.

Apparatus.—The freezing point apparatus was for the most part conventional. Essentially it consisted of a 2.5 × 28 cm. Pyrex tube sealed inside a 5 × 30 cm. tube, with the outer jacket thus formed connected to a 10^{-6} mm. pressure vacuum line. Provision was made to introduce varying amounts of nitrogen gas into the jacket to act as a heat exchanger when desired.

The resistance thermometer sat in a well that went down through the center of the freezing tube. The lower four inches of the well were made of gold-plated copper tubing for rapid heat exchange between the sample and the thermometer; the upper part of the well was made of glass to slow down exchange of heat between the room and the thermometer, and also to allow the upper end of the well to be sealed into a ground glass cap that topped the freezing tube. The exchange fluid in the freezing tube was 2-methylpentane.

Stirring was accomplished with a motor-driven stainless steel coil that moved vertically in the freezing tube at approximately 100 strokes per minute. The stirring wire entered the freezing tube through a section of glass capillary tube sealed into the cap. A flexible plastic sleeve was used to seal the opening between the cap and stirrer, preventing evaporation of sample from, and condensation of moisture into, the sample.

Liquid nitrogen was used as the coolant. Time–temperature cooling curves and occasionally time–temperature melting curves were measured. The solutions generally supercooled, and their freezing points were obtained by extrapolation of the time–temperature curves back across the super-cooled region.

The accuracy of the freezing points of the solutions are estimated to be within ±0.1°. Several of the points along the invariant temperature lines—those with compositions that differed greatly from the eutectic or meritectic composition—had to be obtained without stirring; the uncertainty in such points is considered to be ±1°.

Results

Acetonitrile - Aromatic Systems.—Solid - liquid equilibria data were obtained over the entire range of composition for the three binary systems acetonitrile–benzene, acetonitrile–toluene and acetonitrile–*p*-xylene. The freezing point data for the acetonitrile–benzene system are recorded in Table I, and the phase diagram for this system is shown in Fig. 1. The significant feature in the phase diagram is the meritectic line at 249.15 ± 0.10°K., indicating the presence of a solid phase compound with an incongruent melting point.

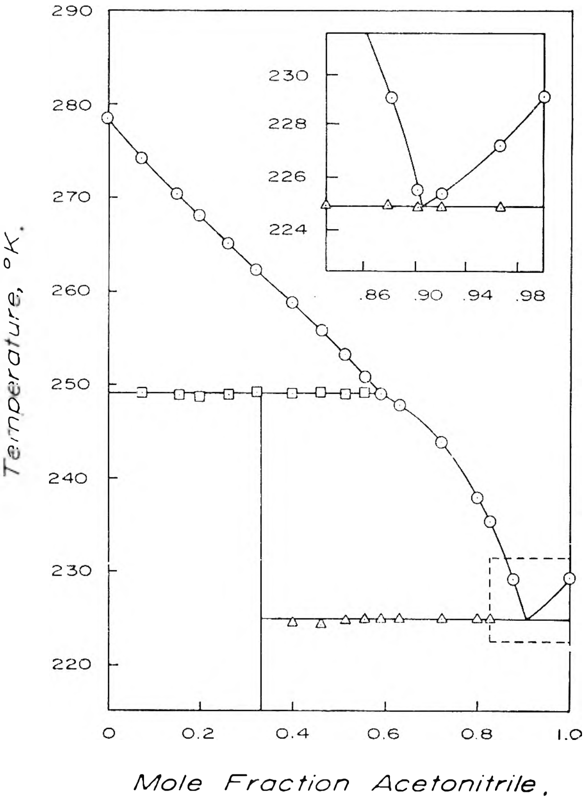

Fig. 1.—Phase diagram of acetonitrile–benzene.

TABLE I

EQUILIBRIUM TEMPERATURES FOR PHASE CHANGES IN THE SYSTEM ACETONITRILE–BENZENE

Mole fraction acetonitrile	Freezing point, °K.	Meritectic point, °K.	Eutectic point, °K.
0.0000	278.66	...	...
.0746	274.38	249.27[a]	...
.1541	270.55	248.95[a]	...
.2009	268.08	248.81[a]	...
.2626	265.15	248.97[a]	...
.3231	262.28	249.19	...
.3993	258.58	249.19	224.48[a]
.4607	255.73	249.16	224.25[a]
.5134	253.14	249.05	224.70
.5574	250.77	249.10	224.73
.5933	249.12	...	224.83
.6305	247.49	...	224.81
.7204	243.80	...	224.83
.8008	237.75	...	224.82
.8256	235.28	...	224.83
.8786	229.09	...	224.83
.8983	225.48	...	224.82
.9200	225.35	...	224.80
.9612	227.18	...	224.72
1.0000	229.30	...	...
0.903 = Eutectic composition	Best value:	249.15 ± 0.1°K.	224.82 ± 0.1°K.

[a] Less accurate values obtained without stirring.

The composition of the compound was determined by plotting the length of the meritectic halt *vs.* mole fraction and extrapolating the two straight lines obtained to their point of intersection. The composition at this point, which is the composition of the compound, is 0.336 mole fraction acetonitrile, or on a molecular ratio basis, two molecules of benzene to one of acetonitrile.

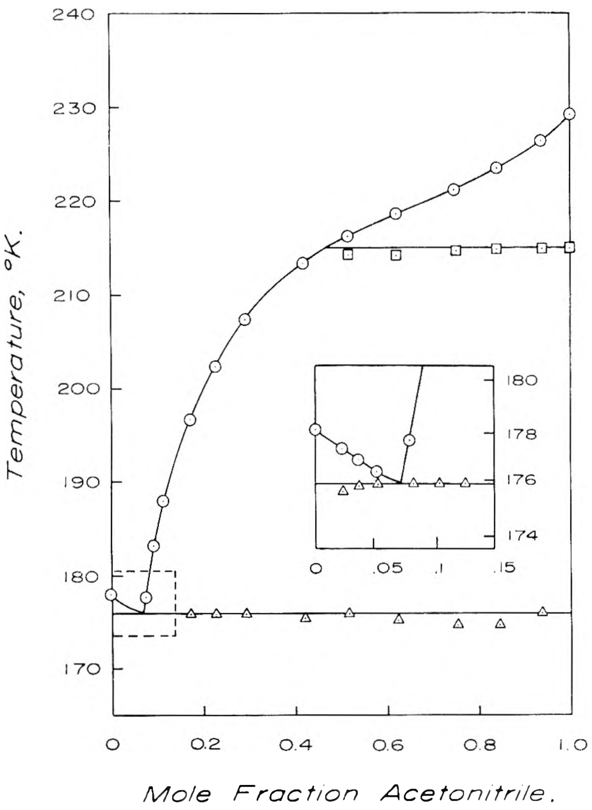

Fig. 2.—Phase diagram of acetonitrile–toluene.

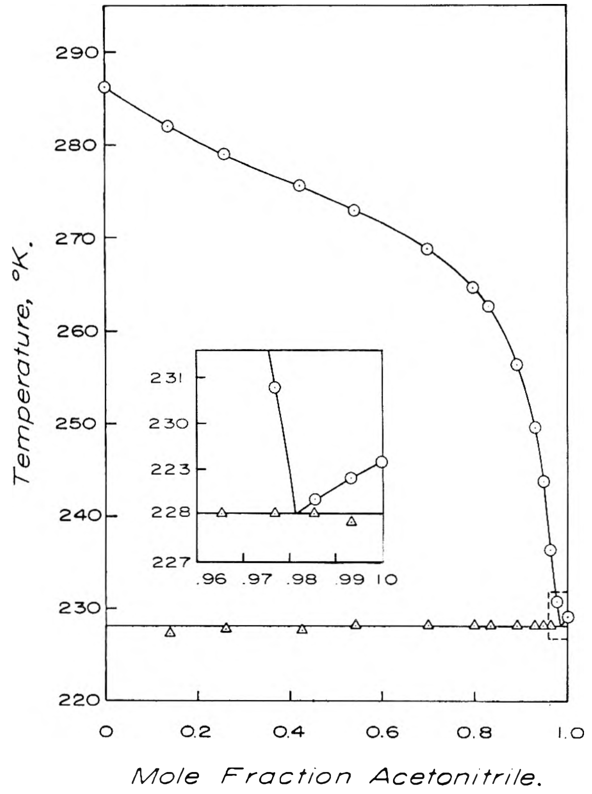

Fig. 3.—Phase diagram of acetonitrile–p-xylene.

The freezing point data for acetonitrile–toluene and acetonitrile–p-xylene systems are recorded in Tables II and III. The phase diagrams for these systems are shown in Figs. 2 and 3. Both systems were investigated very carefully around the compositions corresponding to 1:1 and 2:1 compounds. Very slow cooling, very rapid cooling, and vigorous stirring all were tried. No evidence of compound formation was observed in either system.

TABLE II

EQUILIBRIUM TEMPERATURES FOR PHASE CHANGES IN THE SYSTEM ACETONITRILE–TOLUENE

Mole fraction acetonitrile	Freezing point, °K.	Solid phase transition in acetonitrile, °K.	Eutectic point, °K.
0.0000	178.09	...	...
.0220	177.30	...	175.6
.0317	176.92	...	175.8
.0481	176.39	...	175.8
.0757	177.65	...	175.8
.0953	183.13	...	175.9
.1157	187.78	...	175.9
.1708	196.57	...	175.9
.2297	202.37	...	175.9
.2929	207.40	...	175.9
.4199	213.29	...	175.5
.5180	216.12	214.0	175.8
.6221	218.52	214.1	175.1
.7510	221.16	214.5	174.6^a
.8405	223.23	214.9	174.6^a
.9357	226.18	214.8	175.9^a
1.0000	229.30	215	...
0.073	= Eutectic composition		
	Best value:	215 ± 1 °K.	175.8 ± 0.2° K.

^{a} Less accurate values obtained without stirring.

TABLE III

EQUILIBRIUM TEMPERATURES FOR PHASE CHANGES IN THE SYSTEM ACETONITRILE–p–XYLENE

Mole fraction acetonitrile	Freezing point, °K.	Eutectic point, °K.
0.0000	286.39	...
.1437	282.11	227.39^a
.2608	278.96	227.75^a
.4278	275.36	227.69^a
.5407	272.92	228.07
.7015	268.80	228.10
.8020	264.60	228.10
.8336	262.54	228.10
.8930	256.39	228.10
.9313	249.46	228.09
.9492	243.72	228.10
.9655	236.25	228.09
.9770	230.8	228.09
.9852	228.38	228.04
.9935	228.81	227.87^a
1.0000	229.30	...
0.981	= Eutectic composition	Best value: 228.09 ± 0.10 °K.

^{a} Less accurate values obtained without stirring.

The acetonitrile–toluene system shows a solid transition in the acetonitrile at 215 ± 1 °K. The large uncertainty in the transition temperature occurs because the phase that is stable at the higher temperature supercooled considerably, and even after conversion to the second phase started the rate was slow, requiring several minutes for completion. To obtain a more accurate value, the transition temperature would need to be measured in an apparatus in which the sample could be better thermally insulated from its surroundings.

Exploratory measurements were made on mixtures of several other aromatic hydrocarbons with acetonitrile to check on the possibility of compound formation. The procedure consisted of obtaining freezing curves at several compositions. If all curves showed the same eutectic temperature with no other temperature halts or irregularities, it was concluded that no solid compound existed in the range between the extreme compositions studied. The results are summarized in Table IV.

TABLE IV

ACETONITRILE–AROMATIC SYSTEMS SCREENED FOR SOLID PHASE COMPLEXES

Aromatic component	Range of composition investigated, mole fraction acetonitrile
o-Xylene	0.30–0.69
m-Xylene	.31– .70
Pseudocumene	.31– .94
Anisole	.37– .75
Chlorobenzene	.27– .66
Nitrobenzene	.25– .79
α,α,α-Trifluorotoluene	.25– .74

The hydrocarbons were chosen so as to have a variety of geometrical structures and both low and high electron density in the ring. The range in composition investigated included compositions corresponding to 1:2, 1:1 and 2:1 complexes. No evidence for solid state compound formation was found in any of these mixtures.

Freezing Point of Acetonitrile.—We obtained a value for the freezing point of pure acetonitrile of 229.30 ± 0.05 °K. Eight measurements were made at varying rates of cooling and on samples of acetonitrile from two different lot numbers. The measurements all agreed within 0.02°. This freezing point may be compared with the following values found in the literature: 228.25,[3] 228.15,[2] 227.95,[4] 227.43[5] and 229.28.[6]

The agreement with the last value, obtained by Mathieu,[6] is satisfying. The fact that some of the other values are more than a degree and a half lower is unusual. The solid transition at lower temperatures suggests the possibility that some of the others may have measured a metastable freezing point. However, all attempts by us to supercool the acetonitrile to obtain the metastable freezing point failed.

Acknowledgment.—The authors gratefully acknowledge the support given this project by the National Science Foundation and Research Corporation of America.

---

[3] B. E., *Trav. Bur. Int. Et. Phys.-Chim. Bruxelles, J. chim. phys.*, **27**, 401 (1930).

[4] M. Ewert, *Bull. soc. chim. Belges*, **46**, 90 (1937).

[5] R. R. Dreisbach, "Physical Properties of Chemical Substances," Dow Chemical Co., Midland, Michigan, 1952.

[6] M. P. Mathieu, *Acad. roy. Belg., Classe sci. Mem. Collection in-8*, **28**, No. 2 (1953).

LEAST SQUARES COMPUTER CALCULATIONS OF CHLORIDE COMPLEXING OF TIN(II), THE HYDROLYSIS OF TIN(II), AND THE VALIDITY OF THE IONIC MEDIUM METHOD[1]

BY R. STUART TOBIAS AND Z Z. HUGUS, JR.

Department of Chemistry, University of Minnesota, Minneapolis 14, Minnesota

Received June 15, 1961

The stability constants of the chloro-complexes of Sn^{+2} have been redetermined at 25° for a perchlorate medium at an ionic strength of 3 by e.m.f. measurements using a cell with a tin amalgam electrode. A computer program which permits the assignment of weights to all experimentally determined quantities is outlined and applied to the computation of the constants. The values for the cumulative stability constants are $\beta_1 = 15.12 \pm 0.25\ M^{-1}$, $\beta_2 = 54.9 \pm 2.1\ M^{-2}$, $\beta_3 = 47.3 \pm 4.2\ M^{-3}$ (standard errors). No evidence was found for mixed chlorohydroxo-complexes in solutions with $[H^+]$ from 0.05 to 0.50 M, nor was there any evidence for polynuclear complexes involving chloride bridges.

Introduction

Recently Rabideau and Moore[2] have presented results of least squares calculations of the stability constants of the chloro-complexes of Sn^{+2} using the data of Duke and Courtney[3] and Vanderzee and Rhodes.[4] The first set of data was satisfactorily fitted by three constants for the mono-, di- and trichloro-complexes instead of the four constants given in the original paper. These values apply to a medium 2 M in $[H^+]$ with an ionic strength of 2.03. The total tin(II) concentration was not held constant during the measurements. In the studies of Vanderzee and Rhodes, the total tin(II) concentration was held constant at approximately 0.01 M in a medium with an ionic strength of 3.00. The least squares fitting was carried out with data for solutions with 0.100 and 0.500 M $[H^+]$ and for measurements at four different temperatures. The data for each different temperature and $[H^+]$ were fitted with three parameters corresponding to the coefficients in the power series expansion

$$\exp(-nFE/RT) = 1 + A_1[Cl^-] + \cdots + A_n[Cl^-]^n$$

If only mononuclear chloro-complexes are formed, the parameters are the stability constants; how-

---

[1] This work was supported, in part, by the United States National Science Foundation under grant NSF-14173.

[2] S. W. Rabideau and R. H. Moore, *J. Phys. Chem.*, **65**, 371 (1961).

[3] F. R. Duke and W. G. Courtney, *Iowa State Coll. J. Sci.*, **24**, 397 (1950).

[4] C. E. Vanderzee and D. E. Rhodes, *J. Am. Chem. Soc.*, **74**, 3552 (1952).

ever, significantly different values were found for the two different total hydrogen ion concentrations. Vanderzee and Rhodes interpreted this as evidence for the hydrolysis of tin(II) accompanied by the formation of Sn(OH)Cl, and they used the dependence on $[H^+]$ to calculate the value $2 \times 10^{-2} M$ for the equilibrium constant of $Sn^{+2} + H_2O \rightleftarrows SnOH^+ + H^+$. Rabideau and Moore found, however, that the variation of the parameters determined by the least squares method did not give consistent values for the hydrolysis constant.

Some time ago, one of us published a rather detailed study of the hydrolysis of Sn^{+2} in a medium with the total perchlorate concentration held constant at 3.00 *M*.[5] The lowest total tin(II) concentration studied was 0.0025 *M*, and it was found at this and all higher total tin(II) concentrations that the protolysis of the aquo Sn^{+2} cation was followed by a very rapid condensation of the conjugate base to yield mainly a trimeric species. Because of the pronounced tendency to polymerize, it was possible to get a maximum of only about 8% of the total tin in the form of the mononuclear species $SnOH^+$ even in the most dilute Sn^{+2} solutions. For this reason the value of the constant for the formation of $SnOH^+$, $1 \times 10^{-4} M$ was not accurately determined. Nevertheless, the experimental measurements showed no significant hydrolysis with 0.01 *M* total tin(II) at a hydrogen ion concentration greater than about 3×10^{-2} *M*, and the hydrolysis constant given by Vanderzee and Rhodes to account for the variation in the *A* parameters appeared to be much too large.

Knowledge of the species present in these tin solutions is of value in the interpretation of rates of tin(II)–tin(IV) exchange reactions and rates of oxidation of tin(II) by various reagents, in the calorimetric determination of ligational enthalpies and entropies, and in the interpretation of the absorption spectra of tin solutions. In this respect, it is interesting to note that it has been proposed that the variation in the molar extinction coefficient of Sn(II) in hydrochloric acid solutions as the concentration of HCl is decreased from 12 to 3 *M* is a result of the hydrolysis of Sn^{+2}.[6] The extinction coefficient variations in perchloric and sulfuric acid solutions varying from 1 to 10 *M* in $[H^+]$ also have been attributed to the formation of $SnOH^+$, and a value of 24.5 ± 1 *M* was given for the first hydrolysis constant.[7]

Vanderzee and Rhodes also suggested that substitution of H^+ for Na^+ at constant ionic strength might affect the *A* parameters because of changes in species activities; however they felt that this was not the major cause of the variation in the parameters. Some years ago, it was suggested that probably half of the stability constants reported in the literature were erroneous because of activity variations caused by such medium changes.[8] Since it did not seem likely that mixed chlorohydroxo-complexes were being formed, it appeared that this system might be one in which the constant ionic medium method[9] was proving unsatisfactory.

It also is to be noted that the values obtained by Rabideau and Moore from the data of Duke and Courtney and from those of Vanderzee and Rhodes differ much more than one would anticipate on the basis of any reasonable errors in the determination of the solution concentrations and the potential measurements coupled with the change in the medium.

Considering all of these uncertainties about the species present in tin(II) solutions, it appeared necessary to re-examine the tin(II) chloride system over a wider range of variables before proceeding with further studies on tin(II)–tin(IV) systems. Improved circuits are now generally available for highly accurate e.m.f. measurements, and the use of high speed digital computers makes it possible to carry out least squares calculations of equilibrium constants with many more data items than would normally have been feasible. Stability constants can be obtained with higher accuracy and false hypotheses more easily discarded.

Experimental

Preparation of Solutions.—The Sn^{+2} solutions were prepared by displacement of Cu^{+2} by tin metal in an oxygen-free system which allowed the $Sn(ClO_4)_2$ solutions to be transferred to a storage flask in the thermostat and from there to the buret, all under an atmosphere of nitrogen. The e.m.f. measurements were begun immediately after the tin solutions were prepared. The general design of the apparatus and the preparation of the Sn^{+2} solutions have been described earlier[5]; the latest modification of the preparation train had all ground glass joints and Teflon stopcocks. Copper was determined in the $Cu(ClO_4)_2$ solutions by titration with EDTA using murexide as an indicator. All solutions were prepared from freshly boiled distilled water, and nitrogen gas was passed through the $Cu(ClO_4)_2$ solution for an hour before it was reacted with the metallic tin. The preparation of the tin metal, tin amalgams, the preparation and standardization of the sodium and silver perchlorate solutions, and the purification of the nitrogen gas all have been described earlier.[5] Sodium chloride solutions were standardized by evaporation and drying to a constant weight and also gravimetrically as AgCl. Hydrochloric acid solutions were standardized gravimetrically as AgCl.

E.m.f. Measurements.—The design of the electrochemical cell and the experimental procedure were similar

$$\begin{array}{l} \text{Sn, Hg(satd.)}\,|\text{Tin(II) soln.}\,||3.000\ M\ \text{NaClO}_4\,||0.010\ M \\ \qquad\qquad\qquad\qquad\qquad \text{Ag}^+,\ 2.990\ M\ \text{Na}^+ \quad (1) \\ \qquad\qquad 3.000\ M\ \text{ClO}_4^-\,|\text{AgCl}\,|\text{Ag} \end{array}$$

to that used in the study of the hydrolysis of Sn^{+2} in a perchlorate medium.[5] The titrations were carried out by adding two solutions, one an acidic $Sn(ClO_4)_2$ solution and the other a NaCl or a NaCl–HCl solution. The ionic strength of all solutions was adjusted to 3.00 with $NaClO_4$, and they were deoxygenated prior to use by bubbling nitrogen through them. The measurements with the dilute acid solutions were made with a Rubicon type B potentiometer and a spot light galvanometer, and the data with the 0.5 $M[H^+]$ solutions were determined with a potentiometer-vibrating reed electrometer circuit. A Leeds and Northrup K-3 potentiometer was used to balance all but 1 mv. of the cell e.m.f., and a Cary 31-V electrometer with a Varian G 11-A recorder was used as a null point detector. In this way, when the potentiometer is out of balance by 1 mv., a full scale deflection is registered on the recorder chart. This provides a very sensitive method of determining any drift in the potential values with time. Peak to peak noise was usually of the order of 10 μv.; however, it was not unusual for the potentials to fluctuate over several

---

[5] R. S. Tobias, *Acta Chem. Scand.*, **12**, 198 (1958).

[6] C. I. Browne, R. P. Craig and N. Davidson, *J. Am. Chem. Soc.*, **73**, 1946 (1951).

[7] G. Gordon and C. H. Brubaker, Jr., *ibid.*, **82**, 4448 (1960).

[8] T. F. Young and A. C. Jones, *Ann. Rev. Phys. Chem.*, **3**, 275 (1952).

[9] L. G. Sillén, *J. Inorg. & Nuclear Chem.*, **8**, 176 (1958).

hundredths of a mv. during an hour without showing any consistent drift. The potentials were usually constant within 0.1 mv. overnight. The entire Sn^{+2} preparation train, the electrochemical cell and thermostat, and the electrometer head all were enclosed within an aluminum cabinet serving as a Faraday cage. The oil-bath thermostat was controlled to 25.0 ± 0.1° by pumping water from an external thermostat through copper coils in the oil-bath; an air-driven stirring motor was used for agitation.

Computational Procedure

Input Information.—The usual Leden graphical procedure[10] for treating $C_{Sn(II)}/[Sn^{+2}]$, where $C_{Sn(II)}$ is the total tin concentration and $[Sn^{+2}]$ the equilibrium concentration of the aquo-tin cation, was used to obtain preliminary values for the cumulative stability constants. As a first approximation, it was assumed that $C_{Cl^-} = [Cl^-]$ where C_{Cl^-} is the total chloride concentration and $[Cl^-]$ the equilibrium chloride ion concentration. These preliminary β's together with the sets of data E, σ_E, C_{Cl^-}, σC_{Cl^-}, $C_{Sn(II)}$, $\sigma C_{Sn(II)}$ were used as input for a computer program using the Univac Scientific (ERA 1103) Computer at the University of Minnesota. E is the difference in the potential values of cell (1) with total chloride concentration C_{Cl^-} and with no chloride ion. The σ's are estimated errors in the experimentally determined quantities and were based on the replication experiments and the anticipated errors in the analytical data.

Computation of the β's.—The first step in the program was the calculation of preliminary values for $[Cl^-]$ using the stoichiometric mole balance condition for chloride ion

$$C_{Cl^-} = [Cl^-] + \sum_{n=1}^{N} n\beta_n[Sn^{+2}][Cl^-]^n \qquad (2)$$

The values of $[Sn^{+2}]$ were obtained directly from the input E values, the preliminary β's were used, and values for $[Cl^-]$ were calculated by a Newton–Raphson iteration.[11]

The residuals for the least squares analysis are obtained from the other mole balance condition, that for the total tin(II)

$$C_{Sn(II)} = [Sn^{+2}] + \sum_{n=1}^{N} \beta_n[Sn^{+2}][Cl^-]^n \qquad (3)$$

and the function to be minimized is

$$S = \frac{\sum_{i=1}^{I} w_i(-C_{Sn(II)i} + [Sn^{+2}]_i + \beta_n[Sn^{+2}]_i[Cl^-]_i^{\,n})^2}{\sum_{i=1}^{I} w_i} \qquad (4)$$

In order to obtain the normal equations, the exact residuals are replaced by approximate residuals obtained by expanding the expression for $C_{Sn^{+2}}$ in a power series in the small corrections to be applied to the preliminary β's, neglecting terms of degree higher than the first. The reciprocal of the variance σ_i^2 is chosen for the weight w_i. The variance of the quantity, the residual of which appears in (4), is computed using the provisional β values and the variances $\sigma^2 C_{Sn(II)}$, $\sigma^2 E$ and $\sigma^2 C_{Cl^-}$. If G is the residual in (4), then

$$\sigma^2_G = \left(\frac{\partial G}{\partial C_{Sn(II)}}\right)^2 \sigma^2 C_{Sn(II)} + \left(\frac{\partial G}{\partial E}\right)^2 \sigma^2_E + \left(\frac{\partial G}{\partial [Cl^-]}\right)^2 \left[\left(\frac{\partial [Cl^-]}{\partial C_{Cl^-}}\right)^2 \sigma^2 C_{Cl^-} + \left(\frac{\partial [Cl^-]}{\partial C_{Sn(II)}}\right)^2 \sigma^2 C_{Sn(II)} + \left(\frac{\partial [Cl^-]}{\partial E}\right)^2 \sigma^2_E\right] \qquad (5)$$

The partial derivatives of G are obtained from the mole balance condition for tin (3), and the partials of $[Cl^-]$ are obtained from the mole balance condition for chloride ion. The elements of the matrix formed from the coefficients of the adjustments to the β's in the normal equations are computed, the matrix is inverted, and it then is multiplied into the column vector formed from the constant terms in the normal equations to give the column vector, the elements of which are the adjustments to the β's. The standard errors in the constants were calculated from the relation

$$\sigma^2\beta_n = A_{nn}^{-1}\frac{S}{I - N}$$

where A_{nn}^{-1} is the nth diagonal element in the inverse matrix, S is obtained from (4) with the calculated constants, and $I-N$ is the number of degrees of freedom. The entire cycle of calculations then is repeated in an iterative procedure until convergence is obtained.

The final set of constants together with the final iterated values for $[Cl^-]_i$ and the $C_{Sn(II)i}$ are used in the mole balance expression for tin (3) to calculate values for $[Sn^{+2}]_i$ and hence for the e.m.f. values E_i.

In these calculations σC_{Cl^-} was taken as ±0.4% of the total chloride, and $\sigma_{C_{Sn(II)}}$ was taken as ±0.4% of the total tin(II) concentration. σ_E was estimated from duplicate experiments and observations of the fluctuations in the potentials recorded on the strip charts. The values rose to a maximum of ± 0.5 mv when $0.03\ M < C_{Cl^-} < 0.16\ M$ and then decreased to ± 0.1 mv. for $C_{Cl^-} > 0.28\ M$.

Results

The data are plotted in Fig. 1 as $\eta = \log(C_{Sn(II)}/[Sn^{+2}])$ as a function of the iterated equilibrium chloride ion concentration. The back titration points correspond to a dilution of the tin(II)–chloride system with $Sn(ClO_4)_2$ solution and indicate that the equilibria are reversible. Slow changes are absent, since 3 hours elapsed between the readings. The interesting feature of these data is the absence of any trend in the points as the total analytical hydrogen ion concentration is varied from 0.05 to 0.50 M while maintaining the ionic strength constant at 3.00. Two runs were made with 0.005 M total tin(II) in order to determine if there were any interference from chloride ion bridging to form polynuclear complexes. The points describe the same curve as the 0.01 M tin(II) data and hence polynuclear complexes are absent. These measurements could not be extended to as high ligand concentrations as with the more concentrated tin(II) solutions, for the potentials became erratic at high chloride ion

---

[10] I. Leden, *Z. physik. Chem.*, **A188**, 160 (1941); dissertation, Lund, 1943; see, *e.g.*, J. C. Sullivan and J. C. Hindman, *J. Am. Chem. Soc.*, **74**, 6091 (1952).

[11] E. Whittaker and G. Robinson, "The Calculus of Observations," Fourth Edition, Blackie and Son, Glasgow, 1944, p. 84–87.

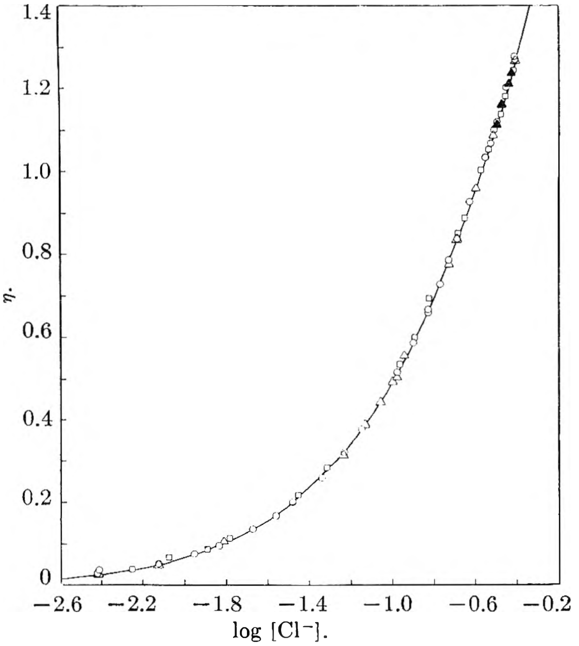

Fig. 1.—η as a function of log [Cl^-]. Concentrations are in moles per liter. The curve is calculated with the set of constants reported in Table I. Δ, data from two runs with [H^+] = 0.500 *M*; □, data from two runs with [H^+] = 0.100 *M*; ○, data from two runs with [H^+] = 0.050 *M*. Only about $^1/_3$ of the experimental points, selected at random, are shown for clarity; ▲, data obtained by dilution with $Sn(ClO_4)_2$–$NaClO_4$ solutions.

concentrations. For this reason, these points were not included in the least squares analysis.

A set of 171 data items was treated in the least squares computation of the equilibrium constants. Since the maximum value of the average ligand number, $\bar{n}$, which was attained in these measurements was about 1.75, the data were fitted in terms of three constants. An attempt to fit them in terms of 4 constants for the mono-, di-, tri- and tetrachloro-complexes gave a negative value for β_4. The average ligand number is given by the slope of the curve in Fig. 1 at a given ligand concentration. The values of the cumulative equilibrium constants for the mono-, di- and trichloro-complexes together with their standard errors are given in Table I. Least squares constants also were calculated from the data of Vanderzee and Rhodes[4] and are included for comparison.

Table I

The Cumulative Stability Constants for the Mono-, Di- and Trichloro-complexes of Sn^{+2} Obtained by the Least Squares Computation

This work	$\beta_1 = 15.12 \pm 0.25\ M^{-1}$
	$\beta_2 = 54.9 \pm 2.1\ M^{-2}$
	$\beta_3 = 47.3 \pm 4.2\ M^{-3}$
Vanderzee and Rhodes	
0.100 *M* [H^+]	$A_1 = 12.98 \pm 0.10\ M^{-1}$
	$A_2 = 44.7 \pm 1.0\ M^{-2}$
	$A_3 = 32.4 \pm 1.7\ M^{-3}$
0.500 *M* [H^+]	$A_1 = 13.71 \pm 0.08\ M^{-1}$
	$A_2 = 49.7 \pm 0.8\ M^{-2}$
	$A_3 = 45.7 \pm 1.4\ M^{-3}$

It should be noted that the standard deviations given for the data of Vanderzee and Rhodes do not indicate the reliability of the constants, since only smoothed data were reported. The data were also insufficient to permit the assignment of weights to all of the experimental parameters, so all of the error was assumed to be in the e.m.f. values; and $\sigma_E = \pm 0.2$ mv. was assigned. This procedure gives virtually the same sets of constants reported for these data by Rabideau and Moore[3] who, in addition, re-evaluated the data of Duke and Courtney and obtained $\beta_1 = 11.4 \pm 0.26\ M^{-1}$, $\beta_2 = 52.3 \pm 1.8\ M^{-2}$, and $\beta_3 = 31.4 \pm 2.3\ M^{-3}$ by a least squares procedure assuming $C_{Cl^-} = [Cl^-]$. Again the standard deviations indicate only the goodness of the fit of a single set of data and not the reliability of the constants. These data were insufficient for use with the computer program described here, since the total tin(II) concentration is given only for the first point in the titration; values cannot be calculated for the other points as the tin(II) solution is diluted by the addition of the chloride solution, for no volume data are given.

The standard errors, σ, of the constants obtained in this work should give a reliable estimate of the accuracy of the constants. Since the number of degrees of freedom is so large, 168, tables of the "*t*" test of significance[12] can be entered using an infinite number of degrees of freedom. Thus 0.674σ is the probable error at the 50% confidence level and 2.576σ is the error at the 99% confidence level.

Discussion

The lack of any evidence for the formation of mixed chlorohydroxo-complexes explains the inability of Rabideau and Moore to obtain consistent values for the hydrolysis constant from the data of Vanderzee and Rhodes. The constants determined in this work for the chloride complexing are slightly larger than those obtained from the data of Vanderzee and Rhodes in the most acid solutions. The values for the smoothed potentials reported by these authors differ by about 4% at high chloride concentrations for the solutions with 0.5 and 0.1 *M* [H^+]. In this work almost all of the e.m.f. values were reproduced within 0.3% at high chloride concentrations by the three constants even though the analytical hydrogen ion concentration was varied by a factor of 10. The values of β_1 and β_3 obtained from the data of Vanderzee and Rhodes are, in turn, considerably larger than the values obtained from the data of Duke and Courtney. The presence of tin(IV) seems to be the most likely reason for these discrepancies, since Duke and Courtney took no special precautions to prevent contamination with tin(IV).

If the simplest ionic model is used to predict the stability of the hydroxo-complex $SnOH^+$ as compared to $HgOH^+$, one would expect similar stability constants for these complexes. The crystal

---

(12) R. A. Fisher, "Statistical Methods for Research Workers," Hafner Publishing Co., New York, N. Y., 1954, p. 174.

radii of Sn^{+2} and Hg^{+2} are given by Wyckoff[13] as 1.02 and 1.04 Å., respectively, and these can be used to approximate the cation radii in the complexes. The hydrolysis of Hg^{+2} has been carefully studied,[14] and one can calculate the value 2×10^{10} M^{-1} for the stability constant of $HgOH^+$ in 0.5 M $NaClO_4$. The hydrolysis constant reported by Vanderzee and Rhodes for a medium with an ionic strength of 3.00 corresponds to a stability constant of 2×10^{12} M^{-1} for $SnOH^+$. The suggestion that Sn^{+2} is hydrolyzed to a significant extent in solutions with a hydrogen ion concentration of 3 M and larger seems even more implausible. The hydrolysis constant reported earlier,[5] which corresponds to a stability constant of 1×10^{10} M^{-1} for $SnOH^+$, is more consistent with this model and the results of this investigation.

This simple ionic model is, however, insufficient to account for the details of the aquo-acidity of Sn^{+2} and Hg^{+2}. The constant for the formation of aqueous $Hg(OH)_2$ from $HgOH^+$ is larger than the formation constant for $HgOH^+$ from the aquo-cation, and no polynuclear complexes are formed. The Hg^{+2} ion frequently forms compounds with two strong bonds at an angle of 180°, and this would account for the hydrolytic behavior. On the other hand, the strength of Sn^{+2} as an aquo-acid is principally a result of the rapid polymerization of the mononuclear conjugate base. The Sn^{+2} ion is known to deviate from spherical symmetry in solid compounds containing tin–oxygen bonds, and this can be explained by the addition of "p" character to the lone pair of 5s electrons[15] giving a "pear shaped" ion. This would tend to account for the formation of two or more strong bonds to oxygen which are directed in such a way as to permit polymerization by ring formation in solution. The Cd^{+2} ion which differs only by the absence of the pair of 5s electrons is an extremely weak aquo-acid; the stability constant for the formation of $CdOH^+$ is only 10^5 M^{-1}.[16]

The absence of any measurable variation in the $\eta([Cl^-])$ curves as H^+ was substituted for Na^+ is encouraging. This indicates that so long as one works with a high concentration of supporting electrolyte, *e.g.*, 3 M, and does not make any more drastic change in the medium than the substitution of up to 16% of one univalent cation by another, activity coefficient effects will be small. It must, of course, be assumed in the interpretation of the data in this work that the substitution of up to 15% of the medium ClO_4^- ions by Cl^- also has a negligible effect on the species activity coefficients.

In the course of this investigation with $Sn(ClO_4)_2$ solutions we have found it essential to carry out the entire procedure for the preparation, handling, and titration of the tin(II) solutions in a glass system with oxygen carefully excluded. Tin(II) perchlorate solutions are strong and fairly rapid reducing agents, and the tin(II)–tin(IV) potential is undoubtedly more positive than the value $E^0_{ox} = -0.15$ v. given in the literature[17] because of the extensive polymerization of tin(IV) hydrolysis products in perchlorate solutions.[18] Exposure of $Sn(ClO_4)_2$ solutions to the atmosphere for short periods of time gave rise to a strong absorption in the blue region of the spectrum, presumably the result of a tin(II)–tin(IV) interaction complex with hydroxo or oxo bridging groups.

Conclusions

The measurements described above show that only the mono-, di- and trichloro-complexes of Sn^{+2} need be considered in systems with $[Cl^-] \leq 0.4$ M and $[H^+] \geq 0.05$ M. No evidence was found for $Sn(OH)Cl$ as required by Vanderzee and Rhodes to fit their data, and this accounts for the inability of Rabideau and Moore to obtain a consistent hydrolysis constant from those data using least squares calculations. The absence of mixed chlorohydroxo complexes in these solutions is in accord with predictions based on ionic models and with independent studies on the hydrolysis of $Sn(ClO_4)_2$ solutions.

---

[13] R. W. G. Wyckoff, "Crystal Structures," Interscience Publishers, New York, N. Y., 1948; $r_{Hg^{2+}}$ calculated from the HgF_2 distance.

[14] S. Hietanen and L. G. Sillén, *Acta Chem. Scand.*, **6**, 747 (1952).

[15] L. E. Orgel, *J. Chem. Soc.*, 3815 (1959).

[16] Y. Marcus, *Acta Chem. Scand.*, **11**, 690 (1957).

[17] W. M. Latimer, "The Oxidation States of the Elements and Their Potentials in Aqueous Solution," 2nd Edition, Prentice-Hall Inc., New York, N. Y., 1952.

[18] J. S. Johnson and K. A. Kraus, *J. Phys. Chem.*, **63**, 440 (1959).

THE KINETICS OF THE THERMAL DECOMPOSITION OF METHYLENECYCLOBUTANE[1]

BY JOHN P. CHESICK

Contribution 1668 from the Sterling Chemistry Laboratory, Yale University, New Haven, Conn.

Received June 13, 1961

Methylenecyclobutane undergoes a homogeneous thermal decomposition to allene and ethylene. This reaction has been studied in the gas phase by static methods from 430 to 470° over a pressure of 0.1 to 25 mm. The reaction is first order with a high pressure rate constant $k = 4.76 \times 10^{16} \exp(-63.3 \text{ kcal.}/RT) \text{ sec.}^{-1}$ At low pressures the rate decreases as predicted for unimolecular reactions in pressure regions where collisional activation starts to become rate controlling. Added nitrogen has the effect of increasing the rate in the low pressure region.

Introduction

In a study of the thermal isomerization of [0,1,2]-bicyclopentane to cyclopentene,[2] it was of interest to know whether a possible product, methylenecyclobutane, was capable of thermal rearrangements to cyclopentene. It was also of interest to investigate the effects of the exocyclic double bond on the stability of the cyclobutane ring through determination of the activation energy for decomposition reactions. Turner's value[3] for the ΔH of hydrogenation of methylenecyclobutane to methylcyclobutane of -29.43 kcal./mole indicated that there should be about 2.5 kcal./mole extra ring strain introduced by the double bond based on the difference in heats of hydrogenation of methylenecyclobutane and methylenecyclopentane.

The thermal reactions of some methylenecyclobutane compounds have been studied. Knoth and Coffman[4] have used the pyrolysis of acetoxymethyl-2,2,3,3-tetrofluorocyclobutane as a way of preparing 1,1-difluoroallenes. This reaction appeared to go through the intermediate methylenecyclobutane. Cripps, *et al.*,[5] have studied the synthesis of substituted methylenecyclobutanes by the addition of allene to various substituted olefins at temperatures from 100 to 250°.

Walters has measured the kinetics of the decompositions of some alkylcyclobutanes which yield ethylene and the appropriate mono-olefin.[6]

Ethylene has been detected as a product of the vacuum ultraviolet irradiation of methylenecyclobutane.[7] However, no gas phase thermal reactions of the unsubstituted methylenecyclobutane have been reported. A kinetic study of the thermal decomposition of methylenecyclobutane therefore was made and is described here.

Experimental

Two samples of methylenecyclobutane were used in this work. The first sample[8] was prepared by the zinc dust debromination of pentaerythrityl tetrabromide and as received contained about 5% spiropentane as an impurity, which was removed by a gas chromatographic separation employing a 30-cm. preparative column packed with silver nitrate in ethylene glycol on 60–80 mesh firebrick. A second batch of methylenecyclobutane was purchased from Columbia Organic Chemicals and was of about 60% purity. This material likewise was purified by gas chromatographic separations using the silver nitrate column and a three-meter 30% hexamethylphosphoramide (HMPA) on 60–80 mesh firebrick column. The purified material from both batches was frozen and thawed in the vacuum system over Ascarite and anhydrous calcium sulfate to remove any water and carbon dioxide. The material was distilled slowly into storage flasks and the usual evacuations were made while the material was frozen at liquid nitrogen temperatures to remove any oxygen present.

Unreacted starting material from high pressure runs likewise was trapped from the analytical separation and processed for re-use. Kinetic results from all three sources of material were compatible. The maximum impurity level of the methylenecyclobutane, as determined by impurity peaks (or absence thereof) in the gas chromatographs, was less than 0.05%.

Matheson prepurified nitrogen as used in the inert gas runs was liquefied under pressure in a trap and gas was taken from this liquid nitrogen to leave frozen any condensable impurities in the nitrogen. Matheson research grade ethylene was used as received, and Columbia Organical Chemicals allene was used after gas chromatographic purification for preparation of calibration mixtures.

The vacuum system with mercury float values and cutoffs, thermostat, and general procedures have been described previously in detail.[9]

An 1800-cc. vessel was used in a static system. Temperatures were monitored with four-junction Chromel–Alumel thermocouples and were checked by comparison with a L. & N. certified No. 8163-C platinum resistance thermometer, L. & N. Mueller bridge, at each temperature employed. Precision of temperature measurement should be ±0.1°. Absolute temperatures should certainly be good to ±0.4°. Quantitative product analyses were performed by gas chromatography using peak area measurements. These were obtained from a Disc Instruments Co. integrater coupled to a L. & N. Speedomax G recorder to which was fed the output of a thermistor catharometer detector. Because of the widely differing thermal conductivities of ethylene, allene, and methylenecyclobutane, calibration mixtures were used to determine the sensitivity factors for peak area ratios. Analytical reproducibility may be assessed by the r.m.s. deviation of less than 2% from the mean observed in the allene–methylenecyclobutane peak area ratios from thirteen duplicate analyses using one calibration mixture. Comparable reproducibility of analyses was obtained from runs where there was enough material for more than one analysis.

A three-meter 30% HMPA on 60–80 mesh firebrick column was used at 25°; reactant and product peaks were all cleanly separated. Because of its short retention time, the ethylene peak was a very sharp spike which was frequently off scale using samples of moderate size. Therefore the allene–methylenecyclobutane area ratio was used for calculation of rate constants. It also was feared that the sharp ethylene peak would unduly tax the time response of the measuring devices and hence would not be reliable. One

---

[1] This work was financed by the United States Air Force through the Air Force Office of Scientific Research, Contract AF49(638)722.

[2] M. Halberstadt and J. Chesick, unpublished work.

[3] R. B. Turner, "Theoretical Organic Chemistry, The Kekule Symposium, 1958," Butterworths, London, 1959.

[4] W. H. Knoth and D. D. Coffman, *J. Am. Chem. Soc.*, **82**, 3873 (1958).

[5] H. N. Cripps, J. K. Williams and W. H. Sharkey, *ibid.*, **80**, 751 (1958).

[6] (a) M. N. Das and W. D. Walters, *Z. physik. Chem. (Frankfurt)*, **15**, 22 (1958); (b) R. E. Wellman and W. D. Walters, *J. Am. Chem. Soc.*, **79**, 1542 (1957).

[7] B. Loeffler, E. Eberlin and L. Pickett, *J. Chem. Phys.*, **28**, 345 (1961).

[8] This sample was provided through the courtesy of Professor W. v.E. Doering.

[9] J. P. Chesick, *J. Am. Chem. Soc.*, **82**, 3277 (1960).

ethylene–allene peak area ratio usually was obtained in the analyses of a run.

Reaction was started by expansion of the methylenecyclobutane from a storage flask into the reaction vessel and was quenched by expansion of the vessel contents into a previously cooled trap at liquid nitrogen temperature.

Mixtures for runs with added inert gas were prepared in a mixing flask equipped with a magnetically driven paddle stirrer. Reaction products were pumped through a three-turn loop of 6 mm i.d. tubing immersed at one end in liquid nitrogen to assure complete freezeout of products and rapid removal of the nitrogen mixture from the vessel.

Results

The products of the reaction, allene and ethylene, were identified by comparison of relative retention times on the HMPA column and on a two-meter silver nitrate column with the times for authentic materials. The separate product peaks also were trapped, and gas infrared spectra of these samples taken on a Perkin-Elmer Model 221 spectrophotometer confirmed the product identification.

The unreacted methylenecyclobutane peak was trapped from one of the runs and passed through a six-meter 30% Dow Corning silicone oil on firebrick column at 50° to see whether any extra products had the same retention time as the reactant on the HMPA column. None was found in the silicone column analysis. Silicone oil and HMPA are sufficiently dissimilar in retention characteristics that this was taken as proof of the purity of the methylenecyclobutane peak.

At the end of run 3 at 1.87 mm. the products quickly trapped to a residual pressure in the system of six microns, which represents an upper bound of 0.4% on the non-condensable content of the product mixture. Since most of this 0.4% gas is still in the vessel, the true figure should be at least a factor of 100 lower. Therefore, essentially no non-condensables, hydrogen or methane were formed. The product allene also is known to be a scavenger for hydrogen atoms.[10]

No other product peaks were observed except in runs at high conversions, such as run 5, which was carried to 70% reaction. Here a peak appeared whose area was about 2% of the allene peak and which has the same retention time as methylacetylene. This peak was usually not observed for conversions of less than 35%. Although it is always difficult to say what smeared out peaks might come out of a gas chromatographic column if one waited long enough after sample injection, it is thought that the product mixtures were free of higher boiling products; no perturbations in the base line were observed which could be attributed to high boiling products even in the course of day long operation.

No products were found at the expected retention times for allene dimer, 1,2-dimethylenecyclobutane, cyclopentene, or 2-methylbutadiene-1,3. An upper limit of 1% may be set for side products relative to allene at a total conversion of 30%.

Figure 1 shows a plot of − log (fraction unreacted) *vs.* time for a series of five runs at one temperature and at approximately the same pressure, 2 to 4 mm. These runs, No. 25, 3, 24, 4 and 5, range from 18 to 70% conversion. The reaction appears to be satisfactorily first order. At 3 mm. the reaction rate is at about 95% of its high pressure limit. The increasing pressure as reaction proceeds might cause an increase in the reaction rate. C_2 hydrocarbons have been found to have relative efficiencies on a pressure basis of about 0.5 with respect to the reactant in energy transfer in the thermal decompositions of methylcyclopropane and cyclobutane.[11] It is not unlikely that similar efficiencies would be found for ethylene and allene with respect to methylenecyclopropane, hence at the relatively high initial pressure, the further increase in total pressure as reaction proceeds should appear to be offset by the expected lower energy transfer efficiencies of the product molecules.

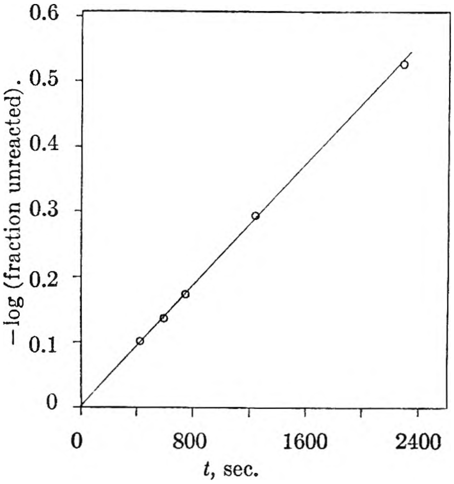

Fig. 1.—First order plot of runs 25, 3, 24, 4, and 5 at 459.2°, and at about 3 mm. initial pressure.

The Appendix shows the ratio of ethylene to allene as a function of pressure at 459.2°. The ratio is unity to ±5%, and no obvious trend with initial pressure or degree of conversion is apparent. The scatter of points is poor because of the previously cited difficulties in the ethylene measurements. Thus at most small amounts of allene are lost through polymerization in the reaction vessel.

The effects of initial reactant pressure and inert gas addition on the first order rate constant are shown on Fig. 2. The corresponding curve for cyclobutane[11] also is included for reference. Addition of a thirteen-fold amount of nitrogen in a series of runs gave only the results predicted on the basis of the effects of inert gases on other unimolecular reactions such as the cyclobutane decomposition. Such an inert gas addition should decrease the rate of diffusion to and from the walls by a factor approaching thirteen. This would be equivalent to changing the surface to volume ratio in testing for homogeneity of reaction. The observed effect of a slight increase in reaction rate is opposite to the decrease expected if a heterogeneous wall reaction is playing an important role.

It is concluded that the thermal decomposition of methylenecyclobutane as studied in this work is a homogeneous unimolecular reaction.

---

[10] A. D. Stepukhovich and L. V. Derevenskikh, *Zhur. Fiz. Khim.*, **29**, 2129 (1955).

[11] H. Pritchard, R. Sowden and A. F. Trotman-Dickenson, *Proc. Roy. Soc.* (*London*), **A218**, 416 (1953).

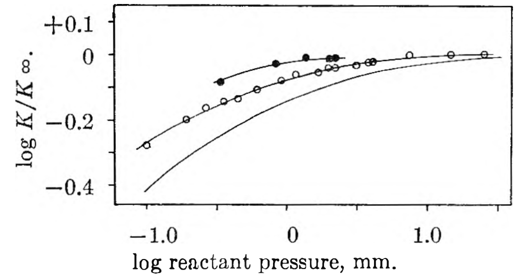

Fig. 2.—Dependence of first order rate constant on reactant partial pressure at 459.2°: ○, no added gas; ●, added nitrogen/methylenecyclobutane = 13.5. Lower curve is for cyclobutane decomposition.[11]

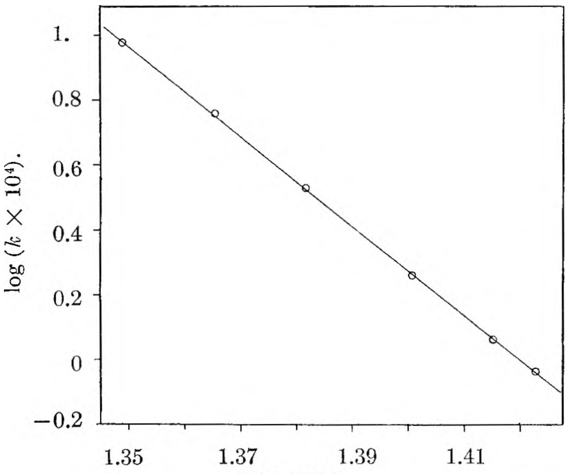

Fig. 3.—Arrhenius plot for initial methylenecyclobutane pressure of 6 mm.

The data for individual runs are tabulated in the Appendix.

The activation energy and hence the pre-exponential factor were extracted from the series of six runs, No. 17, 23, 20, 19, 18 and 33 as plotted in Figure 3.

At 6 mm. initial pressure, the first order rate constant is $4.63 \times 10^{15} \exp(-63.3 \pm 0.5 \text{ kcal.}/RT)$ sec.$^{-1}$. From Fig. 2 this is estimated to be 96 to 97% of the limiting high pressure rate constant. Therefore, the expression for the high pressure rate constant is taken to be $k_\infty = 4.76 \times 10^{15} \exp(-63.3 \pm 0.5 \text{ kcal.}/RT)$ sec.$^{-1}$.

Discussion

The pressure dependence of the rate constant is qualitatively as expected in the Rice–Ramsperger–Kassel model for unimolecular reactions.[12] The Arrhenius factors are similar to those for the cyclobutane decomposition, hence differences in pressure dependence of the two reactions may be attributed to the fact that methylenecyclobutane has three more vibrational degrees of freedom than does cyclobutane. The log (k/k_∞) curve is shifted to lower pressure by about 0.4 unit in log P.[9] An increase in the number of vibrational degrees of freedom of nine in going from cyclopropane to methylcyclopropane shifted the log (k/k_∞) curve for that decomposition reaction to lower pressures by about 1.45 units in log P.[5] On the basis of this somewhat crude comparison of the two reactions, the pressure shift of the curve in this work also appears to be of the correct magnitude. Walters reported a 20% fall in rate constant from its high pressure value, or log $(k/k_\infty) = 0.098$, at 0.1 mm. for the methylcyclobutane decomposition,[5] which corresponds to the further increase of six in vibrational degrees of freedom in going from methylenecyclobutane to methylcyclobutane.

The observed shift of the log (k/k_∞) curve to a lower pressure with the addition of inert gas yields a pressure efficiency of nitrogen relative to methylenecyclobutane in energy transfer of 0.15. This agrees well with the corresponding figure of 0.18 observed in the cyclobutane decomposition.[11]

The observed activation energy for methylenecyclobutane decomposition is 63.3 kcal./mole, larger than the value of 62.5 kcal./mole given for cyclobutane decomposition. Assuming the former figure is high and the latter figure is low, the stated limits of probable errors for these numbers are such that the methylenecyclobutane reaction still would require at least as much activation energy as the cyclobutane decomposition.

The presence of the exomethylene group introduces additional strain in the four-membered ring. This strain energy, 2.5 kcal./mole, may be expected to decrease, rather than to increase, the methylenecyclobutane activation energy relative to that for cyclobutane.

This could be used to support the idea that the cyclobutane reaction occurs through two successive

Appendix

A. Data for Runs without Added Nitrogen

Run	T, °C.	React. P, mm.	$k \times 10^4$, sec.$^{-1}$	Convers., %	Ethylene/ Allene
21	459.2	25.1	5.74	27	0.95
22		15.0	5.86	29	1.00
23		7.38	5.77	26	0.98
24		4.02	5.47	32	1.01
4		3.52	5.48	47	1.03
5		2.89	5.34	70	1.05
25		2.18	5.26	20	1.03
3		1.87	5.27	26	. . .
6		1.54	5.12	24	1.03
26		1.16	4.96	20	1.01
7		0.90	4.80	26	0.94
27		0.61	4.52	33	0.98
8		0.44	4.24	23	1.02
28		0.35	4.18	26	1.05
9		0.26	3.99	21	0.95
29		0.19	3.66	27	0.95
30		0.100	3.16	25	1.08
17	468.1	5.7	9.47	30	1.01
20	450.05	5.5	3.37	24	1.02
18	440.7	5.7	1.82	28	1.03
18	433.4	6.1	1.155	32	1.06
33	429.8	5.98	0.916	27	1.02
B. Data for Runs with Added Nitrogen: Nitrogen/ Methylenecyclobutane = 13.5					
14	459.2	2.26	5.59	65	. . .
12		2.00	5.61	28	. . .
13		1.35	5.71	25	0.99
15		0.82	5.42	27	1.01
16		0.33	4.77	26	1.01

---

[12] N. B. Slater, "Theory of Unimolecular Reactions," Cornell University Press, Ithaca, N. Y., 1959.

bond ruptures rather than as a simultaneous elongation of two opposite carbon–carbon bonds in the ring. Thus a primary reversible ring opening might be easier because of the extra-ring strain energy, but the resulting species 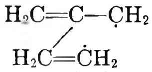 might be more stable than the tetramethylene analog and would require greater energy for complete dissociation to allene and ethylene, giving a larger net activation energy. A check of this point of view might be provided by studies to see if a labeled exo-carbon atom moved into the ring at a rate comparable to or faster than the decomposition reaction. Examination of 1,2-dideuterio or dimethylcyclobutane for *cis-trans* isomerization reaction also would be valuable. On the other hand, increased energy for a single transition state involving ring elongation could be rationalized by the non-linear nature of the allene fragment in the transition state. It would less resemble the linear product molecule than would the non-linear partially formed propylene resemble the non-linear product in the methylcyclobutane decomposition. Thus the activation energy for methylenecyclobutane decomposition could be greater even though the ring strain is also slightly larger than for the alkyl cyclobutanes.

THE HEATS OF DECOMPOSITION OF SOME HIGHER BORON HYDRIDES[1]

By Stuart R. Gunn and LeRoy G. Green

University of California, Lawrence Radiation Laboratory, Livermore, California

Received June 23, 1961

Heats of decomposition of B_4H_{10}, B_5H_9, B_5H_{11} and B_6H_{10} have been determined by explosion of mixtures with SbH_3. Bond energies of boron hydrides are derived and discussed.

Introduction

The heats of decomposition of B_2H_6,[2] B_5H_9[2] and $B_{10}H_{14}$[3] have been determined by a method involving pyrolysis of the compound in a furnace enclosed in a calorimeter. McCoy and Bauer[4] have derived the heat of formation of BH_3 from indirect measurements of the heat of dissociation of B_2H_6. There appear to be no determinations of heats of formation of other boron hydrides; these data are of interest for an understanding of the energetics of interconversion of boron hydrides and the nature of bonding in these unusual compounds. During a recent study of the heat of decomposition of several gaseous hydrides,[5] we determined the heat of decomposition of diborane, obtaining a value in reasonable agreement with that of Prosen. In the present work, we have extended this technique to B_4H_{10}, B_5H_9, B_5H_{11} and B_6H_{10}.

Experimental

B_4H_{10} and B_5H_9 were taken from stocks available in the laboratory. B_5H_{11} was prepared by the reaction of B_2H_6 and B_4H_{10} at 100° for two minutes. B_6H_{10} was prepared by decomposition of the methyl ether adduct of B_5H_{11}.[6] Purifications were performed by bulb-to-bulb distillation on the vacuum line. Infrared spectra were used to follow the course of purification; final spectra of B_4H_{10}, B_5H_9 and B_5H_{11} were in good agreement with those of McCarty, *et al.*[7] Other boron hydrides were not detectable. The final spectrum of B_6H_{10} agreed with an available unpublished spectrum except for the presence of a few per cent. of B_5H_{11}.

Purities of B_4H_{10}, B_5H_9 and B_5H_{11} were checked using a melting-point apparatus similar to that of Skau.[8] A technique was used which permitted approximate evaluation of the heat of fusion and the purity from variation of the melting temperature with fraction melted. The copper-constantan thermocouple was calibrated at the melting point of ammonia and a small linear correction to standard tables applied. The indicated purities and melting points (obtained by extrapolation of the curve of temperature *vs.* reciprocal of fraction melted to zero) were: B_4H_{10}, 99.0%, −121.0° (lit. −119.8)[9]; B_5H_9, 99.3%, −47.2° (lit. −46.8)[10]; B_5H_{11}, 98.3%, −123.5° (lit. −123.4°).[11] It is probable that in all cases the principal contaminants were other boron hydrides, which would have a negligible effect upon the calorimetric results.

The vapor pressure of the B_6H_{10} at 0.0° was 7.3 ± 0.1 mm. in a volume such that 3% was vaporized and 7.2 ± 0.1 mm. with 30% vaporized (lit. 7.2[9]; 6.8, 7.2[12]). At 25.0° it was 28.3 ± 0.2 mm.

The apparatus and techniques were similar to those used for diborane,[6] with modifications to decrease or eliminate (through use of break-seals) exposure of the gases to stopcock grease. Amounts of all reactants were determined by weighing in auxiliary bulbs. B_4H_{10} was transferred from the external bulb to the reaction tube; in all other runs the boron hydride, because of its lower volatility, was initially in the reaction tube and the stibine was in the external bulb. After the run, the hydrogen was transferred through −196° traps to a buret and measured; the traps then were warmed and the condensed gas measured. The lower two-thirds of the reaction tube then was flamed to the softening point of Pyrex to decompose solid hydrides, and the hydrogen was transferred through −196° traps and measured.

Results.—Results of the runs are given in Table I.

---

[1] This work was performed under the auspices of the U. S. Atomic Energy Commission.

[2] E. J. Prosen, W. H. Johnson and F. Y. Pergiel, *J. Research Natl. Bur. Standards*, **61**, 247 (1958).

[3] W. H. Johnson, M. K. Kilday and E. J. Prosen, *ibid.*, **64A**, 521 (1960).

[4] R. E. McCoy and S. H. Bauer, *J. Am. Chem. Soc.*, **28**, 2061 (1956).

[5] S. R. Gunn and L. G. Green, *J. Phys. Chem.*, **65**, 779 (1961).

[6] M. W. Forsyth, W. V. Hough, M. D. Ford, G. T. Hefferan and L. J. Edwards, National Meeting American Chemical Society, Spring, 1959. We are indebted to Dr. Hough for providing further experimental details.

[7] L. V. McCarty, G. C. Smith and R. S. McDonald, *Anal. Chem.*, **26**, 1024 (1954).

[8] E. L. Skau, *Proc. Am. Acad. Arts Sci.*, **67**, 551 (1932); *J. Phys. Chem.*, **37**, 609 (1933); see also J. M. Sturtevant, *Calorimetry* in "Techniques of Organic Chemistry," A. Weissberger, Editor, Vol. 1, "Physical Methods," Part 1, 3rd ed., Interscience Publishers, Inc., New York, N. Y., 1959, p. 608.

[9] A. Stock, "Hydrides of Boron and Silicon," Cornell University Press, Ithaca, N. Y., 1933.

[10] I. Shapiro and J. F. Ditter, *J. Chem. Phys.*, **26**, 798 (1957).

[11] A. Burg and H. I. Schlesinger, *J. Am. Chem. Soc.*, **55**, 4009 (1933).

[12] W. V. Kotlensky and R. Schaeffer, *ibid.*, **80**, 4517 (1958).

TABLE I

HEATS OF DECOMPOSITION OF BORON HYDRIDES

Boron hydride, mmoles	SbH_3	Decomposition %	Condensable %	H_2 in solids %	$-\Delta E$, kcal. mole^{-1}
		B_4H_{10}			
0.409	1.583	97.0	1.2	...	10.9
.498	1.988	95.8	3.2	...	11.0
.573	1.831	95.1	1.4	2.6	12.1
.731	2.194	96.3	1.6	1.1	11.8
.705	1.423	88.1	1.4	4.5	13.2
					11.8
		B_5H_9			
0.423	2.002	89.9	3.6	1.0	12.5
.426	2.008	...	...	...	12.6
.475	2.733	96.0	0.2	1.2	11.4
.502	1.881	...	...	...	12.4
.678	1.725	93.2	5.3	0.6	11.5
.836	2.047	93.1	1.1	...	11.6
					12.0
		B_5H_{11}			
0.406	2.321	97.4	0.8	0.9	18.7
.520	2.032	93.7	3.3	1.5	19.3
.520	2.017	96.9	0.9	1.6	19.2
.709	1.989	85.3	13.0	3.1	20.4
					19.4
		B_6H_{10}			
0.096	1.426	94	4	...	16.2
.099	1.019	101	1	1	15.5
.107	0.613	93	5	5	14.5
.095	0.500	92	4	...	15.2
					15.4

Observed heats have been corrected for the heat of compression, the fuse energy, and the stibine contribution (assuming −34.98 kcal. mole^{-1} for ΔE). Decomposition is calculated from the hydrogen found assuming quantitative decomposition of the stibine, and expressed as per cent. of theoretical. Condensable is assumed to be the unchanged boron hydride and is expressed as per cent. of sample. Hydrogen-in-solids is the non-condensable gas released by flaming the reaction tube, expressed as per cent. of theoretical hydrogen from the boron hydride sample.

ΔE is calculated from the corrected heat and hydrogen produced, it being assumed that no heat was contributed by the boron hydride not decomposed to the elements. There appears to be a slight trend toward larger $-\Delta E$ with smaller decomposition yield, but since the various boron hydrides were run over a similar range of mixture compositions and the results are treated in a relative manner, all runs are weighted equally in the average. The gas from B_5H_9 runs 2 and 4 was lost and a yield of 95% assumed. We estimate the averages to be reliable within ±1 kcal. mole^{-1} for B_4H_{10}, B_5H_9 and B_5H_{11}, and ±2 kcal. mole^{-1} for B_6H_{10}.

Correcting to constant pressure, the heats of decomposition are B_4H_{10} −9.4; B_5H_9, −9.9; B_5H_{11}, −16.7; B_6H_{10}, −13.0. Prosen, *et al.*,[2] found −13.0 for the heat of decomposition of B_5H_9 to amorphous boron, more negative than our result by 3.1 kcal., or 0.62 kcal. (g. atom B)$^{-1}$. Similarly, Prosen's value for B_2H_6, −6.73, is more negative than ours,[4] −5.0, by 0.86 kcal. (g. atom B)$^{-1}$. The agreement would seem to be more than coincidental; it is highly probable that the boron produced by our method of explosive decomposition is more finely divided and has a higher energy than the form produced by passing the gases through a heated tube. Hence we shall adjust our results to Prosen's, in essence taking his form of amorphous boron as the reference state, using 0.7 kcal. (g. atom B)$^{-1}$ for the heat of transition. Applying the usual estimated 0.4 kcal. (g. atom)$^{-1}$ value[13] for the heat of transition from amorphous to crystalline boron, we calculate standard heats of formation of the gases: B_4H_{10}, +13.8; B_5H_{11}, +22.2; B_6H_{10}, +19.6.

Discussion

Adler and Stewart[14] have made measurements of the apparent equilibrium in the system B_5H_{11}–H_2–B_2H_6–B_4H_{10} at various temperatures, obtaining a value of −7.56 kcal. mole^{-1} for ΔH in the range 100–140° and about 1 cal. mole^{-1} deg.$^{-1}$ for ΔC_p of the reaction

$$2B_5H_{11}(g) + 2H_2(g) = 2B_4H_{10}(g) + B_2H_6(g)$$

While this is not a true equilibrium system, since components are being continually removed by competing reactions, it appears from the kinetic data that the equilibrium reaction is rapid compared with others. Our results give −9.3 for ΔH, which is in satisfactory agreement.

Bauer[15] has predicted heats of formation of boron hydrides from a plot of $\Delta H_f^0/n$ *vs.* $1 + p/n$ where the hydride is described as B_nH_{n+p}; the known points for B, B_2H_6, B_5H_9 and $B_{10}H_{14}$ were found to lie on a smooth curve. However, a now obsolete value of +27 for ΔH_f^0 ($B_{10}H_4$, g) was used; substituting the presently accepted value of +2.8[3,16] the point lies far off the curve and it would appear that the relationship was largely fortuitous.

Prosen[17] used the same input data to estimate heats of formation by a different method. He considered four bond types: B–H, B–B, B–H–B and B–B–B, the first two being normal covalent bonds and the last two three-center bonds as formulated by Eberhardt, Crawford and Lipscomb,[18] and solved for the four unknown energies from the four known heats of formation. The procedure neglects resonance energies and changes in single-bond energies indicated by varying lengths and angles, but these may be expected to cancel to some degree in back-calculation of unknown heats of formation.

We shall follow the approach of Prosen and calculate thermochemical bond energies at 298°K. using 135.22 for ΔH_f^0(B, g)[16] and 52.09 for ΔH_f^0 (H, g).[13] From the structural information of Lips-

---

(13) F. D. Rossini, *et al.*, Circular of the National Bureau of Standards, 500, 1952.

(14) R. G. Adler and R. D. Stewart, *J. Phys. Chem.*, **65**, 172 (1961).

(15) S. H. Bauer, *J. Am. Chem. Soc.*, **80**, 294 (1958).

(16) W. H. Evans, E. J. Prosen and D. D. Wagman, "Thermodynamic and Transport Properties of Gases, Liquids, and Solids," American Society of Mechanical Engineers, McGraw-Hill Book Co., New York, N. Y., 1959, p. 226.

(17) E. J. Prosen, American Chemical Society, Spring, 1955; see ref. 15.

(18) W. H. Eberhardt, B. Crawford, Jr., and W. N. Lipscomb, *J. Chem. Phys.*, **22**, 989 (1954).

comb,[19,20] we ascertain the number of bonds of different types; these are listed in Table II together with standard heats of formation and heats of atomization, ΔH_a.

TABLE II

ENERGIES AND BOND TYPES

	ΔH_f^0	ΔH_a	B–H	B–B	B–H–B	B–B–B
BH_3	18 ± 1	273.49	3	0	0	0
B_2H_6	7.5 ± 0.5	575.48	4	0	2	0
B_4H_{10}	13.8 ± 1	1047.98	6	1	4	0
B_5H_9	15.0 ± 0.4	1129.91	5	2	4	1
B_5H_{11}	22.2 ± 1	1226.89	8	0	3	2
B_6H_{10}	19.6 ± 2	1312.62	6	2	4	2
$B_{10}H_{14}$	2.8 ± 1.5	2078.66	10	2	4	6

To calculate the bond energies, we now have seven equations in four unknowns, an over-determined set. The simplest approach is to calculate E(B–H), E(B–H–B) and E(B–B) from BH_3, B_2H_6 and B_4H_{10} successively

$$E(\text{B–H}) = 1/3\ \Delta H_a(BH_3) = 91.16$$

$$E(\text{B–H–B}) = 1/2\ [\Delta H_a(B_2H_6) - 4E(\text{B–H})] = 105.42$$

$$E(\text{B–B}) = \Delta H_a(B_4H_{10}) - 6E(\text{B–H}) - 4E(\text{B–H–B}) = 79.34$$

E(B–B–B) then can be calculated from any higher boron hydride. These solutions are given in Table III where x denotes an input datum.

It is perhaps most reasonable to accept the second set for general use, since B_5H_{11} contains no B–B bonds and hence the B–B–B bonds may be expected to be less perturbed by resonance effects. B_5H_9, B_6H_{10} and $B_{10}H_{14}$ then have resonance stabilization energies of 3, 4 and 42 kcal., respectively.

TABLE III

B–B–B BOND ENERGIES

E(B–B–B)	ΔH_a (calcd.)			
	B_5H_9	B_5H_{11}	B_6H_{10}	$B_{10}H_{14}$
93.75	x	1233.04	1314.82	2054.46
90.68	1126.84	x	1308.68	2036.04
92.65	1128.81	1230.84	x	2047.86
97.78	1133.94	1241.10	1322.88	x
Experimental	1129.91	1226.89	1312.62	2078.66

If for $B_{10}H_{14}$ one assumes a 10–0–4–8 bond configuration instead of 10–2–4–6, the calculated value of ΔH_a in set 2 is 2058.72, deviating only half as much from the experimental. The B–B distance to which the single B–B bonds are assigned in Lipscomb's formulation are only slightly shorter than other B–B distances in the molecule; it may be that the actual electron distribution is such as to make the bonding more uniform throughout the molecule.

The value of 79.3 for E(B–B) is in excellent agreement with the 79.0 calculated from B_2Cl_4[21]; the bond distances are also the same.[19,22]

Acknowledgment.—We wish to thank Edward J. Prosen of the National Bureau of Standards for reading and commenting upon the manuscript.

[19] W. N. Lipscomb, *J. Phys. Chem.*, **22**, 985 (1954).

[20] F. L. Hirschfeld, K. Eriks, R. E. Dickerson, E. L. Tippert, Jr., and W. N. Lipscomb, *ibid.*, **28**, 56 (1958).

[21] S. R. Gunn and L. G. Green, *J. Phys. Chem.*, **63**, 1787 (1959).

[22] M. Atoji, P. J. Wheatley and W. N. Lipscomb, *J. Chem. Phys.*, **27**, 196 (1957).

THE THALLOUS-THALLIC EXCHANGE AT VARIOUS ACIDITIES IN PERCHLORATE MEDIA[1]

BY EDWIN ROIG AND RICHARD W. DODSON

Radioisotope Applications Division, Puerto Rico Nuclear Center, Rio Pedras, Puerto Rico, and Chemistry Department, Brookhaven National Laboratory, Upton, New York

Received June 26, 1961

The Tl(I)–Tl(III) electron exchange rate was measured at 25° in 3 f $NaClO_4$–$HClO_4$ media at various acid concentrations down to 0.1 f. Since the hydrolysis equilibria of Tl(III) have been measured under the same conditions, the results permit a more accurate comparison of the reactivities of Tl^{+++} and $TlOH^{++}$ than has been possible previously. In contrast to results at higher ionic strengths, the rate is found to decrease as the acidity is decreased. The rate law can be written as $R = k_0(Tl^+)(Tl^{+++}) + k_1(Tl^+)(TlOH^{++})$, with $k_0 = 0.253 \pm 0.005\ f^{-1}$ h.$^{-1}$ and $k_1 = 0.089 \pm 0.012\ f^{-1}$ h.$^{-1}$. No evidence is found for an exchange of Tl^+ with $Tl(OH)_2^+$; an upper limit of 0.1 f^{-1} h.$^{-1}$ is assigned to the specific rate of this reaction path. Measurements also were made at 15° and 35°. The activation energy for k_0 is 17.4 kcal./mole.

Introduction

In a number of cases it has been found that the rates of electron exchange reactions in aqueous perchlorate media decrease with increasing concentration of acid. This effect has been ascribed to reaction paths involving hydrolyzed ions, which were concluded to react more rapidly than unhydrolyzed ions. Such indication of hydroxide catalysis has been reported[2–4] for the thallous–thallic exchange, and the rate law has been formulated as $R = k_0(Tl^+)(Tl^{+++}) + k_1(Tl^+)(TlOH^{++})$. From data obtained at ionic strength 6 it was concluded[3,4] that k_0 is negligible compared to k_1. On the other hand, data obtained[2] at ionic strength 3.68 indicated that both terms in the rate law are important. These studies were made before an accurate value for the hydrolysis constant of trivalent thallium was known, and the interpretations were subject to the uncertainty introduced by assuming that activity coefficient ratios are not seriously affected by the substitution of H^+ for Na^+ at constant ionic strength.

Subsequently, Biedermann's careful study[5] of the

---

[1] Research performed under the auspices of the U. S. Atomic Energy Commission.

[2] R. J. Prestwood and A. C. Wahl, *J. Am. Chem. Soc.*, **71**, 3137 (1949).

[3] G. Harbottle and R. W. Dodson, *ibid.*, **73**, 2442 (1951).

[4] R. W. Dodson, *ibid.*, **75**, 1795 (1953).

hydrolysis equilibria of Tl(III) gave values for the equilibrium constants of the first and second hydrolysis steps in 3 f perchlorate solutions at 25°. When these results were used to analyze the rate data for $I = 3.68$ it was concluded[6] that $k_0 = 0.154$ and $k_1 = 1.22\ f^{-1}\ h.^{-1}$. However, this analysis is uncertain because of the somewhat different ionic strength and because at the lowest acidity used in these exchange experiments, $(H^+) = 0.8\ f$, only about 8% of the Tl(III) was present as $TlOH^{++}$.

The present work was undertaken in order to obtain rate data under the same conditions as those used in the equilibrium studies so that a more reliable comparison of the specific rates of the Tl^{+++} and $TlOH^{++}$ reactions could be made. It also was hoped to obtain information about the electron exchange properties of doubly hydrolyzed Tl(III), which may be written as $Tl(OH)_2^+$.

It is necessary to go to quite low acidities to develop significant concentrations of the hydrolyzed ions. Under these conditions, the extremely low solubility of thallic hydroxide ($K_{sp} = (Tl^{+++})(OH^-)^3 = 10^{-45}$)[7] severely limits the total concentration of Tl(III). At micromolar concentrations various side effects become troublesome. In consequence the present work does not yield an estimate for the specific exchange rate of $Tl(OH)_2^+$, although a reasonable upper limit may be assigned. The value of k_1 obtained is not of high accuracy, but it definitely appears that k_1 is less than k_0.

Traces of chloride were a serious problem in this work. It is believed that their effect has been satisfactorily taken into account.

Experimental

Materials.—$TlClO_4$ was prepared by dissolving Tl metal (A. D. MacKay, Inc.) in nitric acid and converting the nitrate into perchlorate by subsequent recrystallizations from perchloric acid. The final product was purified further by recrystallization from water. Stock solutions were analyzed by potentiometric titration with bromate.

$Tl(ClO_4)_3$ stock solutions were obtained by anodic oxidation of $TlClO_4$ aqueous solutions, 2–4 f in $HClO_4$, as described by Biedermann.[5] The $HClO_4$ content was determined by titrating with NaOH after complexing the thallic ion with excess bromide. Stock solutions were analyzed for thallous ion with standard bromate. Total thallium was determined similarly after reduction with hydrogen peroxide.

The $HClO_4$ used was 70% Analytical Reagent (Mallinckrodt and Baker's Analyzed). For some runs the concentrated acid was fumed for 90 hours to minimize chloride impurity. Stock solutions, 3 f, were analyzed by titration with NaOH.

Solutions of $NaClO_4$ were prepared from $HClO_4$ and Baker's Analyzed Na_2CO_3. CO_2 was removed with a stream of nitrogen or by boiling. Different preparations were used in three series of runs. In series I the sodium carbonate and perchloric acid were not purified before use. In series II the chloride impurity was reduced by fuming in the presence of excess acid before final neutralization with recrystallized Na_2CO_3. In series III, doubly recrystallized Na_2CO_3 was employed,[8] without the fuming step. The $NaClO_4$ content was determined by weighing the solid recovered on evaporation. The chloride content of the solutions was estimated from the rate data and in some cases by anodic oxidation to Cl_2, sweeping into a solution of Fast-Green SF, and determining the change in optical density.[9]

The radioactive tracer was 12-day Tl^{202}, obtained by bombardment of mercuric oxide with deuterons at the Brookhaven cyclotron. The target was dissolved in HCl–HNO_3 or HCl–Cl_2 mixtures. Thallium was extracted with diethyl ether from 3 f HCl; the organic phase was washed several times with 3 f HCl and then with 0.5 f HCl. When the target was worked up less than two weeks after bombardment radioactive gold was eliminated by displacement on a copper foil, and the thallium was purified further by ether extraction. The tracer was recovered from the ether phase by extraction with a dilute solution of SO_2. The aqueous solution then was evaporated to dryness (almost invisible residue) and was fumed several times with $HClO_4$. A modification was to omit the SO_2 step, evaporate the ether phase in the presence of water, fume down almost to dryness first with $HClO_4$–HNO_3, then with $HClO_4$ alone. In the resulting solutions the thallium was largely or entirely in the thallous state. Tracer solutions of Tl(III) were prepared as follows: (a) exchange of the active Tl(I) with Tl(III) at 50° in contact with platinum foil for a few days, or (b) electrolytic oxidation.[5] The tracer solutions were analyzed for total thallium, thallous and acid content.

Rate Measurements.—The reaction vessels were volumetric flasks or glass stoppered cylinders. Red Pyrex low actinic glassware was used; alternatively, light was excluded with a wrapping of aluminum foil. Reaction mixtures were prepared by mixing in the reaction vessel appropriate volumes of stock solutions of thallic perchlorate, labelled thallic perchlorate, thallous perchlorate, perchloric acid, sodium perchlorate and triply distilled water. The usual procedure was to add all constituents except the thallous perchlorate, age the mixture in the thermostat for at least 12 hours, and then start the exchange by adding the thallous perchlorate. The same kinetic results were obtained when the aging was omitted, except for indication of a slight amount of reduction of Tl(III) during the early stages of the exchange.

The temperatures of the water-baths used as thermostats were constant within ±0.05°. The thermometers used were checked against thermometers which had been calibrated by the National Bureau of Standards.

For determination of the extent of exchange samples (1 or 2 ml.) were pipetted from the reaction vessel and extracted from an HCl medium with diethyl ether (series I and II) or with methyl isobutyl ketone (series III). These solvents had been purified by distillation through a 20-plate column. The ketone contained 5 volume % n-octanol to aid the separation of the phases. Samples were obtained from each phase by expulsion through a delivery tube into a small glass vial or a test-tube, and were counted in a well-type sodium iodide scintillation counter. No appreciable difference in counting efficiency was found between the organic and aqueous phases. It was found that variations in the wall thickness of the vials were negligible. The precise volume of each sample counted in a vial was calculated from the weight and density. Densities were measured separately. Test-tubes were used in matched pairs which had been found to give the same counting efficiency within 0.3% when filled to a standard depth. The standard deviation due to counting statistics in individual determinations was 1% or less.

Under these conditions, the fraction of the tracer which is in the thallic form is given by

$$\frac{y}{x+y} = \frac{H\left[1 + \dfrac{E_1 + \alpha}{E_3 - E_1}\right] + A\left[\alpha - \dfrac{E_3(E_1 + \alpha)}{E_3 - E_1}\right]}{H + \alpha A}$$

where

x = concn. of tracer in form of Tl(I) in reaction mixture
y = conc. of tracer in form of Tl(III) in reaction mixture
H = counting rate of an arbitrary vol. of the organic phase
A = counting rate of the same vol. of the aqueous phase
E_1 = extraction quotient for Tl(I), *i.e.*, $(Tl^I)_{organic}/(Tl^I)_{aqueous}$
E_3 = extraction quotient for Tl(III)
α = ratio of final vol. of aqueous phase to that of organic phase

The extraction coefficients and phase volume ratios were determined in separate experiments. Their magnitudes were such with the ketone extractant that the approximate expression

---

(5) G. Biedermann, *Arkiv Kemi*, **5**, 441 (1953).

(6) F. J. C. Rossotti, *J. Inorg. & Nuclear Chem.*, **1**, 159 (1955).

(7) P. Schindler, *Helv. Chim. Acta*, **41**, 527 (1958).

(8) We are indebted to Dr. George Biedermann for advice on the purification of sodium carbonate.

(9) H. T. Gordon, *Anal. Chem.*, **24**, 857 (1952).

$$\frac{y}{x+y} = \frac{H}{H+A} - \frac{A}{H+A}\left[(\alpha - 1)\frac{H}{H+A} + E_1\right]$$

was satisfactory. The half-life of the reaction was determined by plotting $1 - x/x_\infty = y/x + y - (b/a)x/(x + y)$ semi-logarithmically *vs.* time, and the second-order specific rate constant was calculated from the expression $k = 0.693/t_{1/2}(a + b)$, where a and b are the concentrations of Tl(I) and Tl(III), respectively, in the reaction mixture. The reactions usually were followed for at least two half-lives. The exchange plots were satisfactorily linear except that there frequently was a slight initial curvature believed to result from reduction of Tl(III). Half-lives were obtained from the linear portion. The concentration of Tl(III) during the exchange was corrected for this reduction by using the magnitude of the zero time intercept. The separation induced exchange in runs where reduction was negligible (less than 1%).

Errors.—We believe that an error of about ±3%, in the sense of a standard deviation, should be attached to the specific rate constants determined in individual runs. This is not a rigorous estimate, but it takes into account the known sources of error, as well as the reproducibility of replicate runs.

Results

At the low Tl(III) concentrations, *e.g.*, about $10^{-5} f$, which were necessary from solubility considerations in much of this work, difficulties were experienced which could be ascribed to traces of chloride in the reaction mixture. These became apparent when the Tl(III) order was checked and it was found to vary from unity to three or greater as the Tl(III) concentration was decreased. The explanation is almost certainly the formation of $TlCl^{++}$ in the reaction mixture. This species is known[10] to be almost inert to electron exchange, having a specific rate less than 1% that of Tl^{+++}. Furthermore, it is very stable,[11] with a formation equilibrium quotient of about 3×10^7 under our conditions.[12] Therefore, when some of the Tl(III) is in this form and the rest is Tl^{+++} (and hydrolyzed species), the observed rate is determined by the uncomplexed Tl(III). When the total Tl(III) concentration is decreased the uncomplexed Tl^{+++} decreases relatively more rapidly, which accounts for the peculiar trend of apparent reaction order. Other complexing anions give similar effects,[13,14] but since chloride is the most likely such impurity in perchlorate media we ascribe the effect to it. This explanation assumes that Tl^{+++} and $TlCl^{+++}$ exchange rapidly with each other so that the entire pool of trivalent thallium is accessible and use of the total Tl(III) concentration is justified in applying the McKay law. The results support the assumption.

The above description implies that the observed specific rate constant is given in good approximation by

$$\frac{\text{Rate}}{(\text{Tl(I)})(\text{Tl(III)})} \equiv k_{\text{obs}} = k\left[1 - \frac{(\text{Cl}^-)}{(\text{Tl(III)})}\right] \quad (1)$$

where k is the true specific rate constant for the system in the absence of chloride. The first-order dependence on (Tl(I)) and (Tl(III)) is substantiated in the present work by the consistency of the k values found. According to (1) a plot of k_{obs} *vs.* 1/(Tl(III)) should be a straight line from whose intercept and slope k and (Cl^-) can be calculated. Such plots are shown in Fig. 1. The two upper curves show data from some runs made in series I. The calculated chloride concentrations are 6.6×10^{-5} and $5.4 \times 10^{-5} f$. From these and similar rate data it was possible to estimate the chloride content of each of the sodium perchlorate and perchloric acid stock solutions used in series I. A least squares fitting procedure was employed. For each run the value of k was calculated from k_{obsd} according to the makeup of the reaction mixture. This procedure is justified in part by the consistent k values obtained. Since not all the stock solutions were analyzed independently for chloride a complete independent verification is not possible. However, the chloride estimates for one of the 3 f $NaClO_4$ stock solutions were $7.4 \times 10^{-5} f$ from rate data and $6.9 \times 10^{-5} f$ by direct analysis. The agreement is satisfactory.

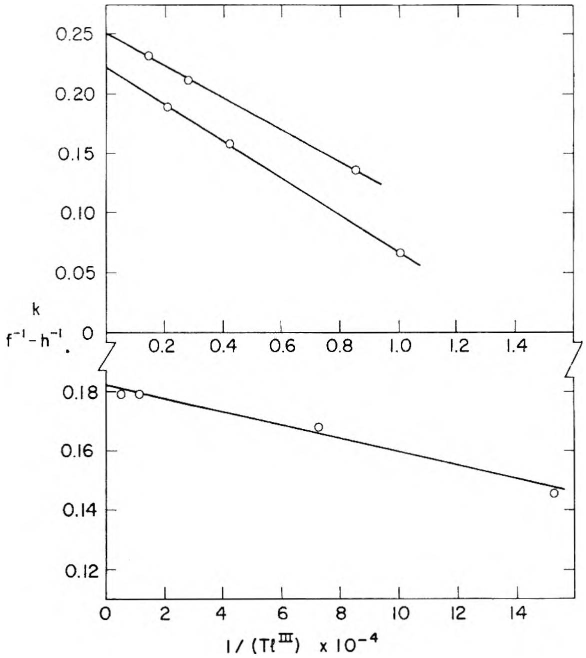

Fig. 1.—Dependence of rate on reciprocal thallic concentration (used for estimation of chloride in reaction mixtures). Upper curve, series I, $(H^+) = 0.81 f$; middle curve, series I, $(H^+) = 0.21 f$; bottom curve, series III, $(H^+) = 2.50 f$.

Although the chloride impurity was reduced by an order of magnitude in series II and III, its effect was still significant. One pair of k values available in series II gives $(\text{Cl}^-) = 1.66 \times 10^{-6} f$ in the 3 f $NaClO_4$ stock solution. Direct analysis gave $1.2 \times 10^{-6} f$. The mean of these, $1.4 \times 10^{-6} f$, was used to correct the rate data. The largest correction amounted to 25%. In series III, runs were made at two different Tl(III) concentrations at every value of (H^+). The results were satisfactorily fit with a chloride estimate of $3.3. \times 10^{-6} f$ in the $NaClO_4$ stock solution. A group of direct analyses gave $3.45 \times 10^{-6} \pm 0.7 \times 10^{-6} f$. It seems reasonable to assign an uncertainty less than 20% to these estimates. The greatest error introduced by the

---

(10) L. Eimer and R. W. Dodson, Brookhaven National Laboratory Quarterly Progress Report, 93(S-8), 67–69 (March 1951).

(11) R. Benoit, *Bull. soc. chim. France*, **16**, 518 (1949).

(12) Private communication from Professor E. L. King.

(13) E. Penna-Franca and R. W. Dodson, *J. Am. Chem. Soc.*, **77**, 2651 (1955).

(14) L. G. Carpenter, M. H. Ford-Smith, R. P. Bell and R. W. Dodson, *Discussions Faraday Soc.*, **29**, 92 (1960).

chloride corrections in series III probably is less than 3.5%.

TABLE I

COMPARISON OF RATE DATA[a] AT 25.0°, ($HClO_4$) 2.50 *f*, (ClO_4^-) 3.68 *f*

(Tl^I), *f*	(Tl^{III}), *f*	k_{obsd}, f^{-1} h.$^{-1}$	Corrected *k*, f^{-1} h.$^{-1}$
0.0501	0.654×10^{-5}	0.146	0.180
.0501	1.37×10^{-5}	.168	.185
.0502	8.72×10^{-5}	.179	.182
.0502	17.5×10^{-5}	.179	.180
		Mean	0.182
		Prestwood and Wahl[2] value	0.182

[a] From series III. Corrected for a chloride concentration of 1.24×10^{-6} *f*, corresponding to 3.3×10^{-6} *f* in the 3 *f* $NaClO_4$ stock solution. (Cl^-) estimated from these data alone is 1.19×10^{-6} *f*.

Additional experiments were considered desirable to validate the chloride correction procedure. A series of exchange rate measurements at (H^+) = 0.2, with $NaClO_4$ omitted, confirmed the fact that the $NaClO_4$ was the source of most of the chloride (90% or more). A set of measurements at high acidity (see Table I) showed the chloride content of the stock perchloric acid to be negligible. In general, it may be said that all of the rate data obtained in this work are consistent with the chloride correction procedure employed, and that the corrections are consistent with the direct chloride determinations which are available. Unsystematic introduction of chloride impurity from run to run (*e.g.*, from the glassware or from laboratory fumes) apparently was negligible. There appeared to be some minor trends in the estimated chloride values which were not accounted for by the correction procedure; but these variations were within the experimental error and were ignored.

It was felt desirable to test the over-all procedure, including the chloride corrections, further by comparing absolute values of *k* with those obtained by other workers under identical conditions except that Tl(III) concentrations were high enough that chloride correction could reasonably be neglected. The measurement of Prestwood and Wahl[2] at 24.9°, ionic strength 3.68, perchloric acid 2.50 *f*, was selected for this purpose. Their experimental value for *k* was 0.183 f^{-1} h.$^{-1}$, which after small corrections to 25° and total perchlorate[15] 3.68 *f*, becomes 0.182 f^{-1} h.$^{-1}$. Our data in Table I give a mean *k* of 0.182 f^{-1} h.$^{-1}$. Prestwood and Wahl also give a set of data, at several different thallium concentrations, from which additional estimates of *k* under the same conditions can be made. The mean of these is 0.186 f^{-1} h.$^{-1}$, again in good agreement. The data of Wiles[16] at ($HClO_4$) = 3.12 also agree with those obtained in the present work within the stated experimental uncertainties. The results of Gilks and Waind[15] are systematically about 15% higher than ours, where comparable; we have no present explanation for this discrepancy.

The results of rate measurements in series I at 25°, ionic strength 3, with acid concentrations between 0.2 and 3.0 *f* are given in Table II. The next to the last column gives the over-all second-order specific rate constants corrected according to eq. 1. The last column gives values calculated from the individual rate constants for the two reaction paths which are believed to prevail, as discussed subsequently. These individual rate constants were evaluated from the results of series II and III, independent of series I. The agreement is satisfactory, with a root mean square deviation of 2.6% and a greatest deviation of 5.1%. Most of the corrected experimental values are slightly higher than those calculated.

TABLE II

ACID DEPENDENCE OF THALLOUS–THALLIC EXCHANGE RATE 25.0°; ionic strength 3; $HClO_4$ 0.2–2.0 *f*; chloride impurity 3–7 × 10^{-5}*f* (Series I).

$HClO_4$, *f*	Tl(I), *f*	Tl(III), *f*	Obsd., *k*, f^{-1} h.$^{-1}$	Cor. *k*, f^{-1} h.$^{-1}$	calcd. *k*, f^{-1} h.$^{-1}$
0.210	0.01994	0.95×10^{-1}	0.0675	0.218	
	.00997	1.20×10^{-4}	.106	.193	
	.00997	2.38×10^{-4}	.158	.223	
	.01994	2.38×10^{-4}	.156	.217	
	.01994	4.76×10^{-4}	.189	.220	
				av. .214	0.203
0.270	0.00997	1.20×10^{-4}	0.124	0.221	.213
.330	.00997	1.20×10^{-4}	.129	.226	.220
.390	.00997	1.20×10^{-4}	.133	.229	.224
.450	.00997	1.20×10^{-4}	.134	.231	.228
.510	.00997	1.20×10^{-4}	.141	.239	.231
.570	.00997	1.20×10^{-4}	.137	.228	
	.01994	1.20×10^{-4}	.140	.233	
	.01994	13.5×10^{-4}	.228	.238	
				av. .233	.233
0.630	.00997	1.20×10^{-4}	.147	.241	.235
.690	.00997	1.20×10^{-1}	.152	.245	
	.01994	1.20×10^{-4}	.150	.242	
	.01994	13.5×10^{-4}	.229	.236	
				av. .241	.237
0.750	0.00997	1.20×10^{-4}	0.151	0.244	0.238
.810	.01994	1.19×10^{-4}	.173	.249	
	.00997	1.20×10^{-4}	.151	.240	
	.01994	1.20×10^{-4}	.147	.233	
	.00339	2.40×10^{-4}	.193	.238	
	.00997	2.40×10^{-4}	.195	.241	
	.01994	3.57×10^{-4}	.212	.249	
	.01994	7.13×10^{-4}	.233	.253	
	.01994	13.5×10^{-4}	.231	.238	
				av. .242	.239
1.050	0.01994	1.20×10^{-4}	.157	.238	
	0.01994	13.5×10^{-4}	.228	.235	
				av. .236	.242
1.530	0.01994	1.20×10^{-4}	.173	.240	
	0.01994	13.5×10^{-4}	.233	.240	
				av. .240	.245
2.01	0.01994	1.20×10^{-4}	.187	.240	
	0.01994	13.5×10^{-4}	.238	.243	
				av. .242	.247

Table III gives the results of series II and III, obtained at 15, 25 and 35° with purified solutions. These data are considered more accurate than those of series I, in part because of the generally smaller chloride corrections. Again, calculated values are shown for comparison with the corrected experimental values of the over-all second-order rate constants. The root mean square deviation is 1.8%, and the greatest deviation is 4.0%.

---

(15) S. W. Gilks and G. M. Waind, *Discussions Faraday Soc.*, **29**, 102 (1960).

(16) D. R. Wiles, *Can. J. Chem.*, **36**, 167 (1958).

Discussion

The data in Tables II and III show that, after appropriate corrections for the inhibiting effect of chloride, the rate law can be written as

$$\text{Rate} = k(\text{Tl(I)})(\text{Tl(III)})$$

where the over-all second-order rate constant k is a function of (H^+). We assume that the acid dependence is due to reaction paths involving unhydrolyzed and hydrolyzed ionic species.

TABLE III

ACID DEPENDENCE OF THALLOUS-THALLIC EXCHANGE RATE

Ionic strength 3; $HClO_4$ 0.100–2.93 f; chloride impurity 1.5–3.3 × 10^{-6} f.

Series	$HClO_4$	Tl(I), f	Tl(III), f	Obsd. k, f^{-1} h^{-1}.	Cor. k, f^{-1} $h.^{-1}$	Calcd. k, f^{-1} $h.^{-1}$
			Temperature 15.0°			
II	0.100	0.01982	5.50×10^{-6}	0.050	0.066	
	.190	.01982	3.82×10^{-5}	.077	.080	
	.40	.01982	3.32×10^{-4}	.087	.087	
	.76	.01982	3.32×10^{-4}	.089	.089	
	1.00	.01982	3.32×10^{-4}	.088	.088	
	1.60	.01982	3.32×10^{-4}	.087	.087	
			Temperature 25.0°			
II	0.100	0.01982	5.50×10^{-6}	0.123	0.163	0.163
III	.100	.05015	1.68×10^{-5}	.129	.158	.163
III	.100	.05015	3.45×10^{-5}	.147	.162	.163
III	.150	.05015	1.71×10^{-6}	.154	.188	.187
III	.150	.05015	5.13×10^{-6}	.173	.184	.187
II	.190	.01982	3.82×10^{-5}	.188	.195	.198
III	.200	.05015	3.47×10^{-6}	.186	.204	.202
III	.200	.05015	7.00×10^{-6}	.193	.202	.202
II	.400	.01982	3.32×10^{-4}	.226	.227	.225
II	.760	.01982	3.32×10^{-4}	.236	.237	.238
II	1.00	.01982	3.32×10^{-4}	.244	.245	.242
III	1.00	.05015	8.72×10^{-6}	.232	.238	.242
III	1.00	.05015	17.4×10^{-6}	.235	.238	.242
II	1.60	.01982	3.32×10^{-4}	.239	.239	.246
III	2.93	.05182	5.14×10^{-6}	.239	.239	.249
III	2.93	.05182	10.19×10^{-6}	.243	.243	.249
			Temperature 35.0°			
II	0.100	0.01982	5.50×10^{-6}	0.255	0.338	
II	.190	.01982	5.50×10^{-6}	.343	.455	
II	.190	.01982	3.82×10^{-5}	.459	.475	
II	.400	.01982	3.32×10^{-4}	.564	.566	
II	.760	.01982	3.32×10^{-4}	.593	.595	
II	1.00	.01982	3.32×10^{-4}	.614	.616	
II	1.60	.01982	3.32×10^{-4}	.625	.626	

The following hydrolysis equilibria are known to prevail in the solutions

$$\text{Tl}^{+++} + \text{H}_2\text{O} = \text{TlOH}^{++} + \text{H}^+, K_1 = \frac{(\text{TlOH}^{++})(\text{H}^+)}{(\text{Tl}^{+++})}$$

$$\text{TlOH}^{++} + \text{H}_2\text{O} = \text{Tl(OH)}_2^+ + \text{H}^+, K_2 = \frac{(\text{Tl(OH)}_2^+)(\text{H}^+)}{(\text{TlOH}^{++})}$$

The equilibrium quotients K_1 and K_2 have been determined by Biedermann at 25° in $NaClO_4$–$HClO_4$ mixtures 3.00 f in total perchlorate. The values are 0.072 and 0.032, respectively, each with an indicated uncertainty of about 20%. The ion association constant of Tl^+ and OH^- is small,[17] so that the thallous species TlOH can be ignored in acid solutions. It is therefore reasonable to seek to represent the rate law as

$$R = k_0(\text{Tl}^+)(\text{Tl}^{+++}) + k_1(\text{Tl}^+)(\text{TlOH}^{++}) + k_2(\text{Tl}^+)(\text{Tl(OH)}_2^+) \quad (2)$$

This may be rewritten as

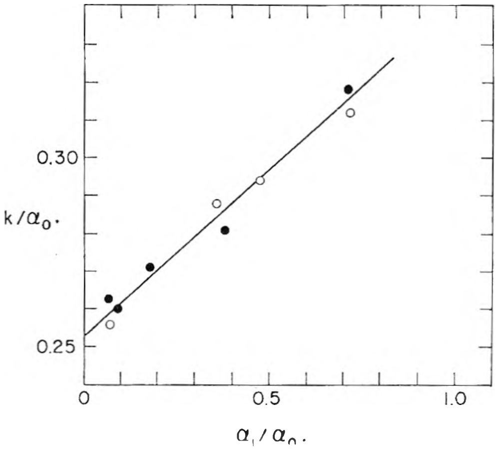

Fig. 2.—Determination of k_0 and k_1 at 25°: solid circles, series II; open circles, series III.

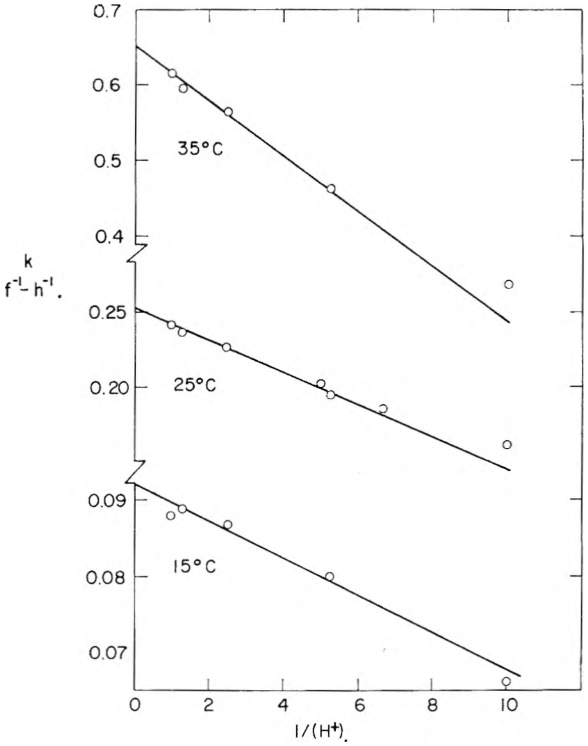

Fig. 3.—Dependence of rate on reciprocal acid concentration (used for approximate estimation of k_0 and k_1).

$$k = \alpha_0 k_0 + \alpha_1 k_1 + \alpha_2 k_2 \quad (3)$$

where $\alpha_0 = (\text{Tl}^{+++})/(\text{Tl(III)})$, $\alpha_1 = (\text{TlOH}^{++})/(\text{Tl(III)})$ and $\alpha_2 = (\text{Tl(OH)}_2^+)/(\text{Tl(III)})$.

The fractions α_i of Tl(III) in its various states of hydrolysis at 25° can be calculated with the aid of the known values of the equilibrium quotients K_1 and K_2; and the exchange rate data may be examined for their consistency with equation 2 by plotting k/α_0 *vs.* α_1/α_0. The graph should be linear as long as the third term of equation 2 is negligible. When it is not, the graph will rise faster than a linear curve. The 25° data of Table III are analyzed in this fashion in Fig. 2. The graph is linear; the greatest departure of any point is 2%, which is within the experimental uncertainty of the rate measurements. From the intercept and slope the values of k_0 and k_1 found are 0.253 ± 0.005 f^{-1}-

---

[17] J. Bjerrum, G. Schwarzenbach and L. G. Sillén, "Stability Constants, Part II," The Chemical Society, London, 1958.

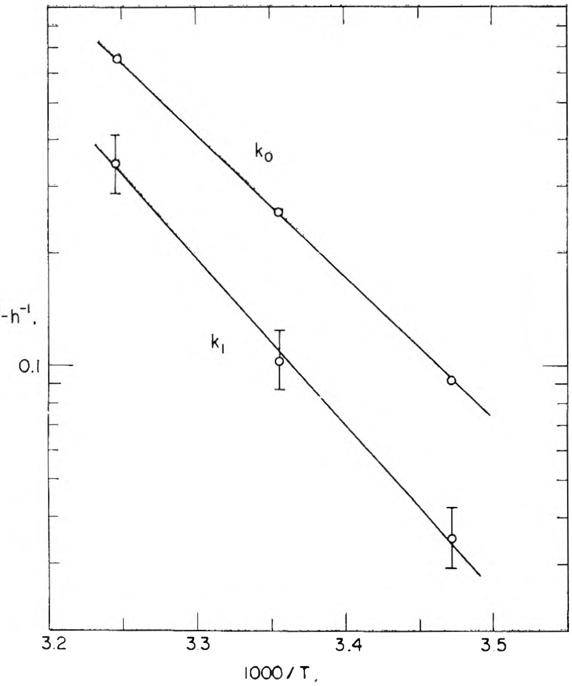

Fig. 4.—Arrhenius plots of k_0 and k_1. A 20% uncertainty is indicated for k_1.

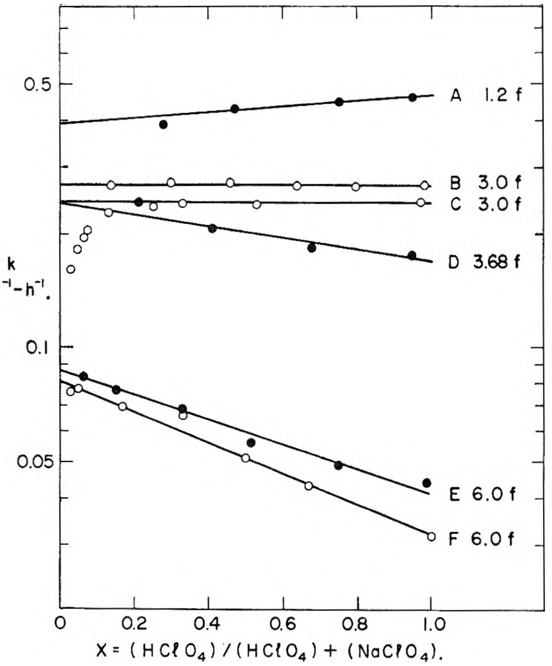

Fig. 5.—Rate as a function of composition at constant ionic strength, at 25°. A, B, E, data from Gilks and Waind[16]; D, data from Prestwood and Wahl[2]; F, data from Harbottle and Dodson[3]; C, present work.

h.$^{-1}$ and 0.089 ± 0.012 f^{-1}h.$^{-1}$, respectively. Uncertainties in the hydrolysis constants and systematic errors in the rate measurements are not included in the error estimates. There is no indication of a contribution from the third term of equation 2, and as an upper limit we estimate $k_2 < 0.1$ f^{-1} h.$^{-1}$.

The data at 15 and 35° cannot be analyzed in this manner since the hydrolysis equilibrium quotients are not known. Approximate estimates of K_1 and K_2, and therefore of k_0 and k_1, could be obtained by assuming plausible values for the enthalpy changes. An alternate approach which does not require as many explicit numerical assumptions is the following. It is found that graphs of k *vs.* $1/(\mathrm{H}^+)$ are surprisingly linear out to large values of $1/(\mathrm{H}^+)$. The series II and III results are plotted in this way in Fig. 3. If one writes equation 3 in explicit form as a function of (H^+), and expands the result in powers of $1/(\mathrm{H}^+)$ one finds

$$k = k_0 + (k_1 - k_0)\frac{K_1}{(\mathrm{H}^+)} + \left[(k_2 - k_0)\frac{K_2}{K_1} + (k_0 - k_1)\right]\frac{K_1{}^2}{(\mathrm{H}^+)^2} + \ldots \quad (4)$$

When k is a linear function of $1/(\mathrm{H}^+)$ the third and higher terms are negligible. (It will be seen by inspection that there is considerable cancellation in the coefficient of the third term.) One can therefore obtain k_0 with good accuracy from the intercepts of the curves in Fig. 3, and can estimate $(k_1 - k_0)K_1$ with fair accuracy from the initial slopes. A value for ΔH_1 then would permit the calculation of k_1. Such estimates are presented in Table IV, on the assumption that $\Delta H_1 = 9$ kcal./mole. This arbitrary value lies in the range of the tabulated[17] heats of hydrolysis of tripositive ions, but has no additional justification. The value of k_1 at 25° obtained by this approach differs by 15% from that found by the more accurate analysis of Fig. 2.

TABLE IV

ESTIMATES OF k_0 AND k_1 FROM $1/(\mathrm{H}^+)$ DEPENDENCE

Temp., °C.	K_1	k_0 f^{-1} h.$^{-1}$	k_1 f^{-1} h.$^{-1}$
15.0	(0.0425)	0.092	0.035
25.0	.072	.253	.104
35.0	(.118)	.651	.343

Arrhenius plots of k_0 and k_1 are shown in Fig. 4. The experimental activation energy found for k_0 is 17.4 kcal./mole, in good agreement with the value 17.6 kcal./mole found by Prestwood and Wahl in solutions of ionic strength 3.68 f. The entropy of activation, calculated in the usual way,[18] is −21 cal./deg.-mole. The line in Fig. 4 for the temperature dependence of k_1 suggests a somewhat greater activation energy than that found for k_0. However, because of the uncertainties introduced by the method of treating the data it does not seem warranted to give a numerical value. It is fair to say that no great difference between the activation energies can be discerned on the basis of the present analysis.

It seems clear from this work that the presence of a hydroxide group in the activated complex does not have the strongly catalytic effect on the thallous–thallic exchange that it does in some other electron exchange reactions, *e.g.*, that between Fe(II) and Fe(III).[19] This statement compares OH^- with $\mathrm{H_2O}$. However, comparison of an OH^- with a chloride, bromide or cyanide places

---

[18] S. Glasstone, K. J. Laidler and H. Eyring, "The Theory of Rate Processes," McGraw-Hill Book Co., Inc., New York, N. Y., 1941, p. 417.

[19] J. Silverman and R. W. Dodson, *J. Phys. Chem.*, **56**, 846 (1952).

it in a very favorable position with respect to these ligands, *i.e.*, their strongly inhibiting effect is not shown by hydroxide. Whether these effects are to be explained by a mechanism involving Tl(II) as an intermediate,[20] or by electronic perturbation due to the ligand,[21] is not clear at the present time.

This reaction system illustrates the difficulty of disentangling medium effects from those due to chemical equilibria in concentrated electrolyte solutions. The medium effects are large in the range (ClO_4^-) 1.2 to 6.0 f, and the kinetic salt effect expected for dilute solutions is reversed. The specific rates decrease with ionic strength, although there is no reasonable doubt that the reactions are between positive ions. This variation has been discussed in earlier publications.[4,15] It is not surprising in view of the fact that the activity coefficients of many ionic solutes increase in this range. Such variations in concentrated solution depend specifically on the nature of the ions. The question naturally arises whether the acid dependence of the thallous–thallic exchange observed in earlier work is due to changes in activity coefficients when hydrogen ion is substituted for sodium ion rather than to shifting hydrolytic equilibria. It seems probable that this is the case.

Bonner and Hunt[22] have discussed this problem in connection with the Co(II)–Co(III) exchange, which also shows an acid dependence in perchlorate media at constant ionic strength. They suggested as a test for medium effects the linearity of a plot of log k *vs.* X, where X is the ratio $(HClO_4)/(HClO_4) + (NaClO_4)$. The test was indecisive. This approach assumes that log F is a linear function of X, where F is the ratio, f_Af_B/f^*, of the product of the activity coefficients of the reactants to the activity coefficient of the activated complex. We are not aware of any convincing demonstration that this simple, linear relationship holds for highly charged ions in concentrated solutions. However, it is of interest to examine the available data for the thallous–thallic exchange on this basis. Such plots are shown in Fig. 5. The graphs are all reasonably linear over most of the acid range. The simplest interpretation is that the changes in the rate of this reaction with acid concentration which have been observed earlier are largely due to medium effects. If this is so, it appears that the logarithm of the activity coefficient ratio does in fact show an approximately linear dependence on the composition of the medium at constant ionic strength in these systems. Measurement of the hydrolysis equilibria of Tl(III) under the same conditions as the various rate measurements would help to test this inference as well as to define further the kinetic properties of $TlOH^{++}$.

Acknowledgment.—We are indebted to many of our colleagues for assistance and advice. We wish particularly to thank R. W. Stoenner for chemical analyses and many of the thallium preparations, J. Hudis for cyclotron bombardments, D. Christman and C. Paul for purifying the organic solvents, and K. T. Brennan for technical assistance. One of us (ER) takes pleasure in acknowledging the hospitality of Brookhaven National Laboratory, where the experimental work was carried out.

---

[20] F. R. Duke and B. Bornong, *J. Phys. Chem.*, **60**, 1015 (1956).

[21] B. N. Figgis, *Trans. Faraday Soc.*, **55**, 1075 (1959).

[22] N. A. Bonner and J. P. Hunt, *J. Am. Chem. Soc.*, **82**, 3826 (1960).

EVIDENCE FOR TWO KINDS OF "H ATOMS" IN THE RADIATION CHEMISTRY OF WATER[1]

BY E. HAYON AND A. O. ALLEN

Chemistry Department, Brookhaven National Laboratory, Upton, Long Island, New York

Received June 26, 1961

Aqueous solutions of a number of chlorinated organic compounds, with concentrations and pH values varied over a wide range, were irradiated with γ-rays. The main reduction products in every case were chloride ion and hydrogen gas. The chloride ion yield always predominated over that of hydrogen at high concentrations of solute or low concentrations of hydrogen ion, while hydrogen predominated in acid solutions at relatively low solute concentrations. The results suggest that the reducing radical, usually called "H," formed from the water by the radiation, reacts with these solutes mainly to form chloride ion; but it also can react with hydrogen ion to yield a different reducing radical, which reacts with the solutes to form hydrogen preferentially. Data obtained with chloroacetic acid solutions were sufficiently extensive to show good quantitative agreement with the competition kinetics suggested by this mechanism, and showed that "H" from water radiolysis reacts 3.4 times as fast with hydrogen ions as with chloroacetic acid molecules.

Water decomposes under ionizing radiations to give H_2, H_2O_2 and oxidizing and reducing radicals usually called OH and H. The nature of the reducing species and the resulting reactions in solution have been much debated.[2-5] It has been postulated that hydrated electrons, neutral hydrogen atoms, or hydrogen molecule ions could be present under certain experimental conditions and enter into chemical reactions. It has not been possible so far to differentiate categorically between the different species.

It was suggested recently from work on the radiation chemistry (200 kv. X-rays) of aqueous solutions of monochloroacetic acid[4] that transient negative radical ions can, under suitable conditions of pH and solute concentration, react with mono-

---

[1] Research performed under the auspices of the U. S. Atomic Energy Commission.

[2] J. Weiss, *Nature*, **165**, 728 (1950).

[3] N. F. Barr and A. O. Allen, *J. Phys. Chem.*, **63**, 928 (1959).

[4] E. Hayon and J. Weiss, *Proc. Second Intern. Conf. Peaceful Uses Atomic Energy (Geneva)*, **29**, 80 (1958).

[5] F. S. Dainton and D. B. Peterson, *Nature*, **186**, 878 (1960).

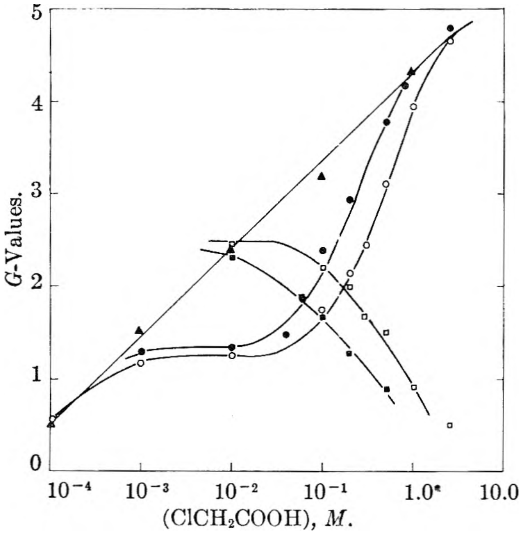

Fig. 1.—Yields of H_2 and Cl^- in γ-radiolysis of air-free solutions of chloroacetic acid: ○, $G(Cl^-)$, pH 1.0; ●, $G(Cl^-)$, pH 1.5; □, $G(H_2)$, pH 1.0; ■, $G(H_2)$, pH 1.5; ▲, $G(Cl^-)$, pH 5.5.

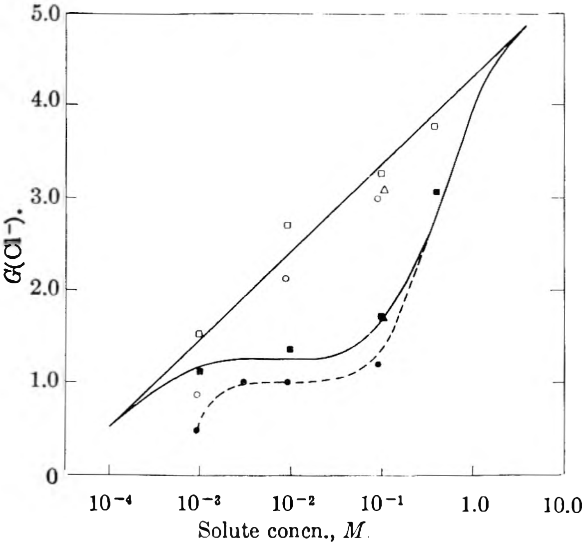

Fig. 2.—Chloride ion yields in γ-radiolysis of air-free solutions of chlorine compounds. Circles, 1,2-dichloroethane; squares, α-chloropropionic acid; triangles, methyl chloride. Open symbols, pH 5.5; filled symbols, pH 1.0. The upper and lower solid curves are for chloroacetic acid at pH 5.5 and 1.0, respectively.

chloroacetic acid to remove the chlorine atom. These ions were considered to be the precursors of hydrogen atoms which react to dehydrogenate the solute molecule. In the present work, aqueous solutions of a number of different chlorinated organic compounds have been irradiated with γ-rays, and kinetic evidence obtained to support the idea that there are two kinds of "H atoms" in the radiation chemistry of water, that one kind is a precursor of the other and can be converted to it by reaction with a hydrogen ion.

Experimental

The cobalt-60 γ-radiation sources that were used have been described previously.[6] The rate of energy absorption was determined by the Fricke ferrous sulfate dosimeter assuming $G(Fe^{3+}) = 15.5$.

The radiation cells used in runs where gaseous products were not determined were Pyrex tubes, 20 cm. long × 1.8 cm. diam., with a ground Pyrex stopper above and a Pyrex stopcock sealed on to a 1.5-cm. diam. frit glass below. Deaeration of the solutions was carried out by bubbling prepurified nitrogen through the frit for about 20 minutes. The stoppers above displaced some of the solution so as to leave no gas space. For the determination of hydrogen yields, the solutions were evacuated as described by Johnson and Allen.[7]

The water used was triply distilled. The solutions were prepared just prior to irradiation and always were kept in darkened bottles. The pH was adjusted with H_2SO_4 or NaOH. Monochloroacetic acid, α- and β-chloropropionic acids, 1,3-dichloroacetone and 1,2-dichloroethane were all "best grade" Eastman Kodak Organic chemicals. Methyl chloride was supplied by Matheson Co. A saturated solution of methyl chloride (0.106 M)[8] was used.

Microquantities of chloride were determined by measuring the turbidity of suspensions of silver chloride formed when a silver salt was added to a solution of chloride in 50% ethanol.[9] The silver reagent contained 1.7 g. of "Baker Analyzed" silver nitrate per liter of 0.2 N nitric acid solution, and was kept in darkened stock bottles. A 20-ml. aliquot of chloride solution was put into a 50-ml. darkened volumetric flask with 20 ml. of ethanol, and 5 ml. of the silver nitrate reagent was added dropwise while swirling the contents of the flask. The volume was made up to the mark with ethanol. The solution first was cooled with tap water and then kept thermostated at 40 ± 0.1° for 30 minutes; then cooled rapidly to room temperature. The turbidity was measured by absorption spectrophotometry at 350 mμ on a Beckman DU spectrophotometer. The reproducibility was ±3%. Blanks were carried out simultaneously for the unirradiated solutions, and in all cases the amount of chloride in the blanks did not exceed 15 μM. In chloroacetic acid solutions above 2.5 M the amount of chloride in the unirradiated solutions increased rapidly and no irradiations were performed.

Hydrogen peroxide was determined by the method of Ghormley.[10] Hydrogen was determined by combustion with oxygen on a platinum filament.

Results

Air-free aqueous solutions of the following chlorinated organic compounds were irradiated with Co^{60} γ-rays: monochloroacetic acid, α- and β-chloropropionic acids, 1,2-dichloroethane, methyl chloride and 1,3-dichloroacetone. The amounts of inorganic chloride and hydrogen found were directly proportional to the dose up to the highest doses used, 1.26×10^{22} e.v./l. (dose rate 4.2×10^{20} e.v./l.-min.). The yields of hydrogen peroxide were determined in all cases and were found for solute concentrations above 10^{-3} M to be of the order of the molecular yield. It was shown for the chloropropionic acids that $G(H_2O_2)$ decreases linearly with the cube root of the solute concentration, and gives a value of $G(H_2O_2)$ at infinite dilution of 0.77 at pH 1.0. At solute concentrations below 10^{-3} M the H_2O_2 concentration leveled off rapidly with dose, in both acid and neutral solutions, indicating that free radicals were destroying the H_2O_2 formed.

Figure 1 shows the yields of chloride obtained from γ-irradiation of air-free solutions of chloroacetic acid as a function of solute concentration at pH 1.0, 1.5 and 5.5. In acid solutions $G(Cl^-)$ is independent of [ClRH] from 10^{-3} to 5×10^{-2} M,

---

(6) H. A. Schwarz and A. O. Allen, *Nucleonics*, **12**, No. 2, 58 (1954).

(7) E. R. Johnson and A. O. Allen, *J. Am. Chem. Soc.*, **74**, 4147 (1952).

(8) D. N. Glew and E. A. Moelwyn-Hughes, *Discussions Faraday Soc.*, **15**, 150 (1954).

(9) E. N. Luce, E. C. Denice and F. E. Akerlund, *Ind. Eng. Chem.*, **15**, 365 (1943).

(10) C. J. Hochanadel, *J. Phys. Chem.*, **56**, 587 (1952).

but starts rising sharply in solutions of higher concentration to a $G(Cl^-)$ of 4.65 in 2.5 *M* chloroacetic acid. This relatively high yield of chloride was found to be independent of dose rate from 2.1 × 10^{19} to 4.2 × 10^{20} e.v./l./min. and presumably does not result from a chain reaction.

Figure 2 shows the yields of chloride from solutions of 1,2-dichloroethane, methyl chloride and α-chloropropionic acid at *p*H 1.0 and 5.5. The full curves drawn are the yields of chloride from solutions of monochloroacetic acid. The dependence of the yields of chloride upon solute concentration and *p*H is much the same from chlorinated hydrocarbons as from chlorinated carboxylic acids in aqueous solution. Figures 3 and 4 show the yields of chloride from β-chloropropionic acid and 1,3-dichloroacetone as a function of solute concentration at *p*H 1.0 and 5.5. The yields in neutral solution of β-chloropropionic acid are about the same as for chloroacetic acid; in acid solution, however, the yields of chloride are lower and do not increase much with increase in solute concentration.

The yields of hydrogen from air-free solutions of monochloroacetic acid at *p*H 1.0 and 1.5 are shown in Fig. 1. Above 10^{-2} *M* $G(H_2)$ starts to decrease with increase in solute concentration, the yields of H_2 being lower the higher the *p*H. As $G(H_2)$ decreases $G(Cl^-)$ increases with increase in chloroacetic acid concentration at any one constant *p*H. It also was found on irradiation of solutions of monochloroacetic acid that at any one solute concentration the yield of H_2 decreased and that of Cl^- increased with increase in *p*H (Fig. 5, for 10^{-1} *M* chloroacetic acid). The sum $G(H_2) + G(Cl^-)$ also is shown, and the slight decrease in the sum with increase in *p*H is due to the change in the radical yields with *p*H.

Figure 6 shows a plot of the sum $G(Cl^-) + G(H_2)$ as a function of chloroacetic acid concentration at *p*H 1.0, 1.5 and 5.5. The hydrogen yields found at the higher *p*H are shown in Table I.

TABLE I

HYDROGEN YIELDS IN MONOCHLOROACETATE SOLUTIONS AT *p*H NEAR 5.5

Concn. ClAc, *M*	$G(H_2)$
0.001	0.80, 0.80
.01	.80, .79
.1	.75, .76
1.0	.65, .63

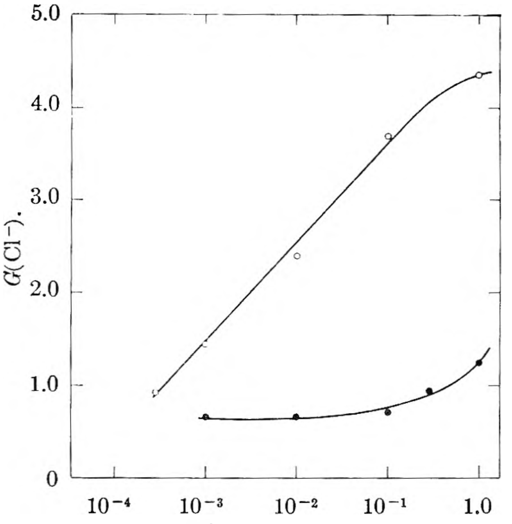

Fig. 3.—Chloride ion yields in γ-radiolysis of air-free solutions of β-chloropropionic acid: open circles, *p*H 5.5; filled circles, *p*H 1.0.

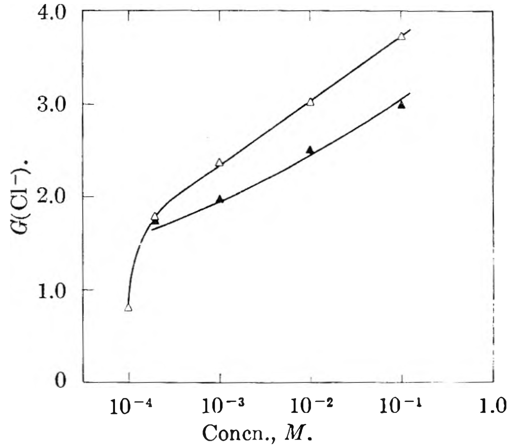

Fig. 4.—Chloride ion yields in γ-radiolysis of air-free solutions of 1,3-dichloroacetone: open symbols, *p*H 5.5; filled symbols, *p*H 1.0.

Discussion

The formation of inorganic chloride on irradiation of deaerated solutions of chlorinated organic compounds is a result of reaction of the reducing species with the solute. The reaction of OH radicals is believed to result in dehydrogenation rather than dechlorination; for instance, OH radicals, produced by Fenton's reaction, attack chloroform but not carbon tetrachloride present in aqueous solution.[11] The sum of $G(H_2)$ and $G(Cl^-)$ at moderately low concentrations agrees with standard values[12] for the sum $G_H + G_{H_2}$ of the yields of hydrogen atoms and molecules produced in γ-radiolysis of water at various *p*H. Thus every reducing radical formed reacts with chloroacetic acid to yield either H_2 or Cl^-.

The following mechanism can account for the yields of H_2 and Cl^- formed on γ-irradiation of air-free aqueous solutions of monochloroacetic acid

$$\text{"H"} + \text{ClRH} \longrightarrow \text{Cl}^- + \text{RH}\cdot \quad (1)$$

$$\text{"H"} + \text{H}^+ \longrightarrow \text{H}' \quad (2)$$

$$\text{H}' + \text{ClRH} \longrightarrow \text{H}^+ + \text{Cl}^- + \text{RH}\cdot \quad (3)$$

$$\text{H}' + \text{ClRH} \longrightarrow \text{H}_2 + \text{ClR}\cdot \quad (4)$$

where "H" is the reducing radical initially produced and H′ is the form resulting from the reaction of "H" with acid. On this mechanism, we expect

$$\frac{G(\text{Cl}^-)}{G(\text{H}_2) - 0.45} = \frac{k_3}{k_4} + \left(1 + \frac{k_3}{k_4}\right)\frac{k_1}{k_2}\frac{(\text{ClRH})}{(\text{H}^+)} \quad (5)$$

where 0.45 is taken as the yield of molecular hydrogen formed from the water.[13] (We neglect the decrease in this molecular yield which might occur in these relatively concentrated solutions.) Figure

---

[11] J. Teply and J. Bednar, *Proc. Second Intern. Conf. Peaceful Uses Atomic Energy (Geneva)*, **29**, 71 (1958).

[12] C. J. Hochanadel and S. C. Lind, *Ann. Rev. Phys. Chem.*, **7**, 83 (1956).

[13] H. A. Schwarz, J. P. Losee, Jr., and A. O. Allen, *J. Am. Chem. Soc.*, **76**, 4693 (1954).

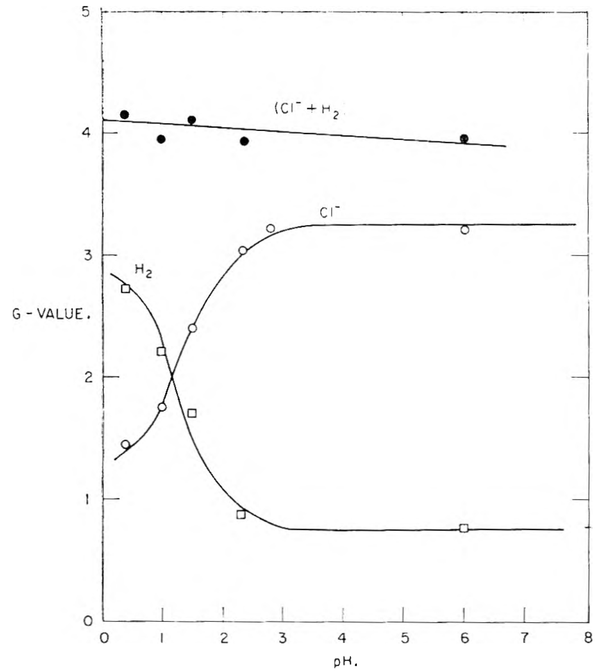

Fig. 5.—Yields of H_2 and Cl^- in γ-radiolysis of 0.1 M air-free solutions of chloroacetic acid plotted as a function of pH.

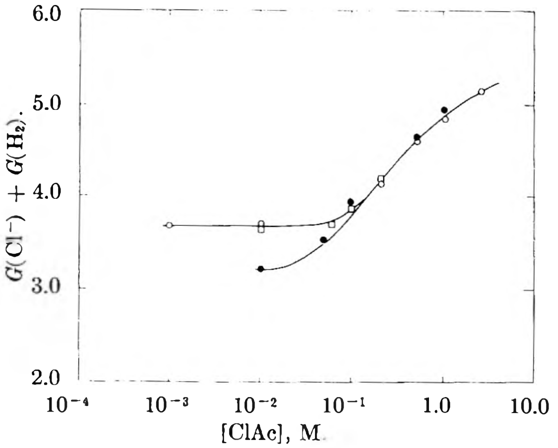

Fig. 6.—Sum of $G(H_2)$ and $G(Cl^-)$ in γ-radiolysis of chloroacetic acid solutions: ○, pH 1.0; □, pH 1.5; ●, pH 5.5.

7 gives results found with monochloroacetic acid at pH 1.0 and 1.5, plotted as suggested by eq. 5. Good straight lines are obtained, with a common intercept $k_3/k_4 = 0.55$, and from the slopes we find $k_2/k_1 = 3.34$ at pH 1.0 and 3.49 at pH 1.5, in good agreement. The kinetic evidence thus shows that H^+ and solute compete for reaction with the reducing radical from water, and that the product of the reaction with H^+ is another reducing agent which in turn reacts with solute to produce either Cl^- or H_2. These results cannot determine whether the two reducing agents involved are a hydrated electron and a hydrogen atom, or a hydrogen atom and a hydrogen molecule ion H_2^+, or other entities not at present clearly envisaged.

The sum of $G(H_2)$ and $G(Cl^-)$ is seen in Fig. 6 to increase markedly with chloroacetate concentration. The effect is probably due to a reduction of the recombination of H and OH in the spurs ("radical scavenging" by the solute) and is similar to the previously reported[14] effect of increasing the concentration of ceric ion in solutions containing ceric and thallous sulfates. The often noted increase in yield of available free radicals in acid solutions, over that found in neutral solutions, is manifested in Fig. 6 by the higher G-values found in acid for the more dilute chloroacetate solutions. This pH effect has been attributed[4] to scavenging of H by H^+, as reaction 2 occurs in the spur. When the chloroacetate concentration exceeds that of H^+, the scavenging effect of the H^+ is swamped out, and the yields at the higher chloroacetate concentrations become independent of pH.

Most of the other organic chlorides studied here behaved very similarly to chloroacetate (Fig. 2), showing the reactivity of the chlorine atom to be similar with respect to competition with H^+ as well as to abstraction by the acid form of the H atom. However, β-chloropropionic acid competes less successfully with hydrogen ion than the others do (Fig. 3), a rather surprising difference. In dichloroacetone (Fig. 4), on the other hand, $G(Cl^-)$ for any concentration is higher than given by the other compounds at all pH, and the chlorine atoms appear unusually reactive here in respect to both competitions.

The behavior of the hydrogen yields with respect to concentration and pH, found here with chlorine compounds, seems to be a quite general phenomenon for aqueous solutions of polar organic compounds of all kinds. It has recently been shown by one of us for solutions of glycolic and acetic acids,[15] and by Allan and Scholes[16] for solutions of isopropyl alcohol containing acetone. The classic paper of Fricke, Hart and Smith[17] shows many examples, including aldehydes, acetone and fatty acids. The hydrogen yields in acid solutions at moderate concentrations approach values around 4, but at higher concentrations $G(H_2)$ decreases; whereas increasing the pH at any constant moderate concentration results in a decrease of $G(H_2)$. In all cases, we suppose that the reducing radical from water radiolysis attacks the electrophilic part of the solute molecule to give mainly products other than hydrogen gas. In acid solutions, the hydrogen ions compete with the solute molecules for reactions with the original reducing radicals, converting them to the acid form, which reacts further mainly by hydrogen abstraction to yield H_2. The results of the present study of chlorinated compounds are thus in no way unusual, but serve to point out more clearly what is occurring, since the alternative product to H_2 is here in every case the easily detected chloride ion, whereas the reduction products of other organic compounds are harder to determine and may include a variety of chemical species.

The data of Fricke, Hart and Smith[17] show that with increasing pH, $G(H_2)$ eventually levels off at a

---

(14) E. Hayon, *J. Phys. Chem.*, **65**, 1502 (1961).

(15) E. Hayon and J. Weiss, *J. Chem. Soc.*, 5091 (1960).

(16) J. T. Allan and G. Scholes, *Nature*, **187**, 218 (1960).

(17) H. Fricke, E. J. Hart and H. P. Smith, *J. Chem. Phys.*, **6**, 229 (1938). The yields reported in that paper in terms of μM/kr. can be converted to G-values on the modern system of dosimetry by multiplication by 0.90.

value which is different for the different compounds. Reported values of $G(H_2)$ for various solutions are shown in Table II. Allan and Scholes have suggested this hydrogen to result from a portion of the reducing radicals which were generated initially in the acid form H′; but if this were its only source, $G(H_2)$ should be the same in alkaline solution for all these organic compounds.

TABLE II

HYDROGEN YIELDS FROM NEAR-NEUTRAL SOLUTIONS OF ORGANIC SOLUTES

Radiation	Solute	Concn. range (M)	$G(H_2)$	Ref.
X-Rays (200 kv.)	Formate	10^{-4}–10^{-1}	1.5	17
	Formaldehyde	10^{-2}	1.2	
	Butyrate	10^{-2}	1.1	
	Methanol	10^{-2}–10^{-1}	2.3	
	Lactate	2×10^{-2}	1.3	[a]
	Methylene blue	10^{-4}		[b]
	plus:			
	Formate	10^{-1}	1.9	
	Ethanol	10^{-1}	2.3	
	Lactate	10^{-1}	1.3	
	Glycolate	10^{-1}-1	1.6	15
	Acetate	10^{-1}-1	2.3	
γ-Rays	Isopropyl alc.			
	plus acetone		1.05	16

[a] G. R. A. Johnston, G. Scholes and J. Weiss, *J. Chem. Soc.*, 3091 (1953). [b] E. Hayon, G. Scholes and J. Weiss, *ibid.*, 301 (1957).

It could be supposed that the basic form has a probability of reacting with the various solutes to give H_2. If this were the case in chloroacetate solutions, $G(H_2)$ should increase with concentration in the same way that $G(Cl^-)$ increases, as the radicals are scavenged out of the spur. Instead, $G(H_2)$ decreases noticeably as the chloroacetate concentration rises from 0.01 to 1.0 M (compare Table I and Fig. 6). This decrease in $G(H_2)$ is about of the magnitude expected for the decrease in the molecular hydrogen yield from water due to scavenging of radicals from the spurs by chloroacetate. It thus seems that the presence of chloroacetate in water near neutrality induces a small additional yield of hydrogen, of magnitude essentially independent of the solute concentration. This yield could arise from some H atoms generated in the acid form, which might be less reactive toward chloroacetate than the basic form and hence be scavenged out of the spurs less efficiently, so that their yield would not change much with increasing chloroacetate concentration. Since $k_3/k_4 = 0.55$, only about 65% of any H atoms generated initially in the acid form should react with chloroacetate to give H_2. The excess $G(H_2)$ in dilute chloroacetate over the molecular yield from water amounts to 0.35, corresponding to an independent yield of H′ (the acid form) of about 0.54, in agreement with Allan and Scholes' estimate of 0.6. The higher H_2 yields from other organic solutions (Table II) still remain to be explained. The mechanism of formation of this hydrogen is not understood. It could possibly arise by partial reaction of the basic form of H with the particular solutes to yield H_2.

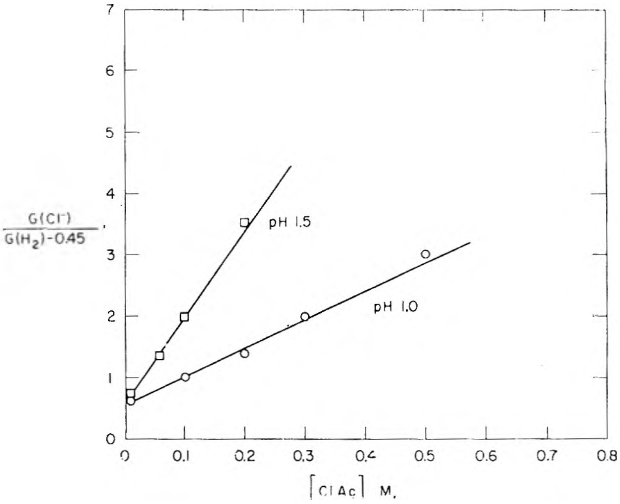

Fig. 7.—Competition plot for chloroacetic acid data at pH 1.0 and 1.5.

However, solutions of hydrogen peroxide and oxygen provide strong evidence against the existence of an initial yield of the acid form of H in neutral solutions. The basic and acid forms of H behave very differently in the competition between O_2 and H_2O_2, and studies of the competitive reduction of these solutes were interpreted[18] as showing that all H were initially generated in the basic form. The data were not precise enough to rule out a small yield of the acid form, but a recent more extensive study in this Laboratory (to be published) shows that all the H (100% ± 4%) are competed for by O_2 and H_2O_2 in the manner characteristic of the basic form. The result casts grave doubt on the interpretation of the organic solution data. More study is clearly called for on hydrogen formation in neutral and alkaline solutions of organic compounds of different types.

---

(18) A. O. Allen and H. A. Schwarz, *Proc. Second Intern. Conf. Peaceful Uses Atomic Energy (Geneva)*, **29**, 30 (1958).

ELECTRON IMPACT SPECTROSCOPY OF TETRAMETHYLSILICON, -TIN AND -LEAD[1]

BY BRICE G. HOBROCK AND ROBERT W. KISER

Kansas State University, Department of Chemistry, Manhattan, Kansas

Received June 26, 1961

Relative abundances and appearance potentials determined with a time-of-flight mass spectrometer are reported for M^+, MCH_3^+, $M(CH_3)_2^+$, $M(CH_3)_3^+$, and $M(CH_3)_4^+$ in the mass spectra of tetramethylsilicon, -tin and -lead. Probable ionization and dissociation processes are given. Heats of formation of the various ions, consistent with the proposed processes, are calculated. The observed ionization potentials for $SiMe_4$ (9.8 ± 0.15 e.v.), $SnMe_4$ (8.25 ± 0.15 e.v.), and $PbMe_4$ (8.0 ± 0.4 e.v.) are compared to those calculated using a modified Hall equivalent-orbital treatment.

Introduction

Various methods have been utilized in making theoretical calculations of ionization potentials for a large number of molecules.[2-5] In these earlier calculations, no attempt was made to study the effect upon the ionization potential when a central atom or group is varied within a family in the periodic table, but in which the ligands remain the same. In an attempt to investigate this effect, we have studied the electron impact spectroscopy of some Group IV organometallics.

An examination of the literature[6] reveals that ionization potentials have been determined for only a very few organometallics. And yet these molecules could conveniently afford suitable data for the desired study; the Group IV tetraalkyls are in most cases low boiling, colorless, liquids with significant vapor pressures at room temperature.

The mass spectral cracking patterns for a number of these compounds have been reported previously by Quinn, Dibeler and Mohler,[7] and agreement of our data with that reported earlier is good. The ionization and appearance potentials reported here are new, with the exception of that of tetramethyllead for which an ionization potential of 11.5 e.v. was reported by Fraser and Jewitt.[8] This is in poor agreement with the value of 8.0 ± 0.4 e.v. determined in this work. Ionization and dissociation processes are postulated for each of the compounds, and the heats of formation for the various ions, as computed for the probable processes, are given.

A variation of the theoretical treatment of the ionization potentials based on the Hall equivalent orbital method[2] gives rather good agreement for the Group IV tetramethyl compounds with the observed ionization potentials for these molecules. The modification deals essentially with the parameter for the methyl group–central atom interaction employed in solving the secular equations.

Experimental

The mass spectra and appearance potentials reported here were obtained with a Bendix model 12–100 time-of-flight mass spectrometer with an analog output system consisting of a monitor and scanner. The instrument has been described previously.[9]

Appearance potentials were determined using the method of extrapolated differences, described by Warren.[10] Ionization efficiency curves were plotted for each determination and the linear portions of the curves forced parallel. The voltage differences at given currents were plotted as a function of the current, and the value of ΔE obtained upon extrapolation to zero current was added algebraically to the ionization potential of the calibration gas employed. Krypton or xenon mixed with the compound being investigated was used to calibrate the ionizing voltage.

Mass spectra for each of the compounds were obtained at nominal electron energies of 70 e.v. Gas chromatographic analyses of the Group IV tetramethyl compounds were made on a Fisher-Gulf model 160 Partitioner, using a 14-foot column of tri-*n*-tolyl phosphate on Celite. Separations were satisfactory for our purposes at 80°; Apiezon-L on Silocel C-22 also has been used for a number of organometallics.[11]

The sample of tetramethylsilicon was obtained from K and K Laboratories. No significant impurities were observed during gas chromatographic analysis of the tetramethylsilicon.

Tetramethyllead was prepared from lead chloride and methylmagnesium bromide in diethyl ether. After acidification, the ether layer was dried over magnesium sulfate, and the tetramethyllead distilled. Gas chromatographic analyses of the sample indicated no impurities.

In the preparation of tetramethyltin, freshly distilled $SnCl_4$ was added to an excess of the Grignard reagent and then 10% HCl was added to decompose the excess Grignard and to effect solution of the solids. The ether layer was dried over magnesium sulfate and distillation gave a rather impure tetramethyltin, as revealed by gas chromatographic analysis. Pure tetramethyltin was obtained by determining the peak due to the tetramethyltin and then trapping it out at 77°K. as it was eluted from the column and detector cell. The tetramethyltin fraction eluted from the gas chromatograph, and trapped, was subsequently found to be quite pure by mass spectrometric analysis.

Results

The appearance potentials for M^+, MCH_3^+, $M(CH_3)_2^+$, $M(CH_3)_3^+$ and $M(CH_3)_4^+$ are summarized in column three of Tables I–III. The probable processes by which the various ions are formed consistent with measured and extrapolated energetics are given in the fourth column. The

---

[1] This work was supported in part by the U. S. Atomic Energy Commission under Contract No. AT(11-1)-751 with Kansas State University. Taken in part from a thesis submitted by B. G. Hobrock to the Graduate School of Kansas State University in partial fulfillment of the requirements for the M.S. degree. Presented at the 140th National Meeting of the American Chemical Society, Chicago, Ill., Sept. 3–8, 1961.

(2) G. G. Hall, *Trans. Faraday Soc.*, **49**, 113 (1953); **50**, 319 (1954).

(3) J. L. Franklin, *J. Chem. Phys.*, **22**, 1304 (1954).

(4) J. J. Kaufman and W. S. Koski, *J. Am. Chem. Soc.*, **82**, 3262 (1960).

(5) A. Streitwieser, Jr., *ibid.*, **82**, 4123 (1960).

(6) R. W. Kiser, "Tables of Ionization Potentials," U. S. Atomic Energy Commission, TID-6142, June 20, 1960.

(7) E. I. Quinn, V. H. Dibeler and F. L. Mohler, *J. Research Natl. Bur. Standards*, **57**, 41 (1956); V. H. Dibeler, *ibid.*, **49**, 235 (1952).

(8) R. G. J. Fraser and T. N. Jewitt, *Proc. Roy. Soc.* (*London*), **A160**, 563 (1937).

(9) E. J. Gallegos and R. W. Kiser, *J. Am. Chem. Soc.*, **83**, 773 (1961).

(10) J. W. Warren, *Nature*, **165**, 811 (1950).

(11) E. W. Abel, G. Nickless and F. H. Pollard, *Proc. Chem. Soc.*, 288 (1960).

TABLE I

APPEARANCE POTENTIALS AND HEATS OF FORMATION OF THE PRINCIPAL IONS OF TETRAMETHYLSILICON

Ion	% abundance (monoisotopic)	Appearance potential (e.v.)	Process	ΔH_f^+ (kcal./mole)
Si^+	2.5	....	$Si(CH_3)_4 \rightarrow Si^+ + 4CH_3$ (?)	(278)[a]
$SiCH_3^+$	11.6	17.1 ± 0.4	$\rightarrow SiCH_3^+ + 3CH_3$	235
$Si(CH_3)_2^+$	1.4	13.9 ± .3	$\rightarrow Si(CH_3)_2^+ + 2CH_3$	194
$Si(CH_3)_3^+$	82.2	11.3 ± .15	$\rightarrow Si(CH_3)_3^+ + CH_3$	166
$Si(CH_3)_4^+$	2.3	9.8 ± .15	$\rightarrow Si(CH_3)_4^+$	163

[a] Taken from ref. 20.

TABLE II

APPEARANCE POTENTIALS AND HEATS OF FORMATION OF THE PRINCIPAL IONS OF TETRAMETHYLTIN

Ion	% abundance (monoisotopic)	Appearance potential (e.v.)	Process	ΔH_f^+ (kcal./mole)
Sn^+	5.7	18.1 ± 0.3	$Sn(CH_3)_4 \rightarrow Sn^+ + 4CH_3$	276
$SnCH_3^+$	14.5	15.7 ± .4	$\rightarrow SnCH_3^+ + 3CH_3$	253
$Sn(CH_3)_2^+$	8.2	13.1 ± .2	$\rightarrow Sn(CH_3)_2^+ + 2CH_3$	225
$Sn(CH_3)_3^+$	69.1	9.9 ± .15	$\rightarrow Sn(CH_3)_3^+ + CH_3$	183
$Sn(CH_3)_4^+$	2.0	8.25 ± .15	$\rightarrow Sn(CH_3)_4^+$	177

TABLE III

APPEARANCE POTENTIALS AND HEATS OF FORMATION OF THE PRINCIPAL IONS OF TETRAMETHYLLEAD

Ion	% abundance (monoisotopic)	Appearance potential (e.v.)	Process	ΔH_f^+ (kcal./mole)
Pb^+	18.2	15.0 ± 0.5	$Pb(CH_3)_4 \rightarrow Pb^+ + 4CH_3$	251
$PbCH_3^+$	29.3	12.4 ± .2	$\rightarrow PbCH_3^+ + 3CH_3$	223
$Pb(CH_3)_2^+$	8.5	11.6 ± .2	$\rightarrow Pb(CH_3)_2^+ + 2CH_3$	236
$Pb(CH_3)_3^+$	44.4	8.9 ± .1	$\rightarrow Pb(CH_3)_3^+ + CH_3$	206
$Pb(CH_3)_4^+$	0.4	8.0 ± .4	$\rightarrow Pb(CH_3)_4^+$	217

calculated heats of formation for the ions are given in the last column.

The heat of formation of tetramethyltin was reported by Lippincott and Tobin[12] as −13.6 kcal./mole; this agrees reasonably well with calculations based on Franklin's method[13] in which we used a heat of formation of −38.1 kcal./mole for tetraethyltin.[14,15] Calculations of heats of formation for the various ions from $SnMe_4$ are based upon the value of −13.6 kcal./mole. To eliminate any possible interferences due to hydride formation, the measurements of appearance potentials were made using the tin isotope with $m/e = 116$, except for the parent ion, where the tin isotope with $m/e = 120$ was utilized to achieve greater detection sensitivity, as well as to prevent determining the appearance potential of the ion of the mass of parent-minus-hydrogen.

TABLE IV

CALCULATED AND OBSERVED IONIZATION POTENTIALS OF GROUP IV TETRAMETHYL COMPOUNDS

Compound	Calcd. I.P. (e.v.)	b parameter	Obsd. I.P. (e.v.)
$C(CH_3)_4$	10.21	1.55	10.29[a]
$Si(CH_3)_4$	(9.8)	1.5	9.8[b]
$Ge(CH_3)_4$	9.1	1.85[c]	9.0[c]
$Sn(CH_3)_4$	(8.3)	2.2	8.25[b]
$Pb(CH_3)_4$	7.8	2.5[c]	8.0,[b] 11.5[d]

[a] D. P. Stevenson, *Discussions Faraday Soc.*, 10, 35 (1951). [b] This work. [c] Interpolated; see accompanying text. [d] See ref. 8.

The heat of formation of tetramethyllead of 32.6 kcal./mole, as determined by Good, *et al.*,[16] was used. This value differs significantly from the value of 3.2 kcal./mole reported by Lippincott and Tobin.[12] Lead has four naturally occurring isotopes; it would have been desirable to have made appearance potential measurements on the lowest masses to minimize any possible contribution from hydride formation. This was not possible because the isotope with lowest mass has an abundance of only 1.3%; the ions containing the isotope of mass 208 therefore were selected to be used in the appearance potential measurements.

The following heats of formation have been used in the calculations with the measured appearance potentials: $\Delta H_f(CMe_4) = -37.6$ kcal./mole[17,18]; $\Delta H_f(SiMe_4) = -63$ kcal./mole[19]; $\Delta H_f(SnMe_4) = -13.6$ kcal./mole[12]; $\Delta H_f(PbMe_4) = 32.6$ kcal./mole[16]; and $\Delta H_f(CH_3) = 32.0$ kcal/mole.[20]

Mass Spectra.—The 70 e.v. mass spectra of these compounds, shown in Fig. 1, are in essential agreement with the spectra reported by Quinn, Dibeler and Mohler.[7] The mass spectra of the Group IV tetramethyl compounds studied are qualitatively similar, with the abundance of the parent molecule-ion being extremely small and the ion containing

---

[12] E. R. Lippincott and M. C. Tobin, *J. Am. Chem. Soc.*, **75**, 4141 (1953).

[13] J. L. Franklin, *Ind. Eng. Chem.*, **41**, 1070 (1949).

[14] G. Grüttner and E. Krause, *Ber.*, **50**, 1802 (1917).

[15] L. H. Long and R. G. W. Norrish, *Trans. Roy. Soc. (London)*, **A241**, 587 (1949).

[16] W. D. Good, D. W. Scott, J. L. Lacina and J. P. McCullough, *J. Phys. Chem.*, **63**, 1139 (1959).

[17] F. D. Rossini and J. W. Knowlton, *J. Chem. Phys.*, **6**, 168 (1938).

[18] "International Critical Tables," E. W. Washburn, editor, Vol. V, McGraw-Hill Book Co., Inc., New York, N. Y., 1929, p. 163.

[19] S. Tannenbaum, S. Kaye and G. F. Lewenz, *J. Am. Chem. Soc.*, **75**, 3753 (1953).

[20] F. D. Rossini, D. D. Wagman, W. H. Evans, S. Levine and I. Jaffe, "Selected Values of Chemical Thermodynamic Properties," National Bureau of Standards Circular 500, U. S. Government Printing Office, Washington, D. C., 1952.

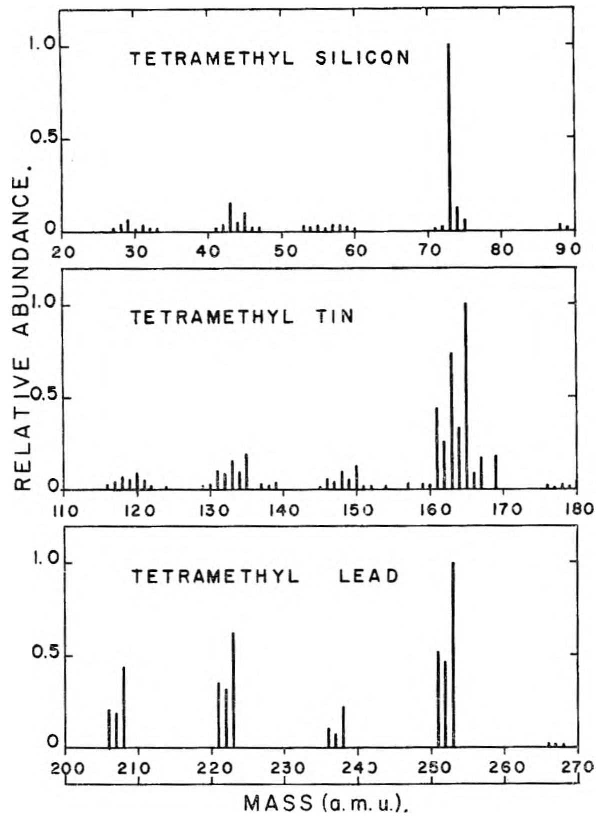

Fig. 1.—Mass spectra of tetramethylsilicon, -tin and -lead.

three methyl groups being the dominant species. It may be noted that the abundances of the smaller fragments increase significantly in intensity in going from tetramethylsilicon to tetramethyllead.

Ionization Potentials.—Calculated and observed ionization potentials for each of the compounds studied are listed in Table IV. Modifying slightly the equivalent orbital treatment due to Hall,[2] ionization potentials were calculated for tetramethyllead and tetramethylgermanium. These calculations were based on methyl group–metal atom interaction parameters interpolated and extrapolated from the parameters of 1.55, 1.5 and 2.2 calculated for neopentane, tetramethylsilicon and tetramethyltin, respectively, using the experimentally determined ionization potentials for these compounds. The following general equation was used

$$(e - I)(f - I) - 4b^2 = 0$$

where e = the ionization potential of the metal hydride (MH_4), f = the ionization potential of methane (13.31 e.v. was used[3]), b = the methyl group–metal atom interaction parameter. and I = the ionization potential of the molecule under consideration. The value of 7.8 e.v. calculated for the ionization potential of tetramethyllead agrees with our experimental value of 8.0 ± 0.4 e.v. (see Discussion).

Discussion

M^+.—From tetramethylsilicon, the ion of m/e = 28 is Si^+. Because of the background at m/e = 28, due to N_2^+, we were unable to determine the appearance potential of the Si^+ ion. All attempts to measure the appearance potential of Si^+ resulted in a value of 15.6 ± 0.1 e.v., the accepted value for the ionization potential of N_2. However, by comparison with the tetramethyltin and tetramethyllead studies, it is believed that the process for the formation of Si^+ also involves the formation of four CH_3 groups as the neutral fragments. The literature value of $\Delta H_f{}^+(Si)$ is 278 kcal./mole.[20,21] Certainly, the appearance potential of Si^+ from tetramethylsilicon is greater than 15.6 e.v.

The ion of m/e = 116 from tetramethyltin can only be Sn^+ and the calculation of its heat of formation gave a value of 276 kcal./mole, considering the neutral fragments to be four CH_3 groups. Although this is greater than the value of 243 kcal./mole reported in the literature,[20] any other process is incompatible with the energetics.

The ion of m/e = 208 in the tetramethyllead spectrum is Pb^+, and is the most abundant isotope of lead. On the basis of the comparison of the literature value of $\Delta H_f{}^+(Pb)$ = 219 kcal./mole[20] with $\Delta H_f{}^+(Pb)$ = 251 kcal./mole, calculated for the accompanying formation of four neutral methyl fragments, we believe the process of formation of Pb^+ from tetramethyllead to be that shown in Table III. The energetics rule out the possible formation of ethane by both the $C_2H_6 + 2CH_3$ and the $2C_2H_6$ processes.

$MCH_3{}^+$.—On the basis of interpolations between the ΔH_f of the other ions, and from an estimation of the energy required to remove successive methyl groups, the ion of m/e = 43 in the tetramethylsilicon spectrum is $SiCH_3{}^+$; it is considered reasonable to have three CH_3 groups as the neutral fragments. The value of the appearance potential and the thermochemical calculations rule out $CH_3 + C_2H_6$ as neutral fragments. Thus, we find that $\Delta H_f{}^+(SiCH_3)$ = 235 kcal./mole.

The heat of formation of the ion of m/e = 131 from tetramethyltin, $SnCH_3{}^+$, is 253 kcal./mole if accompanying it three CH_3 groups are formed as the neutral fragments. Considering the neutral fragments to be $C_2H_6 + CH_3$, a value of $\Delta H_f{}^+(SnCH_3)$ = 337 kcal./mole is calculated; this is considered to be too great, and thus is discarded as a possible process.

The ion of m/e = 223 from tetramethyllead is $PbCH_3{}^+$, with the possibility of some hydride being present; however, near the energy threshold for formation of the ion, the contribution of the hydrides is not considered to be significant. Consideration of the approximate energy necessary to remove a methyl group, and interpolation between the heats of formation of the other ions, indicates that the process involves the formation of three CH_3 radicals as neutral fragments. Therefore the heat of formation of this ion is 223 kcal./mole.

$M(CH_3)_2{}^+$. From the tetramethylsilicon study, the ion $Si(CH_3)_2{}^+$ has a heat of formation of 194 kcal./mole, considering the neutral fragments formed to be $2CH_3$. This value is intermediate between $\Delta H_f{}^+(Si)$ and $\Delta H_f{}^+(SiMe_4)$, as would be expected; thus the assignment of two methyl groups as neutral fragments.

---

(21) F. H. Field and J. L. Franklin, "Electron Impact Phenomena and the Properties of Gaseous Ions," Academic Press, Inc., New York, N. Y., 1957, p. 297.

The process for the formation of the ion of m/e = 146, $Sn(CH_3)_2^+$, from tetramethyltin, is considered to be the same as that for the lead and silicon compounds, with two neutral CH_3 fragments formed. Consideration of the approximate energy necessary to remove a methyl group, and of the fact that the energy for the accompanying formation of an ethane molecule is very great, leads us to conclude that the neutral fragments are two CH_3 radicals. Thus, $\Delta H_f^+(SnMe_2)$ = 225 kcal./mole.

The heat of formation of $Pb(CH_3)_2^+$ is calculated to be 236 kcal./mole. Energetics indicate that the process in Table III, as given for this ion, is the dominant one, involving two methyl groups as neutral products of the dissociative ionization process.

$M(CH_3)_3^+$.—These ions are the dominant species in the mass spectra of all of the compounds considered in this study. The ion of $m/e = 73$ from tetramethylsilicon is $SiC_3H_9^+$. We presume that the structure is that given by $Si(CH_3)_3^+$. Energetics dictate that the neutral fragment is the methyl radical. On this basis, we calculate $\Delta H_f^+(SiMe_3)$ = 166 kcal./mole.

The heat of formation for the dominant species in the tetramethyltin spectrum, $Sn(CH_3)_3^+$, is 183 kcal./mole for the process involving the formation of the neutral fragment CH_3. From energetic considerations, this is the only possible process for the formation of this ion.

$Pb(CH_3)_3^+$ is formed by the removal of a methyl group subsequent to ionization of the parent molecule. The heat of formation for this ion is calculated to be 206 kcal./mole.

$M(CH_3)_4^+$.—This is the parent molecule-ion in the compounds studied. In each of the spectra, this ion is very low in abundance. The heat of formation calculated for $Si(CH_3)_4^+$ from the determined appearance potential is 163 kcal./mole.

The heat of formation for $Sn(CH_3)_4^+$ is 177 kcal./mole; the process of its formation involves the removal of a single electron. Because the Sn^{121} isotope does not occur naturally, the appearance potential of the ion with m/e = 180 definitely is to be attributed to $Sn^{120}(CH_3)_4^+$ and not to $Sn^{121}(CH_3)_3(CH_2)^+$. The ionization potential of $Sn(CH_3)_4$ was found to be 8.25 ± 0.15 e.v.

The parent ion of tetramethyllead, $Pb(CH_3)_4^+$, is of extremely small abundance, and the ionization potential was quite difficult to determine. Only fair agreement was obtained between numerous determinations; therefore an error range of ±0.4 e.v. was assigned to the value of the ionization potential determined. The agreement of this experimental result with the calculations made on the basis of the modified equivalent orbital treatment substantiates our experimental result (see Table IV). Thus, $\Delta H_f^+(PbMe_4)$ = 217 kcal./mole. The ionization potential of 8.0 ± 0.4 e.v. herein reported is 3.5 e.v. lower than that reported by Fraser and Jewitt.[8] The values reported for the ionization potentials of a number of the bis-cyclopentadienyl–metal compounds[22] suggests that the ionization potential for tetramethyllead is indeed much lower than 11.5 e.v., and should be closer to that of the gaseous metal atom. Again, our result of 8.0 ± 0.4 e.v. agrees with this conclusion. It may be noted that the ionization potentials of the tetramethyl organometallics of Group IV decrease in a regular fashion, as expected.

We hope to be able to study experimentally tetramethylgermanium in the near future; it is anticipated that the fragmentation processes will be the same as those observed in this study. From interpolation of the heats of formation of the various ions and by back-calculation, as well as from the interpolation of the appearance potentials, it is estimated that the appearance potentials will be approximately 19, 16, 13.5, 10.5 and 9 e.v., respectively, for the formation of Ge^+, $GeCH_3^+$, $Ge(CH_3)_2^+$, $Ge(CH_3)_3^+$ and $Ge(CH_3)_4^+$ from tetramethylgermanium.

Acknowledgments.—The authors wish to thank Dr. R. L. Soulen for his aid in the preparation of the samples of tetramethyllead and tetramethyltin. Also, we wish to thank Dr. J. L. Franklin for his helpful comments and criticisms of this study.

(22) L. Friedman, A. P. Irsa and G. Wilkinson, *J. Am. Chem. Soc.*, **77**, 3689 (1955).

THE KINETICS OF SINTERING OF PLATINUM SUPPORTED ON ALUMINA

By R. A. Herrmann, S. F. Adler, M. S. Goldstein and R. M. DeBaun

American Cyanamid Company, Stamford, Connecticut

Received June 26, 1961

Various samples of $Pt-Al_2O_3-Cl$ re-forming catalyst were subjected to a series of heat treatments. Examination of the fresh and heated materials by measurement of chemisorptive capacity for H_2, rate of chemisorption of H_2, Pt crystallite size by X-ray line broadening and measurement of Pt solubility in HF lead to the conclusion that Pt is present in the original catalyst in a highly dispersed, perhaps ionic, form and that heat treatment causes the formation of Pt crystallites, and not merely their growth.

Introduction

The state of dispersion of platinum in platinum–alumina re-forming catalysts, both impregnated and cogelled types, has been the subject of an earlier investigation at this Laboratory.[1] Hydrogen chemisorption measurements and X-ray diffraction analyses were employed to describe the nature of platinum and the effect of various treatments on it. These included thermal and hydrothermal treatments, exposure to high temperature hydrogen–hydrocarbon atmosphere (re-forming),

(1) S. F. Adler and J. J. Keavney, *J. Phys. Chem.*, **64**, 208 (1960).

and ordinary catalytic regeneration procedures. The work was independently corroborated,[2] even to quantitative aspects. In these and other papers[3,4] the picture shown, for impregnated catalyst, is of a highly dispersed form of platinum, which undergoes transformation to a clustered and "crystalline" form upon prolonged exposure to various atmospheres at high temperature.

It has been of interest to study the effect of heat treatment on platinum re-forming catalysts of commercial types for two reasons. First, a study of the kinetics of observable changes on heat treatment and the fitting of these into a plausible mechanism may well enable more subtle conclusions to be drawn as to the nature of the reacting material (supported platinum) as originally obtained and as governed by various preparation techniques. Moreover, the stability of the platinum promoter is related to catalyst inactivation in use and is therefore of considerable practical significance.

Our samples of platinum catalysts therefore were subjected to various heat treatments and examined by X-ray line broadening and by hydrogen chemisorption techniques. In the latter technique, both the absolute amounts sorbed and the rates of sorption were studied.

Experimental

Preparation of Catalysts.—All Type A catalysts were prepared in a fashion similar to that previously described[1] under "Impregnated" Catalysts. Subsequent to the normal preparation, samples A_3 and A_4 were prepared from A_1 and A_2 by washing with an ammonia solution to remove chloride, thus modifying the Pt/Cl ratio.

Catalyst B is a commercially used re-forming catalyst. The compositions of this material and all Type A catalysts are given in Table I.

Table I

Catalyst Compositions

	A	A_1	A_2	A_3	A_4	B
% Platinum	0.774	0.787	0.315	0.720	0.300	0.375
% Chloride	0.830	0.920	0.480	0.110	0.040	0.350
% Fluoride	...	...	...	...	...	0.350
Surface area, m.^{2}/g.	225	199	202	199	202	176
Pore volume, cc./g.		0.617	0.625	0.617	0.625	0.940
Alumina	γ	γ	γ	γ	γ	γ
Form	1/16"D × 3/16"L cylinders				1/16" beads	

Heat-Treating Procedure.—Unless otherwise noted, all samples were subjected to a standard calcining procedure of heating to 593° for one hr. in air before division into small samples for further heat-treating and/or chemisorption measurements. Samples to be heat-treated were placed in a quartz "U" tube through which a steady stream of prepurified nitrogen was continuously passed at a rate of 200 cc./min. Approximately 8 g. of catalyst was heat-treated at a time except when samples A and B were treated simultaneously, in which case about 8 g. of each was used.

After placing the sample in the "U" tube containing a thermocouple, the nitrogen stream was allowed to pass over the sample for at least 20 min. before insertion into the hot furnace. This ensured against excess moisture being present which would tend to steam the catalyst in the early stages of heating. The sample temperature was checked several times during a run by means of the thermocouple buried in the catalyst. The furnace temperature was maintained constant to within ±2° with a Wheelco stepless proportioning controller. Following the heat-treatment, samples were cooled in the quartz tube under flowing nitrogen.

Catalyst B always was run simultaneously with sample A The samples were intimately mixed before placing them into the quartz tube, thus ensuring as precise a comparison as possible under exactly the same conditions of temperature and atmosphere. Subsequent separation of these catalysts was greatly facilitated by their different geometrical forms (cylinders and beads), which allowed mechanical separation.

Chemisorptive Measurements.—The procedure and apparatus used for measuring hydrogen chemisorption on supported platinum catalysts already have been described in some detail.[1] Briefly, the chemisorption of hydrogen was measured volumetrically at a pressure of about 9 mm. which was maintained constant to within approximately 10%. The measurements were made with the sample at 200°. Sample preparation consisted of a preliminary outgassing for two hrs., then a short (20 sec.) pretreatment with hydrogen at 500°, followed by overnight pumping to a final pressure of approximately 10^{-6} mm. The uptake of hydrogen at 200° then was followed with time and the volume of hydrogen (STP) adsorbed per gram of platinum at two hr. exposure was taken as a measure of the chemisorptive capacity.

X-Ray Diffraction Line Broadening.—A standard Philips diffractometer was equipped with a "tracergraph" print timer and a programmer to allow point-by-point intensity measurements, recording the time required to accumulate a preset number of counts at a scattering angle, and automatically shifting the diffractometer to the next scattering angle. The reciprocal of the time measured was plotted as a function of scattering angle over a range to cover the platinum (311) reflection. Unfiltered copper radiation and largest slits available were used throughout to ensure maximum intensity from this, the third strongest platinum reflection. Platinum crystallite size determinations were made by standard line broadening techniques using the plotted data.

Solubility of Pt Species in HF.—One to 2 g. samples of powdered catalysts were treated with an excess of an approximately 25% aqueous solution of HF according to an established procedure.[5] The mixtures were filtered after at least one hr. and the filtrates were analyzed for Pt spectrophotometrically.

Results

Table II gives the evaluation of two of the catalyst samples after various heat treatments under dry conditions. Each sample was examined by hydrogen chemisorption (after preliminary pretreatment with hydrogen) and X-ray diffraction. The rate of decrease in chemisorptive capacity was established to be second-order with respect to remaining chemisorptive capacity. This was done using primarily the data for samples A and B, especially at 625° where the data are more complete. Thus, having established the rate dependency, it was assumed to hold for samples A_1, A_2, A_3 and A_4 where there is insufficient data to make a judgment. Each datum was used together with the chemisorptive value of the initial (untreated) sample to calculate an apparent specific second-order rate constant for each material. This constant therefore has dimensions of K = (cc. H_2/g. Pt)$^{-1}$ hr.$^{-1}$. The consistency of the rate constant for sample A at each of the various temperatures is evidence of the second-order relationship, allowing that two of the twelve points represent sufficiently wide deviations from the group to be discounted as incorrect. It should be noted that these data cover a range of loss of chemisorptive power in excess of 80% of the original (untreated) value, showing the observed kinetics to hold over a considerable degree of degradation.

In addition to the total chemisorption, measured

---

[2] L. Spenadel and M. Boudart, *J. Phys. Chem.*, **64**, 204 (1960).

[3] G. A. Mills, S. Weller and E. B. Cornelius, Paper 113, Proceedings 2nd Intern. Catalysis Conference, Paris, France, 1960.

[4] R. C. Pitkethly and A. G. Goble, Paper 91, ref. 3.

[5] K. W. McHenry, R. J. Bertolacini, H. M. Brennan, J. L. Wilson and H. S. Seelig, Paper 117, Proc. 2nd Intern. Catalysis Conference, Paris, France, 1960.

TABLE II

EVALUATION OF HEATED CATALYSTS A AND B

Catalyst and treatment			H_2 chemisorption, cc. H_2/g. catalyst at 120 min.	Chemisorption parameters		Pt crystallites[a]		Second-order sintering rate constant 10^4 (cc. H_2/g. Pt)$^{-1}$ hr.$^{-1}$
Sample	Hr.	T, °C.		α_1	$a_1 \times 10^3$	Size, Å.	Relative amount	
A		Fresh	0.683	56.8	71	...	nil	...
A		Fresh	.674	57.5	68	...	nil	...
A	44	564	.431	69.6	33			1.5
A	47.5	564	.119	233	6.8			11.3[b]
A	70.5	564	.372	84.1	25	170	0.7	1.3
A	167	564	.292	96	7.6	180	1.5	0.9
A	353	564	.116	230	5.5	140	2.3	1.6
A	24	594	.326	87.8	21.3	165	1.0	5.2
A	48	594	.215	134	11.3	180	1.7	5.1
A	93	594	.135	162	7.9	150	2.1	5.0
A	4	625	.355	88.0	22.7	150	1.0	26.0
A	8	625	.141	190	6.9			55.0[b]
A	18	625	.123	192	6.5			25.0
A	40	625	.080	280	4.1	160	2.9	21.0
B		Fresh	0.298	143	13	...	nil	...
B		Fresh	.303	88.2	21	...	nil	...
B	44	564	.136	191	6.8			3.5
B	47.5	564	.057	500	2.2			11.4
B	70.5	564	.045	328	3.2	180	0.4	10.0
B	167	564	.051	411	2.7	170	0.7	3.8
B	353	564	.030	562	1.9	150	1.0	3.2
B	24	594	.117	161	7.6	155	0.7	8.3
B	48	594	.017	264	6.0	165	0.8	7.5
B	93	594	.043	460	2.3	130	0.7	8.2
B	4	625	.088	237	4.9	145	0.7	77.0
B	8	625	.035	585	1.8			120.0
B	18	625	.030	418	2.5			63.0
B	40	625	.023	574	1.8	130	1.1	38.9

[a] By X-ray line broadening. [b] Assumed to be incorrect.

after 120 minutes of exposure to H_2, the rate of uptake of hydrogen in the chemisorption test also was followed. In the calculation of the chemisorption kinetics, the q *vs.* t data were fitted to equation 1.[6] Accordingly, q values were plotted against log t in minutes, as illustrated in Fig. 1. From the slopes of these plots, generally almost linear, values of α_1 and a_1 were estimated from the values of q at 10 and 100 minutes.

$$q = \frac{2.3}{\alpha_1} (\log t + \log a_1 \alpha_1) \qquad (1)$$

This model assumed $a_1\alpha_1t_1 > 1$, as indeed it was found to be.

As can be seen from Table II, the chemisorptive capacity of both samples A and B decreases markedly with both temperature and time of heating. A regularity in this decrease is noted in the opportunity of fitting a second-order model to this data. In Figure 2, the obtained rate constants are plotted against reciprocal absolute temperature to obtain activation energies of about 70 kcal./mole. It is interesting to note that both samples A and B show similar behavior as regards decrease with time of chemisorptive power, even to the effect of temperature.

It is noted that examination of sample A_1 (a nominal duplicate preparation of A), gave similar results, as shown in Table III. Also shown in this table are the results with a version of A containing less platinum (A_2) and also similar catalysts having much lower halogen–platinum ratios. Similar values for both the initial specific chemisorption and also the decrease in chemisorption were observed, although the initial specific chemisorption was decreased somewhat due to the halogen removal procedure.

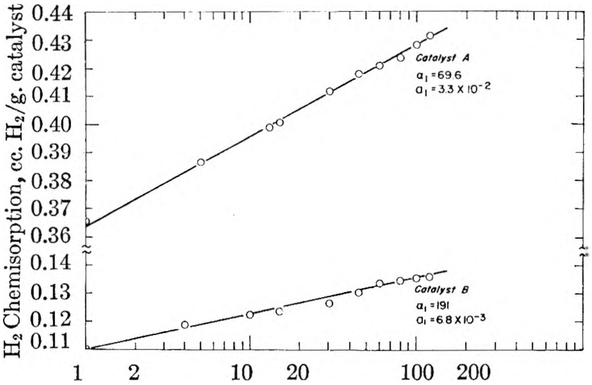

Fig. 1.—Sample plots of chemisorption data. Samples pretreated at 44 hr. at 564°.

Table II indicates that decrease in H_2 chemisorption is accompanied by the appearance of platinum crystallites and that the approximate amounts of crystalline platinum increase with increases in the severity of thermal treatment. It also is interesting to note that this regime does not appear to in-

---

(6) M. J. D. Low, *Chem. Revs.*, **60**, 267, (1960).

Table III

Evaluation of Other Heat Treated Catalyst Samples

Catalyst	Treatment Hr.	Treatment °C.	Pt Crystallites Size, Å.	Pt Crystallites Relative amount	H_2 Chemisorption, cc. H_2/g. catalyst at 120 min.	Sintering rate constant × 10^4 (cc. H_2/g. Pt)$^{-1}$ hr.$^{-1}$
A_1		fresh			0.888, 0.839	...
A_1	4	627	180	1.4	0.344	34
A_1	16	627	180	2.3	0.152	27
A_2		fresh			0.295, 0.269	...
A_2	6	625	...	nil	0.165	13
A_2	12	625	150	.7	0.115	14
A_2	28	625	200	.5	0.107	6.5
A_3		fresh	195	.9	0.390, 0.396	...
A_3	5	625	175	1.6	0.200	35
A_3	20	625	175	2.1	0.094	29
A_4		fresh	...	nil	0.159, 0.171	...
A_4	5	625	...	nil	0.063	59
A_4	20	625	160	.4	0.666	15

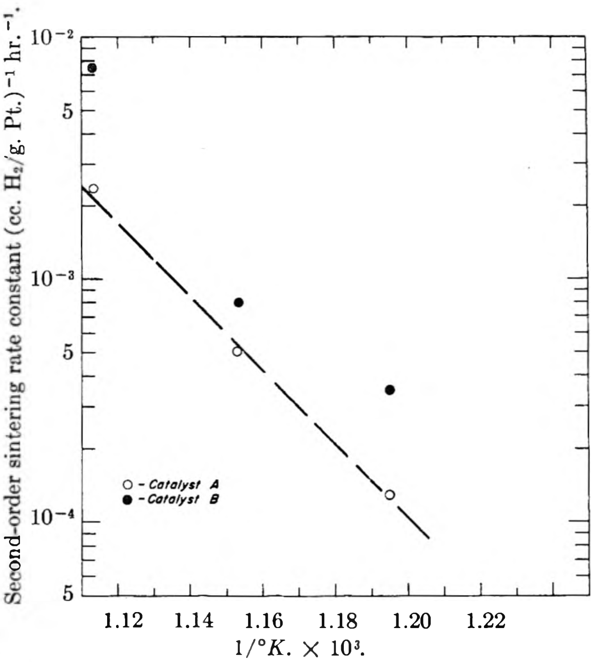

Fig. 2.—Arrhenius plot of sintering rate constants.

crease the size of the crystallites beyond 150–200 Å. Although there may be changes in the distribution of crystallite sizes below this value, it would be difficult to detect them by this method as the X-ray average crystallite size is a volume average crystallite size.

The data also indicate pronounced changes in the apparent values of the parameters in the chemisorption rate expression. These are reminiscent of changes noted with changes in the "cleanliness" of the adsorbing surface or the nature of the adsorbing sites.[6]

Discussion

Fresh catalyst samples A, A_1, A_2 and B all show H/Pt chemisorptive powers of about one and one-half atoms of hydrogen per atom of platinum. This indicates that the platinum is probably highly dispersed in the sample, perhaps even as "monolayer patches" of platinum. This result is borne out by the absence of crystallites detectable by X-ray in the materials. Although the dehalogenated catalysts (A_3 and A_4) possess lower hydrogen/platinum ratios (near one atom H/atom Pt) they are still more highly dispersed as regards platinum than typical cogelled catalysts.[1]

The regularity in decrease of the chemisorptive capacity with time is related to a second-order mechanism with respect to remaining chemisorptive capacity. In the event that the sintering of the platinum is ascribed to a coalition of small crystallites of platinum or to a growth of such crystallites by addition of platinum atoms from an "amorphous" phase, then such second-order dependence on the number of particles would reflect a growth rate depending on the sixth power of the surface area of the crystallites and the sixth power of the chemisorptive capacity. This result is contrary to the observed second-order dependence. What is possibly a more attractive explanation is one in which the chemisorptive capacity of platinum crystallites is taken to be low relative to that of the dispersed platinum and where the original dispersed platinum bodies are sufficiently small so that the chemisorptive capacity is primarily a measure of their number since the crystallites represent a small percentage of the total surface area. In such an event, the second-order decay of chemisorptive capacity with time is explainable as indicating a second-order dependence of the rate of removal of platinum-bearing particles from a highly dilute "solution" or "dispersed" phase to a "crystalline" or "condensed" phase. This notion is supported by the fact that platinum crystallites in the form of three-dimensional aggregates which are 150–200 Å. in size will probably have a maximum H/Pt ratio of about 0.1–0.2, thus contributing very little to the specific chemisorptive capacity of the material. We thus may think of a two-dimensional "solution" of extremely highly dispersed Pt bodies (perhaps as atoms, ionic platinum, or groups of a few atoms) on the surface of the alumina, aggregating by a second-order law to produce deposits of microcrystalline platinum where the crystallites have dimensions of the order 150–200 Å., each thus containing 10^4–10^5 platinum atoms.

On examining the rate of chemisorption of hydrogen as a function of the thermal pretreatment of the catalyst, a regularity in the parameters of the rate equation for chemisorption also is noted. Figures 3 and 4 indicate that the parameters a_1 and α_1 of (1) appear to change quite regularly with changes in total chemisorptive capacity, q, due to various thermal pretreatments.

In the general theory[6] of the kinetics of chemisorption of gases on solids, the coefficient α_1 is highly dependent on the rate of a chain-ending reaction, such as the obliteration of sites on which adsorption could take place as a consequence of adsorption on other sites. Since in our experiments α_1 seems to increase as the total chemisorption decreases, this suggests that heat treatment produces a system in which many adsorption sites are interconnected, such as by a crystalline network of platinum atoms, and that unheated samples possess a system where many more of the sites available for chemisorption are independent of each other, such as by being situated on discrete particles.

These results also can be interpreted in connection with those of McHenry, *et al.*,[5] who showed that fresh impregnated platinum–halogen–alumina catalyst possesses all its platinum in an HF-soluble, ionic form.

A series of our "A" samples was examined in this way, as shown in Table IV. Exposure of the catalysts to H_2, as in the chemisorption test, does not appear to sinter the platinum appreciably as judged by this test. (Other experiments have shown that after pumping off the chemisorbed hydrogen, a second test of chemisorptive capacity gives an H/Pt atomic ratio which is reduced by, at most, 10%). Heat-treatment, however, reduces the soluble platinum markedly as shown by Table IV, and approximately in proportion to the decrease in chemisorptive capacity.

TABLE IV

"SOLUBLE" PLATINUM IN RE-FORMING CATALYSTS

Catalyst	Treatment	% of Pt soluble in HF
A	None	91, 93, 84, 87
A_2	None	91, 89, 92
A	593° for 1 hr.	80, 84
A	593° for 1 hr., subjected to H_2 chemisorption	83, 80
A	593° for 1 hr. + 625° for 4 hr.	56
A	593° for 1 hr. + 625° for 40.5 hr.	27
A	593° for 1 hr. + 625° for 40.5 hr. + subjected to H_2 chemisorption	23, 20

While the crystallite size determination does not appear to add to the picture presented here, it in no way contradicts it. Indeed, just as the same sort of mechanism of sintering appears to be followed by catalysts A and B as judged by the time decay of chemisorptive capacity, so too the increase of crystalline X-ray-visible material in both the samples appears to have similar dependence on both time and temperature.

Examination of the rate constants which characterize the type A catalyst samples (Table III) shows little, if any, difference in sintering rates for these samples even though their platinum contents vary by a factor of as much as 2.5 and the chloride content by a factor of 20. The large variation in platinum to chloride ratio is shown to have little effect on the sintering rate. One then can infer that a chloroplatinate ion is not the only platinum species active in the sintering process. The original presence of halogen may, however, play some part in the distribution of platinum on the alumina surface during impregnation.

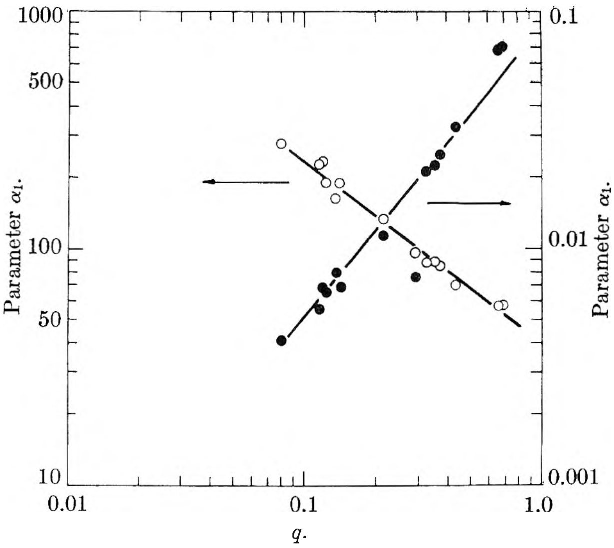

Fig. 3.—Relation of parameters in Elovich rate equation to total chemisorptive capacity (catalyst A).

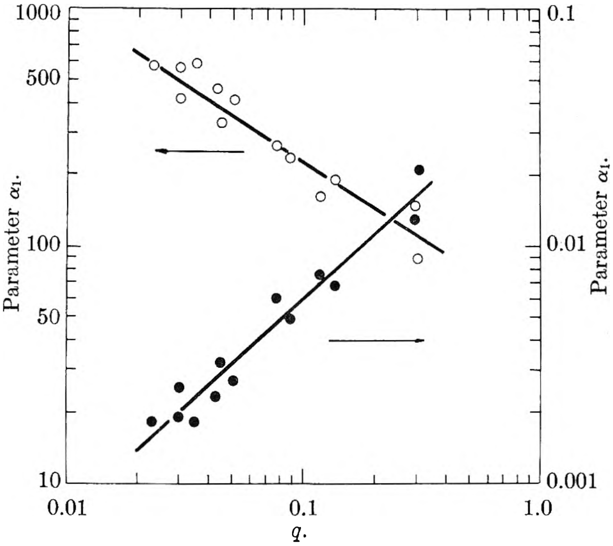

Fig. 4.—Relation of parameters in Elovich rate equation to total chemisorptive capacity (catalyst B).

The second-order rate constants are reported in units of (cc. H_2/g. Pt)$^{-1}$ hr.$^{-1}$, which is related to the fraction of the original chemisorptive capacity remaining. If the distribution of the platinum species on alumina were essentially uniform, then one would expect the kinetics of the sintering process to be linked to the bulk concentration of platinum. In this case, k in units of (cc. H_2/g. catalyst)$^{-1}$ hr.$^{-1}$, rather than in (cc. H_2/g. Pt)$^{-1}$ hr.$^{-1}$, should be constant at different platinum levels. This would be so since the mean distance between the fundamental platinum units would decrease continually as their concentration increases in the manner of the mean-free path of gas molecules with increasing pressure. That this is not so can only be interpreted as meaning that the platinum is non-uniformly distributed and, in fact, must exist in local groupings of more than average density.

Moreover, it has been shown that the number of adsorbing sites relative to total platinum (H/Pt) is independent of platinum concentration. This indicates that the nature of the local grouping of Pt species is unchanged with changes in concentration. As a matter of fact, the only change that could logically occur, in the light of the available data, is in the total number of such groupings. That is to say, increasing the platinum content of the catalyst appears to increase the number of "cities" of relatively fixed dimensions and H_2 chemisorption characteristics.

A non-homogeneous distribution of platinum clusters on an amorphous alumina substrate is not unexpected, since it is well known that such a surface is heterogeneous from a crystallographic point of view. This is, in turn, associated with heterogeneity in the local surface density of hydroxyl groups and perhaps even with the relative acidity or basicity of those groups.[7,8]

Acknowledgments.—We wish to thank Mr. George Yates, who performed the heat treatments and hydrogen adsorption measurements, and Mr. William Doughman, who provided the X-ray data.

---

(7) D. S. Rea and R. Lindquist, Paper 53, 136th National Meeting, Am. Chem. Soc., Atlantic City, September, 1959.

(8) J. B. Peri and R. B. Hannan, *J. Phys. Chem.*, **64**, 1526 (1960).

CHEMISTRY OF COÖRDINATION COMPOUNDS. I. THE KINETICS OF FORMATION OF MONOACETYLACETONATOCOPPER(II) ION

By Alfred V. Celiano,

Department of Chemistry, Seton Hall University, South Orange, N. J.

Michael Cefola and Philip S. Gentile

Department of Chemistry, Fordham University, Bronx 57, N. Y.

Received June 27, 1961

The kinetics of the reaction copper(II) ion + acetylacetone ⇄ monoacetylacetonatocopper(II) ion in methanol was investigated conductometrically in the temperature range −27 to 0°. The reaction obeyed second-order kinetics, first order with respect to copper(II) ion, and first order with respect to the enol form of acetylacetone. The dependence of rate on hydrogen ion concentration indicates that the reaction does not involve prior ionization of the β-diketone, but rather the direct combination of the two reacting species. The enol content of the ligand as well as the energy and entropy of activation were evaluated.

Introduction

The reactions between metal ions and β-diketones have been the subject of considerable investigation. In the sphere of kinetics of complex ions interest has been focused mainly on the mechanism of substitution reactions rather than the rate of complex formation. Rates of reaction of various metals with *o*-phenanthroline[1-3] and α,α'-bipyridyl[4-6] have been determined. Cook[7] has studied the rate of complex formation of metal ions with aqueous 2-thenoyltrifluoroacetone and concluded that, for most metal ions investigated, including Cu^{2+}, the rate of complex formation was identical with the rate of enolization. These investigators also studied the rate of complex formation using acetylacetone and 2,4-hexanedione and found that the rate of complex formation was not the same as the rate of enolization of these β-diketones.

According to the principles enunciated by Bjerrum,[8] complex formation takes place in a series of reversible steps.

$$M^{+n} + HA \rightleftarrows MA^{+(n-1)} + H^{+} \qquad (1)$$

$$MA^{+(n-1)} + HA \rightleftarrows MA_2^{+(n-2)} + H^{+} \qquad (2)$$

In the above scheme, higher complexes are favored at high *p*H. The values for formation constants determined under many environmental conditions[9] indicate a factor $\geqq 10$ for

$$K_1/K_2$$

where K_1 and K_2 are the formation constants for reactions 1 and 2, respectively. In the present study the rate of first complex formation between Cu^{2+} and acetylacetone was followed conductometrically.

Experimental

Materials.—Reagent grade methanol was refluxed for one hour over magnesium methoxide[10] and then distilled through a 90-cm. column. The first portion of distillate was discarded, and a second distillation was made over 2,4,6-trinitrobenzoic acid through a 15-plate Oldershaw column; b.p., 64.5–65.0°, lit.[11] value 64.75°. C.P. acetylacetone was fractionally crystallized, distilled and the middle fraction collected; b.p. 45° (30 mm.) (uncor.); $n^{18.6}D$ 1.4520 ± 0.0001, lit. value 1.45178. Analytical reagent grade Cu-

---

(1) D. W. Margerum, *J. Am. Chem. Soc.*, **78**, 4211 (1956).

(2) W. Brandt and D. Gullstrom, *ibid.*, **74**, 3532 (1952).

(3) T. Leo, I. Kolthoff and D. Leussing, *ibid.*, **70**, 3596 (1948).

(4) P. Krumholz, *J. Phys. Chem.*, **60**, 87 (1956).

(5) J. H. Baxendale and P. George, *Nature*, **162**, 777 (1948).

(6) J. H. Baxendale and P. George, *Trans. Faraday Soc.*, **46**, 736 (1950).

(7) E. Cook, Thesis, "Rate and Equilibrium Studies with Aqueous TTA," Pennsylvania State University, 1953.

(8) J. Bjerrum, "Metal Ammine Formation in Aqueous Solution," P. Haase and Son, Copenhagen, 1941.

(9) R. Taft and E. Cook *J. Am. Chem. Soc.*, **81**, 46 (1959).

(10) A. Weissberger, "Techniques of Organic Chemistry," Vol. VII, "Organic Solvents," Interscience Publishers Inc., New York, N. Y., 1955, p. 336.

(11) G. E. Coates and J. E. Coates, *J. Am. Chem. Soc.*, **55**, 2733 (1933).

$(ClO_4)_2 \cdot 6H_2O$ (G. F. Smith) was dried over phosphorus pentoxide for a minimum of three days.[12] Iodometric analysis of the salt, employing copper metal (99.95% pure) dissolved in perchloric acid as the primary standard,[13] yielded the value 99.60 ± 0.02%. A sample of the salt was heated in a Stanton thermobalance over the temperature range 80–175° and became stable at the latter temperature. Calculations showed that the residue must be $Cu(ClO_4)_2 \cdot 3H_2O$ and subsequent titration on the basis of this formula led to the value 100.1 ± 0.1%. The salt was used without further purification. Analytical reagent grade anhydrous sodium perchlorate (G. F. Smith) was dried at 200°[14] and its purity was determined by an ion-exchange method to be 99.9%. Doubly distilled, lead free, perchloric acid (G. F. Smith) was used without further purification.

Solutions.—Calibrated glassware and weights were used throughout. Stock solutions of $Cu(ClO_4)_2 \cdot 6H_2O$ in methanol were standardized by iodometric titration after evaporation of the methanol. 1 *M* methanolic sodium perchlorate solutions were standardized by an ion-exchange method using Amberlite IR-120. All methanolic solutions were kept in automatic burets and protected from atmospheric moisture and CO_2. Aqueous solutions of perchloric acid were standardized by titration with NaOH. The density of these solutions was determined with a pycnometer and the water content by calculation. Solutions employed in the kinetic determinations were made from the stock solutions to a precision of 0.1%. Acetylacetone was weighed in a pycnometer type cell having side arms of 0.5 mm. capillary to prevent vaporization. The enol content of acetylacetone was determined by the Kurt Meyer bromine titration method as modified by Cooper and Barnes.[15] Approximately 0.04 *M* solutions of the diketone in methanol, containing $NaClO_4$ and water in concentrations used in kinetic determinations, were thermostated in a quartz flask. The indicator was thyodene (Fisher Chemical Co.), which proved to be more sensitive than the usual starch solution.

Reaction Cell.—Preliminary spectrophotometric investigation of the reaction Cu^{2+} + acetylacetone → monoacetylacetonatocopper(II) ion + H^+ indicated that the reaction was far too rapid to be followed by conventional techniques and therefore a continuous flow method was adopted. The cell designed by K. Dalziel[16] was chosen as the prototype and modified for conductometric analysis. These modifications entailed no change whatever in the mixing head, which is the most critical feature of flow reactor design. The reaction tube was a 40-cm. length of precision bore Pyrex tubing (i.d., 2.009 ± 0.004 mm.). Pairs of holes to accommodate the electrodes were drilled opposite one another every 3 cm. along the length of the tube. The reactor volume from mixing head to each observation point then was calculated from the tube dimensions and distance of each set of electrodes from the mixing head.

The electrodes were fashioned from platinum wire (0.032″ diameter) and were ground by placing them in a hole drilled into another piece of 2-mm. capillary. A hard metal wire coated with fine carborundum was placed in the bore of this capillary and rotated. The platinum electrode was gently pushed through the hole onto the revolving wire. The final polishing was done with jeweler's rouge. The electrodes were inserted into the reaction tube and sealed with an epoxy resin (Bondmaster M-654; Rubber & Asbestos Company, Bloomfield, N. J.). Bailar has shown[17] that extended surface catalysts such as Raney nickel and charcoal catalyze the formation of cobalt–nitrogen and chromium–nitrogen bonds. Although no information is available concerning the catalytic action of platinum black on the formation of copper–oxygen bonds, in view of Bailar's findings it was decided not to platinize the electrodes.

The mixing head, consisting of 1-mm. jets backed by 2-mm. capillary, was sealed to the reaction tube with the epoxy resin.

The reagent containers were two-liter suction flasks fitted with a siphon tube and provisions for filling with reactants and introducing and releasing pressure. The reagent containers were connected to the mixing head *via* 3-way stopcocks which enabled each reactant to be passed through the reaction tube separately or mixed with the other reactants. The stopcock plugs were of Teflon and could be tightened by means of a spring and washers. The use of a Teflon plug was found to be extremely important because a tight seal could be developed using only a very fine film of high vacuum silicone grease. The eluent end of the reaction vessel was fitted with a stopcock which enabled "stopped flow" measurements to be made.

Shielded cables were soldered to the electrodes and the entire reaction vessel was placed inside a glass tube 10 cm. in diameter. The outer tube had side arms through which the shielded cable could be taken above the level of the bath liquid. The ends of the outer glass tube were sealed with a metal plate and the resin. The entire assembly was mounted on an aluminum frame and suspended in a constant temperature bath where temperature control was maintained at ±0.01°.

The fluid drive was high purity dry nitrogen and pressure control was accomplished by employing a constant pressure diaphragm valve and a 30-gallon surge tank. Pressure was reproducible to ±0.04 p.s.i.

A conductance bridge similar to that of Luder[18] was constructed, the sole modification consisting of the replacement of the 40-ohm variable resistance in the Wagner Earthing device with a 1000-ohm variable resistance. The oscillator was a General Radio Type 1302-A degeneratively tuned oscillator. The oscillator must have a frequency high enough for the period of oscillation to be small compared to the reaction time; at 50 kc./sec. the period is 2×10^{-5} sec., which is adequate for the present work where the reaction half-lives are $> 10^{-2}$ sec. The use of this high frequency also eliminated much of the polarization effect that would be encountered at lower frequencies because of the use of small, closely spaced electrodes. The oscillator was connected to the bridge by a General Radio Type 578-C, 4-1 step down transformer. The null indicator consisted of a General Radio 1231-B Amplifier and 1231-P5 Filter. The amplifier output was introduced into an oscilloscope.

Measurements.—Ideal operation of the apparatus would involve mixing of equal amounts of both reactants. The true mixing ratio was determined at all experimental temperatures and pressures by mixing methanolic perchloric acid with methanol through the flow system. Aliquots of the undiluted and diluted solutions were titrated in excess water with NaOH, using phenolphthalein as indicator. The mixing ratio, relative delivery from left jet to right jet, was 0.4928 ± 0.0005. Mixing efficiency was assessed by the physical dilution process in which a solution of perchloric acid in methanol was used as one reactant and methanol as the other. Mixing was observed under stopped-flow conditions and was found to be essentially complete by the time the solution reached the first electrode.

The reaction time was determined directly in the stopped-flow method and indirectly in the continuous flow method. For stopped-flow determinations a precision timer reading to 0.01 minute ±0.002 was activated automatically when the eluent stopcock was closed and was stopped by a hard switch when the output from the previously balanced conductance bridge reached a minimum. This device allowed the time to be determined with a precision of ±0.1 second and was generally used for reaction times greater than 2.5 seconds. For the continuous flow method the reaction time was calculated from a knowledge of the flow rate and the volume of the reaction tube to any observaton point. In all cases the rates of flow were in excess of those required to produce turbulent flow,[19] a condition which ensures 99% mixing of the reactants within 5 milliseconds.[20]

The measurements of conductance of the flowing solutions were carried out in the usual manner. For stopped flow methods it was necessary to pre-set the bridge, which involved not only setting a desired value on the resistance box, but also balancing the capacitative reactance and the

---

[12] R. Portillo and L. Albertolas, *Anales soc. espan. fis. quim.*, **28**, 1117 (1930).

[13] J. J. Kolb, *Ind. Eng. Chem., Anal. Ed.*, **16**, 38 (1944).

[14] C. Duval, "Inorganic Thermogravimetric Analysis," Elsevier Publishing Co., New York, N. Y., 1953.

[15] S. R. Cooper and R. P. Barnes, *Ind. Eng. Chem., Anal. Ed.*, **10**, 379 (1939).

[16] K. Dalziel, *J. Biol. Chem.*, **55**, 79 (1953).

[17] J. C. Bailar, *J. Am. Chem. Soc.*, **67**, 176 (1945).

[18] W. F. Luder, *ibid.*, **62**, 89 (1940).

[19] A. Weissberger, ref. 10, Vol. VIII, "Rates and Mechanism of Reactions," Interscience Publishers Inc., New York, N. Y., 1953, p. 680.

[20] K. Dalziel, *J. Biol. Chem.*, **55**, 79 (1953).

Wagner Earthing section. To accomplish this, the reactants were allowed to flow through the tube at other than the aforementioned mixing ratio. Flow was terminated by means of the eluent stopcock and the influent stopcocks then were fully opened. In this way a complete span of resistance values encountered during the reaction could be accurately prebalanced, thus obtaining a sharp minimum in the bridge output.

The ratios of the cell constant at one pair of electrodes (reference cell) to the cell constant at all other electrodes were determined, and all resistance readings were corrected to values that would have been measured at the reference cell. It is known that pressure applied to a system affects the conductance of electrolytic solutions.[21] The expected decrease of resistance with increasing pressure and flow rate was observed to be a linear relationship. All resistance values were corrected to resistance at 7 p.s.i., at which pressure the initial resistance of each solution was determined.

Reaction Medium.—Methanol was chosen as the solvent because of its low freezing point and viscosity and the relatively high solubility of β-diketones in it. It has been shown[22] that the equivalent conductance of H^+ in methanol is extremely sensitive to slight fluctuations in water content when the mole fraction of water is <0.02. Anhydrous $Cu(ClO_4)_2$ cannot be obtained by simple heating of the hydrate since the oxide preferentially forms. The experimental difficulty in obtaining and especially in retaining the anhydrous character of the salt during all the procedures that had to be carried out made the use of the hydrate more feasible. In view of these considerations the *total* water content including the water present in the $Cu(ClO_4)_2$ was made 5.56×10^{-1} M in all solutions. At this concentration the ratio H_2O/Cu^{2+} was 1.1×10^2, and the mole fraction of water in all circumstances was *ca.* 0.02.

During the course of the reaction the ionic strength of the solution varies. There is no prior guarantee that the rate of reaction is independent of this quantity and as a result, all kinetic determinations were made in solutions containing 1×10^{-2} mole/l. of sodium perchlorate. Another reason for employing a neutral salt is the difficulty encountered in balancing the bridge when solutions containing the reactants alone are mixed and allowed to react. At $-17°$ the resistances of 5×10^{-3} M $Cu(ClO_4)_2$ and acetylacetone solutions measured at the reference electrode were, respectively, *ca.* 13×10^3 and 60×10^3 ohms. Assuming that the precision with which the bridge can be balanced is a linear function of per cent. mixing, 99.9% mixing of these solutions without any reaction taking place would allow the bridge to be balanced to ±25 ohms. This value is 2.5% of the total change of resistance which accompanies the reaction and the indeterminacy could lead to serious errors in determining the specific rate constant, especially in the early stages of the reaction. To circumvent this difficulty the $NaClO_4$ was almost entirely added to the solution of acetylacetone, thus allowing the initial resistance of both solutions to have the same value ±100 ohms. In the actual determinations the bridge could be balanced to ±5 ohms at the first few electrodes and ±2 ohms at the remaining electrodes. The initial resistance of the mixed solution was calculated by use of the parallel resistance law applying the proper dilution factors.

Kinetics of First Complex Formation.

The following notations shall be used in the ensuing discussions

$[\ ]$ = concentration

$[HAA]_K$ = β-diketone in the keto form

$[HAA]_E$ = β-diketone in the enol form

$[AA^-]$ = enolate ion

$[CuAA^+]$ = monoenolatocopper(II) ion

$[Cu(AA)_2]$ = bisenolatocopper(II) ion

K_1 = first complex formation constant $= \dfrac{[CuAA^+][H^+]}{[Cu^{2+}][HAA]}$

K_2 = second complex formation constant $= \dfrac{[Cu(AA)_2]\ [H^+]}{[CuAA^+]\ [HAA]}$

K_E = concn. quotient for the process $HAA_K \rightleftarrows HAA_E = \dfrac{[HAA]_E}{[HAA]_K}$

k_1 = specific rate constant for first complex formation

k_2 = specific rate constant for dissociation of first complex

HAA = acetylacetone

Resistance and Per Cent. Reaction.—The reaction between Cu^{2+} and acetylacetone is known to be reversible, although the equilibrium constant for reaction in the environmental conditions obtaining in this study has not been determined. The construction of an experimental curve relating per cent. reaction to resistance values was assessed by two methods based on different assumptions. The linear correspondence of the experimental data obtained by these two independent methods heightened our confidence in the validity and accuracy of the relationship.

In the first approach it was assumed that, if the ratio of metal to chelating agent was $\geqq 5$, the reaction could be considered complete. Determinations were made of the resistance of solutions in which the total Cu^{2+} concentration was 5×10^{-3} and varying amounts of acetylacetone were added, so that the ratio of metal to ligand was $\geqq 5$. It was observed also that the auto-ionization of acetylacetone in the solvent employed was so negligible as to be incapable of detection within experimental error of ±0.05%.

The second approach involved the assumption made by Monk, *et al.*, in the determination of the dissociation constant of condensed phosphates[23-26], namely, that the mobility, and hence conductance, of $NaP_3O_9^{2-}$ ion is two-thirds that of $P_3O_9^{3-}$ ion (*i.e.*, the ratio of charges). We assumed that the mobility of the solvated Cu^{2+} was twice that of solvated $CuAA^+$ and determined the resistance of solutions in which $Cu(ClO_4)_2$ concentration was increased from 5×10^{-3} to 2.5×10^{-3} M, while the concentration of $HClO_4$ was increased from 0 to 5×10^{-3} M, a 1×10^{-3} increase of $HClO_4$ for every 0.5×10^{-3} M decrease of Cu^{2+}.

Figure 1, one of a series of such curves covering all experimental conditions, indicates a linear relationship between resistance and $[H^+]$. The fact that the relationship is linear within experimental error corroborates the fact that hydrolysis of Cu^{2+} in the solvent chosen is negligible and does not have to be taken into account in the kinetic determinations.

Order of Reaction and Integrated Rate Equation.—The order of the reaction between Cu^{2+} and acetylacetone was evaluated from the van't Hoff equation[27] and was found to be second order, first order with respect to Cu^{2+} and first order with respect to acetylacetone. Since complexation is a reversible process, complete determination of its kinetics demands a knowledge of the equilibrium concentration of all the species involved.

---

[21] Kortum and Bockris, "Electrochemistry," Elsevier Publishing Company, New York, N. Y., 1951.

[22] E. Marum and L. Thomas, *Z. physik. Chem.*, **143**, 213 (1929).

[23] C. B. Monk, *J. Chem. Soc.*, **152**, 427 (1949).

[24] R. W. Jones, C. B. Monk and C. W. Davies, *ibid.*, 2693 (1949).

[25] C. W. Davies and C. B. Monk, *ibid.*, 413 (1949).

[26] C. B. Monk, *ibid.*, 423 (1949).

[27] A. A. Frost and R. G. Pearson, "Kinetics and Mechanism," 1st edition, John Wiley and Sons, Inc., New York, N. Y., 1953, p. 44.

Determination of these values cannot be accomplished by simply measuring the conductance of the solution after the reaction is completed because the second complex forms to some extent. Accurate evaluation of equilibrium conditions for first complex formation would be a major task in itself and consequently it was deemed advisable to avoid such a determination if the rate constant of the forward reaction could be evaluated independently.

It has been ascertained (vid. appendix) that the kinetic effect of the reverse reaction is negligible and that k_1 can be evaluated with an accuracy of 2% up to 60% completion. Preliminary investigation of the rate of second complex formation ($k_r = 10^1$ l. mole^{-1} sec.$^{-1}$ at $-17°$), as well as the fact that experimentally determined values of k_1 are constant, indicates that the kinetic effect of second complex formation may be neglected at least up to 60% completion of first complex formation. All rate constants were determined graphically using the integrated equation for non-reversible second-order processes.

An examination of Fig. 2 reveals that the rate constant decreases by 6% of its initial value when the reaction is 60% complete, a decrease three times greater than expected. This decrease led us to suspect that the reacting specie in the "rapid formation" of the complex is the enol form of the β-diketone, a suspicion corroborated by other relationships which shall be discussed subsequently. Taft and Cook also found that the enol form of thenoyltrifluoroacetone complexes with metal ions "instantaneously" compared to the keto form.

Enol Content of Acetylacetone.—Table I lists the percentage enol and the concentration quotient for the reaction $HAA_K \rightleftarrows HAA_E$. Determinations were made on 0.04 M solutions of the diketone in methanol containing $NaClO_4$ and water in concentrations used in the kinetic determinations.

TABLE I

ENOL CONTENT OF ACETYLACETONE

Temp., °C.	% enol	K_E
0	77.8 ± 0.1	3.51
−17.08	74.9 ± .1	2.98
−27.42	73.4 ± .1	2.76

Figure 3 indicates that the rate constant shows no drift, within experimental error, up to 65% completion of reaction when the concentration term for the ligand in the integrated equation is the initial enol concentration. After 65% completion there is an upward drift of the rate constant which is attributed to the formation of the second complex. A series of determinations in which the initial concentration of both the metal ion and acetylacetone were varied yielded the same rate constant and gives conclusive evidence that the rate of first complex formation is second order.

Dependence of Rate of Complex Formation on Hydrogen Ion Concentration.—Acetylacetone is known to be a weak acid, $K_a \cong 10^{-8}$ in H_2O. The conductances of 1×10^{-2} M sodium perchlorate in methanol, and 5×10^{-3} M acetylacetone in a similar solution were determined. There was no apparent difference in conductance of these solutions, from which we can conclude that the hydrogen ion concentration due to ionization is $\leqq 10^{-6}$ M.

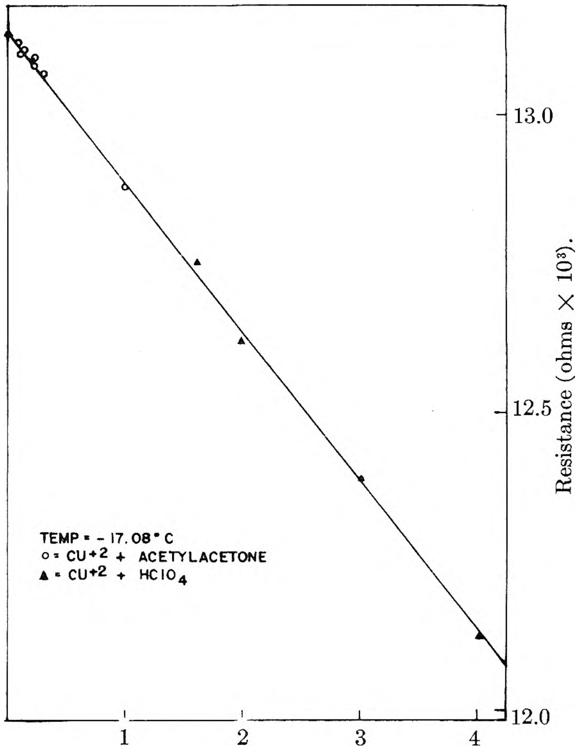

Fig. 1.—Relationship between hydrogen ion concentration and resistance of solutions, measured at the reference electrode, assessed by two independent methods.

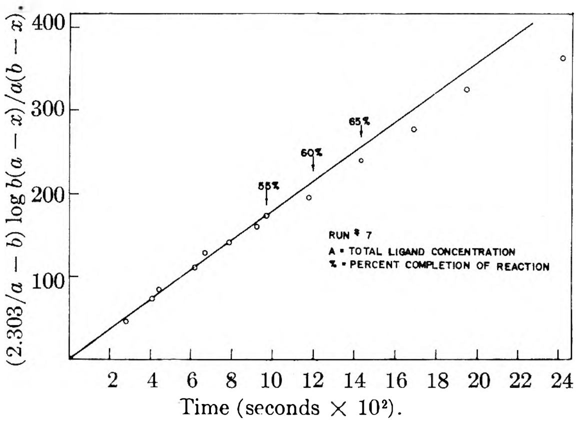

Fig. 2.—Plot of integrated second-order rate equation employing total acetylacetone concentration (see Table II).

Figure 4 indicates that the initial rate is independent of hydrogen ion concentration at least in the range 10^{-6} (run #7) to 2×10^{-3} M (run #11), from which it may be concluded that the following mechanism, capable of explaining the observed second-order kinetics, is definitely eliminated.

Mechanism I.—Consideration of the initial rate

$$HAA \underset{k_R}{\overset{k_I}{\rightleftarrows}} H^+ + AA^- \text{ (rapid)} \tag{3}$$

$$Cu^{+2} + AA^- \underset{k_2}{\overset{k_1}{\rightleftarrows}} Cu(AA)^+ \tag{4}$$

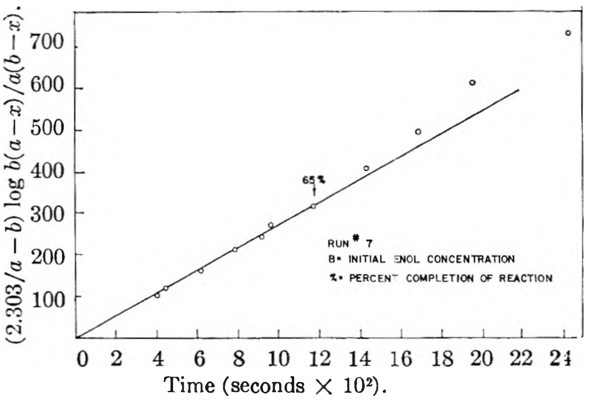

Fig. 3.—Plot of integrated second-order rate equation employing concentration of enol form of acetylacetone.

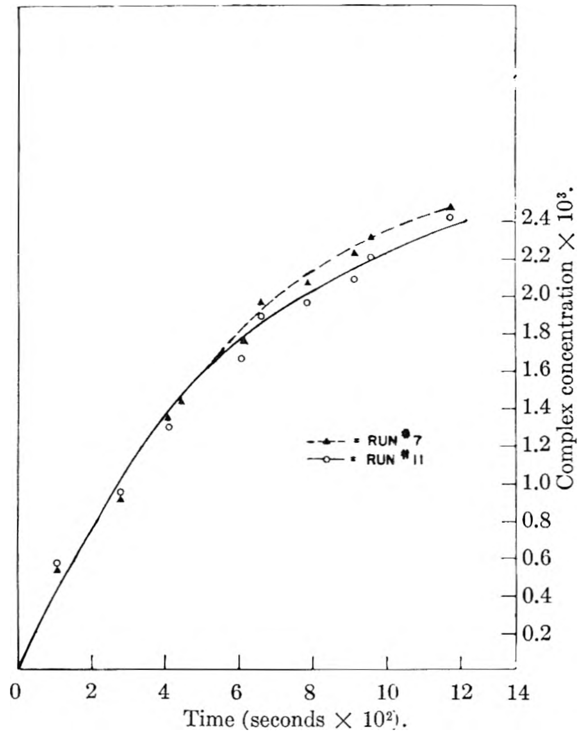

Fig. 4.—Rate of first complex formation as a function of initial perchloric acid concentration. Initial perchloric acid concentration: run #7, $< 10^{-6}\ M$; run #11, $2 \times 10^{-3}\ M$ (see Table II).

$$\frac{dx}{dt} = k_1[\mathrm{Cu}^{+2}]\,[\mathrm{AA}^-] - k_2[\mathrm{Cu(AA)}^+] \tag{5}$$

$$[\mathrm{AA}^-] = \frac{k_\mathrm{I}}{k_\mathrm{R}}\,\frac{[\mathrm{HAA}]}{[\mathrm{H}^+]} \tag{6}$$

$$\frac{dx}{dt} = k_1\,\frac{k_\mathrm{I}}{k_\mathrm{R}}\,\frac{[\mathrm{HAA}]}{[\mathrm{H}^+]}\,[\mathrm{Cu}^{+2}] - k_2\,[\mathrm{CuAA}^+] \tag{7}$$

would eliminate the second term of equation 7 and reduce to

$$\left[\frac{dx}{dt_0}\right] = k_1\,\frac{k_\mathrm{I}}{k_\mathrm{R}}\,\frac{[\mathrm{HAA}]_0}{[\mathrm{H}^+]_0}\,[\mathrm{Cu}^{+2}]_0 \tag{8}$$

If mechanism I obtains in the present reaction, one would expect the ratio of initial rates to have a value of 10^2–10^3 for an equivalent change in initial hydrogen ion concentration. Such a ratio is not observed.

Since the reaction is known to be reversible it may be that the apparent rate of the forward reaction is affected only by initial hydrogen ion concentration insofar as the rate of the reverse reaction is accelerated. In order to check this possibility an integrated rate equation for a second-order reversible reaction in which one of the products is initially present was derived.

Equation for Reversible Second-Order Process When One Product Is Originally Present.—For the reaction

$$\begin{array}{ccccccc} (a-x) & & (b-x) & & (x) & & (x+\delta) \\ \mathrm{A} & + & \mathrm{B} & \underset{k_2}{\overset{k_1}{\rightleftarrows}} & \mathrm{C} & + & \mathrm{D} \end{array} \tag{9}$$

$a = \mathrm{A}_0$; $b = \mathrm{B}_0$; $\delta = \mathrm{D}_0$; $x =$ concn. of product formed by reaction at time t

$$\frac{dx}{dt} = k_1(a-x)\,(b-x) - k_2(x)\,(x+\delta) \tag{10}$$

The integrated form of equation 10 was determined by a method similar to that of Molewyn-Hughes[28] to be

$$x = \frac{ab}{(1-K)}\,[\alpha + \beta \coth\,(k_1 - k_2)\beta t]^{-1} \tag{11}$$

where

$$\alpha = \frac{1}{2}\,\frac{k_1[(a+b) + k_2\delta]}{k_1 - k_2} \tag{12}$$

$$\beta = \frac{1}{2}\,\frac{k_1}{k_1 - k_2}\,\sqrt{(a-b)^2 + 4\,\frac{k_1}{k_2}\,ab + \frac{1}{2}\,\delta(a+b) + \frac{k_2}{4k_1}\,\delta^2} \tag{13}$$

Having already determined k_1 as 2.7×10^3 l. mole^{-1} sec.$^{-1}$ and letting $k_2 = 1.35 \times 10^2$ l. mole^{-1} sec., values of x were calculated using equation 11 in the case where initial [H$^+$] was $2 \times 10^{-3}\ M$. The calculated and observed values agreed within experimental error, thus indicating that the hydrogen ion affects the kinetics only in terms of the reverse reaction.

Specific Rate Constants.—Table II lists the specific rate constants for the first complex formation and the varying conditions of initial concentration and temperature. These constants were determined graphically and the deviation listed is the average deviation of the calculated values from data collected up to 60% completion of reaction.

The temperature coefficient of the specific rate constants (which follows the Arrhenius equation $k = Ae^{-E_a/RT}$ with good precision) was determined by the method of least squares and the entropies of activation were calculated from the relationship

$$k = e\,\frac{kT}{h}\,e^{-E_a/RT}\,e^{\Delta S^*/R}$$

The precision associated with the values of the activation energy and the entropy of activation were evaluated from the precision of the slope and intercept of the plot of log k_1 *vs.* the reciprocal of the absolute temperature. For the reaction studied the energy of activation is 10.8 ± 0.1 kcal. mole^{-1}, and the entropy of activation is -2.6 ± 0.3 e.u.

Appendix

In the case of reversible processes, some investigators have employed the integrated rate

---

(28) E. A. Moelwyn-Hughes, "Physical Chemistry," Pergamon Press, New York, N. Y., 1957, p. 1270.

TABLE II

SPECIFIC RATE CONSTANT FOR FIRST COMPLEX FORMATION EMPLOYING ENOL CONCENTRATION OF ACETYLACETONE

Concentrations listed = initial concentration

Run #	Temp., °C.	$[HAA]_{total} \times 10^3$	$[HAA]_{enol} \times 10^3$	$[Cu^{2+}] \times 10^3$	$[HClO_4] \times 10^3$	k_1 (l. mole^{-1} sec.$^{-1}$)
1	0.00	5.101	3.969	4.928	$<10^{-9}$	$9.76 \times 10^3 \pm 0.7^a$
2	0.00	5.074	3.948	4.928	$<10^{-9}$	$1.02 \times 10^4 \pm .04^a$
3	0.00	4.884	3.800	4.928	$<10^{-9}$	$0.99 \times 10^4 \pm .04^a$
4	−17.08	5.076	3.802	4.923	$<10^{-9}$	$2.67 \times 10^3 \pm .1^a$
5	−17.08	5.059	3.789	2.464	$<10^{-9}$	$2.77 \times 10^3 \pm .1^a$
6	−17.08	10.624	7.958	4.928	$<10^{-9}$	$2.76 \times 10^3 \pm .1^a$
7	−17.08	5.069	3.797	4.925	$<10^{-9}$	$2.67 \times 10^3 \pm .1^a$
9	−17.08	5.040	3.775	4.928	2.00	$2.7 \times 10^3 \pm .2^b$
10	−17.08	5.040	3.775	4.911	2.00	$2.8 \times 10^3 \pm .2^b$
11	−17.08	5.040	3.775	4.928	2.00	$2.7 \times 10^3 \pm .2^b$
12	−27.42	4.953	3.710	4.928	$<10^{-9}$	$1.08 \times 10^3 + .1^a$
13	−27.42	4.953	3.710	4.928	$<10^{-9}$	$1.10 \times 10^3 + .07^a$
14	−27.42	2.281	1.709	4.928	$<10^{-9}$	$1.06 \times 10^3 \pm .05^a$
15	−27.42	2.281	1.709	4.928	$<10^{-9}$	$1.14 \times 10^3 \pm .05^a$

[a] Determined graphically from equation 16. [b] Calculated by equation 11.

equation for a non-reversible process over the first 20–30% of the reaction,[29] especially when equilibrium is displaced far to the right. Such a procedure gave us a value for k_1 of 3×10^3 l. mole^{-1} sec.$^{-1}$ at −17.08°. The region less than 35% completion is precisely that in which rate constants are determined with least accuracy.[30] We were interested in ascertaining to what extent non-reversible rate equations could be used to determine k_1, and with what degree of accuracy. This required an approximate knowledge of K_1.

Since the contribution of the hydrogen ion to conductivity is much larger than that of $Cu(AA)_1^+$, we considered that the total resistance change was a rough estimate of the hydrogen ion produced by both first and second complex formation. Employing the method of successive approximations to make correction for the non-conducting character of $Cu(AA)_2$, and assuming $Cu(AA)^+$ has a specific conductance one quarter that of H^+, the first and second formation constants were roughly evaluated. At −17.08°, when the initial concentration of both reactants was 5×10^{-3} M, the final $[H^+]$ was estimated to be 4.4×10^{-3} M. Assuming[9] $K_1/K_2 \geqq 10$

$$K_1 = \frac{(3.0 \times 10^{-3}) \quad (4.4 \times 10^{-3})}{(0.6 \times 10^{-3}) \quad (1.3 \times 10^{-3})} = 17$$

$$K_2 = \frac{(4.4 \times 10^{-3}) \quad (0.7 \times 10^{-3})}{(3.0 \times 10^{-3}) \quad (0.6 \times 10^{-3})} = 1.7$$

Using the value of $K_1 \cong 17$, and $k_1 \cong 2.8 \times 10^3$ l. mole^{-1} sec.$^{-1}$, k_2 was determined to be 1.65×10^2 l. mole^{-1} sec.$^{-1}$. With these values a hypothetical case was examined in which initial concentrations were those employed in actual experiments. The amount of product, x, formed at any time, t, was calculated from the equation for a reversible second-order process[28]

$$x = \frac{ab}{1 - K} (\alpha + \beta \coth (k_1 - k_2)\beta t)^{-1} \tag{14}$$

where

$$\alpha = \frac{1}{2} \frac{(a + b)}{(1 - K)}; \; \beta = \frac{1}{2(1 - K)} (\sqrt{(a - b)^2 + 4Kab}) \tag{15}$$

a = initial concn. of A; b = initial concn. of B; x = concn. of C and D at time t; $K = k_2/k_1$

The calculated values of x then were introduced into the equation for a non-reversible second-order process

$$k_1 = \frac{1}{t} \times \frac{1}{(a - b)} \ln \frac{b(a - x)}{a(b - x)} \tag{16}$$

and values of k_1 were determined.

Table III lists these values and shows that integrated equations for non-reversible second-order processes may be employed up to 60% completion of the reaction yielding k_1 values which deviate by only 2% from the true value, a deviation which is well within the limits of precision with which rate constants of rapid reactions are determinable.

TABLE III

ACCURACY OF A SPECIFIC RATE CONSTANT OF A REVERSIBLE SECOND-ORDER PROCESS CALCULATED FROM THE INTEGRATED EQUATION FOR A NON-REVERSIBLE PROCESS

$a = 4.925 \times 10^{-3}$; $b = 3.979 \times 10^{-3}$; $k_1 = 2.8 \times 10^3$ l. mole^{-1} sec.$^{-1}$; $x_{equ.} = 3.47 \times 10^{-3}$; $k_2 = 1.65 \times 10^2$ l. mole^{-1} sec.$^{-1}$

Time, sec.	$k_1 \times 10^{-3\,a}$	% Error	% Completion
0.00296	2.80	0.00	4.5
.00742	2.799	.04	10.7
.01188	2.797	.11	16.3
.02375	2.794	.21	28.9
.04454	2.782	.64	45.1
.05938	2.767	1.17	53.5
.07423	2.750	1.79	60.3
.11880	2.678	4.36	74.1
.14846	2.610	6.79	80.0
.17800	2.545	9.10	84.3

[a] Calculated by equation 16.

Acknowledgment.—We are grateful to the Atomic Energy Commission for support of this work *via* the contract AT-(30-1)-906.

---

(29) F. Price and L. Hammett, *J. Am. Chem. Soc.*, **63**, 2387 (1941).

(30) W. E. Roseveare, *ibid.*, **53**, 1651 (1931).

RATE OF REACTION OF METHANE WITH H ATOMS AND OH RADICALS IN FLAMES

By C. P. Fenimore and G. W. Jones

General Electric Research Laboratory, Schenectady, N. Y.

Received June 28, 1961

It was assumed that the irreversible formation of methyl radicals in low pressure flames of CH_4–H_2–O_2–N_2O–Ar occurred at the rate $[CH_4](k_1[H] + k_2[OH] + k_3[O]) = -d[CH_4]/dt$ and k_1, k_2 and k_3 were estimated from the variation of $-d[CH_4]/dt$ with [H], [OH] and [O]. The reaction with O atoms was not very important under the experimental conditions, and k_3 was no larger, therefore, than about 2×10^9 l. mole^{-1} sec.$^{-1}$ at 1600°K. In fuel-rich flames, $[OH]/[H] = 0.06$ to 0.2, and the attack of H atoms predominated; but in lean mixtures, where [OH]/[H] was about 40 times larger, an attack by OH radicals was most important. The constants obtained were $k_1 = 2 \times 10^{11}e^{-11.5/RT}$ l. mole^{-1} sec.$^{-1}$, $k_2 = 3.5 \times 10^{11}e^{-9/RT}$ l. mole^{-1} sec.$^{-1}$, with an uncertainty of 1.5 kcal. in each activation energy.

Introduction

It is convenient to consider that methane burns in two stages. In one stage, methyl radicals are formed by one or more of the reactions

$$\mathrm{H + CH_4 \underset{k_{-1}}{\overset{k_1}{\rightleftharpoons}} CH_3 + H_2} \tag{1}$$

$$\mathrm{OH + CH_4 \rightleftharpoons CH_3 + H_2O} \tag{2}$$

$$\mathrm{O + CH_4 \rightleftharpoons CH_3 + OH} \tag{3}$$

and oxidized at a rate $k_4[O][CH_3]$ to yield carbon monoxide, and hydrogen or water

$$\mathrm{O + CH_3} \xrightarrow{k_4} \ldots \longrightarrow \text{eventually CO} + \ldots \tag{4}$$

Although the intermediate steps of (4) are uncertain, k_4 is known approximately; it is so large that in steady, low pressure flames, where [O] is generally a few per cent. of $[O_2]$, the oxidation of methyl radicals by molecular oxygen is not very important.[1]

Another stage, overlapping the first, is described by the known reactions of O_2–CO–H_2 flames

$$\mathrm{H + O_2 \rightleftharpoons OH + O} \tag{5}$$

$$\mathrm{OH + CO \rightleftharpoons CO_2 + H} \tag{6}$$

$$\mathrm{OH + H_2 \rightleftharpoons H_2O + H} \tag{7}$$

$$\mathrm{O + H_2 \rightleftharpoons OH + H} \tag{8}$$

plus recombinations such as $H + OH + M \rightarrow H_2O + M$, etc.

This paper is concerned with reactions 1, 2 and 3; and we start by assuming that these include all the important ways of forming methyl radicals.[2] If the corresponding reverses are negligible, the sum of the three reactions in the forward direction is $-d[CH_4]/dt$; and by varying [H], [OH] and [O], one might distinguish among (1), (2) and (3). It turns out that (3) is not very important, so only an approximate upper limit for k_3 can be obtained; but k_1 and k_2 can be determined.

k_1 has not been measured before in flames. k_2 was determined recently by Westenberg and Fristrom[3] in a similar way. Their data would not allow an estimate of the temperature dependence, but their and our estimates of the absolute value of k_2 agree.

The Reverse Reactions.—The method just outlined for estimating k_1, k_2 and k_3 requires that the corresponding reactions be irreversible. There is no reason to doubt irreversibility in fuel-lean flames where the only probable reverse reaction, the reverse of (2), is hindered by an activation energy of about 26 kcal. But in rich mixtures containing large $[H_2]$, the reverse of (1) is often important compared to (4) and $-d[CH_4]/dt$ can easily be smaller than the gross rate of formation of methyl radicals.[1]

Therefore we test each fuel-rich run in the following way. We note that whether the reverse of (1) is important or not, the observed decay of methane is the rate of irreversible reaction 4

$$-d[CH_4]/dt = k_4[O][CH_3]$$
$$k_4 \sim 1.9 \times 10^{10} \text{ l. mole}^{-1} \text{ sec.}^{-1},\ ^{1}$$

and an estimate of $[CH_3]$ in the reaction zone can be obtained from $-d[CH_4]/dt$ and [O]. Also, the reverse of (1) is negligible if

$$k_{-1}[H_2][CH_3] << (k_1[H] + k_2[OH] + k_3[O])[CH_4]$$

or if

$$[CH_3] << [CH_3]_{\text{equ.}}\,(1 + k_2[OH]/k_1[H] + k_3[O]/k_1[H])$$

where

$$[CH_3]_{\text{equ.}} = (k_1/k_{-1})[H][CH_4]/[H_2]$$

and[1]

$$(k_1/k_{-1}) \sim 5e^{2/RT}$$

So if the actual $[CH_3]$ deduced from reaction 4 is small compared to the $[CH_3]_{\text{equ.}}$ calculated from [H], $[CH_4]$ and $[H_2]$, the reverse of reaction 1 cannot be important. Although k_4 and (k_1/k_{-1}) are only approximately known, the test has meaning because these constants are correct relative to each other to perhaps 30%.

Estimates of [H], [OH] and [O].—By adding nitrous oxide to the reactants and assuming that its irreversible decomposition occurs mostly by

$$\mathrm{H + N_2O \longrightarrow N_2 + OH} \tag{9}$$
$$k_9 = 4 \times 10^{11}\, e^{-16.3/RT} \text{ l. mole}^{-1} \text{ sec.}^{-1},\ ^{4}$$

[H] can be obtained from $-d[N_2O]/dt$ and $[N_2O]$.

Carbon dioxide is generated by

$$d[CO_2]/dt = k_6[OH][CO] - k_{-6}[H][CO_2]$$
$$k_6/k_{-6} \sim 7.7 \times 10^{-3}e^{23/RT} \text{ at flame temp.}$$
$$k_{-6} = 3 \times 10^{12}e^{-33.3/RT} \text{ l. mole}^{-1} \text{ sec.}^{-1};\ ^{5}$$

---

(1) C. P. Fenimore and G. W. Jones, *J. Phys. Chem.*, **65**, 1532 (1961).

(2) Other ways of forming CH_3 must be unimportant. $CH_4 + O_2 \rightarrow CH_3 + HO_2$ is negligible, among other reasons, because of the large activation energy required[3]; and the same argument eliminates $CH_4 + M \rightarrow CH_3 + H + M$.

(3) A. A. Westenberg and R. M. Fristrom, *J. Phys. Chem.*, **65**, 591 (1961).

(4) C. P. Fenimore and G. W. Jones, *ibid.*, **63**, 1154 (1959).

(5) C. P. Fenimore and G. W. Jones, *ibid.*, **62**, 1598 (1958).

so [OH] can be obtained from $d[CO_2]/dt$, [CO], $[CO_2]$ and [H].

Estimates of [O] are more involved because the same method cannot be used in both fuel-rich and fuel-lean mixtures. In rich flames containing large $[H_2]^1$

$$[O] \sim \frac{-d[O_2]/dt + d[CH_4]/dt}{k_3[H_2]}$$

$$k_3 = 2.5 \times 10^9 e^{-7.7/RT} \text{ l. mole}^{-1} \text{ sec.}^{-1}$$

where it has been assumed that $d[O]/dt$ = zero, and that reaction 3 and the reverse of (8) can be neglected by comparison with (8) itself. The assumptions are reasonable in fuel-rich, but not in lean flames.

In lean flames, however, a few per cent. of any added nitrous oxide forms nitric oxide

$$d[NO]/dt = 2k_{10}[O][N_2O]$$

$$k_{10} = 1 \times 10^{11} e^{-28/RT} \text{ l. mole}^{-1} \text{ sec.}^{-1};\ ^6$$

and since the nitric oxide is essentially inert, its rate of formation can be used to estimate [O]. This determination can be shown to be all right in lean flames because added nitric oxide survives the reaction zone of lean flames almost quantitatively; but in rich flames where nitric oxide reacts appreciably the nitric oxide method cannot be used.

Any of the constants used to determine [H], [OH] or [O] might be systematically wrong by a factor of two, and the radical concentrations must be considered uncertain by this same factor. The ratio [OH]/[H], however, is correct to about 30%.

Procedure.—Just as before,[1,4] reaction rates, corrected for diffusion, were calculated from temperature and composition traverses through flat, low pressure flames burning on water-cooled burners. The only difference was that the required diffusion coefficients were not taken from the literature as before, but were obtained in the following way.

Since carbon dioxide was formed rather late in our flames, we supposed that the carbon dioxide found in regions where the temperature was 400°K. or more below the final temperature had diffused there from hotter parts of the flame. A diffusion coefficient, including temperature dependence over a moderate range, then could be deduced of the form $\log D_{CO_2} = A + n \log T$, where n was found to be 1.6 to 1.9 in various flames. The formula was extrapolated to get D_{CO_2} at higher temperatures; and the diffusion coefficients for other species were calculated assuming an inverse dependence on the square root of molecular weight; $(D_{O_2}/D_{CO_2}) = (44/32)^{1/2}$, etc.

Results

Figure 1 shows traverses through a typical fuel-rich flame. Half of the methane fed reacted in the 0.075 cm. interval between 1200 and 1460°K., and the maximum $-d[CH_4]/dt$ occurred at 1300°. Here $[H] = 110 \times 10^{-7}$ mole l.$^{-1}$ as inferred from the decay of nitrous oxide, [OH]/[H] = 0.12 from the carbon dioxide traverse, and [O]/[H] = 1.0 from the formula for [O] in fuel-rich flames. The mole fraction of hydrogen molecules was 0.16 and the calculated $[CH_3]_{equ.} = (k_1/k_{-1})[H][CH_4]/$

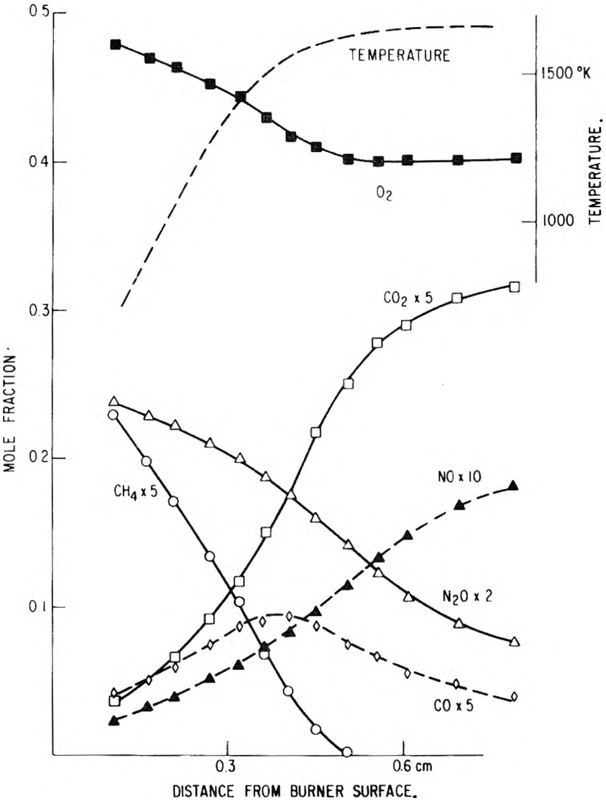

Fig. 1.—Traverses through a fuel-rich flame; $CH_4 + 4.95\ H_2 + 3.17O_2 + 0.64N_2O + 6.21Ar$, burnt at 3 cm. of pressure with a mass flow of 3.78×10^{-3} g. cm.$^{-2}$ sec.$^{-1}$.

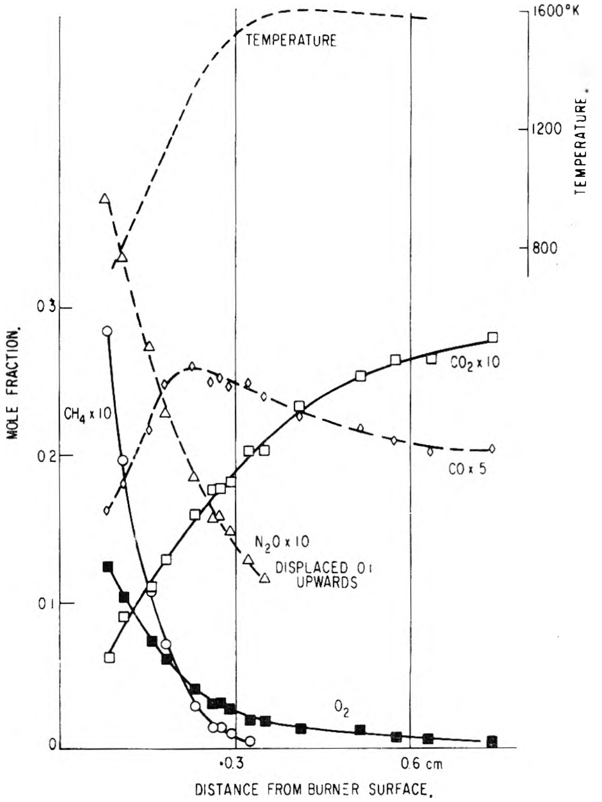

Fig. 2.—A fuel-lean flame; $CH_4 + 7.54O_2 + 1.80N_2O + 4.13Ar$, burnt at 14 cm. of pressure with a mass flow of 2.26 $\times 10^{-3}$ g. cm.$^{-2}$ sec.$^{-1}$.

---

(6) C. P. Fenimore and G. W. Jones, 8th Combustion Symposium at Pasadena, Calif., Sept. 1960.

TABLE I

VALUES OF k_1, k_2 OR k_3 REQUIRED TO ACCOUNT FOR THE OBSERVED $-d[CH_4]/dt$

		Reactants			Reaction zone			Required constants, l. mole^{-1}sec.$^{-1}$ × 10^{-9}		
Fig.	P, cm.	O_2/CH_4	H_2/CH_4	O_2/N_2O	T, °K.	[H] × 10^7, mole l.$^{-1}$	$[CH_3]/[CH_3]_{equ.}$	k_1	k_2	k_3
..	9	1.61	1.16	4.95	1800	32	1.2	3.0	20	9.5
1	3	3.17	4.95	4.95	1300	110	0.1	3.0	26	3.0
..	4	4.23	9.80	5.01	1220	40	.15	2.0	30	3.0
..	5	2.67	10.9	0.25	1790	23	.3	11.3	70	11
..	3	3.55	11.2	2.96	1460	126	.2	4.7	88	11
2	14	7.54	0	4.19	1580	0.4	..	150	16	9
..	12	2.45	0	1.14	1560	3.0	..	38	18	5
..	8	2.42	0	1.35	1800	2.0	..	70	30	5
..	7	6.76	0	5.55	1690	1.3	..	165	21	10
..	5	6.76	1.17	5.54	1445	8.0	..	39	15	5
..	3	9.72	3.04	8.1	1225	37	..	6	10	3

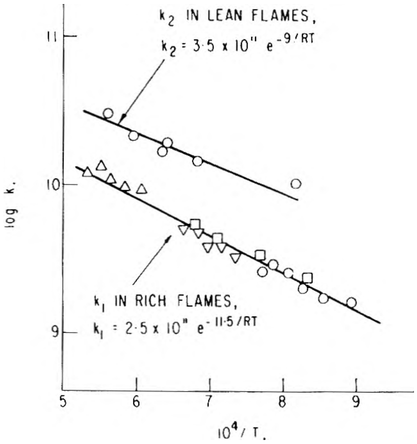

Fig. 3.—Rate constants required to account for the destruction of methane if this occurred entirely by irreversible reaction 1 or irreversible reaction 2.

$[H_2]$ was 10 times the $[CH_3]$ from $-d(CH_4)/dt = k_4[O][CH_3]$. Therefore the reverse of reaction 1 could not have been important. If methane was destroyed only by reaction 1 or only by reaction 3, k_1 or $k_3 = 3 \times 10^9$ l. mole^{-1} sec.$^{-1}$ at 1300°K.; if only by reaction 2, $k_2 = 26 \times 10^9$.

Figure 2 shows a typical fuel-lean flame. The maximum rate was at 1580° where [H] was 275 times smaller than in the rich flame described by Fig. 1; but [OH]/[H] was 78 times larger, and [O]/[H] 17 times larger. For this lean flame, the validity of an estimate of [O] from $d[NO]/dt = 2k_{10}[O][N_2O]$ was demonstrated by repeating the run with the same reactants, except that nitrous oxide was omitted and partly replaced with nitric oxide; and it was observed that nitric oxide was not appreciably destroyed. Values of k_1, k_2 and k_3 appropriate to the hypotheses that methane was destroyed only by reactions 1, 2 or 3 again were calculated.

The other flames resembled Figs. 1 or 2, and the data obtained are summarized in Table I. The column, $[CH_3]/[CH_3]_{equ.}$, shows that the reverse of reaction 1 was important for the first run in the table but for no other flame. The last three columns list the values of k_1, k_2 or k_3 which would be required to account for the destruction of methane if this occurred by only one of reactions 1, 2 or 3 and was irreversible in every case.

Estimates of k_1 and k_2.—Table I is divided into three groups of runs by horizontal lines. The first is the one run which did not give an irreversible formation of methyl radicals and is barred from consideration except when the contrary is specifically stated. The second group is four fuel-rich flames in which [OH]/[H] = 0.06 to 0.2; and the last is six lean flames which are mostly characterized by a forty-fold larger [OH]/[H] ratio. The last entry in the table is exceptional among the lean flames; because of the considerable H_2 fed, it had an [OH]/[H] ratio of only 0.6.

It will be found that reactions 1 and 2 account for the consumption of methane, and that (3) is therefore unnecessary. There are also positive reasons for rejecting (3). It could not be the major route for methane decay in lean flames because of the scatter of the k_3 as a function of temperature.

Nor could (3) be the major route for methane decay in rich flames. If it were, the value obtained for k_3 in the reversible, first run of Table I should be much smaller than the k_3 obtained in the irreversible, rich run at 1790°. Such a difference is not observed for k_3; though it is found for k_1 and k_2.

We conclude that (3) is not the major path for methane decay in any run at 1560 to 1800°, for the required k_3 are all $8 \pm 3 \times 10^9$ in this range and if (3) is unimportant in any of these runs it is unimportant in all. Therefore k_3 must really be no larger, say, then about 2×10^9 l. mole^{-1} sec.$^{-1}$ at 1600°K.

With (3) excluded, we next note that reaction 1 alone could not have destroyed the methane in both rich and lean flames because the k_1 required in most lean flames is much larger than the k_1 required in rich flames at the same temperature. A similar argument shows that methane could not have been destroyed always by (2). Methyl radicals must have been formed chiefly by (1) in rich flames and by (2) in lean flames.

That (2) should be important at all disagrees superficially with some earlier work where it appeared that (2) was unimportant in both rich and moderately lean flames.[7] The earlier flames were not as lean as the present ones, however, and doubtlessly had smaller [OH]/[H] ratios for two reasons. First they contained greater H_2 than most of the

---

[7] C. P. Fenimore and G. W. Jones, *J. Phys. Chem.*, **63**, 1834 (1959).

present ones; and we note that the last run of Table I, which contained 2% H_2 at 1225°, had 16 times smaller [OH]/[H] than the lean flame of Fig. 2, which had only 0.2% H_2 at 1580°. Second, only the early, upstream parts of flames were examined before where [OH]/[H] would be still further decreased by the easier diffusion of H atoms. In the present work, the region studied never extended very far upstream of the maximum $-d[CH_4]/dt$ because some of the radical concentrations became difficult to evaluate.

More of the present results are shown in Fig. 3. The lower curve is a plot of the k_1 values required in rich flames; the points are not the values from Table I, but are separate estimates of k_1 obtained at 0.025-cm. intervals through the reaction zones of each of the four rich runs. The upper plot reproduces the k_2 in lean flames from Table I. There is little to gain by plotting separate values of k_2 because of the small temperature range in each lean flame.

The plots of k_1 and k_2 look satisfactory in rich and lean flames, respectively. Some occurrence of reaction 2 in rich flames is really not excluded, however, because the k_2 which would be required to account for all the consumption of methane in rich flames are only 3 to 5 times larger than the k_2 found in lean flames. Therefore k_1 in Fig. 3 might be too large; and since the error would not depend much on temperature, we round off the pre-exponential factor to 2×10^{11}. A similar correction for k_2 is unnecessary except, perhaps, for the last run in Table I; and the upper curve in Fig. 3 is partly drawn to correct for this run. Hence

$$k_1 = 2 \times 10^{11} e^{-11.5/RT} \text{ l. mole}^{-1} \text{ sec.}^{-1}$$

$$k_2 = 3.5 \times 10^{11} e^{-9/RT} \text{ l. mole}^{-1} \text{ sec.}^{-1}$$

with an uncertainty of 1.5 kcal. in each activation energy.

Comparison with Other Work.—Many earlier estimates at lower temperatures[8] favor an activation energy of 12 to 13 kcal. and a steric factor of about 10^{-1} for k_1, but more recent measurements[8,9] suggest an activation energy of approximately 8 kcal. and a smaller steric factor. If the steric factor associated with the 8 kcal. activation energy is 0.025 as Klein, *et al.*, find, the smaller activation energy predicts the same k_1 at 1600° as does the larger activation energy. Thus we agree in absolute value within a factor of two with a long extrapolation of the results of Klein and co-workers, but the agreement is just as good with much of the older literature. Our activation energy, of course, agrees better with the older literature.

Other estimates of k_1[8] have the same activation energy as Klein and co-workers, 8 kcal., but associate a steric factor of only 10^{-3} or less with it. These estimates with a steric factor of around 10^{-3} or less are incompatible with our measurements.

It might be added that a k_1 much smaller than the value we find also is ruled out by the first, reversible run in Table I. For in this instance, reversibility is supposed to arise from the circumstance that $k_{-1}[H_2][CH_3] >> k_4 [O][CH_3]$; or substituting for $[H_2]$, [O] and k_4, from the condition that $k^{-1} >> 0.2 \times 10^9$ at 1800°K. Using the k_1/k_{-1} given above, our estimate of k_1 gives a reverse constant of $k_{-1} = 0.9 \times 10^9$, which is large enough to permit a considerable degree of eqilibration; but a k_1 smaller by a factor of ten would be inconsistent with such an equilibration either in the first run of Table I, or in a number of rich flames studied previously which also were more or less equilibrated.[1]

Our k_2 agrees very well with other work. Avramenko and Lorentso[10] found $k_2 \sim 10^{11} e^{-8.6/RT}$ at much lower temperatures; and Westenberg and Fristrom[3] showed that if methane reacted *via* (2) in very lean flames at 1650 to 1840°, k_2 must be about 2×10^{10} l. mole^{-1} sec.$^{-1}$. They were not sure that (3) could be excluded, but it is not very important in our work and we find k_2 between 1 and 3×10^{10}.

Westenberg and Fristrom estimated [OH] from reaction 6 with a value of k_6 about 40% smaller than ours at 1750°, and therefore might have been expected to deduce rather smaller k_2 than ours. Also they neglected the reverse of (6), claiming that the omission would introduce little error, and our measurements agree with this claim. In our lean reaction zones, the reverse of (6) varied from about 2% of the forward reaction in the 1580° measurement to 20% of the forward reaction in the 1800° measurement. If they had incurred a little error by omitting the reverse of (6), it would have tended to compensate for the difference between their k_6 and ours.

---

(8) E. W. R. Steacie, "At. and Free Radical Reactions," Reinhold Publ. Corp., New York, N. Y., 1954, p. 448.

(9) R. Klein, J. R. McNesby, M. D. Scheer and L. J. Schoen, *J. Chem. Phys.*, **30**, 58 (1958).

(10) Quoted by N. N. Semenov, "Some Problems of Chemical Reactivity," Vol. 2, Pergamon Press, London, 1959, p. 104.

INFRARED OBSERVATION OF THE O–H BAND OF PURE ETHANOL AND ETHANOL SOLUTIONS TO THE CRITICAL TEMPERATURE[1]

By E. Fishman[2]

Bowne Hall, Syracuse University, Syracuse, New York

Received July 5, 1961

The infrared absorption of pure ethanol and dilute solutions of ethanol dissolved in ethyl ether, ethyl vinyl ether, acetone, acetonitrile, pentane, carbon disulfide and carbon tetrachloride has been determined in the 3 μ region from room temperature to the critical temperatures of the liquids. In the active solvents there is a continuous, linear shift in frequency of the polymer band and no evidence of an equilibrium with free alcohol molecules. The slopes of the frequency *vs.* temperature lines vary from 0.89 for pure alcohol to 0.14 for diethyl ether solution. In the inert solvents, the polymer band behaves as in pure alcohol up to the temperature of its disappearance, but the dimer band seems to depend on the solvent for its frequency and temperature behavior. These observations are discussed in terms of the dimer–polymer models proposed by Pimentel, *et al.*, and the hydrogen bond theory of Finch and Lippincott.

Introduction

The subject of infrared observation of hydrogen bonding has been thoroughly reviewed recently.[3] Briefly, the experimental facts which are the background for this study are as follows. In the vapor phase, the O–H vibration yields a sharp peak at about 3750 cm.$^{-1}$; in liquid alcohol only the broad hydrogen bonded band occurs, centered at about 3350 cm.$^{-1}$. The solvents for alcohol can be divided rather sharply into two distinct categories: hydrogen acceptors which form loose complexes and inert solvents. The spectroscopic distinction is that in the complexing solvents alcohols yield only a broad hydrogen bonded O–H absorption, the central frequency depending on the solvent, whereas the inert solvents yield two bands: the sharp unbonded O–H band, distinct and separate, and the broad complexed O–H band. The relative intensities and positions of these bands depend on the solvent, the concentration of alcohol and the temperature.

In this paper some experimental observations of the effect of extremely high temperatures on the O–H bands in both kinds of solvents will be presented. These results will be discussed in terms of the structures and strengths of the complexes between alcohol molecules themselves and alcohol with complexing solvents.

Experimental

The high temperature infrared cell used in this work is illustrated in Fig. 1. The details of its structure will be published elsewhere, but the main features, sapphire windows and Teflon O-ring seals can be seen in the figure. A brass spacer was machined to keep the windows approximately 0.2 mm. apart. The difference in thermal expansion of sapphire and brass operating over the whole length of the windows increases this separation about 15% from room temperature to 250°. The decrease in the density of a liquid under its own vapor pressure over this temperature range is somewhat greater and definitely non-linear. A precise correction of observed optical densities for these two temperature effects would require calibration of the window separation as a function of temperature *and* pressure, which has not been done. The fact that the two temperature effects are in the opposite direction makes the relative intensities at different temperatures reasonably consistent with each other. However, for experiments done with pure alcohol, with the windows nearly in contact, thermal expansion of a few microns leads to complete opacity in the spectral region of interest. The results on pure alcohol were obtained in a cell made of "Platinite,"[4] an iron–nickel alloy with a coefficient of thermal expansion close to that of sapphire. Nevertheless, the recorded infrared absorption is so sensitive to slight variations in light path that no conclusions can be drawn regarding relative intensities at different temperatures. Reliable infrared spectra, where the absorption never exceeds 75 or 80%, are obtained up to the critical point of the alcohol using this cell.

The alcohol and the active solvents were dried over Linde Molecular Sieves. Inert solvents were used as delivered by the manufacturer.[5] Some separate experiments with added water showed that these results are not altered, hence no special precautions were observed in protecting solutions from the atmosphere or drying inert solvents.

The spectrometer, Perkin–Elmer Model 112 with LiF prism, was modified by the addition of an externally focusing source to reduce the light loss on the walls of the high temperature cell. The entire optical path was enclosed. By sweeping with tank nitrogen, it was possible to reduce the most intense water vapor lines in the 3 μ region to less than 2% absorption, which was quite essential to some of the results reported.

Background curves were run with the pure solvent in the cell. For the solvents acetonitrile, diethyl ether and acetone, it was necessary to extend the background readings over the entire temperature range, since the overtone and combination bands present in the 3 μ region are sensitive in frequency and intensity to temperature variation. In all cases, the background was subtracted point by point using a plexiglass triangle of variable height developed by M. Jean-Jacques Martin at the University of Bordeaux for converting per cent. transmission to optical density.

The frequencies reported here are frequencies of the maximum of optical density. Finch and Lippincott[6] (hereafter referred to as F–L) report frequencies determined by a "center of gravity" method, designed to correct for the dissymmetry of the band. They point out that their method and the method used here give essentially the same results. The prism was calibrated by standard procedures.[7] Considering the broadness of the bonded O–H band and the personal judgment involved in determining the maxima, these frequencies should be considered significant to ±5 cm.$^{-1}$. These estimates are based on the reproducibility of a frequency reading on several independent determinations.

The concentrations of all solutions were 2% alcohol by volume with the exception of the CS_2 and pentane solutions, which were 4%. This range was chosen for spectroscopic convenience, to yield both free and bound O–H in inert solvents, and, at the same time, to avoid a high percentage of self-associated alcohol in the active solvents. In pentane, concentrations of 1, 2 and 4% yielded the same frequencies; only the relative intensities were affected.

---

[1] This research was supported in part by Contract No. AF 49(638)-3 with the Air Force Office of Scientific Research.

[2] This research was carried out while the author was "Professeur Associé" at the University of Bordeaux, France.

[3] G. C. Pimentel and A. L. McClellan, "The Hydrogen Bond," W. H. Freeman and Co., San Francisco, Cal., 1960.

[4] Société Metallurgique d'Imphy, 84 Rue de Lille, Paris (7^{e}).

[5] Grade R. P. chemicals, manufactured by Prolabo, 12 Rue Pelee, Paris XI^{e}. Acetonitrile redistilled over P_2O_5.

[6] J. N. Finch and E. R. Lippincott, *J. Phys. Chem.*, **61**, 894 (1957).

[7] A. R. Downie, M. C. Magoon, T. Purcell and B. Crawford, *J. Opt. Soc. Am.*, **43**, 941 (1953).

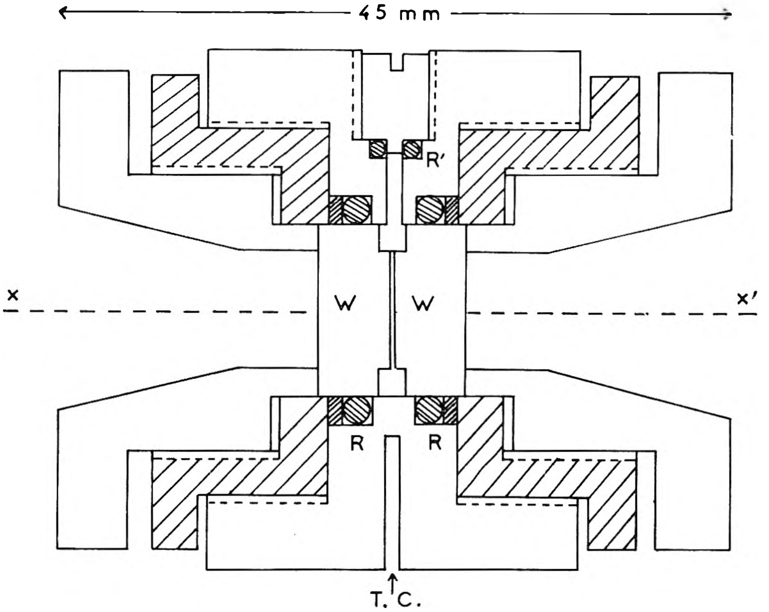

Fig. 1.—High temperature infrared cell: x--x′, light path; W, sapphire windows; R, R′, Teflon O-rings.

Observations

Figure 2 shows the contours of the infrared absorption of pure liquid ethanol from room temperature to its critical point. Note the drastic change in frequency with little change in shape. There is certainly a considerable diminution of integrated intensity with increasing temperature,[8] but little change in half width. As already discussed, changes in path length and liquid density make these curves non-comparable as to integrated intensity.

Figure 3 contains an analogous set of curves drawn for 2% ethanol dissolved in acetonitrile, where the relative integrated intensities have some significance. The band widths at half-maximum absorption are nearly equal at all temperatures, a result noted in all the solvents and previously reported by Becker.[8]

The experimental curves are quite identical in acetone, diethyl ether and ethyl vinyl ether; only the frequencies differ.

Significantly, in the active solvents, at no temperature is there an appearance of an unbonded O–H band indicating an equilibrium between different types of alcohol molecules as is observed in inert solvents. The free O–H band could not have been obscured by atmospheric water vapor which was nearly completely eliminated. Liddel and Becker,[9] in careful measurements of the peak height of the unbonded O–H of methanol in CCl_4 as a function of temperature, report a 50% decrease in peak intensity in going from −10 to 50°. Thus it is possible that we fail to see the free O–H band, not because there is no free O–H present, but due to a decrease in its intensity resulting from some other mechanism.

Ethyl vinyl ether, the weakest hydrogen acceptor solvent used, is an interesting bridging case between the active and inactive solvents. At 150° the frequency of the O–H vibration has reached a value as high as the frequency of the free O–H in some inert solvents. In a sense we have continuously gone over from bound to free O–H.

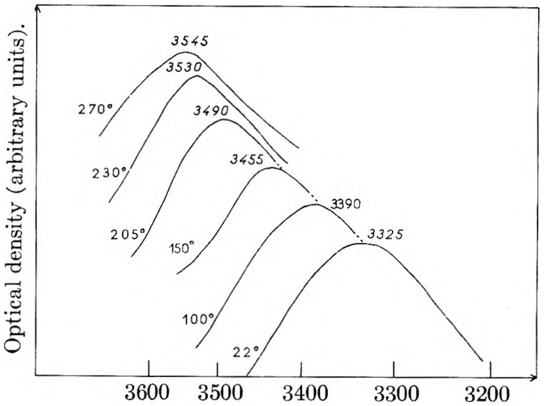

Fig. 2.—Infrared absorption contours of pure ethanol from room temperature to the critical temperature.

The experiments in the inert solvents first were run in order to see if the infrared absorption due to the free O–H vibration simply disappeared at a high enough temperature. Figure 4 shows the result for 2% ethanol in pentane. This result is not in contradiction with Liddel and Becker. The apparent growth of intensity of the free O–H with increasing temperature is related to a displacement of the association equilibrium toward free molecules, but at least it shows that 2% free alcohol at 250° in our cell yields a distinct free O–H band. Thus the absence of this band in active solvents proves that a large fraction of the alcohol molecules remain associated with the solvent, even at the highest temperatures here employed.

Figure 5 shows the peak frequencies of the associated O–H bands as a function of temperature for the various solvents used. All the points are fit very well by straight lines. The slope of the individual lines does not seem to be related to

---

[8] E. D. Becker, *Spectrochim. Acta*, **17**, 436 (1960).

[9] U. Liddel and E. D. Becker, *ibid.*, **10**, 70 (1957).

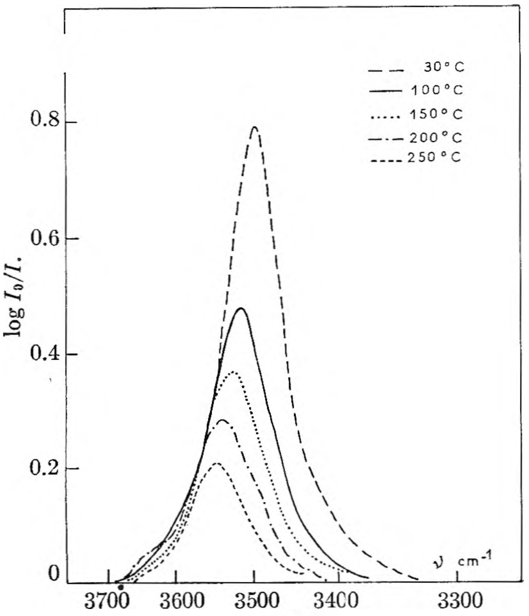

Fig. 3.—Infrared absorption bands of 2% ethanol in acetonitrile.

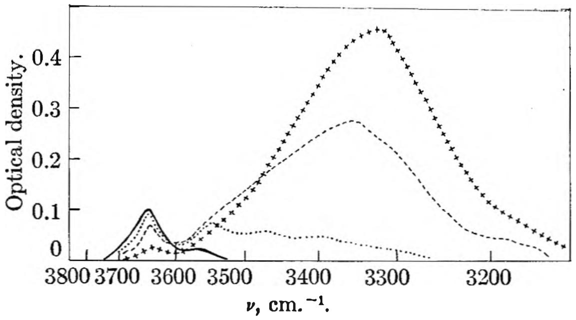

Fig. 4.—Infrared absorption bands of 2% ethanol in pentane: +++, 25°; – – –, 55°; . . ., 100°; ———, 250°.

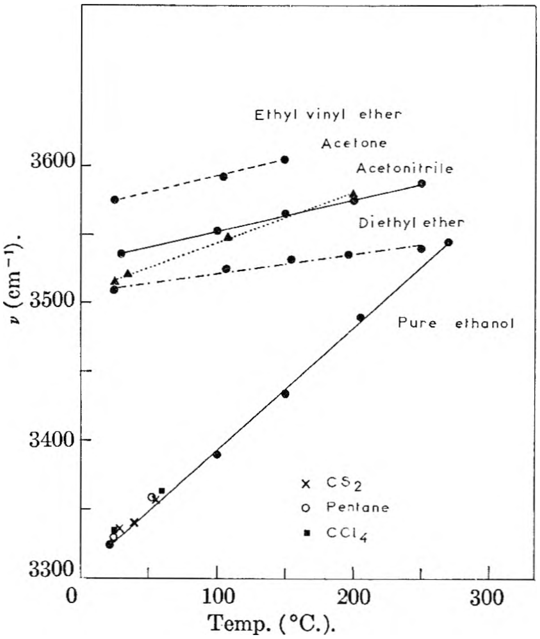

Fig. 5.—Frequencies of the polymer band of ethanol in various solvents as a function of temperature.

$\Delta\nu$, the shift in frequency from its gas phase value, nor does it depend on the thermal expansion coefficient of the solvent. The line representing pure alcohol is characterized both by its large slope and large $\Delta\nu$ at room temperature.

At the lower end of the pure alcohol line are plotted some points representing the frequency of the associated O–H band observed in inert solvents up to the temperature where the displacement of the equilibrium toward free alcohol resulted in the disappearance of this band. These points, representing alcohol in inert solvents associated with itself, fall on the pure alcohol line. They are independent of the particular inert solvent, both in frequency and in slope. This type of hydrogen bonded O–H does not "see" the solvent around it and behaves precisely as it would in pure alcohol to the extent of being independent of the refractive index of the medium. The free O–H band, whose frequency shift with temperature is very small ($d\nu/dt$ is approximately 0.06 cm.⁻¹/deg.) exhibits a considerable change in frequency with solvent.

There is a third O–H band which appears clearly at slightly elevated temperatures near 3500 cm.⁻¹. It shifts toward high frequency with increasing temperature and then disappears as the temperature continues to rise. There has been much discussion as to the reason for this band, often attributed to alcohol dimers, and the form of the hydrogen bond giving rise to it. We present the frequencies of the dimer and free O–H bands, where they have been observed, in tabular form (Table I).

Table I

Vibrational Frequencies of the Free O–H Band and Dimer Band of Dilute Ethanol Solutions at Various Temperatures

	Temp., °C.	Free O–H frequency, cm.⁻¹	Dimer frequency, cm.⁻¹	Slope of dimer *vs.* *T* line, cm.⁻¹/deg.[a]
Solvent pentane	25	3640	. .	
	81	3645	3542	
	100	3647	3545	0.2
	150	3650	3555	
	200	3657	. .	
Solvent CCl_4	25	3632	. .	
	59	3633	3500	
	85	3633	3510	0.5
	105	3635	3520	
	145	3638	3543	
Solvent CS_2	28	3615	. .	
	85	3618	3500	0.9
	110	3615	3522	

[a] These slopes, determined graphically with few experimental points, are very rough estimates.

We note that the 3500 cm.⁻¹ band, whose precise frequency is difficult to determine, does depend on the solvent and follows a temperature behavior analogous with the association bands in active solvents. The conclusion that this band represents an association of the alcohol with the inert solvents is unacceptable for chemical reasons; however, this could be a hydrogen bound O–H of a different type, say the cyclic dimer postulated from observations of the alcohol spectrum in inert matrices.[10] The sketch in Fig. 6 shows a version of the cyclic dimer and the linear polymer, the latter a less realistic version of Fig. 2–2, ref. 1. Note that the solvent could approach the H-bond in the linear polymer only from above or below the plane of the paper, but the H-bond in the cyclic dimer is fully exposed to solvent influence.

It is true that at first the frequency displacement of the dimer band may be only apparent, since the neighboring polymer band changes so drastically with temperature; however, after about 75° the polymer band has all but disappeared and the subsequent displacement must be attributed solely to the dimer band.

The slopes of the frequency of the polymer band *vs.* temperature for the various solvents are presented in Table II. Our value of 0.89 cm.$^{-1}$/deg. is in good agreement with the slope of 0.8 found for the polymer band of ethanol in CCl_4 observed by Liddel and Becker[9] over the temperature range −10 to 50°, but it is in serious disagreement with F–L's value of 0.35, although we observe the same frequencies at room temperature. We have no explanation for this discrepancy. Becker's[8] value of 0.60 cm.$^{-1}$/deg. for ethanol in acetone is also in disagreement with our 0.36 for this same quantity. In Fig. 5 note that the first two points near room temperature for acetone present a quite different slope. A complicating feature in studying the O–H band in acetone is the large absorption at about 3400 cm.$^{-1}$ for acetone itself, a highly temperature dependent band. It now seems desirable in determining the exact shapes of the ν *vs.* T graphs for the same observer to cover the entire temperature range from the freezing point to the critical temperature.

TABLE II

SLOPES OF THE FREQUENCY *vs.* TEMPERATURE LINES FOR THE POLYMER O–H BAND OF ETHANOL IN VARIOUS SOLVENTS. (SEE FIG. 5)

Solvent	$d\nu/dt$, cm.$^{-1}$/deg.
Pure ethanol	0.89
Acetone	.36
Ethyl vinyl ether	.24
Acetonitrile	.24
Diethyl ether	.14

F–L present two arguments for believing that the change in frequency is due to the elongation of the O—O distance rather than various polymer equilibria. One is the independence of the polymer frequency of alcohol to concentration in CCl_4 over a ten-fold range of concentrations. The other is that they can account for their observed range of $d\nu/dT$ values with their theory of hydrogen bonding[11] by allowing the O–H—O unit to absorb energy as a semi-classical harmonic oscillator as the temperature is raised and then calculating the O–H frequency as a function of the increasing O–H—O distance. Their calculated range of slopes, depending on the number of degrees of freedom permitted classical excitation, is 0.20 to 0.64. The fact that their theoretical range nearly brackets our observations with such elevated temperatures tends to confirm their model. However, the variation in slopes reported here are most probably related to differences in acceptor properties rather than to differences in degree of vibrational excitation. Our range of solvents is limited by the fact that many of the strong acceptors polymerize at high temperature.

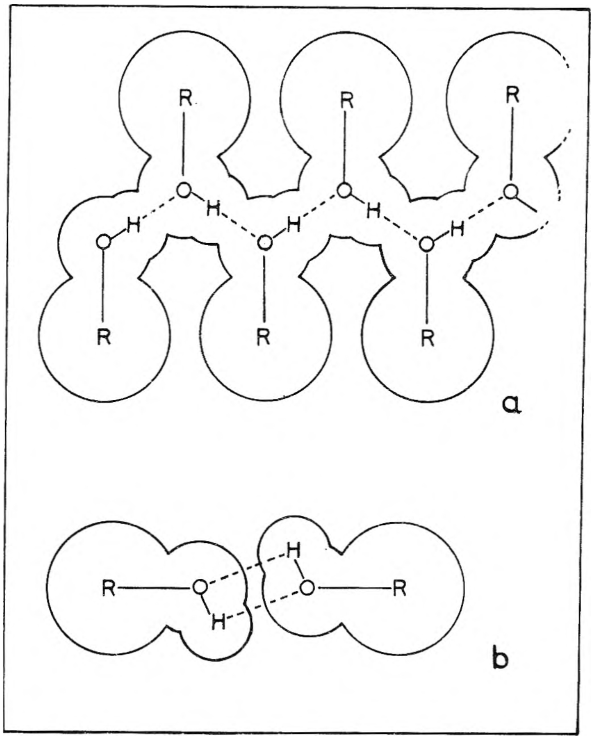

Fig. 6.—Sketch of associated alcohol molecules according to Pimentel, *et al.*: (a) linear polymer; (b) cyclic dimer.

Conclusions

In this paper, the range of state variables over which hydrogen bonding is studied spectroscopically has been enlarged and the new observations have been interpreted by means of models recently proposed. There is still no quantitative theory that ties these models to spectroscopic observations unambiguously; it is hoped that their plausibility has been significantly enhanced by their consistency with these new observations. A major area for contention still remains in the interpretation of the over-all breadth of the bound O–H band. Is its breadth due to a series of n-mers or to a single polymeric species with a vibration band broadened by some mechanical or electronic interaction? The papers of Frisch and Vidale[12] and Reid[13] in addition to F–L show that the broadening can be explained without recourse to n-mer equilibria. The author believes that if the equilibrium model were correct, then one would observe a series of stepwise changes in frequency over a large temperature increment, as in the case of the dimer–polymer equilibrium in inert solvents, instead of the continuous linear change observed. Finally, it may

---

(10) M. van Thiel, E. D. Becker and G. C. Pimentel, *J. Chem. Phys.*, **27**, 95 (1957).

(11) E. R. Lippincott and R. Schroeder, *ibid.*, **23**, 1099 (1955).

(12) H. L. Frisch and G. L. Vidale, *ibid.*, **25**, 982 (1956).

(13) C. Reid, *ibid.*, **30**, 182 (1959).

be hoped that in the future measurements of integrated intensities may be made up to very high temperatures.

Acknowledgments.—The author is deeply indebted to Prof. M. L. Josien for her hospitality and her contagious enthusiasm. He also would like to thank Pierre Saumagne and Jean Lascombe for the interest they have taken in this work. The French Atomic Energy Commission very kindly provided support for the cell construction.

FREEZING POINT DEPRESSIONS IN SODIUM FLUORIDE. EFFECT OF ALKALINE EARTH FLUORIDES[1]

BY STANLEY CANTOR

Oak Ridge National Laboratory,[2] P. O. Box X, Oak Ridge, Tennessee

Received July 7, 1961

Measurements were made of the freezing point depressions of NaF caused by the addition of up to 0.25 mole fraction alkaline earth fluorides. At a fixed concentration the smaller the alkaline earth cation radius, the greater were the deviations from ideal solution behavior. The excess partial molal free energies of solution of NaF, $(\bar{F} - F^0)^E_{NaF}$ evaluated from the measurements were all negative and approached zero asymptotically as the mole fraction of NaF approached unity. $(\bar{F} - F^0)^E_{NaF}$ at fixed concentration was empirically related to $U + nI_2$ where U is the alkaline earth fluoride lattice energy, n is an arbitrary constant, and I_2 is the second ionization potential of the alkaline earth.

Introduction

Understanding the effects of structural parameters, such as radius, charge and polarizability, on thermodynamic properties in fused salt solutions is a large general problem. One approach to solving this problem is to investigate a thermodynamic property of a solvent in which the type and concentration of solutes can be systematically altered, and then relate variations in this property to structural parameters of the pure solutes. The object of this particular investigation was to measure the depressions of freezing point of the solvent, NaF, and correlate the derived thermodynamic information with the structure of the solutes, the alkaline earth fluorides.

The choices of freezing point depression as the measurement and NaF as the solvent were made after reviewing collections[3,4] of solid–liquid phase diagrams of fluorides. Where NaF was a component, the high NaF end of the diagram indicated the absence of solid solutions. In other words, pure crystalline NaF was the primary phase on cooling from the liquid state. Furthermore, the activity of NaF could be accurately evaluated from freezing point data because the heat of fusion and heat capacities of NaF are known.[5]

Some information on the desired freezing points is available from the NaF–BeF_2,[6] –MgF_2,[7,9] –CaF_2,[8] –BaF_2[9] phase diagrams. But these data are not sufficiently precise and consistent to show the relationship between solute structural parameters and the freezing point depression of NaF.

Experimental

Chemicals.—NaF (Mallinckrodt A. R.) was purified by recrystallizing from slowly cooled melts and selecting only clear crystal fragments from the cooled ingot. These melts were contained in graphite or nickel crucibles and were protected by a helium atmosphere. Analyses showed the only impurities exceeding 100 parts per million were Ca, 400 p.p.m.; Al, 300 p.p.m.; O, 300 p.p.m. Commercial CaF_2 (Mallinckrodt A. R.) and BaF_2 (Fisher "Certified") were oven dried at 150° to constant weight before use. Commercial MgF_2 (Baker and Adamson "Purified") and SrF_2 (Baker and Adamson Reagent Grade) were purified in graphite crucibles by first treating with NH_3HF_2 at 250° and then heating to 600° while flushing with a helium stream. Analyses for impurities in MgF_2 in weight per cent. were: Ca, 0.1; Fe, 0.2; Si 0.05; O, 0.11; for SrF_2; Ba, 1.0; Ca, 0.2; K, 0.01; Li, 0.005; Na, 0.02; O, 0.28. BeF_2 (Brush Beryllium) was purified by hydrofluorination at 500°. Impurities in weight per cent. were: O, 0.38; Mg, 0.01; Fe, 0.005; S, 0.058.

Apparatus and Procedures.—The cryoscopic vessel, welded from nickel, provided a cylindrical melt reservoir 6.35 cm. high and 4.8 cm. in diameter, and contained a thermocouple well of 0.64 cm. diameter tubing extending to within 0.64 cm. of the bottom. A vertical tube, 1.3 cm. in diameter and 20.3 cm. high, welded to the top plate of the reservoir, had a side arm through which the vessel could be evacuated. Stirring was accomplished by bubbling argon gas through the melt *via* a long 0.65 cm. diameter tube which passed through the 1.3-cm. vertical tube and was sealed to it by a gas tight Swagelok fitting. The bubbling rate was measured by merely observing the number of bounces per unit time made by the ball float of a sensitive flow meter (Fischer & Porter Flowrator Model 10A1735). The sample sizes (approximately 1.5 moles of NaF) and low vapor pressure ensured that changes in melt composition due to transpiration were negligible.

The vessel was immersed in a Hevi-Duty 5-cm. tube furnace to a depth of 20.3 cm., to prevent appreciable heat loss from the melt reservoir and thermocouple wires. Vessels, after being charged within a dry box, were evacuated for approximately one hr. while the temperature was raised to 700°. Argon then was passed through at the desired rate.

---

[1] Presented, in part, before the Division of Physical Chemistry, American Chemical Society, 138th National Meeting, New York, N. Y., Sept., 1960.

[2] Operated for the United States Atomic Energy Commission by the Union Carbide Corporation.

[3] E. M. Levin, H. F. McCurdie and F. P. Hall, *Phase Diagrams for Ceramists*, Part I (1956), Part II (1959), American Ceramic Society, Columbus, Ohio.

[4] R. E. Thoma (ed.), "Phase Diagrams of Nuclear Reactor Materials," ORNL-2548, Nov. 6, 1959.

[5] C. J. O'Brien and K. K. Kelley, *J. Am. Chem. Soc.*, **79**, 5616 (1957).

[6] E. Thilo and H. Schröder, *Z. physik. Chem.*, **197**, 41 (1951); A. V. Novoselova, M. E. Levina, K. P. Semanov and A. G. Zhasmen, *J. Gen. Chem. U.S.S.R.*, **14**, 385 (1944); D. M. Roy, R. Roy and E. F. Osborn, *J. Am. Ceram. Soc.*, **36**, 185 (1953).

[7] A. G. Bergman and E. P. Dergunov, *Compt. rend. acad. sci. U.R.S.S.*, **31**, 755 (1941).

[8] P. P. Fedotieff and W. P. Iljinskii, *Z. anorg. u. allgem. Chem.*, **129**, 101 (1923).

[9] G. Grube, *Z. Elektrochem.*, **33**, 481 (1927).

The absence of solid solubility in NaF was confirmed by X-ray diffraction and microscopic examination of the cooled melt.

Temperature Measurements and Manipulation.—Temperatures were measured with Pt *vs.* Pt–10% Rh thermocouples in a thermowell extending about 5 cm. into the melt. Periodic calibrations were made against thermocouples calibrated by the National Bureau of Standards. The standard thermocouples were stated to be accurate within ±0.5° up to 1100°. The e.m.f.'s were measured with a Leeds and Northrup Speedomax G recorder with a full chart range of 1 mv. The recorder contained a circuit by which thermocouple outputs could be suppressed in mv steps. The recording unit was calibrated at frequent intervals by means of a Rubicon High Precision type B Potentiometer.

Freezing temperatures with a precision of 0.3° were obtained from cooling curves. The cooling rates of the liquid ranged from 0.3–0.7° per minute. Supercooling, which occurred with most of the samples but seldom exceeded 1°, was easily corrected for by extrapolating the crystallization temperature–time curve back to the liquid curve.

Furnace temperatures were controlled manually by means of a Powerstat.

Results

Melting Point and Thermochemical Properties of Pure NaF.—Pure NaF was found to melt at 1268.0 ± 0.5°K. This temperature agrees with the results of Bredig, *et al.*[10] O'Brien and Kelley,[5] who were primarily interested in high temperature enthalpies, report 1285°K. These authors also give 1300°K. as the melting point of cryolite for which Grjotheim[11] obtained 1282°K. O'Brien and Kelley probably got higher results because their thermocouple, not in contact with the sample container, reflected in part furnace wall temperatures. In this and the two other investigations[10,11] cited, thermocouples were in contact with thermowells which were immersed in the samples. Accordingly, if it is assumed that O'Brien and Kelley have a systematic error of plus 17° and no error in their heat contents, then the recalculated heat of fusion of NaF is 8017 cal., as compared to 8030 cal.

When the temperature dependence of the heat of fusion is taken into account the relation between the activity of NaF(a_{NaF}) and the temperature, T, at which NaF crystallizes out of solution, is

$$-R \ln a_{\mathrm{NaF}} = \left(L_{\mathrm{M}} - \Delta a T_{\mathrm{M}} - \frac{\Delta b}{2} T_{\mathrm{M}}^2\right)\left(\frac{1}{T} - \frac{1}{T_{\mathrm{M}}}\right) + \Delta a \ln \frac{T_{\mathrm{M}}}{T} + \frac{\Delta b}{2}(T_{\mathrm{M}} - T) \quad (1)$$

where L_{M} is the heat of fusion of pure NaF at the melting point (T_{M}); Δa and Δb are constants from the heat capacity–temperature equations.[5]

Freezing Points of NaF Solutions.—The temperatures at which NaF began crystallizing out of solutions containing an alkaline earth fluoride are given in Table I. From these temperatures, values of $\ln a_{\mathrm{NaF}}$ were calculated using equation 1 with $L_{\mathrm{M}} = 8{,}017$, $T_{\mathrm{M}} = 1268$, $\Delta a = 6.00$ and $\Delta b = -3.88 \times 10^{-5}$. For each value of $\ln a_{\mathrm{NaF}}$, $\ln \gamma_{\mathrm{NaF}}$ was obtained (γ_{NaF} is the activity coefficient). The excess partial molal free energy of solution of NaF, $(\bar{F} - F^0)^{\mathrm{E}}{}_{\mathrm{NaF}}$, then was calculated from the equation

$$(\bar{F} - F^0)^{\mathrm{E}}{}_{\mathrm{NaF}} - RT \ln \gamma_{\mathrm{NaF}} \quad (2)$$

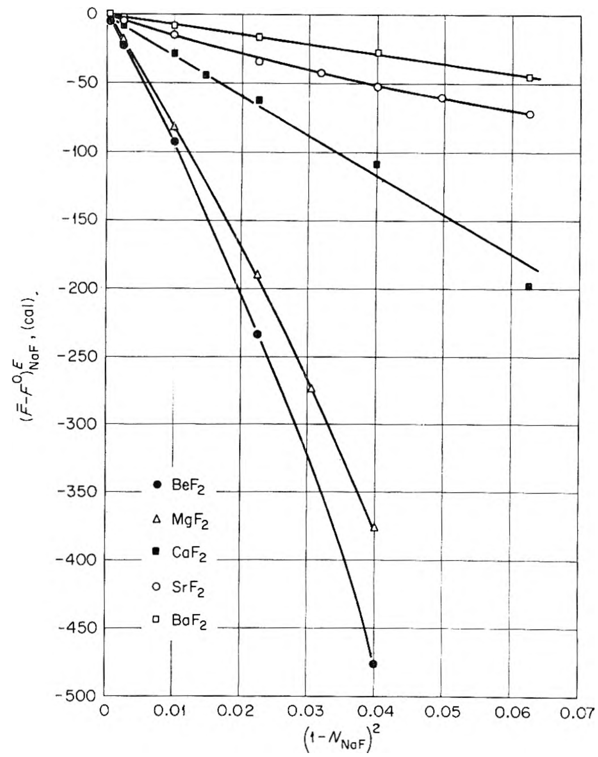

Fig. 1.—Excess partial molal free energy of solution of NaF *vs.* mole fraction squared of the alkaline earth fluoride solute.

Discussion

For the same solute concentrations, lower liquidus temperatures of NaF are found with solutes whose cation sizes are smaller. If the forces in solution are preponderantly coulombic, the higher the electric field strength of the solute cation the more difficult it is for NaF to crystallize out of solution. The thermodynamic quantity, obtained from freezing point depressions, which is the measure of this relative difficulty is the partial molal free energy of solution of NaF.

For all the solutions studied, the partial molal free energy of mixing at the freezing temperatures was always less than $RT \ln N_{\mathrm{NaF}}$, *i.e.*, the excess partial molal free energy of solution of NaF, $(\bar{F} - F^0)^{\mathrm{E}}{}_{\mathrm{NaF}}$, was always negative. But as the mole fraction of NaF approached unity, the excess partial molal free energy of mixing approached zero (see Fig. 1).

TABLE I

OBSERVED FREEZING POINTS OF NAF CONTAINING MF_2 SOLUTES

Mole fraction NaF	Freezing point of NaF, °C.				
	solute				
	BeF_2	MgF_2	CaF_2	SrF_2	BaF_2
1.000	995.0	995.0	995.0	995.0	995.0
0.980	986.2	986.9	986.9	986.9	986.8
.950	971.4	971.9	973.9	973.9	974.2
.900	939.9	941.7	949.8	951.8	952.8
.880	...	...	939.1	...	...
.850	897.3	904.0	924.0	927.8	930.7
.825	...	880.8	...	...	...
$.821_8$	...	...	...	914.4	...
.800	839.7	854.5	895.1	903.7	907.3
$.777_6$	...	...	...	892.5	...
.750	...	...	859.3	878.0	882.4

---

[10] M. A. Bredig, J. W. Johnson and Wm. T. Smith, Jr., *J. Am. Chem. Soc.*, **77**, 307 (1955).

[11] K. Grjotheim, *Norske Videnskaps Selskabs Skrifter*, No. 5 (1956).

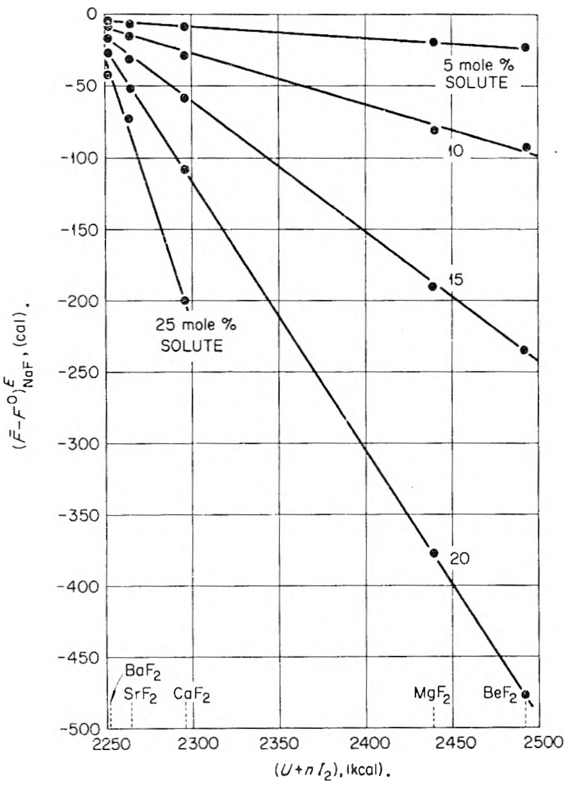

Fig. 2.—Excess partial molal free energy of solution of NaF *vs.* an empirical function of solute structural parameters.

In considering the possibility of regular solution behavior the function $(\bar{F} - F^0)^E{}_{NaF}/(1 - N_{NaF})^2$ was tested for constancy. These solutions did not show regular solution behavior over the entire concentration range. However, when this function was plotted against $(1 - N_{NaF})$ the slopes of these plots were negative for solutions of BeF_2 and MgF_2, close to zero for CaF_2, and positive for SrF_2 and BaF_2. The cation sizes of sodium and calcium are about the same while sodium is smaller than strontium and barium but larger than beryllium and magnesium.

The structural parameter that seems most significant in the interpretation of these data appears to be the ionic radius or interionic distance. However, no simple quantitative relationship between free energy and simple functions of ionic radii or interionic distances was found. A better correlation was obtained by plotting $(\bar{F} - F^0)^E{}_{NaF}$ at constant composition *vs.* the lattice energies of the alkaline earth fluorides (the lattice energy is related to complicated functions of interionic distances). But these plots did not give smooth curves.

As an alternative approach, consideration was given to the possibility that the solute forms complex ions by reactions of the type: $xF^- + MF_2 = [MF_{2+x})^{-x}$. If these complex ions are in ideal solution then the temperature–composition curve for the NaF liquidus may be obtained by suitably altering equation 1.[12] The following complex ions were postulated for the purpose of trial calculations: $[MF_3]^{-1}$, $[M_2F_7]^{-3}$, $[MF_4]^{-2}$, $[M_2F_9]^{-5}$, $[MF_5]^{-3}$, $[MF_6]^{-4}$. If only a single complex species was used over the entire experimental concentration range, the calculated temperatures compared poorly with the temperatures in *any* of the columns of Table I. It was possible to "fit" the observed liquidus temperatures by postulating the presence of two or more complex ions in solution. However, these data are insufficient to establish the equilibria between the complex species that do "fit." The stringent condition of ideality is the main drawback to the use of complex ion models in trying to calculate freezing points. It is doubtful that effects related to the enthalpy of solution are absent.

An empirical method of treating the data is suggested by a relation given in the monograph of Yatsimirskii and Vasilev.[13] These authors show that the free energy of complex formation is equal to the sum of two quantities. The first quantity depends on the volume and charge of the central metal ion. The second quantity is the product of three terms which represent the number of ligands, the polarizability of the ligand and the polarizing effect of the cation. By analogy, it is assumed that $(\bar{F} - F^0)^E{}_{NaF}$ is a linear function of the lattice energy, U, *plus* the second ionization potential, I_2, of the alkaline earth metal multiplied by a constant, n. The purpose of using I_2 was to approximate the polarizing action. The constant, n is purely arbitrary and for BeF_2 solutes was set equal to 4.00 because this is, to a good approximation, the number of nearest neighbors coördinated around Be^{2+} in liquid BeF_2.[14] Since fluoride ions are the ligands throughout they were not put in the function. An excellent fit occurs when the values given in Table II are used for plots of $U + nI_2$ *vs.* $(\bar{F} - F^0)^E{}_{NaF}$ at constant composition (Fig. 2). It must be reiterated that the fit is empirical. Although structural parameters are used, no detailed relationship between $(\bar{F} - F^0)_{NaF}$ and molecular structure is intended.

TABLE II

BORN-HABER LATTICE ENERGY (U), SECOND IONIZATION POTENTIAL (I_2), AND ADJUSTABLE CONSTANT (n) OF THE ALKALINE EARTH FLUORIDES

MF_2	U(kcal.)	I_2 (kcal.)[a]	n
BeF_2	813	420	4.00
MgF_2	692	346.5	5.04
CaF_2	617	273.5	6.14
SrF_2	583	254	6.62
BaF_2	549	230.5	7.38

[a] C. E. Moore, Atomic Energy Levels, National Bureau of Standards Circular 467 (1949–1958).

Acknowledgments.—The author is indebted to Messrs. R. E. Thoma and C. F. Weaver for the X-ray diffraction and petrographic analyses, and to Drs. R. F. Newton, M. Blander and J. Braunstein for many valuable discussions.

---

[12] Reference 11 has several examples of this calculation carried out in the NaF–AlF_3 system.

[13] K. B. Yatsimirskii and Y. P. Vasilev, "Instability Constants of Complex Compounds," Pergamon Press, New York, N. Y., 1960, p. 70.

[14] B. E. Warren and C. F. Hill, *Z. Krist.*, **89**, 481 (1934).

ACID DISSOCIATION CONSTANTS OF PYRIDINE-2-ALDEHYDE AND PYRIDINE-2-ALDOXIME

BY R. W. GREEN AND I. R. FREER

School of Chemistry, Sydney University, Sydney, Australia

Received July 10, 1961

The acid dissociation constants of pyridine-2-aldehyde and its oxime have been measured spectrophotometrically at ionic strengths less than 0.001 in the temperature range 5–60°. Enthalpy and entropy changes associated with the equilibria are reported.

As a preliminary to investigating the complexing powers of pyridine-2-aldehyde and its oxime, a careful determination of their acid–base equilibria was necessary. Ultraviolet spectrophotometry is particularly well suited to this task since pyridine derivatives absorb strongly in two bands near 230 and 280 mμ with an intensity which depends on the degree of protonation of the ring nitrogen.[1] A second strong change in absorption accompanies dissociation of the oxime hydrogen. The high extinction coefficients make it possible to work with solutions more dilute than 10^{-3} *M*, where activity effects are almost negligible and easily calculated.

Experimental

Pyridine-2-aldehyde, supplied by L. Light and Co., after distillation under reduced pressure (25° (1 mm.)) was a colorless liquid ($n^{20}\text{D}$ 1.5382) which became dark brown on prolonged exposure to air. When stored in the dark under nitrogen at 10° it showed no change in one year.

Pyridine-2-aldoxime, also from L. Light and Co., was recrystallized as colorless needles from hot water and dried *in vacuo* at room temperature. Its m.p. (113°) agreed with that reported by Lénhárt.[2]

Stock solutions of both substances were prepared in boiled distilled water, stored in the dark under nitrogen and renewed every three days. Solutions for spectrophotometry were prepared by dilution in glass apparatus rendered water-repellent by treatment with dichlorodimethylsilane and then re-calibrated. Small amounts of sodium hydroxide or perchloric acid were added to adjust the *p*H.

Measurements of *p*H were made with a Radiometer 4 *p*H meter standardized against 0.05 *M* potassium hydrogen phthalate and 0.01 *M* borax[3] at the temperature of the experiment. Solutions were tested in a thermostated cell within a grounded Faraday cage attached to the *p*H meter. Agreement between the two buffer solutions and reproducibility of *p*H measurements generally were found to be better than 0.01 *p*H unit.

Simultaneously with the *p*H measurement, a portion of the same solution was placed in a thermostated 1-cm. silica cell and its optical density at a suitable wave length was measured with a Hilger Uvispek Spectrophotometer. When observations were made below room temperature, a stream of dry nitrogen at the same temperature was passed through the cell compartment to prevent condensation of moisture on the optical faces.

Results

In 0.1 *M* perchloric acid solution, both pyridine-2-aldehyde and its oxime are present entirely in the cationic form, with the ring nitrogen protonated; and at *p*H 6–7 both exist exclusively as the uncharged species. At higher *p*H the oxime hydrogen begins to be titrated and the oxime is wholly anionic at *p*H 12, but the two equilibria do not overlap. It was therefore possible to prepare solutions containing any one species alone, and their absorption spectra at 25° are shown in Figs. 1 and 2. The solutions were found to be stable for several hours over the *p*H and temperature ranges with which we were concerned. The molar extinctions of the single species varied slightly with temperature and, since the precision of the *pK* determinations was closely dependent on these quantities, they were measured at each temperature on several independently prepared solutions of different concentration.

To determine the acid dissociation constants, ten solutions of each substance were prepared with *p*H values in the range *pK* ± 0.5, and their optical densities were measured at 260 mμ for the aldehyde and 295 mμ for the oxime. This was done at several temperatures between 5 and 60°, and the *pK* was calculated from each observation by means of the equation

$$pK = p\text{H} - \log \frac{E_\text{A} - E_\text{obs}}{E_\text{obs} - E_\text{B}} - \log \frac{\gamma_\text{B}}{\gamma_\text{A}} \qquad (1)$$

where *E* denotes molar extinction coefficient and the subscripts A and B refer to acidic and basic forms, respectively. Since the concentrations were all near 10^{-4} *M* and no neutral salt was introduced, the simple Güntelberg[4] formula can be applied to show that the activity correction to *pK* is less than 0.0005 and hence can be neglected here.

TABLE I

ACID DISSOCIATION CONSTANTS

Temp., °C.	Pyridine-2-aldehyde NH⁺ pK_1	Pyridine-2-aldoxime NH⁺ pK_1	Pyridine-2-aldoxime NOH pK_2
5	4.13	3.88	10.25
15	4.00	3.70	10.21
25	3.84	3.56	10.17
30	3.76	3.51	10.13
40	3.57	3.42	10.08
50	3.42	3.39	10.00
60	3.25	3.38	9.91
Equation 2			
A	−4287	+ 26,970	−8786
C	−67.94	+148.38	−112.63
D	− 0.1208	+ 0.2489	− 0.1229

In Table I, pK_1 represents the acid dissociation of the pyridinium group and pK_2 the oxime group. The acid strengths of the pyridinium groups at 25° are of the expected order, since they are markedly stronger than in the unsubstituted pyridinium ion ($pK = 5.18$)[5] but weaker than the same group when

---

(1) R. W. Green and H. K. Tong, *J. Am. Chem. Soc.*, **78**, 4896 (1956).

(2) B. Lénhárt, *Ber.*, **47**, 809 (1914).

(3) V. E. Bowers and R. G. Bates, *J. Research Natl. Bur. Standards*, **59**, 261 (1957).

(4) E. Güntelberg, *Z. physik. Chem.*, **123**, 199 (1926).

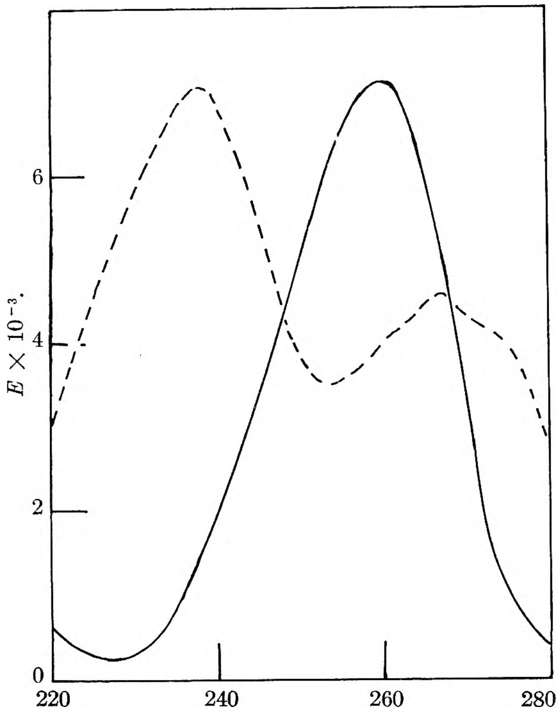

Fig. 1.—Absorption spectra of aqueous solutions of pyridine-2-aldehyde: continuous line, *p*H 1.6; broken line, *p*H 8.

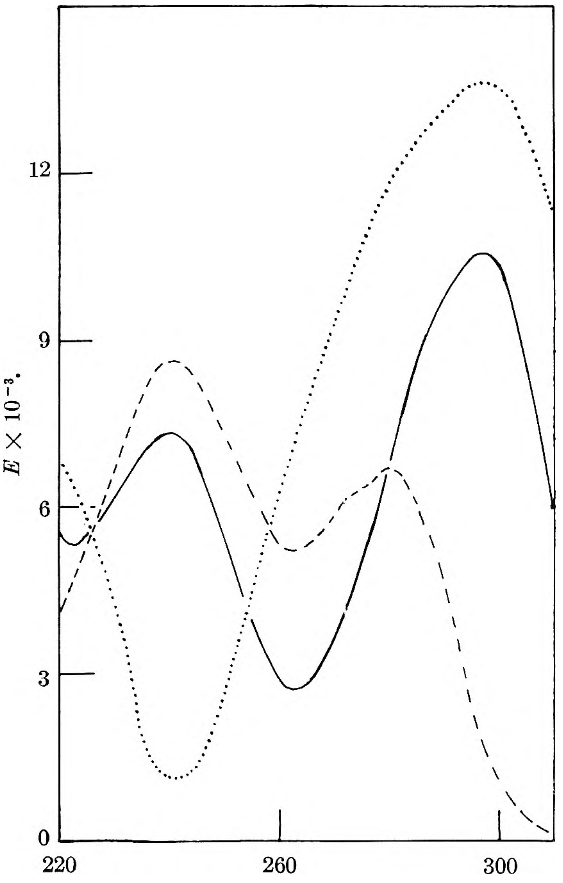

Fig. 2.—Absorption spectra of aqueous solutions of pyridine-2-aldoxime: continuous line, *p*H 1; broken line, *p*H 7; dotted line, *p*H 12.

there is an undissociated carboxyl radical in the 2-position ($pK = 2.21$).[1] The oxime dissociation is slightly stronger than in benzaldoxime ($pK = 10.7$),[6] as would be expected in view of the π-deficient nature of the pyridine ring.[7]

Since all measurements were made at *p*H values near the *pK* of the acid, the second term of eq. 1 was always quite small, so that the maximum error of an individual *pK* estimation should be little greater than that of the *p*H determination itself, namely, ±0.01. The data of Table I, being the means of sets of ten observations, can be expected to have an even higher precision, which justifies their use in calculating enthalpies and entropies of dissociation.

We have followed the procedure of Harned and Robinson[8] and fitted the data of Table I to equations of the form

$$2.303R \log K = -A/T + C - DT \qquad (2)$$

The best values of the parameters A, C and D, obtained by the method of least squares, predict the experimental results with a mean deviation of 0.005. They are presented in Table I.

It follows from eq. 2 that

$$\Delta H^0 = A - DT^2$$

$$\Delta S^0 = C - 2DT$$

and calculated values of these quantities are reported in Table II.

Table II

Thermodynamic Functions

	Pyridine-2-aldehyde		Pyridine-2-aldoxime			
	NH$^+$		NH$^+$		NOH	
Temp., °C.	$\Delta H,^0$ kcal./mole	ΔS^0, e.u.	ΔH^0, kcal./mole	ΔS^0, e.u.	ΔH^0, kcal./mole	ΔS^0, e.u.
5	5.1	− 0.7	7.7	9.9	0.7	−44.3
15	5.7	+ 1.7	6.3	4.9	1.4	−41.8
25	6.5	4.1	4.8	0.0	2.1	−39.3
30	6.8	5.3	4.1	− 2.5	2.5	−38.1
40	7.6	7.7	2.6	− 7.5	3.3	−35.7
50	8.3	10.1	1.0	−12.5	4.0	−33.2
60	9.1	12.6	−0.7	−17.5	4.9	−30.7

Equation 2 implies that, at a temperature $T_{\mathrm{m}} = \sqrt{A/D}$, *pK* passes through a maximum or minimum according to whether A is negative or positive. At the same temperature $\Delta H^0 = 0$. Reference to a compilation of relevant data[9] reveals that A is nearly always positive; and it is well known that *pK* for many common carboxylic acids exhibits a minimum near room temperature. The first dissociation of pyridine-2-aldoxime also follows this general pattern, with a *pK* minimum within the experimental temperature range at about 56°. However, the other two dissociations examined here have negative values of A, implying *pK* maxima. The predicted maximum for pyridine-2-aldehyde is so far outside the experimental range as to be

---

[5] R. K. Murmann and F. Basolo, *J. Am. Chem. Soc.*, **77**, 3484 (1955).

[6] O. L. Brady and R. F. Goldstein, *J. Chem. Soc.*, 1918 (1926).

[7] A. Albert, "Heterocyclic Chemistry," Athlone Press, London, 1959, Chapter 4.

[8] H. S. Harned and R. A. Robinson, *Trans. Faraday Soc.*, **36**, 973 (1940).

[9] R. A. Robinson and R. H. Stokes, "Electrolyte Solutions," Butterworths Scientific Publications, London, 1959, p. 517.

meaningless, but the oxime pK does appear to go through a maximum very near 0°.

Finally, it may be pointed out that the ΔS^0 values are characteristic. Ionization of the pyridinium group presumably follows the equation

$$RNH^+ + H_2O \rightleftharpoons RNH + H_3O^+$$

whose symmetry suggests that the entropy change should be small; but ionization of the oxime group is of the same kind as that of carboxylic acids, which usually is accompanied by a significant decrease of entropy.

THE HEAT OF FORMATION OF TITANIUM DIBORIDE: EXPERIMENTAL AND ANALYTICAL RESOLUTION OF LITERATURE CONFLICT

By WENDELL S. WILLIAMS

Research Laboratory of National Carbon Company, Division of Union Carbide Corporation, Parma 30, Ohio

Received July 10, 1961

Although the literature contains three independent values for the heat of formation of TiB_2 of $\backsim -70$ kcal./mole, the present work shows that this agreement is fortuitous and that each value is in error for a different reason. Brewer and Haraldsen's value, −71.4 kcal., obtained from the reaction $TiN + 2BN = TiB_2 + 3/2\ N_2$, is questionable because of experimental difficulties and a mistake in the tabular data employed. Samsonov's experimental value, −70.04 kcal., obtained from the reaction $2TiO + B_4C = 2TiB_2 + CO_2$, is incorrect because of the use of unreliable thermodynamic data. Samsonov's calculated value, −73 kcal., obtained from an empirical relation between heat of formation and volume change, could not be duplicated. Another value for the heat, −32 kcal., obtained by Schissel and Williams with a mass spectrometer and Knudsen cell, is shown to be low by a stability comparison with TiC and B_4C. When corrected, within appropriate limits of error, the three experiments yield results in agreement with the recent calorimeter value of Lowell and Williams, −50 ± 5 kcal./mole.

I. Introduction

While investigating the vaporization of the refractory hard metal TiB_2 with a mass spectrometer, Schissel and the writer[1] obtained and reported a value of −32 kcal./mole for the heat of formation. This value differs substantially from the four other literature values, all of which are ~ -70 kcal./mole. By a study of the reaction of titanium and boron in a nitrogen atmosphere, Brewer and Haraldsen[2] obtained −71.4 kcal.; by a study of the reduction of TiO_2 by carbon and boron carbide, Samsonov[3] obtained −70.04 kcal.; by use of an empirical formula of Kubaschewski,[4] Samsonov[5] calculated −73 kcal.; and by analysis of the literature data Krestovnikov and Vendrikh[6] selected the value −70.00 kcal. In an attempt to reconcile the conflict, the writer performed several additional experiments and analyzed the papers mentioned.

The additional experiments were of three types: (1) stability comparisons in which bounds were placed on the unknown heat of formation by comparison with other compounds; (2) direct reaction of the elements in a high temperature calorimeter, with Lowell,[7] and (3) a refinement of the Brewer and Haraldsen experiment.[2] A discussion of each of these experiments follows as Section II. In Section III, an analysis of each of the earlier determinations of $\Delta H_f(TiB_2)$ is presented.

II. Description of Present Work

(1) **Stability Comparisons.**—The results of the first stability comparison, presented in Table I, establish the coexistence of TiB_2 and C at temperatures up to 2250°, in agreement with the ternary diagram presented by Brewer and Haraldsen.[2] Thus ΔF and $\Delta H > 0$ for the reaction $TiB_2 + 3/2\ C = TiC + 1/2\ B_4C$. From the heats of formation of B_4C and TiC,[4] $\Delta H_f(TiB_2) < -51 \pm 5$ kcal./mole. This result shows that the −32 value for $\Delta H_f(TiB_2)$ must be in error.

Other comparisons were made against various titanium and boron compounds, but because of a deficiency of thermodynamic data for these materials the results are principally of qualitative interest (Table II).

TABLE I

RESULTS OF INVESTIGATION OF THE REACTION $TiB_2 + 3/2C = TiC + 1/2\ B_4C$

Reactants	Products	Crucible	Temp. (°C.)	Time (hr.)
$TiB_2 + C$	$TiB_2 + C$	TiB_2	1900	1.5
$TiB_2 + C$	$TiB_2 + C$	carbon	2250	8
$TiC + 2B$	$TiB_2 + C$	carbon	2050	4
$TiC + 2B$	$TiB_2 + C$	carbon	2100	3
$2TiC + B_4C$	$2TiB_2 + 3C$	carbon	2000	1

(2) **Direct Reaction Calorimeter.**—In the calorimeter used by Lowell and Williams,[7] titanium and boron powders were mixed in the correct ratio to yield TiB_2, packed in a thermally isolated graphite capsule and heated *in vacuo*. At a temperature of 1500° an exothermic reaction occurred, raising the temperature of the capsule above that of the heater by 1000° in 0.2 second. By X-ray diffraction analysis of a pulverized sample the product was shown to be all TiB_2. The temperature rise of the capsule was followed with a calibrated photo-

---

[1] P. O. Schissel and W. S. Williams, *Bull. Am. Phys. Soc. Ser. II*, **4**, No. 3 (1959).

[2] L. Brewer and H. Haraldsen, *J. Electrochem. Soc.*, **102**, 399 (1955).

[3] G. V. Samsonov, *Zhur. Priklad. Khim.*, **28**, 1018 (1955).

[4] O. Kubaschewski and E. L. Evans, "Metallurgical Thermochemistry," Third Ed., Pergamon Press, 1958.

[5] G. V. Samsonov, *Zhur. Fiz. Khim.*, **30**, 2057 (1956).

[6] A. N. Krestovnikov and M. S. Vendrikh, *Izvest. Vyssikh Ucheb. Zavednii Tsvet. Metall.*, No. 2, 54 (1959).

[7] C. E. Lowell and W. S. Williams, *Rev. Sci. Instr.*, in press.

TABLE II

ADDITIONAL STABILITY COMPARISONS

Reactants	Products	Type of analysis	Container	Mode of heating	Temp. (°C.)	Time (hr.)
$TiB_2 + Mo$	β(Mo–Ti)B	X-Ray diff. and emission spectroscopy	TiB_2 crucible	Induction	1900	1.5
$TaB_2 + Ti$	TiB + TaB	X-Ray diff.	Ta tube	Resistance	2250	8
$TiB_2 + Ta$	TiB + TaB	X-Ray diff.	TiB_2 crucible	Electron bombardment	2000 2200	5 1/4
$TiB_2 + W$	W_2B	X-Ray diff.	W strip (free surface)	Resistance	2300	1/2

tube feeding a recording galvanometer. From the corrected ΔT, the number of moles of C, Ti and B determined by weighing, and heat capacities for the elements given by Stull and Sinke,[8] the heat of formation of TiB_2 was found to be ΔH_f (TiB_2) = -50 ± 5 kcal./mole.

(3) **Nitride Transition.**—Brewer and Haraldsen studied the reaction $TiN + 2BN = TiB_2 + 3/2N_2$ and reported a temperature at which ΔF reaction $\cong 0$, hereafter called the transition temperature T_t. Above this temperature $\Delta F_{\text{reaction}} < 0$, and below, $\Delta F_{\text{reaction}} > 0$. Once this temperature was known, they used extrapolated literature values of ΔF_f for TiN and BN to compute ΔH_f (TiB_2). It was decided to repeat their experiment, avoiding the use of a molybdenum crucible, which reacts with TiB_2 as shown in Table II, and using more than the two reaction temperatures employed by these workers.

Two different experimental geometries were used, both leading to a value of $T_t = 2150 \pm 25$°K. (Brewer and Haraldsen's value was 1820°K.) In the first method, BN capsules filled with BN–TiN mix were heated in a miniature graphite tube furnace. Five runs were made at different temperatures in 1/2 atmosphere of N_2. Pyrometer readings were made on a small hole in the side of the graphite tube and corrected for losses through the chamber wall. The contents of the BN capsule were analyzed by X-ray diffraction after each run. The results are summarized in Table III. Visually, the three phases in runs 3 and 5 were randomly dispersed, indicating temperature uniformity. The transition temperature indicated by this experiment is 2140°K.

TABLE III

RESULTS OF SEARCH FOR TRANSITION TEMPERATURE IN REACTION $2BN + TiN = TiB_2 + 3/2\ N_2$.

T, °K.	Time (hr.)	Products
(Control sample)		BN, TiN
2300	0.5	TiB_2
2033	1.25	BN, TiN
2163	1.5	BN, TiN, TiB_2
2128	1	BN, TiN
2148	3.5	BN, TiN TiB_2(weak)
1870	30	BN, TiN

The second geometry employed induction heating. The powders were contained in a BN crucible in a graphite susceptor. Temperature readings were made *via* a prism and Pyrex flat in a hole in the top of the crucible. The transmission coefficient for the optical system was determined using a flat-filament lamp, and checked against the melting point of gold. X-Ray analysis was used after three runs at different but constant temperature in N_2 and placed bounds on the location of T_t. In several later runs a manometer was connected to the system and the N_2 pressure monitored as a function of temperature. A rise in pressure was taken as an indication of the conversion of the two solid nitrides to the boride, releasing nitrogen to the gas phase. The value of T_t found in this way (2159°K.) lay between the limits set by the X-ray results on the second set of constant-temperature runs. The value adopted on comparing the two sets of measurements was $T_t = 2150 \pm 25$°K.

The above result can be criticized on the grounds that equilibrium has not been demonstrated: the transition from the nitrides to the boride might be rate-limited by diffusion or some other process and hence the true value of T_t should be lower than observed. In an attempt to test this hypothesis, the transition was sought from the high-temperature side. No reversal in the direction of the reaction was detected on lowering the temperature. Then TiB_2 powder was heated in a graphite tube in successive atmospheres of N_2 and ammonia at temperatures below even Brewer and Haraldsen's reported transition. In each case the TiB_2 showed no evidence of conversion to the nitrides of boron and titanium. Because of this experimentally observed lack of reversibility of the reaction, due possibly to surface contamination of the TiB_2 with oxides, the value of T_t obtained in these experiments represents an upper bound. The agreement between runs and under slightly varying experimental conditions—*e.g.*, amount of previous outgassing before introduction of N_2 atmosphere, extent of compaction of powders—suggests, however, that 2150°K. might indeed be a good value. Additional evidence that T_t is higher than that reported by Brewer and Haraldsen comes from the writer's observation that mixed TiN and BN in N_2 do not convert to TiB_2 at 1870°K. after holding at temperature for 30 hours. This result is significant because Brewer and Haraldsen found TiB_2 after reacting Ti, B, and N_2 at a temperature 50° lower.

Using the above value of T_t for the purposes of calculation, the heat of formation of TiB_2 is obtained as follows: entropy, enthalpy and heat capacity data for N_2 and B are from Stull and Sinke; the values for BN are from the National Bureau of Standards tabulation,[9] which is more reliable for this compound than The U. S. Bureau of Mines Bulletins[10] No. 426 or 584. A discussion of this

---

(8) D. R. Stull and G. C. Sinke, "Thermodynamic Properties of the Elements," Adv. in Chem. No. 18, Am. Chem. Soc., 1956.

(9) National Bureau of Standards, "Selected Values of Chemical Thermodynamic Properties," Series III.

(10) K. K. Kelley, "Contributions to the Data on Theoretical Metallurgy," U. S. Bur. Mines Bull. 476 and 584.

point is given in Section III (1). The Dworkin, Sasmor and Van Artsdalen[11] value of ΔH_f(BN) = -60.7 kcal./mole at 298°K. is adopted. The highest temperature given for the thermodynamic quantities in the NBS table is 1200°K., leading directly to ΔH_f(BN) = -59.8 at 1200°K. Adjusting to the observed transition temperature gives ΔH_f(BN) = -59.0 at 2150°K. Using ΔS appropriate to 2150°K. gives ΔF_f(BN) = -15.9 kcal./mole at 2150°K. The other quantity needed is ΔF_f(TiN) at 2150°K. The NBS table gives values up to 1500°K. Using a linear extrapolation, we obtain -34.6 kcal./mole for the required quantity. Then $\Delta F_f(TiB_2) = \Delta F_f(TiN) + 2\Delta F(BN) =$ -66 kcal./mole at 2150°K. Except for a slight correction for the ΔF of fusion of Ti, this value represents the $\Delta H_f(TiB_2)$ at 298°K. generated by this experiment and the supplementary data available.

A substantial difference exists between the calorimeter value of Lowell and Williams, -50 kcal./mole, and the nitride transition value described above, -66 kcal./mole. This difference cannot be attributed to lack of equilibrium in the present nitride transition experiment since if the true transition temperature were lower than that observed, the computed heat of formation would be even more negative than -66 kcal./mole. Cumulative uncertainty in the thermodynamic data employed and the high temperature extrapolations of these quantities probably are responsible. Ten per cent. uncertainty in each value, which is reasonable, makes them overlap.

III. Analysis of Earlier Experiments

(1) **Brewer and Haraldsen.**[2]—In the nitride transition experiment discussed in Section II (3) and originally performed by Brewer and Haraldsen, two general sources of error can exist. One is the experimental determination of the transition temperature, which established $\Delta F = 0$ in the reaction $TiN + 2BN = TiB_2 + 3/2\ N_2$, and the other is the thermodynamic values from the literature for ΔF_f(TiN) and ΔF_f(BN). The present work indicates that both types of error were included.

In computing ΔF_f(BN) at their transition temperature, Brewer and Haraldsen evidently used heat content and heat capacity data from U. S. Bureau of Mines Bulletin 476, tabulated by K. K. Kelley. These values, in turn, were taken from the experimental work of Magnus and Danz,[12] but their data referred to one-half mole. Thus, Bulletin 476 and its successor, Bulletin 584, contain values for BN heat content and heat capacity that are too low by a factor of two since they are intended to refer to one mole. This point has been confirmed by Kelley.[13] With the use of the corrected heat capacity equation, the Brewer and Haraldsen experiments yield $\Delta H_f(TiB_2) = -84$ kcal./mole.

The above remarks have dealt only with the second type of error. As mentioned in Section II (3), the value reported here for the transition temperature T_t does not agree with that found by Brewer and Haraldsen. In their original experiment, two runs were made in the attempt to find T_t: at 2270°K., TiB_2 formed in abundance from a mixture of Ti, B and BN heated in N_2; at 1820°K., only the elemental powders of Ti and B were used as solid reactants, and a small amount of TiB_2 was formed along with a large amount of TiN and possibly a trace of BN. This temperature, 1820°K., was taken by Brewer and Haraldsen as the desired T_t for computing $\Delta H_f(TiB_2)$. The absence of BN X-ray diffraction peaks comparable in intensity with those found for TiN requires explanation.

A possibility is that the amorphous boron did not react with N_2 at 1820°K. in the period of time employed (50 minutes), but instead reacted with the Ti to form TiB_2. To investigate this point, the writer heated amorphous boron in one atmosphere of N_2 to a temperature 50° higher than the Brewer and Haraldsen value of T_t. At the end of one hour no X-ray diffraction peaks for BN were found. Presumably the lack of reaction is due to surface contamination of the boron particles, although in the writer's experiment the boron powder was outgassed *in vacuo* at 1500°K. for an hour before the N_2 was admitted to the system. (At 2270°K., the same experiment yielded about 50% conversion of amorphous boron to BN.) In the calorimeter experiment of Lowell and Williams it was shown that Ti and amorphous B react to form TiB_2 at a temperature below 1820°K., and other work with the same apparatus demonstrated that TiN is formed at 1300°K.

Thus a mixture of elemental Ti and B heated in an N_2 atmosphere even below T_t would be expected to yield only TiB_2. In the Brewer and Haraldsen experiment, much of the boron reacted with the molybdenum crucible, leaving an excess of titanium over that required to combine with the remaining boron as TiB_2. The excess titanium formed TiN. As discussed in Section II (3), the writer has found that TiB_2 does not react in a period of several hours with N_2 at any temperature, due again to some surface contamination, so the TiB_2 formed would be stable during a 50-minute experiment. A false conclusion about T_t is the result. Thus even if corrections are made in the thermodynamic data employed by Brewer and Haraldsen, the resulting value of $\Delta H_f(TiB_2)$ is too negative because of experimental problems in determining T_t.

(2) **Samsonov.**[3]—Samsonov[3] studied the reduction of TiO_2 with carbon and boron carbide. The analysis given by him is appropriate to the reaction $2TiO + B_4C + C = 2TiB_2 + CO$. Since the value of $\Delta H_f(TiB_2)$ obtained from his data and this reaction does not agree with his value, it is likely that the reaction investigated was really that given by Krestovnikov and Vendrikh[6] in discussing Samsonov's work: $2TiO + B_4C = 2TiB_2 + CO_2$. Lack of identification of solid or gaseous products makes evaluation difficult. If the latter reaction is correct, the value of $\Delta H_f(TiB_2)$ calculated by Samsonov is still unreliable because of the choice of some questionable thermodynamic quantities from the Russian literature. In particular, the

---

[11] A. S. Dworkin, D. J. Sasmor and E. R. Van Artsdalen, *J. Chem. Phys.*, **22**, 837 (1954).

[12] A. Magnus and H. Danz, *Ann. Physik*, **81**, [4], 407 (1926).

[13] K. K. Kelley, private communication.

heat of formation of boron carbide used differs from the value of Smith, Dworkin and Van Artsdalen[14] by 52 kcal./mole. If the latter value is substituted, the value of $\Delta H_f(\mathrm{TiB_2})$ generated by Samsonov's experiment is -44 ± 6 kcal./mole—a value consistent with the calorimeter value of Lowell and Williams.

(3) **Samsonov.**[5]—In a separate paper Samsonov[5] gives the value $\Delta H_f(\mathrm{TiB_2}) = -73$ kcal./mole which he obtained from an empirical relation by Kubaschewsky and Evans[4] between the heat of formation of a compound and the change in molar volume on forming the compound from the elements. The writer has not been able to duplicate this calculation using the Kubaschewsky and Evans formula and both Russian and American values of atomic volumes of Ti and B.

(4) **Krestovnikov and Vendrikh.**[6]—An abstract[15] of a paper by Krestovnikov and Vendrikh[6] implied that an experimental study of the stability of $\mathrm{TiB_2}$ has been made, but the paper itself contains only review and discussion of (1), (2) and (3) above.

(5) **Schissel and Williams.**[1]—The mass spectrometer experiment performed by Schissel and Williams[1] involved the measurement of the equilibrium titanium partial pressure over $\mathrm{TiB_2}$ mixed with excess boron in a $\mathrm{TiB_2}$ Knudsen cell contained in a tungsten jacket.

To bring their value, -32 kcal./mole, into agreement with the calorimeter value of -50, the temperature determination for the former would have to have been in error (too high) by several hundred degrees or the Ti vapor pressure measurement would have to have been in error (too high) by two orders of magnitude. Neither of these errors is likely. The geometry of the Knudsen cell radiation sighting hole was favorable for black-body conditions (depth = 10 × radius, diameter = $^1/_8$"), and the window was calibrated with a flat-filament lamp and protected with an internal shield when readings were not being taken. A 50° uncertainty was allowed by the authors. The Ti pressure was measured using both an absolute calibration against a weighed amount of silver and a relative calibration against the known silver vapor pressure; the Ti pressures so determined agreed within a factor of two.

A more plausible explanation is that the Ti pressure was in fact too high because of the vaporization of Ti from some other source. Analysis of material chipped from around the orifice of the tungsten outer jacket of the Knudsen cell showed $\mathrm{W_2B}$ by X-ray diffraction and only W and B by spectrographic analysis. Thus the titanium that must have interacted with the tungsten cell *via* the vapor phase evidently re-evaporated. (This conclusion is in agreement with the results of the experiment listed in Table II: $\mathrm{TiB_2}$ powder heated on a tungsten strip *in vacuo* formed $\mathrm{W_2B}$ and lost Ti by vaporization.) The collimation of the molecular beam effusing from the Knudsen cell was such as to give line geometry, while the orifice of the cell was circular. Thus Ti atoms vaporizing from the tungsten lid on either side of the orifice could enter the beam, giving rise to a spurious Ti flux.

Recently the mass spectrometer experiment has been repeated by Schissel and Trulson,[16] using $\mathrm{TiB_2}$ powder in a graphite crucible. The resulting value for $\Delta H_f(\mathrm{TiB_2})$, -52 ± 6 kcal./mole, is in agreement with the calorimeter result of Lowell and Williams.

Acknowledgments.—The writer is grateful to Alan W. Searcy for his continued interest in this problem and for many helpful comments on the manuscript. P. O. Schissel and O. C. Trulson have generously allowed mention of their results before full publication. Appreciation also is due to C. E. Lowell, J. Weigel and R. D. Schaal for assistance during the work.

---

[14] D. Smith, A. S. Dworkin and E. R. Van Artsdalen, *J. Am. Chem. Soc.*, **77**, 2654 (1955).

[15] A. N. Krestovnikov and M. S. Vendrikh, *Chem. Abstr.*, **52**, 18613g (1959).

[16] P. O. Schissel and C. Trulson, private communication.

INFRARED SPECTRA OF COMPLEXES OF 2-PYRIDINALDOXIME

BY RONALD A. KRAUSE, NORMAN B. COLTHUP AND DARYLE H. BUSCH

A Contribution from the McPherson Chemical Laboratory of The Ohio State University, Columbus, Ohio, and the Central Research Division, Chemical Research Department and the Research Service Department, American Cyanamid Company

Received July 11, 1961

Infrared spectra of nickel(II), palladium(II), palladium(IV), platinum(II) and platinum(IV) complexes of 2-pyridinaldoxime are reported. Assignments have been made for four pyridine ring bands, the acyclic C=N vibration and the N–O stretching mode. The pyridine ring bands appear in the range expected for 2-substituted pyridines; the frequency of the C=N stretching mode, however, is very dependent on the complex type. As oxime protons are removed from the complex, the C=N vibration shifts from the normal range (1654–1614 cm.$^{-1}$) to the range 1519–1505 cm.$^{-1}$ for the uncharged complexes. The N–O vibration shifts toward higher frequencies as oxime protons are removed.

Introduction

During the course of a study of the nickel(II), palladium(II), palladium(IV), platinum(II) and platinum(IV) complexes of 2-pyridinaldoxime,[1] the infrared spectra of these compounds were recorded. In the present paper assignments for the C=N, N–O and four pyridine ring bands have been made for these compounds. Perhaps the most

---

[1] R. A. Krause and D. H. Busch, *J. Am. Chem. Soc.*, **82**, 4830 (1960); R. A. Krause, D. C. Jicha and D. H. Busch, *ibid.*, **83**, 528 (1961). The preparation of dibromobis-(2-pyridinaldoximo)-palladium(IV) and dibromobis-(2-pyridinaldoximo)-platinum(IV) has been described by R. A. Krause, Ph.D. dissertation. The Ohio State University, 1959.

interesting observation is the unusual position of the C=N stretching mode in complexes containing the $C{=}N{-}O^{\ominus}\cdots HO{-}N{=}C$ and the $C{=}N{-}O^{\ominus}$ groups.

Experimental

The preparation of the compounds under consideration in the present paper already has been reported.[1] Preparation of the ligand hydrochloride and ligand potassium salt is described below.

2-Pyridinaldoxime Hydrochloride.—2-Pyridinaldoxime was dissolved in hydrochloric acid and evaporated to dryness. After recrystallizing from hot, absolute ethanol the golden, crystalline solid was dried over P_2O_5. *Anal.* Calcd. for $C_6H_7N_2OCl$: C, 45.43; H, 4.45; N, 17.66; Cl, 22.36. Found: C, 45.78; H, 4.53; N, 17.91; Cl, 22.09.

2-Pyridinaldoxime, Potassium Salt.—Ten grams of 2-pyridinaldoxime and 4.6 g. of potassium hydroxide were dissolved in 200 ml. of absolute ethanol. After adding 145 ml. of benzene the water was azeotroped out and the solution evaporated to dryness. Although the bright yellow solid contained some 2-pyridinaldoxime it was considered to be sufficiently pure for infrared examination.

TABLE I

INFRARED ABSORPTION BANDS.[a] LIGAND AND LIGAND SALTS

HPOX[b]	HPOX·HCl	KPOX
3410sh	3100m	3000s-b
3300sh	3020s	2350w-b
3230sh	2970sh	1620w
3194s	2950sh	1595sh
3104sh	2920vs	1591s-sp
3070s	2860vs	1573sh
3003s-sp	2760s	1562m
2880b	1635m	1530sh
2791s	1620m-sp	1517s
2767sh	1605s-sp	1509sh
1625w	1580w	1500sh
1600s-sp	1525m	1477sh
1569s-sp	1515w	1470s
1520s	1470w	1460sh
1477s-sp	1455s-sp	1440s
1439s-sp	1445sh	1430sh
1386vw	1425sh	1337sh
1327s	1375m	1332s
1298m	1370sh	1306m
1267w	1357w	1292m
1254w	1320m	1260w
1231s	1293s-sp	1235m
1159s-sp	1285sh	1217m
1103s-sp	1243m-sp	1175w
1056w	1232s-sp	1149m-sp
1046w	1195w	1140m-sp
1005m	1163m	1109s
996sh	1095w	1090sh
985s	1045w	1075s
979s	1002vs-sp	1052s
962m	958m-sp	1035s
946s	933m-sp	986s
892m	926w	962m
879s	915w	901sh
828m-b	790s-sp	890s
778s	745m	866m
771s	731m	862sh
741s	664m-sp	777sh
668s		771s
		740s
		734s
		675s

[a] s = strong, m = medium, w = weak, b = broad, sh = shoulder, sp = sharp, v = very. [b] In this and the following tables, HPOX refers to 2-pyridinaldoxime, while POX refers to its uninegative anion.

TABLE II

INFRARED ABSORPTION BANDS. COMPLEXES CONTAINING THE —C=N—OR GROUP

Ni-$(HPOX)_3$-$I_2 \cdot 2H_2O$	Ni-$(HPOX)_2$-Cl_2	Ni-$(HPOX)_2$-$(OAc)_2$	$[Pd(POX{-}COCH_3)Cl_2]$	$[Pt(POX{-}COCH_3)_2]Cl_2$
3299sh-b	3406vw	3424m	3408m	3405s
3060s-b	3160s	3084sh	3178w	3112sh
1633w-sh	3082s	3007w	3031m-sp	3067s-sp
1614sh	3015s	2932sh	1790s-sp	2995sh
1599s-sp	2779vw	1760m-b	1752sh	2920w
1563w	1654m-sp	1644m	1615w-b	2054w
1478s-sp	1611s-sp	1613s	1590m-sp	1780s
1443m	1574w	1576sh	1565w	1750sh
1383m	1559sh	1550s	1477m-sp	1731sh
1292sh	1490s-sp	1481m	1446w	1720sh
1279s	1480sh	1440sh	1426m-sp	1633sh
1252s	1438vw	1410s-b	1369s-sp	1614sh
1239s	1388vw	1343sh	1356m-sp	1595m-sp
1218w	1318s	1334w	1298m	1564w
1158m	1307s	1247m-b	1254w	1485s-sp
1108w-b	1257m	1217m	1214s-sp	1454sh
1070sh	1215m	1163m	1173vs	1443m
1036vs	1158m	1152m	1161sh	1425sh
1022sh	1087vw	1104sh	1108m	1416sh
956w-b	1055vs	1069s-b	1061m-vb	1373sh
921w	1018w	1015w	1045m	1366sh
891m	946w	925sh	1034m	1360s-sp
775s-b	937m	916m	1011s	1335m-sp
746w-b	886m	888m	981m	1271sh
676m	782sh	879sh	954s-sp	1250m
670m	776s	791vw	910sh	1227s
	754m	778sh	904s	1183s-b
	673s	776s	896sh	1162s
		756m	853sh	1111m-sp
		751m	841s	1068w
		681s	773vs	1040m
		659s	737m	1021sh
			704s	1017sh
			668m	1009s
			658m	1004sh
				998sh
				983m
				959sh
				949s
				928s
				898s
				833m
				828sh
				778s
				673s
				659m

Infrared Spectra.—The infrared spectra of all complexes were recorded on a Perkin-Elmer model 21 spectrophotometer using the KBr disk technique. The spectra of the ligand and ligand salts were run using the Nujol mineral oil mull technique; spectra were obtained on both Nujol mineral oil and halocarbon mulls.

Discussion

Tables I–IV list infrared bands for the complexes under consideration, while Table V gives assignments which were made in the present study. The 2-substituted pyridine ring should give rise to four ring stretching frequencies between 1640 and 1425 cm.$^{-1}$ and a band at 790–740 cm.$^{-1}$ originating

TABLE III

INFRARED ABSORPTION BANDS. COMPLEXES CONTAINING THE —C=N—O⁻. . .HO—N=C— GROUP

[Ni(POX)-(HPOX)(OAc)-(H_2O)]	[Ni(POX)-(HPOX)(Py)$_2$]I	[Ni(POX)-(HPOX)]I	[Pd(POX)-(HPOX)]Cl
3395s-b	3465sh	3363s	3408s
1772m-vb	3409m	3050sh-b	3085m
1637w	3025m	1626sh	2977m
1607m	1630sh	1608s-sp	1630sh
1568sh	1606s-sp	1588sh	1610m
1547m	1585sh	1547sh	1594m
1529sh	1553sh	1535sh	1580m
1515sh	1544m	1526m	1556s
1480m	1527sh	1510sh	1546sh
1428sh	1522sh	1477s-sp	1526sh
1397s-b	1511sh	1435w	1510sh
1333m	1489sh	1337w	1479s-sp
1256sh	1478s-sp	1300m	1425w-b
1221w	1460sh	1253m	1348s-sp
1150w	1442s-sp	1216m	1303m
1051s-b	1418sh	1151w	1233s-sp
1021w-b	1340m	1128sh	1206w
920w	1303m	1118w	1167sh
885m-b	1246sh	1090m-b	1150s
777s-b	1242sh	1045s	1114m-sp
753vw	1215m	1023sh	1074m
694sh	1157m	886w	1024m
681m-b	1118m	775s	915m-b
662m	1093m	749m	895m-b
	1065m	678m	765s
	1056sh	669w	714m-b
	1041m		665sh
	1015m		659m
	953m		
	906m-b		
	775m		
	756m		
	754m		
	750m		
	700m		
	683m		
	660w-b		

TABLE IV

INFRARED ABSORPTION BANDS. COMPLEXES CONTAINING THE —C=N—O⁻ GROUP

[Ni-(POX)$_2$]	[Pd-(POX)$_2$]	[Pt-(POX)$_2$]	[Pd-(POX)-Cl]$_2$	[Pt-(POX)$_2$-Br$_2$]	[Pd-(POX)$_2$-Br$_2$]
3353s-b	3320sh	3361s-b	3410s	3389s	3410s-b
1634sh	3177s-b	3030sh	1630sh	2995m	2988s
1608s-sp	3019sh	1661sh	1604s	1633w	1622w
1583sh	1659w	1616s-sp	1567sh	1610m-sp	1595s-sp
1549sh	1605s-sp	1564vw	1528sh	1562w	1559w
1519m-b	1561vw	1515sh	1517m	1524sh	1523sh
1504sh	1513sh	1505m	1490s	1517s-sp	1509s
1478s-sp	1505s	1491s	1477m	1505sh	1500sh
1464sh	1482s	1465sh	1435m	1488s-sp	1475s
1436w	1463sh	1433s	1349s	1479sh	1460sh
1340m	1424m	1348s	1297w-b	1463sh	1448wh
1304w	1344s	1255s	1256sh	1436sh	1428s
1256w	1315sh	1182s	1249m	1426s-sp	1409sh
1227m	1246s	1157s	1225m	1416sh	1396sh
1154sh	1175s	1118w	1183w-b	1401sh	1360s
1120s	1150m	1054s-b	1148m	1360s-sp	1307s
1094s	1131sh	907w-b	1131s	1342sh	1288sh
1019w	1108sh	828m-b	1125sh	1326m-sp	1259s
890m-b	1057vw	805w-b	1101s	1312sh	1229s
775s	1039w	768m-b	897w-b	1229sh	1216sh
749m	1029w	679m	880w-b	1258s-sp	1190s
680m-b	892m	664m	776sh	1206sh	1152s
	833m		767m-b	1196sh	1108m
	775s		712w	1191s	1052sh
	678m		701m	1160m-sp	1043m
	668vw		676w	1149sh	1029m
	658w-b		667w	1117m-sp	912w
				1062m	892m
				1052m	826s-b
				1037m-sp	808sh
				1008w	802vw
				993w	776s-b
				988sh	752sh
				924w-b	737m
				906sh	672s
				898m	668sh
				883sh	666sh
				838m-b	
				778s-b	
				744m	
				678s	
				667m	

from the four adjacent (ring) hydrogen wagging vibration.[2] 2-Substituted pyridine ring bands are expected at 1615–1585, 1576–1568, 1477–1465 and 1438–1428 cm.$^{-1}$; 2-substituted pyridine N-oxide ring bands are expected at 1640–1600, 1577–1557, 1540–1480 and 1445–1425 cm.$^{-1}$.[2] Normal oximes[3,4] have bands at 3300–3150 cm.$^{-1}$ (OH stretch), 1690–1620 cm.$^{-1}$ (C=N stretch) and near 950 cm.$^{-1}$ (N-O stretch); benzaldoxime absorbs at 3280, 1632 and 945 cm.$^{-1}$.

In the present study the C=N (acyclic) vibrational frequency is assigned after first locating the four ring bands from the above data. There was usually a distinct fifth band in this region unassignable to the pyridine ring; this must be assigned as the C=N band.

Between 950 and 1200 cm.$^{-1}$ there was a very strong band (or group of bands), usually the strongest in the spectrum. These were assigned to the N-O stretching vibration on the basis of intensity. This band was not always unambiguously assignable since three equally intense bands occasionally occurred in this region. In these cases, the band in the middle of the group was arbitrarily chosen as representing the N-O band.

The infrared spectrum of 2-pyridinaldoxime differs from that of a conventional oxime by the broad OH band (*ca.* 3250 cm.$^{-1}$) being replaced by multiple bands between 3194 and 2791 cm.$^{-1}$; the strongest of these lies at 2791 cm.$^{-1}$. This implies much stronger hydrogen bonding than in other oximes. The band assigned to C=N (acyclic) at 1520 cm.$^{-1}$ is considerably lower than normal; one might attribute this lowering to structures of the type (I) in which the oxime proton

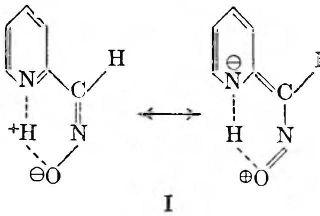

I

is partially ionized. This effect is verified by the abnormally low C=N absorption frequency (1517

---

(2) A. R. Katritzky, *Quart. Revs.* (*London*), **13**, 353 (1959).

(3) J. Fabian, M. Legrand and P. Poirier, *Bull. soc. chim. France*, **23**, 1499 (1956).

(4) J. F. Brown, Jr., *J. Am. Chem. Soc.*, **77**, 6341 (1955).

TABLE V

ASSIGNMENTS FOR LIGAND, LIGAND SALTS AND COMPLEXES. FREQUENCIES IN CM.$^{-1}$

Compound	C=N	N–O	Ring I	Ring II	Ring III	Ring IV
Ligand and ligand salts						
HPOX·HCl	1620m-sp	1002vs-sp	1605s-sp	1580w	1525m	1455s-sp
HPOX	1520s	985s	1600s-sp	1569s-sp	1477s-sp	1439s-sp
KPOX	1517s	1075s	1591s-sp	1573sh	1470s	1440s
Complexes containing the —C=N—O—R group						
$Ni(HPOX)_3I_2$	1633w-sh	1036vs	1599s-sp	1563w	1478s-sp	1443m
$Ni(HPOX)_2Cl_2$	1654m-sp	1055vs	1611s-sp	1574w	1490s-sp	1438vw
$Ni(HPOX)_2(OAc)_2$	1644m	1069s-b	1613s	1576sh	1481m	1440sh
$Pd(POX{-}Ac)Cl_2$	1615w-b	Interference	1590m-sp	1565w	1477m-sp	1426m-sp
$Pt(POX{-}Ac)_2Cl_2$	1614sh	Interference	1595m-sp	1564w	1485s-sp	1443m
Complexes containing both —C=N—OH and —C=NO$^-$ groups						
$Ni(POX)(HPOX)(OAc)(H_2O)$	1547m	1051s-b	1607m	1568sh	1480m	1428sh
$Ni(POX)(HPOX)(Py)_2I$	1544m	1041m	1606s-sp	1553sh	1478s-sp	1442s-sp
Ni(POX)(HPOX)I	1526m	1045s	1608s-sp	1588sh	1477s-sp	1435w
Pd(POX)(HPOX)Cl	1556s	1150s	1610m	1580m	1479s-sp	1425w-b
Complexes containing the —C=N—O$^-$ group						
$Ni(POX)_2$	1519m-b	1120s	1608s-sp	1583sh	1478s-sp	1436w
$Pd(POX)_2$	1505s	1175s	1605s-sp	1561vw	1482s	1424m
$[Pd(POX)Cl]_2$	1517m	1131s	1604s	1567sh	1490s	1435m
$Pt(POX)_2$	1505m	1182s	1616s-sp	1564vw	1491s	1433s
$Pd(POX)_2Br_2$	1509s	1190s	1595s-sp	1559w	1475s	1428s
$Pt(POX)_2Br_2$	1517s-sp	1191s	1610m-sp	1562w	1488s-sp	1426s-sp

cm.$^{-1}$) observed in the spectrum of the potassium salt of 2-pyridinaldoxime (II).

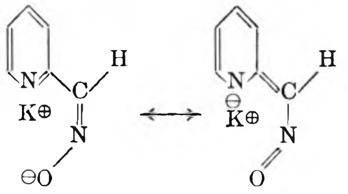

II

A single strong band at 982 cm.$^{-1}$ in the free ligand is assigned to the N–O stretching vibration and a broad medium intensity band at 822 cm.$^{-1}$ is assigned to the out of plane wag of the hydrogen bonded oxime proton (this latter band disappears in the potassium salt). Ring bands appear at 1597, 1568, 1472 and 1440 cm.$^{-1}$ in the free ligand.

The ligand hydrochloride (HPOX·HCl) is closer to a normal oxime in its infrared spectrum. Placement of the hydrochloride proton on the pyridine nitrogen prevents an O---H---N hydrogen bond, and reduces the polar character of the bond to the oxime proton. The C=N vibration is assigned to the 1620 cm.$^{-1}$ band.

In Table V assignments for the complexes have been listed in three different groups; the first group consists of complexes containing —C=N—O—R (with R being H or $COCH_3$), the second contains complexes having the functional group —C=N—O$^{\ominus}$. . .HO—N=C— (the oximes may or may not be hydrogen bonded), while the third group contains complexes having —C=N—O$^{\ominus}$. The effect of proton removal from the oxime function on the absorption frequency of the —C=N— group is quite dramatic. Those complexes containing un-ionized oxime groups have a —C=N— absorption in the range 1654–1614 cm.$^{-1}$, quite in keeping with that observed for normal oximes and the ligand hydrochloride. In those complexes containing the —C=N—O. . .HO—N=C— and —C=N—O$^{\ominus}$ groups, however, the —C=N— absorption frequency drops to the range 1556–1526 and 1519–1505 cm.$^{-1}$, respectively. There is an inverse change in the N–O absorption frequency in this series; the first group shows this absorption in the range 1069–1036 cm.$^{-1}$, the second group in the range 1150–1041 cm.$^{-1}$, and the third group in the range 1191–1120 cm.$^{-1}$.

The observed position of the —C=N— absorption in the ligand hydrochloride (1620 cm.$^{-1}$) and in the potassium salt of the ligand (1517 cm.$^{-1}$) lends support to the assignments for the complexes. As the oxime proton becomes more ionic, there is probably more contribution of —N=O— to the structure, the —C=N— vibration consequently shifts to lower frequency and the N–O vibration shifts to higher frequency. (Bellamy[5] lists the N=O absorption in C-nitroso monomers at 1600–1500 cm.$^{-1}$)

The four pyridine ring bands for the complexes lie in the range 1616–1590, 1588–1553, 1491–1475 and 1443–1424 cm.$^{-1}$. These observed ranges agree quite well with those expected for 2-substituted pyridines and 2-substituted pyridine N-oxides.

---

(5) L. J. Bellamy, "The Infrared Spectra of Complex Molecules," John Wiley and Sons, Inc., New York, N. Y., 1958, pp. 305–306.

THE EFFECT OF IONIC STRENGTH ON EQUILIBRIUM IN SILVER-HYDROGEN ION EXCHANGE[1]

By Leslie Leifer, Arthur W. Davidson and William J. Argersinger, Jr.

Chemical Laboratory of The University of Kansas, Lawrence, Kan.

Received July 12, 1961

From data on exchange equilibrium at 25° between Dowex 50 of 10.5% divinylbenzene content and aqueous silver nitrate–nitric acid solutions at ionic strengths of 0.1, 0.3 and 1.0 molal, values were determined for the selectivity coefficients K_m for silver–hydrogen over a wide range of resin compositions. For the two higher concentrations, the presence of a sharp minimum in the value of K_m in resins of low silver content was confirmed. From the K_m values and previously determined Ag^+–H^+ activity coefficient ratios in the aqueous solution, values were calculated for the thermodynamic equilibrium constant K for the silver–hydrogen exchange. Extrapolation of these values to zero ionic strength gives the figure 10.9 as the best value as yet available for this constant, and one which shows good consistency with previously determined constants for resins of lower and higher divinylbenzene content, as well as with the best previously determined constants for sodium–hydrogen and silver–hydrogen exchange on the same resin.

Introduction

Detailed studies have been reported previously for silver–hydrogen exchange on Dowex 50 of 10.5% divinylbenzene content with dilute solutions (0.02 and 0.1 molal)[2] and with solutions of 1 molal total ionic strength.[3] Despite the use of widely different methods of analysis and the overall 50-fold variation in ionic strength, the values determined in these two investigations for the selectivity coefficients K_m (defined by the equation

$$K_m = \frac{m_{H^+}N_{Ag\ Res}}{m_{Ag^+}N_{H\ Res}}$$

in which m represents molality in the aqueous solution and N mole fraction in the resin) are in fair agreement over a wide range of resin compositions. Högfeldt, Ekedahl and Sillén, however, reported a minimum value for the selectivity coefficient at $N_{Ag\ Res} = 0.15$, whereas the data from our Laboratory did not extend to $N_{Ag\ Res}$ values lower than 0.18. Studies have been reported also for the same exchange, at 0.1 molal ionic strength, on similar resins of 8 and 16% divinylbenzene content;[4] here a minimum in the selectivity coefficient–resin composition curve was found for the latter resin only, at $N_{Ag\ Res} = 0.25$.

Since the mean activity coefficient ratios $\gamma_{HNO_3}/\gamma_{AgNO_3}$ in mixed aqueous solutions of ionic strengths from 0.1 to 1.0 molal are known for the entire range of compositions,[5] values can be found readily for the revised selectivity coefficients K_a, defined by the equation

$$K_a = K_m\left(\frac{\gamma_{HNO_3}}{\gamma_{AgNO_3}}\right)^2 = K_m\left(\frac{\gamma_{H^+}}{\gamma_{Ag^+}}\right)$$

and from these values, by a process of graphical integration,[6,7] the value of the thermodynamic equilibrium constant K, defined by the equation

$$K = K_a\left(\frac{f_{Ag\ Res}}{f_{H\ Res}}\right) = \frac{a_{H^+}a_{Ag\ Res}}{a_{Ag^+}a_{H\ Res}}$$

can be determined. The Swedish workers, on the assumption of unit activity coefficient ratio in dilute aqueous solutions, calculated from their data a value of 9.8 for K, whereas the early data from this Laboratory yielded a K value of 13.7.

The purpose of the investigation here reported was threefold: (1) to determine whether or not the sharp increase in silver–hydrogen selectivity coefficient previously observed in resins of low silver content could be confirmed; (2) to observe the variation with ionic strength of values obtained for the thermodynamic equilibrium constant K for the silver–hydrogen exchange; (3) to compare the best K value obtainable directly from silver–hydrogen exchange data with the value calculated (from the constants previously found in this Laboratory for sodium–hydrogen[8] and silver–sodium[9] exchanges on the same resin) by means of the simple relationship

$$K_H{}^{Ag} = K_H{}^{Na}K_{Na}{}^{Ag}$$

where in each case $K_Y{}^X$ represents the thermodynamic equilibrium constant for the reaction

$$X^+ + Y\ Res = Y^+ + X\ Res$$

Experimental Methods

The resin used throughout was taken from a single large sample of Dowex 50 of 10.5% divinylbenzene content. It had been "recycled" three times between the hydrogen and sodium forms, a treatment which tends to minimize variation in capacity and selectivity. Visual inspection of the resin particles showed them to be of uniform color, and they were limited to a uniform narrow size range by the use of standard sieves. In most of the exchange experiments, the initial resin was pure hydrogen resin, obtained by repeated circulation of 20% hydrochloric acid through the sodium resin, followed by thorough washing with distilled water and partial drying in air at room temperature. Since it had been observed that extensive air drying tends to bring about fracture of the resin particles, with appreciable alteration of their exchange capacity, resin samples to be used for exchange always were left in a moist, tacky state.

The equivalent weight of the hydrogen resin was determined in the following manner. Three weighed samples of the air dried material were subjected to exhaustive exchange with sodium chloride solution and the eluted acid was titrated with sodium hydroxide solution. A fourth weighed sample of the same resin was completely dried

---

[1] From part of a thesis submitted by Leslie Leifer in partial fulfillment of the requirements for the degree of Doctor of Philosophy, The University of Kansas, 1959.

(2) E. Högfeldt, E. Ekedahl and L. G. Sillén, *Acta Chem. Scand.*, **4**, 1491 (1950).

(3) O. D. Bonner, W. J. Argersinger, Jr., and A. W. Davidson, *J. Am. Chem. Soc.*, **74**, 1044 (1952).

(4) O. D. Bonner and V. Rhett, *J. Phys. Chem.*, **57**, 254 (1953).

(5) O. D. Bonner, A. W. Davidson and W. J. Argersinger, Jr., *J. Am. Chem. Soc.*, **74**, 1047 (1952).

(6) W. J. Argersinger, Jr., A. W. Davidson and O. D. Bonner, *Trans. Kansas Acad. Sci.*, **53**, 404 (1950).

(7) E. Ekedahl, E. Högfeldt and L. G. Sillén, *Acta Chem. Scand.*, **4**, 556 (1950).

(8) A. W. Davidson and W. J. Argersinger, Jr., *Ann. N. Y. Acad Sci.*, **57**, 105 (1953).

(9) G. E. Wilson, A. W. Davidson and W. J. Argersinger, Jr., *J. Am. Chem. Soc.*, **76**, 3824 (1954).

by being heated to constant weight in an oven at 115° and its water content thus determined. The equivalent weight, calculated on the basis of the dry resin, was found to be 199.2 ± 0.5.

Samples of from 4 to 10 g. of hydrogen resin were agitated at 25° for suitable periods (varying from 2 to 36 hrs.), in blackened ground-glass stoppered flasks with 100- to 350-ml. samples of mixed silver nitrate–nitric acid solutions of various compositions at fixed ionic strengths of 1.0, 0.3 and 0.1 molal. In general, duplicate runs were not made at a single solution composition, but rather the compositions were varied slightly to give separate individual points on the exchange curve. Thus the general smoothness of the curve, rather than agreement of different runs for a single point, gives an indication of the reliability of the measurements.

After equilibration the resin was allowed to settle and the equilibrium solution was pipetted off. The residue was placed in a large büchner funnel to which suction was applied, and washed by flooding with distilled water until the washings no longer gave a test for silver ion; this washing procedure usually was completed in 10–15 seconds. Since analyses for silver and hydrogen could be carried out on the same sample of equilibrium resin, the degree of dryness of the resin was not critical; hence the resin samples to be analyzed were merely superficially dried by pressure between pads of filter paper.

The density of each equilibrium solution was determined by means of a pycnometer, and samples were analyzed for acidity by titration with standard sodium hydroxide solution and for silver content by one of the following methods. For solutions 0.01 to 0.1 molal in silver nitrate, titration with standard potassium iodide solution in the presence of ceric ammonium sulfate[10] proved to be satisfactory. At concentrations between 0.0001 and 0.01 molal, silver was determined by electrometric titration with standard potassium iodide solution; many of the results at these lower concentrations were checked by means of electrodeposition of silver from ammoniacal solution on a platinum gauze cathode.

Weighed samples of the equilibrium resin were subjected to exhaustive exchange with concentrated sodium nitrate solution until free of silver ion or, in the case of resin of low silver content, until the pH of the effluent solution was the same as that of the eluent. The eluate then was analyzed for acidity and for silver ion as already described. From two to five analyses were made on each solution and resin sample, and selectivity coefficients were calculated from the mean of the results.

Results

In Fig. 1, values of the logarithm of K_a, the revised selectivity coefficient, calculated from our exchange data and the known $HNO_3/AgNO_3$ activity coefficient ratios, are plotted against the degree of exchange or mole fraction of silver resin, $N_{Ag\ Res}$. From these plots were determined by graphical integration the activity coefficients of the resin components at selected compositions, as shown in Table I, and also values for K, the thermodynamic equilibrium constant.

TABLE I

ACTIVITY COEFFICENTS OF RESIN COMPONENTS

Ionic strength	0.1 M		0.3 M		1.0 M	
$N_{Ag\ Res}$	$f_{Ag\ Res}$	$f_{H\ Res}$	$f_{Ag\ Res}$	$f_{H\ Res}$	$f_{Ag\ Res}$	$f_{H\ Res}$
0	..	1.00	..	1.00	..	1.00
.2	1.13	1.00	1.16	0.96	1.31	1.01
.4	1.09	1.02	1.10	0.98	1.21	1.05
.6	1.05	1.05	1.05	1.03	1.11	1.14
.8	1.02	1.15	1.02	1.11	1.05	1.32
1.0	1.00	..	1.00	..	1.00	..
	$K =$	11.7	$K =$	12.3	$K =$	13.3

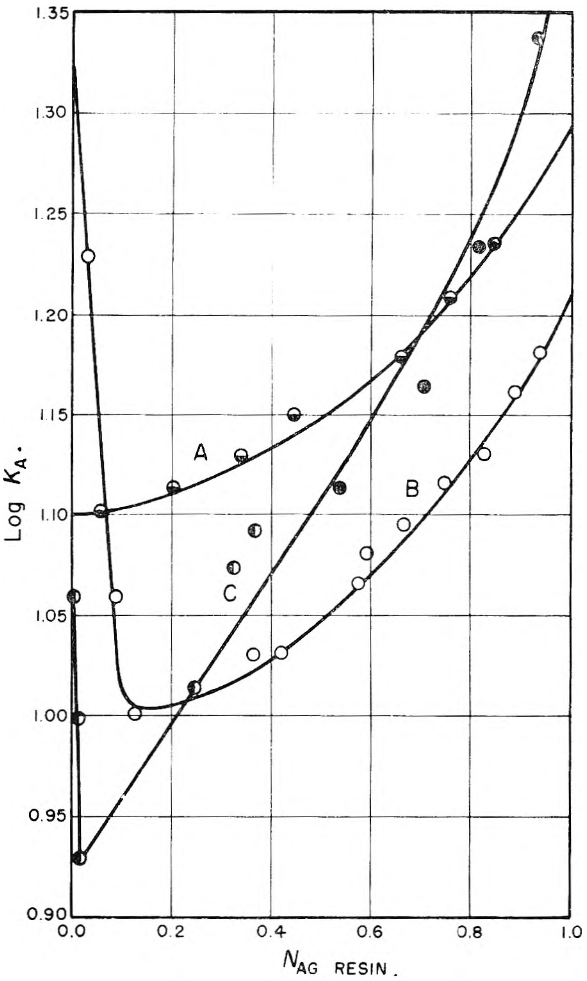

Fig. 1.—Silver–hydrogen exchange at several ionic strengths: (A) 0.1 molal; horizontally half-filled circles; subtract 0.1 from ordinate scale. (B) 0.3 molal, open circles; (C) 1.0 molal, vertically half-filled circles, data from present work; filled circles, data from ref. 3.

Discussion

In most ion-exchange equilibria, the revised selectivity coefficients $K_{a\ Y}{}^{X}$ tend toward unity with increase in N_X; in other words, the resin shows increasing selectivity for the "preferred" ion with increasing content of the other ion.[11] In this respect the course of the selectivity curve for the silver–hydrogen exchange must be regarded as "abnormal," since throughout at least a large fraction of the composition range $K_{aH}{}^{Ag}$ *increases* with increasing $N_{Ag\ Res}$. It may be noted, however, that the results obtained for 0.3 and 1.0 molal solutions in the present study again exhibit the sharp increase in $K_{a\ H}{}^{Ag}$ with decreasing $N_{Ag\ Res}$, for resins of low silver content, that first was observed in the earliest investigation of this exchange system,[2] and later also for a more highly cross-linked resin.[4] For 0.1 molal solutions, however, our data (curve A in Fig. 1) show no such minimum, at least down to an $N_{Ag\ Res}$ value as low as 0.057. It is, of course, conceivable that a minimum might occur at a still lower silver content, but investi-

---

(10) A. Bloom and W. M. McNab, *Ind. Eng. Chem., Anal. Ed.*, **8**, 167 (1936).

(11) J. A. Kitchener, *Physical Chemistry of Ion-Exchange Resins*, in J. O'M. Bockris, "Modern Aspects of Electrochemistry," No. 2. Academic Press, Inc., New York, 1954, p. 119.

gation of this region would necessitate accurate determination of silver ion at concentrations so low as to be inaccessible to the usual methods of chemical analysis.

The variation in the calculated values of the thermodynamic equilibrium constant K with ionic strength remains to be considered. First, there is a possibility of the incidence of error in the determination of resin composition in consequence of exchange during the washing of the equilibrium resin. The very short duration of the washing procedure (10–15 sec.), however, argues against sufficiently extensive exchange to alter significantly the equilibrium resin composition. The procedure described removes adsorbed, invaded, and superficial electrolyte, but leaves essentially unchanged the composition of the equilibrium resin itself, in terms of which the process equilibria have been formulated.

The major source of the variation of calculated values of K with ionic strength is no doubt the fact that, in our formulation of the exchange reaction, we have neglected both the transfer of water between solution and resin and changes in the amount of adsorbed electrolyte. It has been shown[8] that in the case of sodium–hydrogen exchange consideration of the first of these factors alone sufficed to bring the K values for various ionic strengths into satisfactory agreement. A further modification of the equilibrium equation to include changes in adsorbed electrolyte also has been discussed.[12,13] The application to the silver–hydrogen exchange of these more sophisticated treatments, however, would require much additional data, as yet unavailable, with regard not only to water and electrolyte uptake by the equilibrium resin, but also to water activity in the equilibrium solution. Since all of the disturbing effects diminish with increasing dilution, the best presently available value of the equilibrium constant is that obtained by extrapolation of the observed values to infinite dilution. When our values of K are plotted against the square root of the ionic strength an almost straight line is obtained, which yields by extrapolation a limiting value, K^0, of 10.9. It is of interest to compare this value of K^0 with those obtained from two other sources. Linear interpolation of the values obtained by Bonner and Rhett[4] for resins of 8 and 16% divinylbenzene content with 0.1 molal solutions gives for 10.5% divinylbenzenes the figure 9.05, which, corrected for the activity coefficient ratio, becomes 10.2. On the other hand, the product of the limiting value of K_{Na}^{Ag}, 6.54,[9] and that of K_{H}^{Na}, 1.64[11], is 10.7. In view of the wide diversity of the experimental sources from which they are calculated, the approximate concordance of these three K^0 values appears to be not without significance.

Acknowledgment.—This work was supported in part by contract DA-23-072-ORD-222 with the Office of Ordnance Research.

(12) G. L. Gaines, Jr., and H. C. Thomas, *J. Chem. Phys.*, **21**, 714 (1953).

(13) E. W. Baumann and W. J. Argersinger, Jr., *J. Am. Chem. Soc.*, **78**, 1130 (1956).

A POLAROGRAPHIC STUDY OF EXCESS LEAD DISSOLVED IN MOLTEN LEAD CHLORIDE

By J. J. Egan[1]

Max-Planck-Institut für physikalische Chemie, Göttingen, Germany

Received July 13, 1961

The constitution of a solution of excess lead in molten lead chloride equilibrated with liquid Au–Pb alloys at 518° was studied with the help of a polarographic technique. Limiting currents for the oxidation of subhalide at a platinum microelectrode as anode were obtained and used as a measure of the concentration of dissolved excess lead, which was found to be proportional to the activity of lead. It is concluded that excess lead dissolves in the melt as Pb_2^{++} ions.

Introduction

When lead is brought in contact with molten lead chloride it has been found[2] that a small amount of the lead dissolves in the chloride. This is a general phenomenon that occurs in many metal–metal halide systems. The form in which the excess metal exists in the salt has been the subject of experimentation and speculation for many years. In the Cd–$CdCl_2$ system, for example, both freezing point depression[3] and magnetic susceptibility[4] measurements have indicated that Cd dissolves in the melt as Cd_2^{++} ions, although later analysis[5] using revised heat of fusion data shows the necessity of postulating more complex species.

The dissolution of excess lead in molten lead chloride may be assumed to be due (1) to the formation of monovalent lead ions

$$Pb + Pb^{++} = 2Pb^{+} \qquad (1)$$

or (2) to the formation of Pb_2^{++} ions analogous to the species Hg_2^{++} prevailing in a solution of mercurous nitrate

$$Pb + Pb^{++} = Pb_2^{++} \qquad (2)$$

Since the solubility of excess lead in molten lead chloride is as low as 6×10^{-3} mole % at 500° according to Corbett and von Winbush,[2] the ac-

---

(1) Brookhaven National Laboratory, Upton, L. I., New York, U. S. A.

(2) J. D. Corbett and S. von Winbush, *J. Am. Chem. Soc.*, **77**, 3964 (1955).

(3) K. Grjotheim, F. Grönvold and J. Krogh-Moe, *ibid.*, **77**, 5824 (1955).

(4) J. Farquharson and E. Heymann, *Trans. Faraday Soc.*, **31**, 1004 (1935).

(5) L. E. Topel and A. S. Landis, *J. Am. Chem. Soc.*, **82**, 6291 (1960).

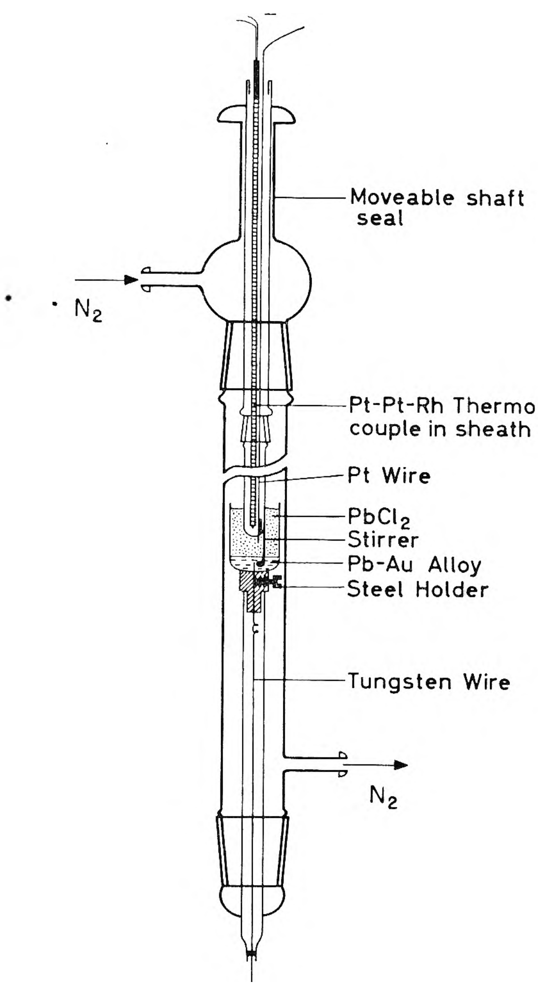

Fig. 1.—Polarographic apparatus using a platinum microelectrode.

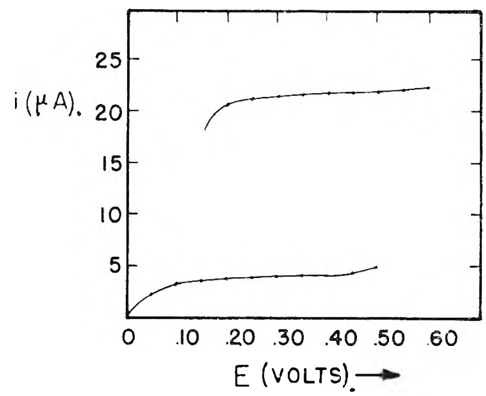

Fig. 2.—Typical current *vs.* voltage curves obtained.

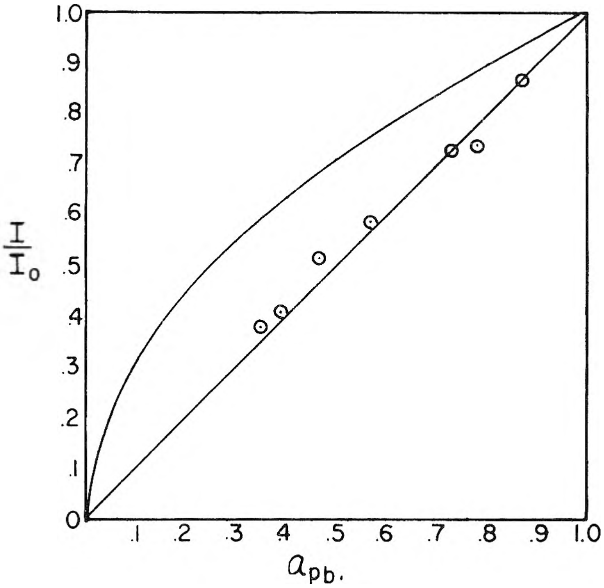

Fig. 3.—I/I_0 values for Au–Pb alloys. Experimental points are compared with straight line and parabola.

tivity of Pb^+ or Pb_2^{++} can be assumed to be proportional to its concentration. Thus on formulating the law of mass action the content of excess Pb dissolved in molten lead chloride is proportional to the square root of the activity a_{Pb} of lead in the case of reaction 1, but proportional to the first power of a_{Pb} in the case of reaction 2. With the help of measurements of the content of excess lead in molten lead chloride as a function of a_{Pb} by equilibrating molten lead chloride with lead alloys involving known values of a_{Pb}, one may, therefore, decide whether reaction 1 or reaction 2 prevails. Analogous investigations have been conducted by Heymann, Martin and Mulcahy[6] for the systems Na–NaBr, Cd–CdCl$_2$ and CdBr$_2$ and by Cubicciotti[7] for the system Ca–CaCl$_2$ using conventional chemical analysis.

As an alternative, equations 1 and 2 may be written with electrically neutral species, *i.e.*, $PbCl_2$, $PbCl$ and Pb_2Cl_2 or $Pb + PbCl_2$. The consequences resulting from the law of mass action, however, are not affected by writing equations 1 and 2 with electrically neutral molecular species.

In this study a polarographic method is employed to analyze for relative amounts of metal dissolved in the salt phase. This method is particularly suited to systems where only a small amount of metal dissolves in its salt. The feasibility of using solid microelectrodes for analysis of fused salt solutions has been demonstrated by Laitinen, Liu and Ferguson[8] as well as many others. References to various specific cases may be found in the article by Laitinen, *et al.* Topel and Osteryoung[9] have used the method to study solutions of Bi in BiCl$_3$. Here the microelectrode is operated as the anode where excess lead is oxidized to the normal divalent state.

The limiting current corresponding to the oxidation of Pb^+ or Pb_2^{++} is essentially proportional to the concentration of these species. Thus, denoting the current corresponding to $a_{Pb} = 1$ by I_0, one has in the case of reaction 1

$$I/I_0 = a_{Pb}^{1/2} \quad (3)$$

whereas in the case of reaction 2

$$I/I_0 = a_{Pb} \quad (4)$$

---

[6] E. Heymann, R. Martin and M. Mulcahy, *J. Phys. Chem.*, **47**, 473 (1943).

[7] D. Cubicciotti, United States Atomic Energy Report MDDC-1058, 1946.

[8] H. A. Laitinen, C. H. Liu and W. S. Ferguson, *Anal. Chem.*, **30**, 1266 (1958).

[9] L. E. Topel and R. A. Osteryoung, *J. Electrochem. Soc.*, **108**, 573 (1961).

Experimental

The lead chloride was prepared by precipitating it with hydrochloric acid from a lead nitrate solution, which previously had been filtered to remove an unknown black residue. It then was dried and melted for 24 hours under hydrogen chloride gas. The gas previously had been treated by running it over charcoal at 250°, powdered alumina, and anhydrous aluminum trichloride.

The apparatus is shown in Fig. 1. The molten metal and lead chloride were contained in a Solidex glass cup. Electrical contact with the metal, which served as a cathode, was maintained by a tungsten wire sealed into the bottom of the cup. The platinum microelectrode was sealed into a glass tube and could be positioned in the melt with the moveable shaft seal. The electrode had an area of approximately 3.5 mm.^{2}. This assembly was contained in a Solidex tube through which purified nitrogen flowed, and was heated with a wire-wound resistance furnace.

For the measurements of the polarographic current, voltages ranging from 0 to 0.6 volt were supplied by a 2 v. storage battery in conjunction with a 100 Ω potentiometer. Currents were measured with a Multiflex galvanometer connected through an Ayrton shunt.

After the current I_0 had been measured for lead chloride coexisting with pure lead, known amounts of bismuth or gold were added for measurements corresponding to values of $a_{Pb} < 1$. A stirrer shown in Fig. 1 was used in order to obtain a liquid alloy of uniform composition. Only values obtained with gold alloys are considered to be relevant for reasons discussed below.

Results and Conclusions

Figure 2 shows two current *vs.* voltage curves obtained with the apparatus. The top curve represents the current obtained from pure lead in equilibrium with lead chloride. Currents below 0.2 volt could not be measured because the platinum electrode alloys with lead at these low voltages. The bottom curve shows the residual current obtained from lead chloride in contact with pure gold. This current was subtracted from all measured currents. Tungsten was tried as microelectrode material but the limiting currents were not constant with increasing voltage.

Measurements with successive additions of gold were made at 518°. Values of I/I_0 *vs.* a_{Pb} for an applied voltage of 0.40 volt are plotted in Fig. 3 with values based on mole fractions and the results of e.m.f. measurements published by Kleppa.[10] No experiments were performed below a lead activity of 0.3, where the lead-gold alloys are solid[11] for the temperatures used here. The results are in agreement with reaction 2. Thus Pb_2^{++} ions are the predominant form in which excess lead dissolves in lead chloride.

To some extent, however, Pb_2^{++} ions dissociate into 2 Pb^{++} ions and two excess electrons, as has been shown recently by Herzog and Klemm[12] with the help of transference measurements.

Attempts also were made to use Pb–Bi alloys but it was found that pure bismuth gave currents slightly higher than pure lead. These measurements were disregarded. It is believed that bismuth reacts to a small extent with lead chloride, then a small amount of excess bismuth dissolves in the resulting bismuth trichloride producing a current at the microelectrode.

Karpachev, Stromberg and Jordan[13] have studied the cell

$$\begin{array}{c} Pb|PbCl_2||PbCl_2|C \\ (+Pb)\ (+Pb) \end{array}$$

at 700° and with varying amounts of Pb in the right-hand compartment. They conclude that Pb^+ is the predominant subhalide species. At present there is no explanation of this discrepancy.

It can be seen easily from equation 4 that such a polarographic method may be used to measure activities in alloys if the species of subhalide is known. The alloying elements must be more noble than the metal forming the subhalide so that no reaction will take place with the salt. Also subhalides of the second metal must not be formed as was believed to have happened with the Pb–Bi system.

Acknowledgments.—The author would like to express his appreciation to Professor Carl Wagner for suggesting this problem and for helpful discussions concerning the experiments and manuscript. He also is indebted to Dr. George Simkovich for supplying the lead chloride. A grant from Associated Universities, Inc. also is very gratefully acknowledged.

[10] O. J. Kleppa, *J. Am. Chem. Soc.*, **71**, 3275 (1949).

[11] M. Hansen and K. Anderko, "Constitution of Binary Alloys," McGraw-Hill Book Co., New York, N. Y., 1958.

[12] W. Herzog and A. Klemm, *Z. Naturforsch.*, **16a**, 523 (1961).

[13] S. Karpachev, A. Stromberg and E. Jordan, *Comp. rend. acad. sci. U.R.S.S.*, **36**, 101 (1942).

ON THE FROST-MUSULIN REDUCED POTENTIAL ENERGY FUNCTION

BY YATENDRA PAL VARSHNI[1] AND RAMESH CHANDRA SHUKLA

Department of Physics, Allahabad University, Allahabad, India

Received July 13, 1961

The values of α_e and $\omega_e x_e$ have been calculated for 23 molecules by the Frost-Musulin reduced potential energy function for diatomic molecules, and discussed with reference to the question of the existence of a "universal" potential energy curve.

Introduction

Like the reduced equation of state, Frost and Musulin[2] have investigated the possibility of the existence of a reduced potential energy function for diatomic molecules. To define a reduced potential energy (U') as a function of reduced internuclear distance (R'), one possibility is

$$U' = U/D_e \text{ and } R' = R/R_e \qquad (1)$$

where D_e is the dissociation energy and R_e is the equilibrium internuclear distance. In terms of

---

[1] Division of Pure Physics, National Research Council, Ottawa 2, Canada.

[2] A. A. Frost and B. Musulin, *J. Am. Chem. Soc.*, **76**, 2045 (1954).

TABLE I

Diatoms	α_e (obsd.) cm.$^{-1}$	α_e (calcd.) cm.$^{-1}$	% error	$\omega_e x_e$ (obsd.), cm.$^{-1}$	$\omega_e x_e$ (calcd.), cm.$^{-1}$	% error	$\omega_e x_e . \mu_A \times (R_e - R_{ij})^2 \times 10^{18}$
H_2^+	1.4	0.578	−58.7	62.00	47.04	−24.1	35.447
H_2	2.993	1.4628	−51.1	117.995	102.398	−13.2	30.980
CH	0.534	0.4174	−21.8	64.3	55.78	−13.3	30.983
OH	.714	.5508	−22.9	82.81	73.544	−11.2	30.248
HCl	.3019	.2521	−16.5	52.05	48.154	− 7.5	29.043
HCl^+	.3183	.2114	−33.6	53.5	38.40	−28.2	37.459
KH	.0673	.0644	− 4.3	14.65	12.592	−14.0	31.279
ZnH	.2500	.3586	+43.4	55.14	67.266	+22.0	22.039
HBr	.226	.2102	− 7.0	45.21	45.077	− 0.3	26.965
CdH	.218	.3098	+42.1	46.30	67.388	+45.5	18.478
HI	.183	.1677	− 8.4	39.73	41.584	+ 4.7	25.687
HgH	.312	.4368	+40.0	83.01	102.934	+24.0	21.692
Li_2	.00704	.008243	+17.1	2.592	2.911	+12.3	23.958
O_2	.01579	.01486	− 5.9	12.073	12.090	+ 0.1	26.865
O_2^+	.01984	.01612	−18.7	16.53	13.30	−19.6	33.418
ClF	.00436	.004763	+ 9.2	4.00	5.904	+47.6	18.214
Na_2	.00079	.001199	+51.8	0.726	0.850	+17.1	22.975
P_2	.00142	.001493	+ 5.1	2.804	2.973	+ 6.0	25.355
Cl_2	.0017	.001625	− 4.4	4.00	3.155	−21.1	34.083
K_2	.000219	.0003491	+56.1	0.354	0.406	+14.7	23.433
Br_2	.000275	.0003664	+33.2	1.07	1.320	+23.4	23.324
ICl	.000536	.0005755	+ 7.4	1.465	1.693	+15.6	23.265
I_2	.000117	.0001335	+14.1	0.6127	0.7392	+20.6	22.283
Average			24.9			17.7	26.847

these variables the potential energy minima would be at $U' = -1$ and $R' = 1$.

To express the potential energy function as a function of more general reduced internuclear distance they argued as follows: The curvature at the minima which is related to the force constant (k_e) will vary considerably from molecule to molecule, since the inner shell repulsion for atoms other than hydrogen should influence the internuclear distance at the minimum. To take this into account they used the reduced distance variable

$$U' = U/D_e \text{ and } R' = (R - R_{ij})/(R_e - R_{ij}) \quad (2)$$

where R_{ij} is a constant for a given molecule and is a measure of the inner shell radii of atoms i and j. Here again the minima is given by

$$U' = -1 \text{ and } R' = 1$$

In case of H_2 and H_2^+, R' of (2) is identical with R' of (1) since $R_{ij} = 0$.

Assuming U' as a universal function of R' (eq. 2), independent of which molecule is being considered

$$\frac{d^2U'}{dR'^2} = K, \text{ a dimension-less constant}$$

Since

$$\frac{d^2U}{dR^2} = k_e$$

we get by virtue of (2)

$$k_e(R_e - R_{ij})^2/D_e = K \quad (3)$$

or

$$R_{ij} = R_e - (KD_e/k_e)^{1/2} \quad (4)$$

They obtained $K = 4$ from the data for H_2^+ and H_2. Thus R_{ij} can be calculated for each molecule.

Frost and Musulin[2] have examined the validity of this idea by examining the constancy of the coefficients of the higher terms such as $L/6$, $M/24$ in the expansion

$$U' = -1 + (K/2)(R' - 1)^2 + (L/6)(R' -)1^3 + (M/24)(R' -)1^4 + \ldots .$$

where

$$L = \left(\frac{d^3U'}{dR'^3}\right)_{R'=1} \text{ and } M = \left(\frac{d^4U'}{dR'^4}\right)_{R'=1}$$

For L and M they obtained the relations

$$L = \frac{(R_e - R_{ij})^3}{D_e}\left(\frac{d^3U}{dR^3}\right)_{R=R_e} \quad (5)$$

$$M = \frac{(R_e - R_{ij})^4}{D_e}\left(\frac{d^4U}{dR^4}\right)_{R=R_e} \quad (6)$$

The average values of L and M, for 23 molecules, were found to be (−15.06) and 43.48, respectively. The mean deviations of L and M from their averages were 13.2 and 42%, respectively.

However, a more direct test of this concept is to test for the reproducibility of the molecular constants α_e (vibration-rotation interaction constant) and $\omega_e x_e$ (anharmonicity constant).

We have applied this test in the present note. The method of obtaining α_e and $\omega_e x_e$ from a potential function is explained by Varshni.[3] By this we get the following expressions for α_e and $\omega_e x_e$ in terms of L and M

$$\alpha_e = \left[-\frac{L}{3K}\frac{R_e}{(R_e - R_{ij})} - 1\right]\frac{6B_e^2}{\omega_e} \quad (7)$$

$$\omega_e x_e = \left[\frac{5}{3}\left(\frac{L}{K}\right)^2 - \frac{M}{K}\right]\left[\frac{R_e}{R_e - R_{ij}}\right]^2 \frac{W}{\mu_A R_e^2} \quad (8)$$

where $W = 2.1078 \times 10^{-16}$ and μ_A is the reduced mass in atomic weight units.

The observed and calculated values for α_e and $\omega_e x_e$, for the 23 molecules considered by Frost and Musulin, are compared in Table I.

---

[3] Y. P. Varshni, *Rev. Mod. Phys.*, **29**, 664 (1957); **31**, 839 (1959).

The necessary data have been taken from their paper and Herzberg.[4]

Equations 7 and 8 can be recast as

$$(\alpha_e\omega_e/6B_e^2 + 1)(R_e - R_{ij}) = -L/3K \qquad (9)$$

and

$$(\omega_e x_e)\mu_A(R_e - R_{ij})^2 = W\left[\frac{5}{3}\left(\frac{L}{K}\right)^2 - \frac{M}{K}\right] \qquad (10)$$

which suggests another possibility of testing the constancy of the L.H.S. of the expressions 9 and 10, respectively. This is equivalent to testing the constancy of L and $(L^2/K - M)$, respectively. As L has been examined by Frost and Musulin, we have investigated expression 10 only. The results are given in the last column of Table I. It may be noted that our procedure of examining $(L^2/K - M)$ does not involve α_e, though L involves α_e.

The average value of the L.H.S. in (10) comes out to be 26.847.

Discussion

The problem of a "Universal" potential energy function also has been discussed by Varshni,[3] who found that though rigorously speaking a "Universal" potential energy function does not exist, it is still possible to find approximate "Universal" relations for α_e and $\omega_e x_e$ in terms of the Sutherland parameter $\Delta(= k_e r_e^2/2D_e)$.

The average percentage errors for α_e and $\omega_e x_e$ are seen to be 24.9 and 17.7. These may be compared with corresponding average percentage errors 22.1 and 11.1 found by Varshni[3] for 23 molecules, 18 of which are common with the present list.

The average percentage error for $\omega_e x_e$ is only 17.7, while for L and M the corresponding values were 13.2 and 42, respectively. $\omega_e x_e$ depends on both the third and the fourth derivatives. The low error in the case of $\omega_e x_e$ is due to the fact that for most of the molecules, errors in L and M were in the same direction. A happy cancellation of the errors has led to the good results for $\omega_e x_e$.

For most of the molecules, expression 10 is seen to be near the average value. Four molecules, *viz.*, H_2^+, HCl^+, O_2^+ and Cl_2 give specially high values. Three of these are ionized molecules. The case of Cl_2 is interesting. Varshni[3] (see Fig. 6 and Table XII) and Varshni and Shukla[5] also found that the reported experimental value of $\omega_e x_e$ for Cl_2 deviates widely from the calculated values by other methods. The experimental value of $\omega_e x_e$ for Cl_2 has been obtained from levels observed only up to $x'' = 3$. The uncertainty in the determination of $\omega_e x_e$ from the observed data has been discussed by Varshni and Shukla.[5] It appears that the reported value $\omega_e x_e = 4$ is not satisfactory. A value of $\omega_e x_e \simeq 3$ would be in accord with the considerations of references 3 and 5 and the present paper.

Acknowledgments.—The authors are thankful to Prof. D. S. Kothari (Delhi) for his kind interest in the work, and to the Council of Scientific and Industrial Research for the financial assistance.

(4) G. Herzberg, "Spectra of Diatomic Molecules," D. Van Nostrand Co., Inc., New York, N. Y., 1951.

(5) Y. P. Varshni and R. C. Shukla, *Trans. Faraday Soc.*, **57**, 537 (1961).

PHASE EQUILIBRIA IN FUSED SALT SYSTEMS: BINARY SYSTEMS OF PLUTONIUM(III) CHLORIDE WITH THE CHLORIDES OF MAGNESIUM, CALCIUM, STRONTIUM AND BARIUM[1]

BY K. W. R. JOHNSON,[2] MILTON KAHN[3] AND J. A. LEARY[2]

University of New Mexico, Albuquerque, New Mexico, and the Los Alamos Scientific Laboratory, Los Alamos, New Mexico

Received July 14, 1961

Thermal and differential thermal analysis techniques, supplemented by microscopic examination of cooled melts, were used to investigate phase equilibrium diagrams for the binary systems: $PuCl_3$–$MgCl_2$, $PuCl_3$–$CaCl_2$, $PuCl_3$–$SrCl_2$, $PuCl_3$–$BaCl_2$. The $PuCl_3$–$MgCl_2$ and $PuCl_3$–$CaCl_2$ systems are characterized by single eutectic points: the $PuCl_3$–$SrCl_2$ and $PuCl_3$–$BaCl_2$ systems are characterized by peritectic transformations and solid solutions. Compounds of the type M_3PuCl_9 (M = Sr or Ba) are associated with the peritectic transformation and solid solutions occur in compositions which are rich in $SrCl_2$ or $BaCl_2$.

Introduction

Phase equilibria in the binary system $PuCl_3$–alkali chloride were reported recently by this Laboratory.[4,5]

This investigation extends the previous work to include the systems $PuCl_3$–$MgCl_2$, $PuCl_3$–$CaCl_2$, $PuCl_3$–$SrCl_2$ and $PuCl_3$–$BaCl_2$. A combination of thermal and differential thermal analysis, supplemented by microscopic examination of cooled melts, was used to study temperature–composition diagrams for these systems.

Experimental

Preparation of Materials.—The preparation of $PuCl_3$ has been described.[6]

Pure $MgCl_2$ was prepared by repeated fractional recrystallization of $MgCl_2 \cdot 6H_2O$. The $MgCl_2 \cdot 6H_2O$ was dehydrated by slowly heating to 250° under an HCl atmosphere and subsequently sublimed *in vacuo*.

$CaCl_2$ was prepared from spectroscopically pure CaO that

(1) Taken from a dissertation by K. W. R. Johnson submitted in partial fulfillment of the requirements for the degree of Doctor of Philosophy in Chemistry at the University of New Mexico.

(2) Los Alamos Scientific Laboratory, P.O. Box 1663, Los Alamos, N. M.

(3) Chemistry Department, University of New Mexico, Albuquerque, N. M.

(4) C. W. Bjorklund, J. G. Reavis, J. A. Leary and K. A. Walsh, *J. Phys. Chem.*, **63**, 1774 (1959).

(5) R. Benz, M. Kahn and J. A. Leary, *ibid.*, **63**, 1983 (1959).

had been prepared by Roberts' method.[6] The CaO was converted to $CaCl_2 \cdot 6H_2O$ by dissolution in HCl and subsequent crystallization; this purified salt was dehydrated by heating with an excess of sublimed NH_4Cl.[7]

High purity $SrCl_2$ and $BaCl_2$ were prepared by repeated fractional crystallization of the respective hydrated salts followed by dehydration by heating with an excess of NH_4Cl.

Each of the anhydrous alkaline earth chloride salts was cast into stick form to facilitate subsequent handling.

Chemical analyses and melting points of $PuCl_3$ and the other components used in this investigation are summarized in Table I.

TABLE I

SALT ANALYSIS

Compound	Composition, % by wt. Cation Found	Cation Theor.	Chloride Found	Chloride Theor.	Freezing point, °C. Found	Lit.
$PuCl_3$	69.33	69.20	30.7	30.80	767.4	767–769[4,5]
$MgCl_2$	25.59	25.54	74.4	74.46	713.9	708–714[8–12a]
$CaCl_2$	36.12	36.11	63.9	63.89	774.5	770–773[8,10,11,12b,13,14]
$SrCl_2$	55.2	55.27	44.7	44.73	875.2	872–873[11,12c]
$BaCl_2$	66.1	65.95	33.9	34.05	961.9	960–962[11,12b,13,14]

Apparatus.—The apparatus used for the thermal and differential thermal analyses was a slight modification of apparatus previously described.[4]

External equipment for controlling the heating and cooling rates, and for measuring the temperature of the salt system was similar to that used previously.[4] In addition to measuring temperatures with a Brown Electronik continuous recorder, the temperatures also could be measured with a Rubicon Model No. 2780 Precision Potentiometer.

The thermocouple for measuring temperatures was calibrated using U. S. Bureau of Standards Zn and Al and J. T. Baker Chemical Co. NaCl as standards. Freezing points of these standards were reproducible to 0.1°. No interference from polymorphic transformations within the equipment was observed.

A Bausch and Lomb Co. petrographic microscope, mounted in an inert atmosphere glove box, was used to examine samples of the cooled salt melts.

Procedure.—In a typical experiment, weighed portions (7–15 g.) of the components were placed in the equilibration chamber and the apparatus was assembled. A flow of HCl gas, which had been dried by passage through $Mg(ClO_4)_2$, was passed through the equilibration chamber at a rate of 10–15 g./hr. After the temperature was increased to 75° above the liquidus point of the mixture, the HCl gas tube was lowered into the melt. Complete solution of the two components was effected by bubbling gas through the melt for 2 hours.

At the end of the mixing period the gas tube was withdrawn from the melt and the gas flow reduced to 5 g./hr. As the salts were cooled at a constant rate (usually 1.5°/min.), both temperature and differential temperature were recorded. These recordings were compared to determine approximate transition temperatures and the degree, if any, of supercooling. It was found that errors caused by supercooling of the melt could be eliminated by placing a rubber-tipped vibrator in contact with the equilibration chamber.

The salts were re-heated to the same initial temperature and again cooled at a constant rate. Measurements with the precision potentiometer were taken each minute starting at least 10 minutes before an anticipated transition. The precise transition temperature then was determined

TABLE II

THERMAL ANALYSIS OF $PuCl_3$–MCl_2 SYSTEMS

Second component	Melt composition, mole % $PuCl_3$	Transition temperatures, °C. First	Second	Third
$MgCl_2$	0	714		
	10.0	699	648	
	20.0	683	648	
	30.0	664	650	
	35.9	653	650	
	40.0	652	650	
	40.8	651	650	
	48.0	671	650	
	50.0	674	650	
	52.3	680	648	
	58.0	690	650	
	65.0	701	651	
	70.0	712	[a]	
	80.0	731	649	
	90.0	748	649	
	91.0	752	[a]	
	100.0	767		
$CaCl_2$	0	774		
	9.1	742	606	
	20.0	700	609	
	30.0	660	611	
	40.0	619	611	
	42.1	614	607	
	44.4	614	609	
	60.0	677	610	
	75.0	714	607	
	90.0	747	602	
	100.0	767		
$SrCl_2$	0	876		
	9.8	849	629	
	20.0	805	628	
	25.6	782	628	
	30.0	748	630	
	35.0	722	628	616
	41.6	673	628	615
	43.5	660	628	619
	44.1	626	619	
	50.0	618	615	
	50.0	622	[a]	
	56.0	623	612	
	59.3	652	616	
	70.0	690	616	
	79.3	718	615	
	90.0	745	614	
	100.0	767		
$BaCl_2$	0	961	925	
	10.0	939	759	
	20.0	895	754	
	25.0	870	758	
	30.0	832	758	642
	33.0	812	759	641
	35.0	800	756	643
	40.0	750	644	
	55.0	689	649	
	62.0	656	646	
	65.0	662	648	
	73.0	687	648	
	85.0	727	647	
	100.0	767		

[a] Not cooled sufficiently to detect lower temperature transitions.

---

(6) R. N. Roberts, U. S. Atomic Energy Comm. Report LA-1936 (1957).

(7) J. C. Bailar, Ed., "Inorganic Syntheses," Vol. IV, McGraw-Hill Book Co., Inc., New York, N. Y., 1953, pp. 104–111.

(8) "Soviet Research in Fused Salts," Chemistry Collection No. 1, Structure and Properties (1949–1955).

(9) K. K. Kelley, U. S. Bur. Mines Bull. 477, 1950.

(10) G. E. Moore, *J. Am. Chem. Soc.*, **65**, 1700 (1943).

(11) Alvin Glassner, U. S. Atomic Energy Comm. Report ANL-5750, Table IV.

(12) D. Hodgman, R. C. Weast and S. M. Selby, Ed., "Handbook of Chemistry and Physics," 42nd ed., Chemical Rubber Publishing Co., 1960, (a) p. 601; (b) p. 551; (c) p. 563; (d) p. 539.

(13) David T. Peterson and J. A. Hinkelbein, *J. Phys. Chem.*, **63**, 1360 (1959).

(14) D. Cubicciotti, U. S. Atomic Energy Comm. Report MDDC-1058 (1946).

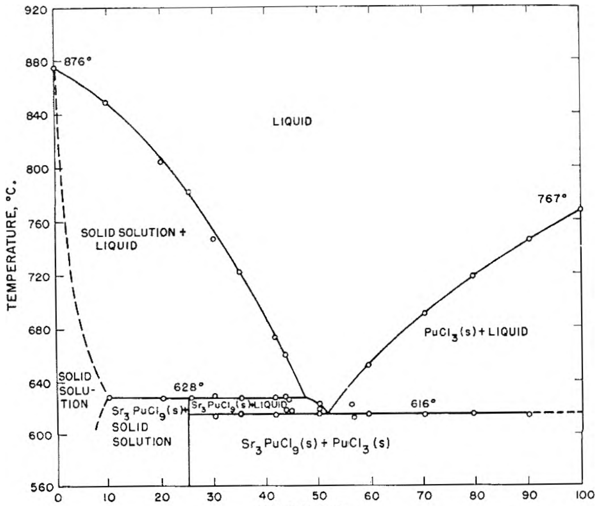

Fig. 1.—The plutonium(III) chloride–strontium chloride system.

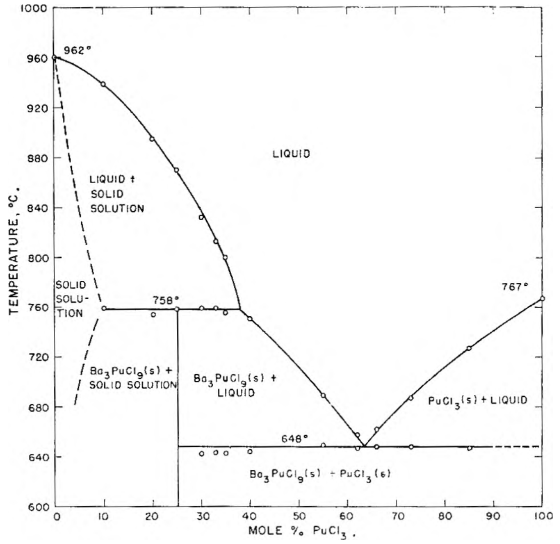

Fig. 2.—The plutonium(III) chloride–barium chloride system.

from a temperature *vs.* time plot of the precision potentiometer data.

Upon completion of a cooling curve, a calculated quantity of alkaline earth chloride was added to the equilibration through the sidearm provided for this purpose. The maximum temperature was re-adjusted, the added salt was dissolved in the melt, and the thermal analysis procedure was repeated.

When thermal analysis of the second composition was completed, the temperature was raised again to above the liquidus point. To obtain samples for chemical analyses the gas tube again was lowered into the melt and partially filled with salt by decreasing the gas pressure in the tube to below atmospheric pressure. The molten salt rapidly solidified. The gas tube then was raised above the heated zone of the equilibration chamber and the furnace was turned off. The salt samples were cooled to room temperature and divided into several portions in an inert atmosphere glove box. One portion was dissolved in dilute $HClO_4$ for chemical analysis, and a second portion was stored under argon for microscopic examination.

Results

The results of thermal analysis and differential thermal analysis are shown in Table II. In all four systems the first transition temperature with two component mixtures was typical of a liquidus point. Second and third transition temperatures were typical of eutectic and peritectic arrests.

The $PuCl_3$–$MgCl_2$ system can be represented by a simple phase diagram that contains one eutectic point at 38 mole % $PuCl_3$ and 650°. The diagram was confirmed by microscopic examination at room temperature of samples from the melts on both sides of the eutectic point. The 40% $PuCl_3$ composition revealed discrete crystals of $PuCl_3$ plus intergrowths of the eutectic composition. The eutectic appeared as bundles of acicular crystals of $PuCl_3$ in a matrix of $MgCl_2$. Samples of the 30% $PuCl_3$ melt contained discrete crystals of $MgCl_2$ plus intergrowths of the eutectic composition.

The $PuCl_3$–$CaCl_2$ phase diagram also is simple, containing one eutectic point at 43 mole % $PuCl_3$ and 610°. Samples of the cooled 40% $PuCl_3$ melt contained primary crystals of $CaCl_2$ plus eutectic intergrowths. The cooled 45% $PuCl_3$ melt contained primary $PuCl_3$ crystals, plus eutectic.

The $PuCl_3$–$SrCl_2$ system (Fig. 1) is characterized by a eutectic point, a peritectic transformation and solid solution. The eutectic point occurs at 52 mole % $PuCl_3$ and 616°, the peritectic transformation occurs at 46 mole % $PuCl_3$ and 628° and is accompanied by the formation of a compound with the empirical formula Sr_3PuCl_9, and solid solution occurs in strontium chloride-rich compositions.

The empirical formula Sr_3PuCl_4 was assigned to the compound that melts incongruently, based on the absence of the 616° eutectic arrest at 25.6 and 20.0 mole % $PuCl_3$. This eutectic arrest, however, was clearly discernable at 30 mole % $PuCl_3$. Microscopic examination of the cooled crystals from the 25.6 mole % $PuCl_4$ melt indicated essentially one phase of refractive index 1.77 ± 0.02. Crystals from the 30 mole % $PuCl_3$ melt appeared to be predominantly this same phase, with intergrowths of eutectic mixture.

Evidence for the existence of solid solution is based principally on microscopic examination of samples from the 9.8 mole % $PuCl_3$ melt. Under the microscope the predominant phase appeared unlike pure $SrCl_2$ in that the refractive index was variable and somewhat higher than that of $SrCl_2$. A very small amount of Sr_3PuCl_9 was present along the grain boundaries of the "$SrCl_2$-like" phase. The possibility that this change in refractive index was due to the solubility of HCl in $SrCl_2$ was not supported by chemical analysis. Furthermore, on repeating the thermal analysis using Ar instead of HCl, identical cooling curves and microscopic specimens were obtained.

The formation of a solid solution also was corroborated by thermal analysis. In the range 44.1 to 9.8% $PuCl_3$, the duration of the 628° arrest decreased uniformly from 74 min. to less than 8 min. per mole of melt.

A second sample of the same composition (9.8 mole % $PuCl_3$) was cooled from above the liquidus point to room temperature at 1.5°/min. Discrete crystals of $SrCl_2$ and Sr_3PuCl_9 were visible under the polarizing microscope, indicating that the slope of the solid solution line below the peritectic temperature must be toward the $SrCl_2$ axis. Microscopic examination of the 90% $PuCl_3$ melt indicated no solid solution for compositions rich in $PuCl_3$. No polymorphic transformations were observed at any of these compositions when thermal analysis was carried down to 25°.

The $PuCl_3$–$BaCl_2$ system (Fig. 2) is quite similar to the $PuCl_3$–$SrCl_2$ system. A eutectic point occurs at 64 mole % $PuCl_3$ and 648°, and a peritectic transformation occurs at 38 mole % $PuCl_3$ and 758° with the accompanying production of a compound to which we have assigned the empirical formula Ba_3PuCl_9. The compound has a refractive index of 1.76 ± 0.02. Except for pure $BaCl_2$, no polymorphic transformations were observed when any of these compositions were cooled to 25°. Microscopic evidence for the existence of solid solution is based on samples from the 10% $PuCl_3$ melt. The predominant phase was cubic and was of variable and somewhat lower refractive index than pure $BaCl_2$. A trace of Ba_3PuCl_9 was discernable along grain boundaries. It is noteworthy that below 925° the cubic structure is more stable. Evidently the cubic modification is stabilized by the solubility of $PuCl_3$ in $BaCl_2$. The duration of thermal arrests at 759° supports the microscopic evidence for solid solution. For 30% $PuCl_3$ the thermal arrest was 70 min. per mole of melt, whereas for 10% $PuCl_3$, the thermal arrest was much less than 10 min.

Acknowledgments.—The authors wish to express their gratitude to W. J. Maraman for advice and to the members of the Analytical Group under the direction of C. F. Metz for the chemical analyses involved in this investigation. This work was performed under the auspices of the U. S. Atomic Energy Commission.

METHANETHIOL AND CARBON DISULFIDE: HEATS OF COMBUSTION AND FORMATION BY ROTATING-BOMB CALORIMETRY[1]

BY W. D. GOOD, J. L. LACINA AND J. P. MCCULLOUGH

Contribution No. 108 from the Thermodynamics Laboratory, Petroleum Research Center, Bureau of Mines, U. S. Department of the Interior, Bartlesville, Oklahoma

Received July 17, 1961

The heats of combustion of methanethiol and carbon disulfide were measured by rotating-bomb calorimetry. For combustion calorimetry of methanethiol, normal boiling point 5.96°, liquid samples were sealed in borosilicate glass ampoules rigid enough to withstand the high vapor pressure at room temperature. Samples of carbon disulfide were sealed in polyester bags. The derived values of $\Delta Hf°_{298.16}$ for formation in the gaseous state from graphite, gaseous hydrogen and rhombic sulfur are: methanethiol, -5.46 kcal. mole^{-1}; carbon disulfide, 27.98 kcal. mole^{-1}.

Methods for precision combustion calorimetry of organic sulfur compounds are well established.[2–4] Until the present investigation, however, the modern methods had not been used to measure the heats of combustion of two common and important sulfur compounds, methanethiol and carbon disulfide. These compounds presented special experimental problems because both are highly volatile and contain a high proportion of sulfur. In a continuing Bureau of Mines program of thermodynamic studies of organic sulfur compounds, these problems were solved, and accurate values of the heats of combustion and formation were obtained.

Experimental

Materials.—The sample of methanethiol was prepared at the Laramie Petroleum Research Center of the Bureau of Mines as part of American Petroleum Institute Research Project 48A.[5] The purity of this material was 99.94 ± 0.06 mole %, as determined by the time–temperature freezing point method. The sample used for the combustion experiments was dried by passing the vapors through magnesium perchlorate.

The sample of carbon disulfide was obtained from a commercial source and was distilled in an efficient fractionating column.[6] The purity of the distilled sample, measured by the time–temperature freezing point method, was 99.98 mole %. A study by gas–liquid chromatography also indicated a purity of 99.98–99.99 mole %. The sample used for combustion calorimetry was dried by passing the vapors through phosphorous pentoxide.

Apparatus and Procedures.—The rotating-bomb calorimeter used in the study of methanethiol, laboratory designation BMR-II, has been described.[7] The measurements on carbon disulfide were made in a new but essentially identical calorimeter, laboratory designation BMR-III. Platinum-lined bomb Pt-3b,[8] internal volume 0.350 l., was used for both compounds.

Except for the methods of sample confinement discussed in the following section, experimental details were about the same as those described in ref. 3.

Sample Containers.—Spherical Pyrex ampoules, weighing 100 to 200 mg., were used as sample containers for methanethiol. These ampoules had to withstand the vapor pressure of liquid methanethiol (about 2 atm. at room temperature) internally and the pressure of oxygen in the bomb (30 atm.) externally. Empty ampoules were tested by sealing the capillary stems and subjecting them to an external pressure of 35 atm. The ends of the capillary stems were broken off those that survived this test, and the ampoules

---

[1] This investigation was part of American Petroleum Institute Research Project 48A on "The Production, Isolation and Purification of Sulfur Compounds and Measurement of Their Properties," which the Bureau of Mines conducts at Bartlesville, Okla., and Laramie, Wyo.

[2] S. Sunner, (a) *Svensk Kem. Tidskr.*, **58**, 71 (1946); (b) Thesis, University of Lund, 1950.

[3] W. N. Hubbard, C. Katz and G. Waddington, *J. Phys. Chem.*, **58**, 142 (1954).

[4] G. Waddington, S. Sunner and W. N. Hubbard, "Experimental Thermochemistry," F. D. Rossini, Editor, Interscience Publishers, Inc., New York, N. Y., 1956, Chapter 7, pp. 149–179.

[5] J. C. Morris, W. J. Lanum, R. V. Helm, W. E. Haines, G. L. Cook and J. S. Ball, *J. Chem. Eng. Data*, **5**, 112 (1960).

[6] The authors thank Mr. H. J. Coleman of this Center for his careful purification of the sample of carbon disulfide used in this investigation.

[7] W. D. Good, D. W. Scott and G. Waddington, *J. Phys. Chem.*, **60**, 1080 (1956).

[8] W. D. Good, D. R. Douslin, D. W. Scott, A. George, J. L. Lacina J. P. Dawson and G. Waddington, *ibid.*, **63**, 1133, (1959).

Table I

Energy of Idealized Combustion Reactions[a]

Methanethiol

$m'(\mathrm{CH_3SH})$, g.	0.81607	0.81805	0.91328	0.90716	0.83621	0.81247	0.64729	0.91185	0.94488
m'' (oil), g.	0.18052	0.17903	0.11227	0.11602	0.16636	0.18100	0.29449	0.11359	0.09129
$\Delta t_c = t_f - t_i - \Delta t_{\mathrm{cor.}}$, deg.	2.02463	2.02452	2.02075	2.01862	2.02400	2.02022	2.01966	2.02023	2.02097
$\mathcal{E}(\mathrm{Calor.})(-\Delta t_c)$, cal.	−8101.88	−8101.44	−8086.35	−8077.83	−8099.36	−8084.23	−8081.99	−8084.27	−8087.23
$\mathcal{E}(\mathrm{Cont.})(-\Delta t_c)$,[b] cal.	−28.19	−28.24	−28.16	−28.16	−28.18	−28.95	−28.81	−28.96	−28.98
$\Delta E_{\mathrm{ign.}}$, cal.	0.78	0.45	0.50	1.41	0.42	0.72	0.68	0.78	0.55
$\Delta E^{f}_{\mathrm{dec.}}(\mathrm{HNO_3 + HNO_2})$, cal.	7.44	10.79	9.56	7.41	8.01	9.72	7.22	7.05	9.27
ΔE, cor. to st. states,[c] cal.	0.64	0.58	−0.75	−0.65	0.37	0.65	2.56	−0.70	−1.24
$-m''\Delta Ec^\circ/M$(oil), cal.	1982.83	1966.44	1233.24	1274.37	1827.30	1988.10	3234.76	1247.65	1002.73
$-m'''\Delta Ec^\circ/M$(fuse), cal.	4.21	5.03	4.09	4.78	4.50	6.00	5.23	5.71	5.15
$m'\Delta Ec^\circ/M(\mathrm{CH_3SH})$, cal.	−6134.17	−6146.39	−6867.87	−6818.67	−6286.94	−6107.99	−4860.35	−6852.74	−7099.75
$\Delta Ec^\circ/M(\mathrm{CH_3SH})$, cal. g.$^{-1}$	−7516.72	−7513.46	−7520.00	−7516.50	−7518.38	−7517.80	−7508.76	−7515.21	−7513.92

Av. value and standard dev. of the mean: −7515.64 ± 1.11 cal. g.$^{-1}$.

Carbon Disulfide

$m'(\mathrm{CS_2})$, g.	0.50678	0.50504	0.50056	0.51320	0.50929	0.50925	0.66346[d]	0.66384[d]	0.29135	0.66013[d]
m''(oil), g.	.47182	.46880	.47061	.46629	.46750	.46763	.39290	.39412	.57062	.39610
m'''(polyester), g. at (% rel. hum.)	.03943 (52)	.04573 (59)	.04455 (51)	.04413 (51)	.04482 (51)	.04432 (52)	.04566 (55)	.04318 (59)	.04415 (56)	.04394 (55)
$\Delta t_c = t_f - t_i - \Delta t_{\mathrm{cor.}}$, deg.	2.00087	1.99921	1.99709	2.00123	1.99963	1.99948	2.00137	2.00222	1.99533	2.00387
$\mathcal{E}(\mathrm{Calor.})(-\Delta t_c)$, cal.	−8054.58	−8047.90	−8039.37	−8056.03	−8049.59	−8048.99	−8056.59	−8060.02	−8032.28	−8036.66
$\mathcal{E}(\mathrm{Cont.})(-\Delta t_c)$,[b] cal.	−27.68	−27.65	−27.57	−27.52	−27.51	−27.54	−27.56	−27.56	−27.51	−27.61
$\Delta E_{\mathrm{ign.}}$, cal.	0.69	0.64	0.62	0.92	0.97	0.82	1.00	0.97	1.33	0.62
$\Delta E_{\mathrm{dec.}}(\mathrm{HNO_3 + HNO_2})$, cal.	10.22	10.38	11.24	9.33	9.59	8.33	19.33	23.57	6.81	22.01
ΔE, cor. to st. states,[c] cal.	2.22	2.26	2.30	2.16	2.21	2.22	−0.46	−0.53	4.77	−0.43
$-m''\Delta Ec^\circ/M$(oil), cal.	5182.55	5149.36	5169.23	5121.77	5135.02	5136.43	4315.62	4329.12	6267.81	4350.82
$-m'''\Delta Ec^\circ/M$(polyester), cal.	215.41	249.74	243.39	241.09	244.86	242.12	249.40	235.81	241.15	240.01
$-m''''\Delta Ec^\circ/M$(fuse), cal.	4.30	4.62	4.42	4.13	3.97	4.54	5.07	4.34	4.26	4.26
$m'\Delta Ec^\circ/M(\mathrm{CS_2})$, cal.	−2666.87	−2658.55	−2635.74	−2704.15	−2680.48	−2682.07	−3494.19	−3494.30	−1533.66	−3476.98
$\Delta Ec^\circ/M(\mathrm{CS_2})$, cal. g.$^{-1}$	−5262.38	−5264.04	−5265.58	−5269.20	−5263.18	−5266.71	−5266.61	−5263.77	−5263.98	−5267.12

Average value and standard dev. of the mean: −5265.26 ± 0.68 cal. g.$^{-1}$.

[a] The symbols and abbreviations in this table are those used in ref. 11, except as noted. [b] $\mathcal{E}^i(\mathrm{Cont.})(t_i - 25^\circ) + \mathcal{E}^f(\mathrm{Cont.})(25^\circ - t_f + \Delta t_{\mathrm{cor.}})$ [c] Items 81–85, incl., 87–91, incl., 93 and 94 of the computation form of ref. 11. [d] In these experiments five atmospheres of air was used in the bomb instead of the usual one atmosphere.

then were weighed. The ampoules were filled by a method previously described,[9] with the ampoule receiver cooled by an ice-bath. The filled ampoules were removed individually from the receiver, and the bulb was immediately packed in crushed ice. A stream of warm, dry air was brushed on the capillary tip extending from the ice until all the material had evaporated from the stem and a small bubble appeared in the bulb. The bulb was removed from the ice and immediately packed in powdered solid carbon dioxide to reduce the vapor pressure enough to permit sealing the capillary stem. The stream of dry air was kept on the capillary tip so that the chilled sample would not adsorb moisture from the laboratory air. The ampoule was sealed and then removed from the solid carbon dioxide and allowed to warm to room temperature. It was possible after a little experience to make the volume of the bubble in the ampoule negligibly small at room temperature. Combustion reactions were initiated with the hydrocarbon oil previously described (Sample USBM-P3a).[7] The combustion reactions were violent, a characteristic of highly volatile samples sealed in strong ampoules. In only nine experiments out of 23 was complete combustion obtained.

Samples of carbon disulfide were confined in polyester bags by a technique previously described.[8] The same hydrocarbon oil was used as an auxiliary kindling material.

Units of Measurements and Auxiliary Quantities.—All data reported are based on the 1951 International Atomic Weights[10a] and fundamental constants[10b] and the definitions: 0 °C. = 273.15°K.; 1 cal. = 4.184(exactly) joules. The laboratory standard weights had been calibrated at the National Bureau of Standards.

In reducing weights in air to *in vacuo*, in converting the energy of the actual bomb process to the isothermal bomb process, and in reducing to standard states,[11] the following values (for 25°) of density, ρ, specific heat, c_p, and $(\partial E/\partial P)_T$ for the various substances were used.

	ρ, g. ml.$^{-1}$	c_p, cal. deg.$^{-1}$ g.$^{-1}$	$(\partial E/\partial P)_T$, cal. atm.$^{-1}$ g.$^{-1}$
Methanethiol	0.861	0.45	....
Carbon disulfide	1.255	.239	−0.0109
Auxiliary oil	0.87	.53	− .0060
Polyester film	1.38	.315	− .00069

Calibration.—During the study of methanethiol, the energy equivalent, $\mathcal{E}$(Calor.), of calorimetric system BMR-II was determined by combustion of benzoic acid (National Bureau of Standards standard sample 39g with a certified heat of combustion of 26.4338 ± 0.0026 abs. kj./g. mass under certificate conditions). Twelve calibration experiments gave the value, $\mathcal{E}$(Calor.) = 4001.66 ± 0.14 cal. deg.$^{-1}$ (mean and standard deviation). During the study of carbon disulfide, the energy equivalent of calorimetric system BMR-III was determined by combustion of benzoic acid (National Bureau of Standards standard sample 39h with a certified heat of combustion of 26.434 ± 0.003 abs. kj./g. mass under certificate conditions). Seven calibration experiments gave the value, $\mathcal{E}$(Calor.) = 4025.54 ± 0.19 cal. deg.$^{-1}$ (mean and standard deviation).

Results

Calorimetric Results.—The calorimetric results for methanethiol and carbon disulfide are summarized in Table I. The experimental values of $\Delta Ec^\circ/M$ apply to the idealized combustion reactions 1 and 2 for methanethiol and carbon disulfide at 298.15°K.

---

(9) G. B. Guthrie, Jr., D. W. Scott, W. N. Hubbard, C. Katz, J. P. McCullough, M. E. Gross, K. D. Williamson and G. Waddington, *J. Am. Chem. Soc.*, **74**, 4662 (1952).

(10) (a) E. Wichers, *ibid.*, **74**, 2447 (1952); (b) F. D. Rossini, F. T. Gucker, Jr., H. L. Johnston, L. Pauling and G. W. Vinal, *ibid.*, **74**, 2699 (1952).

(11) W. N. Hubbard, D. W. Scott and G. Waddington, "Experimental Thermochemistry," F. D. Rossini, Editor, Interscience Publishers, Inc., New York, N. Y., 1956, Chapter 5, pp. 75–128.

$$CH_3SH(liq.) + 7/2\ O_2(g) + 29\ H_2O(liq.) = CO_2(g) + H_2SO_4{\cdot}30H_2O(liq.) \quad (1)$$

$$CS_2(liq.) + 4\ O_2(g) + 92\ H_2O(liq.) = CO_2(g) + 2H_2SO_4{\cdot}45H_2O(liq.) \quad (2)$$

Apart from the violence of the combustion reactions of methanethiol, no difficulty was encountered in obtaining complete oxidation of the sample to CO_2 and aqueous H_2SO_4. However, complete oxidation of carbon disulfide could be obtained only if a relatively large amount of auxiliary oil was burned with the sample. Experiments were made with various ratios of carbon disulfide to auxiliary oil, and complete oxidation resulted only when less than 45% of the total measured energy came from the combustion of carbon disulfide. In some of the experiments with carbon disulfide, 5 atmospheres of air (instead of the usual one atmosphere) was charged to the bomb before charging to a total pressure of 30 atmospheres with pure oxygen. It was hoped that fixation of more than the normal amount of nitrogen oxides would promote complete oxidation. This expedient did allow a significant increase in the ratio of carbon disulfide to auxiliary oil. As the detailed results in Table I show, the measured heat of combustion of carbon disulfide was not affected when the ratio of carbon disulfide to auxiliary oil was varied in such a way that carbon disulfide contributed between 20 and 45% of the total measured energy. The results for methanethiol also were unaffected by relatively large changes in the ratio of that compoun to auxiliary oil (Table I).

Recovery of sulfuric acid in the combustion products of both compounds was 100.0 ± 0.1% of that expected from the stoichiometry of the combustion reaction. Quantitative recovery of sulfuric acid indicates that the compounds were pure and that the chemistry of the combustion reaction is properly described. Mass spectroscopic examination of the gaseous combustion products of both compounds did not show significant amounts of any product other than carbon dioxide.

Derived Results.—Derived results for both compounds are given in Table II. The values of $\Delta Ec°_{298.15}$ and $\Delta Hc°_{298.15}$ are for the idealized combustion reactions 1 and 2. To calculate the standard heats of formation of methanethiol and carbon disulfide, values of the heats of formation of carbon dioxide and water were taken from National Bureau of Standards Circular 500[12], and $\Delta H°_{298.15}$ for the reactions

$$S(c,\ rhombic) + 3/2\ O_2(g) + 31\ H_2O(liq.) = H_2SO_4{\cdot}30H_2O(liq.) \quad (3)$$

and

$$S(c,\ rhombic) + 3/2\ O_2(g) + 46\ H_2O(liq.) = H_2SO_4{\cdot}45H_2O(liq.) \quad (4)$$

was taken to be −143.50 and −143.63 kcal., respectively. These values were obtained by applying appropriate dilution corrections[12] to the value of the heat of formation of $H_2SO_4{\cdot}115H_2O$(liq.) recently determined in this Laboratory.[13] The heat of vaporization of carbon disulfide is from unpublished measurements of this Laboratory. The value used for the heat of vaporization of methanethiol was obtained by a short extrapolation of the results of Russell, *et al.*[14]

TABLE II[a]

DERIVED RESULTS AT 298.15°K., KCAL. MOLE^{-1}

Property	State	Methanethiol	Carbon disulfide
$\Delta Ec°$	Liquid	-361.56 ± 0.12	-400.91 ± 0.12
$\Delta Hc°$	Liquid	$-363.04 \pm .12$	-402.69 ± 0.12
$\Delta Hf°$	Liquid	$-11.15 \pm .13^b$	21.37 ± 0.17^b
$\Delta Hv°$		$5.69 \pm .02$	6.61 ± 0.02
$\Delta Hf°$	Gas	$-5.46 \pm .14^b$	27.98 ± 0.19^b

[a] Uncertainties are the "uncertainty interval" equal to twice the final over-all standard deviation of the mean (F. D. Rossini, ref. 4, p. 319). [b] Reference state for sulfur is S (rhombic).

Discussion

The only previously published experimental value of the heat of formation of gaseous methanethiol,[12] −2.97 kcal. mole^{-1}, is from the pioneering work of Thomsen.[15] From bond energy considerations Allen[16] recently predicted that the heat of formation of gaseous methanethiol should be −5.4 kcal. mole^{-1}. This prediction is in excellent agreement with the experimental value from this research.

The heat of formation of gaseous carbon disulfide has been derived from the experimental results of several investigators, including heats of combustion measured by Thomsen,[15] Berthelot[17] and Guerin, *et al.*[18] These measurements of the heat of combustion of carbon disulfide are quite discordant. The heat of formation given in NBS Circular 500,[12] 27.55 kcal. mole^{-1}, apparently was calculated directly from the results of Terres and Wesemann's[19] studies of the equilibria of the reactions

$$CO_2 + H_2S = COS + H_2O \quad (5)$$

$$COS + H_2S = CS_2 + H_2O \quad (6)$$

Values of $\Delta H°_{298.15}$ for these reactions, computed from the measured equilibrium constants and free energy data, show significant trends with reaction temperature. For example the three values of $\Delta H°_{298.15}$ for reaction 6 that may be calculated from Terres and Wesemann's results show a trend with reaction temperature of almost 0.5 kcal. mole^{-1}. These and other uncertainties in the result obtained from the equilibrium studies account for the discrepancy between the earlier value of the heat of formation of carbon disulfide and the more accurate result of this investigation.

---

(12) F. D. Rossini, D. D. Wagman, W. H. Evans, S. Levine and I. Jaffe, "Selected Values of Chemical Thermodynamic Properties," Natl. Bur. Standards Circular 500, 1952.

(13) W. D. Good, J. L. Lacina and J. P. McCullough, *J. Am. Chem. Soc.*, **82**, 5589 (1960).

(14) H. Russell, Jr., D. W. Osborne and D. M. Yost, *ibid.*, **64**, 165 (1942).

(15) J. Thomsen, "Thermochemische Untersuchungen," Barth, Leipzig (1882–1886).

(16) T. L. Allen, *J. Chem. Phys.*, **31**, 1039 (1959).

(17) (a) M. P. E. Berthelot, *Ann. chim. phys.*, **23**, 209 (1881); (b) **28**, 126 (1893).

(18) H. Guerin, M. Bastick, J. Bastick and J. Adam-Gironne, *Compt. rend.*, **228**, 87 (1949).

(19) E. Terres and H. Wesemann, *Angew. Chem.*, **45**, 795 (1932).

MECHANISM OF THE PHOTO-INITIATED POLYMERIZATION OF METHYL METHACRYLATE AT ZINC OXIDE SURFACES[1]

By Joseph C. Kuriacose and M. Clare Markham

Chemistry Department, Saint Joseph College, West Hartford, Conn.

Received July 18, 1961

Detailed investigation of the photosensitized polymerization of methyl methacrylate in suspensions of zinc oxide in various solvents, irradiated by near ultraviolet light at 365 mμ, demonstrates conclusively that surface-adsorbed oxygen is essential to chain initiation. Polymers of high molecular weight, *ca.* 10^6, are obtained with oxygen-free solutions, and untreated zinc oxide surfaces. Zinc oxide reduced under hydrogen, or heated to remove surface oxygen during evacuation, results in greatly suppressed polymerization. Presence of oxygen in solution yields a larger number of chains initiated, but lower molecular weight. Excess oxygen inhibits polymerization completely. Comparison of polymerizations in various solvents indicates that solvents having high dielectric constants coupled with good proton-donating or hydrogen-bonding characteristics favor chain initiation *via* excited oxygen on the surface. This photo-activated oxygen is formed on the surface of zinc oxide during irradiation and the polymer chains initiated by it continue to grow for some time in the dark. Evidence that the excited oxygen may be an anion initiator stems from the observation that methyl methacrylate and acrylonitrile polymerize readily in these systems, but styrene not at all. Electron spin resonance spectra show that both oxygen and water adsorbed in the dark are able to trap all the conduction electrons in heated, evacuated zinc oxide, but light is necessary for initiation of polymerization. Ultraviolet light at 365 mμ therefore is believed to produce an excited oxygen, probably anion radical, at the surface of the zinc oxide.

Introduction

Formation of hydrogen peroxide in dilute aqueous suspensions of zinc oxide containing organic material is the characteristic effect of irradiation at 365 mμ.[2-4] Organic substances vary considerably in their ability to promote peroxide formation. An essential condition is rapid entrainment of air or vigorous shaking to bring molecular oxygen in continuous contact with the photocatalytic surface of the zinc oxide. In the absence of organic matter a low steady-state level of peroxide is formed, indicating a reversible reaction. Proposed mechanisms for the formation of peroxide have postulated intermediate free radicals from either oxygen or water.

Observation that irradiated zinc oxide could initiate polymerization of some vinyl monomers in dilute aqueous solution, apparently only in absence of air, suggested possible direct dissociation of water at the catalyst surface. The present studies were undertaken to clarify the mechanism of initiation of polymerization in these systems, particularly the effects of previous treatment of the catalyst, removal of oxygen from the solution, and the influence of the solvent.

Experimental

Apparatus and Materials.—The 365 mμ line of a Hanovia high pressure quartz mercury arc was used as the exciting light. Radiation above 380 mμ is not absorbed by zinc oxide or any of the materials in these systems. Shorter wave lengths, below 330 mμ, are filtered out by using Pyrex reaction vessels and a thick Pyrex shield over the arc. Thus the only light absorption is by zinc oxide at 365 mμ.

A simple water-jacketed Pyrex tube with provision for transferring samples under nitrogen was used for preliminary comparison of relative efficiencies (in promoting polymerization) of solvents and types of photocatalysts. For studies of the rate of polymerization a similar, but larger, vessel was designed, using standard Pyrex creosote flasks for the inner vessel and employing a magnetic stirrer. It soon was discovered that both nitrogen stirring and magnetic stirring interfered with the growth of polymer chains. A 250-ml. Pyrex flask of the erlenmeyer type with a large surface on which the catalyst could be distributed for light absorption proved to be most convenient.

Materials.—Methyl methacrylate, inhibitor-free, was supplied by courtesy of Monsanto Chemical Co., Springfield, Mass. Formamide, N,N-dimethylformamide and N-methylformamide were Matheson Coleman & Bell highest purity, 99% or better. Absolute methanol was ACS reagent grade. Spectroscopically pure zinc oxide and zinc sulfide were obtained from the New Jersey Zinc Company. This company also supplied samples of zinc oxide specially prepared to be (1) photoconducting, (2) charge-accepting and (3) charge-rejecting. When no other type is specified the term zinc oxide will refer to the spectroscopically pure sample, which however gives the same results as ordinary analyzed reagent grade commercially available zinc oxide.

Measurement of Molecular Weights of Polymers.—A specially constructed viscometer was designed for intrinsic viscosity measurements to determine approximate molecular weights of polymers dissolved in benzene. A reservoir bulb of large cross-section made possible progressive dilutions without intermediate emptying and refilling of the viscometer. Values of K and α used were, respectively, 7.45×10^{-5} and 7.575×10^{-1}.[5]

Dielectric Constants.—Dielectric constants of solvent mixtures were measured with a Sargent Oscillometer calibrated with the pure liquids.

Usual Experimental Conditions.—Unless otherwise stated all data in tables were obtained using 0.15 g. of zinc oxide, 50 ml. of water and 1 ml. of methyl methacrylate. The usual temperature was 30°. The suspension was allowed to settle giving a uniform distribution of zinc oxide on the bottom of a 250-ml. erlenmeyer flask. The system then was evacuated, irradiated for 2.5 hours, and allowed to stand 18 hours in the dark before adding dilute sulfuric acid to terminate the reaction.

Electron Paramagnetic Resonance Measurements.—These studies were carried out by irradiating specially prepared zinc oxide samples with the Hanovia H-4 lamp described above in the cavity of a Varian, 100 Kc. spectrometer, through the courtesy of Dr. P. H. Bray's laboratory, Physics Department of Brown University.

Results and Discussion

The extent and characteristics of polymerization of methyl methacrylate in dilute solution, initiated by light absorbed by a photocatalytic solid, are influenced by the following factors: (1) the nature and pre-treatment of the photocatalyst; (2) the concentration of oxygen present in solution or supplied during irradiation; (3) physical conditions of irradiation such as quantity of photocata-

---

[1] This work was carried out under Contract No. AF 19(604)-7224, with the Geophysics Research Directorate, Air Force Cambridge Research Laboratories, Air Force Research Division.

[2] M. C. Markham and K. J. Laidler, *J. Phys. Chem.*, **57**, 363 (1953).

[3] J. G. Calvert, K. Theurer, G. T. Rankin and W. M. MacNevin, *J. Am. Chem. Soc.*, **76**, 2575 (1954).

[4] G. M. Schwab, *Advances in Catalysis*, **9**, 229 (1957).

[5] J. H. Baxendale, S. Bywaters and M. G. Evans, *J. Polymer Sci.*, **1**, 237 (1946).

lyst, stirring, duration of irradiation, temperature; (4) time and temperature of standing after irradiation before termination; (5) the nature and concentration of the monomer; (6) the nature of the solvent.

(1) **Nature and Pre-treatment of the Photocatalyst.**—The study of the kinetics and mechanism of photo-catalytically initiated polymerization of methyl methacrylate has been carried out with spectroscopically pure zinc oxide. A few preliminary experiments with various photocatalytic solids indicate that zinc sulfide is also a good initiator for these polymerizations.

Of the various preparations of zinc oxide tested, both the ordinary analytical reagent grade of zinc oxide and the specially prepared charge-accepting zinc oxide also showed good ability to initiate polymerization. The photoconducting and charge-rejecting zinc oxides were much less effective. These latter two samples have been prepared in such a way as to contain more excess zinc and possess better thermal conductivity. The charge-accepting zinc oxide is a poorer conductor. Since it gives off hydrogen sulfide on treatment with dilute acid, it must contain zinc sulfide. At any rate higher conductivity does not appear to be favorable to initiation of polymerization at the photocatalyst surface.

In every case adsorbed oxygen was found to be necessary for initiation of polymerization. Zinc oxide reduced under hydrogen is not effective. Table I shows the effect of pre-treatment of the zinc oxide.

TABLE I

EFFECT OF PRE-TREATMENT OF CATALYST AND SUSPENSION

Treatment of ZnO	Treatment of suspension	Polymer wt., g.	Mol. wt. $\times 10^{-6}$	Min. no. chains $\times 10^{-17}$
Heated	Evacuated	0.3240	2.167	0.906
Unheated	Evacuated	.3724	1.981	1.139
Unheated	Not evacuated	.2077	0.543	2.317

Discussion I.—Heating the zinc oxide under vacuum increases the molecular weight of the polymer but reduces the number of chains. It seems that this effect is not due to sintering, since heating produces the same effect on 0.15 g. of zinc oxide as on 0.25 g. A decrease in surface area would not be expected to reduce the efficiency of 0.25 g. of heated zinc oxide to less than that of 0.15 g. of unheated zinc oxide.

(2) **Effect of Oxygen Present in Solution.**—Comparison of the evacuated and non-evacuated suspensions in Table I shows that the more oxygen there is in the system the less the molecular weight, and the greater the number of chains initiated. The total weight of polymer is least when the system is not evacuated, and greatest when the zinc oxide is not heated and the system is evacuated. It would appear from these results that oxygen is required for the initiation process, but too much oxygen in solution serves as an inhibitor. Table II gives more complete data on the effect of oxygen on the course of the polymerization.

TABLE II

EFFECT OF TIME OF IRRADIATION

Irradiation time, hr.	Polymer wt., g.	Mol. wt. $\times 10^{-6}$	Min. no. chains $\times 10^{-17}$
	System evacuated		
0.5	0.0867	1.923	0.273
1.5	.2963	1.469	1.222
2.0	.3525	1.816	1.176
2.5	.3724	1.981	1.139
	System not evacuated		
0.5	0.0326	...	...
1.0	.0912	0.432	1.278
1.5	.1456	.543	1.624
2.5	.2077	.543	2.317
5.5	.3798	.589	3.908

Discussion II.—With increase in time of irradiation there are more chains initiated whether the system is evacuated or not; the molecular weight remains about the same. The initiating species must be formed during the period of irradiation. The inhibiting effect of extra oxygen can be compensated for by longer irradiation as far as total amount of polymer is concerned, but in the presence of excess oxygen the molecular weight always remains low, and the number of chains increases.

(3) **Physical Conditions of Irradiation.**—For best results the zinc oxide should be spread uniformly over a large surface. In a 250-ml. erlenmeyer flask, containing 1 ml. of methyl methacrylate in 50 ml. of water, 0.15 g. of zinc oxide gave maximum polymerization. Results are remarkably reproducible, producing polymers of high, uniform average molecular weight. Under these conditions 2.5 hr. irradiation is sufficient for maximum amount of polymer provided polymerization is allowed to go to completion in the dark as described below. It is very important to allow the solution to remain undisturbed during polymerization as the data of Table III clearly show.

TABLE III

EFFECT OF STIRRING

Conditions	Polymer wt., g.	Mol. wt. $\times 10^{-6}$	Min. no. chains $\times 10^{-17}$
No stirring	0.3724	1.991	1.139
Stirred every $^1/_2$ hr. during irradiation	0.3637	1.096	2.010
Vigorous stirring with magnetic stirrer	trace	...	...

Discussion III.—Vigorous stirring during irradiation prevents polymerization. Occasional stirring decreases the molecular weight but also results in a larger number of chains formed. Stirring therefore appears to favor chain termination. The influence of temperature during irradiation can be seen best in Table IVB where it is compared with the effect of temperature in the dark period following irradiation.

(4) **Time and Temperature Variables.**—

Discussion IV.—During the period of irradiation the total weight of polymer formed is almost the same whether the system is evacuated or not. Even after the period of irradiation, chains seem to be initiated. In an evacuated system the period after irradiation results in increased weight

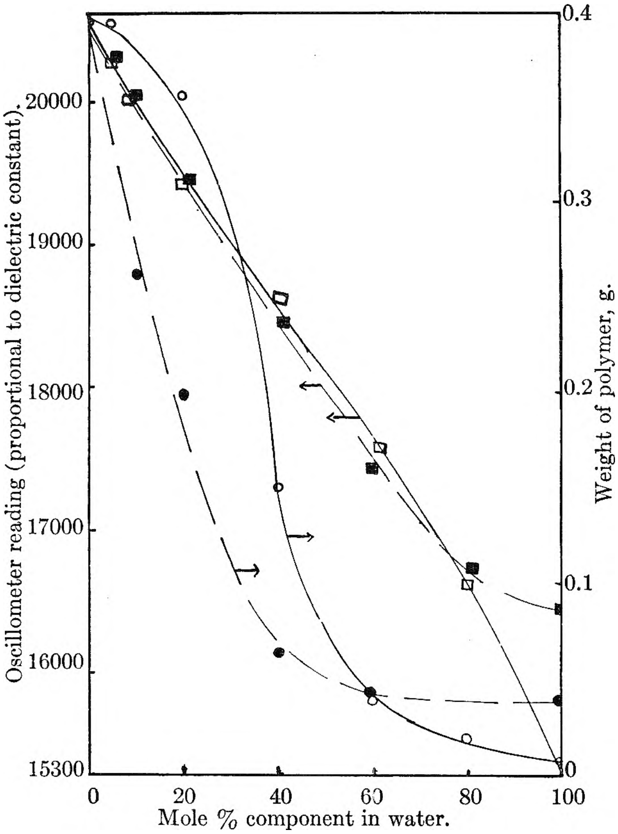

Fig. 1.—Influence of mixtures of solvents on extent of polymerization of methyl methacrylate at irradiated zinc oxide surface, showing relationship to dielectric constant of mixture: ●, weight of polymer and ■, dielectric constant, in mixtures of N,N-dimethylformamide and water; ○, weight of polymer and □, dielectric constant, in mixtures of methanol and water. 0.15 g. ZnO, 1 ml. methyl methacrylate, 50 ml. solvent, irradiated 2.5 hr., acid added to terminate polymerization after 18 additional hr. in the dark.

TABLE IVA

EFFECT OF DARK PERIOD ON POLYMER GROWTH

Total time before adding acid, hr.	Polymer wt., g.	Mol. wt. $\times 10^{-6}$	Min. no chains $\times 10^{-17}$
System evacuated			
2.5	0.1539	1.310	0.712
6.0	.3205	1.413	1.375
21.0	.3724	1.981	1.139
System not evacuated			
2.5	0.1476	0.678	1.275
21.0	0.2077	0.543	2.317

of polymer chiefly through increased average molecular weight. In a non-evacuated system the average molecular weight remains about the same; only the apparent number of chains initiated increases.

The effect of raising the temperature is to increase the weight of polymer formed, both during and after the period of irradiation. In the evacuated systems the average molecular weight remains around 1.5 × 10^6; the apparent number of chains initiated again appears to increase during the dark period. These effects are much smaller in the non-evacuated systems, with average molecular weights of 0.5 × 10^6, and a large number of chains already formed at the end of the 2.5 hours irradiation.

TABLE IVB

EFFECT OF TEMPERATURE

Total time before adding acid, hr.	Temp., °C.	Polymer wt., g.
System evacuated		
2.5	20	0.183
2.5	30	.264
2.5	40	.283
21.0	20	.288
21.0	30	.390
21.0	40	.529
System not evacuated		
2.5	20	0.139
2.5	30	.148
2.5	40	.222
21.0	20	.188
21.0	30	.208
21.0	40	.250

These results could mean any of the following: (1) More polymer chains are really initiated in the dark; this condition could be realized only if the photo-reactive oxygen formed by light on the zinc oxide surface is a very stable free radical or excited species which takes a long time to react with monomer molecules; (2) The monomer molecules which have reacted with the photo-activated oxygen need time to grow to a detectable size which can be precipitated and filtered out of the reaction mixture after adding acid to dissolve the zinc oxide.

It already has been shown that vigorous stirring results in apparently complete suppression of polymerization. Nevertheless, the oxygen must have been photo-activated on irradiating the zinc oxide in the stirred vessel also, and monomer molecules must have come in contact with the surface more frequently. Chain propagation therefore seems to be a slower process than chain initiation or termination. The effect of stirring seems to be largely chain termination, whereas the increase in temperature seems to affect the extent of chain propagation and thus the number of chains counted in the analytical process. This interpretation is strengthened by considering the effect of increasing monomer concentration.

(5) The Nature and Concentration of the Monomer.—

TABLE V

EFFECT OF CONCENTRATION OF METHYL METHACRYLATE

Vol. methyl methacrylate, ml.	Polymer wt., g.	Mol. wt. $\times 10^{-6}$	Min. no. chains $\times 10^{-17}$
0.5	0.1439	0.750	1.103
1.0	.3724	1.981	1.139
2.0	.4515	2.565	1.067

Discussion V.—Increases in both temperature and concentration yield higher total weights of polymer. In the case of increasing concentration the effect is to increase molecular weight only, whereas the temperature affected primarily the apparent number of chains initiated. The usual experimental condition, 1 ml. of methyl methacrylate in 50 ml. of water, already exceeds slightly the solubility of methyl methacrylate in water. The addition of more methyl methacrylate cannot increase the concentration of monomer in solution, but only serves to maintain a saturated solution for a longer period of time, and thus keep up a steady rate of addition to growing chains, thereby increasing the average molecular weight. The rise in temperature increases both the solubility of monomer and the rate of diffusion. Once a layer of polymer has formed on the surface of zinc oxide, the diffusion of monomer to add to initiated chains becomes increasingly difficult. Some chains apparently fail to reach a detectable size unless the temperature is increased, or polymerization is allowed to continue for a long time in the dark.

Both acrylonitrile and methyl methacrylate have been found to polymerize readily in these systems. Styrene does not polymerize to any measurable extent when irradiated in a suspension of zinc oxide in water. Since styrene is known to be susceptible to polymerization only by free radicals or cations,[6] it is possible that the photo-initiator may be an anion. These considerations prompted an investigation of the nature and role of solvents favorable to these polymerizations.

(6) **The Role of the Solvent.**—

TABLE VI

EFFECT OF DIELECTRIC CONSTANT

Solvent (dielectric constant)	Polymer wt., g.	Mol. wt. $\times 10^{-6}$	Min. no. chains $\times 10^{-17}$
CH_3OH (33)	0.01	...	...
$HCON(CH_3)_2$ (37)	.0417	...	...
H_2O (80)	.3681	1.694	1.316
$HCONH_2$ (109)	.4620	0.543	5.153
$HCONH(CH_3)$ (190)	.0249	...	...

Discussion VI.—Methyl methacrylate is much more soluble in the three amides (formamide, N-methylformamide and N,N-dimethylformamide) and in methanol, than in water. One might have thought that dielectric constant was the most important property of the solvent for this polymerization, except that there is very little polymerization in N-methylformamide which has the highest dielectric constant of all. Figure 1 illustrates the effect of mixture of solvents.

The drop in weight of polymer is much greater on adding small amounts of N,N-dimethylformamide to water than on adding methanol. Independent studies in this Laboratory have shown that the rate of oxidation of methanol is greater than that of the amides in irradiated aqueous suspensions of zinc oxide. Therefore it is improbable that the inefficiency of the polymerization in these solvents is due to competing reactions of oxidation of the solvent on the zinc oxide surface. Addition of either N-methylformamide or N,N-dimethylformamide to formamide lowers the extent of polymerization almost equally. These facts indicate that neither the dielectric constant nor the solubility is the unique determining property. The ability of the solvent to furnish protons or form hydrogen bonds seems to be one of the most influential characteristics.

N-Methyl groups in the amides serve to prevent intermolecular association, thus allowing the unshared electron pair on the nitrogen to bind its own protons more strongly and increasing the nucleophilic character. The suitability of formamide as a solvent for the photo-initiated polymerization appears to be related to its more electrophilic nature.

When methanol is added to water it increases the solubility of methyl methacrylate as would N,N-dimethylformamide. Water, however, is a good proton donor, and methanol is more akin to water than N,N-dimethylformamide in its electron attracting properties. Therefore methanol in small concentrations causes a smaller decrease in polymer yield than N,N-dimethylformamide. The higher the concentration of methanol or dimethylformamide the smaller the molecular weight of the polymer.

Formamide itself gives rise to a low molecular weight polymer, similar to that obtained in water when the system is not evacuated. The number of chains initiated in formamide is more than double that in water. Irradiation of pure zinc oxide in formamide results in a decrease in absorption of the irradiated formamide at 290 mμ as shown by difference spectra *vs.* unirradiated formamide as the blank. The same effect in the spectrum can be obtained in limited degree by addition of hydrogen peroxide to formamide.

Electron paramagnetic resonance studies show that the solvent may influence the properties of zinc oxide even in the dark. Good conduction signals are obtained from zinc oxide only after heating and evacuation. Signals obtained in the dark from these samples are very little altered on irradiation at 365 mμ. Introduction of either oxygen or water completely obliterates this conduction electron signal, which is not restored on irradiation. These effects are in striking confirmation of observations in the infrared spectral measurements being conducted in the laboratories of the National Research Council, Ottawa.[7] The electron paramagnetic resonance effects certainly merit further study. To the present, only a very slight increase in the conduction electron signal has been observed on irradiating an oxygen-covered zinc oxide surface in contact with water.

Summary and Conclusions

The data outlined above lead to the following general interpretation of the mechanism of the photo-initiated polymerization of methyl methacrylate at zinc oxide surfaces.

The photo-initiator formed at the surface of zinc oxide is certainly a form of oxygen. The polymerization process initiated in the light is completed in the dark.

The light must produce an excited state of oxygen, not merely an electron-transfer to oxygen, since electron paramagnetic resonance studies show that oxygen has indeed already trapped all the conduction electrons of the zinc oxide, even in the dark. Furthermore, samples of zinc oxide spe-

---

[6] D. C. Pepper, *Quart. Revs.* (London), **8**, 88 (1954).

[7] J. H. Taylor and C. H. Amberg, *Can. J. Chem.*, **39**, 535 (1961).

cially made to be good conductors do not favor the polymerization.

The fact that styrene will not polymerize in these systems whereas monomers containing electrophilic groups such as acrylonitrile and methyl methacrylate polymerize readily seems to suggest that the photo-activated oxygen may be anionic in character, possibly a radical-anion, such as excited $\cdot O_2^-$. Styrene is less soluble in water than methyl methacrylate, but the failure to observe polymerization of styrene is not due to limited solubility, since it will not polymerize when the solvent is formamide, in which styrene has a much greater solubility.

The polymerization must not be anion-propagated, even though it may be anion-initiated, because the process has many features characteristic of free radical chain polymerizations. Vigorous stirring increases chain termination. If the reaction mixture is not disturbed reproducible polymers of high average molecular weight are obtained in evacuated systems. Oxygen present in solution shortens the chain length. Solubility of monomer and rate of diffusion are important factors.

The role of the solvent is incompletely understood. Neither dielectric constant nor solubility of the monomer is a unique determining characteristic. Ability to donate protons, or to solvate and stabilize the chain-initiator through hydrogen-bonding, seems to be an important feature.

An excited oxygen radical-ion may be able to fulfill all these requirements. It would initiate polymerization only of monomers susceptible to anion-initiation. Since it also has a free-radical character, neutralization of the anion character of the initiated polymer chain by a solvent which can furnish protons would still leave an ordinary free radical chain propagation process.

THE INFRARED SPECTRA OF THE OCTAHEDRAL COMPLEXES OF IRON(II), COBALT(II) AND NICKEL(II) WITH BIACETYL-BIS-METHYLIMINE AND PYRIDINAL METHYLIMINES

By Paul E. Figgins and Daryle H. Busch

McPherson Chemical Laboratory, The Ohio State University, Columbus, Ohio

Received July 19, 1961

The infrared spectra of the iron(II), cobalt(II) and nickel(II) complexes of biacetyl-bis-methylimine (BMI), 2-pyridinal methylimine (PMI) and 2,6-pyridindial-bis-methylimine (PDMI) have been recorded and interpreted. Opposing effects are associated with complexing, depending on the extent of metal–ligand pi-bonding. With PMI, cobalt(II) and nickel(II) cause an increase in the bond order of the acyclic methine group, while iron(II) exhibits the reverse effect. The stereochemical and electronic relationships associated with a planar tridentate ligand, such as PDMI, favor spin pairing in the d^7 cobalt(II) ion. Conjugative metal–ligand d π-p π bonding is maximized in the complexes of BMI, particularly that of iron(II).

Introduction

Although the first octahedral complex containing an α-diimine probably was prepared by Blau,[1] detailed studies of these interesting ligands were initiated by Krumholz.[2] That investigator demonstrated the close similarity in spectral properties between iron(II) complexes of such diimines as biacetyl-bis-methylimine and those of 1,10-phenanthroline and 2,2′-bipyridine. Subsequently, magnetic measurements,[3,4] infrared, visible and ultraviolet spectral studies,[4] and the synthesis and characterization of analogous 2-pyridinal imine[4–7] and 2,6-pyridindial diimine[7,8] complexes have demonstrated the strong donor properties of the general class of ligands having conjugated dimethine and trimethine functions. These results have served to justify the contention that the great affinities exhibited by 2,2′-bipyridine and 1,10-phenanthroline for transition metal ions arise from the conjugated diimine groupings contained in their structures.

Because of this profound complexing ability, the details of the various studies, and the moderate base strengths of heterocyclic aromatic amines, the recurrent suggestion appears in the literature that the peculiar efficacy in chelation of these ligands arises from their ability to form conjugated double bonds with suitable central metal ions. Infrared spectral measurements provide one of the most promising techniques for the investigation of ligand–metal π-bonding in systems of this class. The synthesis[7] of the complete series of octahedral complexes of cobalt(II), nickel(II) and iron(II) with biacetyl-bis-methylimine, 2-pyridinal methylimine and 2,6-pyridindial-bis-methylimine provides a useful series of complexes for these studies. The infrared spectra of these complexes are discussed in detail below.

Experimental

The methods of preparation of the compounds of interest were reported previously.[7]

The infrared spectra over the range 650–4000 cm.$^{-1}$ were obtained by using a Perkin–Elmer Model 21 recording spectrophotometer, equipped with sodium chloride optics. Potassium bromide or potassium iodide pellets were used for the solid samples, and the spectra of liquid 2-pyridinal

---

[1] F. Blau, *Monatsh.*, **19**, 647 (1898).

[2] P. Krumholz, *J. Am. Chem. Soc.*, **75**, 2163 (1953).

[3] K. Sone, *Naturwissenschaften*, **5**, 104 (1956).

[4] D. H. Busch and J. C. Bailar, Jr., *J. Am. Chem. Soc.*, **78**, 1137 (1956).

[5] G. Bähr and H. Thamlitz, *Z. anorg. u. allgem. Chem.*, **282**, 3 (1955).

[6] R. C. Stoufer and D. H. Busch, *J. Am. Chem. Soc.*, **78**, 6016 (1956).

[7] P. E. Figgins and D. H. Busch, *ibid.*, **82**, 820 (1960).

[8] F. Lions and K. V. Martin, *ibid.*, **79**, 2733 (1957).

TABLE I

INFRARED BANDS AND ASSIGNMENTS (CM.$^{-1}$) FOR 2-PYRIDINAL METHYLIMINE AND ITS COMPLEXES

Abbreviations used: w, weak; m, medium; s, strong; ua, unassigned; PMI, 2-pyridinal methylimine; d, deformation; st, stretch; r, rock; d-s symmetrical deformation.

Assignment	PMI- (liq.)	[Fe- (PMI)$_3$]I$_2$	[Co- (PMI)$_3$](BF$_4$)$_2$	[Ni- (PMI)$_3$](BF$_4$)$_2$	[Cu- (PMI)Cl$_2$]	[Hg- (PMI)Cl$_2$]	PMI- (cryst.)
H$_2$O	3425m	3447s	3388m	3378m	3412m	3401s	3459
ring C–H, st	3058w	3015 to	3090w	3082m	3026w	.....	3061sh
	3012w	2968					3005s
chain C–H, st	2959w	...	...	...	...	...	2873s
	2890s						2799s
C=N, st	1634s	1558w	1652m	1654s	1655m	1660s	?
Py, Band I	1587s	1619s	1602s	1604s	1609s	1596s	1596s
Py, Band II	1567s	1599w	1570w	1570w	1573w	1573w	1574s
Py, Band III	1468s	1475s	1480m	1482m	1481m	1481m	1473–1457s
Py, Band IV	1435s	1436s	1446s	1441s	1447s	1440s	1430s
N–CH$_3$, d–s	1344m	1365m	1373w	1371m	1373m	1367w	1364w
ua	1216w	1236s	1226s	1225s	1228s	1223s	1235m
ua	1144w	1150m	*a*	*a*	1159m	1157	1152–1136s
ua	1005m	1021m	*a*	*a*	1028s	1012s	1018s
"Breathing" mode	989s	969w	*a*	*a*	983w	973m	997m
C–H, d	862s	878w	878w	875w	882m	873m	987s
C–H, r	774s	772s	779s	774s	781s	783–778s	783s
ua	742m	748w	748w	749w	743w	742w	752s
C–H, d	659w	667m	670w	668m	670w	...	679s

[a] This region of spectrum obscured by BF$_4^-$ band.

methylimine and 2,6-pyridindial-bis-methylimine were obtained with liquid films between sodium chloride plates. All data have been corrected.

Results and Discussion

The Complexes of 2-Pyridinal Methylimine.—Infrared spectral bands and assignments for 2-pyridinal methylimine (structure I) and its complexes with iron(II), cobalt(II), nickel(II), copper(II) and mercury(II) are listed in Table I. The vibrational frequencies of the pyridine ring and of the C=N side chain (which, together, constitute the chelate ring) should be found in the portion of the spectrum between 1700 and 1400 cm.$^{-1}$.

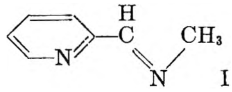
I

In an unconjugated acyclic system the C=N band usually is found in the range from 1690 to 1640 cm.$^{-1}$, and appears to be variable in intensity.[9] However, the acyclic C=N group in 2-pyridinal methylimine is conjugated, and the interaction of the π-electrons of the side chain group with the π-electron system of the pyridine ring can be described in terms of resonance structures such as that shown below (II).

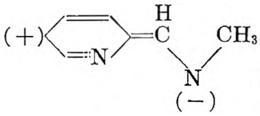
II

As a consequence of such structures, the bond order of the side-chain C=N group would be decreased, causing a shift in the C=N stretching frequency toward the lower values. In the free ligand, the acyclic C=N stretching frequency occurs at 1634 cm.$^{-1}$ (Table I), in agreement with this view.

For the complexes listed in Table I, the assignment of the C=N stretching frequency is unambiguous in every case except that of the iron(II) complex. For this reason, the spectrum of the iron (II) complex will be considered after discussion of the spectra of the remaining complexes.

Complexing with cobalt(II) and nickel(II) increases the frequency of this band from 1634 to 1652 and 1654 cm.$^{-1}$, respectively. Since these bands appear at frequencies in the range observed for unconjugated C=N stretching frequencies, there is probably very little interaction between the pyridine ring and this acyclic function. The complexes of copper(II) and mercury(II) exhibit similar absorptions at 1655 and 1660 cm.$^{-1}$, respectively, and therefore indicate even less conjugation.

On the basis of the ring vibrations of pyridine,[10–12] the four bands at 1587, 1567, 1468 and 1435 in the spectrum of 2-pyridinal methylimine (Table I) may be assigned to the pyridine ring. The basic pattern of these four bands is evident throughout the series of spectra of the complexes, although some shifting of bands and changes in intensities do occur. In all of the complexes, band I is the strongest of the four and it is one of the strongest absorptions in the double bond region. Band II is greatly reduced in intensity and often is hardly more than a shoulder. Bands III and IV are usually of medium or strong intensity, with band IV being the stronger of the two. Band IV occurs in the region where a CH$_3$ deformation frequency should be located. Weak bands or shoulders are sometimes apparent, and the band is

---

(9) L. J. Bellamy, "Infrared Spectra of Complex Molecules," John Wiley and Sons, Inc., New York, N. Y., 1954, p. 226.

(10) C. H. Kline, Jr., and J. Turkevich, *J. Chem. Phys.*, **12**, 300 (1944).

(11) L. Corrsin, B. J. Fax and R. C. Lord, *ibid.*, **21**, 1170 (1953).

(12) F. A. Andersen, B. Bak, S. Broderson and J. Rastrup-Andersen, *ibid.*, **23**, 1047 (1955).

of variable intensity. The CH_3 band may be responsible for these variations.

The infrared spectra of the complexes of cobalt(II), nickel(II), copper(II) and mercury(II) all show a shift of band I to higher frequencies. The magnitude and direction of these shifts is comparable with the shifts observed for the methine group.

The highest frequency bands below 1700 cm.$^{-1}$ in the spectrum of the iron(II) complex occur at 1619 and 1599 cm.$^{-1}$. The first is strong in intensity and the second is much less intense. In this respect they resemble bands I and II of the aromatic ring vibrations. The next band, at 1558 cm.$^{-1}$, is fairly sharp and of medium intensity. The two remaining bands occur at 1475 and 1436 cm.$^{-1}$. These two absorptions agree well with bands III and IV as observed in the other complexes.

An earlier paper[4] tentatively assigned the band observed at 1558 cm.$^{-1}$ to the C=N side chain stretching frequency on the basis that the higher bands in the double bond region are consistent in intensity and position with assignment to vibrations associated with the pyridine ring. The occurrence of this high frequency band at 1619 cm.$^{-1}$ would represent a substantial increase in frequency upon coördination for the corresponding ring vibration (band I). Nonetheless, it has been shown that the ring vibrations generally shift toward higher frequencies upon complexing with iron (II).[4]

In the case of the iron(II) complex, the frequency of the acyclic methine group shifts to a lower value indicating decreased double bond character in the C=N group. Such an effect can be explained, as has been suggested previously,[4] in terms of π-bond formation between the ligand and the metal ion.

Since both cobalt(II) and nickel(II) contain unshared pairs of d-electrons, some π-electron interaction of this class should be expected. However, the π-bonding effect may be small in these cases. In this respect, the spectrum of the mercuric complex of PMI is significant. In this case, no π-bonding is anticipated because there are no electrons in orbitals of appropriate energy and symmetry. It is, therefore, interesting to find that the acyclic C=N stretching vibration of PMI exhibits its maximum frequency in the mercury complex (1660 cm.$^{-1}$).

It was noted in an earlier paper[1] that the liquid ligand PMI very slowly converts into a crystalline material. This solid melts at 208–210° and appears to have a doubled molecular weight. The infrared spectrum of the crystalline material (Table I) closely resembles that of the liquid, with one striking exception. The C=N stretching frequency (1634 cm.$^{-1}$ in the liquid) is absent from the spectrum of the solid. The explanation which appears to fit all the experimental facts involves the condensation of two molecules of the imine (structure III).

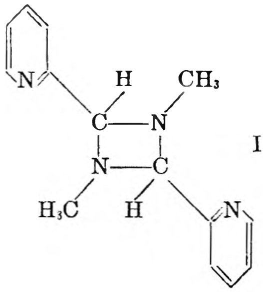

III

TABLE II

INFRARED BANDS (CM.$^{-1}$) AND ASSIGNMENTS FOR 2,6-PYRIDINDIAL-BIS-METHYLIMINE AND ITS COMPLEXES

Abbreviations used: w, weak, m, medium; s, strong; v, very; sh, shoulder; ua, unassigned, PDMI, 2,6-pyridindial-bis-methylimine; ?, questionable assignment; st, stretch; d, deformation; r, rock; d-s, symmetrical deformation.

Assignment	PDMI	[Fe-(PDMI)$_2$]-$I_2 \cdot 2H_2O$	[Co-(PDMI)$_2$]-$I_2 \cdot H_2O$	[Ni-(PDMI)$_2$]-$I_2 \cdot H_2O$
H_2O	3461m	3412	3458	3434
ring C–H, st	3064w	...	...	...
chain C–H, st	2962sh 2892s	2968s	2958	2944
C=N, st	1660s	1532s	1643w	1643w
Py, Band I	1596s	1607m	1594s	1593vs
Py, Band II	1578s	1580w	1553w	sh
Py, Band III	1460s	1452sh	1473m	1472sh
Py, Band IV	1442sh	1434s	1432s	1434s
ua	1408s	1404w	1404s	...
N–CH_3, d-s	1348vs	1355m	1356m	1361m
C–N, st	...	1388 ?vs	1267s	1289s
ua	1225m	1219w	1214w	1213m
ua	1156w	1164m	1167s	1159s
ua	1008s	1037w	1016w	sh
ua	952s	919m	915s	924m
C–H, r	811s	798s	798s	780s
ua	743s	750s	744s	742s
C–H, d	684m	672m	675m	676m

The Complexes of 2,6-Pyridindial-bis-methylimine.—In the complexes with cobalt(II) and nickel(II) with this ligand (structure IV), the bands assigned to the C=N stretching vibration are found at 1643 cm.$^{-1}$ and are greatly reduced in intensity (Table II). In the cobalt(II) complex it is hardly more than a shoulder. The magnitude of the shift due to complexing (17 cm.$^{-1}$) is approximately the same as was observed for the cobalt(II) complexes of 2-pyridinal methylimine, but the direction of the shift is reversed, implying an increased interaction between the side chain C=N group and the pyridine ring upon complexing.

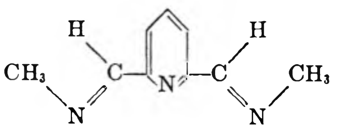

The orientation of π-orbitals in octahedral complexes containing planar tridentate chelating agents of this class provides a tentative explanation. First it is to be noted that all four of the side chain donor atoms coördinate in a single plane of the octahedron (call it the XY plane). Further, the p_z-orbitals of the coördinated nitrogen atoms in these groups are properly oriented to overlap the d_{xy}-orbital of the central atom. On the other hand, the pyridine nitrogen atoms (on plus and minus Z)

may each overlap a central-atom d-orbital which is available for their exclusive interaction. Two significant consequences follow. The sharp distinction between d_{xy} on the one hand and the pair of energy levels d_{xz} and d_{yz} on the other is equivalent to the imposition of a tetragonal distortion on the octahedral structure. In fact, it may be concluded that strong π-bonding in octahedral complexes containing coplanar tridentate chelating agents should lead to appreciable tetragonal distortions in complexes containing these tridentate ligands.

This particular cobalt(II) compound is especially interesting in view of the coincident requirement of a tetragonal structure by the π-bonding system of the trimethine ligand, PDMI, and by Jahn–Teller distortions in the case of the spin-paired d^7 cobalt(II) ion ($\mu_{\text{eff}} = 2.31$ Bohr magnetons). The significance of these relationships is emphasized if one recalls that π-bonding had already been invoked to account for spin-pairing in the iron(II) complexes containing dimethine and trimethine ligands. The considerations presented here account for the more common occurrence of spin-paired cobalt(II) complexes among tridentate rather than bidentate ligands of this class.[7]

If π-bonding between metal ion and ligand is of principal importance in determining the relative stabilities of complexes with these ligands, the bidentate ligands might be expected to form the more stable complexes. This comes about because of the symmetrically conjugated nature of the π-electron system in the bidentate case.

The spectrum of the bis-(2,6-pyridindial-bis-methylimine)-iron(II) compound exhibits the same type of anomalous behavior as was observed in the spectrum of tris-(2-pyridinal methylimine)-iron(II) iodide. The highest bands in the 1700–1400 cm.$^{-1}$ region appear at 1607, 1580 and 1532 cm.$^{-1}$ (Table II). On the basis of the shapes and intensities, the two higher frequency bands have been assigned to bands I and II of the pyridine ring. The next band at 1532 cm.$^{-1}$ then must be the C=N stretching frequency. This frequency is 26 cm.$^{-1}$ lower than the corresponding band for the iron(II) complex of 2-pyridinal methylimine. The shoulder appearing at 1452 cm.$^{-1}$ in the spectrum of the iron(II) complex has been assigned to band III of the pyridine ring.

The Complexes of Biacetyl-bis-methylimine.—The infrared spectra of the tris cobalt(II) and nickel(II) complexes of biacetyl-bis-methylimine may be characterized by their simplicity in comparison to the infrared spectra discussed above (Table III). The highest frequency bands in the 1700-1400 cm.$^{-1}$ region appear at 1608 and 1612 cm.$^{-1}$ for the cobalt(II) and nickel(II) complexes, respectively, and have been assigned to the C=N stretching frequency. These values are well below those observed for the other nickel(II) and cobalt(II) complexes during this investigation, and well below the values given in the literature for unconjugated acyclic methine groups. From this it might be inferred that there is a considerable amount of π-electron interaction between the ligand and the metal ion, such as is shown in structure V. However, it should be pointed out that the butadiene-like conjugation of the free ligand could contribute to the low value of this vibration. Since all attempts to synthesize the free ligand failed,[7] this possibility could not be subjected to experimental test. This conjugative effect does not approach that observed for iron(II) with the ligands previously discussed.

TABLE III

INFRARED BANDS (cm.$^{-1}$) AND ASSIGNMENTS FOR BIACETYL-BIS-METHYLIMINE COMPLEXES

Abbreviations used: w, weak; m, medium; s, strong; ua, unassigned; sh, shoulder; BMI, biacetyl-bis-methylimine; st, stretch; d-a, asymmetrical deformation; d-s, symmetrical deformation.

Assignment	[Fe-(BMI)$_3$]I$_2$	[Co-(BMI)$_3$]I$_2$	[Ni-(BMI)$_3$]I$_2$
H_2O	3426	3438	3397
C–H, st	2891	2919	2884
C=N, st	?	1608s	1612s
CH_3(d–a)	1426s	1430s	1427s
CH_3(d–s)	1388s	1390s	1384sh
		1374sh	1373s
C–N, st	1331s[a]	1306s	1301s
ua	1204s	1194s	1194s
ua	1139s	1143m	1141w
ua	1061m	1094m	1092w
ua	1049m	1054sh	1044s
		1043s	
ua	1004m	1006m	1005m
		970w	
ua	962s	901s	901s
	898w		
ua	. . .	755s	754s

[a] Band included under this assignment for convenience of tabulation. See text.

In the case of the cobalt(II) and nickel(II) complexes of biacetyl-bis-methylimine, there appears a characteristic doublet in the region 1450–1350 cm.$^{-1}$. Each maximum of this doublet shows either a definite shoulder or tends to be broadened. These two peaks have been assigned to asymmetrical and symmetrical deformations of the methyl groups, the asymmetrical being at the higher frequency. In the ligand, there are two types of CH_3 groups, those attached to carbon and those attached to nitrogen atoms. It is these two types of CH_3 groups which account for the splitting or broadening of the two main bands. The strong band in the vicinity of 1300 cm.$^{-1}$ has been assigned to a C–N stretching frequency.

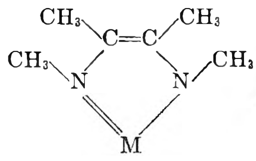

V

The anomalous infrared spectrum of tris-(biacetyl-bis-methylimine)-iron(II) iodide as reported earlier[4] has been confirmed during the course of this investigation (Table III). In the region below 1700 cm.$^{-1}$, the first absorption band appears at 1426 cm.$^{-1}$. If this were assigned to a C=N stretching mode it would represent a shift of almost 200 cm.$^{-1}$ from the position of the corresponding absorption in the spectra of the other complexes.

However, the band at 1426 cm.$^{-1}$ is accompanied by another at 1388 cm.$^{-1}$. These are similar to those which were assigned to the asymmetric and symmetric CH_3 deformations in the spectra of the cobalt and nickel complexes. Consequently, any other assignments would be very difficult to justify.

The next band, at 1331 cm.$^{-1}$ has been listed as a C–N stretching frequency on the basis of its similarity to the corresponding band in the cobalt(II) and nickel(II) complexes. However, in the case of the iron(II) complex, two distinct features are observed. The band is from 25–30 cm.$^{-1}$ higher than that found in either the cobalt(II) or nickel(II) complex. In addition, the band in the iron(II) complex is of greater intensity, being the most intense in the spectrum. If, as has been suggested previously,[4] the structure involving double bonds with the iron(II) ion (structure V) represents the predominate form of the iron(II) methine type of complexes, the double bond character of the C=N function would be greatly reduced. In the extreme case, the chelate ring would form a completely conjugated five-membered ring with many of the characteristics of an aromatic ring. This is in agreement with the profound changes in the spectrum of the iron(II) complex, as compared to those of cobalt(II) and nickel(II).

The remainder of the bands in the spectra of the iron(II), cobalt(II) and nickel(II) complexes of biacetyl-bis-methylimine have not been assigned. However, it should be pointed out that the striking difference in the spectrum of the iron(II) complex in the region 957–650 cm.$^{-1}$ also can be interpreted as indicative of radical changes taking place in the ligand. The vanishing or extreme alteration of the group frequencies expected for the ligand biacetyl-bis-methylimine upon coördination with iron(II) provides a direct demonstration of the strong coupling between the π-electron system of the ligand and the t_{2g} set of d-orbitals of the iron(II) atom. This contention is supported by the appearance of strong absorptions assignable to the C=N groups in the spectra of the corresponding cobalt(II) and nickel(II) complexes.

MOLAL VOLUMES AND REFRACTIVE INDEX INCREMENTS OF $BaCl_2$–HCl SOLUTIONS. MIXTURE RULES[1]

BY RICHARD M. RUSH AND GEORGE SCATCHARD[2]

Chemistry Div., Oak Ridge National Lab., Oak Ridge, Tenn.

Received July 31, 1961

An equation for the apparent molal volumes of mixed electrolyte solutions in terms of the apparent molal volumes of the single electrolytes is derived from the excess free energy relationship of Scatchard. This equation represents adequately the specific volumes of solutions containing both the 1-1 electrolyte HCl and the 2-1 electrolyte $BaCl_2$. An equation which correlates empirically the solute refractive index increments also is given.

Young and Smith[3] express the apparent molal volume and apparent molal enthalpy in a solution of two salts by an equation which in our symbols becomes

$$\Phi = \Phi_A x_A + \Phi_B x_B + k_{AB} x_A x_B I \qquad (1)$$

in which x_A and x_B are the mole fractions of the solute components, $n_A/(n_A + n_B)$ and $n_B/(n_A + n_B)$, and Φ_A and Φ_B are the apparent molal volumes (or enthalpies) in the two-component solutions at the same ionic strength, I. For the apparent molal volume

$$\Phi = (V - n_0 V_0)/(n_A + n_B) \qquad (2)$$

if V is the volume of the system, V_0 the molal volume of the solvent, and n_0, n_A and n_B are the numbers of moles of solvent and solutes. For the partial molal enthalpy, V and V_0 are replaced by the corresponding enthalpies H and H_0.

For the solutions of 1-1 electrolytes to which they applied it, equation 1 is identical with that yielded by the equation for the free energy of mixed salt solutions[4] with only the first deviation from additivity, $B^{(0,1)}$, which gives Harned's rule. For different valence types, however, $B^{(0,1)}$ leads to the equation

$$\Phi = \Phi_A x_A + \Phi_B x_B + k_{AB}^{(0,1)} x_A x_B (m_A + m_B) \qquad (3)$$

in which m_A and m_B are the molalities of the two salts. The difference is not great, for the important thing is that the three apparent molal quantities are measured at the same ionic strength.

As part of an investigation of the behavior of three-component mixtures in the ultracentrifuge, the densities and refractive index increments of a number of aqueous solutions containing hydrochloric acid and barium chloride have been measured. The specific volumes $v = 1/d$, are correlated by equation 3 and the refractive index increments, $\Delta n/c$, by equation 4

$$\Delta n/c = (\Delta n/c_A)^0 x_A + (\Delta n/c_B)^0 x_B + K_{AB} x_A x_B c \qquad (4)$$

in which $c = (c_A + c_B)$ is the sum of the molar concentrations of the salts and $(\Delta n/c_A)^0$ and $(\Delta n/c_B)^0$ are the values of $\Delta n/c$ for the two component systems at the same c.

Experimental

The solutions were prepared by weighing solid $BaCl_2 \cdot 2H_2O$, a stock solution of HCl standardized by weight titrations and water into a volumetric flask.

The densities were measured at 25.0° with a 24-ml. pycnometer. The precision of these measurements is about 3

---

(1) Work performed for the U. S. Atomic Energy Commission at the Oak Ridge National Laboratory, operated by the Union Carbide Corporation, Oak Ridge, Tennessee.

(2) Department of Chemistry, Massachusetts Institute of Technology, Cambridge, Massachusetts; Consultant, Chemistry Division, Oak Ridge National Laboratory.

(3) T. F. Young and M. B. Smith, *J. Phys. Chem.*, **58**, 716 (1954).

(4) G. Scatchard, *J. Am. Chem. Soc.*, **83**, 2636 (1961).

parts in 10^5. There may, however, be a systematic error of 0.2% in the concentrations.

The refractive indices were measured at 25° with a Brice–Phoenix differential refractometer using light of 436, 546 and 589 mμ wave length. The mixtures were measured *vs.* various HCl solutions to keep the measured refractive index difference within the range of the instrument. The HCl solutions were measured stepwise *vs.* each other and water so that the refractive index of the mixtures *vs.* water, Δn, could be obtained directly. The refractometer was calibrated with KCl solutions from the data of Kruis.[5] The precision of the measurement of $\Delta n/c$ is about 1 part in 10^3.

Molal Volumes.—To determine the volume of a ternary solution, we rearrange equation 13 of reference 4 to

$$G^e = RT[A_An_A^* + A_Bn_B^* + B_{AB}^{(0)}n_A^*n_B^*/(n_A^* + n_B^*) + B_{AB}^{(1)}n_A^*n_B^*(n_A^* - n_B^*)/(n_A^* + n_B^*)^2] \quad (5)$$

in which $n_A^* = n_A\Sigma_i\nu_{iA}z_i^2/2 = I_An_0w_0$, and w_0 is 0.001 times the molecular weight of the solvent. Then

$$\begin{aligned} V^e &= \partial G^e/\partial P \\ &= a_An_A^* + a_Bn_B^* + b_{AB}^{(0)}n_A^*n_B^*/(n_A^* + n_B^*) + b_{AB}^{(1)}n_A^*n_B^*(n_A^* - n_B^*)/(n_A^* + n_B^*)^2 \quad (6) \end{aligned}$$

where $a_A = RT\partial A_A/\partial P$, $b_{AB}^{(0)} = RT\,\partial B_{AB}^{(0)}/\partial P$, etc. The ideal volume

$$V^I = V_0n_0 + V_An_A + V_Bn_B = V_0n_0 + V_A^*n_A^* + V_B^*n_B^* \quad (7)$$

and the total volume

$$\begin{aligned} V &= V^I + V^e = V_0n_0 + (V_A^* + a_A)n_A^* + (V_B^* + a_B)n_B^* + b_{AB}^{(0)}n_A^*n_B^*/(n_A^* + n_B^*) + b_{AB}^{(1)}n_A^*n_B^*(n_A^* - n_B^*)/(n_A^* + n_B^*)^2 \\ &= V_0n_0 + (n_A^* + n_B^*)\,[(V_A^* + a_A)y_A + (V_B^* + a_B)y_B + b_{AB}^{(0)}y_Ay_B + b_{AB}^{(1)}y_Ay_B(y_A - y_B)] \quad (8) \end{aligned}$$

in which y_A is the ionic strength fraction of A, $n_A^*/(n_A^* + n_B^*) = I_A/I$. If we define Φ^* analogously to Φ

$$\Phi^* = (V - V_0n_0)/(n_A^* + n_B^*) = \Phi(n_A + n_B)/(n_A^* + n_B^*) \quad (9)$$

so

$$\Phi^* = \Phi_A^*y_A + \Phi_B^*y_B + b_{AB}^{(0)}y_Ay_B + b_{AB}^{(1)}y_Ay_B(y_A - y_B) \quad (10)$$

$$= \Phi_A^*y_A + \Phi_B^*y_B + (d_{AB}^{(0,1)}I + d_{AB}^{(0,2)}I^2 + \ldots)y_Ay_B + (d_{AB}^{(1,2)}I^2 + \ldots)y_Ay_B(y_A - y_B) \quad (11)$$

in which the d_{AB}'s are independent of I. If we drop the terms in I^2 and higher powers of I, we may write

$$\Phi = \Phi_Ax_A + \Phi_Bx_B + (d_{AB}^{(0,1)}n_An_B/n_A^*n_B^*)x_Ax_B(m_A + m_B) \quad (12)$$

which is identical with equation 3 if

$$k_{AB}^{(0,1)} = d_{AB}^{(0,1)}n_An_B/n_A^*n_B^* \quad (13)$$

The extension to higher terms is so much simpler for Φ^* than for Φ that it is convenient to calculate Φ^* in terms of ionic strengths from equation 10, then calculate Φ from equation 9. The extension to more complicated solutions from equation 4 of reference 4 is direct though complex. The application to enthalpies differs from that to volumes only in replacing $\partial G/\partial P$ by $\partial(G/T)/\partial(1/T)$.

For the hydrochloric acid–barium chloride–water system we obtain

$$\Phi^* = (18.026 + 0.9181\sqrt{I} - 0.03275I)y_A + (8.109 + 1.0315\sqrt{I} + 0.0784I)y_B + 0.10y_Ay_BI \quad (14)$$

$$\Phi = (18.026 + 0.9181\sqrt{I} - 0.03275I)x_A + (24.328 + 3.0945\sqrt{I} + 0.2353I)x_B + 0.30x_Ax_B(m_A + m_B) \quad (15)$$

It follows that the partial molal volumes are

$$\bar{V}_{HCl} = (18.026 + 1.3772\sqrt{I} - 0.06550I)y_A + (18.026 + 1.4338\sqrt{I} + 0.1457I)y_B \quad (16)$$

$$\bar{V}_{BaCl_2} = (24.328 + 4.4717\sqrt{I} + 0.4371I)y_A + (24.328 + 4.6418\sqrt{I} + 0.4706I)y_B \quad (17)$$

Young and Smith[3] obtained from the data of Wirth[6] for HCl the equation

$$\Phi = 18.052 + 1.00096\sqrt{I} - 0.06736I \quad (18)$$

and from the measurements of Palitzsch,[7] Kohner,[8] Shibata and Holeman,[9] and Jones and Dole[10] on $BaCl_2$ solutions we calculate

$$\Phi = 24.08 + 3.36\sqrt{I} + 0.125I \quad (19)$$

Both equations for $BaCl_2$ are very different from

TABLE I

DEVIATIONS FROM MIXTURE RULES

Δ refers to the observed minus the calculated value

m_{HCl}	m_{BaCl_2}	$\Delta v \times 10^6$	$\Delta(\Delta n/c) \times 10^6$		
			436 mμ	546 mμ	589 mμ
0.5070	0	0	5	3	4
1.5450	0	−1	−10	−4	−6
2.4033	0	0	−2	−1	0
3.5248	0	2	8	3	5
4.3586	0	0	4	3	4
4.9446	0	0	−7	−4	−4
0	0.3037	0	−6	2	1
0	0.6108	−2	12	−6	−3
0	0.9249	2	−5	5	0
0	1.2436	1	−2	2	5
0	1.5792	−1	1	−3	−3
0.5119	0.4090	1	−4	24	25
0.3078	0.5116	3	−2	14	11
0.5172	0.5176	3	16	27	30
0.7238	0.5166	8	13	20	25
0.5162	0.6186	10	13	17	25
1.5610	0.4184	0	12	14	13
1.3561	0.5221	4	12	16	16
1.5812	0.5271	−1	15	9	11
1.7910	0.5274	−1	7	−7	−5
1.5763	0.6315	−3	11	1	3
0.4180	1.0432	2	−23	8	12
1.0393	0.8379	1	−8	7	5
0.2098	1.2566	9	−38	−24	−31
0.8420	1.0534	1	3	−9	−8
1.0589	1.0603	−6	2	−13	−12
0.4206	1.2611	−2	−4	−3	−5
0.6343	1.2677	−1	−5	−16	−18
1.2720	1.0607	−8	−10	−34	−48
0.4222	1.3731	−6	1	−15	−18
1.0550	1.1691	−4	−15	−33	−33

---

[5] A. Kruis, *Z. physik. Chem.*, **B34**, 13 (1936).

[6] H. E. Wirth, *J. Am. Chem. Soc.*, **62**, 1128 (1940).

[7] S. Palitzsch, *Z. physik. Chem.*, **A138**, 379 (1928).

[8] H. Kohner, *ibid.*, **B1**, 427 (1928).

[9] Z. Shibata and P. Holeman, *ibid.*, **B13**, 347 (1931).

[10] G. Jones and M. Dole, *J. Am. Chem. Soc.*, **52**, 2245 (1930).

that of Gucker,[11] copied by Harned and Owen,[12] which is in error because Gucker interpreted the symbol C_v in Geffcken's review[13] as moles per liter rather than equivalents per liter. The differences between the equations for the two-component systems determined from our measurements and those from the results of other observers may be caused by systematic errors in our concentrations. For comparison with the three component systems, we have preferred to use our own results, measured over the same concentration range and under the same conditions.

The deviations, Δv, of the measured specific volumes from those calculated by equation 15 are shown in Table I.

Refractive Index Increments.—The equations for the refractive index increments are

$$\Delta n_{436}/c = (0.0090667 - 0.0002273c + 0.0000158c^2)x_A + (0.0318274 - 0.0017776c + 0.0002335c^2)x_B + 0.000268x_Ax_Bc \quad (20)$$

$$\Delta n_{546}/c = (0.0086264 - 0.0001911c + 0.0000112c^2)x_A + (0.0309489 - 0.0018557c + 0.0002878c^2)x_B + 0.000252x_Ax_Bc \quad (21)$$

$$\Delta n_{589}/c = (0.0085459 - 0.0002054c + 0.0000135c^2)x_A + (0.0307106 - 0.0018472c + 0.0002924c^2)x_B + 0.000225x_Ax_Bc \quad (22)$$

The deviations of the measured refractive index increments $\Delta(\Delta n/c)$, from those calculated by equations 20, 21 and 22 are shown in Table I.

Acknowledgment.—The authors express their appreciation to Drs. J. S. Johnson, K. A. Kraus and T. F. Young for helpful discussion and to Neva E. Harrison for valuable technical assistance.

[11] F. T. Gucker, *Chem. Revs.*, **13**, 111 (1933).

[12] H. S. Harned and B. B. Owen, "Physical Chemistry of Electrolytic Solutions," Third Edition, Reinhold Publ. Corp., New York, N. Y., 1958, p. 361.

[13] W. Geffcken, *Z. physik. Chem.*, **A155**, 1 (1931).

POLARIMETRIC DETERMINATION OF ABSORPTION SPECTRA OF THIN FILMS ON METAL. I. INTERPRETATION OF OPTICAL DATA[1,2]

BY L. S. BARTELL AND D. CHURCHILL

Institute for Atomic Research and Department of Chemistry, Iowa State University, Ames, Iowa

Received July 31, 1961

A polarimetric method for the determination of electronic absorption spectra of films of molecular thickness adsorbed on polished metal surfaces is described. Schemes for finding the thickness, refractive index, and absorption coefficient of adsorbed films are discussed. The practicability of the method is demonstrated by a determination of the absorption spectrum of a 1 *M* dispersion of tetraphenylporphine in a film of collodion 31 Å. thick, on chromium. The spectrum of the 31 Å. dispersion was found to be similar to the spectrum of a bulk solution of the compound in benzene. It is shown also that direct photometric measurements of reflectivities from surfaces may yield useful spectral information about films.

Electronic spectra of substances in solution and in the solid state have played an important role in the study of intermolecular interactions and complex formation. The possibility of applying spectroscopic techniques in surface chemistry to elucidate the nature of electronic interactions associated with adsorption, where our picture of molecular forces is more speculative than for bulk phases, seems particularly attractive. A number of investigations have been made of absorption spectra of compounds adsorbed on transparent solids where many layers of adsorbed molecules may be traversed by the incident radiation.[3] A series of informative studies of infrared spectra of molecules adsorbed on metals have been published,[4,5] notably by Eischens and co-workers. In these investigations, spectra were inferred from intensity loss suffered upon multiple reflection. Analogous studies of electronic spectra of molecular films on metals so far have eluded observation, however, principally because of the diffuseness of electronic spectra as compared with infrared spectra, and because of the small amount of absorbing material in a monolayer.

In principle, a polarimetric measurement of amplitude and phase changes of light reflected from a metallic surface gives a more direct and complete characterization of optical constants of thin films on the surface than does a study of reflected intensities. Accordingly, an investigation of the polarimetric method was initiated with a view to its possible application to the determination of electronic spectra of molecular films on metals. A preliminary experimental study in which an indirect measure of phase shift on reflection was made revealed that the polarimetric method is indeed capable of sufficient sensitivity for the purpose.[6] Therefore, a rigorous polarimetric investigation of films on metals in the visible and near ultraviolet regions was undertaken.

The theory relating polarimetric measurements to optical properties of thin films was developed by Drude over seventy years ago but seems never to have been applied directly to the present problem. The purpose of this paper is two-fold. First, a scheme is presented for interpreting polarimetric measurements directly in terms of the thickness, refractive index, n, and absorption coefficient, k,

---

[1] Work was performed in the Ames Laboratory of the U. S. Atomic Energy Commission. Contribution No. 1045.

[2] Based on a dissertation by D. Churchill to the Graduate School, Iowa State University, in partial fulfillment of the requirements for the degree of Doctor of Philosophy, 1960.

[3] See for example J. H. deBoer, "Electron Emission and Adsorption Phenomena," Cambridge University Press, New York, N. Y., 1935.

[4] R. P. Eischens and W. A. Pliskin, "Advances in Catalysis," Vol. 10, Academic Press, Inc. New York, N. Y., 1958.

[5] S. A. Francis and A. H. Ellison, *J. Opt. Soc. Am.*, **49**, 131 (1959).

[6] L. S. Bartell, *J. Chem. Phys.*, **24**, 1108 (1956).

(and the spectral behavior of n and k) for adsorbed films on metals. Secondly, the practicability of the approach is tested experimentally by studying a 1 molar dispersion of the dye tetraphenylporphine (TPP) in collodion in a 31 Å. film on metal. The application of the method to chemical problems has yielded several interesting results which will be presented in paper II.

Theory

The theory of the polarimetric method for determining the optical properties of thin films has been discussed by several authors.[7-9] It will be presented in the following only in sufficient detail to make understandable the equations essential in the analysis of optical data.

When plane polarized light is reflected from a metal surface at other than normal incidence it becomes elliptically polarized, in general. The ellipticity may be characterized by the phase difference, Δ, between the components of the light vibrating in the plane of incidence and perpendicular to the plane of incidence, and the amplitude ratio, $\tan \psi$, of the two components. The alteration of polarization on reflection is determined by the optical properties of the surface. The presence of a thin film on the surface changes the effective optical constants of the surface and this, in turn, further modifies the ellipticity of the reflected light.

Our primary objective is to show how the optical constants of a surface film can be deduced from the modification of ellipticity of light. Before treating this, it is helpful to consider the equations of ordinary metallic reflection. These also will be useful later in the comparison of the polarimetric method with the method of measuring reflectivity in the inference of absorption spectra.

Reflection of Light by Metals.—Let the amplitude of the incident light beam, plane polarized at an azimuth of 45° to the plane of incidence, be $\sqrt{2}\,\mathcal{E}$. The components of the reflected wave perpendicular and parallel to the plane of incidence, $\mathcal{R}_s' = \mathcal{R}_s^0 \exp(i\,\delta_s')$ and $\mathcal{R}_p' = \mathcal{R}_p^0 \exp(i\delta_p')$, are governed by the Fresnel reflection equations

$$\mathcal{R}_s' = -\,\mathcal{E} \sin(\phi - \chi')/\sin(\phi + \chi') \qquad (1)$$

$$\mathcal{R}_p' = \mathcal{E} \tan(\phi - \chi')/\tan(\phi + \chi') \qquad (2)$$

where ϕ is the angle of incidence and χ' for a dielectric is the angle of refraction.[10] For a metal, χ' is a complex quantity defined, by analogy to Snell's law, by the relation

$$\sin \chi' = (\sin \phi)/\bar{n}' \qquad (3)$$

where $\bar{n}' = (n' - ik')$ is the complex refractive index of the metal with a real component of refractive index, n', and an absorption coefficient, k'. Accordingly, it can be seen that

$$\begin{aligned}\mathcal{R}_p'/\mathcal{R}_s' &= -\cos(\phi + \chi')/\cos(\phi - \chi')\\ &= \mathcal{R}_p^0 \exp(i\delta_p')/\mathcal{R}_s^0 \exp(i\delta_s')\\ &= \tan \psi' \exp(i\Delta') \qquad (4)\end{aligned}$$

Equation 4 directly relates ψ' and Δ' to χ' and hence to $\bar{n}'$. The determination of $\bar{n}'$ from ψ' and Δ' is required for the analysis of the next section. Explicit equations for this purpose are[11]

$$\begin{aligned}n' &= \{[(A^2 + B^2)^{1/2} + A]/2\}^{1/2}, \text{ and}\\ k' &= \{[(A^2 + B^2)^{1/2} - A]/[(A^2 + B^2)^{1/2} + A]\}^{1/2}\\ &\quad \text{where } A = u^2 - v^2 + \sin^2 \phi,\ B = 2uv\\ u &= (\sin \phi \tan \phi \cos 2\psi')/(1 + \cos \Delta' \sin 2\psi'), \text{ and}\\ v &= (\sin \phi \tan \phi \sin \Delta' \sin 2\,\psi')/\\ &\qquad (1 + \cos \Delta' \sin 2\,\psi') \qquad (5)\end{aligned}$$

The reflectivities R_p' and R_s' of a metal with refractive index $\bar{n}'$ are $|\mathcal{R}_p'/\mathcal{E}|^2$ and $|\mathcal{R}_s'/\mathcal{E}|^2$, respectively. The reflectivities R_p and R_s of a metal with a film can be computed from experimental values of ψ and Δ in exactly the same way by calculating an effective complex refractive index for the composite metal–film surface, using eq. 5, and substituting the result into Fresnel's eq. 1 and 2. Of principal concern to us in the following will be the reflectivity ratios R_p/R_p' and R_s/R_s'. In the event that it is desired to calculate reflectivity ratios from optical constants of the film instead of from ψ and Δ, it is convenient to use the relations developed by Fry.[12]

Optical Constants of Film from Ellipticity of Reflected Light.—The modification of the ellipticity on reflection from a surface with a film is conveniently characterized by a variable, σ, defined by

$$\mathcal{R}_p/\mathcal{R}_s = (\mathcal{R}_p'/\mathcal{R}_s')(1 + i\sigma) \qquad (6)$$

where the unprimed quantities refer to reflection from a surface with a film. It can be seen from eq. 4 that

$$1 + i\sigma = (\tan \psi/\tan \psi')[\cos(\Delta - \Delta') + i \sin(\Delta - \Delta')] \qquad (7)$$

The dependence of σ, which itself may be complex, upon the experimental variables, is[7,8]

$$\sigma = \frac{4\,\pi L}{\lambda} \sin \phi \cos \phi \left(\frac{\epsilon - 1}{\epsilon}\right) \times \frac{\epsilon'(\epsilon - \epsilon')}{(\epsilon' - 1)(\epsilon' - \tan^2 \phi)} \qquad (8)$$

provided the film is isotropic and much thinner than the wave length of light, where

ϵ = complex dielectric constant of the film
ϵ' = complex dielectric constant of the substrate
L = thickness of the film
λ = wave length of the incident light in air
ϕ = angle of incidence

The dielectric constant is the square of the complex refractive index, $\bar{n} = (n - ik)$, discussed in the preceding section, and can be determined experimentally for the substrate by measurements of Δ', ψ' and ϕ according to eq. 5.

The purpose of the present study was to investigate the feasibility of measuring, polarimetrically, the optical parameters characterizing an adsorbed film, namely the thickness, L, the refractive index, n, and the absorption coefficient, k. The variation of absorption coefficient with wave

---

(7) P. Drude, "Lehrbuch der Optik," Leipzig, 1900; *Ann. Physik*, **36**, 532 (1889); **36**, 865 (1889); **39**, 481 (1890).

(8) F. A. Lucy, *J. Chem. Phys.*, **16**, 167 (1948).

(9) O. S. Heavens, "Optical Properties of Thin Solid Films," Academic Press, Inc., New York, N. Y., 1955.

(10) The convention will be adopted in this paper of letting primed optical quantities represent reflection from a surface with no film and unprimed quantities represent reflection from a surface with a film. Sign conventions follow Drude's Lehrbuch, ref. 7.

(11) "Handbuch der Physik," Vol. 20, J. Springer, Berlin, 1928, pp. 240–245. Sign conventions used in eq. 5 above follow Drude, ref. 7, and hence eq. 5 differs from those in the Handbuch.

(12) T. C. Fry, *J. Opt. Soc. Am.*, **22**, 307 (1932).

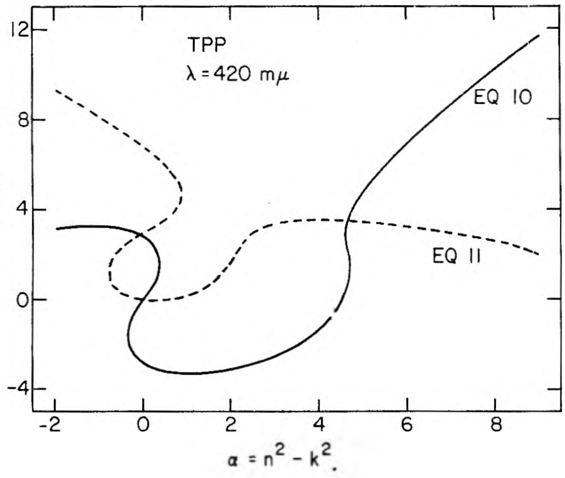

Fig. 1.—Functional relationship between optical constants of film according to eq. 10 and 11.

length, of course, constitutes the absorption spectrum of the film.

The real and imaginary parts of σ, which can be deduced from optical data with the aid of eq. 7, provide two independent relations. From these, any two of the film parameters, n, k and L, can be found using eq. 8, if the third is known. In practice, it is usually not difficult to recognize regions in the spectrum of a film where the absorption coefficient, k, is very small. At these wave lengths n and L can be calculated directly. If the optical thickness of a given film is considered to be constant over the spectrum, it then becomes possible to determine n and k for all wave lengths.

The mechanics of deducing the constants is simplified if the following transformations are made

$$a = n'^2 - k'^2 \qquad b = 2n'k'$$
$$\alpha = n^2 - k^2 \qquad \beta = 2nk$$
$$c = (4\pi/\lambda) \sin \phi \cos \phi$$

Equation 8 becomes

$$\sigma = \frac{cL}{(r^2 + s^2)} \times \frac{(a - ib)(\alpha - 1 - i\beta)(\alpha - i\beta - a + ib)(r + is)}{(\alpha - i\beta)} \qquad (9)$$

where

$$r = a^2 - a - a \tan^2 \phi - \tan^2 \phi - b^2$$

and

$$s = b(2a - 1 - \tan^2 \phi)$$

The determination of L may be accomplished by taking β to be zero, substituting eq. 9 into eq. 7, and solving for α and L as described by Lucy.[8] The thicknesses found in this manner, to be sure, are valid at best only at wave lengths where k is negligible, but the appropriate value to be taken can be recognized by inspection in favorable cases.

Once L has been found the equations can be solved for α and β, from which n and k may be calculated. The simultaneous equations resulting from the substitution of eq. 9 into eq. 7 are

$$0 = \beta^3 y + \beta^2 (\alpha x + G) + \beta(\alpha^2 y + H) + x (\alpha^3 - \alpha^2 a - \alpha^2 + \alpha a) - yb(\alpha^2 - \alpha) - \alpha^2(r^2 + s^2) (\tan \psi/\tan \psi') \times [\sin(\Delta - \Delta')]/cL \qquad (10)$$

and

$$0 = -\beta^3 x + \beta^2 (\alpha y + M) + \beta(-\alpha^2 x + N) + y(\alpha^3 - \alpha^2 a - \alpha^2 + \alpha a) + xb (\alpha^2 - \alpha) + \alpha^2 (r^2 + s^2) \times [(\tan \psi/\tan \psi') \cos(\Delta - \Delta') - 1]/cL \qquad (11)$$

where

$$x = ar + bs$$
$$y = as - br$$
$$G = -x(a + 1) - by - (r^2 + s^2) (\tan \psi/\tan \psi') \times [\sin(\Delta - \Delta')]/cL$$
$$H = bx - ay$$
$$M = -y(a + 1) + bx + (r^2 + s^2) [(\tan \psi/\tan \psi') \times \cos(\Delta - \Delta') - 1]/cL$$
$$N = ax + by$$

The solution of eq. 10 and 11 for α and β is readily accomplished by the Newton-Raphson Method[13] with the aid of an electronic computer. In Fig. 1 is shown the functional relation between α and β according to eq. 10 and 11 for a film 31 Å. thick. It may be noted that a spurious solution and a trivial solution with $\alpha = \beta = 0$ exist in addition to the desired solution, so that some care must be taken in making the initial guesses of α and β for solution by successive approximation.

Experimental

Polarization Spectrometer.—Polarization spectrometers similar in principle to the instrument used in this investigation have been described in the literature.[14] A 1000-watt tungsten filament projection bulb was used for a light source. Some effort was made to use a xenon arc lamp, which has a more intense emission in the ultraviolet, but its stability was found to be insufficient for precise measurements. The light beam was focused on the entrance slit of a Bausch and Lomb Model 33-86-40 grating monochromator. The emergent beam, with a band width of 1.5 mμ, was focused at infinity by a quartz collimating lens and passed through a calcite Glan-Thompson polarizing prism set at an azimuth of 45° to the plane of incidence. The resultant polarized light was reflected from the specimen slide which was held vertically by light spring clips to an adjustable specimen stage. After reflection, the ellipticity of the light was determined by means of a quartz Babinet-Soleil compensator and the analyzer of a Rudolph Model 80-200 photoelectric polarimeter. The analyzer was equipped with a search unit of a Photovolt Model 520-M multiplier photometer. Power supplies for the light source and photometer were stabilized to 0.5%.

The compensator was specially constructed by the Gaertner Scientific Company with thin wedges giving a compensation at 400 mμ of approximately 10° per turn of the micrometer screw. The fineness of subdivision of the micrometer scale permitted readings with a sensitivity of 0.01°.

In the following experiments an angle of incidence of 68.45° was used. The fast axis of the compensator was set parallel to the plane of incidence. In this position, the settings of the compensator and analyzer for maximum extinction of the reflected light are essentially independent of each other.[15]

Photometeric balancing of the analyzer for maximum extinction of the reflected light was done by the "Method of Symmetric Angles."[16] The average deviation within a set of analyzer settings was about 0.005°. A similar technique was used for balancing of the compensator. The average deviation in the determination of the phase difference between the two components of elliptically polarized light was seldom greater than 0.015°.

In making an experimental run, a clean slide was mounted on the specimen stage. The monochromator was set at the smallest wave length for which readings were desired and the compensator and analyzer readings for maximum extinc-

---

(13) H. Margenau and G. M. Murphy, "The Mathematics of Physics and Chemistry," Second Edition, D. Van Nostrand Co., Inc., Princeton, N. J., 1956.

(14) A. B. Winterbottom, *J. Opt. Soc. Am.*, **38**, 1074 (1948).

(15) R. E. Hartman, *ibid.*, **41**, 244 (1951).

(16) H. J. Rudolph, *ibid.*, **45**, 50 (1955).

tion of the reflected light were recorded. The wave length setting was increased and the procedure repeated. After readings had been completed over the desired spectral range for the clean surface, a film was deposited upon the slide and the readings were repeated.

Preparation of Films.—The chromium surfaces used in the investigation were cut from commercial chromium-plated steel ferrotype plates. The 1″ × 1″ slides were polished by hand on Buehler Ltd. finest quality microcloth impregnated with Linde A alumina. The polishing was done in a water-bath. The slides were rinsed with doubly distilled water, dried over the flame of a Meker burner and held briefly in the hottest part of the flame. These surfaces gave clear breath figures and readily formed films of *n*-octadecylamine by adsorption from a 0.08% solution of the amine in cetane.

The $\alpha,\beta,\gamma,\delta$-tetraphenylporphine (TPP) used was the product of a reaction of pyrrole with benzaldehyde and contained a large concentration of α, β, γ, δ-tetraphenyl chlorine. The crude product was dissolved in benzene and percolated through a column of activated alumina. No further purification was attempted. The TPP and an equal amount by weight of collodion solids were dissolved in *n*-amyl acetate. A drop of this dilute solution was spread on a clean slide and the film was formed as the solvent evaporated.

There were two reasons for dispersing the dye in a collodion matrix. Since the optical theory for films has been fully developed only for isotropic films, the collodion was introduced to discourage the preferential orientation normally expected for dye molecules at an interface. Secondly, it was hoped that the collodion would tend to inhibit aggregation of dye molecules and lead to an absorption spectrum similar to that found in solution.

Results

Table I shows the data obtained from readings taken for a clean chromium surface and the surface with a film of collodion and TPP. For the sake of brevity, the intervals listed are twice as great as those actually measured. The film thickness listed in Table I was calculated at each wave length assuming $k = 0$. The resultant values for L were found to vary inversely with absorption by the film. The actual film thickness was estimated from the values obtained at wave lengths where the solution spectrum showed little absorption and the calculated thickness approached an upper limit. The calculated thicknesses weighted most heavily in this estimate are underlined in Table I. A value of 31 Å. was considered to be the most probable thickness and the refractive indexes and absorption coefficients were calculated on this basis. Figure 2 shows the absorption coefficient and index of refraction plotted as a function of the wave length. These may be compared with the absorption spectrum of a solution of the TPP in benzene, plotted in Fig. 3.

TABLE I

RESULTS FOR COLLODION FILM 1.1 *M* IN TETRAPHENYLPORPHINE ON CHROMIUM (ϕ = 68.45°)

λ	Δ	Δ'	ψ	ψ'	L, Å.[a]
330	101.170	110.467	35.095	34.062	29.81
350	104.499	113.330	34.832	34.037	26.71
370	107.581	116.145	34.525	33.745	27.14
390	111.009	118.927	34.726	34.176	24.45
410	114.595	122.317	33.981	34.151	16.37
420	115.054	123.919	34.140	34.511	17.20
440	117.885	126.934	34.394	34.041	26.93
460	121.485	130.078	33.908	33.492	28.08
470	123.111	131.435	33.720	33.220	29.40
480	124.484	132.625	33.600	33.032	30.89
500	126.944	134.605	33.511	33.082	28.61
510	128.288	135.768	33.523	33.161	27.66
520	129.177	136.975	32.878	32.509	29.09
530	129.805	137.167	32.188	31.765	29.22
540	130.055	137.219	32.413	31.949	30.11
550	131.552	138.566	32.845	32.387	30.47
560	131.778	139.066	31.682	31.258	30.64
575	132.899	139.636	31.447	30.992	30.60

[a] Calculated assuming $k = 0$.

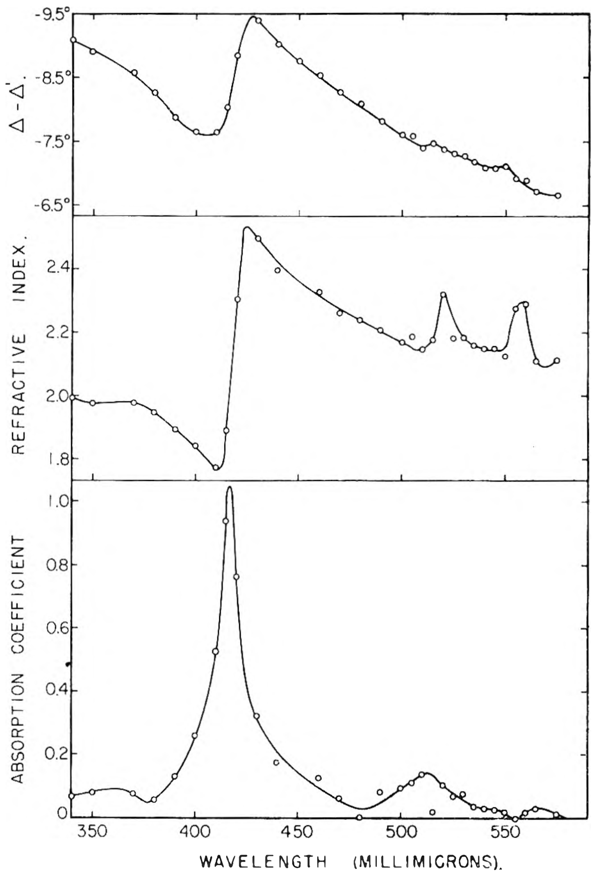

Fig. 2.—Calculated phase-shift and optical constants for a 31 Å. film of collodion 1 *M* in the dye tetraphenylporphine.

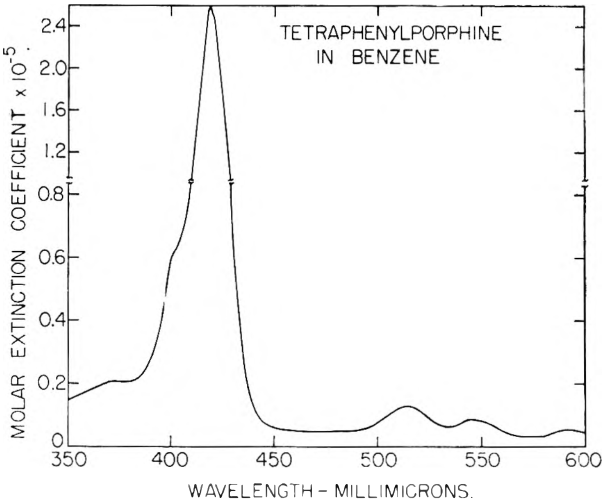

Fig. 3.—Absorption spectrum of bulk solution of tetraphenylporphine in benzene.

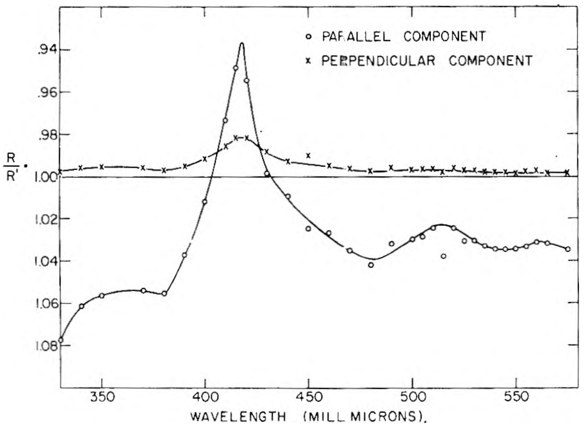

Fig. 4.—Ratio of reflectivity with film to reflectivity without film of tetraphenylporphine in collodion. Calculated from experimental values of ψ, ψ', Δ and Δ' using Fresnel's reflection equations.

An estimate of the standard error in the determination of n, k and L for the film arising from errors in the experimental determination of Δ, Δ', ψ and ψ' was made. The sensitivity of optical constants to ellipticity measurements is given in eq. 7 and 8, from which standard errors can be determined by the relation

$$\sigma_u = \left\{\sum_i (\partial u/\partial \xi_i)^2 \sigma_{\xi_i}{}^2\right\}^{1/2} \tag{12}$$

where u represents n, k or L and ξ_i represents ψ, ψ', Δ and Δ'. For the sake of argument, standard errors in amplitudes and phases were taken as 0.01 and 0.02°, respectively, slightly in excess of the values suggested by the scatter in experimental readings in individual runs at a given wave length. Calculation by eq. 12 for λ = 410 mμ implied errors of about 0.01 for n and k. At 480 mμ the calculated error was 0.3 Å. for L. These values include no allowance for disturbances in apparatus between readings without films and readings with films, for the time-dependent contamination of surfaces and mechanical instability in the equipment or for errors in null settings of the instrument. Nevertheless, the scatter in the experimental values of n and k indicates that the calculated uncertainties are not greatly off in magnitude. In this work, the absolute accuracy is less important than the precision with which the inflections representing absorption bands can be detected.

Molar extinction coefficients were estimated for the various absorption peaks in the film spectrum so that a direct comparison of the molecular film and bulk solution properties could be made. This was done by comparing the defining relations for the absorption coefficient, k, and the molar extinction coefficient, E, which are

$$\ln (I_0/I) = 4\pi kL/\lambda \tag{13}$$

and

$$\log (I_0/I) = Ecd \tag{14}$$

where c represents the molar concentration and d the length of the absorption cell in cm. It is necessary to know the density of the dye–collodion film mixture in order to calculate c. From a knowledge of the composition of collodion solids and the density of dyes of structure similar to TPP, it was estimated that the film had a density of 1.4, and that c was about 1.1 M.

A comparison of solution and film absorption parameters is presented in Table II. It must be pointed out that the scatter of the experimental values of k in the present data precludes any very definitive characterization of the weakest absorption by the film in the vicinity of 550 mμ. The distinct anomaly in the refractive index for the film at 550 mμ strongly suggests the existence of a peak corresponding to the weak peak in dilute solution, however.

TABLE II

MOLAR EXTINCTION COEFFICIENTS FOR ABSORPTION PEAKS IN SPECTRA OF $\alpha,\beta,\gamma,\delta$-TETRAPHENYLPORPHINE IN SOLUTION AND IN 31 Å. FILM

	Concn., moles/l.	λ_{max}, mμ	k	Molar extinction coefficient
Solution	6.5×10^{-5}	418		26.0×10^4
(benzene)		514		1.3×10^4
		547		0.9×10^4
Film	1.1	417	1.0	12×10^4
		513	0.14	1.3×10^4
		$\backsim$550	$\backsim$0.03	$\backsim 0.3 \times 10^4$

It is interesting to consider what the outcome would be if direct measurements of reflected intensities were made analogous to those determined in the infrared by Francis and Ellison.[5] The completeness of optical information derived by the present method makes it possible to calculate the result of such a measurement as discussed in the section on metallic reflection. The calculated ratio, R/R', of reflectivity with film to reflectivity without the 31 Å., 1 M dye film is shown in Fig. 4.

Discussion

This work confirms the feasibility of using a polarimetric method to study absorption spectra of surface films of molecular thickness. The spectrum of TPP determined polarimetrically was found to agree very satisfactorily with the solution spectrum, considering the difference in solvents and the enormous difference in concentration. Not only was the strong principal peak found but also the weak subsidiary peaks.

As is well-known, the anomalous dispersion exhibited by the refractive index of a medium in the vicinity of an absorption maximum serves as a useful measure of the absorption itself. The anomalies are clearly evident for TPP in Fig. 2. It is instructive to observe from eq. 7 and 8 or, most directly from eq. 10, that for very thin films of low absorption coefficient

$$(\Delta - \Delta') \sim K(n^2 - 1)/n^2$$

where K is generally a smoothly varying, mild function of the wave length. Therefore, it follows that the "phase dispersion," $(\Delta - \Delta')$, should itself exhibit the anomalies associated with the refractive index of the film. This is verified readily by inspection of Fig. 2 and suggests that a simple measurement of $(\Delta - \Delta')$ may be sufficient in some cases to characterize the spectrum of adsorbed films. The "ellipsometer readings" of reference 6, which are approximately proportional to $(\Delta - \Delta')$, made use of this property.

The appreciable manifestation of the absorption spectrum in the reflectivity ratio, illustrated in Fig. 4, is impressive testimony of the efficiency of interaction of a given dye molecule with radiation incident upon its geometric area. The reflectivity ratio for the component of radiation parallel to the plane of incidence is, as expected, much more sensitive to the film than the ratio for the perpendicular component. The strikingly faithful reproduction of the detail of the absorption spectrum by the reflectivity ratio indicates that a direct photometric inference of electronic absorption spectra of molecular films on metals should prove entirely practicable.

Acknowledgment.—We wish to thank Mr. B. L. Carroll for assistance in the spectrometer measurements and numerical computations. We also are greatly indebted to the National Institutes of Health for making available the polarimetric apparatus used in this research.

THE BISULFATE ACID CONSTANT FROM 25 TO 225° AS COMPUTED FROM SOLUBILITY DATA[1]

By M. H. Lietzke, R. W. Stoughton and

Chemistry Division, Oak Ridge National Laboratory, Oak Ridge, Tenn.

T. F. Young

Department of Chemistry, University of Chicago, Chicago, Illinois

Received August 4, 1961

The bisulfate acid constant has been computed from 25 to 225° from data on the solubility of Ag_2SO_4 in H_2SO_4 solutions. In the small temperature range (25–55°) where a comparison can be made the results agree very well with those of other investigations. In addition the thermodynamic constants for the reaction $HSO_4^- = H^+ + SO_4^=$ are presented.

In a previous series of papers a study of the solubility of Ag_2SO_4 in a variety of electrolyte media has been described.[2] In this work it was shown that the concentration dependence of the logarithms of the equilibrium quotients and solubility products could be expressed by single-parameter expressions of the type $S\sqrt{I}/(1 + A\sqrt{I})$, where S is the appropriate Debye–Hückel limiting slope, I is the ionic strength of the solution, and A is an adjustable parameter. These expressions were shown to hold for ionic strengths as high as 4.0 and from 25 to 275°. In the present paper the data on the solubility of Ag_2SO_4 in H_2SO_4 solutions are used to compute values of the bisulfate dissociation constant K_2

$$HSO_4^- = H^+ + SO_4^= \quad K_2$$

from 25 to 225°.

Method of Calculation.—In carrying out the calculations it was assumed that only the species Ag^+, H^+, $SO_4^=$ and HSO_4^- existed in a solution of Ag_2SO_4 dissolved in H_2SO_4. If s is the molal solubility of Ag_2SO_4 in H_2SO_4 of molality m, and x and y are taken as the $SO_4^=$ and H^+ concentrations, then the molality solubility product of the Ag_2SO_4 is given by

$$S = 4s^2x \tag{1}$$

By conservation of acid hydrogen, the HSO_4^- concentration is seen to be equal to $2m$ less the H^+ concentration y, and the bisulfate dissociation quotient becomes

$$Q_2 = \frac{xy}{2m - y} \tag{2}$$

The equation for the conservation of total sulfate is

$$m + s = 2m - y + x$$

or

$$s + y - x - m = 0 \tag{3}$$

Equations 1, 2 and 3 represent three equations in the three unknowns (s, x and y) which may be solved for any particular values of S and Q_2.

In accordance with previous calculations[2] it was assumed that

$$\ln Q_2 = \ln K_2 + 4S_T\left[\frac{\sqrt{I}}{1 + A\sqrt{I}}\right] \tag{4}$$

and

$$\ln S = \ln 4s_0^3 + 6S_T\left[\frac{\sqrt{I}}{1 + P\sqrt{I}} - \frac{\sqrt{3s_0}}{1 + P\sqrt{3s_0}}\right] \tag{5}$$

where K_2 is the bisulfate acid constant, S_T is the Debye–Hückel limiting slope at temperature T for a singly charged ion, s_0 is the solubility of Ag_2SO_4 in water at temperature T, P and A are adjustable parameters and I is the ionic strength of the solution, given by

$$I = m + s + 2x \tag{6}$$

Thus, the over-all problem involves the evaluation of $\ln K_2$, A and P by a non-linear least squares procedure, subject to the restrictions represented by equations 1, 2, 3 and 6.

The criterion adopted in solving the above set of equations was that $\sum_i (s_{\text{obsd.}} - s_{\text{calcd}})_i^2$ be a minimum, where the summation is taken over the different solubilities (at different values of m) at any tem-

---

[1] This paper is based upon work performed for the United States Atomic Energy Commission at the Oak Ridge National Laboratory operated by Union Carbide Corporation.

[2] M. H. Lietzke and R. W. Stoughton, *J. Phys. Chem.*, **63**, 1183, 1186, 1188, 1190, 1984 (1959); **64**, 816 (1960).

perature. Accordingly a series expansion of s was made in terms of the partial derivatives with respect to the three adjustable parameters K_2, P and A as

$$s_{\text{obsd.}} = s_{\text{calcd.}} + \frac{\partial s}{\partial \ln K_2}\Delta \ln K_2 + \frac{\partial s}{\partial P}\Delta P + \frac{\partial s}{\partial A}\Delta A \tag{7}$$

in which $s_{\text{calcd.}}$ and the partial derivatives are evaluated for approximate values of $\ln K_2$, P and A. The increments $\Delta \ln K_2$, ΔP and ΔA then give approximate corrections to these parameters. Since, however, the solubility of Ag_2SO_4 has been measured as a function of temperature in only three different concentrations of H_2SO_4 it was decided to omit the evaluation of $\partial s/\partial P$ directly. Rather, values of $\ln K_2$ and A were obtained over a selected range of values of P. Then that value of P was chosen for the final calculations which gave a most nearly temperature independent value of A (consistent with previous calculations[2] in which it was shown that temperature independent values of P and A could be used to describe the system).

The procedure used to carry out the computation of $\ln K_2$ was as follows.

(a) Quadratic analytical expressions representing the solubilities of Ag_2SO_4 in each concentration of H_2SO_4 (0.1, 0.5 and 1.0 m) *vs.* temperature were obtained by the method of least squares. These equations were solved at 25° intervals from 25 to 225° to give the solubilities.

(b) At each temperature a preliminary value of I was computed (with equation 6) for each solubility from an estimated (first approximation) value of the sulfate concentration x and the experimental values of m and s. (In subsequent iterations the calculated values of s and x are used in computing I.)

(c) The preliminary value of I was substituted into equations 4 and 5 along with initial guesses (*i.e.*, first approximations) of the values of $\ln K_2$ and A, and the selected value of P.

(d) With the values of Q_2 and S so obtained equations 1, 2 and 3 were solved simultaneously by the Newton–Raphson method,[3] which lends itself readily to computations on a high speed computer. The method involves linearizing the non-linear equations 1 and 2 by expansion in a Taylor's series through the first derivative to give equations 8 and 9, respectively

$$s + (s_0/2x_0)x - (s_0 + S/3\,s_0x_0) = 0 \tag{8}$$

$$y_0x + (x_0 + Q_2)y - (x_0y_0 + 2mQ_2) = 0 \tag{9}$$

where the subscript 0 refers to initial estimates on the values of s, x and y. The solutions of equations 1, 2 and 3 then are obtained by solving (itetatively) the linear equations 8, 9 and 3 using standard matrix techniques until converged values of s, x and y result. While equations 8 and 9 are only approximate (because only first derivatives are used in the Taylor's expansion), no error results, *i.e.*, the final converged values obtained are the correct solutions for the non-linear equations 1 and 2 and the linear equation 3.

(e) After the converged values of s, x and y had been obtained approximate values for the partial derivatives $\partial s/\partial \ln K_2$ and $\partial s/\partial A$ were computed for each solubility by incrementation of the current estimate of $\ln K_2$ and A by 1% and the assumption that

$$\frac{s(\ln K_2 + \delta) - s(\ln K_2)}{\delta(\ln K_2)} \simeq \frac{\partial s}{\partial \ln K_2}$$

$$\frac{s(A + \delta) - s(A)}{\partial A} \simeq \frac{\partial s}{\partial A}$$

(f) The values of the partial derivatives for each solubility at a particular temperature then were used to form a matrix

$$X = \begin{pmatrix} \left(\dfrac{\partial s}{\partial \ln K_2}\right)_1 & \left(\dfrac{\partial s}{\partial A}\right)_1 \\ \left(\dfrac{\partial s}{\partial \ln K_2}\right)_2 & \left(\dfrac{\partial s}{\partial A}\right)_2 \\ \left(\dfrac{\partial s}{\partial \ln K_2}\right)_3 & \left(\dfrac{\partial s}{\partial A}\right)_3 \end{pmatrix}$$

where the subscripts $_1$, $_2$, $_3$ denote the solubilities in the three concentrations of H_2SO_4. The matrix X was transposed to give X^T and the matrix product X^TX was formed

$$X^TX = \begin{pmatrix} \sum\limits_i \left(\dfrac{\partial s}{\partial \ln K_2}\right)_i^2 & \sum\limits_i \left(\dfrac{\partial s}{\partial \ln K_2}\right)_i \left(\dfrac{\partial s}{\partial A}\right)_i \\ \sum\limits_i \left(\dfrac{\partial s}{\partial \ln K_2}\right)_i \left(\dfrac{\partial s}{\partial A}\right)_i & \sum\limits_i \left(\dfrac{\partial s}{\partial A}\right)_i^2 \end{pmatrix}$$

(g) A vector V was computed as

$$V = \begin{pmatrix} \sum\limits_i \left[(s_{\text{obsd}} - s_{\text{calcd}})\dfrac{\partial s}{\partial \ln K_2}\right]_i \\ \sum\limits_i \left[(s_{\text{obsd}} - s_{\text{calcd}})\dfrac{\partial s}{\partial A}\right]_i \end{pmatrix}$$

As mentioned previously the vector solution, $\Delta \ln K_2$ and ΔA, of the matrix equation

$$X^TX\begin{pmatrix} \Delta \ln K_2 \\ \Delta A \end{pmatrix} = V$$

constituted corrections for modifying the initial estimates of $\ln K_2$ and A. This procedure (steps b through g) was repeated with the new values of $\ln K_2$ and A and with the most recently calculated values of s, x, y and I until two successive values of both $\ln K_2$ and A differed by less than 0.1%. Then the entire calculation (steps b through g) was repeated with a series of values of P. (It should be mentioned that steps e through g represent an application of the standard least squares technique.)

(h) The computations were repeated for 25° intervals from 25 to 225° (the highest temperature at which solubility data were available). Then the values of $\ln K_2$ were chosen corresponding to that value of P for which the value of A was most nearly temperature independent, *i.e.*, $P = 0.72$. (Actually the values of $\ln K_2$ and A were not particularly sensitive to the values of P. A variation in the value of P from 0.6 to 0.8 caused a maximum deviation in the value of $\ln K_2$ of only 2%.)

(i) The values of $\ln K_2$ obtained as a function of temperature were fitted by the method of least squares to give equation 10.

$$\ln K_2 = -\frac{1283.108}{T} + 12.31995 - 0.04223215T \tag{10}$$

where T is the absolute temperature.

---

[3] H. Margenau and G. M. Murphy, "The Mathematics of Physics and Chemistry," D. Van Nostrand Co., Inc., New York, N. Y., 1943, p. 475.

Results and Discussion

The values of ln K_2 obtained in this work were compared with those of previous investigators. The value of K_2 at 25° as calculated from equation 10 is 0.01032, which compares very well with reported values.[4] The only previous work as a function of temperature was that of Young, Klotz and Singleterry[5] in which K_2 was determined over the range of 5 to 55° and an equation 11 was obtained for K_2 *vs.* temperature to 155° by utilization of the conductivity data of Noyes.[6]

$$\ln K_2 = -\frac{1785.390}{T} + 15.99658 - 0.04892367T \quad (11)$$

In Table I are summarized values of log K_2 *vs.* temperature as computed from the solubilities at each temperature, as calculated from equation 10, and as obtained from equation 11.

TABLE I

VALUES OF LOG K_2 AS A FUNCTION OF TEMPERATURE

t	$-\log K_2$ (from solubilities)	$-\log K_2$ (eq. 10)	$-\log K_2$ (eq. 11)
25	1.891	1.987	1.988
50	2.374	2.301	2.318
75	2.699	2.636	2.677
100	3.010	2.987	3.059
125	3.334	3.352	3.460
150	3.688	3.728	3.876
175	4.087	4.113	
200	4.489	4.506	
225	4.941	4.905	

In Table II are summarized the thermodynamic constants for the reaction

$$HSO_4^- = H^+ + SO_4^=$$

from 25 to 225° as computed by using equation 10.

All calculations in this paper were carried out on an IBM-7090 computer.

TABLE II

THERMODYNAMIC CONSTANTS FOR THE REACTION $HSO_4^- = H^+ + SO_4^=$

t	ΔF^0, cal.	ΔH^0, cal.	ΔS^0, e.u.
25	2.712	− 4.911	−25.6
50	3.403	− 6.214	−29.8
75	4.200	− 7.623	−34.0
100	5.102	− 9.136	−38.2
125	6.108	−10.750	−42.4
150	7.219	−12.480	−46.5
175	8.436	−14.310	−50.7
200	9.757	−16.240	−54.9
225	11.183	−18.280	−59.1

It is interesting to note that the entropy of dissociation of HSO_4^- is negative and attains a higher negative value the higher the temperature. A similar effect was found[2] for the dissociation of UO_2SO_4 into UO_2^{++} and SO_4^{--}, and for the dissolution of Ag_2SO_4. Thus it appears that the formation of SO_4^{--} in water increased the amount of "order" or "structure" shown by the solvent at any temperature and that this effect is much greater the higher the temperature.

Acknowledgments.—The authors wish to thank Dr. H. A. Levy and Mrs. M. P. Lietzke for helpful advice on the mathematical procedures and the computer programming.

---

(4) R. A. Robinson and R. H. Stokes, "Electrolyte Solutions," Academic Press, Inc., New York, N. Y., 1955, p. 374.

(5) I. M. Klotz and C. R. Singleterry, Theses, University of Chicago, 1940; R. A. Robinson and R. H. Stokes, "Electrolyte Solutions," Academic Press, Inc., New York, N. Y., 1955 p. 376; T. F. Young, L. F. Maranville and H. M. Smith, "The Structure of Electrolytic Solutions," edited by W. J. Hamer, John Wiley and Sons, Inc., New York, N. Y., 1949, Chap. 4; T. F. Young, unpublished work.

(6) A. A. Noyes, "The Electrical Conductivity of Aqueous Solutions," The Carnegie Institution of Washington, Washington, D. C., 1907.

THERMODYNAMIC PROPERTIES OF SOME OXIDES OF NITROGEN[1]

BY I. C. HISATSUNE

Department of Chemistry, Pennsylvania State University, University Park, Pa.

Received August 4, 1961

Available spectroscopic and structural data have been used to calculate the thermodynamic functions for N_2O_3, N_2O_4 and N_2O_5, and dissociation equilibria of these oxides. For the N_2O_5 dissociation, the necessary functions for NO_3 radical were estimated from vibrational frequencies calculated with Urey–Bradley force constants. These data together with those obtained from other sources lead to the following estimated properties for ideal gases at one atmosphere and 25°.

	C_p^0(cal./deg. mole)	S^0(cal./deg. mole)	ΔH_f^0 (kcal./mole)	ΔF_f^0 (kcal./mole)
NO_3	11.22	60.36	16.95	27.36
N_2O_3	15.68	73.92	20.00	33.49
N_2O_4	18.47	72.73	2.54	23.66
N_2O_5	20.22	85.00	3.35	28.18

Introduction

The oxides of nitrogen, which form a "happy hunting ground"[2a] for chemical kineticists and have been subjected to extensive kinetic investigations,[2b] are of considerable interest in air pollution, geophysics[3] and recently in astrophysics[4] as well. There are approximately twenty of these oxides

---

(1) Supported by the PHS Grant RG-8192 and the Air Force Geophysics Research Directorate.

(2) (a) F. Daniels, *Chem. Eng. News* **33**, 2370 (1955); (b) see for recent reviews S. W. Benson, "The Foundation of Chemical Kinetics," McGraw-Hill Book Co., Inc., New York, N. Y., 1960.

(3) L. E. Miller, "The Chemistry and Vertical Distribution of the Oxides of Nitrogen in the Atmosphere," U. S. Air Force Geophysical Research Paper No. 38, AFCRC-TR-56-207, 1954.

(4) C. C. Kiess, C. H. Corliss and H. K. Kiess, *Science*, **131**, 1319 (1960); F. J. Heyden, C. C. Kiess and H. K. Kiess, *ibid.*, **130**, 1195 (1959).

including ions which have been characterized chemically. However, with only few exceptions, the physical properties such as the important thermodynamic functions for these compounds have not been established satisfactorily. These oxides, especially the higher oxides, are reactive and often exist in equilibrium mixtures so that they are difficult to handle experimentally. Direct calorimetric measurements on them do not appear possible and one must resort to estimation of thermodynamic functions from statistical calculations using spectroscopic data.

Vibrational frequencies of the higher oxides can be obtained directly by using low temperature methods of infrared spectroscopy. At sufficiently low temperatures, the compounds can be stabilized so that satisfactory spectra can be obtained. Furthermore, the interpretation of these low temperature data is usually simplified because the equilibria are shifted to one extreme. Even when frequencies cannot be determined experimentally, we now have sufficient normal coördinate analysis data to allow us to make reasonable estimates of the force constants and calculate these frequencies. These calculated frequencies are reliable enough to be used in the computations of thermodynamic functions. In this paper we report the thermodynamic functions for N_2O_3, N_2O_4 and N_2O_5, and their dissociation equilibria estimated from spectroscopic and limited kinetic and thermochemical data.

Calculations

Statistical equations and physical constants necessary to calculate the standard thermodynamic functions were taken from Pitzer's textbook.[5] Equations for internal rotations and tables of harmonic oscillator contributions from this source also were used. Each nitrogen oxide was assumed to behave as an ideal gas with all internal vibrations being harmonic and with only rigid rotations allowed. Vibrational frequencies and molecular geometries used in our calculations were as follows.

N_2O_3.—The geometry of this oxide was estimated previously from the interpretation of its vibrational spectrum in terms of Urey–Bradley force field calculations.[6] The best estimates were nitroso bond 1.12 Å., nitro bond 1.18 Å. nitro angle 134°, nitroso ON–N angle 110° and NN bond 2.08 Å. Vibrational frequencies were taken to be 1863, 1589, 1297, 783, 627, 407, 313 and 253 cm.$^{-1}$. We assumed free rotation about the NN bond as suggested from the entropy consideration.[7]

N_2O_4.—Accurate geometric parameters reported by Smith and Hedberg[8] were used for this molecule, *i.e.*, NN bond 1.750 Å., nitro bond 1.180 Å., nitro angle 133.7°, and V_h molecular symmetry. Frequencies used were 1748, 1710, 1373, 1261, 812, 750, 675, 480, 385, 260 and 50 cm.$^{-1}$.[9]

N_2O_5.—The geometric parameters for the structure O_2NONO_2 were estimated to be: nitro bond 1.18 Å., nitro angle 137°, central NO bond 1.47 Å., and central N–O–N angle 127°. These estimations were made from N_2O_4 and HNO_2 structures.[8, 10] We also tried 150° for the central N–O–N angle, but this produced only insignificant differences in the calculated results. Frequencies of 2 × 1728, 1338, 1247, 860, 3 × 743, 614, 577, and 2 × 353 cm.$^{-1}$ were employed in the calculations. The two torsional modes were assumed to be free rotations. One additional frequency corresponding to the central N–O–N angle bending mode could not be determined experimentally. This frequency was taken to be 170 cm.$^{-1}$, which forced the calculated entropy to agree with the experimental value.[11] The vibrational spectrum of this molecule and the structure will be discussed elsewhere.

NO_3.—Structural and spectroscopic data for this free radical are lacking. Such information therefore was deduced in the following manner. The molecular symmetry of NO_3 was taken to be D_{3h} because, according to Walsh's LCAO–MO correlation diagram,[12] this radical is formed by the removal of one electron from a bonding MO in NO_3^- with no change in molecular symmetry. From the changes in bond distance in N_2 and N_2^+, we estimate that there will be about 2% elongation of the NO bond in NO_3^- when one bonding electron is removed. Thus, the estimated bond distance and angle in the radical are 1.27 Å. and 120°.

Vibrational frequencies for the planar modes were calculated from the equations given by Janz and Mikawa for the Urey–Bradley force field treatment of D_{3h} tetra-atomic systems.[13] The Urey–Bradley force constants for the radical were estimated as follows. The K_{NO} was found to be 3.50 millidyne/Å. from an approximate linear relationship between K_{NO} and r_{NO} for the nitrogen oxides N_2O_4, NO_2, NO_2^-, NO_3^-, and the nitryl halides XNO_2. The Urey–Bradley force constants for these species, except for the nitrate ion, had been reported earlier.[14] The nitrate K_{NO} was taken from the work of Janz and Mikawa.

The bending constant H was taken to be the same as in NO_3^- but was corrected for the scaling bond distance to give 0.53 millidyne/Å. This bending constant was found in our earlier calculations[14] to be related to the quadratic non-bonded atom interaction constant F through the sum $F + 2H$. Among structurally related molecules this sum for the nitro group appeared to be relatively invariant: $ClNO_2$, 2.65; O_2NNO_2, 2.66; ONO_2^-, 2.67. Thus F for the radical was evaluated from $F + 2H = 2.67$ with $H = 0.53$ to get $F = 1.61$ millidyne/Å. The remaining linear repulsive constant F' was taken to be $-0.1\ F$ as is usually done. The calculated planar mode frequencies were 2 × 1158, 940 and 2 × 704 cm.$^{-1}$. The out-of-

---

[5] K. S. Pitzer, "Quantum Chemistry" Prentice-Hall, Inc., New York, N. Y., 1953.

[6] J. P. Devlin and I. C. Hisatsune, *Spectrochim. Acta*, **17**, 218 (1961).

[7] I. C. Hisatsune and J. P. Devlin, *ibid.*, **16**, 401 (1960).

[8] D. W. Smith and K. Hedberg, *J. Chem. Phys.*, **25**, 1282 (1956).

[9] I. C. Hisatsune, J. P. Devlin and Yasuo Wada, *ibid.*, **33**, 714 (1960).

[10] L. H. Jones, R. M. Badger and G. E. Moore, *ibid.*, **19**, 1599 (1951).

[11] J. D. Ray and R. A. Ogg, Jr., *ibid.*, **26**, 984 (1957).

[12] A. D. Walsh, *J. Chem. Soc.*, 2301 (1953).

[13] G. J. Janz and Y. Mikawa, *J. Mol. Spectroscopy*, **5**, 92 (1960).

[14] I. C. Hisatsune, J. P. Devlin and S. Califano, *Spectrochim. Acta*, **16**, 450 (1960); J. P. Devlin and I. C. Hisatsune, *ibid.*, **17**, 206 (1961).

plane wagging frequency was taken to be 765 cm.$^{-1}$, the same as in gaseous nitric acid.[15]

Results

Thermodynamic functions calculated on the basis of molecular geometries and frequencies described above for N_2O_3, N_2O_4, N_2O_5 and NO_3 are listed, respectively, in Tables I to IV. These results together with those available for nitric oxide[16] and NO_2[17] then were used to calculate the enthalpy and free energy changes and equilibrium constants for the dissociation equilibria of N_2O_3, N_2O_4 and N_2O_5.

TABLE I

THERMODYNAMIC FUNCTIONS FOR N_2O_3 (CAL./DEG. MOLE)

T, °K.	C_p^0	$(H^0 - H_0^0)/T$	$-(F^0 - H_0^0)/T$	S^0
100	10.35	9.27	50.63	59.90
200	13.50	10.64	57.45	68.09
250	14.71	11.34	59.90	71.24
275	15.23	11.67	61.00	72.67
298.16	15.68	11.96	61.96	73.92
300	15.72	11.98	62.03	74.01
325	16.17	12.29	63.00	75.29
350	16.60	12.58	63.92	76.50
400	17.39	13.13	65.64	78.77
500	18.73	14.12	68.68	82.80
600	19.82	14.99	71.33	86.32
700	20.69	15.74	73.70	89.44
800	21.39	16.41	75.84	92.25
900	21.94	16.99	77.81	94.80
1000	22.38	17.51	79.63	97.14
1100	22.73	17.97	81.32	99.29
1200	23.02	18.38	82.90	101.3
1300	23.25	18.74	84.38	103.1
1400	23.44	19.07	85.79	104.9
1500	23.61	19.37	87.11	106.5

TABLE II

THERMODYNAMIC FUNCTIONS FOR N_2O_4 (CAL./DEG. MOLE)

T, °K.	C_p^0	$(H^0 - H_0^0)/T$	$-(F^0 - H_0^0)/T$	S^0
100	11.06	9.57	47.57	57.14
200	15.11	11.32	54.71	66.04
250	16.93	12.27	57.34	69.61
275	17.76	12.73	58.53	71.26
298.16	18.47	13.15	59.58	72.73
300	18.53	13.18	59.66	72.84
325	19.25	13.62	60.73	74.35
350	19.92	14.04	61.76	75.80
400	21.16	14.86	63.69	78.55
500	23.24	16.34	67.17	83.50
600	24.86	17.63	70.26	87.89
700	26.13	18.76	73.07	91.86
800	27.12	19.74	75.64	95.38
900	27.89	20.61	78.01	98.62
1000	28.49	21.37	80.27	101.6
1100	28.98	22.04	82.44	104.5
1200	29.37	22.63	84.24	106.9
1300	29.69	23.16	86.24	109.4
1400	29.95	23.64	87.85	111.5
1500	30.16	24.07	89.45	113.5

TABLE III

THERMODYNAMIC FUNCTIONS FOR N_2O_5 (CAL./DEG. MOLE)

T, °K.	C_p^0	$(H^0 - H_0^0)/T$	$-(F^0 - H_0^0)/T$	S^0
100	11.89	10.53	57.75	68.28
200	16.13	12.24	65.54	77.77
250	18.30	13.23	68.37	81.61
275	19.32	13.74	69.66	83.40
298.16	20.22	14.21	70.79	85.00
300	20.28	14.25	70.87	85.12
325	21.19	14.75	72.04	86.78
350	22.04	15.24	73.15	88.39
400	23.58	16.19	75.24	91.43
500	26.11	17.93	79.05	96.98
600	28.03	19.46	82.46	101.9
700	29.49	20.79	85.56	106.4
800	30.61	21.95	88.41	110.4
900	31.48	22.97	91.06	114.0
1000	32.15	23.84	93.51	117.4
1100	32.69	24.63	95.83	120.5
1200	33.12	25.32	97.95	123.4
1300	33.47	25.94	100.1	126.0
1400	33.76	26.49	102.0	128.5
1500	34.00	26.98	103.9	130.8

TABLE IV

THERMODYNAMIC FUNCTIONS FOR NO_3 (CAL./DEG. MOLE

T, °K.	C_p^0	$(H^0 - H_0^0)/T$	$-(F^0 - H_0^0)/T$	S^0
100	7.97	7.95	42.66	50.61
200	9.02	8.15	48.21	56.35
250	10.10	8.42	50.06	58.48
275	10.68	8.60	50.87	59.47
298.16	11.22	8.79	51.57	60.36
300	11.26	8.80	51.62	60.42
325	11.83	9.01	52.34	61.35
350	12.37	9.23	53.01	62.25
400	13.21	9.62	54.25	63.87
500	14.96	10.59	56.54	67.13
600	16.11	11.42	58.54	69.96
700	16.92	12.15	60.36	72.51
800	17.51	12.79	62.02	74.81
900	17.95	13.34	63.56	76.90
1000	18.28	13.82	64.99	78.81
1100	18.53	14.23	66.33	80.56
1200	18.73	14.60	67.58	82.18
1300	18.89	14.92	68.76	83.69
1400	19.02	15.21	69.88	85.09
1500	19.12	15.47	70.94	86.41

The enthalpy change at 0°K. for the N_2O_3 dissociation equilibrium was calculated from the experimental data reported by Beattie and Bell.[18] Verhoek and Daniels[19] also reported some data for this equilibrium, but entropy calculations reported earlier[7] showed that their data were not as reasonable as those reported by Beattie and Bell. However, ΔH_0 for the NO_2–N_2O_4 equilibrium was evaluated from the experimental data reported by Verhoek and Daniels.[19] In the case of N_2O_5 dissociation equilibrium, ΔF_0(460°K.) of + 6.3 kcal./mole reported by Schott and Davidson[20] was used to estimate ΔH_0. The thermodynamic functions

---

[15] H. Cohn, C. K. Ingold and H. G. Poole, *J. Chem. Soc.*, 4272 (1952).

[16] "Selected Values of Properties of Hydrocarbons," Natl. Bur. of Standards Circ. No. 461 (1947).

[17] A. P. Altshuller, *J. Phys. Chem.*, **61**, 251 (1957).

[18] I. R. Beattie and S. W. Bell, *J. Chem. Soc.*, 1681 (1957).

[19] F. H. Verhoek and F. Daniels, *J. Am. Chem. Soc.*, **53**, 1250 (1931).

[20] G. Schott and N. Davidson, *ibid.*, **80**, 1841 (1958).

Table V

Thermodynamic Functions for $N_2O_3 \rightleftarrows NO + NO_2$ (ΔH_0^0 = 8.63 Kcal./Mole)

T, °K.	ΔH^0 (kcal./mole)	ΔF^0 (kcal./mole)	K_{eq} (atm.)
100	9.24	6.16	3.46×10^{-14}
200	9.59	2.92	6.58×10^{-4}
250	9.66	1.25	8.15×10^{-2}
275	9.68	0.42	4.61×10^{-1}
298.16	9.69	−0.38	1.91
300	9.69	−0.45	2.11
325	9.69	−1.28	7.20
350	9.69	−2.13	2.13×10
400	9.67	−3.82	1.22×10^{2}
500	9.59	−7.19	1.38×10^{3}
600	9.48	−10.53	6.87×10^{3}
700	9.33	−13.86	2.12×10^{4}
800	9.18	−17.16	4.88×10^{4}
900	9.01	−20.44	9.20×10^{4}
1000	8.84	−23.71	1.52×10^{5}

Table VI

Thermodynamic Functions for $N_2O_4 \rightleftarrows 2NO_2$ (ΔH_0^0 = 12.69 Kcal./Mole)

T, °K.	ΔH^0 (kcal./mole)	ΔF^0 (kcal./mole)	K_{eq} (atm.)
100	13.32	9.35	3.61×10^{-21}
200	13.62	5.24	1.86×10^{-6}
250	13.66	3.15	1.78×10^{-3}
275	13.65	2.09	2.16×10^{-2}
298.16	13.64	1.12	1.51×10^{-1}
300	13.64	1.04	1.74×10^{-1}
325	13.62	−0.01	1.01
350	13.59	−1.05	4.52
400	13.50	−3.14	5.18×10
500	13.29	−7.27	1.51×10^{3}
600	13.03	−11.36	1.38×10^{4}
700	12.74	−15.40	6.44×10^{4}
800	12.43	−19.40	2.00×10^{5}
900	12.10	−23.36	4.71×10^{5}
1000	11.76	−27.24	8.95×10^{5}

Table VII

Thermodynamic Functions for $N_2O_5 \rightleftarrows NO_2 + NO_3$ (ΔH_0^0 = 20.51 Kcal./Mole)

T, °K.	ΔH^0 (kcal./mole)	ΔF^0 (kcal./mole)	K_{eq} (atm.)
100	21.05	17.97	5.25×10^{-40}
200	21.29	14.78	7.01×10^{-17}
250	21.33	13.15	3.19×10^{-12}
275	21.33	12.33	1.58×10^{-10}
298.16	21.33	11.57	3.28×10^{-9}
300	21.33	11.52	4.08×10^{-9}
325	21.32	10.70	6.40×10^{-8}
350	21.32	9.88	6.78×10^{-7}
400	21.27	8.26	3.08×10^{-5}
500	21.23	4.99	6.56×10^{-3}
600	21.15	1.76	2.30×10^{-1}
700	21.05	−1.47	2.88
800	20.94	−4.68	1.90×10
900	20.82	−7.87	8.17×10
1000	20.70	−11.07	2.62×10^{2}
1100	20.55	−14.23	6.70×10^{2}
1200	20.41	−17.44	1.50×10^{3}
1300	20.25	−20.52	2.82×10^{3}
1400	20.10	−23.65	4.92×10^{3}
1500	19.93	−26.77	7.94×10^{3}

for equilibria of N_2O_3, N_2O_4 and N_2O_5 dissociations are given in Tables V to VII.

Discussion

Among the higher oxides of nitrogen considered here, only N_2O_4 has a known molecular structure. No experimental geometric parameters are available for the remaining oxides. Even the vibrational frequencies are not known unequivocally. It was necessary to assume free internal rotations in both N_2O_3 and N_2O_5 and the torsional frequency in N_2O_4 also was estimated theoretically. All vibrational frequencies of NO_3 and one bending frequency in N_2O_5 were estimated values. In view of these uncertainties, we must consider the reliability of the calculated thermodynamic functions reported here.

It was found earlier[7] that the uncertainty in the geometry of N_2O_3 did not affect the calculated entropy value very much. When the geometric parameters were varied over a wide but reasonable range of values, only about 0.5 cal./deg. mole change was produced in the calculated total entropy at 25°. There are two other evidences which show that the estimated thermodynamic functions, at least in the room temperature region, are reliable. The change in entropy for the reaction $N_2O_3 \rightleftarrows NO + NO_2$ at 25° is 33.78 e.u. from our calculations, and this compares well with the experimental value of 33.25 ± 0.35 e.u. reported by Beattie and Bell.[18] If we take the standard heat of formation of NO_2 as 8.09 kcal./mole,[21] then the ΔH_f (25°) of 20.0 is obtained for N_2O_3 from our results This value is in agreement with that reported by Abel and Proisl.[22]

Extensive thermodynamic data on the NO_2–N_2O_4 system had been reported earlier by Giauque and Kemp.[23] Our free energy functions in the temperature range 275 to 400°K. are larger by approximately 0.5 to 0.3 e.u. than those reported by Giauque and Kemp. Our ΔH_0^0 of 12.69 kcal./mole may be compared to 12.88 kcal./mole estimated by these investigators. These differences are due to the use of more recent vibrational frequencies in our work. In order to check whether the torsional frequency deduced from the difference between the experimental and spectroscopic entropy was reasonable or not, we had calculated earlier[24] the C_p values in the temperature range of 20 to 260°K. for solid N_2O_4 using the method of Lord.[25] We also calculated the entropy of the solid at 262°K., and we obtained good agreement between the calculated and observed values for both the entropy and the heat capacities. Our assignment of the N_2O_4 spectrum also had been used by Monse[26] to calculate the equilibrium constant for the NO_2–N_2O_4 nitrogen isotope exchange reaction. Satisfactory agreement between

---

[21] "Selected Values of Chemical Thermodynamic Properties," Natl. Bur. Standards Circ. No. 500 (1952).

[22] E. Abel and J. Proisl, *Z. Elektrochem.*, **35**, 712 (1929) cited in ref. 23.

[23] W. F. Giauque and J. D. Kemp, *J. Chem. Phys.*, **6**, 781 (1938).

[24] I. C. Hisatsune, "Proceedings of International Meeting on Molecular Spectroscopy Bologna, Italy, 1959," Pergamon Press, London, in press.

[25] R. C. Lord, Jr., *J. Chem. Phys.*, **9**, 693 (1941).

[26] E. U. Monse, *ibid.*, **33**, 312 (1960).

experiment and theory was obtained there, too.

Adequate data are not available for either N_2O_5 or NO_3 to really test the reliability of our calculated thermodynamic functions. However, the results obtained here for these species and for the equilibrium are essentially the same as those estimated by Schott and Davidson,[20] and therefore they are probably as good as any estimates that can be made at this time. A few more thermochemical measurements on N_2O_5 and investigation of the vibrational spectrum of NO_3 by matrix isolation methods, for example, will help to remove some of the uncertainties.

In Table VIII the standard enthalpies and free energies of formation and the entropies of these oxides at 25° are summarized. The heat of formation of N_2O_5 is the value reported by Ray and Ogg[27] but it has been corrected to include the new results on NO_2 and N_2O_4.

TABLE VIII

STANDARD STATE ENTHALPY AND FREE ENERGY OF FORMATION AND ENTROPY OF SOME OXIDES OF NITROGEN AT 25°

	ΔHf^0 (kcal./mole)	ΔFf^0 (kcal./mole)	S^0 (cal./deg. mole)
NO_3	16.59	27.36	60.36
N_2O_3	20.00	33.49	73.92
N_2O_4	2.54	23.66	72.73
N_2O_5	3.35	28.18	85.00

---

(27) J. D. Ray and R. A. Ogg, Jr., *J. Phys. Chem.*, **61**, 1087 (1957).

A STUDY OF THE RATE OF ISOTOPIC EXCHANGE FOR Zn^{65} IN MOLTEN ZINC-ZINC CHLORIDE SYSTEMS AT 433-681°

BY A. G. BUYERS[1]

Hughes Research Laboratories, Malibu, California

Received August 4, 1961

It is the purpose of this research to identify the controlling rate and the mechanism for transfer of Zn^{65} from molten zinc to zinc chloride in stirred melts with constant interfacial area of contact. This has been accomplished by measuring the temperature dependence for the rate of exchange of Zn^{66} between molten zinc and zinc chloride in isothermal contact in the temperature range 433-681°. Accordingly, studies were carried out which included: one series of exchange experiments wherein both phases of this two phase melt were saturated with each other; and a second group of experiments using unsaturated phases. The temperature dependence for the exchange half-time expressed below applied, respectively, to these series $\log t_{1/2} = -1.220 + 2120/T$ and $\log t_{1/2} = -1.800 + 2092/T$. Interpretation of these results and examination of prior data have disclosed that the rate-controlling step for the transfer of Zn^{65} from molten zinc to zinc chloride is an interfacial reaction which may involve the formation and dissociation of Zn_2^{+2}. An average activation energy for this transfer process was calculated to be 9.8 ± 1 kcal./mole.

A survey of the literature revealed only the referenced research concerned with the kinetics and mechanism for attaining isotopic equilibrium in heterogeneous non-aqueous, inorganic, liquid systems at elevated temperatures.[2,3] In view of the increasing importance of this high temperature, physical chemical phenomenon in missile and nuclear technology, research was carried out to examine the rate of isotopic exchange for Zn^{65} in the system molten zinc-molten zinc chloride.

Experimental

Experimental procedures were designed to complete preparation of pure melt components and measurement of exchange half-time as a function of temperature in melts at solubility equilibrium as well as those in which saturation and exchange equilibria must be attained. All experiments were carried out at 650 ± 50 r.p.m. stirrer speed and in quartz tubes of internal diameter 29 mm.

1. **Preparation of Anhydrous Zinc Chloride.**—Mallinckrodt analytical grade hydrated zinc chloride was melted with ammonium chloride in a 4:1 weight ratio. Melt temperature was maintained at 300 ± 2° under a vacuum of 10^{-3} to 10^{-4} atmospheres until vigorous boiling ceased. Then the temperature of the system was held at 480 ± 2° until no further evaporation of ammonium chloride was noticeable. The dry product was removed into a dry box and transferred into a previously dried Vycor tube equipped with a quartz wool filter. The loaded tube was removed from the dry box and heated under partial vacuum to 400 ± 2°. Filtrates were removed and ground in a dry atmosphere. Chemical analysis of the final product revealed it to be pure anhydrous zinc chloride within the limit of analytical accuracy, *i.e.*, ±1% error.

2. **Zinc Metal Containing Zn^{65} as Radioactive Tracer.**—Cleaning of the non-radioactive zinc metal, analysis 99.99% zinc, for experiments in melts already at solubility equilibrium was accomplished by a dilute nitric acid wash followed immediately by a water rinse and drying. Irradiated precast zinc needles, nvt 10^{12} to 10^{14}, were added during experiment. These needles were precast to permit rapid introduction into the melt and were made light in weight to avoid breaking the apparatus.

For experiments in which unsaturated melt components were used, non-radioactive and irradiated zinc were melted with stirring under a dry helium atmosphere until a homogeneous distribution of Zn^{65} had been achieved. Acid wash, rinsing and drying were carried out as before.

3. **Experimental Apparatus.**—Apparatus used for carrying out exchange studies is described as a mechanical force pump, three-stage glass diffusion pump and Pyrex vacuum manifold, together with an inert gas drying train containing Drierite and magnesium perchlorate. A small Bodine motor with variable speed control was used to rotate a Pyrex shaft fitted with a graded seal to a quartz shaft with concurrently acting blades, four in each phase. This shaft was introduced into the standard taper fitter cap of the Vycor exchange chamber through a water-cooled, ground glass seal designed for stirring organic liquids. The melt itself was contained within an open quartz tube inserted into an outer Vycor sleeve. The cap at the top of the Vycor envelope was equipped with a standard taper glass plug which when removed permitted radioactive zinc needles to be dropped into the melt. At all times a positive pressure of dry, inert

---

(1) Work performed at Atomics International, a Division of North American Aviation, Canoga Park, California.

(2) (a) BNL-LMFR Report for September (1957); (b) PR CM-10A-Progress Report, Chemistry Metallurgy Division, Chalk River, April 1, 1957 to June 30, 1957.

(3) R. T. Lofberg, "An Investigation of the Heterogeneous Isotopic Exchange Between Sn(liquid) and $SnCl_2$(liquid)," Master of Science Thesis, Department of Chemistry, New Mexico Highlands University, June, 1956.

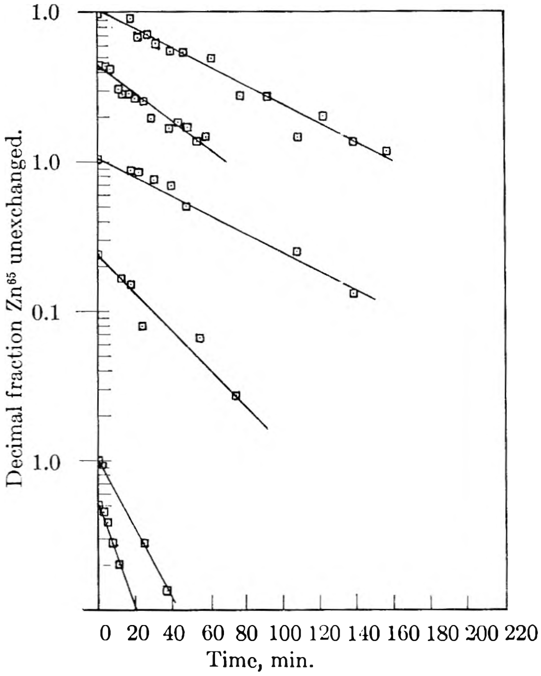

Fig. 1.—Isotopic exchange rates, Zn^{65}–ZnCl$_2$ (melts at solubility equilibrium, log decimal fraction Zn^{65} unexchanged *vs.* time in minutes). (From top to bottom curves—433, 513, 451, 591, 606, 681.)

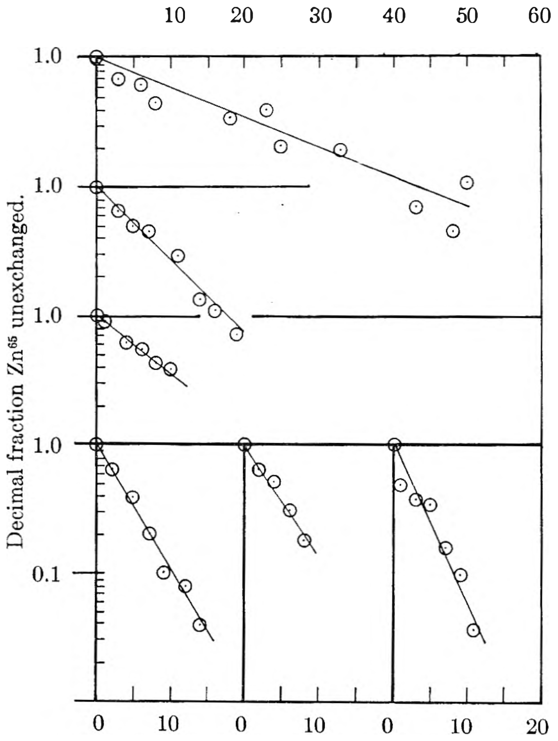

Fig. 2.—Isotopic exchange rates Zn^{65}–ZnCl$_2$ (melts not at solubility equilibrium, log decimal fraction Zn^{65} unexchanged *vs.* time in minutes). (From top to bottom curves—442, 503, 561; from left to right curves—624, 661, 668°.)

gas within the system prevented moisture from contacting the melt.

A one-quarter inch thick iron cylindrical sleeve encompassed the Vycor exchange chamber to provide an isothermal zone containing the two phase chemical system. Inside this sleeve a Pt + /Pt/10% Rh thermocouple attached to a potentiometer measured uncorrected melt temperatures. Heat was supplied by a 110 v. Marshall furnace used with a Chromel-Alumel thermocouple and Paravane Controller.

4. **Exchange Experiments in Melts at Solubility Equilibrium.**—Exchange experiments in melts at solubility equilibrium were initiated using a dry box in which pure, nonradioactive zinc and zinc chloride were placed into a quartz tube. The tube was inserted into the vacuum system under a dry helium flow, immediately after removal of a rubber stopper. The system was flushed twice with dry helium. After heating the melt to 440°, the stirring system was introduced and activated. The molten mass was rapidly heated to and held at the desired temperature for at least 18 hr. Weighed, precast, irradiated zinc metal needles were dropped into the melt through the opening at the top of the chamber. The stirring mechanism was reactivated after all of the needles had melted and the melt temperature had stabilized at that for operation. In these systems it was possible to carry out determination of exchange half times for more than one temperature using the same melt. After exchange equilibrium had been achieved for the initial addition of radioactivity, the melt temperature was increased and 18 hr. of agitated contact at the new temperature was permitted. A new addition of radioactive zinc needles was performed and determination was made of the rate of disappearance of Zn^{65} from the metal as a function of time.

The beginning of agitation was designated as zero time for exchange calculations. After stopping the stirrer, molten metal samples were removed using 3-mm. internal diameter Pyrex tubes attached to a hypodermic syringe. Sampling tubes were capped and inserted into the melt to the bottom of the metal phase prior to withdrawing molten metal samples. At withdrawal, the time was recorded. Samples were washed with water, dissolved in dilute nitric acid and diluted to 25 ml. One-ml. aliquots were counted using a Nuclear Chicago γ-scintillation well counter.

5. **Exchange Experiments in Melts not at Solubility Equilibrium.**—For experiments using zinc-zinc chloride systems not at solubility equilibrium, it was necessary to melt fresh salt and prepared radioactive metal together. Then the stirrer was inserted and activated at the temperature of experiment. Zero time again was the time of stirrer activation. Molten metal samples were withdrawn and used as in experiments with saturated melts.

6. **Limits of Accuracy for Experimental Data.**—The statistical error for γ-counting methods was $\pm 2\%$ of the total count for a given sample; of more significance is the definition of the limits of accuracy for the two most important experimental variables measured herein, *i.e.*, melt temperature and zero time for exchange.

A. **Temperature.**—During experiment it was not possible to insert a thermocouple directly into the stirred melt. Experimental temperatures were measured by means of a thermocouple inside the circular iron sleeve. These recorded temperatures were remeasured using a Leeds and Northrup potentiometer in conjunction with a Chromel-Alumel thermocouple immersed in an unstirred non-radioactive melt. Furnace temperature calibration curves, applicable to the kinetic data for melts initially at solubility equilibrium, were prepared. The data revealed that all furnace temperatures recorded must be corrected by adding 11° to yield actual melt temperatures to within ±2°.

Temperature *vs.* time plots were prepared for use as calibration curves for experiments in which initially solid, unsaturated melt components were melted together and then heated to the temperature for experiment. Since the exchange half-times were short (2.4–13.2 min.) for these experiments, mean melt temperatures were measured for recorded data corresponding to those time intervals near peak furnace temperatures. To determine real melt temperatures, measured experimental furnace temperatures must be corrected by the difference between peak furnace and mean melt values. As indicated in Table I, the magnitude of this correction increased with temperature from $-7°$ at a peak furnace temperature of 447 to $+24°$ at a peak furnace temperature of 651°. Temperatures for experiments in unsaturated melts were accurate to within ± the correction value for each peak furnace temperature.

B. **Zero Time for Exchange.**—As previously mentioned, zero time for exchange was taken as the time of stirrer activation. For exchange studies in melts initially at solubility equilibrium there were two sources of error in zero time inherent in the experimental method: first, the time for ex-

TABLE I

TEMPERATURE CORRECTIONS—EXCHANGE EXPERIMENTS WITH UNSATURATED MELTS

Peak furnace temp., °C.	Mean melt temp., °C.	Correction, °C.
447	440	− 7
525	532	+ 7
582	592	+10
628	646	+18
651	675	+24

change which occurred prior to melting of the radioactive zinc needles during their addition to the saturated zinc–zinc chloride melt. This exchange would take place during the passage of the solid zinc needles through the molten zinc chloride. The resulting error in zero time for exchange was found to be small. Second, after the radioactive zinc needles had melted into the molten zinc phase, Zn^{65} was not homogeneously distributed for periods of time varying from 1 to 3 min. Activation of the stirring mechanism held this period to a minimum, but the initial metal samples taken revealed inhomogeneity.

For kinetic experiments in zinc–zinc chloride melts initially not at solubility equilibrium, there was one major source of error in zero time for exchange. This was the time for exchange which took place after melting of the zinc chloride and during heating to the desired temperature for experiment. In this instance, negligible exchange would initially occur between molten zinc chloride and solid zinc. After the zinc melted, Zn^{65} would exchange into the zinc chloride from the molten zinc as the melt temperature was raised to that for operation. However, the stirrer was not activated until this latter furnace temperature was reached. Earlier experiments had revealed exchange half times which were 1.5 to 2 hr. in unstirred melts. Therefore, the exchange of Zn^{65} was small during the period of melting and heating to the temperature for experiment.

In summary, the magnitude of error in zero time for exchange for all melts was demonstrated by the deviation from time zero of plotted data (Figs. 1 and 2) at the initiation of each exchange experiment. This error did not exceed three minutes for melts initially at solubility equilibrium and was less than one minute for melts initially not at solubility equilibrium.

Results

Experimentally determined isotopic exchange rate data are plotted in Figs. 1 and 2. Summarized in Fig. 1 are data obtained from melts at solubility equilibrium. Data obtained from melts not at solubility equilibrium are found in Fig. 2. These representations have disclosed that the time of exchange was an exponential function of the fraction of radioisotope remaining in the zinc phase.

Calculations from raw to plotted data were carried out and summarized in Table II.

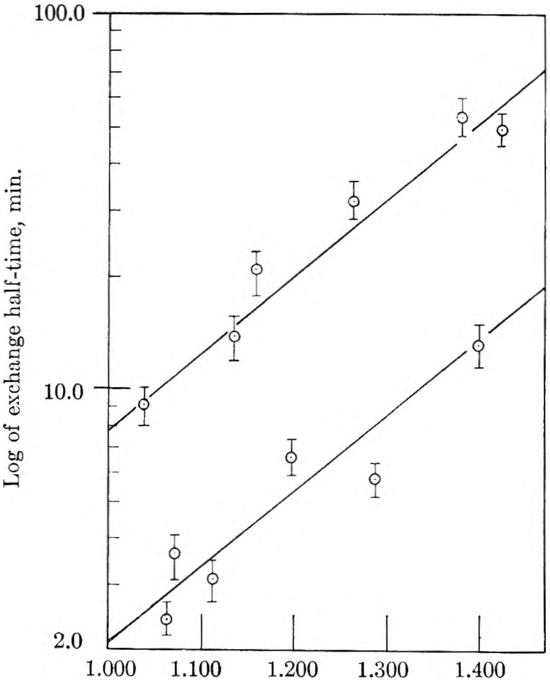

Fig. 3.—Arrhenius plot for isotopic exchange Zn^{65}–$ZnCl_2$, log $t_{1/2}$ in minutes *vs.* $1/T \times 10^3$ (2.0–100.0, 1.000–1.400) (melt at solubility equilibrium—top curve; melt not at solubility equilibrium—bottom curve).

For melts in which more than one rate of isotopic exchange was measured, successive specific activity calculations were made on the basis of the total counts present in the whole system at the attainment of the first equilibrium plus the added new radioactivity. Therefore, the fraction of Zn^{65} remaining in the metal phase at zero time was not 1.000 in all experiments. The half-time for exchange is that time at which the value of the fraction of Zn^{65} remaining in the zinc phase has decreased to one-half that at zero time. Exchange half-times and the corresponding temperatures at which they were measured are listed in Table III. A plot of the Arrhenius relation using these data was made in Fig. 3. Activation energies were calculated for the two slopes depicted and were found to be nearly equal at a value of 9.8 kcal./mole, accurate to within ±1.0 kcal./mole based on an error in slope of ±10%. The temperature dependence of the half-time for exchange for melts at solubility equilibrium was determined from the best line drawn by eye through the plotted data. It was written

$$\log t_{1/2} = -1.220 + 2120/T$$

For melts initially not at solubility equilibrium, the temperature coefficient was expressed by

$$\log t_{1/2} = -1.800 + 2092/T$$

It was interesting to note that the slopes of the two curves in Fig. 3 reflected the same controlling rate process, but a difference in the amount of exchange between melts initially at solubility equilibrium and in those in which this was not the case.

Discussion

It generally is assumed that the rates of inorganic reactions in molten high temperature systems are quite rapid and that equilibrium is achieved very soon after contacting of two liquid phases. As exchange occurs at the liquid–liquid interface reacting species are depleted at the interface in one phase and reaction products appear at the interface in the second liquid phase. In order for the exchange to continue, reacting material must diffuse through one liquid phase to the interface and product species must diffuse away from the interface through the second molten phase.

In this work the same area of liquid–liquid interfacial contact was maintained while each phase was stirred separately in an effort to replace diffusion to the interface with transport by turbulence. Nevertheless it follows that there are three competing processes which are concurrent, any one of which can be rate controlling. These are:

Table II

Equations for Calculation from Raw to Plotted Data

$$S_t = \frac{(\text{Zn}^{65}\ \gamma \text{ counts/min.})\ (\text{Aliquot factor})}{\text{Wt. of withdrawn Zn sample}} = \text{Zn}^{65} \text{ specific activity at time } t$$

$$S_0 = \frac{(\text{Total Zn}^{65}\ \gamma \text{ counts/min. at time } 0) - (\text{Total counts/min. withdrawn to time } t)}{\text{Total wt. of Zn phase at time, } t} = \text{specific}$$

activity at zero time

$$S_\infty = \frac{(\text{Total Zn}^{65}\ \gamma \text{ counts/min. at time } 0) - (\text{Total counts/min. withdrawn at time } t)}{\text{Total wt. of Zn in the two phase system}} = \text{specific}$$

activity at infinite time (exchange equilibrium)

$$\text{Decimal fraction Zn}^{65} \text{ unexchanged} = \frac{S_t - S_\infty}{S_0 - S_\infty}$$

Table III

Isotopic Exchange Rate Data

Zn^{65}-$ZnCl_2$

°C.	$10^3/T$ °K.	Exchange half-time, min.	Remarks
433	1.416	50	Melts at solubility equilibrium at beginning of exchange
451	1.381	54	
513	1.272	32	
591	1.157	21	
606	1.138	14	
681	1.048	9	
442	1.400	13.2	Melts fresh, not at solubility equilibrium at beginning of exchange
503	1.289	5.8	
561	1.199	6.6	
624	1.115	3.1	
661	1.071	3.6	
668	1.063	2.4	

(a) diffusion of reacting or product species through the liquid metal; (b) diffusion of reactants or products through the molten salt; and (c) reaction at the interface.

It seems reasonable that interfacial processes will be the slowest or controlling rate and that the role of diffusion within a phase may be fast in comparison. For ionic salts there exists some supporting evidence for this postulate. Experiments have been reported in which radioactive cerium was dissolved in liquid bismuth and contacted with the molten ternary eutectic, $MgCl_2$-KCl-NaCl.[2a] Experimental conditions included large interfacial area and thin liquid phases. Equilibrium was established for cerium extraction within 30 seconds, at a rate controlled by an unidentified interfacial process. Elsdon and Fletcher have studied the isotopic exchange between molten cadmium metal, spiked with Cd^{115}, and cadmium chloride,[2b] revealing complete exchange at 600° after 15 minutes. Their melts were contained in sealed quartz tubes which were oscillated to cause extremely intimate mixing of liquid phases. In a more covalent melt, further evidence for a rate-controlling interfacial reaction was found in an unpublished research in the liquid tin-stannous chloride system.[3] These workers have shown that a plot of exchange half-time *vs.* stirrer speed was hyperbolic, *i.e.*, as the exchange half-time approached zero the speed of the stirrer became infinitely large. Thus, the controlling rate for isotopic exchange was an interfacial one.

The activation energy for viscous flow of molten zinc for an average temperature of 850° was reported to be 3.09 kcal./mole.[4] Since in molten metals the activation energies for viscous flow and for self-diffusion are nearly equal, this activation energy, 3.09 kcal., is that for diffusion of Zn in itself in the liquid state. Reported research has disclosed that the activation energy for the diffusion of zinc in molten zinc bromide is 16.0 ± 3 kcal./mole in the temperature range 402–636°.[5] The structure of molten zinc chloride is not different appreciably from that of zinc bromide. Liquid phases of either salt at the same temperature have similar degrees of association, indicating zinc diffusion rates of the same order of magnitude in each covalent salt. It is concluded that the activation energy, 9.8 ± 1 kcal./mole, obtained experimentally by equilibration of molten zinc and zinc chloride, not initially homogeneous in Zn^{65}, reflects an interfacial process which is the controlling rate in the redistribution mechanism. However, this interfacial process has not been identified. The gross exchange rate difference between fresh melts and those at solubility equilibrium has disclosed that the isotopic interphase transfer rate is changed by the solution of zinc. Since zinc chloride is not appreciably soluble in zinc metal, *i.e.*, less than 0.05 mole % at 1000°,[6] and the solubility of zinc metal in zinc chloride at 498° is 0.182 mole %, it seemed likely that the solubility phenomenon causing the difference in rate was occurring in the zinc chloride phase. Corbett, Von Winbush and Albers have found that zinc dissolves in molten zinc halides by forming the subhalide, Zn_2X_2.[7] Thus it is reasonable to postulate that the transition of the salt–metal phase boundary by Zn^{65} is the result of the presence at the interface of the equilibrium, $2Zn^{++} + 2e^- \rightarrow Zn_2^{++}$. Excess divalent zinc is always available on the metal side of the phase boundary causing formation of monovalent zinc in the salt constituting the other interface material. Accordingly it is suggested, but unproven, that shifts in the equilibrium between di- and monovalent zinc is the mechanism by which Zn^{65} crosses the line of demarcation between phases.

---

(4) S. Glasstone, K. J. Laidler and H. Eyring, "The Theory of Rate Processes," McGraw-Hill Book Co., Inc., New York, N. Y., 1941, p. 496.

(5) E. and L. A. Wallen von Lars, *Z. Naturforschung*, **14**, 262 (1959).

(6) S. J. Yosim and E. B. Luchsinger, *Ann. N. Y. Acad. Sci.*, **79**, 1079 (1960).

(7) J. D. Corbett, S. Von Winbush and F. C. Albers, *J. Am. Chem. Soc.*, **79**, 3020 (1957).

Conclusions

The following conclusions are drawn from this study which has determined the temperature dependence for the rate of isotopic exchange of Zn^{65} between molten zinc and zinc chloride in the temperature range 433–681°:

1. The temperature dependence for the isotopic exchange half time for saturated melts is expressed by the equation

$$\log t_{1/2} = -1.220 + \frac{2120}{T}$$

2. The temperature dependence for the isotopic exchange half-time for fresh melts is expressed by the equation

$$\log t_{1/2} = -1.800 + \frac{2092}{T}$$

3. The controlling rate in the isotopic exchange mechanism is an interfacial process which involves the equilibrium between mono- and divalent zinc ions which can exist in molten zinc chloride–zinc metal systems.

Acknowledgment.—The author wishes to express his appreciation to the Atomic Energy Commission and Atomics International, under whose auspices this work was carried out.

INTRAMOLECULAR REARRANGEMENTS. IV. PHOTOLYSIS OF 2-PENTANONE-4,5,5-d_3[1]

By R. P. Borkowski[2] and P. Ausloos

National Bureau of Standards, Washington, D. C.

Received August 7, 1961

The photolysis of 2-pentanone-4,5,5-d_3 in the vapor and liquid states yields $D_2C{=}CHD$ and $DHC{=}CHD$. These ethylenes are formed by intramolecular rearrangements in which either an H or a D-atom is transferred to the carbonyl group.

$$D_2C{=}CHD + CH_3COCH_3 \ (I) \longleftrightarrow CH_3COCH_2CHDCD_2H + h\nu \longleftrightarrow DHC{=}CHD + CH_3COCH_2D \ (II)$$

In the vapor phase the quantum yield of ethylene is independent of concentration, temperature and intensity, whereas it decreases with increasing wave length and oxygen pressure. The effect of oxygen is more pronounced at longer wave lengths and lower temperatures, which indicates that oxygen interacts only with molecules excited to a low vibrational level. The ratio $C_2D_3H/C_2H_2D_2$ is independent of intensity, but increases with increasing wave length and ketone concentration, and diminishes with increasing temperature and oxygen pressure. These effects may be explained qualitatively in terms of the difference in the bond strength of C–D and C–H. In the liquid phase the quantum yield of ethylene increases, and the ratio $C_2D_3H/C_2H_2D_2$ decreases with increasing temperature. A difference of activation energy of about 1 kcal./mole was obtained for D and H transfer in the intramolecular rearrangement.

Introduction

In addition to undergoing radical dissociative processes, ketones which have hydrogen atoms in the γ-position relative to the carbonyl group decompose photochemically by an intramolecular rearrangement yielding olefins and simpler ketones.[3] Recent work on the photolysis of 2-hexanone-5,5-d_2,[4] in which indirect evidence has been obtained for the formation of the enol form of acetone, suggests that the rearrangement takes place *via* a six-membered ring. The isolation and identification of 1-methylcyclobutanol as a product from the photolysis of 2-pentanone in the liquid[5,6] and vapor[6] phases, respectively, provides further support for the postulation of a six-membered cyclic intermediate.

It has been observed recently that oxygen and nitric oxide inhibit the intramolecular rearrangement in the vapor-phase photolysis of 2-pentanone,[6] although no inhibition had been observed in earlier work on 2-hexanone.[7] In order to clarify this point a comprehensive study was undertaken of the effects of oxygen on the quantum yield of the intramolecular rearrangement at different wave lengths and temperatures. The compound chosen to be investigated was 2-pentanone-4,5,5-d_3 in the hope that a better understanding of the primary process may be obtained by studying the effect of various parameters not only on the quantum yield of the total ethylene, but also on the ratio of the two ethylenes produced in primary processes I and II.

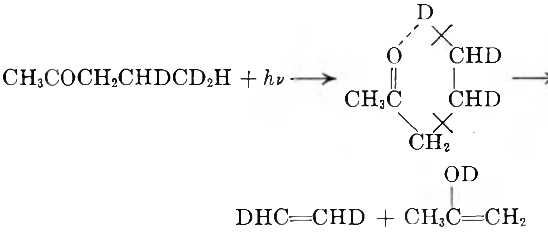

$$DHC{=}CHD + CH_3C(OD){=}CH_2 \quad (I)$$

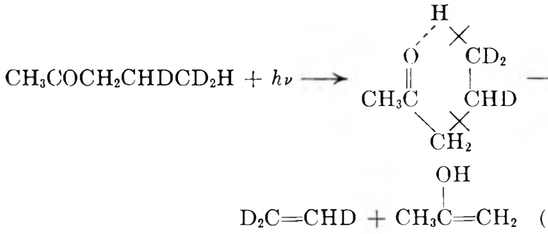

$$D_2C{=}CHD + CH_3C(OH){=}CH_2 \quad (II)$$

The effect of temperature and wave length on the liquid phase photolysis of this compound also was investigated.

---

[1] This research was supported by a grant from the U. S. Public Health Service, Department of Health, Education, and Welfare.

[2] National Academy of Sciences–National Research Council Postdoctoral Research Associate 1961–1962.

[3] For a review see: J. N. Pitts, Jr., *J. Chem. Educ.*, **34**, 112 (1957).

[4] R. Srinivasan, *J. Am. Chem. Soc.*, **81**, 5061 (1959).

[5] N. C. Yang and D-D. H. Yang, *ibid.*, **80**, 2913 (1958).

[6] P. Ausloos and R. E. Rebbert (to be published).

[7] V. Brunet and W. A. Noyes, Jr., *Bull. soc. chim. France*, 121 (1958).

Experimental

(a) **Apparatus.**—The vapor-phase experiments were conducted in a cylindrical quartz cell with a volume of approximately 175 cc. (10 cm. in length and 5 cm. in diameter). The cell was centered in an aluminum block furnace provided with double quartz windows. The temperature of the furnace was controlled to ±2°. The cell was attached to a standard type of vacuum system generally used in photochemical work.

An Osram-100 lamp was used in all of the direct photolytic experiments. A combination of Corning filters 7–54 and 0–54 was used, to obtain the 3130 Å group of lines, and a filter composed of 1,4-diphenylbutadiene in diethyl ether[8] isolated the 2537–2650 Å. lines. A neutral density filter was used to vary the intensity by a factor of twenty. A low-pressure mercury arc in combination with Corning filter 9–54 was used in the $Hg(^3P_1)$-sensitized experiments. Quantum yields were determined at 2537 and 3130 Å. by measuring the carbon monoxide yield from the photolysis of 3-pentanone at 87 and 145°, respectively.

The short wave length experiments were carried out by using a Hanovia hydrogen discharge lamp. The space between the lamp and the cell was evacuated. The cell was provided with thin high quality quartz windows which transmit down to 1700 Å.

The 2000-Curie Co^{60} source at the National Bureau of Standards was used to irradiate the vapor phase.

The liquid-phase experiments were conducted in a quartz cell having a volume of approximately 0.35 cc. (0.05 cm. in depth and 3 cm. in diameter). The cell was provided with two outlets, one of which could be sealed after filling, and the other with a breakseal. It was immersed in a Pyrex dewar flask which had double quartz windows. A water-bath was used for experiments conducted above 0°, and ethanol was used as the refrigerant for those conducted below 0°. A Hanovia SH-100 lamp was used in combination with Corning filter 0–53 to obtain the 3130 Å. group of lines, whereas the 0–53 filter was replaced by the 1,4-diphenylbutadiene filter to obtain the 2537–2650 Å. lines. The liquid phase work was conducted at constant incident intensity.

In the majority of the experiments conversions never exceeded 0.5%.

(b) **Analysis.**—The analytical system consisted of a solid nitrogen trap, a modified Ward Still, an automatic Toepler pump and a Toepler-gas buret. The carbon monoxide–methane fraction was removed at −210°. The C_2 fraction was removed at −170°. At the lower temperatures this fraction contained mainly C_2D_3H, $C_2H_2D_2$ and traces of C_2H_6. On a few occasions a C_3 fraction was removed at −150°. All of these fractions were analyzed mass spectrometrically using a Consolidated Mass Spectrometer Model 21-101. The analyses for fractions boiling higher than C_3 were not attempted.

(c) **Materials.**—2-Pentanone-4,5,5-d_3 was obtained from the Merck Company, Ltd. and was used without further purification. A chemical purity analysis by a Perkin–Elmer "A" column at 82° indicated that the compound was 98% pure. The 2% of impurity consisted mainly of compounds having boiling points higher than that of the 2-pentanone-4,5,5-d_3. Mass spectrometric analysis of this compound indicated that it contained a maximum of 4% 2-pentanone-d_2. This impurity would contribute primarily to the production of $C_2H_2D_2$, and thus the $C_2D_3H/C_2H_2D_2$ ratios indicated in the paper may be low by as much as 4%. Since the amount of $C_2H_2D_2$ produced from the impurity was not known, no correction was made for this error.

2-Pentanone and 3-pentanone were obtained from Eastman Kodak Co. and were distilled on a spinning band column. In each case a middle fraction was used.

Oxygen of assayed reagent grade quality was obtained from Air Reduction Company, Inc. It was contained in a one-liter bulb behind a mercury cut-off which was attached directly to the reaction section.

The two ethylenes, $D_2C{=}CHD$ and $DHC{=}CHD$, were obtained from Merck Company, Ltd. and their mass spectrometric cracking patterns were determined. The $D_2C{=}CHD$ spectrum had to be corrected for an impurity of 8.2% $C_2H_2D_2$, and the $DHC{=}CHD$ spectrum was corrected for an impurity of 3.6% $H_2C{=}CHD$. These cracking patterns were used to interpret the mass spectra obtained from the C_2 fraction.

Results and Discussion

Vapor Phase. The Effect of Concentration.—The results in Table I indicate that at 3130 and 2537 Å. the quantum yield of ethylene is within experimental error independent of concentration.[9] At 3130 Å. the ratio $C_2D_3H/C_2H_2D_2$ increases with concentration of the ketone, indicating that the probability of a D atom transfer to the carbonyl group decreases with increase in concentration. This observation may be interpreted in terms of a collision-induced vibrational deactivation of the excited ketone molecule. In view of the difference in bond strengths between C–H and C–D, it may indeed be expected that the higher the level of vibrational excitation the more a D atom transfer will be favored over a H atom transfer.

It may be noted that methyl acetate is about as efficient a deactivator as the ketone itself. In contrast, carbon monoxide, which has been added at a higher concentration of the ketone, had no noticeable effect on the ratio $C_2D_3H/C_2H_2D_2$. However, in the latter case the possibility exists that at a concentration of the ketone of 14×10^{-6} moles/cc., the ratio, $C_2D_3H/C_2H_2D_2$, has reached its maximum value. It indeed can be seen that the value of the ethylene ratio obtained at this concentration is comparable to the one obtained in the liquid phase photolysis at approximately the same temperature.

At 2537 Å. the effect of concentration on the ratio of the ethylenes is small, but the results follow the same trend as those at 3130 Å.

The Effect of Wave Length.—The results in Table I show that the quantum yield of ethylene increases with decrease in wave length. However, the sum Φ_{CO}[10] + Φ_{ethylene} remains approximately constant.

It can be seen that the ratio $C_2D_3H/C_2H_2D_2$ diminishes with decrease in wave length. This trend is consistent with the view that the probability of a D atom transfer to the carbonyl group as compared to a H atom transfer increases with increase in absorbed energy. It is interesting to note that the ratios $C_2D_3H/C_2H_2D_2$ obtained in the $Hg(^3P_1)$-sensitized experiments are higher than those obtained in the direct photolysis at 2537–2650 Å. This may be attributed to the possibility that not all of the energy absorbed by the Hg atom is transferred to the ketone as vibrational excitation energy. The laws of conservation of energy and momentum require that some of the energy will be imparted to the mercury atom as kinetic energy. Consistent with this interpretation are the somewhat lower values for the ratio 1-butene/2-butene recently found in the $Hg(^3P_1)$-sensitized decomposition of 4-methyl-2-hexanone as compared to the direct photolysis of this compound at 2537 Å.[11]

Experiments carried out with the hydrogen dis-

---

[8] M. Kasha, *J. Opt. Soc. Am.*, **38**, 929 (1948).

(9) It may be noted that a twenty-fold reduction of the intensity has no effect on either the quantum yield of ethylene or on the ratio of the ethylenes.

(10) The quantum yields of CO were measured at temperatures above 100° to ensure that all of the CH_3CO formed in the dissociative process underwent thermal decomposition.

(11) P. Ausloos, *J. Phys. Chem.*, **65**, 877 (1961).

TABLE I

VAPOR PHASE PHOTOLYSIS OF $CH_3COCH_2CHDCD_2H$. THE EFFECT OF CONCENTRATION, INTENSITY, TEMPERATURE AND WAVE LENGTH ON THE RATIO $D_2C{=}CHD/DHC{=}CHD$

	Ketone concn. (moles/cc.) $\times 10^6$	I_a (quanta/cc./sec.) $\times 10^{-13}$	T (°K.)	Φ_{CO}	$\Phi_{ethylene}$	$C_2D_3H/C_2H_2D_2$
(A) 3130 Å.						
(1) Effect of concn.	0.27	1.57	305		0.27	2.00
	0.85	1.57	305		.27	2.00
	1.60	1.57	305		.29	2.30
	1.65[a]	1.57	306		.34	2.72
	3.74	1.57	307		...	2.41
	14.1	1.57	305		.28	2.62
	14.1	0.078	305		.27	2.69
	14.2	0.078	306		.29	2.72
	14.1[b]	1.57	306		.27	2.67
	14.2	1.57	305		.24	2.72
(2) Effect of temp.	1.60	1.57	305		.29	2.30
	1.60	1.57	420		.32	1.47
	10.2	1.57	306		.27	2.60
	10.2	1.57	359		.26	1.93
	10.2	1.57	420	0.58	.28	1.42
(B) 2537–2650 Å.	1.38	0.1	306		.39	0.90
	2.82	.1	306		...	0.96
	14.1	.1	308		.40	1.00
	10.8	.1	398	0.42	.42	0.92
(C) Hg($^3P_1$)-sensitized	1.65	...	306		...	1.01
	14.3	...	307		...	1.16

[a] 16.5×10^{-6} moles/cc. CH_3COOCH_3 added. [b] 28.2×10^{-6} moles/cc. CO added.

charge lamp (1700–1900 Å.) at 300°K. gave a value of 0.65 for the ratio $C_2D_3H/C_2H_2D_2$, whereas radiolysis in the vapor phase gave a value of 0.58. It thus can be seen that at high energies the ratio $C_2D_3H/C_2H_2D_2$ approaches the statistical value of 0.5. In this connection it is of interest to point out that the mass-spectrum of 2-pentanone-4,5,5-d_3 at low energies (13 e.v.) yielded a value of 0.50 for the mass ratio 58/59. Because the masses 58 and 59 may be ascribed to the ions $CH_3\overset{\displaystyle OH}{\overset{|}{C}}{=}CH_2^+$ and $CH_3\overset{\displaystyle OD}{\overset{|}{C}}{=}CH_2^+$, respectively, it thus may be concluded there is no isotope effect for the olefin split-out process which the ketone ion undergoes.

Effect of Temperature.—The results of Table I indicate that at 3130 Å. an increase in temperature leads to a pronounced decrease in the ratio $C_2D_3H/C_2H_2D_2$. The decrease, which is due to an increase in vibrational energy is, as may be expected, considerably less at the shorter wave lengths. It can be seen also that the effect of concentration on the ratio of the ethylenes is less at 420 than at 305°K. The latter observation indicates a shorter dissociative lifetime of the excited ketone molecule at the higher temperatures.

Effect of Oxygen.—The results in Table II show that, at the wave lengths used in this work, the quantum yield of ethylene and the ratio $C_2D_3H/C_2D_2H_2$ decrease with increase in the pressure of oxygen. The effect of oxygen is considerably more pronounced at 3130 than at 2537 Å. It also is more important at 305 than at 420°. Thus, it appears that oxygen preferentially interacts with molecules excited to lower vibrational levels.

TABLE II

VAPOR PHASE PHOTOLYSIS OF $CH_3COCH_2CHDCD_2H$. THE EFFECT OF OXYGEN

(A) 3130 Å.

Ketone pressure = 26.5 mm. $I_a = 1.57 \times 10^{13}$, quanta/cc./sec.

P_{O_2}, mm.	T, °K.	$\phi_{ethylene}$	$C_2D_3H/C_2H_2D_2$
...	305	0.28	2.62
0.36	305	.24	2.62
.39	305	.24	2.62
.75	305	.18	2.36
1.5	305	.16	2.22
5.5	305	.10	1.96
26.2	305	.07	1.78
53.5	305	.08	1.65
56.0	305	.06	1.71
1.25	420	.18	1.44
28.0	420	.14	1.40

(B) 2537–2650 Å.

Ketone pressure = 26.5 mm. $I_a = 0.1 \times 10^{13}$, quanta/cc./sec.

P_{O_2}, mm.	T, °K.	$\phi_{ethylene}$	$C_2D_3H/C_2H_2D_2$
...	308	0.40	1.00
1.25	307	.42	1.00
33.0	307	.36	0.92
2.7	423	.39	0.88

The effect of oxygen on the quantum yield of ethylene in the photolysis of 2-pentanone has been reinvestigated at 3130 Å. and 305° K. The results (Table III), which are in good agreement with those recently reported,[6] show that the inhibitory effect of oxygen is not of the same magnitude as in the case of 2-pentanone-4,5,5-d_3, under the same experimental conditions. This difference may be due to a shorter dissociative lifetime of 2-

pentanone as compared to that of 2-pentanone-4,5,5-d_3. Since 2-pentanone has three H atoms in the γ-position, while 2-pentanone-4,5,5-d_3 has only one H atom and two more strongly bonded D atoms in this position, 2-pentanone would have a relatively higher probability of undergoing a molecular elimination than 2-pentanone-4,5,5-d_3.

TABLE III

VAPOR PHASE PHOTOLYSIS OF $CH_3COCH_2CH_2CH_3$. THE EFFECT OF OXYGEN AT 3130 Å.

Ketone pressure = 26.5 mm. I_a = 1.57 × 10^{13} quanta/cc./sec.

P_{O_2}, mm.	T, °K.	$\Phi_{ethylene}$
...	305	0.30
1.4	306	.25
6.4	303	.20
56.5	305	.13

Liquid Phase.—In the liquid phase (Table IV) the ratio $C_2D_3H/C_2H_2D_2$ decreases with an increase in temperature. A plot of log $C_2D_3H/C_2H_2D_2$ against $1/T$ yields a difference of 1.15 ± 0.15 kcal./mole in the activation energy for the transfer of a D atom and an H atom. Since the point obtained at 2537 Å. lies on the same line of the Arrhenius plot, the ratio $C_2D_3H/C_2H_2D_2$ is independent of wave length. It may indeed be expected that in the liquid phase, collisional deactivation is important. The mean energy level from which decomposition occurs does, however, depend on the equilibrium temperature. It is interesting to note that in the vapor phase at 3130 Å. the effect of temperature on the ratio $C_2D_3H/C_2H_2D_2$ is of the same order of magnitude. This is not surprising in view of the fact, as was pointed out before, that the ratios of the ethylenes in the two phases are comparable.

TABLE IV

LIQUID PHASE PHOTOLYSIS OF $CH_3COCH_2CHDCD_2H$

λ, Å.	T, °K.	$R_{ethylene}$ × 10^4 (cc./min.)	$C_2D_3H/C_2H_2D_2$
3130	198	5.40	6.40
3130	214	6.55	5.37
3130	273	27.8	3.44
2537	296	...	2.76
3130	343	26.2	2.12

The relative quantum yield of ethylene is within experimental error constant from 343 to 273°K. At temperatures below 273°K., however, there is a pronounced decrease in the yield of ethylene. Because ethylene can be formed only by a molecular elimination process, cage recombination cannot be invoked to explain the reduction in quantum yield. It is more likely that an activation energy of a few kcal./mole is required for the decomposition process.

NOTES

THE ELECTRODE POTENTIALS OF GERMANIUM: SOME COMMENTS ON THE INTERPRETATION BY LOVREČEK AND BOCKRIS

By J. I. Carasso, M. M. Faktor and H. Holloway

Post Office Research Station, Dollis Hill, London N.W. 2, England

Received March 20, 1961

In a recent paper[1] Lovreček and Bockris have described measurements of the electrode potentials of germanium over a range of pH in deoxygenated solutions. These potentials were interpreted as mixed potentials arising from the simultaneous occurrence of the two electrode reactions

$$Ge + H_2O \longrightarrow GeO + 2H^+ + 2e^- \quad (1)$$

$$2H^+ + 2e^- \longrightarrow H_2 \quad (2)$$

These authors showed that the resultant overall corrosion reaction

$$Ge + H_2O \longrightarrow GeO + H_2 \quad (3)$$

would be thermodynamically feasible only in solutions which are in equilibrium with a low pressure of hydrogen. (The maximum hydrogen pressure for which the postulated process is possible depends upon the form of GeO involved, being about 10^{-3} atm. for brown GeO and about 10^{-8} atm. for yellow GeO.) Such low hydrogen pressures might well have been attained in the solutions which Lovreček and Bockris swept with helium. However, replacement of the atmosphere of helium by one of hydrogen would render the postulated corrosion reaction 3 impossible. Yet the authors have reported that the measured potentials were unaffected by sweeping with hydrogen. The only possible conclusion appears to be that at least one of the two postulated electrode reactions 1, 2 does not contribute to the measured potentials, and that, if corrosion does occur in deoxygenated solutions, it does so by a process other than the postulated corrosion reaction 3.

A further objection to the interpretation by Lovreček and Bockris concerns their claim that the difference between the measured mixed potentials and the reversible potentials for the anodic reaction is not more than 20 mv. This result was derived from the assumption that the corrosion current in deoxygenated solutions and the exchange current for the anodic reaction are both about 2 × 10^{-6} amp. cm.$^{-2}$.

The value assumed for the corrosion current was derived from the results of Brattain and Garrett[2] who do not appear to have deoxygenated

---

[1] B. Lovreček and J. O'M. Bockris, *J. Phys. Chem.*, **63**, 1368 (1959).

[2] W. H. Brattain and C. G. B. Garrett, *Phys. Rev.*, **94**, 750 (1954); *Bell System Tech. J.*, **34**, 129 (1955).

their solutions. Harvey and Gatos[3] have found that the rate of dissolution of germanium in oxygenated aqueous solutions at 35° is about 1 μg. cm.$^{-2}$hr.$^{-1}$ which corresponds to a corrosion current of about 10^{-6} amp. cm.$^{-2}$. More recently an investigation of the polarized germanium electrode by Paleolog, Tomashov and Fedotova[4] has shown directly that the corrosion current in air saturated solutions is about 10^{-6} amp. cm.$^{-2}$ at 25°. Harvey and Gatos[3] found that in deoxygenated solutions the corrosion rate was much less than 1 μg. cm.$^{-2}$ hr.$^{-1}$ and this implies that the value of the corrosion current (2×10^{-6} amp. cm.$^{-2}$) assumed by Lovreček and Bockris is much too high.

The value of the exchange current for germanium oxidation quoted by Lovreček and Bockris was stated to be "extrapolated from Turner."[5] In fact, the reference quoted does not imply a value for this exchange current. Turner's paper gives the slope of the Tafel line for germanium dissolution and, less accurately, its position. In order to derive a value for the exchange current one also must know either the position and slope of the Tafel line for the reverse reaction (deposition of germanium from solution) or the reversible potential for the anodic reaction. Neither of these pieces of information is given by Lovreček and Bockris so that the source of their value for the exchange current is a matter for conjecture. There is the further point that Turner's Tafel slope applies at current densities where germanium has been shown to be oxidized to the quadrivalent state[6] and a different Tafel slope might apply to the postulated oxidation to the divalent state.

In the absence of any information about the relative magnitudes of the corrosion current and the exchange current, consideration must be given to the possibility that the mixed potential which is measured is very different from the reversible anodic potential. Thus, if the corrosion current is one or two orders of magnitude greater than the anodic exchange current, the reversible anodic potential may be 120 to 240 mv. more negative than the mixed potential. This would admit the possibility that the anodic reaction is oxidation of germanium to the quadrivalent state, for example

$$\mathrm{Ge} + 2\mathrm{H_2O} \longrightarrow \mathrm{GeO_2} + 4\mathrm{H^+} + 4e^- \text{ or}$$
$$\mathrm{Ge} + 3\mathrm{H_2O} \longrightarrow \mathrm{H_2GeO_3} + 4\mathrm{H^+} + 4e^-$$

Our conclusions are: 1. the potential of the germanium electrode in deoxygenated solutions is not determined by the corrosion reaction which has been postulated by Lovreček and Bockris. 2. Lovreček and Bockris' statement that the corrosion current and the exchange current for the anodic reaction are of comparable magnitude appears to be quite unjustified. Therefore the proximity of the measured potentials to reversible potentials calculated for the reaction

$$\mathrm{Ge} + \mathrm{H_2O} \rightleftarrows \mathrm{GeO} + 2\mathrm{H^+} + 2e^-$$

is not evidence that the latter reaction has any potential determining significance.

Acknowledgment is due to the Engineer-in-Chief of the British Post Office for permission to publish.

---

[3] W. W. Harvey and H. C. Gatos, *J. Electrochem. Soc.*, **105**, 654 (1958).

[4] E. N. Paleolog, N. D. Tomashov and A. Z. Fedotova, *Zhur. Fiz. Khim.*, **34**, 1027 (1960).

[5] D. R. Turner, *J. Electrochem. Soc.*, **103**, 252 (1956).

[6] F. Jirsa, *Z. anorg. u. allgem. Chem.*, **268**, 84 (1952).

THE REACTIVITY OF HYDROGEN ATOMS IN THE LIQUID PHASE: THE LACK OF EFFECT OF LINEAR ENERGY TRANSFER IN THE RADIOLYSIS OF HYDROCARBONS

By W. G. Burns

Chemistry Division, Atomic Energy Research Establishment, Harwell, Didcot, Berkshire, England

Received May 29, 1961

An encouraging trend in the radiation chemistry of alkane hydrocarbons has been the explanation of some features of the product yields in terms of the reaction behavior of atoms and radicals determined in the gas phase when generated by means other than radiation.[1,2] Hardwick[3] has recently attempted to show that the collision yields of many reactions of the type H· + paraffin, which occur in the radiolysis of the liquids, are roughly the same as found in the gas phase (*i.e.*, $\sim 10^{-7}$), the reason for high rate constants in the liquid phase being the large frequencies ($\sim 10^{14}$ sec.$^{-1}$ molecule^{-1}) for solute–solvent collisions.[4] The atoms considered are scavengeable, and not "hot."

If the kinetic interpretation [5,6] of the decrease in radiolytic hydrogen yield with scavengers present is correct, there are two characteristics of the hydrogen yields from pure cyclohexane and pure *n*-hexane which seem to require explanation. They are: 1. The apparent lack of contribution to the hydrogen yield by the reaction H· + H· → $\mathrm{H_2}$ for radiation of low LET[3]; 2. The invariance of the yields with changing LET of the radiation.[7,8]

In the reaction scheme

$$\mathrm{H\cdot} + \mathrm{H\cdot} \longrightarrow \mathrm{H_2} \quad k_1 \tag{1}$$
$$\mathrm{H\cdot} + \mathrm{C_6H_{12}} \longrightarrow \mathrm{H_2} + \mathrm{C_6H_{11}\cdot} \quad k_2 \tag{2}$$

we have $k_2 = 6.6 \times 10^9$ cc. mole^{-1} sec.$^{-1}$ (ref. 3), and if we take $k_1 = 6 \times 10^{12}$ cc. mole^{-1} sec.$^{-1}$, the value used for H atoms in water,[9,10] reaction 1 can provide effective competition for reaction 2 if [H·] approaches (k_2/k_1) [$\mathrm{C_6H_{12}}$], *i.e.*, $\sim 10^{-2}$ *M*. Such concentrations of hydrogen atoms might be exceeded in the center of the track left by a densely ionizing particle if they were formed very near the center of the track. For example, in a column of 10 A. radius in which G(H·) $\sim$4 (the value for cyclohexane)[6,11] for radiation of LET 5 e.v./Å., the concentration of H atoms is 1.1 *M*. To reduce the recombination to negligible proportions this concen-

---

[1] J. H. Futrell, *J. Am. Chem. Soc.*, **81**, 5921 (1959).

[2] T. J. Hardwick, *J. Phys. Chem.*, **64**, 1623 (1960).

[3] T. J. Hardwick, *ibid.*, **65**, 101 (1961).

[4] E. A. Moelwyn-Hughes, *J. Chem. Soc.*, 95 (1932).

[5] G. E. Adams, J. H. Baxendale and R. D. Sedgwick, *J. Phys. Chem.*, **63**, 854 (1959).

[6] J. G. Burr and J. D. Strong, Abstracts of the 137th National Meeting of the A.C.S. p. 43-R.

[7] R. H. Schuler and A. O. Allen, *J. Am. Chem. Soc.*, **77**, 507 (1955).

[8] H. A. Dewhurst and R. H. Schuler, *ibid.*, **81**, 3210 (1959).

[9] A. K. Ganguly and J. L. Magee, *J. Chem. Phys.*, **25**, 129 (1956).

[10] P. J. Dyne and J. M. Kennedy, *Can. J. Chem.*, **38**, 61 (1960).

[11] P. J. Dyne and W. M. Jenkinson, *ibid.*, **38**, 539 (1960).

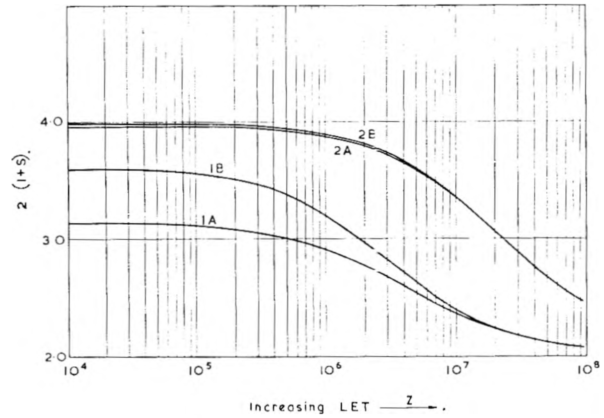

Fig. 1.—Expected $G(H_2)$ from cyc ohexane due to atomic abstraction and recombination, for different values of track radius: 1A: $D = 2 \times 10^{-5}$ cm.²/sec.; $k_1 = 9 \times 10^{12}$ cc. mole⁻¹ sec.⁻¹; $t_0 = 1.25 \times 10^{-10}$ sec.; $r = 10$ Å.; 1B: $D = 2 \times 10^{-4}$ cm.²/sec.; $k_1 = 9 \times 10^{13}$ cc. mole⁻¹ sec.⁻¹; $t_0 = 1.25 \times 10^{-10}$ sec.; $r = 30$ Å.; 2A: $D = 2 \times 10^{-5}$ cm.² sec.; $k_1 = 9 \times 10^{12}$ cc. mole⁻¹ sec.⁻¹; $t_0 = 1.25 \times 10^{-8}$ sec.; $r = 100$ Å.; 2B: $D = 10^{-4}$ cm.²/sec.; $k_1 = 9 \times 10^{13}$ cc. mole⁻¹ sec.⁻¹; $t_0 = 1.25 \times 10^{-8}$ sec.; $r = 300$ Å.

tration would need to be reduced by a factor between 10^2 and 10^3, *i.e.*, the "initial" radius r of the track increased by a factor between 10 and 32.

In a more quantitative approach, values of S, the total fraction of radicals which react with scavenger, have been calculated using the model of Ganguly and Magee[9] for various values of the parameters k_1, $q = k_2C_8t_0$, and $Z = 1/(2 - \eta)$ $(-dE/dx)_0$ in 100 e.v. per cm., where η is the mean LET/initial LET. The parameter Z depends on the radiation type and is designed to take account of the increasing LET with penetration for a given particle; it has a value of $\sim 10^{-4}$ for fast electrons, 1.8×10^6, 5.6×10^6, and 1.3×10^7 (100 e.v.) cm.⁻¹ for 20 M.e.v. deuterons, 40 and 10 M.e.v. α-particles. With the following constants: $D = 2 \times 10^{-5}$ cm.²/sec., $t_0 = 1.25 \times 10^{-10}$ sec., *i.e.*, $r_0 = 10$ Å., $k_1 = 9 \times 10^{12}$ cc. mole⁻¹ sec.⁻¹, number of radicals per spur of 100 e.v. = 4, $k_2 = 6.6 \times 10^9$ cc. mole⁻¹ sec.⁻¹, $C_8 = 9.3 \times 10^{-2}$ mole cc.⁻¹ (the last three values appropriate to cyclohexane), values of $G(H)$ $(1 + S)/2$ have been found and are given in Fig. 1 curve 1A as a function of Z. This represents the expected $G(H_2)$ since reaction 2 results in abstraction, and the expected G-value is seen to decrease with increasing LET. The additional $G(H_2)$ due to unimolecular processes is considered not to vary with radiation type.

The diffusion constant is that used for H atoms in water,[9,10] and is appropriate for the interdiffusion of medium sized molecules[12] such as benzene,[13] but for hydrogen atoms in cyclohexane this value may be too low. However S will not be very dependent on D since reaction 1 is thought to be diffusion controlled, and any increase in S on increasing D caused by favoring reaction 2 will be partly offset by the increase in k_1, proportional to D. Curve 1B was calculated with $D = 2 \times 10^{-4}$ cm.²/sec. (obtained for H atoms in cyclohexane by using the method of ref. 12) and with k_1 increased by a factor 10. The effect of an increase in t_0 by a factor 100 is shown in curves 2A and 2B from which it is clear that the conditions for densely ionizing radiation are not so sensitive to changes in D and k_1 as those at low LET, but that a value of $t_0 \approx 10^{-8}$ sec. is sufficient to reduce the dependence of S on the radiation type to about the required limits. Further increases of t_0 will cause the drop in $2(1 + S)$ to occur at higher values of Z.

The lack of dependence of the G-values of alkane decompositions on radiation type is remarkable when it appears that we can calculate k_2 and show that there is the possibility of effective competition between the bimolecular and unimolecular reaction of hydrogen atoms. Even in the case of benzene,[14,15] where the G-values for gas production show a decided dependence on LET (possibly explained on an excited molecule basis), the simplicity of the gas products, consisting only of hydrogen and acetylene, even at a linear energy deposition rate of $\sim$26 e.v./Å. is striking.

It is suggested that a possible explanation of these effects is that the initial decomposition, *e.g.* to hydrogen atoms, occurs at larger distances (perhaps 100–300 Å.) from the position of energy deposition than is sometimes supposed in models for the radiation chemistry of water ($\sim$10 Å.). This may be the result of an intermolecular dispersal of energy, or a diffusion of molecules without decomposition (or possibly the latter following the former).

---

(12) S. Glasstone, K. J. Laidler and H. Eyring, "The Theory of Rate Processes," New York, N. Y., 1941.

(13) K. Graupner and E. R. S. Winter, *J Chem. Soc.*, 1445 (1952).

(14) W. G. Burns, W. Wild and T. F. Williams, *Proc. 2nd Intern. Conf. Peaceful Uses Atomic Energy*, **29**, 266, 1958.

(15) W. G. Burns, "Rassegna Internationale Elettronica and Nucleare, Sezione Nucleare," Vol. VI, Rome, 1959, p. 99.

THE RELATIONSHIP OF BOND DISSOCIATION ENERGIES, METHYL AFFINITIES AND RADICAL REACTIVITIES

BY L. A. ERREDE

Contribution No. 204 from the Central Research Laboratories of the Minnesota Mining and Manufacturing Company, St. Paul, Minn.

Received June 12, 1961

It was reported in a previous publication[1] that the energy (D) required to dissociate an organic molecule R_i-R_j into its radical fragments $R_i\cdot$ and $R_j\cdot$, can be calculated by means of equation 1

$$D = 71\epsilon_i\epsilon_j \qquad (1)$$

where ϵ_i and ϵ_j are the characteristic binding coefficients for the groups forming the bond in question. For monovalent atoms H, F, Cl, Br and I, ϵ is given approximately by equation 2

$$\epsilon_x = E^{1/2}/r \qquad (2)$$

where E is Pauling's electronegativity[2] of the atom and r is the corresponding C–X bond length (in Ångstrom units).

The ϵ_g of a group $R_1R_2R_3C$– can be calculated by equation 3 provided that the groups (or atoms) R_1,

---

(1) L. A. Errede, *J. Phys. Chem.*, **64**, 1031 (1960). The ϵ-value for C_6H_5 listed in Table I should read 1.18 instead of 1.11.

(2) L. Pauling, "The Nature of the Chemical Bond," 2nd Ed., Cornell University Press. Ithaca, N. Y., 1948, p. 58.

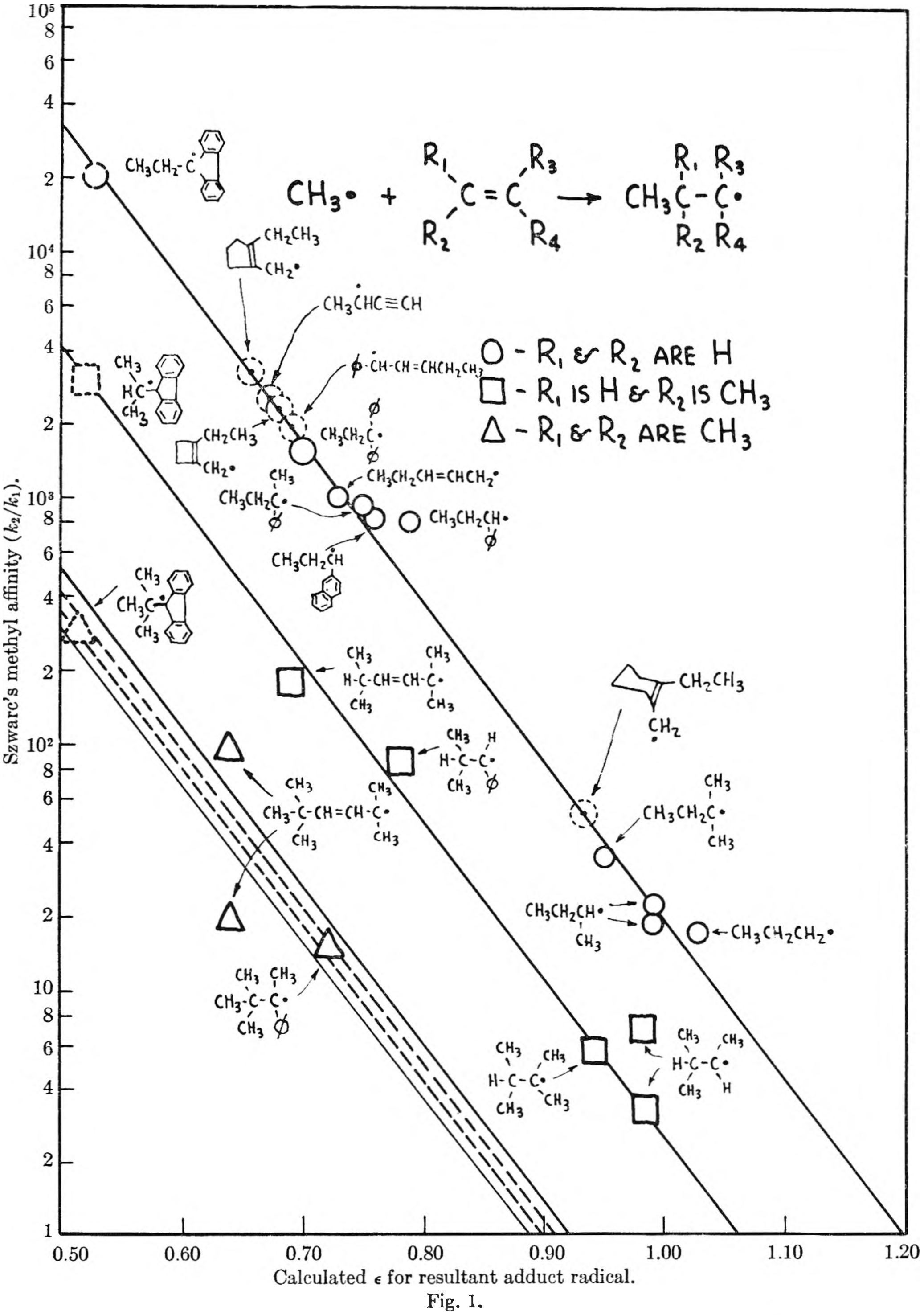

Fig. 1.

R_2 and R_3 do not have a center of unsaturation α to one of the central carbon atoms.

$$\epsilon_g = 0.43 + 0.162(\epsilon_1 + \epsilon_2 + \epsilon_3) \qquad (3)$$

The ϵ_g of radicals such as $\cdot CH_2C_6H_5$, $\cdot CH(C_6H_5)_2$ and $\cdot CH_2—CH=CH_2$ cannot be calculated by eq. 3, but rather must be determined experimentally.[1] However, once the ϵ-value is determined for one member of a homologous series such as CR_1R_2A (or $CR_1A_1A_2$), where A is a group with a center of unsaturation α to the central atom, the ϵ for all other members of that series can be calculated by means of equation 3, since ϵ'_A for $\geq C—A$ can be deduced from the value determined experimentally and then used in conjunction with ϵ_1 and ϵ_2 to calculate the ϵ_g of any other homolog.

The basic ϵ-values that could be deduced from available bond dissociation energy data[3-5] are collected in Table I of reference 1. Although these

---

(3) M. Szwarc, *Chem. Revs.*, **47**, 75 (1950).

(4) A. H. Sehon and M. Szwarc, *Ann. Rev. Phys. Chem.*, **8**, 439 (1957).

(5) T. L. Cottrell, "The Strengths of Chemical Bonds," 2nd Ed., Butterworth's Scientific Publications, London, 1958.

TABLE I

ε-VALUES FOR HYDROCARBON RADICALS CALCULATED FROM SZWARC'S METHYL AFFINITY DATA

Olefin	k_2/k_1	Ref.	Radical (R)	ε	Calcd. B.D.E. in kcal. for R–H	R–CH_3
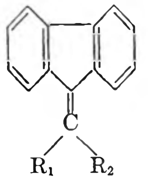			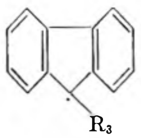			
H H	20,000	7	Et	0.53	50	41
H CH_3	2,900	7	*i*-Pr	.52	49	40
CH_3 CH_3	300	7	*t*-Bu	.51	48	39
			H	.57	53	44
$C_6H_5(CH{=}CH)_2H$	2,000	7	$C_6H_5\dot{C}HCH{=}CHCH_2CH_3$	.69	65	53
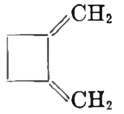	2,375	9	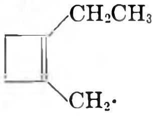	.68	64	52
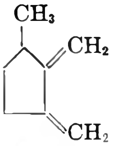	3,288	9	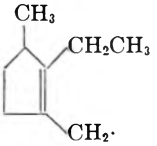	.66	62	51
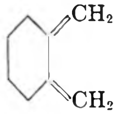	508	9	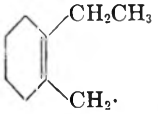	.93	87	71

data[1a] now can be used to calculate the bond dissociation energy of a large number of bonds not yet determined experimentally, there are still many classes of bonds such as X–CR_2A, where A is $\overset{\mathrm{O}}{\overset{/\!/}{\mathrm{C}}}$—OR, $-\overset{\mathrm{O}}{\overset{\|}{\mathrm{C}}}\mathrm{R}$, CN, SO_2R, etc., for which the key experimental bond dissociation energy data to find the respective ϵ_A' are lacking.

It has been pointed out by Walling[6] that the methyl affinities, as determined by Szwarc[7] and his students, can be used to calculate the dissociation energy of C–H bonds α to some of these centers of unsaturation. Szwarc's data are given in the form of k_2/k_1 ratios that indicate the rate of addition of methyl radicals to olefins (k_2) relative to the rate of hydrogen abstraction from isoöctane (k_1).

$$CH_3\cdot + M \xrightarrow{k_2} CH_3M\cdot \quad (4)$$

$$CH_3\cdot + HS \xrightarrow{k_1} CH_4 + S\cdot \quad (5)$$

Walling[6] reported that log k_2/k_1 is related to the bond dissociation energy of the bond CH_3M–H according to the equation

$$\log k_2/k_1 = 11.36 - 0.104[R_m + D(R-H)] \quad (6)$$

where R_m is the "resonance energy" of the olefin M and D(R–H) is the B.D.E. of the bond CH_3M–H. Unfortunately, only a few R_m values are known and consequently only a few new D(R–H) were calculated by Walling. These are given here in kcal. directly above the bond in question.[8]

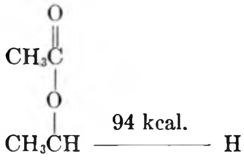

$$CH_3\overset{\overset{\mathrm{O}}{\|}}{C}{-}O{-}CH_3CH \overset{94\ \mathrm{kcal.}}{\text{———}} H$$

$$\overset{EtO}{|}\!CH_3CH \overset{94\ \mathrm{kcal.}}{\text{———}} H$$

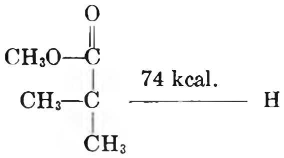

$$CH_3O{-}\overset{\overset{\mathrm{O}}{\|}}{C}{-}\underset{CH_3}{\underset{|}{C}}(CH_3) \overset{74\ \mathrm{kcal.}}{\text{———}} H$$

The magnitude of the R_m term in equation 6, however, is relatively small (usually < 4 kcal.) and actually it often falls within the experimental error for determination of many B.D.E. values. An equivalent straight line relationship with a slightly less negative slope also is obtained if one ignores R_m and simply plots log k_2/k_1 as a function of D(R–H), or as a function of ϵ_R, since $D(R-H) = 71\epsilon_H\epsilon_R$. In Fig. 1, Szwarc's methyl affinities[7,9] of olefinic hydrocarbons are plotted as a function of the ϵ_g value calculated for the corresponding radical adduct.

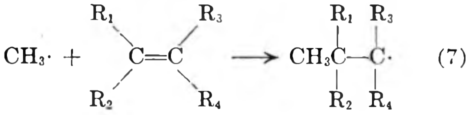

$$CH_3\cdot + \overset{R_1}{\underset{R_2}{}}C{=}C\overset{R_3}{\underset{R_4}{}} \longrightarrow CH_3\overset{R_1}{\underset{R_2}{C}}{-}\overset{R_3}{\underset{R_4}{C}}\cdot \quad (7)$$

It is noted that the three straight lines representing addition of methyl radicals to $CH_2{=}C<$, CH_3-$CH{=}C<$ and $(CH_3)_2C{=}C<$, respectively, are

---

(6) C. Walling, *J. Phys. Chem.*, **64**, 166 (1960).

(7) M. Szwarc and J. H. Binks, "Theoretical Organic Chemistry," The Kekule Meeting, London, 1958; Butterworth's Scientific Publications, London, 1959.

(8) The bond dissociation energy of $(EtO)CH_3CH$–H also can be calculated using equations 1 and 3 and the appropriate ε-values listed in Table I of ref. 1. The value calculated for this bond was 93 kcal., which is in good agreement with that calculated by Walling (94 kcal.).

(9) J. Gresser, A. Rajbenbach and M. Szwarc, *J. Am. Chem. Soc.* **82**, 5820 (1960).

TABLE II

ϵ-VALUES FOR RADICALS HAVING C=O AND CN GROUPS CALCULATED FROM SZWARC'S METHYL AFFINITY DATA[10]

	Olefin	k_2/k_1	Radical	ϵ	Calcd. B.D.E. in kcal. for R-H	R-CH_3
A	$CH_2{=}CH{-}\overset{\overset{O}{\|}}{C}CH_3$	1900	$CH_3CH_2CH\overset{\overset{O}{\|}}{C}CH_3$	0.69^a	65	53
	$CH_2CH{-}\overset{\overset{O}{\|}}{C}{-}OCH_3$	1030	$CH_3CH_2\dot{C}HCO_2CH_3$	$.73^a$	68	56
	$CH_2{=}\overset{\overset{CH_3}{\mid}}{C}{-}\overset{\overset{O}{\|}}{C}{-}OCH_3$	1440	$CH_3CH_2\dot{C}(CH_3)CO_2CH_3$	$.71^a$	67	55
	$CH_2{=}CHCN$	1730	$CH_3CH_2\dot{C}HCN$	$.70^a$	66	54
	$CH_2{=}\overset{\overset{CH_3}{\mid}}{C}{-}CN$	2120	$CH_3CH_2\dot{C}(CH_3)CN$	$.68^a$	64	52
B	$CH_3CH{=}CH\overset{\overset{O}{\|}}{C}{-}OCH_3$	68	$(CH_3)_2CH{-}\dot{C}HCO_2CH_3$	0.78^b		
				$.72^c$	67	55
	$CH_3CH{=}CHCN$	73	$(CH_3)_2CHCHCN$	$.77^b$		
				$.69^c$	65	53
C	$(CH_3)_2C{=}CH\overset{\overset{O}{\|}}{C}{-}OCH_3$	12	$(CH_3)_3C{-}CHCO_2CH_3$	$.74^b$		
				$.71^c$	67	55
	$(CH_3)_2C{=}CHCN$	24	$(CH_3)_3C{-}\dot{C}HCN$	$.70^b$		
				$.69^c$	65	53
D	...	...	$\cdot CH_2\overset{\overset{O}{\|}}{C}CH_3$	$.73^c$	68	56
	...	...	$\cdot CH_2CN$	$.74^c$	69	57
	...	...	$\cdot CH_2CO_2CH_3$	$.77^c$	72	59
	...	...	$\cdot C(CH_3)_2CO_2CH_3$	$.69^c$	65	53
	...	...	$CH_3CHO\overset{\overset{O}{\|}}{C}CH_3$	1.00^d	94	77
	...	...	$CH_3CHOCH_2CH_3$	1.00^d		
				0.99^e	93	76

[a] Calculated by means of equation 8 for addition of CH_3 to $CH_2{=}$ end groups. [b] Calculated by means of equation 8 for addition of $CH_3\cdot$ to $CH_3CH{=}$ end groups. [c] Calculated by means of equation 3 using data for radicals in Group A. [d] Calculated using equation 1 and the D(R–H) reported by Walling.[6] [e] Calculated using equation 3 and the appropriate ϵ-values given in Table I of ref. 1.

parallel to each other. Hence, the following general equation was calculated for addition of $CH_3\cdot$ to olefinic hydrocarbons.

$$\log k_2/k_1 = 3.40 + 4.00(\epsilon_1 + \epsilon_2) - 6.44\epsilon_g \qquad (8)$$

where ϵ_1 and ϵ_2 are the ϵ-values for the substituents (H or CH_3) attached to the carbon atom site where addition of the methyl radical to the olefin occurs.

Thus, the methyl affinities as determined by Szwarc can be used to determine for many radicals the ϵ-values which are not available from bond dissociation energy data. A few such examples are shown in Fig. 1 and Table I. The fluorenyl radicals are worthy of special comment. The ϵ-value for the ethylfluorenyl radical was calculated using equation 8 and the methyl affinity for fulvene. Equation 3 then was used to calculate the ϵ for isopropyl- and *t*-butylfluorenyl radicals, and when these data were tested in the methyl affinity–ϵ plot, it was noted that the points fell on the parallel lines for addition to $CH_3CH{=}C{<}$ and $(CH_3)_2C{=}C{<}$, respectively, as shown in Fig. 1.

Recently, Herk, Stefani and Szwarc[10] have reported methyl affinities for olefins containing electronegative substituents. Their data were used to calculate the ϵ-value of the resultant adduct radical using equation 8 and the results are summarized in Table II. The ϵ-values of groups B and C in Table II also were calculated using equation 3 and the ϵ-values in group A. It is seen that there is relatively good agreement for the radicals in group C but not for those in group B. The ϵ-values of the more simple radicals in each series were calculated from the data in groups A and C and are shown in group D for purposes of comparison.

Tables I and II (also Table I of ref. 1) show that the ϵ-values of radicals $\cdot CH_2A$ decrease as the stabilizing effect of A increases owing to increased electronic interaction of A with the unpaired electron. This behavior is consistent with the well established order of stability for some organic radicals. Thus, the relative ϵ-values for $\cdot CH_2C_6H_5$, $\cdot CH(C_6H_5)_2$, $\cdot C(C_6H_5)_3$ and fluorenyl radical are 0.83, 0.74, 0.65 and 0.57, respectively. Those for the allyl radicals are 0.74, 0.68, 0.66 and 0.93, respectively. The decrease in ϵ noted for the cyclobutene and cyclopentene species is consistent with the increased opportunity for electronic interaction due

$CH_3CH{=}CHCH_2\cdot$

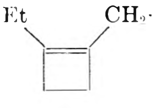

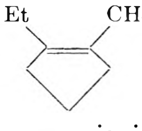

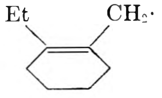

---

[10] L. Herk, A. Stefani and M. Szwarc, *J. Am. Chem. Soc.*, **83**, 3008 (1961).

to the already planar structure of these radicals; but the magnitude of increase in ϵ for the cyclohexene radical is surprising and requires further consideration. Szwarc[9] points out, however, that the vinyl groups of 1,2-dimethylenecyclohexane, to which $CH_3\cdot$ adds giving the corresponding cyclohexene radical, are not coplanar; hence, this might account for the abnormally low k_2/k_1 ratio (or high ϵ-value). The ϵ-values for the radicals listed in Table I of reference 1 and Fig. 1 of this publication parallel the order of stability anticipated on the basis of the inductive and hyperconjugative effects for primary, secondary and tertiary radicals and for the relative stabilizing effects of halogen atoms.

Thus the ϵ-values determined from kinetic data can be used with equation 1 to calculate approximately the bond dissociation energies of many bonds (Tables I and II) that cannot be determined experimentally by the usual methods. The converse also should be true; that is the ϵ-values calculated from bond dissociation energy data should be applicable to kinetic studies involving reactions of free radicals *via* coupling, abstraction and addition to centers of unsaturation. This inverse relationship, however, is not as straightforward as it first appears.

In a homologous series of organic compounds RX having a common atom X, where X is H, F, Cl, Br or I, the energy required to dissociate the bond R–X into its radical fragments $R\cdot$ and $\cdot X$ increases with increase in the binding coefficient ϵ of the radical $R\cdot$, as indicated by equation 1. Inversely, the higher the ϵ value of a given radical R, the greater is its tendency to re-form a covalent bond to give a stable organic molecule. Hence, the ϵ-value might be considered the idealized index of reactivity of the radical with respect to forming a more stable species *via* reactions involving free radical coupling, abstraction and addition to centers of unsaturation.

The qualification "idealized" is stressed to indicate an imaginary ability to keep other factors constant, since the binding coefficient is in reality only one of three important parameters that determine the rate of forming covalent bonds *via* free radical reactions. For example, many polymer chemists have demonstrated[11,12] the marked effect that polar and steric factors have on the rate of addition of a series of free radicals to a given olefinic monomer; and recently experiments were reported[13] which demonstrate the importance of these parameters in free radical abstraction reactions.

Qualitatively, the ϵ-value of a radical is a reciprocal function of Price's Q-values for monomer-radical reactivity.[11] Similarly Szwarc's[7] relative reactivities of different radicals toward the same set of monomers bears only a qualitative relationship to the corresponding ϵ-values. Thus, the relative reactivities of $CH_3\cdot$, $Et\cdot$, n-$Pr\cdot$, $CCl_3\cdot$ and polystyryl radicals for addition to unsaturated molecules[7] are in the respective order 1:1:1:0.56:0.60, whereas the corresponding ϵ-values are 1.08, 1.05, 1.03, 0.94 and 0.79.

---

[11] T. Alfrey, Jr., J. J. Bohrer and H. Mark, "Copolymerization," Interscience Publishers, Inc., New York, N. Y., 1950, Chapters III and IV.

[12] P. J. Flory, "Principles of Polymer Chemistry," Cornell University Press, Ithaca, N. Y., 1953, Chapters IV and V.

[13] F. W. Evans, R. J. Fox and M. Szwarc, *J. Am. Chem. Soc.*, **82**, 6415 (1960).

WETTING PROPERTIES OF POLYHEXAFLUOROPROPYLENE

By Marianne K. Bernett and W. A. Zisman

U. S. Naval Research Laboratory, Washington, D. C.

Received June 14, 1961

Until recently, polytetrafluoroethylene was known to have the lowest surface energy of all polymeric solids studied. Its critical surface tension of wetting (γ_c) of 18.5 dynes/cm.[1] is characteristic of a surface consisting essentially of close-packed perfluoromethylene $-CF_2-$ groups. In a recent study[2] it was shown that copolymers of tetrafluoroethylene and hexafluoropropylene exhibit even lower values of γ_c than polytetrafluoroethylene; depending upon the molar proportions of the two polymer constituents, the γ_c value of the respective copolymer decreases as perfluoromethylene groups in each surface are replaced by perfluoromethyl groups. It also was predicted that a 100% HFP polymer thus would exhibit an even lower γ_c. The present investigation reports on the wettability of such a solid polymer prepared by Eleuterio[3] from hexafluoropropylene only.

Experimental

The four polymers studied were experimental samples furnished by the Polychemicals Department of the du Pont Co. They were of different molecular weights and were received in the form of thin sheets, 0.013 inch thick. The specimens varied from very brittle to flexible. Since the surfaces were not sufficiently smooth for wetting studies, the specimens were prepared by pressing them between clean, dry, acid-cleaned Pyrex plates at 4000 lb. pressure and 200° for two hours and then cooling them under pressure for at least 16 hours.[4] Although the sheets emerged somewhat warped, the surfaces thus obtained were smooth and specular. The liquids for the wetting studies and the method used for measuring contact angles were the same as described previously.[2] All data were observed at 25 ± 1° and 50 ± 2% R.H.

Results and Discussion

Figure 1 shows the wetting curves for the solid hexafluoropropylene polymer specimens B 6007 A, B, C and D (code names by du Pont). These curves were obtained by plotting cos θ of each liquid n-alkane against the liquid surface tension γ_{LV}. On specimens A, C and D the contact angles of the respective alkanes coincide within ±1° whereas on specimen B, all values are higher by a few degrees (cos θ is lower). This specimen has been denoted by du Pont to be of intermediate molecular weight; the others are of either higher or lower molecular weights. The value of γ_c thus obtained is 16.2 dynes/cm. for B, and 17.1 dynes/cm. for the other three samples. In accordance with previous observations which showed that the surface energy of $-CF_3$ groups in a surface is lower than

---

[1] H. W. Fox and W. A. Zisman, *J. Colloid Sci.*, **5**, 514 (1950).

[2] M. K. Bernett and W. A. Zisman, *J. Phys. Chem.*, **64**, 1292 (1960).

[3] H. S. Eleuterio, U. S. Patent 2,958,685 (Nov. 1, 1960).

[4] M. K. Bernett and W. A. Zisman, *J. Phys. Chem.*, **63**, 1241 (1959).

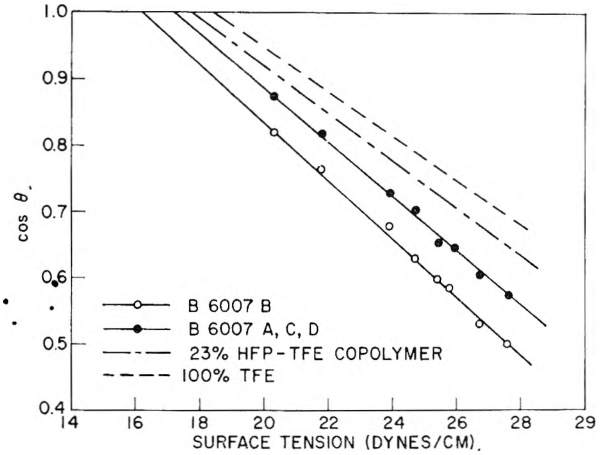

Fig. 1.—Wettability of HFP polymer by *n*-alkanes.

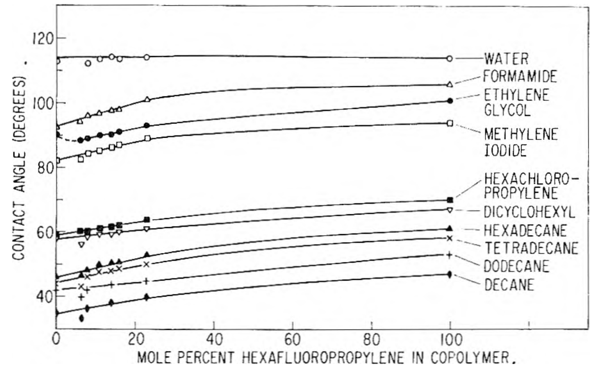

Fig. 2.—Wetting of HFP polymer and HFP–TFE copolymers by miscellaneous liquids.

that of $-CF_2-$ groups,[1,5] the γ_c value of a 100% hexafluoropropylene polymer shows the lowest surface energy encountered to date in a bulk solid.

It was predicted by extrapolating the results of wetting studies on TFE–HFP copolymers,[2] that a 100% HFP polymer will exhibit a γ_c of 15.5 dynes/cm. The actual value obtained in this study is 16.2 dynes/cm. This is in reasonably good agreement with the predicted value, if one considers the extent of extrapolation from 23 to 100 mole % HFP. (A 23 HFP mole % was the highest available in the studies of TFE–HFP copolymers.) The extrapolation was made with the assumption that a graph of contact angle *vs.* mole % HFP for any given liquid will continue in a straight line throughout the total mole % range, as it did for polymers containing up to 23 mole % HFP.[2] This linearity was considered only a convenient approximation. Figure 2 shows the complete graph obtained when the observed θ values for the 100% HFP also are plotted. It can be seen that slight deviations from a straight line resulted with each alkane liquid, and greater deviations with the hydrogen-bonding liquids, such as formamide and ethylene glycol. This is in general accordance with the earlier investigation of halogenated organic solid surfaces.[6]

That the actual value of γ_c of the 100% HFP is so close to the predicted one, and not to the calculated one of 13.3 dynes/cm.[2], is undoubtedly due to the effect of steric hindrances and restricted flexibility of these linear polymer molecules. The $-CF_2-$ and $-CF_3$ groups thus are prevented from being distributed in the same arrangement along the free surface of the solid as they are in any individual polymer molecule. The necessity of pressures from 2000 to 10,000 atmospheres and temperatures above 200° in the preparation of the poly HFP[3] are a strong indication that restrictions arise from the steric configurations and the limited accessibility of the bonds of the monomers.

---

(5) H. W. Fox and W. A. Zisman, *J. Colloid Sci.*, **7**, 228 (1952).

(6) A. H. Ellison and W. A. Zisman, *J. Phys. Chem.*, **58**, 260 (1954).

HEAT CONTENTS, $H_T - H_{298.1°K}$, FOR SOME HALIDES OF MERCURY, CADMIUM AND BISMUTH AT THEIR MELTING POINTS[1]

By L. E. Topol and L. D. Ransom

Research Division, Atomics International, A Division of North American Aviation, Inc., Canoga Park, California

Received June 5, 1961

In previous investigations[2] the heats of fusion and heat capacities of $BiCl_3$, $BiBr_3$, $HgCl_2$, $CdCl_2$, $CdBr_2$ and CdI_2 near the melting point were measured. However, the heat contents relative to 298.15°K. were not published for these halides at the melting point. Since it recently was pointed out[3] that such data would be of value, the $H_{m.p.} - H_{298.1°K}$ increments as well as the heat capacities (assuming they are constant) of the solid salts for the same temperature range are listed in Table I. Although the agreement between the heat content increment of this study and that of an earlier work[4] for $CdCl_2$ is poor, the present value as well as those of all the other salts except the bismuth halides are in excellent agreement with literature estimates[5] (Table I). Included in Table I with the heat capacities for the temperature range 298°K. to the melting point are those values found near the melting points of the salts. As can be seen, there is virtually no change in the heat capacity with temperature for any of the solid salts except $CdCl_2$ and $CdBr_2$. Since these two halides have

TABLE I

HEAT CONTENTS, $H_T - H_{298.1°K}$, AT MELTING POINT AND HEAT CAPACITY DATA FOR $HgCl_2$, $BiCl_3$, $BiBr_3$, $CdCl_2$, $CdBr_2$ AND CdI_2

Salt	M.p., °K.	$H_{m.p.} - H_{298.1°K}$ (kcal./mole) This work	Lit.[5]	Heat capacity (cal./deg.mole) m.p. to 2981.°K.	near m.p.
$HgCl_2$	552.7	4.93	5.1	19.4	19.2
$BiCl_3$	506.6	5.27	4.6	25.3	26.1
$BiBr_3$	492.2	5.11	4.3	26.3	26.0
$CdCl_2$	842.1	11.21	10.9, 13.1[4]	20.6	28.5
$CdBr_2$	841.2	11.06	10.9	20.4	22.8
CdI_2	661.2	7.36	7.3	20.3	21.5

---

(1) This work was performed under contract to the U. S. Atomic Energy Commission.

(2) (a) L. E. Topol, S. W. Mayer and L. D. Ransom, *J. Phys. Chem.*, **64**, 862 (1960); (b) L. E. Topol and L. D. Ransom, *ibid.*, **64**, 1339 (1960).

(3) L. Brewer, private communication.

(4) A. N. Krestovnikov and G. A. Karetnikov, *Legkie Metal.*, **4**, 35 (1935).

(5) L. Brewer, *et al.*, "The Chemistry and Metallurgy of Miscellaneous Materials: Thermodynamics," ed. by L. L. Quill, McGraw-Hill Book Co., New York, N. Y., 1950.

much higher melting points than do the others, the occurrence of an increase in heat capacity over this larger temperature interval is not unexpected. However, the reason for the much larger change for $CdCl_2$ than for $CdBr_2$ is not clear in view of the similar nature of these salts.

PARTIAL MOLAL VOLUMES IN LIQUID-LIQUID MIXTURES

By Ryoichi Fujishiro, Kōzō Shinoda and J. H. Hildebrand

Department of Chemistry, University of California, Berkeley 4, Cal.

Received June 19, 1961

The work here reported is part of a study of the role of expansion in the theory of solution. The magnitude of this factor first became strikingly evident by the observation of Glew[1] that the partial molal volume, $\bar{v}_2$, of iodine in *f*-heptane at 25° and at virtually infinite dilution (mole fraction 1.8×10^{-4}) is 100 cc., a 70% expansion over its (extrapolated) liquid molal volume, 59 cc. Its partial molal volumes in a number of other solvents were measured by Shinoda and Hildebrand.[2] Smith, Walkley and Hildebrand[3] obtained figures for the partial molal volumes of bromine and stannic iodide at high dilution in the same series of solvents. Jolley and Hildebrand[4] published values of the partial molal volumes of gases. Walkley and Hildebrand[5] found that $\bar{v}_2$ for H_2 in benzene and in toluene exceeds that of D_2 by 10%.

The paper by Smith, Walkley and Hildebrand compared the partial molal volumes of one solute in a series of solvents; this research compares a series of solutes in the same solvent.

The method used was the simple, rapid, accurate one described in ref. 2. A long, thin glass capsule containing a small, weighed amount of a solute is dropped into a large bulb filled with a solvent through its capillary stem. The capsule is broken and the solute dissolved by means of a large glass ball within the bulb. The partial molal volume is calculated from the rise of the liquid in the capillary stem. The amounts of the solvent and solute are such that the values of $\bar{v}_2$ are virtually those for infinite dilution (mole fraction $\approx 10^{-3}$). The materials used were purified by methods previously described.[2]

The values of $\bar{v}_2$ thus obtained are given in Table I, together with the molal volumes, $\bar{v}_2^0$, and the solubility parameters of the pure components, δ. The values of $\bar{v}_2$ are the means of two or more determinations agreeing well within 1%.

Figure 1 is a plot of $[(\bar{v}_2 - \bar{v}_2^0)/\bar{v}_2^0]^{1/2}$ *vs.* solubility parameters in the two solvents, CCl_4 and CS_2. This method of plotting is suggested by the equation

$$\bar{v}_2 - v_2^0 = n\beta_1 RT \ln \gamma_2 \qquad (1)$$

where β_1 is the compressibility of the solvent when the solute is very dilute, as in these experiments; γ_2 is the activity coefficient of the solute, and n is the ratio $(\partial E_1/\partial V_1)_{P,T}$ to $\Delta E_1^v/v_1$. E is energy in cal./mole, ΔE^v is energy of vaporization. Equation 1, without the factor, n, was given by Hildebrand and Scott.[6] Inclusion of the factor, n, is explained in a more detailed derivation to be given in a book now in press.[7] Upon combining equation 1 with the simple equation for regular solutions

$$RT \ln \gamma_2 = v_2^0 \phi_1^2 (\delta_2 - \delta_1)^2 \qquad (2)$$

where ϕ_1 is the volume fraction of the solvent, here ~1, we obtain

$$\frac{\bar{v}_2 - v_2^0}{v_2^0} = \pm(\delta_2 - \delta_1)(n\beta_1)^{1/2} \qquad (3)$$

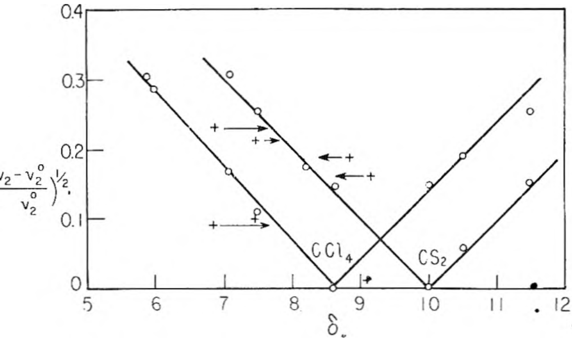

Fig. 1.—Partial excess volumes at high dilution and solubility parameters.

We see from Fig. 1 that the left-hand member is closely proportional to $\pm(\delta_2 - \delta_1)$ except in the cases of n-C_7H_{16}, i-C_8H_{18}, C_6H_6 and 1,2,3-$C_6H_3(CH_3)_3$, the points for which are designated by crosses. The slopes of the lines are almost exactly 45°, hence the proportionality constant is close to 0.1. The wide range of expansion covered by this regularity, up to 9%, is especially noteworthy.

Table I

Partial Molal Volumes of Solutes, $\bar{v}_2$, at 25° and High Dilution

Solute	δ	v_2^0	$\bar{v}_2$ in CS2	$\bar{v}_2$ in CCl4	$\bar{v}_2$ in n-C7H16
C_7F_{16}	5.85	225.5	...	246.5	254.6
c-$C_6F_{11}CF_3$	6.0	195.8	...	211.6	218.3
i-C_8H_{18}	6.85	166.1	172.2	167.5	167.4
c-$C_4Cl_2F_6$	7.1	142.5	155.5	146.6	153.6
n-C_7H_{16}	7.45	147.5	154.4	149.1	...
$CCl_2F \cdot CClF_2$	7.5	119.8	127.7	120.9	124.5
c-C_6H_{12}	8.2	108.8	112.1	...	...
CCl_4	8.6	97.1	99.2	...	98.2
s-$C_6H_3(CH_3)_3$	8.8	139.6	144.5	...	...
C_6H_6	9.15	89.3	91.6	...	91.0
C_6H_5Cl	9.5	102.1	...	...	105.5
CS_2	10.0	60.7	...	62.0	63.4
$CHBr_3$	10.5	87.8	88.1	90.9	92.1
Br_2	11.5	51.5	52.6	54.75	...

This empirical constant does not agree very well with values of $(n\beta)^{1/2}$. The compressibilities of CCl_4 and CS_2 are 1.11×10^{-4} and 0.93×10^{-4} atm.$^{-1}$, respectively, and the n-values are, respectively,[8] 1.07 and 0.89. The figures for β are

---

[1] D. N. Glew and J. H. Hildebrand, *J. Phys. Chem.*, **60**, 618 (1956).

[2] K. Shinoda and J. H. Hildebrand, *ibid.*, **62**, 272 (1958).

[3] E. B. Smith, J. Walkley and J. H. Hildebrand, *ibid.*, **63**, 703 (1959).

[4] J. E. Jolley and J. H. Hildebrand, *J. Am. Chem. Soc.*, **80**, 1050 (1958).

[5] J. Walkley and J. H. Hildebrand, *ibid.*, **81**, 4439 (1959).

[6] J. H. Hildebrand and R. L. Scott, "Solubility of Nonelectrolytes," Reinhold Publ. Corp., New York, N. Y., 1950, p. 141.

[7] J. H. Hildebrand and R. L. Scott, "Regular Solutions," Prentice-Hall, New York, N. Y., 1962, in press.

[8] Ref. 6, p. 97.

in atm.$^{-1}$; to convert them to the units used for δ, cal. cc.$^{-1}$, we introduce the factor 41.3 and obtain for the theoretical values of $(n\beta)^{1/2}$ 0.070 and 0.058, respectively, for the two solvents, considerably less than the experimental value, 0.1.

The points for i-C_8H_{18} are found far to the left of the lines in both solvents. Its solubility parameter would have to be 7.7 instead of 6.85, as derived from its energy of vaporization, in order to agree with the other solutes. Its solubility relations with such diverse substances as C_7F_{16}[9] and I_2[10] yield the values 7.9 and 7.95 for its solubility parameter, in good agreement with the value 7.7 above. The much smaller discrepancies for n-C_7H_{16} correspond similarly to an adjusted solubility parameter.

The point for cyclohexane in CS_2 falls upon the line. This substance, although a hydrocarbon, is compact. In its solvent power for iodine it is likewise quite normal. Evidently the behavior of i-C_8H_{18} is to be referred primarily to loose structure.

We have added in Fig. 1 a point for benzene in carbon tetrachloride obtained from measurements by Scatchard, Wood and Mochel.[11] Plotting their values of $\Delta v^m/v^0$ *vs.* $x_2(C_6H_6)$, the slope at $x_2 = 0$ gives $\bar{v}_2 - v_2^0 = 1.45 \times 10^{-4}$ whence $(\bar{v}_2 - v_2^0/v_2^0 = 0.012$.

The points for benzene and mesitylene also depart from the general relation depicted in Fig. 1. The molecules of these solvents have π-electrons, whereas those that agree with the relation all have non-bonding electrons. Walkley, Glew and Hildebrand[12] showed that these two classes of solvents fall into different groups with respect to their effect upon the wave length of the visible peak of iodine.

The values of $\bar{v}_2$ for various solutes in n-heptane as solvent, given in Table I, yield points that are somewhat scattered when plotted as in Fig. 1, as might be expected.

The study confirms (a) the intimate relation between excess volumes and solubility and (b) the role that differences in the type of molecular electronic structure may play in solubility relations.

We gratefully acknowledge support of this work by the Atomic Energy Commission and by the National Science Foundation.

---

[9] J. Hildebrand, B. B. Fisher and H. A. Benesi, *J. Am. Chem. Soc.*, **72**, 4348 (1950).

[10] G. R. Negishi, L. H. Donnally and J. H. Hildebrand, *ibid.*, **55**, 4793 (1933).

[11] G. Scatchard, S. E. Wood and J. M. Mochel, *ibid.* **62**, 712 (1940).

[12] J. Walkley, D. N. Glew and J. H. Hildebrand, *J. Chem. Phys.*, **33**, 621 (1960).

THE THERMAL DECOMPOSITION OF METHYLENECYCLOBUTANE[1]

By R. L. Brandaur,[2] B. Short[2] and S. M. E. Kellner[3]

Department of Chemistry of the University of Rochester, Rochester, N. Y.

Received June 26, 1961

In considering the influence of the side chain constituent on the rate and mechanism of decomposition of substituted cyclobutanes, a study of the pyrolysis of methylenecyclobutane was of interest since this molecule represents a structure intermediate between the alkylcyclobutanes on the one hand and cyclobutanone and other carbonyl-group containing cyclobutanes on the other.

Experimental

Materials.—The methylenecyclobutane was obtained from Reaction Products, Inc. After fractionation in this Laboratory through an 85-cm. Lecky–Ewell column (b.p. 41.0 ± 0.5° at 760 mm.) this sample was used directly for the preliminary experiments. Since the sample subsequently was found to contain a trace of 2-methyl-1-butene and about 7% of spiropentane, it was purified further by vapor fractometry before use in the kinetic experiments. No evidence of impurities was found by either infrared spectrometry or gas chromatography after this treatment.

The allene used in this work was prepared by Dr. M. Szwarc of the New York State College of Forestry and was fractionated in this Laboratory in a Podbielniak column. The middle fraction (b.p. −35°) was used after repeated degassing at −160°.

Ethylene from the Phillips Petroleum Company (research grade, 99.9% min. purity) was subjected to trap-to-trap distillation and degassed at −196°.

Apparatus.—The early experiments were performed in a 500-ml. Pyrex reaction vessel with a conventional furnace and temperature control system. The effect of increased surface area was tested by use of a vessel packed with thin-walled Pyrex capillary tubing so as to have a surface-to-volume ratio 34 times that of the unpacked vessel. The final kinetic experiments were carried out in a cylindrical 320-ml. vessel contained in an electrically heated furnace mounted with the axis of the cylinder in a vertical position. Platinum, platinum–13% rhodium thermocouples attached to a Leeds and Northrup type K-2 potentiometer were used for the temperature measurements. The pressure in the reaction vessel was measured with a 3-mm. bore capillary mercury manometer for the high pressures (45–65 mm.), and with a 20-mm. bore mercury manometer read with a cathetometer for pressures below 12 mm.

Infrared absorption measurements were made on a Perkin–Elmer Model 21 double beam infrared spectrometer equipped with a one meter path length gas cell. Chromatographic analyses were performed on a Perkin–Elmer Model 154B Vapor Fractometer, separations being effected by tetraisobutylene on firebrick or diisodecyl phthalate on Celite. Synthetic mixtures of reaction products served as standards for quantitative determinations.

Results

Preliminary Experiments.[4]—Methylenecyclobutane was found to decompose in the gas phase near 450°. The principal products first were identified as ethylene and allene by infrared absorption measurements. Subsequently the combined products from the decomposition at 460° of two 11-mm. samples were separated into a fraction volatile at −139° and one volatile at −78°. Mass spectrometric analysis[5] confirmed ethylene and allene as the chief constituents of the two respective fractions.

Since for 45 to 65 mm. of methylenecyclobutane

---

[1] This work was supported by a grant from the National Science Foundation.

[2] Participants in the NSF Summer Research Program for Science Teachers during 1959 and 1960, respectively.

[3] (a) Department of Chemistry, St. Michael's College, Winooski, Vermont; (b) Postdoctoral fellow during the summer of 1960 under a research grant from the Shell Companies Foundation, Inc.

[4] Performed by Eugene Johnson and M. N. Das in this Laboratory. The work of E. J. was part of a senior research problem for the B.S. degree and was mentioned in footnote 24 of W. B. Guenther and W. D. Walters, *J. Am. Chem. Soc.*, **81**, 1314 (1959). M. N. D. was working as a postdoctoral fellow under a research grant from the Celanese Corporation of America.

[5] Performed by Consolidated Engineering Corporation, Pasadena, California.

at 450–470° the pressure in the reaction vessel did not rise to twice the initial pressure, it was thought that a pressure-decreasing process, perhaps a reaction of the product allene, might be occurring along with the decomposition of methylenecyclobutane in the latter stages. However, in the initial stages of experiments with 6 to 11 mm. of methylenecyclobutane at 450–460° the pressure increase was essentially equal to the pressure of the −139° fraction (principally ethylene) and also to the pressure of the −78° fraction (chiefly allene). Under such conditions the pressure increase appeared to be a satisfactory measure of the amount of decomposition.

The quarter-time for the decomposition in the packed vessel at 460° for 7 experiments averages 7.4 minutes, that for 11 experiments in the unpacked vessel 7.5 minutes. The decomposition, therefore, is not influenced significantly by the amount of surface present and appears to be a homogeneous gas phase reaction.

Products and Stoichiometry.—On the basis of the early experiments the reaction mixture at the conclusion of an experiment was divided into four fractions by differences in volatility: (1) products non-condensable at −196°, (2) products volatile at −160°, but condensable at −196°, (3) products volatile at −100°, but condensable at −160°, (4) products condensable at −100°. The amount of noncondensables was negligibly small. Fraction 2 consisted of ethylene and a trace of allene. Fraction 3 contained allene and small amounts of ethylene and methylenecyclobutane. Fraction 4 contained methylenecyclobutane and a trace of allene. Comparison of retention times of the products on the Vapor Fractometer with those of known samples confirmed the identity of the products. Moreover, there were no other products, such as isomers of methylenecyclobutane, detectable on the Vapor Fractometer.

A good mass balance was obtained by gas buret measurements on the separated fractions and subsequent quantitative vapor fractometry of each fraction. The pressure increase corresponds closely to both the pressure of ethylene and to that of allene (Table I). The ratio of the initial pressure in the reaction vessel to the sum of the pressure of undecomposed methylenecyclobutane and one-half the pressure of products is 0.98 ± 0.04. Thus any polymerization reaction must be negligibly small. It appears that the only significant reaction occurring in the pyrolysis of methylenecyclobutane between 410 and 460° at low pressures and less than 30% conversion can be represented by

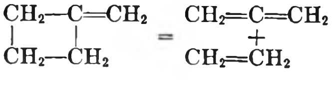

Moreover, these results confirm the earlier conclusion that the pressure increase is a good measure of the amount of decomposition under these conditions.

Kinetics.—Pressure–time curves were used to determine reaction rates. These curves show no induction period and have the general appearance of first-order curves. Plots of log $(P_0/(2P_0 - P_t))$ *vs.* time are linear up to at least 30% reaction. The ratio of the quarter-time to the eighth-time for 11 experiments averaged 2.13, which is within experimental error of the theoretical value of 2.15 for first-order reactions. The pressure range studied was limited for reasons outlined above, but a nearly three-fold increase in the initial pressure had no significant effect on the first-order rate constant.

The temperature dependence of the pyrolysis was studied by means of sixteen experiments at seven temperatures from 410 to 470° and with initial pressures of 2.3 to 10.4 mm. Rate constants were calculated from quarter-times and eighth-times using the integrated first-order rate equation. The value of the activation energy for the Arrhenius equation $k = A \exp(-E/RT)$ determined from the slope of the best straight line through the points of a plot of log k *vs.* $1/T$ is 61.4 ± 0.5 kcal./mole. A least squares analysis of these sixteen experiments yields an activation energy and standard deviation of 61.6 ± 0.6 kcal./mole. For nine experiments in the pressure range 6.4 to 10.4 mm. the least squares value is 61.5 ± 0.4 kcal./mole. Using $E = 61.5$, the average value of A and its standard deviation were computed for the latter experiments as $1.22 \pm 0.03 \times 10^{15}$ sec.$^{-1}$. The first-order rate constant may be expressed as

$$k = 1.22 \pm 0.03 \times 10^{15} \exp(-61{,}500/RT) \text{ sec.}^{-1}$$

It is to be noted that for a given k value a 0.1 kcal./mole change in E will cause a 7% change in A at 450°. The entropy of activation ΔS^* obtained from the frequency factor $A = \kappa e(kT/h) \exp(\Delta S^*/R)$ for a unimolecular reaction[6] by taking the transmission coefficient κ as unity is 6.7 cal./deg. mole at 450°. The positive value of ΔS^* is expected for a ring cleavage reaction.

Discussion.—The kinetics of the pyrolysis of methylenecyclobutane resembles that of the alkylcyclobutanes[7] rather than that of the carbonyl-containing cyclobutanes[8] (Table II). The smaller rate constant for methylenecyclobutane as compared with the alkylcyclobutanes at 450° appears to

TABLE I

COMPARISON OF OBSERVED AND CALCULATED PRESSURES IN THE DECOMPOSITION OF METHYLENECYCLOBUTANE

P_0,[a] mm.	ΔP,[b] mm.	P_E,[c] mm.	P_A,[c] mm.	P_M,[c] mm.	$P_M + 1/2(P_E + P_A)$, mm.	T, °C.
6.65	0.89	0.86	0.92	5.87	6.76	410.2
7.81	1.29	1.55	1.56	6.77	8.33	420.2
6.44	2.03	2.18	2.10	4.45	6.59	430.2
7.19	2.15	2.22	2.17	5.42	7.61	440.8
8.43	2.44	2.48	2.44	5.84	8.30	459.8

[a] P_0 is the initial pressure of methylenecyclobutane. [b] ΔP is the measured pressure increase in the reaction vessel, corrected for dead space. [c] P_E, P_A and P_M are the pressures of ethylene, allene and unreacted methylenecyclobutane in the reaction mixture.

---

(6) S. Glasstone, K. J. Laidler and H. Eyring, "The Theory of Rate Processes," McGraw-Hill Book Co., New York, N. Y., 1941, p. 295.

(7) (a) F. Kern and W. D. Walters, *Proc. Natl. Acad. Sci.*, **38**, 937 (1952); C. T. Genaux, F. Kern and W. D. Walters, *J. Am. Chem. Soc.*, **75**, 6196 (1953); (b) M. N. Das and W. D. Walters, *Z. physik. Chem.*, **15** (Bonhoeffer Gedenkband), 22 (1958).

(8) (a) M. N. Das, F. Kern, T. D. Coyle and W. D. Walters, *J. Am. Chem. Soc.*, **76**, 6271 (1954); (b) L. G. Daignault and W. D. Walters, *ibid.*, **80**, 541 (1958).

TABLE II

KINETIC DATA FOR SOME CYCLOBUTANES[a]

Substance	10^4k, sec.$^{-1}$	E_a, kcal.	A, sec.$^{-1}$	ΔS^*, cal./deg. mol.	Ref.
Cyclobutane	5.15 (450°)	62.5	4.0×10^{15}	9.0 (449°)	7a
Methylcyclobutane	7.75 (450°)	61.2	2.4×10^{15}	8.1 (450°)	7b
Methylenecyclobutane[b]	3.18 (450°)	61.5	1.2×10^{15}	6.7 (450°)	..
Cyclobutanone	6.9 (368°)	52.0	3.6×10^{14}	4.6 (368°)	8a
Methyl cyclobutyl ketone	6.8 (400°)	54.5	3.4×10^{14}	4.3 (400°)	8b

[a] k is the first-order rate constant, E_a the activation energy, A the frequency factor, and ΔS^* the entropy of activation. [b] At 6–10 mm. initial pressure.

be due to the difference in the entropies of activation. One might expect less randomness of motion in an incipient allene molecule than in the corresponding structure for an alkyl-substituted ethylene.

The present results on the thermal decomposition of methylenecyclobutane are of interest in connection with some exploratory pyrolytic experiments on spiropentane performed in this Laboratory,[9] and confirmed by one of us (S.M.E.K.). Spiropentane (99+ %)[10] was subjected to decomposition in a static system at 420° and initial pressures near 10 mm. The combined reaction mixture from several experiments was separated into three fractions on the basis of volatility and the infrared spectra were determined. The chief products were found to be ethylene, allene and methylenecyclobutane. From the data it appears that spiropentane simultaneously undergoes an isomerization to methylenecyclobutane and a ring cleavage to yield allene and ethylene. As the present study shows, methylenecyclobutane decomposes to form ethylene and allene, but the rate is not sufficient to account for the major part of the ethylene and allene observed in the initial stages of the decomposition of spiropentane.

Acknowledgment.—The authors wish to thank Professor W. D. Walters for his helpful suggestions and encouragement, and Mr. C. A. Whiteman, Jr., for his assistance with the infrared absorption measurements and the least squares calculations.

[9] Experiments of R. W. Roberts as part of his senior research problem for the B.S. degree, 1956.

[10] Obtained from Dr. Guy Waddington.

A COMPARATIVE STUDY OF THE DECARBOXYLATION OF MALONIC ACID AND OXANILIC ACID IN ETHERS AND IN TERTIARY AMINES

BY LOUIS WATTS CLARK

Department of Chemistry, Western Carolina College, Cullowhee, North Carolina

Received July 14, 1961

Numerous studies have been reported in the literature on the decarboxylation of malonic acid alone and in solution.[1] The rate-determining step of the reaction apparently involves the coördination of the polarized electrophilic carbonyl carbon atom of the acid with an unshared pair of electrons on a nucleophilic atom of solvent.[1b] It has been observed recently that oxanilic acid undergoes smooth decarboxylation when warmed in polar solvents, particularly in primary and in tertiary amines,[2] according to the equation

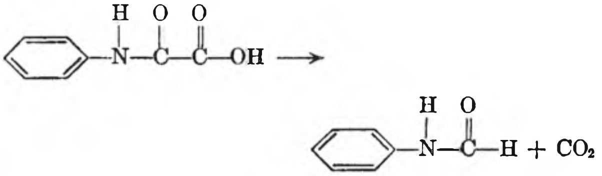

Since oxanilic acid may be regarded as a type of α-keto acid, and malonic acid as a type of β-keto acid, information furnished by these studies should be applicable to other members of these two homologous series.

Up to the present time only bases have been employed as catalysts for the oxanilic acid reaction. It was deemed worthwhile to extend the range of catalysts to include a number of liquids containing nucleophilic atoms other than nitrogen. Anisole, phenetole and β-chlorophenetole were selected for this purpose. A third tertiary amine, N,N-dimethylaniline, also was included in these studies. In order to obtain a comprehensive comparison of the results of these studies with those on malonic acid, kinetic experiments were carried out on the decarboxylation of malonic acid in two additional solvents, phenetole and β-chlorophenetole. Results of this investigation are recorded herein.

Experimental

Reagents.—(1) Both the oxanilic acid and the malonic acid used in this investigation were Reagent Grade, 100.0% assay. (2) All the solvents were Reagent Grade or Highest Purity reagents. Each sample of each liquid was distilled at atmospheric pressure directly into the dried reaction flask immediately before the beginning of each decarboxylation experiment.

Apparatus and Technique.—The details of the apparatus and technique have been described previously.[3] In these experiments a sample of malonic acid weighting 0.1870 g., or a sample of oxanilic acid weighing 0.2968 g. (corresponding to 40.0 ml. of CO_2 at STP on complete reaction) was weighed into a fragile glass capsule weighing approximately 0.1 g. blown from 6-mm. soft-glass tubing. A weighed quantity of solvent (saturated with dry CO_2 gas) was placed in the 100-ml. 3-neck, standard-taper flask immersed in the oil-bath. The temperature of the thermostat-controlled oil-bath (maintained to within ±0.01°) was determined using a thermometer graduated in tenths of a degree and calibrated by the U. S. Bureau of Standards.

---

[1] (a) C. N. Hinshelwood, *J. Chem. Soc.*, **117**, 156 (1920); (b) G. Fraenkel, R. L. Belford and P. E. Yankwich, *J. Am. Chem. Soc.*, **76**, 15 (1954); (c) L. W. Clark, *J. Phys. Chem.*, **64**, 677 (1960), and previous articles in this series.

[2] (a) L. W. Clark, *ibid.*, **65**, 572 (1961); (b) *ibid.*, **65**, 542 (1961).

[3] L. W. Clark, *ibid.*, **60**, 825 (1956).

Results

Decarboxylation experiments were carried out in each solvent at three different temperatures over a 20° temperature range. Experiments at each temperature were repeated a sufficient number of times to obtain complete assurance of their validity and reproducibility. In one case the experiment was performed eight times at the same temperature. In the case of each of the solvents used in this investigation the log $(V_\infty - V_t)$ was a linear function of time over practically the entire course of the reaction.

The average rate constants, calculated in the usual manner from the slopes of the experimental logarithmic plots, are brought together in Table I. The parameters of the Eyring equation, based upon the data in Table I, are shown in Table II, along with corresponding data for malonic acid previously obtained in anisole and the three tertiary amines.

TABLE I

APPARENT FIRST-ORDER RATE CONSTANTS FOR THE DECARBOXYLATION OF OXANILIC ACID AND MALONIC ACID IN SEVERAL SOLVENTS

System	Temp., °C. cor.	No. of runs	$k \times 10^4$, sec.$^{-1}$	Av. dev.
Anisole + oxanilic acid	128.44	3	0.98	±0.01
	139.02	5	3.17	.01
	148.10	8	8.25	.02
Phenetole + oxanilic acid	137.87	3	2.99	.01
	148.05	3	7.82	.02
	156.89	2	18.47	.02
β-Chlorophenetole + oxanilic acid	128.18	2	1.12	.01
	137.82	3	2.86	.01
	148.00	4	7.44	.02
N,N-Dimethylaniline + oxanilic acid	139.42	3	2.33	.01
	150.16	3	7.67	.01
	158.15	2	17.88	.03
Phenetole + malonic acid	139.80	2	1.74	.01
	149.38	3	3.86	.01
	159.59	3	9.43	.01
β-Chlorophenetole + malonic acid	128.49	2	1.34	.01
	138.02	4	3.08	.02
	147.90	3	6.99	.01

TABLE II

KINETIC DATA FOR THE DECARBOXYLATION OF MALONIC ACID AND OXANILIC ACID IN SEVERAL SOLVENTS[a]

	Malonic acid		Oxanilic acid	
Solvent	$\Delta H^\ddagger$, kcal./mole	$\Delta S^\ddagger$, e.u./mole	$\Delta H^\ddagger$, kcal./mole	$\Delta S^\ddagger$, e.u./mole
Anisole[4]	30.2	− 3.7	35.6	+11.1
Phenetole	29.0	− 6.0	32.6	+ 4.0
β-Chlorophenetole	27.8	− 7.9	31.3	+ 0.7
Quinoline[5,2b]	26.7	− 2.4	38.6	+16.0
N,N-Dimethylaniline[6]	26.2	− 6.6	37.6	+15.3
8-Methylquinoline[5,2b]	24.4	−10.5	35.6	+10.0

[a] The first superscript after the name of the solvent refers to the source of the malonic acid data, the second (if any) to that of oxanilic acid.

Discussion of Results

Inspection of lines 1 and 2 of Table II reveals that the enthalpy of activation of the malonic acid reaction decreases regularly with increasing basicity (nucleophilicity) of the solvent. The changes in $\Delta S^\ddagger$ on proceeding down the column are consistent with the differences in the steric effects of the solvents[2b,4-6]

If oxanilic acid forms an activated complex with a solvent in a manner analogous to malonic acid, the $\Delta H^\ddagger$ of the reaction in a given solvent would be expected to be somewhat higher than that in the case of malonic acid, since the effective positive charge on the polarized carbonyl carbon atom taking part in the rate-determining step is lower in oxanilic acid than in malonic acid.[2] Inasmuch as dicarboxylic acids associate past the dimer stage whereas monocarboxylic acids do not,[7] the activated complex in the case of malonic acid would be expected to be somewhat bulkier than in the case of oxanilic acid, so that, in a given solvent, oxanilic acid should possess a higher entropy of activation than malonic acid. These deductions are seen to be substantially verified in the case of the first three solvents listed in Table II—anisole, phenetole and β-chlorophenetole. The $\Delta H^\ddagger$ and $\Delta S^\ddagger$ values for the oxanilic acid reaction in each of these solvents are somewhat larger than they are for malonic acid. Also, the $\Delta H^\ddagger$ of the oxanilic acid reaction, as in the case of malonic acid, decreases as the nucleophilicity of the solvent increases. These data are consonant with the hypothesis that oxanilic acid, like malonic acid, forms an activated complex with the solvent prior to cleavage.

On passing from β-chlorophenetole to the first tertiary amine, quinoline, it will be seen that the $\Delta H^\ddagger$ of the oxanilic acid reaction increases abruptly instead of continuing to follow the decreasing trend shown by malonic acid. However, from quinoline on, the $\Delta H^\ddagger$ decreases regularly with increasing nucleophilicity of the solvent. The high values of $\Delta H^\ddagger$ are indicative of a weaker attraction between solute and solvent. This may be caused by the residual positive charge on the anilide nitrogen atom of oxanilic acid attracting the nucleophilic nitrogen atom of a solvent molecule.

Acknowledgments.—The support of this research by the National Science Foundation, Washington, D. C., is gratefully acknowledged.

---

(4) L. W. Clark, *J. Phys. Chem.*, **62**, 1468 (1958).

(5) L. W. Clark, *ibid.*, **62**, 500 (1958).

(6) L. W. Clark, *ibid.*, **61**, 1975 (1957).

(7) W. Hückel, "Theoretical Organic Chemistry," Vol. II, Elsevier Publ. Co., New York, N. Y., 1958, p. 329 *et seq.*

KINETICS OF RING SPLITTING OF METHYLCYCLOPENTANE OVER ALUMINA

BY J. H. SINFELT AND J. C. ROHRER

Esso Research and Engineering Company, Linden, New Jersey

Received July 20, 1961

Alumina is a catalyst for a variety of hydrocarbon reactions. For example, alumina is known to catalyze certain ring splitting reactions of saturated cyclic hydrocarbons, such as the conversion of cyclopropane to propylene[1] and of methylcyclo-

---

(1) V. N. Ipatieff and W. Huhn, *Ber.*, **36**, 2014 (1903).

TABLE I

RING SPLITTING OF METHYLCYCLOPENTANE (MCP): PRODUCT DISTRIBUTIONS AND RATES

Temp., °C.	471	471	471	471	471	499	499	499	499	499
MCP pressure, atm.	1.0	1.0	1.0	1.0	10.0	1.0	1.0	1.0	1.0	10.0
H_2 pressure, atm.	0^a	2.0	6.0	20.0	20.0	0^a	2.0	6.0	20.0	20.0
F/W^b	0.13	0.13	0.13	0.13	0.13	0.25	0.25	0.25	0.25	0.25
% of MCP^c converted to:										
C_1–C_5	0	0.8	1.2	2.4	2.4	0	0.5	1.6	3.7	5.8
Hexanes + hexenes	0.6	1.6	4.1	7.5	14.4	0.4	2.1	3.5	7.8	12.0
Total ring splitting, %	0.6	2.4	5.3	9.9	16.8	0.4	2.6	5.1	11.5	17.8
Rate of ring splitting, $r,^d \times 10^4$	8	31	69	130	220	10	65	130	290	450
Paraffin/olefin ratio										
Propane/propylene		0.2	0.9	7.4	8.0		0.2	0.8	7.3	4.9
Butanes/butenes		.2	.8	8.1	8.5		.2	.6	8.1	3.4
Hexanes/hexenes	0.2	.3	.6	3.6		0.2	.3	.5	3.1	2.8

[a] N_2 at 6.0 atm. substituted for H_2. [b] Moles of methylcyclopentane charged per hour per g. of catalyst. [c] Conversion to cyclohexane less than 0.1% in all cases. [d] Moles of methylcyclopentane converted per hour per g. of catalyst.

propane to 2-butene and isobutylene.[2] A similar ring splitting reaction is observed when methylcyclopentane is passed over alumina. The present paper reports the results of a kinetic study of the latter reaction, including the effects of hydrogen pressure on the reaction rate. A knowledge of the reactivity of methylcyclopentane over alumina provides some insight into the nature of the interaction of saturated hydrocarbons with an acidic surface such as alumina. Furthermore, this information is important in understanding the role of alumina as a support in bifunctional catalysts such as platinum on alumina.

Experimental

Procedure.—Reaction rates were measured using a flow reactor technique, as described in previous papers.[3,4] In the present work, methylcyclopentane was passed over alumina in the presence of hydrogen, and the reaction products were analyzed by a combination of chromatographic columns coupled directly to the reactor outlet. At each set of conditions, the methylcyclopentane was fed continuously to the reactor for a 30-minute reaction period. Between reaction periods pure hydrogen was passed over the alumina for 90 minutes at the pressure to be used in the following reaction period. Reaction products were sampled near the ends of the reaction periods to ensure the attainment of steady-state conditions prior to sampling.

The reactor was a $^1/_2$ inch i.d. stainless steel tube with a total volume of about 20 cc., and was surrounded by an electrically heated aluminum block to maintain isothermal operation. A catalyst charge of 15 g. was used. The chromatographic columns contained squalane and hexamethylphosphoramide, both impregnated on firebrick. The hexamethylphosphoramide column ($^1/_4$ inch i.d., 16 meters in length) was operated at 40°, and was used for analysis of C_5 and lighter hydrocarbons. The squalane column ($^1/_4$ inch i.d., 4 meters in length) was operated at 95°, and was used for analyses of C_6 hydrocarbons. The squalane column did not give complete resolution of the hexenes from the hexanes. To resolve hexenes from hexanes, samples were analyzed before and after absorption of the olefins in sulfuric acid.

Materials.—Phillips pure grade methylcyclopentane (> 99 mole % purity) was used throughout. The methylcyclopentane and hydrogen were dried to less than 5 p.p.m. by weight of water, using procedures described previously.[3,4] The catalyst used in this work was η-alumina,[5] prepared by calcining β-alumina trihydrate, obtained from Davison Chemical Co., in air for four hours at 593°. The surface area was 210 m.^{2}/g.

Results

The products of ring splitting of methylcyclopentane are hexenes, hexanes and lower carbon number (C_1–C_5) olefins and paraffins. In addition to ring splitting, small amounts of isomerization to cyclohexane and dehydrogenation to methylcyclopentenes are detected.

The kinetics of the ring splitting reaction were studied at low conversion levels (1 to 18%) to obtain initial rates of conversion. Conversions and rates at 471 and 499° are shown as a function of methylcyclopentane and hydrogen pressures in Table I. The reaction rate r is given by

$$r = \frac{F}{W} \Delta x \qquad (1)$$

where F represents the feed rate of a particular reactant in g. moles per hr., W is the weight of catalyst in grams, and Δx is the fraction of reactant converted. As applied to the ring splitting reaction of methylcyclopentane, F refers to the methylcyclopentane feed rate and Δx refers to the fraction of the methylcyclopentane converted to hexenes, hexanes and C_1–C_5 paraffins and olefins.

In the absence of hydrogen, the ring splitting reaction was found to proceed at a measurable rate, as shown by the results obtained when nitrogen was substituted for hydrogen. However, the rates were found to be higher in the presence of hydrogen and to increase with increasing hydrogen pressure throughout. Over the range from 2 to 20 atm., the rate was found to increase slightly more than four-fold.

Increasing methylcyclopentane pressure from 1 to 10 atm. was found to increase the rate of ring splitting by 50 to 70%, so that the rate is roughly proportional to the 0.2 power of the methylcyclopentane pressure.

The ratio of paraffins to olefins in the reaction product was found to increase markedly with increasing hydrogen pressure, as shown in Table I. In the case of C_3 and C_4 products, the ratio of paraffin to olefin increased by about 40-fold when the hydrogen pressure was increased from 2 to 20 atm., while the ratio of hexanes to hexenes increased by 10 to 12-fold. However, in no case

---

[2] M. N. Dojarenko, *Ber.*, **59**, 2933 (1926).

[3] J. H. Sinfelt, H. Hurwitz and J. C. Rohrer, *J. Phys. Chem.*, **64**, 892 (1960).

[4] J. H. Sinfelt, H. Hurwitz and R. A. Shulman, *ibid.*, **64**, 1559 (1960).

[5] H. C. Stumpf, A. S. Russell, J. W. Newsome and C. M. Tucker, *Ind. Eng. Chem.*, **42**, 1398 (1950).

did the ratio approach the equilibrium value. For example, the equilibrium value of propane/propylene at 20 atm. hydrogen pressure is about 100 times as high as the value found in this work.[6]

Typical isomeric distributions of some of the products are given in Table II. In the case of the olefins, only the distribution of the butenes is given, since the distributions of the higher molecular weight olefins were not well determined by the chromatographic analyses. For the butenes, the distribution is roughly in accord with that at equilibrium. In the case of the butanes and pentanes, the isoparaffins predominate in the products. For the butanes, the distribution is the inverse of the equilibrium distribution. The distribution of the hexanes which were observed in the product was not far different from that at equilibrium. However, essentially no dimethylbutanes were observed, whereas at equilibrium there should be about 28% present.

TABLE II

TYPICAL ISOMERIC DISTRIBUTIONS OF PRODUCTS

	Composition, mole %			
	Obsd.[a]		Equilibrium[b]	
	471°	499°	471°	499°
Butanes				
n-Butane	36	38	67	68
Isobutane	64	62	33	32
Pentanes				
n-Pentane	33	25	32	31
Isopentane	67	75	68	67
Hexanes[b]				
n-Hexane	30	30	35	35
2-Methylpentane	44	45	40	39
3-Methylpentane	26	25	25	26
Butenes				
Butene-1[c] Isobutene[c]	64	61	56	56
trans-Butene-2	20	24	25	25
cis-Butene-2	16	15	19	19

[a] H_2 pressure = 20.0 atm., methylcyclopentane pressure = 1.0 atm., 10–12% conversion. [b] Less than 1% dimethylbutanes observed in hexanes fraction; comparison with equilibrium data based only on the three isomers shown. [c] Butene-1 and isobutene not resolved.

Discussion

The observed hydrogenation activity of alumina in this work is in line with the observations of other workers who found that alumina was active for hydrogenation of ethylene at about the same temperatures as were used in the present study.[7,8] Hydrogen transfer reactions also occur to some extent, as evidenced by the fact that some hexanes are observed in the reaction products even when the reaction is carried out in the absence of hydrogen.

The promotional effect of hydrogen pressure on the rate of the ring splitting reaction could conceivably be due to several factors. One possibility is that hydrogen increases the rate of desorption of products *via* hydrogenation Another is that hydrogen serves to keep the surface free of carbonaceous residues arising from side reactions involving extensive dehydrogenation and polymerization. It is also conceivable that increasing hydrogen pressure may increase the concentration of acidic sites (protons) on the surface, which in turn may be important in the initial formation of carbonium ion type intermediates.

The small effect of methylcyclopentane pressure on the rate of the ring splitting reaction suggests that the active catalyst sites are well covered with hydrocarbon intermediates over the range of pressures studied. The apparent activation energy of the reaction is about 30 kcal./mole.

It is significant that the predominant reaction of methylcyclopentane over alumina is ring splitting with essentially no isomerization to cyclohexane, whereas over platinum supported on the same alumina appreciable isomerization–dehydroisomerization to cyclohexane and benzene is observed.[9] This suggests that the intermediates involved in these reactions are different in detail, although both are presumably of the carbonium ion type.

---

[6] "Selected Values of Physical and Thermodynamic Properties of Hydrocarbons and Related Compounds," API Research Project 44, Carnegie Press, Inc., New York, N. Y., 1953.

[7] V. C. F. Holm and R. W. Blue, *Ind. Eng. Chem.*, **43**, 501 (1951).

[8] S. W. Weller and S. G. Hindin, *J. Phys. Chem.*, **60**, 1501 (1956).

[9] J. H. Sinfelt and J. C. Rohrer, *ibid.*, **65**, 978 (1961).

INFLUENCE OF MOLECULAR WEIGHT DISTRIBUTION ON VISCOELASTIC PROPERTIES OF POLYMERS AS EXPRESSED BY THE ROUSE AND ZIMM THEORIES

BY STUART E. LOVELL AND JOHN D. FERRY

Department of Chemistry, University of Wisconsin, Madison, Wisconsin

Received July 24, 1961

At very low frequencies, the limiting value of the storage compliance of an uncross-linked polymeric system with any arbitrary distribution of molecular weight can be derived[1] from the Rouse theory[2] in terms of certain molecular weight averages. The calculation assumes that the effective monomeric friction coefficient is the same for all modes of motion which perceptibly influence the viscoelastic behavior at very low frequencies. If one compares the steady-state compliance of a homogeneous polymer (J_{eh}) with that of a sample with molecular weight distribution having the same number-average molecular weight (J_{en}), the result is

$$J_{en}/J_{eh} = \bar{M}_{z+1}\bar{M}_z/\bar{M}_w\bar{M}_n \qquad (1)$$

where the various molecular weight averages have their usual symbols.

Somewhat similar calculations have now been made for other viscoelastic functions based on the same assumptions. At very low frequencies, the storage and loss moduli G' and G'' are proportional to ω^2 and ω, respectively. The constants of proportionality can be formulated in terms of molecular weight averages by either the Rouse or the Zimm[3] theory. For example, the Rouse theory provides for a homogeneous polymer when $\omega^2\tau_1^2 << 1$

---

[1] J. D. Ferry, M. L. Williams and D. M. Stern, *J. Phys. Chem.*, **58**, 987 (1954).

[2] P. E. Rouse, Jr., *J. Chem. Phys.*, **21**, 1272 (1953).

[3] B. H. Zimm, *ibid.*, **24**, 269 (1956).

$$G'_{\mathrm{h}} = (\rho RT/M)\omega^2 \sum_{p=1} \tau_1{}^2/p^4 = 1.082(\rho RT/M)\omega^2\tau_1{}^2 \quad (2)$$

The corresponding expression for any distribution of molecular weights[4] $\varphi(M)$ such that $\int M\varphi(M)\cdot \mathrm{d}M = \bar{M}_{\mathrm{n}}$ is

$$G' = (\rho RT/\bar{M}_{\mathrm{n}})\omega^2 \int_0^\infty \Sigma(a^2Z^2\zeta_0/6\pi^2p^2kT)^2\varphi(M)\mathrm{d}M$$
$$= 1.082(\rho RT/\bar{M}_{\mathrm{n}})\omega^2(a^2\zeta_0/6\pi kTM_0{}^2)^2\bar{M}_{z+1}M_zM_wM_n \quad (3)$$

Here ρ is the density, ω the circular frequency, τ_1 the thermal relaxation time ($= a^2Z^2\,\zeta_0/6\pi^2kT$), a^2 the mean square molecular length per monomer unit, Z the degree of polymerization, ζ_0 the monomeric friction coefficient and M_0 the monomer molecular weight. If one again compares a polydisperse sample with a homogeneous polymer when the number-average molecular weights are the same, the ratio of the storage moduli of the two samples at a given low frequency is

$$G'_{\bar{\mathrm{n}}}/G'_{\mathrm{h}} = (\bar{M}_{z+1}\bar{M}_z\bar{M}_w/\bar{M}_n{}^3)(\zeta_{0\bar{\mathrm{n}}}/\zeta_{0\mathrm{h}})^2 \quad (4)$$

where the subscript $\bar{\mathrm{n}}$ refers to the polydisperse material. The last factor is necessary because the effective friction coefficients in the two samples will not in general be the same.[5] For a "most probable" distribution of molecular weights, the factor involving the molecular weight averages is 24 and it is still larger for broader distributions; the ratio of the friction coefficients also will usually be greater than unity.

Similar calculations provide the ratios $G''_{\bar{\mathrm{n}}}/G''_{\mathrm{h}}$, $G'_{\bar{\mathrm{w}}}/G'_{\mathrm{h}}$, and $G''_{\bar{\mathrm{w}}}/G''_{\mathrm{h}}$, where the subscript $\bar{\mathrm{w}}$ denotes a polydisperse sample with the same *weight*-average molecular weight as the homogeneous sample with which it is being compared. The results are presented in Table I for the Rouse and the Zimm theories. Here the solvent contribution $\omega\eta_s$ has been subtracted from the loss modulus so that the expressions are applicable to dilute solutions as well as to concentrated and undiluted systems. In the Zimm expressions, η_z is the effective local viscosity encountered by moving segments, tentatively identified with the solvent viscosity. The symbol $\bar{M}^{3/2}$ represents $\int_0^\infty M^{3/2}\varphi(M)\mathrm{d}M$. The effect of molecular weight distribution is less marked in the Zimm expressions, because the relaxation times of individual species are proportional to $M^{3/2}$ rather than M^2 as in the Rouse theory.

TABLE I

RATIOS OF DYNAMIC MODULI AT VERY LOW FREQUENCIES FOR POLYDISPERSE AND HOMOGENEOUS POLYMER SAMPLES

Polydisperse/ Homogeneous	Rouse	Zimm
$G'_{\bar{\mathrm{n}}}/G'_{\mathrm{h}}$	$(\bar{M}_{z+1}\bar{M}_z\bar{M}_w/\bar{M}_n{}^3)$ $\times\ (\zeta_{0\bar{\mathrm{n}}}/\zeta_{0\mathrm{h}})^2$	$(\bar{M}_z\bar{M}_w/\bar{M}_n{}^2)$ $\times\ (\eta_{z\bar{\mathrm{n}}}/\eta_{z\mathrm{h}})^2$
$(G''_{\bar{\mathrm{n}}} - \omega\eta_s)/$ $(G''_{\mathrm{h}} - \omega\eta_s)$	$(\bar{M}_w/\bar{M}_n)$ $\times\ (\zeta_{0\bar{\mathrm{n}}}/\zeta_{0\mathrm{h}})$	$(\bar{M}^{3/2}/\bar{M}_n{}^{3/2})$ $\times\ (\eta_{z\bar{\mathrm{n}}}/\eta_{z\mathrm{h}})$
$G'_{\bar{\mathrm{w}}}/G'_{\mathrm{h}}$	$(\bar{M}_{z+1}\bar{M}_z/\bar{M}_w{}^2)$ $\times\ (\zeta_{0\bar{\mathrm{w}}}/\zeta_{0\mathrm{h}})^2$	$(\bar{M}_z/\bar{M}_w)$ $\times\ (\eta_{z\bar{\mathrm{w}}}/\eta_{z\mathrm{h}})^2$
$(G''_{\bar{\mathrm{w}}} - \omega\eta_s)/$ $(G''_{\mathrm{h}} - \omega\eta_s)$	$\zeta_{0\bar{\mathrm{w}}}/\zeta_{0\mathrm{h}}$	$(\bar{M}^{3/2}/\bar{M}_w{}^{3/2})$ $\times\ (\eta_{z\bar{\mathrm{w}}}/\eta_{z\mathrm{h}})$

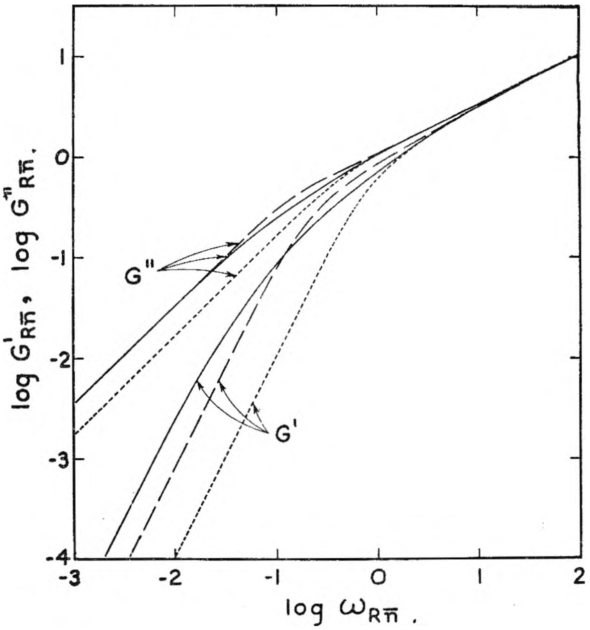

Fig. 1.—Dimensionless Rouse plots for the shear storage and loss moduli of a polymer with a most probable distribution of molecular weights (solid curves). The relative positions (on unreduced scales) of the moduli for monodisperse polymers of the same M_n and of the same $\bar{M}_w$ are shown by the curves with short and long dashes, respectively.

The magnitudes of the ratios of ζ_0's and η_z's will depend on the type of system. In dilute solution, where the polydisperse and homogeneous polymers are of course to be compared at equal weight concentrations, if η_z can be identified with the solvent viscosity then the η_z ratios are unity. In concentrated solutions and undiluted polymers, the Rouse theory specifies[5] that $\zeta_{0\bar{\mathrm{n}}}/\zeta_{0\mathrm{h}} = \eta_{\bar{\mathrm{n}}}\bar{M}_n/\eta\bar{M}_w$, while $\zeta_{0\bar{\mathrm{w}}}/\zeta_{0\mathrm{h}} = \eta_{\bar{\mathrm{w}}}/\eta_{\mathrm{h}}$; here the η's are the respective steady flow viscosities. Thus insofar as the viscosity is a function of the weight-average molecular weight in polydisperse systems, $\zeta_{0\bar{\mathrm{w}}}/\zeta_{0\mathrm{h}} = 1$. The ratio $\eta_{0\bar{\mathrm{n}}}/\eta_{0\mathrm{h}}$ is greater than unity to an extent that depends on the breadth of distribution and also whether the concentration and average molecular weight are sufficiently high for long-range coupling entanglements.

It is of interest to examine the shapes of the functions G' and G'' for a specific molecular weight distribution, the most probable,[6] as predicted by the Rouse theory. For this purpose, the equivalent formulation of Blizard[7,8] is more convenient because of its closed form. Calculations[9] were made with a Bendix G-15D computer, generously made available by the Theoretical Chemistry Laboratory, to obtain the complex dimensionless modulus of Blizard for a most probable molecular length distribution. The most probable distribution was approximated by the form, valid except when $\bar{M}_n$ is very small, of $\varphi(M) = e^{-\mu}/\bar{M}_n$; here $\mu = M/\bar{M}_n$. Blizard's expression then becomes

---

(4) J. D. Ferry, "Viscoelastic Properties of Polymers," John Wiley and Sons, Inc., New York, N. Y., 1961, p. 172, eq. (51).

(5) Reference 4, p. 169 ff.

(6) P. J. Flory, "Principles of Polymer Chemistry," Cornell University Press, Ithaca, N. Y., 1953, pp. 319, 335.

(7) R. B. Blizard, *J. Appl. Phys.*, **22**, 730 (1951).

(8) B. Gross, *J. Polymer Sci.*, **20**, 123 (1956).

(9) The authors can furnish upon request a more detailed report together with numerical tables including evaluations of the Rouse and Zimm theories for homogeneous systems.

$$A(iH) = \int_0^\infty e^{-\mu}[\mu(iH)^{1/2} \coth \mu(iH)^{1/2} - 1]\, d\mu \quad (5)$$

where H is Blizard's reduced frequency. The results of eq. 5 were subsequently expressed in terms of the reduced variables corresponding to the Rouse theory

$$G'_{R\bar{n}} = G'\bar{M}_n/cRT \quad (6)$$

$$G''_{R\bar{n}} = (G'' - \omega\eta_s)\bar{M}_n/cRT \quad (7)$$

$$\omega_{R\bar{n}} = \omega\tau_{1\bar{n}} = \omega a^2 Z_n^2 \zeta_0/3\pi^2 kT \quad (8)$$

By identifying the results of the Blizard and Rouse formulations at low and high frequencies, it can be shown that $G'_{R\bar{n}} + iG''_{R\bar{n}} = A/2$, and $\omega_{R\bar{n}} = H/\pi^2$.

In Fig. 1, $G'_{R\bar{n}}$ and $G''_{R\bar{n}}$ are plotted against $\omega_{R\bar{n}}$. The only difference in shape from the familiar curves for a polymer homogeneous in molecular weight is a more gradual curvature where the slopes change. Curves also are drawn to show the relative positions (*i.e.*, relative for unreduced scales, G' and G'' *vs.* ω directly) for homogeneous samples with the same number and weight average molecular weights, respectively, taking the ζ_0-ratios as unity. At high frequencies, the curves all coincide; at low frequencies, their separations on the modulus scale are all in agreement with the formulas given in Table I. These calculations are valid, of course, only for systems in which there is no entanglement coupling.

Experiments on dilute solutions of homogeneous and polydisperse polymers are in progress. For concentrated and undiluted systems, it will be necessary to extend the calculations to take entanglement coupling into account, except when the entire range of molecular weights is below the critical entanglement limit.

Acknowledgment.—This work was supported in part by a grant from the National Science Foundation.

COMMUNICATION TO THE EDITOR

POLYMERIZATION OF SOLID ETHYLENE BY IONIZING RADIATION: EVIDENCE FOR ION-MOLECULE CONDENSATION

Sir:

A recent study from this Laboratory[1] disclosed that irradiation of liquid propylene gives dimer olefin derived in part by direct condensation of two propylene molecules, with all their hydrogen atoms retained in the product. This was taken as support for an ion–molecule mechanism that was proposed originally for 1-hexene radiolysis:[2]

$$C_nH_{2n}^+ + C_nH_{2n} \longrightarrow C_{2n}H_{4n}^+ \xrightarrow{e^-} C_{2n}H_{4n}$$

However, proof was lacking that propagation could proceed to give the higher polymers

$$C_{2n}H_{4n}^+ + C_nH_{2n} \longrightarrow C_{3n}H_{6n}^+, \text{ etc.}$$

It now has been found that ethylene irradiated at −196° gives low molecular weight, mostly branched polymers, >90% monoölefins, of carbon number through C_{18}. Products from the irradiation of an equimolar mixture of C_2D_4 and C_2H_4 were separated by gas chromatography, and mass spectra of the major C_4 (1-butene), C_6, C_8, and C_{10} components recorded. Corrections were made in the parent ion region of the mass spectra for contributions by C^{13} and by the light hydrogen isotopic impurity in the C_2D_4 (0.83%). Corrections for fragment ions were necessary only for 1-butene; these were applied assuming no isotope effect, a correction leading to some error, but not a serious one. Data are shown in the table.

TABLE I

ISOTOPIC DISTRIBUTION OF PRODUCTS OF C_2D_4–C_2H_4 RADIOLYSIS AT −196°: SPECIES DISTRIBUTION IN EACH CARBON NUMBER, MOLE PER CENT.

	d_0	d_1	d_2	d_3	d_4	d_5	d_6	d_7	d_8	d_9	d_{10}	d_{11}	d_{12}	d_{13}	d_{14}	d_{15}	d_{16}	d_{17}	d_{18}	d_{19}	d_{20}
C_4	22	3	7	8	32	2	6	2	18												
C_6	15	3	2	4	29	5	1	6	22	3	1	3	6								
C_8	9	1	1	1	25	4	1	4	30	3	2	1	15	1	1	0	4				
C_{10}	4	2	0	2	14	0	2	4	28	0	2	4	25	0	2	2	9	0	0	0	<4

The strong maxima at species with deuterium atoms in multiples of four make it clear that hydrogen exchange between monomer and propagating polymer is negligible. It is also clear that the initiating species must contain two carbon atoms and four hydrogen atoms, and cannot be a vinyl or an ethyl entity. An initiating species with the formula C_2H_4 could be the molecule ion, $C_2H_4^+$, or some excited state of the molecule. We believe only the molecule ion could supply the driving force for carbon–carbon bond formation at such a low temperature.

The character of this initiating ion contrasts with that of the *t*-butylcarbonium ion, which appears to initiate the radiation-induced polymerization of isobutylene. It has been noted[3] that the ion–molecule reaction to form *t*-butyl ion

$$C_4H_8^+ + C_4H_8 \longrightarrow C_4H_9^+ + C_4H_7\cdot$$

is exothermic. In contrast, the comparable reaction with ethylene is endothermic

$$C_2H_4^+ + C_2H_4 \longrightarrow C_2H_5^+ + C_2H_3\cdot$$

---

[1] C. D. Wagner, *Tetrahedron*, **14**, 164 (1961).

[2] P. C. Chang, N. C. Yang, and C. D. Wagner, *J. Am. Chem. Soc.*, **81**, 2060 (1959).

[3] F. W. Lampe, *J. Phys. Chem.*, **63**, 1986 (1959).

This may explain the different mode of initiation.

Further studies are underway to explore the mode of propagation to form the branched olefins.

Shell Development Company
Emeryville, California
C. D. Wagner

Received October 14, 1961

ADDITIONS AND CORRECTIONS

1960, Vol. 64

Thomas H. Donnelly. The Study of Limited Molecular Weight Distribution by the Use of Equilibrium Ultracentrifugation.

Page 1832. In eq. (15) the exponent should read: $(\beta_i/\beta_0) - 1$).

Page 1834. In col. 1, line 7, "Eq. 33" should read "Eq. (34)."—T. H. Donnelly.

1961, Vol. 65

M. Shanin and K. O. Kutschke. Formation of Methyl Hydroperoxide in the Photoöxidation of Azomethane.

Page 189. In the authors name line, for "Shanin" read "Shahin."—M. Shahin.

W. J. Thomas and I. A. Furzer. The Computation of the Path Difference Function for the Calculation of Diffusion Coefficients by the Gouy Method.

Pages 439–440. Equation (1) should read

$$f(z) = \mathrm{erf}(Z) - (2/\sqrt{\pi})ze^{-z^2}$$

$f(z)$	e^{-z^2}	$f(z)$	e^{-z^2}
Corrections		0.037	0.86760
		0.038	0.86526
0.0299	0.88492	0.039	0.86294
0.154	0.66548	0.040	0.86064
		0.041	0.85837
Omissions		0.042	0.85611
		0.043	0.85337
0.031	0.88215	0.044	0.85165
0.032	0.87966	0.045	0.84945
0.033	0.87720	0.046	0.84726
0.034	0.87476	0.047	0.84509
0.035	0.87235	0.048	0.84294
0.036	0.86996	0.049	0.84080

W. J. Thomas and I. A. Furzer

W. A. Rosser, Jr., and H. Wise. The Rate of Reaction of Hydrogen with Nitrogen Dioxide.

Pages 533–534. Equation (8) should read

$$k_1/k_2 = 0.16 \times e^{3130/RT}$$

This correction affects the equations shown in Fig. 2 and the ration A_1/A_2, which occurs twice. The derived value of the specific rate constant k_1 is not affected by the error in eq. (8).—Willis A. Rosser, Jr.

Andrew G. De Rocco. On the Second Virial Coefficient for Uncharged Spherical Macromolecules.

Page 778. In col. 2, line 10 below eq. (10), for "δ" read "$\delta - 1$."

Page 779. In col. 1, line 4, for "$\theta = 0$" read "$H = 0$." In eq. (18), for "+0.9489" read "−0.4477."—Andrew G. De Rocco.

K. Nishikawa, D. Patterson and G. Delmas. Critical Phenomena in Thin Films using the Bragg-Williams Approximation.

Page 1228. Table I, mentioned after eq. (30), was omitted.

Table I

Values of τ_c

	$\xi_- = 0$				$\xi_+ = 0$	
	ξ_+ m 0.2	0.5	1.0	2.0	ξ_- m 0.1	0.2
3	0.850	0.83	0.81	0.77	0.85	0.82
5	.928	.91	.90	.88	.92	.88
7	.957	.95	.94	.93	.95	
9	.971	.96	.96	.96	.96	
14	.986	.98	.98	.98		
19	.991	.98	.98	.98		
6	.946	.93	.92	.91	.94	
	(.946)	(.92)				

C. Peterson and T. K. Kwei. The Kinetics of Polymer Adsorption onto Solid Surfaces.

Page 1332. Equation (5) should read

$$-\ln 1 - (1 + k_1/k_1C)\theta = (k_1C + k_1)t = k_1Ct \text{ (for small } k_{-1})$$

Clarke M. Peterson

M. O'Keeffe and W. J. Moore. Diffusion of Oxygen in Single Crystals of Nickel Oxide.

Page 1438. In equation (2) of this paper we put $\alpha = \beta/3$ instead of the correct $\alpha = \beta$. The diffusion data have been recalculated. The new and corrected diffusion coefficient for ^{18}O in NiO is $D = 6.2 \times 10^{-4} \exp(-57{,}500 \text{ cal.}/RT)$ cm.^{2} sec.$^{-1}$. The value in the paper was $D = 10^{-5} \exp(-54{,}000)/RT)$. The general conclusions of the paper are not changed.—Walter J. Moore.

Author Index to Volume LXV, 1961

Subject Index to Volume LXV, 1961

No. 26 in the Advances in Chemistry Series

NONMILITARY DEFENSE

Chemical and Biological Defenses in Perspective

This complete text of the Symposium on Nonmilitary Defense at the ACS spring meeting in 1960 is both timely and significant. It offers 11 papers by specialists from industry, from health and defense departments of the government, from the American Medical Association, the President's office, the Rockefeller Foundation.

Chemical and biological weapons are nearly on a par with nuclear weapons. This book shows why. It provides a point by point comparison between chemical, biological and nuclear weapons . . . full description of the threat . . . discussion of medical problems in protecting citizens . . . of questions of early warning and detection . . . of research still needed.

All chemists and laymen concerned with the weapons aspects of defense will want this marshalling of the facts.

100 pages. **Paper bound.** **Price: $2.00**

Order from:

Special Issues Sales / American Chemical Society / 1155 Sixteenth Street, N.W. / Washington 6, D.C.

- **Increasingly, authors are asked to prepare abstracts of their papers to accompany the complete papers when published in primary journals.**
- **Scientists must frequently index their own books.**
- **Industrial organizations routinely build collections of abstracts and indexes with emphasis on their own special interests.**

CA TODAY

This informative 130 page clothbound volume describes for the reader the interworkings of the world's largest and most successful abstracting undertaking.

All scientists and organizations interested in producing abstracts and/or indexes will find this book on the production of CHEMICAL ABSTRACTS an invaluable aid.

CA Today tells how source material is gathered, explains the assignment of abstracts, and the problems of recording, editing, and classifying abstracts. Indexing procedures are explained, methods of printing are discussed, and research, administration, housing and equipment, nomenclature, and records are amply described in separate chapters. The total concept behind the development of successful abstracting is presented for the first time in one reference.

Clothbound. . . . .**130 pages**. **$3.50**

order from

Special Issues Sales
AMERICAN CHEMICAL SOCIETY
1155 16th Street, N. W.
Washington, D. C.

THE RING INDEX *Second Edition*

A List of Ring Systems Used in Organic Chemistry

by Austin M. Patterson
Leonard T. Capell
Donald F. Walker

This index, published in 1960, provides a single source where structural formulas, names and numberings of the thousands of parent organic ring systems can be found. Since the first edition (1940) the number of ring systems has almost doubled.

features This new edition lists 7727 organic ring systems—almost a hundred percent increase over the first edition. It has been enlarged to 1425 pages to cover the abstracted literature through 1956. Each ring system contains: (1) a structural formula showing the standard numbering system in accord with the 1957 *Definitive Rules for the Nomenclature of Organic Chemistry* of the IUPAC; (2) other numberings that have appeared in the literature; (3) a serial number which identifies the system; (4) the preferred name and other names given to the system; (5) identifying references to the original literature.

arrangement The ring systems are arranged from the simplest to the most complex, beginning with single rings, then systems of two rings and so on up to twenty-two-ring complexes.

uses The Ring Index is an indispensable reference for organic chemists and for others who work with cyclic organic compounds. You can use it for determining accepted structure of a ring system . . . finding name or names of the system if structure is known . . . finding the numbering of a system . . . identifying a system if there are two or more isomeric forms . . . discovering what systems have been reported in the literature and where . . . naming and numbering a newly discovered ring system . . . as a reference book in teaching.

1425 pages. ***Cloth bound.*** ***Price: $20.00***

Order from:

Special Issues Sales / American Chemical Society / 1155 Sixteenth Street, N.W. / Washington 6, D.C.